THE INFLUENCE OF BIOLOGICAL RHYTHMS ON THE BENEFICIAL EFFECTS OF GRAPE SEED PROANTHOCYANIDIN EXTRACT (GSPE) ON LIVER METABOLISM IN HEALTH AND DISEASE

Romina Mariel Rodriguez

THE INFLUENCE OF BIOLOGICAL RHYTHMS ON THE BENEFICIAL EFFECTS OF GRAPE SEED PROANTHOCYANIDIN EXTRACT (GSPE) ON LIVER METABOLISM IN HEALTH AND DISEASE

ROMINA MARIEL RODRIGUEZ

DOCTORAL THESIS
2022

UNIVERSITAT ROVIRA i VIRGILI

UNIVERSITAT ROVIRA I VIRGILI
THE INFLUENCE OF BIOLOGICAL RHYTHMS ON THE BENEFICIAL EFFECTS OF GRAPE SEED PROANTHOCYANIDIN EXTRACT (GSPE) ON LIVER METABOLISM IN HEALTH AND DISEASE
Romina Mariel Rodriguez

UNIVERSITAT ROVIRA I VIRGILI
THE INFLUENCE OF BIOLOGICAL RHYTHMS ON THE BENEFICIAL EFFECTS OF GRAPE SEED PROANTHOCYANIDIN EXTRACT (GSPE) ON LIVER METABOLISM IN HEALTH AND DISEASE
Romina Mariel Rodriguez

Romina Mariel Rodríguez

THE INFLUENCE OF BIOLOGICAL RHYTHMS ON THE BENEFICIAL EFFECTS OF GRAPE SEED PROANTHOCYANIDIN EXTRACT (GSPE) ON LIVER METABOLISM IN HEALTH AND DISEASE

DOCTORAL THESIS

Supervised by Dr. Miquel Mulero Abellán

UNIVERSITAT ROVIRA i VIRGILI

Nutrigenomics Research Group

Department of Biochemistry and Biotechnology

Tarragona 2022

UNIVERSITAT ROVIRA I VIRGILI
THE INFLUENCE OF BIOLOGICAL RHYTHMS ON THE BENEFICIAL EFFECTS OF GRAPE SEED PROANTHOCYANIDIN EXTRACT (GSPE) ON LIVER METABOLISM IN HEALTH AND DISEASE
Romina Mariel Rodriguez

UNIVERSITAT ROVIRA i VIRGILI

DEPARTAMENT DE BIOQUÍMICA I BIOTECNOLOGIA
Campus Sescelades
C/ Marcel·lí Domingo, 1
43007 Tarragona
Tel. +34 977 55 95 21
Fax +34 977 55 82 32

FAIG CONSTAR que aquest treball, titulat "**The influence of biological rhythms on the beneficial effects of Grape seed proanthocyanidin extract (GSPE) on liver metabolism in health and disease**" que presenta **Romina Mariel Rodríguez** per a l'obtenció del títol de doctorat, ha estat realitzat sota la meva direcció al Departament de Bioquímica i Biotecnologia de la Universitat Rovira i Virgili i que compleix els requisits per a l'obtenció de la Menció Internacional de Doctorat.

HAGO CONSTAR que el presente trabajo, titulado "**The influence of biological rhythms on the beneficial effects of Grape seed proanthocyanidin extract (GSPE) on liver metabolism in health and disease**", que presenta **Romina Mariel Rodríguez** para la obtención del título de Doctor, ha sido realizado bajo mi dirección en el Departamento Bioquímica y Biotecnologia de la Universitat Rovira i Virgili y que cumple con los requisitos para la obtención de la Mención Internacional de Doctorado.

I STATE that the present study, entitled "**The influence of biological rhythms on the beneficial effects of Grape seed proanthocyanidin extract (GSPE) on liver metabolism in health and disease**", presented by **Romina Mariel Rodríguez** for the award of the degree of Doctor, has been carried out under my supervision at the Department of Biochemistry and Biotechnology of the Universitat Rovira i Virgili and that is eligible to apply for the International Doctoral Mention.

Tarragona, 8 de Juny de 2022/Tarragona, 8 de Junio de 2022/Tarragona, June 8th, 2022

El director de la tesi doctoral

El director de la tesis doctoral

Doctoral thesis supervisor

Dr. Miquel Mulero Abellán

UNIVERSITAT ROVIRA I VIRGILI
THE INFLUENCE OF BIOLOGICAL RHYTHMS ON THE BENEFICIAL EFFECTS OF GRAPE SEED PROANTHOCYANIDIN EXTRACT (GSPE) ON LIVER METABOLISM IN HEALTH AND DISEASE
Romina Mariel Rodriguez

This thesis was carried out at the Nutrigenomics Research Group of the Universitat Rovira i Virgili (URV) thanks to the award of a URV predoctoral grant Martí i Franqués Program, grant number 2018PMF-PIPF-11. The research work performed in this thesis was supported by the grant AGL2016-77105-R from the Spanish Ministry of Economy and Competitiveness (MINECO). An international research stay was carried out at the Institute of Neurobiology of the Center of Brain, Behavior and Metabolism (CBBM), Universität zu Lübeck (Germany), under the supervision of Prof. Dr. Henrik Oster. This international stay was supported by the international mobility grant (ERASMUS+) for internships (2021/22) and by the Spanish Society of Genetics travel grant (2021).

UNIVERSITAT ROVIRA i VIRGILI

Grup de Recerca
NUTRIGENÒMICA URV

MARTÍ i FRANQUÈS
DOCTORAL PROGRAMME
Universitat Rovira i Virgili

GOBIERNO DE ESPAÑA
MINISTERIO DE ECONOMÍA Y COMPETITIVIDAD
Unión Europea
Fondo Europeo de Desarrollo Regional

Erasmus+

UNIVERSITAT ROVIRA I VIRGILI
THE INFLUENCE OF BIOLOGICAL RHYTHMS ON THE BENEFICIAL EFFECTS OF GRAPE SEED PROANTHOCYANIDIN EXTRACT (GSPE) ON LIVER METABOLISM IN HEALTH AND DISEASE
Romina Mariel Rodriguez

A mis padres,

mis hermanos y amigos.

A mi sobrina Ada.

UNIVERSITAT ROVIRA I VIRGILI
THE INFLUENCE OF BIOLOGICAL RHYTHMS ON THE BENEFICIAL EFFECTS OF GRAPE SEED PROANTHOCYANIDIN EXTRACT (GSPE) ON LIVER METABOLISM IN HEALTH AND DISEASE
Romina Mariel Rodriguez

AGRADECIMIENTOS

"La felicidad sólo es real cuando es compartida"

"Compartir és viure, i viure és estimar"

Al momento de escribir estas líneas, me recorre una sensación inmensa de gratitud, y sé que no alcanzarán las palabras para agradecer a todos los que de alguna u otra forma me han acompañado y han compartido conmigo esta desafiante y maravillosa etapa de mi vida.

Me gustaría agradecer en primer lugar a la Universitat Rovira i Virgili, y en especial, al Grupo de Investigación en Nutrigenómica por haberme brindado esta gran oportunidad de llevar a cabo mis estudios de doctorado, por proveerme con las herramientas y permitirme seguir capacitándome.

GRACIAS a Miquel, por haber confiado en mí y ser tan comprensivo desde el inicio, sobre todo con las peripecias de mi incorporación. Gracias por guiarme durante estos años, por tu apoyo en todo momento, por las palabras de aliento y motivación en cada correo, en cada reunión. Gracias por enseñarme que a veces hay que mirar por el espejo retrovisor y seguir. Me llevo muchísimas enseñanzas y muy bonitos recuerdos como el congreso en Londres o las tardes de inglés. Gracias por levantarme los ánimos más de una vez y sacarme una carcajada cuando las cosas no salían como esperábamos, porque si hay algo que no le faltaba a este equipazo era actitud positiva. Gracias por estar al pie del cañón siempre, por la dedicación y el esfuerzo que has puesto en esta tesis, sé que has sido fundamental para que hoy pueda estar cumpliendo este objetivo.

GRACIAS a Braulio y a Rosa, porque además de estar siempre predispuestos a ayudar, me han levantado el ánimo con sólo una palabra o una sonrisa por los pasillos incontables veces.

Quiero dedicarle un GRACIAS enorme a la que considero de las más valiosas y auténticas. Gracias Niurkita por todo el cariño y la ayuda que me brindaste estos años. Gracias porque siempre has estado para resolverme las dudas y

explicarme las cosas con mucha paciencia. Sin duda voy a extrañar los cafecitos, las charlas y los looks. Pero espero que nunca olvides que tu niña del puente te admira y quiere muchísimo.

Muchas GRACIAS a mis compañeros que me han acompañado en este camino. Desde luego estos años han sido mucho más llevaderos gracias a ustedes. Juntos hemos pasado por todos los colores jaja…las verdes, las rojas, las rosas y las amarillas!, el viaje a Parma, los Re-Cumples, las expediciones al tanque de nitrógeno, las dietas de cafetería y las tardes rotulando tubitos, las calçotadas… Me llevo muy lindos recuerdos. Gracias Jorge, Vero, Raúl, Pauli, Néstor, Marta, Iván y Rafa por compartir conmigo esta etapa. Gracias Alba además por todo lo que compartimos como compis de piso, yo también he disfrutado mucho las tardes de body-pump y las de ocio jeje, gracias por los ánimos y los consejos a la hora de escribir. Gracias Marina, Jose y Èlia también por las meriendas y las tardes de playa, por los cafés, las birras, las cenas y las salidas. Han sido una parte muy importante, ¡muchas gracias por todos los lindos momentos compartidos!

GRACIAS Carme bonita por estar siempre predispuesta a ayudarme, ya sea para cosas del laboratorio como para mudanzas/viajes acarreando valijas por Tarragona, por los mates y las charlas podcast acompañadas de vermut (sigo pensando que nos iría muy bien jaja). Me has demostrado que puedo contar contigo en las buenas y en las malas y te voy a estar por siempre agradecida. GRACIAS a la italiano-argentina por todo el aguante en estos años, por las aventuras que hemos vivido juntas, por las cenas y comidas taaan deliciosas por hacerlo todo con tanto amor. Gracias por escucharme y aconsejarme tanto en el lab como en la vida. En sí, gracias Fra por tanto, ti voglio bene.

GRACIAS Álvaro por tu amistad incondicional, por haberle dado color a mi vida. Si pienso en las mejores cosas que me dio esta etapa, haberte conocido sin duda lo es. Gracias por todo lo vivido, por estar siempre presente, por creer en mí y darme ánimos, sin ti esto no hubiera sido posible. Gracias por permitirme conocer a Pau, a la que también quiero agradecer de corazón

por todo el aguante, sobre todo en los momentos más difíciles. Atesoro increíbles momentos con ustedes, pero sé que nos esperan muchas más aventuras juntos.

GRACIAS a Naty y Carmen, por ser más que compis de piso, por compartir mis alegrías y mis tristezas, por aguantar mis momentos de crisis con el doctorado y ser tan buenas amigas. Naty siempre predispuesta a ponerme bella, gracias a ti aprendí a maquillarme jaja. Carmen, no sé qué hubiera sido de mí durante la pandemia sin las tardes de terracita y vermut, o las maratones de Netflix, o las clases de la Patri, o tus bizcochos de plátano, corrección: o tus bizcochos jaja. Siempre me tendrás para hacer catarsis o para unos episodios de Friends con pochoclos y me pone muy feliz seguir compartiendo momentos juntas. Me gustaría también darle las GRACIAS a Blanca, sobre todo por ayudarme con los contratos en alemán y ser mi instructora de mails, he disfrutado compartiendo piso y helados contigo.

GRACIAS a Anna y María porque me han aconsejado y ayudado siempre. Me lo he pasado muy bien estos años compartiendo cenas, gin tonics y también gimnasio jaja. GRACIAS Kathe y Eli por haberme hecho parte de su familia y amigos, he disfrutado muchísimo los viajes y las juntadas al estilo latino. Han estado siempre y han sido un sostén muy importante para mí en estos años. ¡¡¡Mil gracias!!!

A mis amigos de Barcelona, GRACIAS porque todo esto empezó con ustedes. Su amistad y todo lo hermoso que vivimos hicieron que quisiera volver a estas tierras. A mis nenis, Carla, Paola y Ainhoa, porque a pesar de la distancia cada vez que nos vemos me alegran el corazón y sé que seguiremos sumando historias y aventuras juntas. Les estimo moltíssim! A Marc, mi gran amigo y compi de estudio, por haberme alojado en los inicios de esta etapa, que gracias a ti han sido más llevaderos. Te agradezco por estar siempre presente y por todos los lindos momentos que compartimos, desde tu viaje a Argentina hasta las excursiones por Tarragona. Graciaas bdoo! Jaja

GRACIAS a mi veci José por ser tan buena onda, por darme siempre una mano cuando lo necesitaba, por las veces que me has llevado a Reus para hacer experimentos o buscado del aeropuerto. Me alegra haberte conocido y sabes que puedes contar conmigo siempre.

A mis amigas de la carrera, Meli y Ceci porque a la distancia han aguantado todos mis dramas, y me han apoyado y animado en todo momento. GRACIAS Me, disfruté muchísimo y me ha encantado tenerte cerca esos meses de estancia, sin duda no hubiera sido igual sin tus matecitos y charlas en el Dräger park o las noches de karaoke y guitarra en el puerto de Rostock. GRACIAS Ce por venir a compartir conmigo este día tan especial, me pone muy feliz tenerte de este lado del mapa y sé que seguiremos sumando historias juntas. Mil gracias amigas. ¡Las adoro!

A mis amigas de toda la vida, la Flia E., GRACIAS porque a pesar de que pasen los años y la distancia no nos permita vernos, nuestra amistad es eterna, y sé que estarán ahí para apoyarme. ¡Las quiero mucho amis! Muchas GRACIAS Vi, mi hermanita de corazón, porque estuviste siempre y cuando más te necesitaba, escuchándome y aconsejándome. Gracias por compartir conmigo a la distancia los nuevos retos de los 30 jaja.

One of the most beautiful experiences was my doctoral stay at the Institute of Neurobiology in Lübeck. As well as learning new techniques and a bit of German, in particular vital words such as „Dunstabzugshaube" I met such nice and wonderful people from all over the world. First of all, I would like to thank Dr. Henrik Oster for giving me the opportunity to carry out my research at the Institute. Thanks so much Leo for all your patience, for taking the time to teach me and always answering all my doubts, and ALSO for the nice "Spanish-Portuguese" coffee talks rsrsrs. A very special thanks to my Gilmore girls, Isa and Ankita. I'm so glad to have met you girls. Thanks for the long nights of games/talks (never watched a single episode but it will always be Gilmore girls' night), I keep the best memories in my heart. Thank you so much Lina, it was very nice to have you as a lab partner, but what I enjoy most is to have you as a friend. Although the word friendship has an

end (but not lab partner), I know that no matter the distance or time our friendship will last. It was great to see you again, thanks for coming to Tarragona! Also, thanks to the rest of the Lulú-club, to Xenia, Iwona and Nane, I really enjoyed working with you, sharing scientific views and why not some beers too.

Lübeck también me permitió conocer personas geniales fuera del ámbito "académico". Gracias a mis compis de "la Cueva" Undji y Moritz por todo lo compartido juegos, risas, pelis, cenas y sobre todo las "dance sessions" desestresantes. Quiero darle las gracias al alma de la Cueva, al mexicano más copado y divertido por mostrarme a Alemania desde otra perspectiva. GRACIAS Mau por ser tan bueno conmigo, por los desayunos y las charlas filosóficas después de un largo día de trabajo con un Malbec (cómo extraño Alemania por esto jaja) en la cueva o la terraza del Hansemuseum. Gracias por presentarme a la banda Latina y hacerme sentir como en casa. Tu amistad es uno de los grandes tesoros que me dio esta hermosa experiencia.

Por último, pero no menos importante quiero darle las GRACIAS a mi familia por haberme acompañado en todo momento, cerca y sobre todo a lo lejos. A mis padres por ser mis pilares, por enseñarme a volar alto y ser mi ejemplo de esfuerzo y constancia; y a mis hermanos Cristy, Iván y Maury por el apoyo y el cariño incondicional. ¡Los amo y extraño un montón!

Como dije al principio, me considero muy afortunada y estoy muy agradecida por tener en mi vida personas tan valiosas, a las que he conocido durante esta etapa y también a las que me siguieron acompañando en estos años.

Porque las palabras nunca alcanzan, cuando lo que hay que decir desborda el alma: ¡¡¡MUCHÍSIMAS GRACIAS A TODOS!!!

UNIVERSITAT ROVIRA I VIRGILI
THE INFLUENCE OF BIOLOGICAL RHYTHMS ON THE BENEFICIAL EFFECTS OF GRAPE SEED PROANTHOCYANIDIN EXTRACT (GSPE) ON LIVER METABOLISM IN HEALTH AND DISEASE
Romina Mariel Rodriguez

Discovery is seeing what everybody else has seen
and thinking what nobody else has thought
Albert Szent-Györgyi

UNIVERSITAT ROVIRA I VIRGILI
THE INFLUENCE OF BIOLOGICAL RHYTHMS ON THE BENEFICIAL EFFECTS OF GRAPE SEED PROANTHOCYANIDIN EXTRACT (GSPE) ON LIVER METABOLISM IN HEALTH AND DISEASE
Romina Mariel Rodriguez

TABLE OF CONTENTS

SUMMARY

Biological rhythms are internal timing mechanisms that allow organisms to adapt and anticipate cyclical changes in the environment caused by the rotation of the earth around its axis (circadian rhythms) and around the sun (circannual rhythms). Disruption of these mechanisms have been associated with impairment of metabolic homeostasis. Nowadays, excessive consumption of high-calorie foods has not only been shown to promote metabolic dysfunction, but also to cause circadian disturbances leading to Metabolic syndrome (MS) and non-alcoholic fatty liver disease (NAFLD). Proanthocyanidins, including grape seed proanthocyanidin extract (GSPE), are secondary plant metabolites that are considered beneficial in treating metabolic diseases. It has been reported that GSPE is able to modulate the circadian clock machinery, thus influencing the internal rhythmicity of metabolic processes. Therefore, the main aim of the present thesis was to evaluate if diurnal rhythms (day/night) and seasonal rhythms (photoperiods) can influence the beneficial effects of GSPE consumption on liver metabolism. To fulfill this objective, we carried out animal experiments and analyzed lipid and glucose-related parameters in blood and liver in relationship with the liver clock function. Firstly, we assessed the alteration of the hepatic metabolic rhythms caused by an obesogenic diet intake and demonstrated that the restorative effect of GSPE depends on the timing of administration. Most of its beneficial effects were found when GSPE was administered at the onset of the dark phase, the beginning of the active phase in rats. Secondly, we determined the photoperiod-dependent response of GSPE effects over serum hormones and liver metabolism under physiological conditions. Finally, we evidenced the strong influence of day length on the beneficial effects of GSPE consumption to treat MS and NAFLD. These findings highlight the importance of considering biological rhythms when studying the therapeutic actions of proanthocyanidins in MS-associated diseases in order to maximize their benefits.

UNIVERSITAT ROVIRA I VIRGILI
THE INFLUENCE OF BIOLOGICAL RHYTHMS ON THE BENEFICIAL EFFECTS OF GRAPE SEED PROANTHOCYANIDIN EXTRACT (GSPE) ON LIVER METABOLISM IN HEALTH AND DISEASE
Romina Mariel Rodriguez

RESUMEN

Los ritmos biológicos son mecanismos de cronometraje internos que permiten a los organismos adaptarse y anticiparse a los cambios cíclicos del entorno causados por la rotación de la tierra alrededor de su eje (ritmos circadianos) y del sol (ritmos circanuales). La alteración de estos mecanismos está asociada al deterioro de la homeostasis metabólica. Actualmente, el consumo excesivo de alimentos calóricos no sólo favorece la disfunción metabólica, sino que también provoca alteraciones circadianas conduciendo al síndrome metabólico (SM) y a la enfermedad del hígado graso no alcohólico (HGNA). Las proantocianidinas, incluido el extracto de proantocianidina de semilla de uva (GSPE), son metabolitos vegetales secundarios, beneficiosos para tratar enfermedades metabólicas. El GSPE es capaz de modular el reloj circadiano, influyendo en el ritmo de los procesos metabólicos. Por consiguiente, el objetivo principal esta tesis fue evaluar si los ritmos diurnos (día/noche) y estacionales (fotoperiodos) pueden influir en los efectos beneficiosos del consumo de GSPE en el metabolismo hepático. Para ello, realizamos experimentos con animales y analizamos parámetros lipídicos y la glucídicos en sangre e hígado relacionándolos con la función del reloj hepático. Primero, evaluamos la alteración de los ritmos metabólicos hepáticos causada por una dieta obesogénica y demostramos que el efecto restaurador del GSPE depende del momento de administración. Mayores beneficios se observaron cuando se administró GSPE al inicio de la fase oscura, el comienzo de la fase activa en ratas. Luego, determinamos que el efecto del GSPE sobre las hormonas séricas y el metabolismo hepático es dependiente del fotoperiodo en condiciones fisiológicas. Por último, evidenciamos la influencia de la duración del día en los efectos beneficiosos del GSPE sobre SM y el HGNA. Estos resultados manifiestan la importancia de considerar los ritmos biológicos al estudiar las acciones terapéuticas de las proantocianidinas en las enfermedades asociadas a SM para maximizar sus beneficios.

UNIVERSITAT ROVIRA I VIRGILI
THE INFLUENCE OF BIOLOGICAL RHYTHMS ON THE BENEFICIAL EFFECTS OF GRAPE SEED PROANTHOCYANIDIN EXTRACT (GSPE) ON LIVER METABOLISM IN HEALTH AND DISEASE
Romina Mariel Rodriguez

RESUM

Els ritmes biològics són mecanismes de cronometratge interns que permeten als organismes adaptar-se i anticipar-se als canvis cíclics de l'entorn causats per la rotació de la terra al voltant del seu eix (ritmes circadians) i del sol (ritmes circanuals). L'alteració d'aquests mecanismes està associada al deteriorament de l'homeòstasi metabòlica. Actualment, el consum excessiu d'aliments calòrics no només afavoreix la disfunció metabòlica, sinó que també provoca alteracions circadianes conduint a la síndrome metabòlica (SM) i a la malaltia del fetge gras no alcohòlic (HGNA). Les proantocianidines, inclòs l'extracte de proantocianidines de llavor de raïm (GSPE), són metabòlits vegetals secundaris, beneficiosos per tractar malalties metabòliques. El GSPE és capaç de modular el rellotge circadià, influint en el ritme dels processos metabòlics. Per tant, l'objectiu principal aquesta tesi va ser avaluar si els ritmes diürns (dia/nit) i estacionals (fotoperíodes) poden influir en els efectes beneficiosos del consum de GSPE en el metabolisme hepàtic. Per això, realitzem experiments amb animals i analitzem paràmetres lipídics i glucídics en sang i fetge relacionant-los amb la funció del rellotge hepàtic. Primer, avaluem l'alteració dels ritmes metabòlics hepàtics causada per una dieta obesogènica i demostrem que l'efecte restaurador del GSPE depèn del moment d'administració. Més beneficis es van observar quan es va administrar GSPE a l'inici de la fase fosca, el començament de la fase activa en rates. Després determinem que l'efecte del GSPE sobre les hormones sèriques i el metabolisme hepàtic és dependent del fotoperíode en condicions fisiològiques. Finalment, evidenciem la influència de la durada del dia als efectes beneficiosos del GSPE sobre SM i HGNA. Aquests resultats manifesten la importància de considerar els ritmes biològics en estudiar les accions terapèutiques de les proantocianidines en les malalties associades a SM per maximitzar-ne els beneficis.

UNIVERSITAT ROVIRA I VIRGILI
THE INFLUENCE OF BIOLOGICAL RHYTHMS ON THE BENEFICIAL EFFECTS OF GRAPE SEED PROANTHOCYANIDIN EXTRACT (GSPE) ON LIVER METABOLISM IN HEALTH AND DISEASE
Romina Mariel Rodriguez

ABBREVIATIONS

ACC Acetyl-coenzyme A carboxylase

ADP Adenosine diphosphate

AGPAT1/2 1-acylglycerol-3-phosphate O-acyltransferase 1/2

Akt Akt serine threonine kinase

AMP Adenosine monophosphate

AMPK Adenosine monophosphate-activated protein kinase

AP-1 Activator protein 1

ATF4/6 Transcription factor 4/6

ATP Adenosine triphosphate

AVP Arginine vasopressin

BCAAs Branched-chain amino acids

BMAL1 Brain and muscle Arnt-like 1

CAF Cafeteria diet

cAMP Cyclic adenosine monophosphate

CD36 Cluster of differentiation 36, Fatty acid translocase

CHGA Chromogranin A

CHOP CCAAT/enhancer binding homologous protein

CLOCK Circadian locomotor output cycles kaput

CPT1 Carnitine palmitoyltransferase 1

CRF Corticotrophin-releasing factor

CRY Cryptochrome

CS Citrate synthase

CSNK1δ/ ε Casein kinase 1 delta/epsilon

CVDs Cardiovascular diseases

CYP7A1 Cholesterol 7 α-hydroxylase

DGAT2 Diacylglycerol O-acyltransferase 2

DIO2 Type II iodothyronine deiodinase

DIO3 Type III iodothyronine deiodinase

DMSO Dimethylsulfoxide

DNM2 Dynamine 2

DRP1 Dynamin-related protein 1

ERAD Endoplasmic reticulum (ER)-associated degradation

EYA3 Eyes absent 3

F344 Fischer 344

FASN Fatty acid synthase gene

FATP5 Fatty acid transporter 5

FGF15 Fibroblast growth factor 15

FIS1 Fission 1

FXR Receptor farnesoid X receptor

G6P Glucose-6-phosphate

G6Pc Glucose-6-phosphatase, catalytic subunit

G6PD Glucose-6-phosphate dehydrogenase

GC-qTOF Gas chromatography coupled with quadrupoletime-of-flight mass spectrometry

GK Glucokinase

GLUT2 Glucose transporter 2

GLUT4 Glucose transporter 4

GPAT Glycerol-3-phosphate acyltransferase

GRP78 Glucose-regulated protein 78

GSK3β Glycogen synthase kinase 3 beta

GSPE Grape seed proanthocyanidin extract

HDL High density lipoprotein

HFD High-fat diet

HPA Hypothalamic pituitary adrenal

HPLC/ESI-MS/MS High-performance liquid chromatography/electrospray ionization tandem mass spectrometry

IL-6 Interleukin 6

IMM Inner-mitochondrial-membrane

IR Insulin resistance

IRE1α Inositol-requiring enzyme 1α

IRS-1 Insulin receptor substrate 1

JNK c-Jun N-terminal kinase 1

L12 12 hours of light/day

L18 18 hours of light/day

L6 6 hours of light/day

LDL Low density lipoprotein

LPIN1/2 Lipin 1/2

MESOR Midline Estimating Statistic of Rhythm

MFN1/2 Mitofusin 1/2

miR MicroRNA

MS Metabolic syndrome

mTORC1 /2 Mammalian target of rapamycin complex 1/2

NAD Nicotinamide adenine dinucleotide

NAFLD Non-alcoholic fatty liver disease

NAMPT Nicotinamide phosphoribosyltransferase

NASH Nonalcoholic steatohepatitis

NF-κB Nuclear factor kappa B

NPAS2 Neuronal PAS domain protein 2

NR1D1 Nuclear receptor subfamily 1, group D, member 1

OMM Outer mitochondrial membrane

OPA1 Optic atrophy 1

p Phosphorylated

PACs Proanthocyanidins

PARKIN Parkin RBR E3 Ubiquitin Protein Ligase

PAS-bHLH PAS-basic helix-loop-helix transcription factor

PCA Principal component analysis

PCK1 Phosphoenolpyruvate carboxykinase 1

PER Period

PERK protein kinase RNA-like endoplasmic reticulum kinase

PFKL Phosphofructokinase 1, liver type

PGC1α/ β Peroxisome proliferator-activated receptor gamma coactivator 1-alpha/beta

PI3K Phosphatidylinositol 3-kinase

PINK1 PTEN-induced kinase 1

PLS-DA Partial least squares discriminant analysis

PPARα Peroxisome proliferator-activated receptor alpha

PT Pars tuberalis

RORE ROR/REV-ERB-response element

RORα RAR-related orphan receptor alpha

ROS Reactive oxygen species

SCN Suprachiasmatic nucleus

SGLT1 Sodium/glucose cotransporter 1

SHP Small heterodimer partner

SIRT1 Sirtuin 1

SLC2A2 Solute Carrier Family 2 Member 2

SREBP1 Sterol regulatory element-binding protein 1

SS simple steatosis

STD Standard diet

T2DM Type 2 diabetes mellitus

T3 Triiodothyronine

T4 Thyroxine

TAG Triacylglycerol

TCA Tricarboxylic acid

TH Thyroid hormone

TNF-α Tumor necrosis factor alpha

TSHβ Thyroid stimulating hormone beta

UCP2 Uncoupling protein 2

UPR Unfolded protein response

VH Vehicle

VIP Vasoactive intestinal peptide

VLDL Very low-density lipoproteins

ZT Zeitgeber time

α-HB 2-hydroxybutyric acid, alpha-hydroxybutyrate

β-HB 3-hydroxybutyric acid, beta-hydroxybutyrate

I. INTRODUCTION

UNIVERSITAT ROVIRA I VIRGILI
THE INFLUENCE OF BIOLOGICAL RHYTHMS ON THE BENEFICIAL EFFECTS OF GRAPE SEED PROANTHOCYANIDIN EXTRACT (GSPE) ON LIVER METABOLISM IN HEALTH AND DISEASE
Romina Mariel Rodriguez

1 BIOLOGICAL RHYTHMS

Due to its rotation, the earth is periodically exposed to the radiation of the sun, which generates predictable changes in light and temperatures in addition to fluctuations in relative humidity of the air and oxygen in aquatic environments [1]. Therefore, almost every living organism on earth faces fluctuating environmental conditions. As a result, most species have evolved internal timing mechanisms that enable them to anticipate and cope with these rhythmic changes in the environment, thereby ensuring their survival [2]. These resulting timing mechanisms are known as circadian, from Latin *circa* meaning “around” and *diem* meaning “day”, or circannual (around a year) rhythms.

1.1 Properties of Circadian Rhythms

The first property of circadian rhythms was demonstrated more than 200 years ago by the French geophysicist, astronomer and most notably, chronobiologist, Jean-Jacques d'Ortous de Mairan, who placed his *Mimosa* plant, which rises its leaves by day and lowers them by night, inside his closet under constant darkness, isolated from diurnal variation on day light [3]. He was surprised to observe that the plant continued to open and close its leaves on the same schedule. By doing this he proved circadian rhythms have a self-sustained nature. In other words, almost all diurnal rhythms that occur under natural conditions are also observed under laboratory conditions despite the absence of external cues such as constant light or constant darkness [4].

Under constant conditions, the time that it takes to complete one cycle of a circadian oscillation is known as the free-running period. This brings us to the second distinctive attribute of circadian rhythms: these cycles persist with a period that approximates but does not equal 24 hours [5]. The

period offset from 24 hours is not a result of imprecision but rather is an important hallmark of circadian rhythm. This near 24-hour period is necessary for the circadian rhythm to achieve a stable phase relation with the environmental cycle, allowing organisms to adapt more precisely to seasonal changes in day length [6]. In fact, Pittendrigh showed that this deviation from the 24-hour cycle provides an opportunity for the internal time-keeping system to continuously align by and to the light-dark cycle [7]. As a result of the continuous adjustment of the expressed rhythms (controlling the timing or phase) a little drift is allowed prior to the rhythm being reset to its correct phase, giving more precise control.

The third characteristic feature of circadian rhythms, and one of the most important ones, is their capability to be synchronized by external stimuli, such as the light-dark cycle. The act of synchronizing a rhythm with an external cue is called entrainment. Therefore, under normal conditions, circadian rhythms are not free running, rather, they are entrained to the local environment.

Therefore, a rhythm is considered to be “circadian” if the oscillation has a period of approximately 24 h and continues in constant conditions, this means is not driven by responses to periodic external time cues or “Zeitgebers” (from German: time-giver) but can be also synchronized or entrained by environmental time cues.

1.2 Circadian Rhythms parameters

A rhythm can be defined as a regularly repeating oscillation, which its unit of repetition is called a cycle. When studying biological rhythms, there are certain rhythmic parameters that are usually measured, including period, phase, amplitude and MESOR (Midline Estimating Statistic of Rhythm) [8].

The period represents the duration of time necessary to complete one cycle, normally measured from peak to peak (Figure 1A). In the case of a circadian rhythm, as its name implies, the period lasts approximately 24

hours (one day), while circannual rhythms have a period of about one year [9]. Phase, also known as acrophase, is the time that separates the maximum of the variation (the peak), from the origin or reference time point (Figure 1B). Amplitude refers to half of the difference between the highest and the lowest point, the peak and trough respectively, of a certain variable (Figure 1C) [10]. The overall average of a rhythm will not be correctly represented by the arithmetic mean of the values as it will be biased towards the higher density of the samples. Therefore, it is necessary to calculate a rhythm-adjusted mean defined by a mathematical model such as the cosine curve [11]. This parameter is called MESOR and represents the value midway between the highest and the lowest values of the sinusoidal function or cosine procedure [12] (Figure 1D).

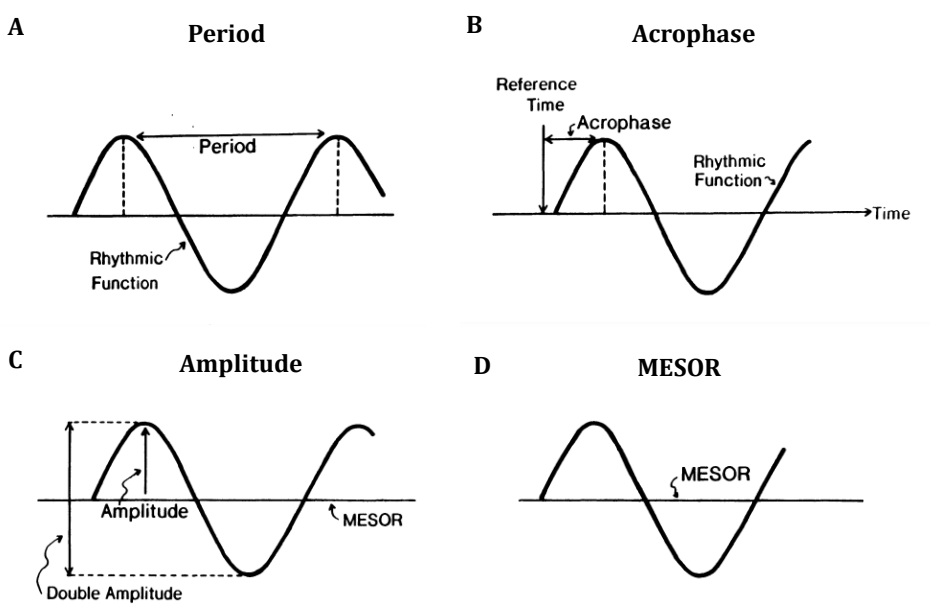

Figure 1. Definition of parameters of a rhythmic function. Adapted from [13].

1.3 The mammalian circadian system

In order to adapt and anticipate daily environmental changes, most organisms have developed a synchronization system, the so-called molecular circadian clock system [14]. In mammals, this complex and

coordinated system is composed of a central and several peripheral clocks that display endogenous oscillations of approximately 24 hours regulating many physiological processes such as feeding, sleep-wake, locomotor activity and metabolic homeostasis [15].

1.3.1 The Central Circadian Clock

The persistence of a rhythm in the absence of an external Zeitgeber, such as the dark-light cycle, certainly could be indicative for the presence of an internal timekeeper mechanism or biological clock. In fact, nowadays it is well known that mammals possess a central pacemaker that coordinates their behavior and metabolism in accordance with the rising and setting of the sun [16]. This master clock resides in the suprachiasmatic nucleus (SCN), which is located in the anterior region of the hypothalamus immediately dorsal, or superior (hence *supra*) to the optic chiasm (Figure 2). The SCN contains roughly 20.000 neurons, which form a neuronal network responsible for controlling circadian rhythms [17]. External information is received from the photosensitive ganglion cells of the retina via the retinohypothalamic tract to the SCN, generating neuronal and hormonal responses that regulate many different body functions in a 24-hour cycle [18].

There are two distinct sections of the SCN, depending on the neuropeptide expression. Vasoactive intestinal peptide (VIP)-expressing cells form the SCN core. In response to light, the retina sends information to the VIP part, which triggers gene expression and allows synchronization and entrainment [19]. The other section consists mainly of arginine vasopressin (AVP) expressing cells. Inputs to AVP primarily come from the cortex, basal forebrain, and hypothalamus. Hence, once SCN integrates direct photic input from the retina through the optic nerve and from other brain regions, it sends information to other hypothalamic nuclei as well as to the pineal gland in order to modulate hormone productions, including

melatonin, forming a network of neuronal and hormonal connections that affect all parts of the body [20].

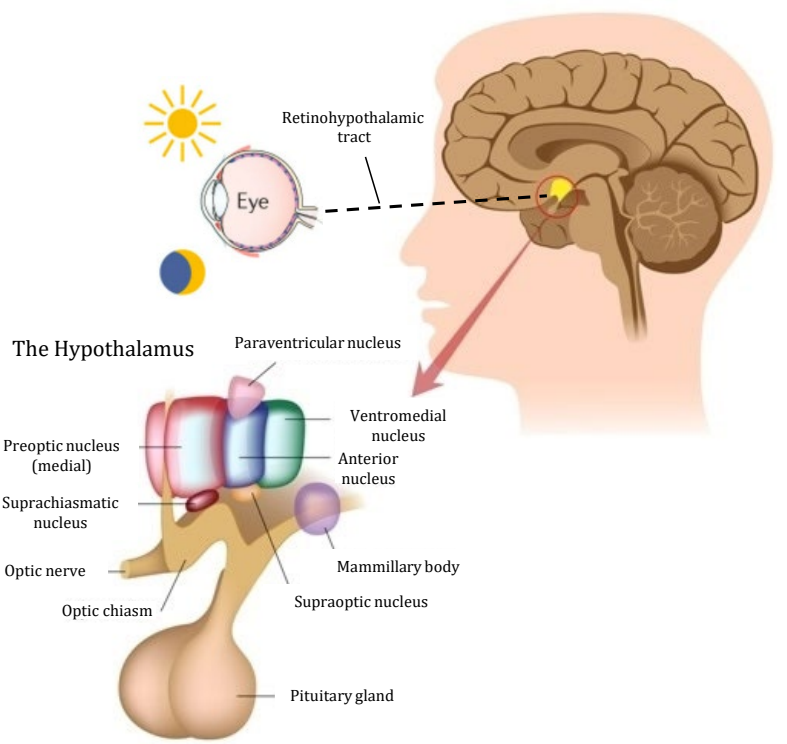

Figure 2. The master clock resides in the suprachiasmatic nucleus (SCN) of the hypothalamus. Adapted from [21].

1.3.2 Molecular components of circadian clocks

In the past decades remarkable progress has been made in understanding the molecular process that is responsible for the generation of rhythmicity in the SCN. It is now widely accepted that the circadian timekeeping system consists of a cell-autonomous transcription-translation auto-regulatory feedback loop involving a core set of genes that are highly conserved among animals [22].

The molecular components of the mammalian circadian clock consist of several transcription factors including Circadian Locomotor Output Cycles Kaput (CLOCK) and its paralogue neuronal PAS domain protein 2 (NPAS2),

which form together with Brain-muscle Arnt like 1 protein (BMAL1) the positive arm of this core loop, whereas Period (PER 1,2,3) and Cryptochrome (CRY 1,2) constitute the negative arm [23]. During the day, CLOCK which is a PAS-basic helix-loop-helix transcription factor (PAS-bHLH), interact with BMAL1 through its bHLH-PAS domains to drive the expression of several clock-controlled genes, including those encoding their own inhibitors, *Per* and *Cry,* by binding to the E-box element present in the promoter of these genes [24]. Consequently, the resulting PER and CRY proteins after reaching a critical concentration heterodimerize, translocate to the nucleus and interact with the CLOCK–BMAL1 complex in order to hamper their own transcription [25]. This PER–CRY repressor complex is degraded during the night, allowing CLOCK–BMAL1 complex to restore the cycle of transcription [26,27]. It takes approximately 24 hours to complete the entire cycle with CLOCK-BMAL1 being high during the light period and PER-CRY being elevated during the dark period regardless of whether the animal is diurnal or nocturnal. There is a secondary loop, although it is not involved in rhythm generation, which is believed to confer stability and robustness to the molecular clock, by controlling the phase and the amplitude of gene expression [28]. The elements in this feedback loops include the nuclear receptor subfamily 1 group D (NR1D1) also known as reverse rythroblastosis virus alpha (*Rev-Erbα*), its paralog REV-ERB beta (NR1D2) and retinoic acid related-orphan receptors RORs. All of them bind to the retinoic acid-related orphan receptor response elements (ROREs) in CLOCK and BMAL1 regulatory sequences. While REV-ERBs strongly represses *Bmal1* transcription, RORs positively regulate expression of CLOCK and BMAL1. *Rev-Erbs* and *RORs* are transcriptionally controlled by the same mechanism as that of *Per* and *Cry* genes. CLOCK-BMAL1 complex activates transcription of *Rev-Erbα* and *Rev-Erbβ*, which subsequently compete with ROR, in order to inhibit transcription of *Clock* and *Bmal1*. Therefore, it is called the second negative regulatory feedback loop in the circadian clock system [29] (Figure 3).

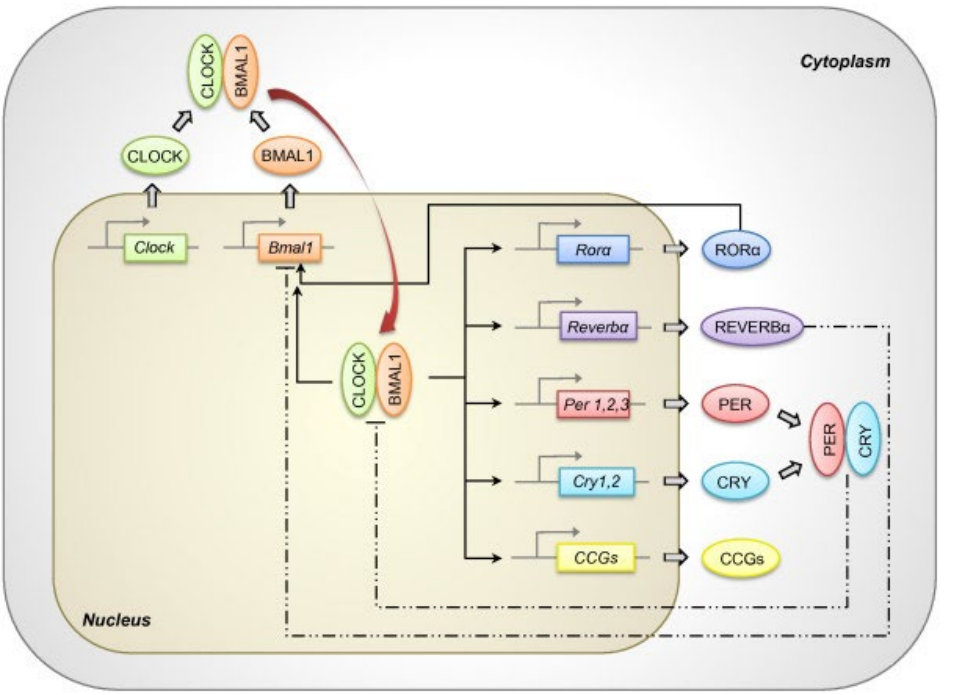

Figure 3. Molecular machinery of the circadian clock. Extracted from [30].

The CLOCK:BMAL1 heterodimer also regulates the transcription of many clock-controlled genes by binding to the E-boxes of their promoters [31]. One of the most important is the nicotinamide phosphoribosyl transferase (*Nampt*), which encodes for the rate-limiting enzyme in NAD+ biosynthesis [32].

Recent evidence has shown that circadian clock proteins have also another post-translational control which involves the phosphorylation by multiple kinases of these circadian transcription factors. PER proteins are phosphorylated by Casein kinase 1 delta and epsilon (CSNK1δ and CSNK1ε), thereby reducing their stability, and targeting them for polyubiquitylation and degradation by the 26S proteasomal pathway. Meanwhile, PER1 and PER2, which have been accumulating during the night, are progressively phosphorylated, ensuring to complete correct cycle of clock genes transcription [33]. Moreover, SIRT1, a NAD+-dependent protein deacetylase, promotes the deacetylation and

degradation of PER2 [34]. In addition, positive regulators CLOCK and BMAL1 are phosphorylation targets of glycogen synthase kinase 3 beta (GSK3β) which reduces their stability and increases transcriptional activity [35]. In hepatocytes, BMAL1 is also phosphorylated at Serine 42 by the protein kinase B, also known as Akt2, to promote its cytoplasmic localization [36]. Another study demonstrated that phosphorylation of CLOCK by AKT on Serine 845 regulates its nuclear translocation and consequently the circadian genes expression levels in insulin sensitive tissues, such as liver and skeletal muscle [37]. Likewise, it has been determined that the AMP-activated protein kinase (AMPK) can stimulate NAMPT transcription through phosphorylation and inhibition of CRY [38]. Altogether, these post-translational modifications and subsequent degradation of circadian clock proteins are crucial steps for determining circadian periodicity of the clock. As a matter of fact, 5 to 10 per cent of transcripts in any given tissue are thought to be expressed in a circadian manner [39]. Thus, to maintain a correct circadian expression of the transcriptome, the activity of these transcription factors must be tightly controlled.

1.3.3 The circadian clock in peripheral tissues

In the past decades, researchers have been surprised to evidence that these circadian rhythms could persist in isolated tissues from lungs, livers, and other tissues grown in a culture dish (i.e., *in vitro*) that were not under the control of the SCN [40]. Thus, revealing the presence of circadian clocks in several peripheral organs and tissues outside the brain. This was confirmed by experiments using damaged-SCN animals in which circadian rhythms of peripheral tissues were not abolished, suggesting the existence of organ-specific synchronizers of circadian rhythms at the cell and tissue levels [41]. It is now well established that circadian clocks are widely distributed in almost every cell in mammals and exhibit tissue-specific rhythmicity, driven by the master circadian clock in the SCN. These so-

called peripheral clocks are able to generate oscillations with a periodicity of roughly 24 h in a self-sustained manner [42].

Several studies using gene expression techniques such as microarrays, demonstrate that the same molecular components present in the SNC are responsible for circadian oscillations in peripheral tissues [43,44]. Although peripheral oscillators are coordinated by the central pacemaker, they are only weakly coupled to the SCN. In this sense, an experimental design where 'jet lag' was induced in rats by advancing or delaying 6 hours the light cycle demonstrate SCN can quickly adjust to the switch whereas it took over a week for peripheral clocks to re-synchronize [40]. Synchronization takes place via neural, hormonal, and behavioral signals.

Regardless of the progress in the area, it remains unclear how central control of circadian rhythms by the SCN is transferred to the periphery. Two mechanisms about how the pacemaker in the SCN transduces its regulation of the peripheral tissue clocks have been proposed. The first one involves the sympathetic and parasympathetic nervous systems, as both receive input from the hypothalamus and change their activity with the light/dark cycle. Neurons of the autonomic nervous system innervate almost all peripheral organs and tissues including muscle, heart, kidney, liver, pancreas, white adipose tissue, and ovary. Moreover, the sympathetic branch regulates the output of melatonin through innervation of the pineal gland. Melatonin, secreted from the pineal gland during the dark period, plays a major role in the regulation of sleep and wake cycles [45]. The second mechanism providing circadian rhythmicity to peripheral tissues is the hypothalamic pituitary adrenal (HPA) axis, responsible for the neuroendocrine adaptation component of the stress response [46,47]. This response is characterized by hypothalamic release of corticotrophin-releasing factor (CRF). The SCN innervate and imparts circadian rhythmicity to hypothalamic neurons responsible of producing CRF. Once CRF binds to its receptors on the anterior pituitary gland, triggers the

secretion of adrenocorticotrophic hormone. This hormone stimulates adrenal cortex to synthesize and release glucocorticoids in a rhythmic way. Unlike melatonin release, light has not such influence on the HPA axis, enabling both diurnal and nocturnal animals to phase shifting. For diurnal animals, glucocorticoids, cortisol for instance in case of humans, peak during the transition from the dark/inactive period to the light/active period, and for nocturnal animals the peak occurs in the opposite way [48]. Essentially, rhythmic glucocorticoid secretion enables animals to prepare for the approaching period of activity and feeding and may influence gene expression in virtually all tissues.

Hence, peripheral oscillators located in many peripheral organs such as liver, pancreas, kidney, heart, skeletal muscles, and adipose tissues, are controlled at multiple levels. Apart from the entraining signals they receive from the central clock, other factors such as food, immune challenges, stress, locomotor activities, and circulating hormones such as glucocorticoids and the circadian variation in body temperature can also potentially act as entraining cues for peripheral clocks, allowing cell-autonomous peripheral oscillators to operate independently of the SCN [49,50] (Figure 4). Therefore, although there is a central pacemaker, it rarely has exclusive control over the multiple clocks within the body of a multicellular organism.

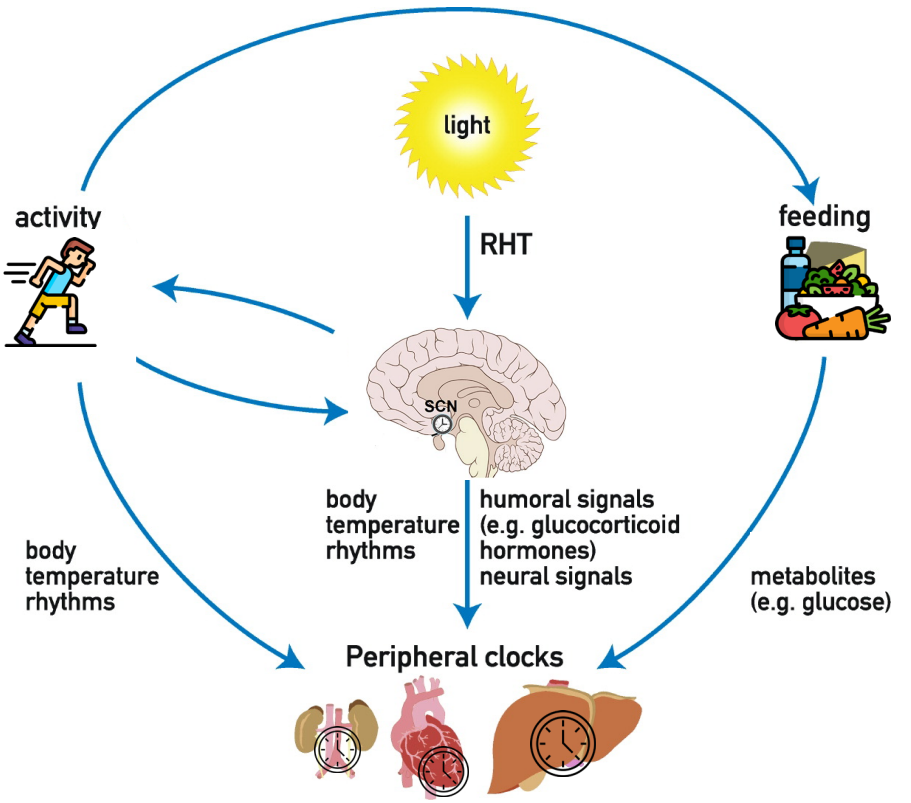

Figure 4. Entrainment of peripheral clock by the SCN and external cues. RHT, retinohypothalamic tract. Adapted from [51].

1.4 Circannual Rhythms

At the same time as the Earth rotates around its axis, it is also moving around the sun, creating circannual rhythms, which determines the day length variations and seasons [52] (Figure 5). Circannual rhythm is an evolutionary process that relies on long-term timing mechanisms residing in all tissues, but with dominant pacemaker systems in the brain and pituitary gland, synchronizing the annual environmental cycle, notably photoperiod, with physiological and behavioral processes [53,54]. Thus, in natural conditions, circannual rhythm is mainly determined by light, responding to the absolute day length of the seasons [55]. This year-round clock allows organisms to measure changes in the seasons, enabling them to adapt to the environmental variations [56]. In this regard, many

biological activities, including migration and reproduction, are restricted to a specific period of the year [57].

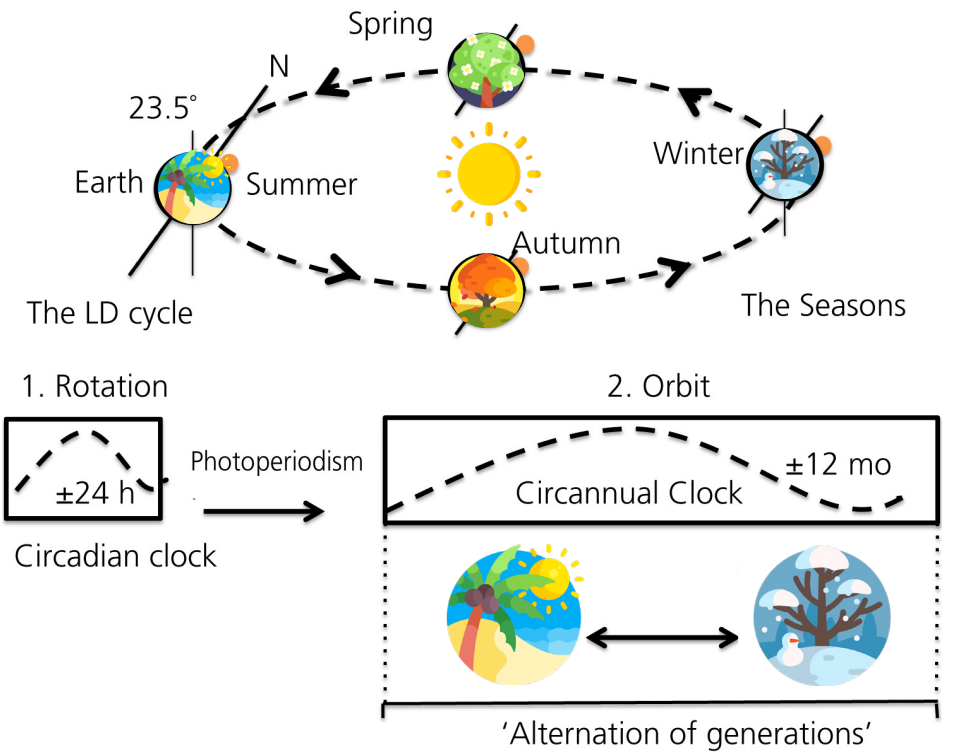

Figure 5. Endogenous clocks anticipate the Earth's periodicity. The circadian clocks anticipate the time of day and circannual clocks predict the seasons. LD, light/dark. Adapted from [54].

1.4.1 Central Circannual Pacemakers

In mammals, significant progress has been made on characterizing the central circannual timing system [58,59]. In this sense, melatonin-responsive thyrotroph cells residing in the *pars tuberalis* (PT) of the hypophysis have been pointed out as the master regulators of seasonal biology due to its function as the first transducer of the photoperiodic signal [60]. Information about the length of the day is sent to the pineal gland which, as was mentioned before, produces the melatonin hormone. Seasonal variations in darkness length determine the duration of melatonin release by the pineal gland, acting over melatonin-sensitive

tissues that control specific aspects of seasonal physiology and behavior [61,62]. In addition, the transcriptional coactivator eyes absent 3 (EYA3), which is modulated by CLOCK-BMAL1 heterodimer, plays a pivotal role in the regulation of seasonal responses entrained by the photoperiod, inducing transcription of the thyroid stimulating hormone beta (TSHβ) subunit in the PT thyrotroph cells [63]. As it is a clock-controlled gene product, EYA3 protein displays circadian patterns increasing its expression 12 hours after the onset of darkness [63]. Thus, in long days it reaches its peak in light conditions whether in short days its expression is mainly decreased by melatonin release due to dark conditions. Therefore, activation of transcription co-activators EYA3 and TSHβ proteins via exposure to long photoperiod melatonin signals initiates the summer neuroendocrine response together with suppression of chromogranin-A (CHGA) production in thyrotroph cells in the PT [54]. Moreover, tanycytes, ependymal cells found in the third ventricle of the brain, have proven to be involved in the generation and maintenance of the circannual timing system, regulating the hormonal and gene pathways that orchestrate the circadian phenotype [64]. In this sense, during long day season, PT-derived TSHβ enhance the transcription of type II iodothyronine deiodinase (DIO2) in tanycytes, which in turn promote the activation of thyroid hormones (TH), converting the inactive form thyroxine (T4) to the active triiodothyronine (T3). Meanwhile during short day season, Dio2 expression is inhibited, and the expression of type III iodothyronine deiodinase (Dio3) is promoted which catalyzed the conversion of T3 into the inactive form rT3 or T4 into inactive diiodothyronine (T2) [65] (Figure 6).

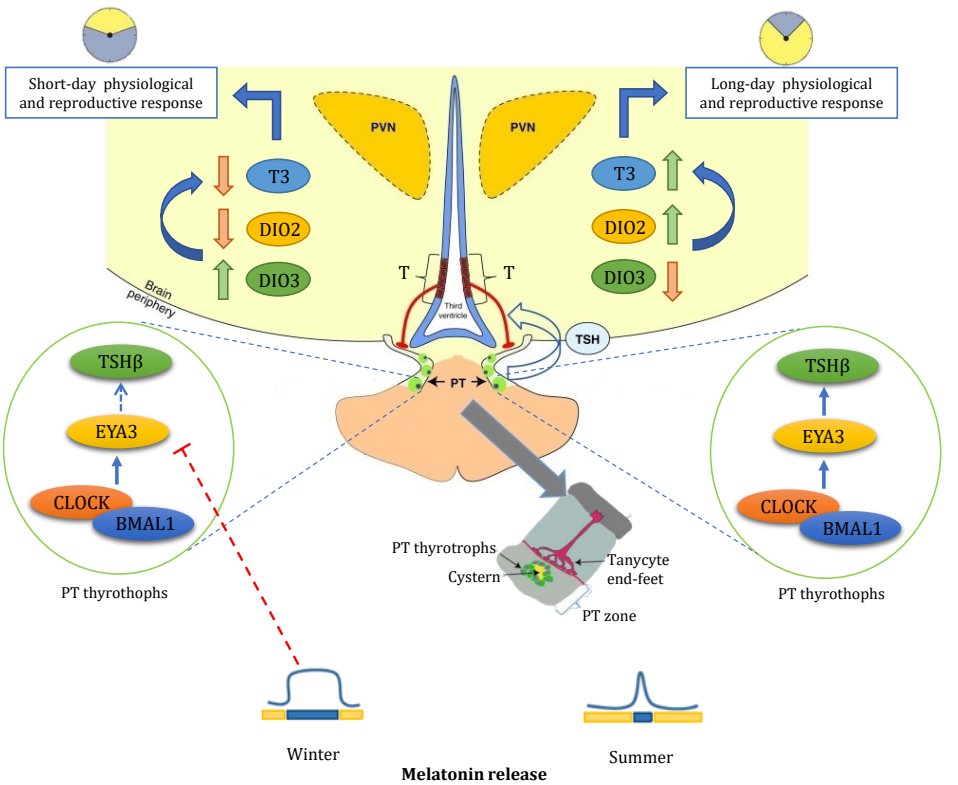

Figure 6. Molecular mechanisms involved in the physiological response to seasonal day length variations. T, tanycytes. Adapted from [52].

1.5 Chrononutrition

Circadian timing and metabolic physiology have recently been associated with nutrition, creating a relatively new area of research [66]. In fact, the term "Chrononutrition" first appeared in a Japanese book about nutrition and health published in 2005 [67]. In addition to studying how timing of food consumption and biological rhythms may impact our health and metabolism, Chrononutrition also investigates how nutrition (composition of meals and portion sizes) may influence our internal clocks [68]. This discipline specifically proposes that nutrients can modulate the circadian clock system [57], and that alterations of biological clocks can negatively impact the consumption and timing of meals [69,70].

2 CIRCADIAN RHYTHMS IN LIVER FUNCTION

In terms of circadian transcription, the liver is the most extensively studied organ. A bunch of independent studies have revealed that about 1000 transcripts exhibit circadian expression in the hepatic tissue [71–75]. However, recent proteomic and metabolomic studies have shown that some metabolic enzymes display oscillations whereas their transcripts are relatively constant throughout the day, demonstrating that posttranscriptional mechanisms are also involved in circadian regulation of liver functions [76–78]. Notably, but not unexpectedly, most of the rhythmically expressed hepatic genes encode for key enzymes involved in metabolic pathways and energy homeostasis [20]. In this sense, carbohydrate, lipid, amino acid and bile acid metabolism, xenobiotics' detoxification and synthesis of plasma protein are carried out by the liver and rhythmically regulated by its clock. The hepatic rhythmicity is able to oscillate the expression of genes related to all these metabolic pathways and also the inflammatory, oxidative stress and mitochondrial dynamic pathways [79,80]. Thus, the liver is a crucial and essential player in metabolism as key physiological functions are subject to daily oscillations and regulated by its circadian clock (Figure 7).

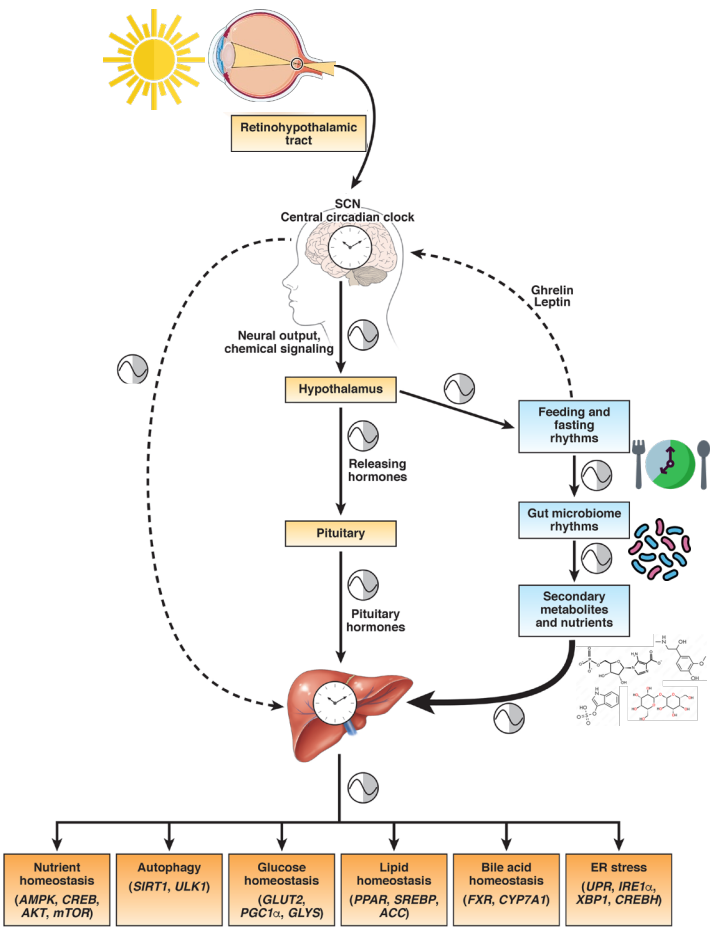

Figure 7. Signals influencing liver peripheral clock and liver circadian clock regulated functions. Adapted from [81].

Time-related changes in gene expression are crucial to ensure the proper functioning of incompatible metabolic processes that are taking place in the liver [82]. As an example, simultaneous high expressions of glycogen synthase and glycogen phosphorylase would not enable glucose to be converted into glycogen and vice versa during the absorptive and postabsorptive phases, respectively. Thus, it is likely that there is a physiological meaning behind the temporal separation into different time windows of expression of these two enzymes in the liver [83]. Therefore, the antiphasic expression of genes involved in chemically incompatible

processes may constitute one of the major tasks of the hepatic circadian clock [84].

2.1 Circadian rhythms in carbohydrates metabolism

The liver is a central metabolic organ and its role in homeostasis of glucose metabolism has been well studied [85,86]. The first step in glucose metabolism involved the transport of glucose into hepatocytes. This action is accomplished by the GLUT2 transporter [87]. Loss of GLUT2 circadian expression was observed in mice with liver-specific deletion of *Bmal1* leading to metabolic glucose abnormality [88]. Once inside the cell, glucose is rapidly phosphorylated to glucose-6-phosphate by the enzyme glucokinase (GK), which acts as a blood glucose sensor maintaining hepatic glucose homeostasis, together with glycogen phosphorylase enzyme [89,90]. Expression of GK was observed to undergo circadian control reaching its peak during the transition from the rest phase to the active phase [91,92]. Furthermore, insulin and glucagon, which play a key role in the regulation of glucose metabolism, were found to exhibit rhythmicity [93,94]. Thus, their rhythmicity patterns are transmitted to the liver via their signaling pathways [92]. Insulin, for instance, influences glycogen synthase activity by controlling the expression of glycogen synthase kinase 3 in a circadian manner; and regulates REV-ERB stability which has an impact on the rhythmic regulation of other metabolic processes [95,96].

2.2 Circadian rhythms in lipid and bile acid metabolism

In lipogenesis acetyl-CoA is transformed into malonyl-CoA by the rate-limiting enzyme ACC1. Circadian control of this step is provided by AMPK, which inhibits fatty acid synthesis and stimulates β-oxidation through the inactivation of ACC1. Additionally, the transcription of *Elovl3* and *Fasn*, which encodes important enzymes in *de novo* synthesis of fatty acids, are subjected to circadian regulation [97]. Circadian control has been also observed in β-oxidation and ketogenesis processes through the expression of *Cpt1/2* and *Hmgcs2* genes, respectively [98,99]. Moreover, crucial genes

encoding enzymes in charge of triglyceride biosynthesis such as *Gpat2*, *Agpat1/2*, *Lpin1/2*, and *Dgat2*, exhibit rhythmic expressions, thus resulting in oscillations of hepatic triglycerides [100]. In addition, it was observed that hepatic production of phosphatidylcholine, the most abundant phospholipid in VLDL, is regulated by REV-ERBα/β [101].

The NAD+-dependent deacetylase SIRT1 has been shown to activate many important metabolic players, including AMPK, PPARG coactivator 1 alpha (PGC1α), peroxisome proliferator-activated receptor alpha (PPARα), a nuclear receptor that regulates lipid metabolism, sterol regulatory element-binding protein 1c (SREBP-1c), a transcriptional factor that regulates the activation of *de novo* lipogenesis in the liver, and CLOCK-BMAL1 heterodimer. Furthermore, PGC1α activates PPARα, and both are able to increase the activity of the CLOCK-BMAL1 heterodimer [102,103]. A key role in the crosstalk between the circadian clock and the metabolic pathways is played by PGC1α as it modulates hepatic gluconeogenesis, fatty acid β-oxidation, and mitochondrial biogenesis. Furthermore, PGC1α is capable of sensing nutritional status and coordinate with the circadian signals communicating extracellular inputs to the biological clock [104]. In this sense, AMPK functions as a metabolic sensor and SIRT1 is mainly responsible for the interaction between the circadian clock and metabolism [105].

In the bile acid synthesis, the rate-limiting enzyme is cholesterol 7α-hydroxylase (*Cyp7a1*), and its transcription is known to be stimulated by REV-ERBα [106]. Moreover, hepatics nuclear receptor farnesoid X receptor (FXR) and small heterodimer partner (SHP), and intestinal hormone fibroblast growth factor 15 (FGF15), which are under the control of circadian clocks, are also in charge of the control of *Cyp7a1* expression [107].

2.3 Circadian rhythms in mitochondrial homeostasis

An important parameter linking metabolism and the liver clock is mitochondrial function [108]. Mitochondria are essential organelles for cellular function and homeostasis due to, among other processes, the production of ATP through oxidative phosphorylation [98]. They are therefore critical in the regulation of energy metabolism [109]. In addition, mitochondria are highly dynamic organelles in both form and function. Their activities vary according to the nutritional state of the cell at different times of the day [110]. In this sense, recent studies demonstrate that mitochondrial functions, including mitochondrial dynamics, biogenesis, and cellular respiration, undergo circadian regulation [98,111–113]. Moreover, a variety of metabolites related to mitochondrial metabolism, such as levels of NAD+ [114,115], ATP, ROS, and Krebs cycle metabolites [116], were found to have rhythmicity, both in cultured cells as well as in animal models. Additionally, daily oscillations in some mitochondrial rate-limiting enzymes involved in lipid and carbohydrates metabolism were observed to be dependent on clock proteins PER1/2 in mice liver [117]. In consequence, it is likely to assume that these metabolic rhythms also provide feedback into the clock functions [118].

Mitochondrial dynamics is the process by which mitochondria continuously fuse (fusion) and divide (fission) and is involved in multiple cellular functions. These two opposing processes are in balance to maintain the morphology, mitochondrial function, and dynamic network of the mitochondrion [109]. Indeed, it allows the mitochondrial cellular network to modulate its bioenergetic properties according to the nutritional demands of the organism, regulate mitochondrial motility and act as a quality control mechanism by facilitating the removal of damaged mitochondria through mitophagy [119]. In the cell, mitochondrial content is determined by the balance between mitochondrial biogenesis and mitophagy. While PGC1α and PGC1β proteins are considered to be in

charge of mitochondrial biogenesis, PINK1, PARKIN and BNIP3 are the key proteins for mitophagy. On the other hand, mitochondrial fusion is regulated by the GTPases MFN1 (Mitofusin 1), MFN2 (Mitofusin 2) and OPA1 (Optic atrophy 1), while mitochondrial fission is controlled by the GTPase DRP1 (Dynamin-related protein 1), DNM2 (Dynamine 2) and FIS1 (Fission 1) [120] (Figure 8).

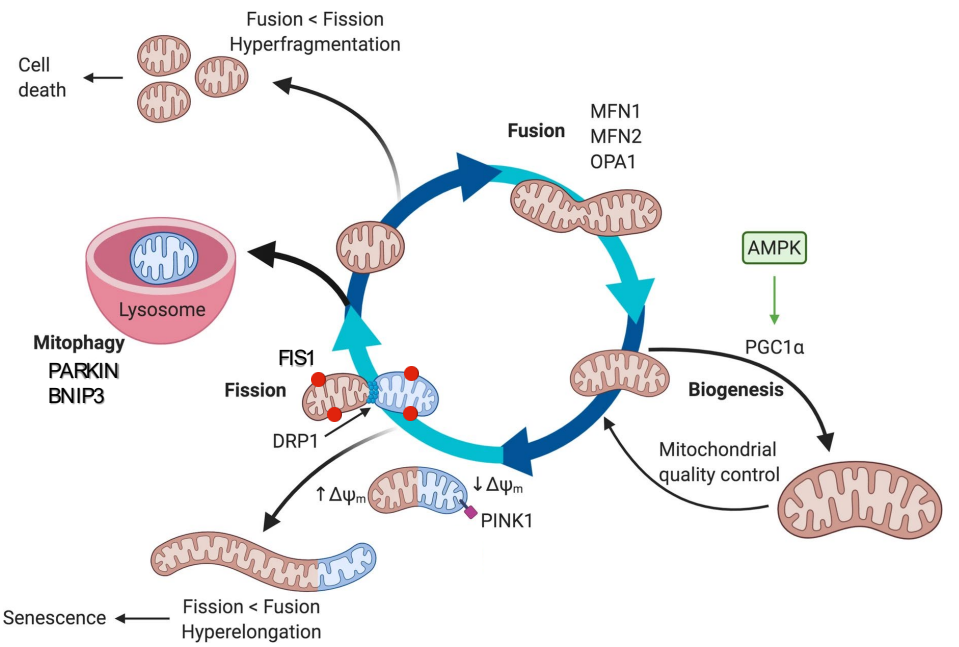

Figure 8. Representation of mitochondrial dynamics and the proteins involved. Adapted from [121].

In the process of mitochondrial fragmentation, mitochondria become rounder and smaller, however, in fusion, mitochondria undergo elongation due to increased dimerization [122,123]. A possible model for circadian control of mitochondrial homeostasis, depicted in Figure 9, suggests that CLOCK-BMAL1 heterodimer may influence key proteins involved in mitochondrial dynamics as well as it stimulates mitochondrial biogenesis and mitophagy through activation of SIRT1, which interacts with the transcription factor of PGC1α involved in mitochondrial biogenesis.

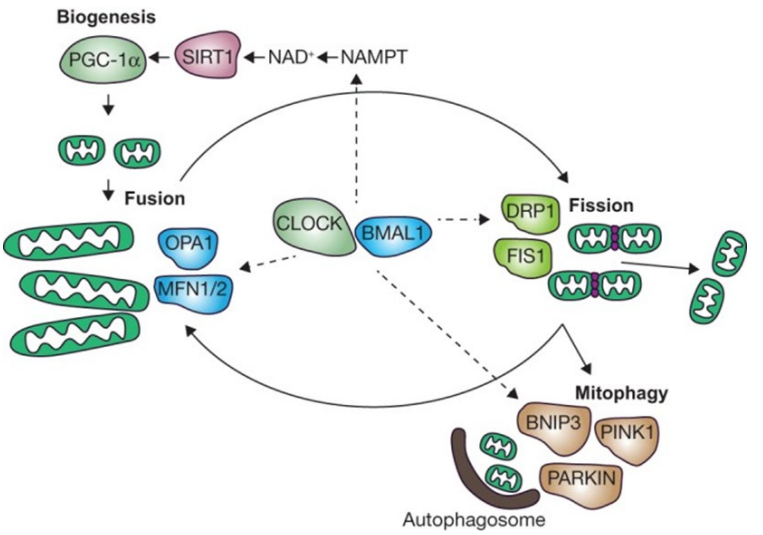

Figure 9. Model for circadian regulation of mitochondrial homeostasis. Extracted from [98].

3 CIRCADIAN DISRUPTION AND METABOLIC DISEASES

There is growing evidence suggesting that circadian regulation is closely linked to metabolic homeostasis, and that dysregulation of circadian rhythms, as a consequence of the artificial light and air conditioning invention, as well as sedentary lifestyles and the continued availability of food, can lead to metabolic diseases. In turn, metabolic cues also interact with the circadian system, providing feedback and thereby modulating circadian gene expression and behavior [124].

3.1 Metabolic Syndrome

In mammals, the circadian clock plays a critical role in the liver by regulating lipid, carbohydrate, and xenobiotic metabolism. Disturbance of this rhythm has been implicated in several pathologies such as metabolic syndrome (MS) [125]. The MS is an unhealthy status defined by a set of components reflecting overeating, sedentary lifestyle, and the resulting excess in adiposity (weight gain). The clustering of components includes abdominal obesity, insulin resistance, hypertension, dyslipidemia, low high-density lipoprotein (HDL) cholesterol and hyperglycaemia.

Additionally, MS is characterized by increasing the risk of suffering type 2 diabetes mellitus (T2DM), cardiovascular diseases (CVDs) and non-alcoholic fatty liver disease (NAFLD) [126].

Both animal and human studies have evidenced the involvement of circadian misalignment in weight gain and obesity development [127–132]. A high-fat diet [133,134], jet lag [135], mistimed feeding [136,137], and shift work [138] have all been found to disrupt circadian alignment, resulting in weight gain in human and animal experiments. Moreover, mouse models lacking circadian clock genes developed obesity and MS [139–143]. The association between circadian disruption and obesity in humans has largely been investigated through observational studies among shift workers. In this sense, a negative change in food consumption patterns was observed on late-time workers [144–147], and social jet lag individuals [148–150], leading to an increase in the risk for obesity, T2DM, MS and CVDs [151].

3.2 Non-alcoholic fatty liver disease

An excessive accumulation of lipids due to disorders in liver lipid metabolism could lead to the development of liver steatosis, which when not related to chronic alcohol consumption, is called non-alcoholic fatty liver disease (NAFLD). The term includes a wide spectrum of conditions from simple steatosis (SS) to nonalcoholic steatohepatitis (NASH), through fibrosis and cirrhosis which may progress to hepatocellular carcinoma (HCC).

The NAFLD association with obesity has been well-established [152,153], as it is considered the hepatic manifestation of the MS. Furthermore, increasing prevalence and severity of NAFLD has been related to the rising trends in obesity. In this regard, it is not surprising to confirm that the prevalence of NAFLD in obese individuals is higher than that of the general population (30%). Moreover, obesity seems to increase the liver-

associated mortality among NAFLD patients [154]. Even though the vast majority of NAFLD patients are obese, a few have normal weight and normal body mass index. In these patients, it is believed that genetic rather than environmental factors could play a central role[155].

Obesity is involved in both the initial process leading to SS, but also in its progression to NASH. When the adipose tissue is unable to store an excess of energy due to a high-calorie diet, the hepatocytes accumulate the extra lipids leading to SS. This incapacity of hepatocytes to handle such excess of fat facilitates inflammation and lipo-apoptosis, which are basic features of NASH [156].

Being a disease with a complex pathophysiology, the development and progression of NAFLD encompasses multifactorial causes. Day and colleagues postulated the so-called double-hit hypothesis to try to explain the etiology of hepatic steatosis. On one hand, the first impact (i.e, insulin resistance) causes a metabolic change which increases lipolysis in adipose tissue and creates an influx of free fatty acids into the liver. On the other hand, the second impact appears when lipid accumulation becomes toxic (lipotoxicity) and induces an oxidative stress response in the liver, involving inflammatory processes [157].

Thus, the main cause of steatosis has been associated with insulin resistance. When there is a failure of insulin binding or insulin receptor substrate protein, a disruption in the balance between intracellular lipids and glucose occurs, thus accumulating fatty acid metabolites into hepatocytes. This induces defects in insulin signaling pathways due to abnormal phosphorylation of insulin receptors through serine-kinase activation and contributes to an insulin resistance state [158]. Insulin not only is responsible for cell glucose uptake, but also has an anti-lipolytic effect, which is impaired in insulin resistance states. As a result of the decreased suppression of adipose tissue lipolysis and the inhibition of β-

oxidation, hepatic lipids accumulation and *de novo* lipogenesis in the liver takes place [159]. Additionally, hepatic triglyceride incorporation into new VLDL and secretion is inhibited through microsomal triglyceride transfer protein blocking, leading to dysregulation of VLDL metabolism and secretion and accumulation of triglycerides in the liver, promoting steatosis [160]. The exposure of hepatocytes to high lipid and carbohydrate levels causes lipotoxicity and glucotoxicity, respectively, and the consequent activation of inflammatory pathways.

However, according to Buzzetti *et al*., this point of view is too simplistic for describing the development and progression of NAFLD where multiple parallel factors, acting synergistically in genetically predisposed individuals, are implicated. In this sense, it was proposed a new multiple parallel-hit model in which there were other important factors like gut microbiota and genetic inheritance are intimately associated with NAFLD progression, aside from the aforementioned factors implicated [161].

The inflammatory state is characterized by abnormal cytokine production such as TNF-α and IL-6, increased acute-phase reactants and other mediators, and activation of a network of inflammatory signaling pathways [162]. According to Hotamisligil, c-Jun N-terminal kinase 1-Activator protein 1 (JNK-AP-1) and IκB kinase-nuclear factor kappa B (IKK-NF-κB) are two main inflammatory pathways which are critically related to the development of chronic inflammation in NAFLD [163]. If inflammation is sustained for a significant period of time, activation of hepatic stellate cells, that are responsible for liver fibrosis, occurs and the mechanism of hepatic tissue regeneration are impaired. This can result in necrotic cell death, apoptosis, and lead to NASH. Successively, these events predispose to cirrhosis and, in many cases, can lead to liver cancer [164] (Figure 10).

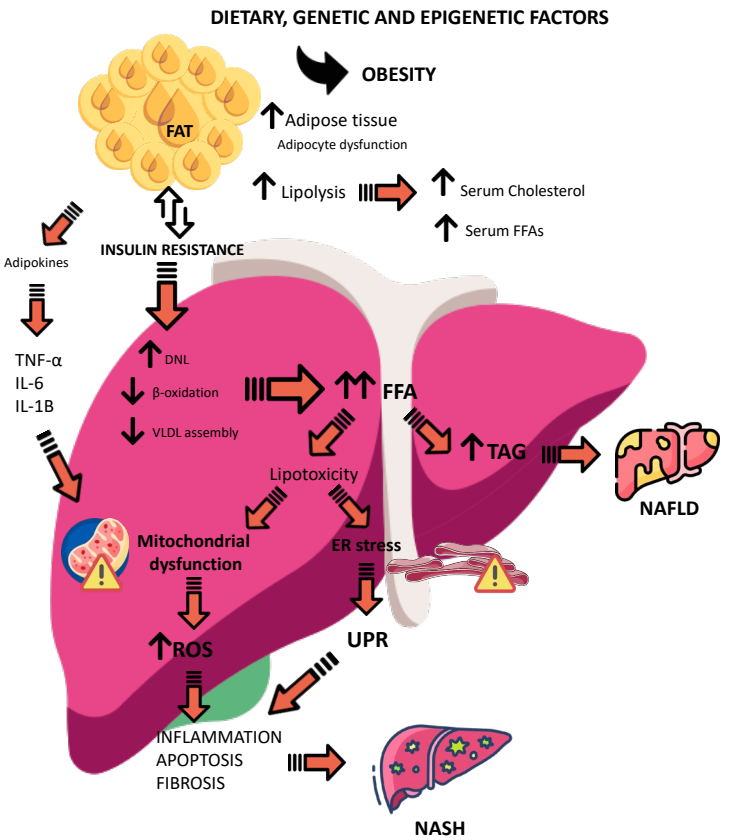

Figure 10. Molecular pathways in NAFLD pathogenesis. Adapted from [161].

Several studies on animals have linked circadian clock genes with the pathogenesis of NAFLD [165]. In this sense, mice with whole-body or liver-specific knockout clock genes or clock-controlled genes, such as *Pparα*, developed hepatic steatosis [166–170]. Moreover, wild-type mice subjected to HFD exhibit significantly changes in mRNA levels of clock genes *Bmal1*, *Per1-3*, and *Cry 1-2* [171].

3.2.1 The Unfolded Protein Response

Many liver diseases, such as NAFLD, are associated with disruption of the endoplasmic reticulum homeostasis, named ER stress. In response to this disruption, the highly conserved signaling pathway called unfolded protein response (UPR) is triggered. UPR is responsible for regulating protein

synthesis and re-establishing homeostasis after a cell is stressed by excessive protein load or accumulation of unfolded or misfolded proteins. Moreover, the UPR seems to be related to lipid and membrane biosynthesis, insulin activity, inflammation, and apoptosis [172,173]. In addition, mitochondrial homeostasis and lipid metabolism are closely related as it was demonstrated that the UPR activates SREBP-1c pathways, consequently promoting lipid accumulation which aggravates ER stress and UPR itself [174]. Furthermore, UPR also triggers JNK activation, which activity is linked to insulin signalling impair and to the development of inflammation and cell death [175].

Glucose-regulated protein 78 (GRP78) is a chaperone that binds unfolded proteins and initiates the UPR activating three different pathways involving three proteins: protein kinase RNA-like endoplasmic reticulum kinase (PERK), the inositol-requiring enzyme 1α (IRE1α), and transcription factor 6 (*Atf6*) [176]. Activation of PERK leads to the selective translation of certain proteins and, on the other hand, also promotes the translation inhibition of others during stress conditions. Among these selected proteins there are the activating transcription factor 4 (*Atf4*) and CCAAT/enhancer binding homologous protein (*Chop*) [177]. While it provides transcriptional signals that promote ER homeostasis, ATF4 can also induce the expression of the proapoptotic protein called CHOP. Activated IRE1α splices *Xbp1* mRNA and releases a transcriptionally active XBP1s variant to alleviate the ER load [178]. On the other hand, upon UPR activation, ATF6 translocates to Golgi and its proteolytic maturation results in a transcriptional program to restore ER homeostasis and support endoplasmic reticulum (ER)-associated degradation (ERAD). ATF6 also induces CHOP expression and thus contributes to cell death [179] (Figure 11).

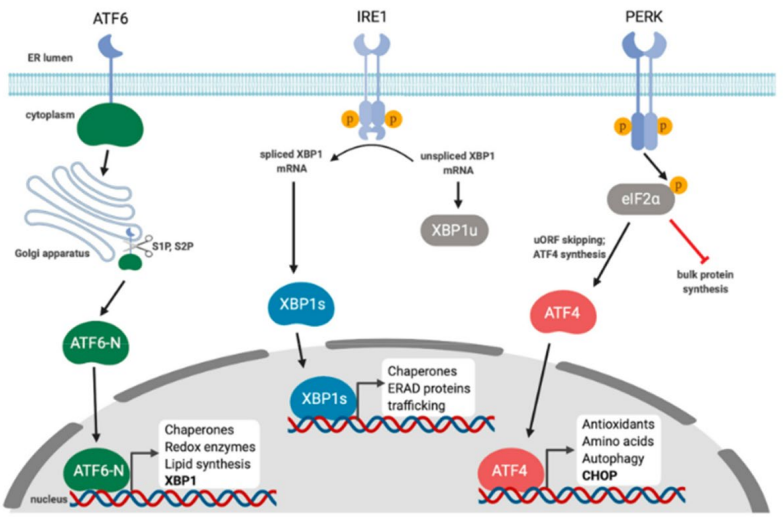

Figure 11. Triggering of the unfolded protein response due to ER stress. Extracted from [180].

Cretenet and colleagues demonstrated that the IRE1α-XBP1 pathway might be regulated by circadian rhythms in the liver. The authors observed a rhythmically 12-hour expression of IRE1α and XBP1 in hepatocytes [181]. Moreover, they observed that knockout-mice of the circadian clock genes exhibit constitutive activation of the UPR pathway and, importantly, showed a loss of circadian expression of enzymes involved in the regulation of hepatic lipid metabolism and triglyceride accumulation [181].

It has been demonstrated that activation of the UPR could trigger changes in mitochondrial function and mitophagy. In this sense, the UPR stimulates mitophagy to eliminate stress-damaged mitochondria, controls mitochondrial bioenergetics by influencing the mitochondria-associated membrane and impairs mitochondrial membrane potential [182]. Therefore, these mitochondrial alterations, cause depletion of mitochondrial DNA, morphological and ultrastructural changes, variation of the respiratory chain and mitochondrial β-oxidation dysfunction, contributing to the pathogenesis of NAFLD [183]. Moreover, as a result of

the increased lipid flux, the respiratory oxidation collapse, generating toxic metabolites and excessive production of reactive oxygen species (ROS) thereby contributing to worsening mitochondrial damage. Moreover, ROS along with oxidized low-density lipoprotein (LDL) particles conduct to inflammation and fibrosis via activation of Kupffer and hepatic stellate cells [184].

3.2.2 Disturbances on Mitochondrial Dynamics

Mitochondrial fission and fusion are the most important structural changes that occur in mitochondria. However, perturbations in the balance between these two processes affect mitochondrial function and lead to mitochondrial dysfunction [123].

Recent research links mitochondrial dynamics to energy demand and nutrient intake, suggesting that mitochondrial changes serve as a mechanism for metabolism to adapt to dietary demands [185]. In fact, several studies have found that mitochondria play a crucial role in the pathophysiology of metabolic disorders such as obesity, dyslipidemia and NAFLD [186]. Neufeld-Cohena and collaborators showed that diurnal regulation of mitochondrial respiration was lost in the liver of HFD mice [117]. Moreover, it has been shown that obesity and excess energy intake alter the balance of mitochondrial dynamics, thereby contributing to progressive mitochondrial dysfunction and metabolic deterioration [109]. It is therefore suggested that excess dietary fat affects both mitochondrial biogenesis, structure, and function [187,188]. Indeed, it has been found that cells exposed to a nutrient-rich environment tend to maintain their mitochondria in a fragmented state, whereas the mitochondria of starved cells tend to be elongated [122]. Furthermore, it was observed that this mitochondrial plasticity is lost as NAFLD progresses. The unbalance in mitochondrial dynamics may disrupt mitophagy, leading to the accumulation of damaged mitochondria, promoting oxidative stress, and enhancing the UPR [189]. Consequently, altered mitochondrial dynamics

may underlie the pathogenesis of NAFLD producing aberrant phenotype organelles which may lead to more serious complications beyond fatty liver (e.g., hepatocellular carcinoma) [190].

4 POLYPHENOLS

Polyphenols are secondary metabolites synthesized by plants in metabolic pathways, which are commonly involved in chemical defense against pathogens, UV radiation and other stress factors, as well as for nutrition growth and reproduction [191].

They present a varied structure and, approximately more than 8.000 phenolic structures have been described, but not all of them are present in all plant species [192]. The main characteristic of polyphenols is the presence of at least two phenol rings and one or more hydroxyl substituents in their structure [193].

4.1 Classification of phenolic compounds

Based on their structures, and according to certain characteristics such as the number of phenolic rings, the number and arrangement of their carbon atoms and also the structural elements that can bind to the phenol ring (e. g. sugars and organic acids), polyphenols can be classified into two main families: flavonoids and non-flavonoids [194].

4.1.1 Flavonoids

The term flavonoid generally refers to phenolic compounds sharing the same basic phenyl benzopyran chemical structure with a 15-carbon skeleton of a C6–C3–C6 connected to two aromatic rings by a heterocyclic ring [195]. Flavonoids can be classified into different subclasses depending on the oxidation and hydroxylation pattern of the central ring: flavan-3-ols, flavanones, flavonols, flavones, isoflavones, and anthocyanins [194], (Figure 12).

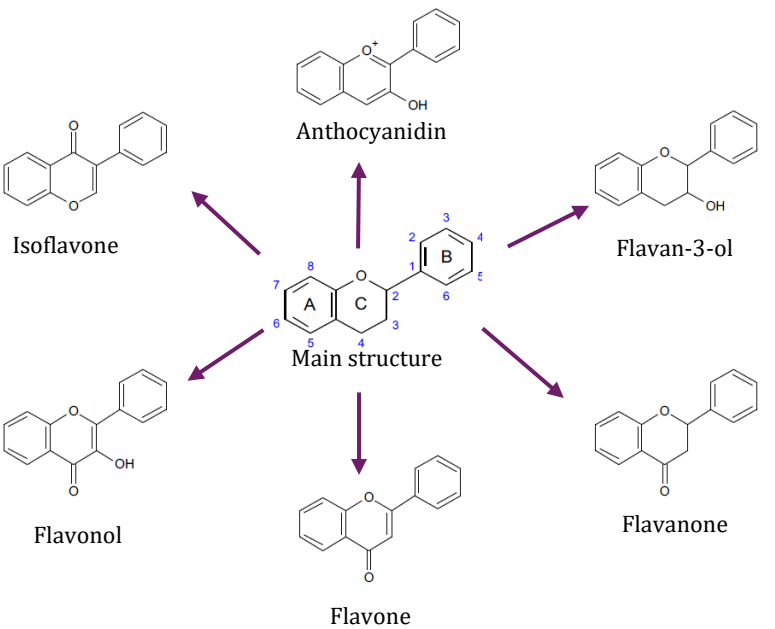

Figure 12. Flavonoid subclasses and their basic chemical structures. Adapted from [194].

The most complex subclass of flavonoids are flavan-3-ols present in many sources of food such as grapes, apricots, apples, cinnamon or cocoa beans and beverages like wine, tea, or beer, and are responsible for giving them the astringent and bitterness characteristic [196]. A particularity of this group is that, unlike the other flavonoids, flavan-3-ols are not present in a glycosylated form in food but either they appear in free forms or as gallic acid esters [197]. They exist in both monomeric units, catechins, and in oligomeric and polymeric forms, proanthocyanidins (PACs). PACs are polymers of catechins linked by bonds between C4 and C8 or C6. Among the various flavan-3-ols phenolic species (+)-catechin and (-)-epicatechin are the most widespread in nature, although they are commonly conjugated with gallic acid to form the so called gallate flavon-3-ols (epicatechin gallate, catechin gallate, epigallocatechin gallate and gallocatechin gallate) [198]. This group of phenolic compounds are widely present in the human diet with different beneficial effects largely demonstrated by the scientific community during the last years as

antihypertensive, protective against MS, improving insulin resistance, inflammation, and lipid metabolism [199].

Flavanones exist as hydroxyl, glycosylated, and O-methylated derivatives and are extensively found in citric fruits, being naringenin of grapefruit and hesperidin of orange the most popular ones [200]. Flavonols are the most ubiquitous flavonoids found all over the plant kingdom [194] commonly glycosylated, being kaempferol, quercetin, isorhamnetin, and myricetin the principal dietary flavonols found not only in onions, broccoli, curly kale, tomatoes, peaches, blueberries, and cherries, but also in beverages like red wine and tea [201,202]. Flavones encompass the less prevalent and hydrophobic flavonoids, which include apigenin, baicalein, luteolin, wogonin and nobiletin present in the skin of citrus fruits as well as in parsley, celery, and some herbs [203]. Isoflavones are found exclusively in legumes, with daidzein and genistein being the main representatives which are present principally in soybean [204]. Anthocyanins are water soluble pigments that confer the characteristic red, blue, and purple color to plants. They are widely found in red grapes, cherries, and berries, being cyanidin the most widespread anthocyanin [205].

4.1.2 Non-Flavonoids

Non-flavonoid compounds include phenolic acids, stilbenes, lignans, tannins and xanthones. The principal non-flavonoid of dietary significance is represented by phenolic acids, mainly benzoic acid and cinnamic acid derivatives. They are present in several fruits such as apricot, cherries with higher concentrations in dried fruits, and also in eggplant, cereals and spinach vegetables [206]. Stilbenes represent a small class of non-flavonoids with resveratrol as the most common and studied compound in this group. It can be found in grapes, peanuts, and berries, and has demonstrated beneficial effects on human health [207]. Lignans are widespread in the plant kingdom and form a large part of the human diet,

being present in rice, legumes, seeds, and vegetable oils. The most relevant dietary lignans are secoisolariciresinol, matairesinol, lariciresinol, pinoresinol, medioresinol, and syringaresinol [208]. Tannins are water soluble phenolic compounds which can be found in beans, berries, and nuts [208]. Xanthones consist of a tricyclic xanthene-9-one structure whose principal natural sources are mangosteen and mango fruit [209].

4.2 Polyphenols and health

Phenolic compounds, and particularly flavonoids, have been shown to exert many beneficial effects on human health thus becoming a field of interest for biomedical research. In this sense, there is increasing evidence showing the anti-inflammatory, antimicrobial, anticancer, antiallergic, and antioxidant attributes of these bioactive compounds [210–213]. There are also a bunch of epidemiological studies associating the consumption of phenol-rich fruits and vegetables with the protection against chronic diseases, such as cardiovascular and neurodegenerative diseases [214–217]. Their beneficial health properties rely on their interaction with key intermediates of vital physiological processes, such as inflammatory and stress responses as well as metabolic regulation [218].

4.2.1 Effects of Flavonoids on Metabolic Syndrome

A wide range of studies have demonstrated that flavonoids exert beneficial effects in the prevention and management of several MS risk factors such as obesity, dyslipidemia, hypertension, and insulin resistance [219–221].

The occurrence of obesity appears to precede the occurrence of the other risk factors that comprise MS [126]. In this regard, the consumption of PACs has been shown to reduce fat deposition and body weight in experiments with diet-induced obese animals, rats, and mice [222–225]. In addition, several studies about dietary consumption of flavonoids rich food showed a correlation between increased phenolic diet consumption and maintenance or even decrease of body weight in adults [226,227]. The

possible mechanisms involved in weight loss through flavonoid consumption include control of appetite and decrease food intake, modulation of adipogenesis, lipolysis, β-oxidation, energy expenditure stimulation and reduction of intestinal fat absorption as well as amelioration of gut microbiota dysbiosis [228]. However, these mechanisms may be involved in other beneficial health effects in addition to the anti-obesity effect.

Dyslipidemia represents an abnormal and unhealthy amount of lipids in the blood. Several studies have shown associations between serum levels of lipids and lipoproteins and the intake of phenolic rich fruit and beverages. In this sense, green tea has shown to reduce total serum cholesterol in adults, men, and women [229]. Moreover, daily consumption of anthocyanins was found to improve HDL cholesterol levels in a Chinese population while a high intake of flavonoids was associated with a decrease on serum triglycerides concentrations in women but not in men subjects [230].

On the other hand, a negative correlation has been shown between the incidence of hypertension, one major risk factor associated with CVDs, and the consumption of flavonoids [231–233]. In this sense, dietary flavonoid intake mitigates the risk of CVDs by improving endothelial dysfunction and decreasing blood pressure [234]. Over the past years, several epidemiological and experimental trials have evidenced the medical benefits of polyphenols intake on CVDs and hypertension incidence. For example, in a study involving 156,957 north American participants, consumption of anthocyanins and flavan-3-ols have shown to contribute to the prevention of hypertension [235]. Many other studies conducted in obese human patients and hypertensive rats demonstrated that flavonoids intake, in particular cranberry beverage, black and green tea, quercetin, anthocyanin, naringenin among several other, have favorable effects in protecting against CVDs. Results from these studies showed that the intake

of the mentioned phenolic compounds improved the cardiovascular function, reduced systolic blood pressure and LDL cholesterol, showing, in addition, a positive effect on atherosclerosis increasing redox status, vasodilation and HDL cholesterol [236–238].

Due to its increasing prevalence, T2DM is becoming a global health concern. Moreover, 7.5 % of the adult population is affected by impaired glucose tolerance, also called prediabetes, and non-diabetic hyperglycaemia [239]. There have been various epidemiological studies showing that diet can affect the risk of developing impaired glucose tolerance and T2DM. A diet poor in fruits and vegetables (main sources of polyphenols) is associated with an increased risk of T2DM [240]. In this regard, an inverse correlation has been observed between the consumption of grapes and T2DM development risk in a study involving 45,411 Asian participants [241]. The prevention of T2DM due to the intake of flavonoid-enriched food may be related to, among others, the anti-inflammatory effects and the direct actions on the glucose metabolic pathway (insulin sensitivity) [242]. In this sense, *in vitro* studies demonstrated that flavonoids treatment enhanced expression of GLUT4, PI3K, p-IRS-1 and p-Akt while decreased the expression of SGLT1, GLUT2 and GLUT5 leading to a glucose uptake reduction [243–245].

In summary, the antioxidative and anti-inflammatory effects of flavonoids, together with its interaction with genes and proteins involved in key metabolic pathways, have been hypothesized to have a major role in their preventive action on MS [246,247] (Figure 13). Despite this, although flavonoids seem to mitigate MS risk factors and prove to be effective as a preventive measure against the main pathological hallmarks of MS, some studies remain inconclusive, probably due to the complex interactions among individual risk factors, the abundance of naturally occurring flavonoids, and their multiple effects on the body.

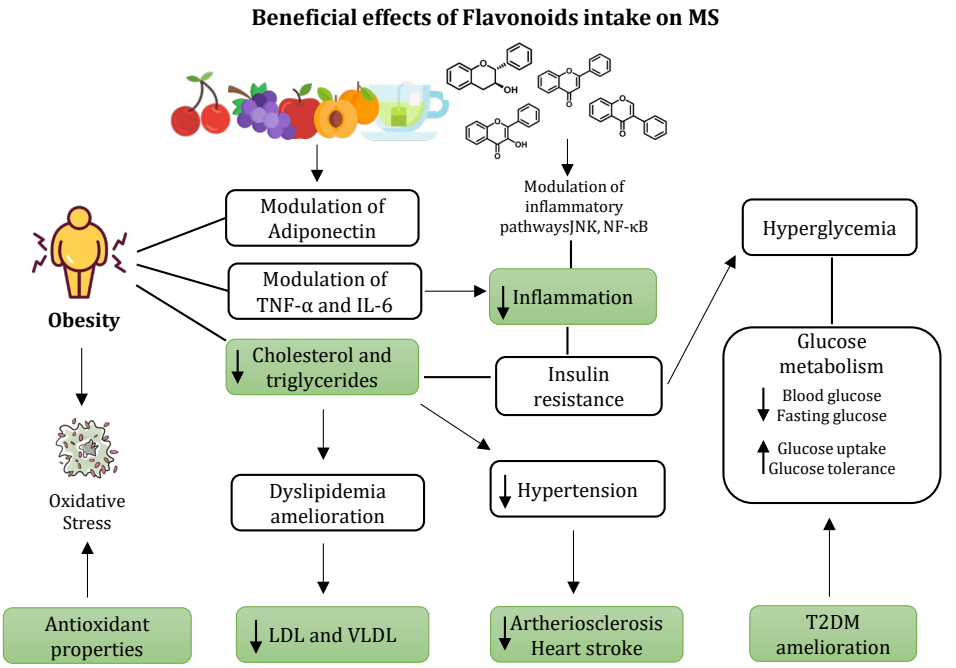

Figure 13. Schematic representation of the beneficial effects of flavonoid intake on MS. Adapted from [221].

4.2.2 Effect of Grape Seed Procyanidin Extract on Metabolic syndrome

Grape Seed Procyanidin Extract (GSPE), a complex mix of several phenolic compounds enriched in PACs (catechin, dimeric and oligomeric procyanidins, epicatechin, epigallocatechin, epicatechin gallate, and epigallocatechin gallate), has been one of the main study targets of the Nutrigenomics Research group. Comprehensive surveys have been conducted over the last years, studying the biological effects of GSPE on lipid and carbohydrate homeostasis, its regulation of cell signaling and metabolism and its hypotensive properties. In this sense, studies involving diet-induce obese rats showed that GSPE was able to improve dyslipidemia, lowering triglycerides and LDL cholesterol levels, mainly by inhibiting key hepatic lipogenic regulators such as SREBP-1c, *Fasn* and diacylglycerol Oacyltransferase 2 (*Dgat2*) [248,249]. In addition, the interaction and repression of microRNAs (miR) miR-33a and miR-122,

major regulators of hepatic lipid metabolism, have been attributed to its hiperlipidemia amelioration [250–252].

Furthermore, chronic administration of GSPE is able to attenuate hypertension associated with MS in rats characterized by a cafeteria diet induced obesity [253]. Other studies evidenced the corrective effects on obesity-related disturbed glucose homeostasis of GSPE administration, as it lowers glucose blood level, increased glucose uptake and improved insulin resistance states [254–256].

In addition to the liver, several experiments have demonstrated that GSPE is also able to modulate the function of adipose tissue and skeletal muscle. In this regard, researchers demonstrated that a chronic ingestion of this bioactive compound reduced adipocyte size in white adipose tissue [257]. Moreover, a very recent study has also shown the GSPE improvement over size of inguinal subcutaneous white adipose cells, in addition to a downregulation of fatty acid metabolic genes in a time-dependent manner [258]. Casanova and colleagues demonstrate an amelioration in adipose mitochondrial functionality by GSPE administration in rats, and a preventive effect over ROS production and damage [259]. Furthermore, anti-inflammatory effects of GSPE consumption were demonstrated in white adipose tissue of obese-feeding rats by a decrease of TNF-a and IL-6 production [260].

The main GSPE effects on skeletal muscle are associated with the activation of AMPK. It is known that AMPK activation suppresses lipogenesis and stimulates fat oxidation [261]. In this sense, it has been shown that PACs increased AMPK phosphorylation, resulting in increased thermogenesis and energy expenditure, stimulated mitochondrial functionality and oxidative capacity via up-regulation of uncoupling protein 2 (*Ucp2*) muscle gene expression [262].

Altogether, these studies exhibit the antioxidant, anti-inflammatory, antihypertensive and hypolipidemic properties of GSPE, demonstrating

that it can be considered as a potential natural compound to protect against MS.

4.2.3 Effect of Grape Seed Procyanidin Extract on circadian rhythms

As the circadian clock has become a focus on metabolic research, the Nutrigenomic Research group has also carried out studies to analyze the relationship between GSPE with the central and peripheral clocks. In this regard, Ribas-Latre and collaborators demonstrated that GSPE was able to modulate the levels of melatonin, a main regulator of the sleep-wake cycle, increasing its plasma concentration when it was administered at ZT0, the beginning of the light phase, in rats [263]. In the same study, these investigators also observed a GSPE modulation of the expression pattern of *Bmal1*, a master regulator of the molecular clock, and *Nampt,* a clock-controlled gene, in the hypothalamus [263].

Besides acting on a central level, GSPE may also influence clock components in peripheral tissues. The first studies using HepG2 cells suggested a modulation of the liver clock via an increase of the transcriptional activity of *Rorα* and subsequently enhancing *Bmal1* expression [264]. In addition, an acute study in healthy rats, also suggested *Bmal1* and *Nampt* as possible targets for GSPE to modulate the circadian clock in the liver [265]. In this study, researchers observed a modulation of NAD+ content by GSPE. NAD+ has a central role in the liver for the synchronization of metabolism and it is regulated by its rate limiting enzyme NAMPT. In this regard, GSPE was capable of modulating *Nampt* and NAD+ levels, increasing *Nampt* gene and protein expressions thereby raising NAD+ concentrations when it was administered at ZT12, the beginning of the dark phase. Moreover, the authors only observed a modulation of clock genes expression patterns in the acute treatment at ZT12, highlighting the importance of the timing of administration in the effects of these compounds [265]. It has also been observed that chronic consumption of GSPE modulates the expression of clock and clock-

controlled genes in the gut and white adipose tissue, as well as in the liver, in healthy and obese rats [266]. In this sense, not only animal trials but also cell experiments confirm that this phenolic PACs-rich extract is able to interact and modulate daily rhythms by interacting with components of the core clock machinery in central and peripheral tissues, modifying their expression, which may have an impact on the regulation of metabolism.

5 REFERENCES

1. Kriegsfeld, L.J.; Nelson, R.J. Biological Rhythms. *Handbook of Neuroscience for the Behavioral Sciences* **2009**, doi:10.1002/9780470478509.NEUBB001005.
2. Ince, L.M. Introduction to Biological Rhythms: A Brief History of Chronobiology and Its Relevance to Parasite Immunology. *Parasite Immunology* **2022**, *44*, e12905, doi:10.1111/PIM.12905.
3. de Mairan, J.-J. Observation Botanique. *Histoire de l'Académie Royale des Sciences Paris* **1729**.
4. Vitaterna, M.H.; Takahashi, J.S.; Turek, F.W. Overview of Circadian Rhythms. *Alcohol Research & Health* **2001**, *25*, 85.
5. Halberg, F. Circadian (about Twenty-Four-Hour) Rhythms in Experimental Medicine [Abridged]. *Proc R Soc Med* **1963**, *56*, 253, doi:10.1177/003591576305600404.
6. Moore-Ede, M.C.; Czeisler, C.A.; Richardson, G.S. Circadian Timekeeping in Health and Disease. *New England Journal of Medicine* **1983**, *309*, 469–476, doi:10.1056/NEJM198308253090806.
7. Pittendrigh, C.S. Circadian Rhythms and the Circadian Organization of Living Systems. *Cold Spring Harbor Symposia on Quantitative Biology* **1960**, *25*, 159–184, doi:10.1101/SQB.1960.025.01.015.
8. Biologic Rhythms in Clinical and Laboratory Medicine. *Biologic Rhythms in Clinical and Laboratory Medicine* **1992**, doi:10.1007/978-3-642-78734-8.
9. Reinberg, A.; Smolensky, M.H. Introduction to Chronobiology. **1983**, 1–21, doi:10.1007/978-1-4613-9496-9_1.
10. Halberg, F. Chronobiology. *Annual Review of Physiology* **1969**, *31*, 675–726, doi:10.1146/annurev.ph.31.030169.003331.
11. Lee, R.; Balick, M.J. Chronobiology: It's About Time. *Explore: The Journal of Science and Healing* **2006**, *2*, 442–445, doi:10.1016/j.explore.2006.06.022.
12. Cornelissen, G. Cosinor-Based Rhythmometry. *Theoretical Biology and Medical Modelling* **2014**, *11*, 1–24, doi:10.1186/1742-4682-11-16/FIGURES/9.
13. Haus, E.; Touitou, Y. Principles of Clinical Chronobiology. *Biologic Rhythms in Clinical and Laboratory Medicine* **1992**, 6–34, doi:10.1007/978-3-642-78734-8_2.
14. Cagampang, F.R.; Bruce, K.D. Horizons in Nutritional Science The Role of the Circadian Clock System in Nutrition and Metabolism., doi:10.1017/S0007114512002139.
15. Takahashi, J.S.; Hong, H.K.; Ko, C.H.; McDearmon, E.L. The Genetics of Mammalian Circadian Order and Disorder: Implications for Physiology and Disease. *Nat Rev Genet* **2008**, *9*, 764, doi:10.1038/NRG2430.
16. Bell-Pedersen, D.; Cassone, V.M.; Earnest, D.J.; Golden, S.S.; Hardin, P.E.; Thomas, T.L.; Zoran, M.J. CIRCADIAN RHYTHMS FROM MULTIPLE

OSCILLATORS: LESSONS FROM DIVERSE ORGANISMS. **2005**, doi:10.1038/nrg1633.

17. Welsh, D.K.; Takahashi, J.S.; Kay, S.A. Suprachiasmatic Nucleus: Cell Autonomy and Network Properties. *Review in Advance on Annu. Rev. Physiol* **2010**, *72*, 551–577, doi:10.1146/annurev-physiol-021909-135919.

18. Colwell, C.S. Linking Neural Activity and Molecular Oscillations in the SCN. *Nature Reviews Neuroscience 2011 12:10* **2011**, *12*, 553–569, doi:10.1038/nrn3086.

19. Aton, S.J.; Herzog, E.D. Come Together, Right...Now: Synchronization of Rhythms in a Mammalian Circadian Clock. *Neuron* **2005**, *48*, 531–534, doi:10.1016/J.NEURON.2005.11.001.

20. Dibner, C.; Schibler, U.; Albrecht, U. The Mammalian Circadian Timing System: Organization and Coordination of Central and Peripheral Clocks. *Annu. Rev. Physiol* **2010**, *72*, 517–549, doi:10.1146/annurev-physiol-021909-135821.

21. Hannibal, J.; Fahrenkrug, J. Neuronal Input Pathways to the Brain's Biological Clock and Their Functional Significance. *Adv Anat Embryol Cell Biol* **2006**, *182*, 1–71, doi:10.1007/3-540-27789-7.

22. Takahashi, J.S.; Hong, H.K.; Ko, C.H.; Mcdearmon, E.L. The Genetics of Mammalian Circadian Order and Disorder : Implications for Physiology and Disease. **2008**, *9*, doi:10.1038/nrg2430.

23. Zhang, E.E.; Kay, S.A. Clocks Not Winding down: Unravelling Circadian Networks. *Nature Reviews Molecular Cell Biology 2010 11:11* **2010**, *11*, 764–776, doi:10.1038/nrm2995.

24. Jordan, S.D.; Lamia, K.A. AMPK at the Crossroads of Circadian Clocks and Metabolism. *Molecular and Cellular Endocrinology* **2013**, *366*, 163–169, doi:10.1016/j.mce.2012.06.017.

25. Lee, C.; Etchegaray, J.; Cagampang, F.R.A.; Loudon, A.S.I.; Reppert, S.M. Posttranslational Mechanisms Regulate the Mammalian Circadian Clock. **2001**, *107*, 855–867.

26. Saran, A.R.; Dave, S.; Zarrinpar, A. Circadian Rhythms in the Pathogenesis and Treatment of Fatty Liver Disease. *Gastroenterology* **2020**, *158*, 1948, doi:10.1053/J.GASTRO.2020.01.050.

27. Wang, Z.; Wu, Y.; Li, L.; Su, X.D. Intermolecular Recognition Revealed by the Complex Structure of Human CLOCK-BMAL1 Basic Helix-Loop-Helix Domains with E-Box DNA. *Cell Research* **2013**, *23*, 213, doi:10.1038/CR.2012.170.

28. Mirsky, H.P.; Liu, A.C.; Welsh, D.K.; Kay, S.A.; Doyle, F.J. A Model of the Cell-Autonomous Mammalian Circadian Clock. *Proc Natl Acad Sci U S A* **2009**, *106*, 11107–11112, doi:10.1073/PNAS.0904837106.

29. Guillaumond, F.; Dardente, H.; Giguère, V.; Cermakian, N. Differential Control of Bmal1 Circadian Transcription by REV-ERB and ROR Nuclear Receptors. *J Biol Rhythms* **2005**, *20*, 391–403, doi:10.1177/0748730405277232.

30. Zanquetta, M.M.; Corra-Giannella, M.L.; Monteiro, M.B.; Villares, S.M.F. Body Weight, Metabolism and Clock Genes. *Diabetology and Metabolic Syndrome* **2010**, *2*, 1–10, doi:10.1186/1758-5996-2-53/FIGURES/2.

31. Golombek, D.A.; Bussi, I.L.; Agostino, P. v. Minutes, Days and Years: Molecular Interactions among Different Scales of Biological Timing. *Philosophical Transactions of the Royal Society B: Biological Sciences* **2014**, *369*, doi:10.1098/RSTB.2012.0465.

32. Rutter, J.; Reick, M.; Wu, L.C.; McKnight, S.L. Regulation of Crock and NPAS2 DNA Binding by the Redox State of NAD Cofactors. *Science (1979)* **2001**, *293*, 510–514, doi:10.1126/SCIENCE.1060698/SUPPL_FILE/RUTTERWEB.PDF.

33. Meng, Q.; Logunova, L.; Maywood, E.S.; Gallego, M.; Lebiecki, J.; Brown, T.M.; Semikhodskii, A.S.; Glossop, N.R.J.; Piggins, H.D.; Chesham, J.E.; et al. Article Setting Clock Speed in Mammals : The CK1 3 Tau Mutation in Mice Accelerates Circadian Pacemakers by Selectively Destabilizing PERIOD Proteins. **2008**, 78–88, doi:10.1016/j.neuron.2008.01.019.

34. Asher, G.; Gatfield, D.; Stratmann, M.; Reinke, H.; Dibner, C.; Kreppel, F.; Mostoslavsky, R.; Alt, F.W.; Schibler, U. SIRT1 Regulates Circadian Clock Gene Expression through PER2 Deacetylation. *Cell* **2008**, *134*, 317–328, doi:10.1016/J.CELL.2008.06.050.

35. Spengler, M.L.; Kuropatwinski, K.K.; Schumer, M.; Antoch, M.; Spengler, M.L.; Kuropatwinski, K.K.; Schumer, M.; Antoch, M.; Spengler, M.L.; Kuropatwinski, K.K.; et al. A Serine Cluster Mediates BMAL1-Dependent CLOCK Phosphorylation and Degradation A Serine Cluster Mediates BMAL1-Dependent CLOCK Phosphorylation and Degradation. **2016**, *4101*, doi:10.4161/cc.8.24.10273.

36. Dang, F.; Sun, X.; Ma, X.; Wu, R.; Zhang, D.; Chen, Y.; Xu, Q.; Wu, Y.; Liu, Y. Insulin Post-Transcriptionally Modulates Bmal1 Protein to Affect the Hepatic Circadian Clock. *Nature Communications 2016 7:1* **2016**, *7*, 1–12, doi:10.1038/ncomms12696.

37. Luciano, A.K.; Zhou, W.; Santana, J.M.; Kyriakides, C.; Velazquez, H.; Sessa, W.C. CLOCK Phosphorylation by AKT Regulates Its Nuclear Accumulation and Circadian Gene Expression in Peripheral Tissues. *The Journal of Biological Chemistry* **2018**, *293*, 9126, doi:10.1074/JBC.RA117.000773.

38. Puig, L.S.; Valera-Alberni, M.; Cantó, C.; Pillon, N.J. Circadian Rhythms and Mitochondria: Connecting the Dots. *Frontiers in Genetics* **2018**, *9*, 452, doi:10.3389/FGENE.2018.00452/BIBTEX.

39. Panda, S.; Hogenesch, J.B.; Kay, S.A. Circadian Rhythms from Flies to Human. *Nature 2002 417:6886* **2002**, *417*, 329–335, doi:10.1038/417329a.

40. Yamazaki, S.; Numano, R.; Abe, M.; Hida, A.; Takahashi, R.I.; Ueda, M.; Block, G.D.; Sakaki, Y.; Menaker, M.; Tei, H. Resetting Central and Peripheral Circadian Oscillators in Transgenic Rats. *Science (1979)* **2000**, *288*, 682–685, doi:10.1126/SCIENCE.288.5466.682.

41. Yoo, S.H.; Yamazaki, S.; Lowrey, P.L.; Shimomura, K.; Ko, C.H.; Buhr, E.D.; Siepka, S.M.; Hong, H.K.; Oh, W.J.; Yoo, O.J.; et al. PERIOD2::LUCIFERASE Real-Time Reporting of Circadian Dynamics Reveals Persistent Circadian

Oscillations in Mouse Peripheral Tissues. *Proc Natl Acad Sci U S A* **2004**, *101*, 5339–5346, doi:10.1073/PNAS.0308709101.

42. Barclay, J.L.; Tsang, A.H.; Oster, H. Interaction of Central and Peripheral Clocks in Physiological Regulation. *Progress in Brain Research* **2012**, *199*, 163–181, doi:10.1016/B978-0-444-59427-3.00030-7.

43. Almon, R.R.; Yang, E.; Lai, W.; Androulakis, I.P.; Dubois, D.C.; Jusko, W.J. Circadian Variations in Liver Gene Expression: Relationships to Drug Actions. *J Pharmacol Exp Ther* **2008**, *326*, 700, doi:10.1124/JPET.108.140186.

44. Panda, S.; Antoch, M.P.; Miller, B.H.; Su, A.I.; Schook, A.B.; Straume, M.; Schultz, P.G.; Kay, S.A.; Takahashi, J.S.; Hogenesch, J.B. Coordinated Transcription of Key Pathways in the Mouse by the Circadian Clock. *Cell* **2002**, *109*, 307–320, doi:10.1016/S0092-8674(02)00722-5.

45. Altun, A.; Ugur-Altun, B. Melatonin: Therapeutic and Clinical Utilization. *International Journal of Clinical Practice* **2007**, *61*, 835–845, doi:10.1111/J.1742-1241.2006.01191.X.

46. Schibler, U.; Brown, S.A. Enlightening the Adrenal Gland. *Cell Metab* **2005**, *2*, 278–281, doi:10.1016/J.CMET.2005.10.001.

47. Buijs, R.M.; Kalsbeek, A. Hypothalamic Integration of Central and Peripheral Clocks. *Nature Reviews Neuroscience 2001 2:7* **2001**, *2*, 521–526, doi:10.1038/35081582.

48. Challet, E. Minireview: Entrainment of the Suprachiasmatic Clockwork in Diurnal and Nocturnal Mammals. *Endocrinology* **2007**, *148*, 5648–5655, doi:10.1210/EN.2007-0804.

49. van der Veen, D.R.; Riede, S.J.; Heideman, P.D.; Hau, M.; van der Vinne, V.; Hut, R.A. Flexible Clock Systems: Adjusting the Temporal Programme. *Philosophical Transactions of the Royal Society B: Biological Sciences* **2017**, *372*, doi:10.1098/RSTB.2016.0254.

50. Agorastos, A.; Nicolaides, N.C.; Bozikas, V.P.; Chrousos, G.P.; Pervanidou, P. Multilevel Interactions of Stress and Circadian System: Implications for Traumatic Stress. *Frontiers in Psychiatry* **2020**, *10*, 1003, doi:10.3389/FPSYT.2019.01003/BIBTEX.

51. Schibler, U.; Sassone-Corsi, P. A Web of Circadian Pacemakers. *Cell* **2002**, *111*, 919–922, doi:10.1016/S0092-8674(02)01225-4.

52. Wood, S.; Loudon, A. Clocks for All Seasons: Unwinding the Roles and Mechanisms of Circadian and Interval Timers in the Hypothalamus and Pituitary. *Journal of Endocrinology* **2014**, *222*.

53. Hazlerigg, D.G.; Lincoln, G.A. Hypothesis: Cyclical Histogenesis Is the Basis of Circannual Timing. *Journal of Biological Rhythms* **2011**, *26*, 471–485, doi:10.1177/0748730411420812.

54. Lincoln, G. A Brief History of Circannual Time. *Journal of Neuroendocrinology* **2019**, *31*, e12694, doi:10.1111/JNE.12694.

55. Prendergast, B.J. Internalization of Seasonal Time. *Hormones and Behavior* **2005**, *48*, 503–511, doi:10.1016/J.YHBEH.2005.05.013.

56. Helm, B.; Ben-Shlomo, R.; Sheriff, M.J.; Hut, R.A.; Foster, R.; Barnes, B.M.; Dominoni, D. Annual Rhythms That Underlie Phenology: Biological Time-Keeping Meets Environmental Change. *Proc Biol Sci* **2013**, *280*, doi:10.1098/RSPB.2013.0016.

57. Oike, H.; Oishi, K.; Kobori, M. Nutrients, Clock Genes, and Chrononutrition. *Current Nutrition Reports* **2014**, *3*, 204, doi:10.1007/S13668-014-0082-6.

58. Wood, S.H.; Christian, H.C.; Miedzinska, K.; Saer, B.R.C.; Johnson, M.; Paton, B.; Yu, L.; McNeilly, J.; Davis, J.R.E.; McNeilly, A.S.; et al. Binary Switching of Calendar Cells in the Pituitary Defines the Phase of the Circannual Cycle in Mammals. *Curr Biol* **2015**, *25*, 2651–2662, doi:10.1016/J.CUB.2015.09.014.

59. Dupré, S.M.; Burt, D.W.; Talbot, R.; Downing, A.; Mouzaki, D.; Waddington, D.; Malpaux, B.; Davis, J.R.E.; Lincoln, G.A.; Loudon, A.S.I. Identification of Melatonin-Regulated Genes in the Ovine Pituitary Pars Tuberalis, a Target Site for Seasonal Hormone Control. *Endocrinology* **2008**, *149*, 5527–5539, doi:10.1210/EN.2008-0834.

60. Nakao, N.; Ono, H.; Yamamura, T.; Anraku, T.; Takagi, T.; Higashi, K.; Yasuo, S.; Katou, Y.; Kageyama, S.; Uno, Y.; et al. Thyrotrophin in the Pars Tuberalis Triggers Photoperiodic Response. *Nature 2008 452:7185* **2008**, *452*, 317–322, doi:10.1038/nature06738.

61. Arendt, J. Melatonin, Circadian Rhythms, and Sleep. *New England Journal of Medicine* **2000**, *343*, 1114–1116, doi:10.1056/NEJM200010123431510.

62. Lincoln, G.A.; Anderson, H.; Loudon, A. Clock Genes in Calendar Cells as the Basis of Annual Timekeeping in Mammals--a Unifying Hypothesis. *J Endocrinol* **2003**, *179*, 1–13, doi:10.1677/JOE.0.1790001.

63. Dardente, H.; Wyse, C.A.; Birnie, M.J.; Dupré, S.M.; Loudon, A.S.I.; Lincoln, G.A.; Hazlerigg, D.G. A Molecular Switch for Photoperiod Responsiveness in Mammals. *Current Biology* **2010**, *20*, 2193–2198, doi:10.1016/J.CUB.2010.10.048.

64. Thrun, L.A.; Dahl, G.E.; Evans, N.P.; Karsch, F.J. A Critical Period for Thyroid Hormone Action on Seasonal Changes in Reproductive Neuroendocrine Function in the Ewe. *Endocrinology* **1997**, *138*, 3402–3409, doi:10.1210/ENDO.138.8.5341.

65. Yoshimura, T.; Yasuo, S.; Watanabe, M.; Iigo, M.; Yamamura, T.; Hirunagi, K.; Ebihara, S. Light-Induced Hormone Conversion of T4 to T3 Regulates Photoperiodic Response of Gonads in Birds. *Nature* **2003**, *426*, 178–181, doi:10.1038/nature02117.

66. Johnston, J.D.; Ordovás, J.M.; Scheer, F.A.; Turek, F.W. Circadian Rhythms, Metabolism, and Chrononutrition in Rodents and Humans. *Advances in Nutrition* **2016**, *7*, 399, doi:10.3945/AN.115.010777.

67. Oda, H.; Kato, H.; Seki, T. *Health Nutrition: Nutritional Physiology as Health Science*; Kyoritsu Shuppan (in Japanese): Tokyo, Japan, **2005**; ISBN 9784320061538.

68. Tahara, Y.; Shibata, S. Chrono-Biology, Chrono-Pharmacology, and Chrono-Nutrition. *J Pharmacol Sci* **2014**, *124*, 320–335, doi:10.1254/JPHS.13R06CR.

69. Aparecida Crispim, C.; Carliana Mota, M. New Perspectives on Chrononutrition. *https://doi.org/10.1080/09291016.2018.1491202* **2018**, *50*, 63–77, doi:10.1080/09291016.2018.1491202.

70. Garrido, M.; Terrón, M.P.; Rodríguez, A.B. Chrononutrition against Oxidative Stress in Aging. *Oxidative Medicine and Cellular Longevity* **2013**, doi:10.1155/2013/729804.

71. Duffield, G.E.; Best, J.D.; Meurers, B.H.; Bittner, A.; Loros, J.J.; Dunlap, J.C. Circadian Programs of Transcriptional Activation, Signaling, and Protein Turnover Revealed by Microarray Analysis of Mammalian Cells. *Curr Biol* **2002**, *12*, 551–557, doi:10.1016/S0960-9822(02)00765-0.

72. Kornmann, B.; Schaad, O.; Bujard, H.; Takahashi, J.S.; Schibler, U. System-Driven and Oscillator-Dependent Circadian Transcription in Mice with a Conditionally Active Liver Clock. *PLOS Biology* **2007**, *5*, e34, doi:10.1371/JOURNAL.PBIO.0050034.

73. Miller, B.H.; McDearmon, E.L.; Panda, S.; Hayes, K.R.; Zhang, J.; Andrews, J.L.; Antoch, M.P.; Walker, J.R.; Esser, K.A.; Hogenesch, J.B.; et al. Circadian and CLOCK-Controlled Regulation of the Mouse Transcriptome and Cell Proliferation. *Proc Natl Acad Sci U S A* **2007**, *104*, 3342–3347, doi:10.1073/PNAS.0611724104/SUPPL_FILE/11724TABLE9.DOC.

74. Oishi, K.; Amagai, N.; Shirai, H.; Kadota, K.; Ohkura, N.; Ishida, N. Genome-Wide Expression Analysis Reveals 100 Adrenal Gland-Dependent Circadian Genes in the Mouse Liver. *DNA Research* **2005**, *12*, 191–202, doi:10.1093/dnares/dsi003.

75. Oishi, K.; Miyazaki, K.; Kadota, K.; Kikuno, R.; Nagase, T.; Atsumi, G.I.; Ohkura, N.; Azama, T.; Mesaki, M.; Yukimasa, S.; et al. Genome-Wide Expression Analysis of Mouse Liver Reveals CLOCK-Regulated Circadian Output Genes *. *Journal of Biological Chemistry* **2003**, *278*, 41519–41527, doi:10.1074/JBC.M304564200.

76. Eckel-Mahan, K.L.; Patel, V.R.; Mohney, R.P.; Vignola, K.S.; Baldi, P.; Sassone-Corsi, P. Coordination of the Transcriptome and Metabolome by the Circadian Clock. *Proc Natl Acad Sci U S A* **2012**, *109*, 5541–5546, doi:10.1073/PNAS.1118726109/SUPPL_FILE/SD04.XLSX.

77. Mauvoisin, D.; Wang, J.; Jouffe, C.; Martin, E.; Atger, F.; Waridel, P.; Quadroni, M.; Gachon, F.; Naef, F. Circadian Clock-Dependent and -Independent Rhythmic Proteomes Implement Distinct Diurnal Functions in Mouse Liver. *Proc Natl Acad Sci U S A* **2014**, *111*, 167–172, doi:10.1073/PNAS.1314066111/SUPPL_FILE/SD03.XLS.

78. Robles, M.S.; Cox, J.; Mann, M. In-Vivo Quantitative Proteomics Reveals a Key Contribution of Post-Transcriptional Mechanisms to the Circadian Regulation of Liver Metabolism. *PLOS Genetics* **2014**, *10*, e1004047, doi:10.1371/JOURNAL.PGEN.1004047.

79. Schwabe, R.F.; Wiley, J.W.; Reinke, H.; Asher, G. Circadian Clock Control of Liver Metabolic Functions. *Gastroenterology* **2016**, *150*, 574–580, doi:10.1053/J.GASTRO.2015.11.043.

80. Gnocchi, D.; Custodero, C.; Sabbà, C.; Mazzocca, A. Circadian Rhythms: A Possible New Player in Non-Alcoholic Fatty Liver Disease Pathophysiology.

Journal of Molecular Medicine 2019 97:6 **2019**, *97*, 741–759, doi:10.1007/S00109-019-01780-2.

81. Saran, A.R.; Dave, S.; Zarrinpar, A. Circadian Rhythms in the Pathogenesis and Treatment of Fatty Liver Disease. *Gastroenterology* **2020**, *158*, 1948-1966.e1, doi:10.1053/J.GASTRO.2020.01.050.

82. Green, C.B.; Takahashi, J.S.; Bass, J. The Meter of Metabolism. *Cell* **2008**, *134*, 728–742, doi:10.1016/J.CELL.2008.08.022.

83. Ishikawa, K.; Shimazu, T. Circadian Rhythm of Liver Glycogen Metabolism in Rats: Effects of Hypothalamic Lesions. *https://doi.org/10.1152/ajpendo.1980.238.1.E21* **1980**, *1*, 21–25, doi:10.1152/AJPENDO.1980.238.1.E21.

84. Schibler, U. Dialogues in Clinical Neuroscience The Daily Timing of Gene Expression and Physiology in Mammals. **2007**, doi:10.31887/DCNS.2007.9.3/uschibler.

85. Postic, C.; Dentin, R.; Girard, J. Role of the Liver in the Control of Carbohydrate and Lipid Homeostasis. *Diabetes & Metabolism* **2004**, *30*, 398–408, doi:10.1016/S1262-3636(07)70133-7.

86. Sherwin, R.S. Role of Liver in Glucose Homeostasis. *Diabetes Care* **1980**, *3*, 261–265, doi:10.2337/DIACARE.3.2.261.

87. Adeva-Andany, M.M.; Pérez-Felpete, N.; Fernández-Fernández, C.; Donapetry-García, C.; Pazos-García, C. Liver Glucose Metabolism in Humans. *Bioscience Reports* **2016**, *36*, 416, doi:10.1042/BSR20160385.

88. Lamia, K.A.; Storch, K.-F.; Weitz, C.J. Physiological Significance of a Peripheral Tissue Circadian Clock. *Harvard Medical School* **2008**.

89. Matschinsky, F.M.; Wilson, D.F. The Central Role of Glucokinase in Glucose Homeostasis: A Perspective 50 Years after Demonstrating the Presence of the Enzyme in Islets of Langerhans. *Frontiers in Physiology* **2019**, *10*, 148, doi:10.3389/FPHYS.2019.00148/BIBTEX.

90. Han, H.S.; Kang, G.; Kim, J.S.; Choi, B.H.; Koo, S.H. Regulation of Glucose Metabolism from a Liver-Centric Perspective. *Experimental & Molecular Medicine* **2016**, *48*, e218, doi:10.1038/EMM.2015.122.

91. Udoh, U.S.; Swain, T.M.; Filiano, A.N.; Gamble, K.L.; Young, M.E.; Bailey, S.M. Chronic Ethanol Consumption Disrupts Diurnal Rhythms of Hepatic Glycogen Metabolism in Mice. *American Journal of Physiology - Gastrointestinal and Liver Physiology* **2015**, *308*, G964, doi:10.1152/AJPGI.00081.2015.

92. Vollmers, C.; Gill, S.; DiTacchio, L.; Pulivarthy, S.R.; Le, H.D.; Panda, S. Time of Feeding and the Intrinsic Circadian Clock Drive Rhythms in Hepatic Gene Expression. *Proc Natl Acad Sci U S A* **2009**, *106*, 21453–21458, doi:10.1073/PNAS.0909591106/SUPPL_FILE/0909591106SI.PDF.

93. Aronoff, S.L.; Berkowitz, K.; Shreiner, B.; Want, L. Glucose Metabolism and Regulation: Beyond Insulin and Glucagon. *Diabetes Spectrum* **2004**, *17*, 183–190, doi:10.2337/DIASPECT.17.3.183.

94. Jiang, G.; Zhang, B.B. Glucagon and Regulation of Glucose Metabolism. *Am J Physiol Endocrinol Metab* **2003**, *284*, doi:10.1152/AJPENDO.00492.2002.

95. Tseng, H.L.; Yang, S.C.; Yang, S.H.; Shieh, K.R. Hepatic Circadian-Clock System Altered by Insulin Resistance, Diabetes and Insulin Sensitizer in Mice. *PLOS ONE* **2015**, *10*, e0120380, doi:10.1371/JOURNAL.PONE.0120380.

96. Cho, H.; Zhao, X.; Hatori, M.; Yu, R.T.; Barish, G.D.; Lam, M.T.; Chong, L.W.; Ditacchio, L.; Atkins, A.R.; Glass, C.K.; et al. Regulation of Circadian Behaviour and Metabolism by REV-ERB-α and REV-ERB-β. *Nature 2012 485:7396* **2012**, *485*, 123–127, doi:10.1038/nature11048.

97. Gooley, J.J. Circadian Regulation of Lipid Metabolism. *Proceedings of the Nutrition Society* **2016**, *75*, 440–450, doi:10.1017/S0029665116000288.

98. de Goede, P.; Wefers, J.; Brombacher, E.C.; Schrauwen, P.; Kalsbeek, A. Circadian Rhythms in Mitochondrial Respiration. *J Mol Endocrinol* **2018**, *60*, R115–R130, doi:10.1530/JME-17-0196.

99. Chavan, R.; Feillet, C.; Costa, S.S.F.; Delorme, J.E.; Okabe, T.; Ripperger, J.A.; Albrecht, U. Liver-Derived Ketone Bodies Are Necessary for Food Anticipation. *Nat Commun* **2016**, *7*, doi:10.1038/NCOMMS10580.

100. Adamovich, Y.; Rousso-Noori, L.; Zwighaft, Z.; Neufeld-Cohen, A.; Golik, M.; Kraut-Cohen, J.; Wang, M.; Han, X.; Asher, G. Circadian Clocks and Feeding Time Regulate the Oscillations and Levels of Hepatic Triglycerides. *Cell Metab* **2014**, *19*, 319–330, doi:10.1016/J.CMET.2013.12.016.

101. Gréchez-Cassiau, A.; Feillet, C.; Guérin, S.; Delaunay, F. The Hepatic Circadian Clock Regulates the Choline Kinase α Gene through the BMAL1-REV-ERBα Axis. *Chronobiol Int* **2015**, *32*, 774–784, doi:10.3109/07420528.2015.1046601.

102. Zhou, B.; Zhang, Y.; Zhang, F.; Xia, Y.; Liu, J.; Huang, R.; Wang, Y.; Hu, Y.; Wu, J.; Dai, C.; et al. CLOCK/BMAL1 Regulates Circadian Change of Mouse Hepatic Insulin Sensitivity by SIRT1. *Hepatology* **2014**, *59*, 2196–2206, doi:10.1002/HEP.26992.

103. Stenvers, D.J.; Scheer, F.A.J.L.; Schrauwen, P.; la Fleur, S.E.; Kalsbeek, A. Circadian Clocks and Insulin Resistance. *Nature Reviews Endocrinology 2018 15:2* **2018**, *15*, 75–89, doi:10.1038/s41574-018-0122-1.

104. Li, S.; Lin, J.D. Molecular Control of Circadian Metabolic Rhythms. *Journal of Applied Physiology* **2009**, *107*, 1959–1964, doi:10.1152/JAPPLPHYSIOL.00467.2009/ASSET/IMAGES/LARGE/ZDG01 00986930001.JPEG.

105. Peng, X.; Li, J.; Wang, M.; Qu, K.; Zhu, H. A Novel AMPK Activator Improves Hepatic Lipid Metabolism and Leukocyte Trafficking in Experimental Hepatic Steatosis. *J Pharmacol Sci* **2019**, *140*, 153–161, doi:10.1016/J.JPHS.2019.05.008.

106. Duez, H.; van der Veen, J.N.; Duhem, C.; Pourcet, B.; Touvier, T.; Fontaine, C.; Derudas, B.; Baugé, E.; Havinga, R.; Bloks, V.W.; et al. Regulation of Bile Acid Synthesis by the Nuclear Receptor Rev-Erbα. *Gastroenterology* **2008**, *135*, 689-698.e5, doi:10.1053/J.GASTRO.2008.05.035.

107. Eggink, H.M.; Oosterman, J.E.; de Goede, P.; de Vries, E.M.; Foppen, E.; Koehorst, M.; Groen, A.K.; Boelen, A.; Romijn, J.A.; la Fleur, S.E.; et al. Complex Interaction between Circadian Rhythm and Diet on Bile Acid Homeostasis in Male Rats. *Chronobiol Int* **2017**, *34*, 1339–1353, doi:10.1080/07420528.2017.1363226.

108. Rey, G.; Reddy, A.B. Protein Acetylation Links the Circadian Clock to Mitochondrial Function. *Proc Natl Acad Sci U S A* **2013**, *110*, 3210–3211, doi:10.1073/PNAS.1300419110/ASSET/150C0D4F-EDC4-430C-857D-102AFA4CA65D/ASSETS/PNAS.1300419110.FP.PNG.

109. Jheng, H.-F.; Tsai, P.-J.; Guo, S.-M.; Kuo, L.-H.; Chang, C.-S.; Su, I.-J.; Chang, C.-R.; Tsai, Y.-S. Mitochondrial Fission Contributes to Mitochondrial Dysfunction and Insulin Resistance in Skeletal Muscle. *Molecular and Cellular Biology* **2012**, *32*, 309–319, doi:10.1128/mcb.05603-11.

110. Oliva-Ramírez, J.; Moreno-Altamirano, M.M.B.; Pineda-Olvera, B.; Cauich-Sánchez, P.; Javier Sánchez-García, F. Crosstalk between Circadian Rhythmicity, Mitochondrial Dynamics and Macrophage Bactericidal Activity. *Immunology* **2014**, *143*, 490, doi:10.1111/IMM.12329.

111. Peek, C.B.; Affinati, A.H.; Ramsey, K.M.; Kuo, H.Y.; Yu, W.; Sena, L.A.; Ilkayeva, O.; Marcheva, B.; Kobayashi, Y.; Omura, C.; et al. Circadian Clock NAD+ Cycle Drives Mitochondrial Oxidative Metabolism in Mice. *Science* **2013**, *342*, doi:10.1126/SCIENCE.1243417.

112. Jacobi, D.; Liu, S.; Burkewitz, K.; Kory, N.; Knudsen, N.H.; Alexander, R.K.; Unluturk, U.; Li, X.; Kong, X.; Hyde, A.L.; et al. Hepatic Bmal1 Regulates Rhythmic Mitochondrial Dynamics and Promotes Metabolic Fitness. *Cell Metabolism* **2015**, *22*, 709–720, doi:10.1016/j.cmet.2015.08.006.

113. Ezagouri, S.; Asher, G. Circadian Control of Mitochondrial Dynamics and Functions. *Current Opinion in Physiology* **2018**, *5*, 25–29, doi:10.1016/J.COPHYS.2018.05.008.

114. Nakahata, Y.; Sahar, S.; Astarita, G.; Kaluzova, M.; Sassone-Corsi, P. Circadian Control of the NAD+ Salvage Pathway by CLOCK-SIRT1. *Science (1979)* **2009**, *324*, 654–657, doi:10.1126/SCIENCE.1170803/SUPPL_FILE/NAKAHATA.SOM.PDF.

115. Ramsey, K.M.; Yoshino, J.; Brace, C.S.; Abrassart, D.; Kobayashi, Y.; Marcheva, B.; Hong, H.K.; Chong, J.L.; Buhr, E.D.; Lee, C.; et al. Circadian Clock Feedback Cycle through NAMPT-Mediated NAD+ Biosynthesis. *Science (1979)* **2009**, *324*, 651–654, doi:10.1126/SCIENCE.1171641/SUPPL_FILE/RAMSEY.SOM.PDF.

116. Schmitt, K.; Grimm, A.; Dallmann, R.; Oettinghaus, B.; Restelli, L.M.; Witzig, M.; Ishihara, N.; Mihara, K.; Ripperger, J.A.; Albrecht, U.; et al. Circadian Control of DRP1 Activity Regulates Mitochondrial Dynamics and Bioenergetics. *Cell Metabolism* **2018**, *27*, 657-666.e5, doi:10.1016/J.CMET.2018.01.011.

117. Neufeld-Cohen, A.; Robles, M.S.; Aviram, R.; Manella, G.; Adamovich, Y.; Ladeuix, B.; Nir, D.; Rousso-Noori, L.; Kuperman, Y.; Golik, M.; et al. Circadian Control of Oscillations in Mitochondrial Rate-Limiting Enzymes and Nutrient Utilization by PERIOD Proteins. *Proc Natl Acad Sci U S A*

2016, *113*, E1673–E1682, doi:10.1073/PNAS.1519650113/SUPPL_FILE/PNAS.1519650113.SD07.XLSX.

118. Asher, G.; Sassone-Corsi, P. Time for Food: The Intimate Interplay between Nutrition, Metabolism, and the Circadian Clock. *Cell* **2015**, *161*, 84–92, doi:10.1016/J.CELL.2015.03.015.

119. Westermann, B. Bioenergetic Role of Mitochondrial Fusion and Fission. *Biochimica et Biophysica Acta (BBA) - Bioenergetics* **2012**, *1817*, 1833–1838, doi:10.1016/J.BBABIO.2012.02.033.

120. Westermann, B. Mitochondrial Fusion and Fission in Cell Life and Death. *Nature Reviews Molecular Cell Biology 2010 11:12* **2010**, *11*, 872–884, doi:10.1038/nrm3013.

121. Garbern, J.C.; Lee, R.T. Mitochondria and Metabolic Transitions in Cardiomyocytes: Lessons from Development for Stem Cell-Derived Cardiomyocytes. *Stem Cell Research & Therapy 2021 12:1* **2021**, *12*, 1–25, doi:10.1186/S13287-021-02252-6.

122. Liesa, M.; Shirihai, O.S. Mitochondrial Dynamics in the Regulation of Nutrient Utilization and Energy Expenditure. *Cell Metab* **2013**, *17*, 491–506, doi:10.1016/J.CMET.2013.03.002.

123. Lima, A.R.; Santos, L.; Correia, M.; Soares, P.; Sobrinho-Simões, M.; Melo, M.; Máximo, V. Dynamin-Related Protein 1 at the Crossroads of Cancer. *Genes 2018, Vol. 9, Page 115* **2018**, *9*, 115, doi:10.3390/GENES9020115.

124. Green, C.B.; Takahashi, J.S.; Bass, J. The Meter of Metabolism. *Cell* **2008**, *134*, 728–742, doi:10.1016/J.CELL.2008.08.022.

125. Maury, E.; Ramsey, K.M.; Bass, J. Circadian Rhythms and Metabolic Syndrome: From Experimental Genetics to Human Disease. *Circ Res* **2010**, *106*, 447, doi:10.1161/CIRCRESAHA.109.208355.

126. Cornier, M.A.; Dabelea, D.; Hernandez, T.L.; Lindstrom, R.C.; Steig, A.J.; Stob, N.R.; van Pelt, R.E.; Wang, H.; Eckel, R.H. The Metabolic Syndrome. *Endocrine Reviews* **2008**, *29*, 777–822, doi:10.1210/ER.2008-0024.

127. Bray, M.S.; Young, M.E. Chronobiological Effects on Obesity. *Curr Obes Rep* **2012**, *1*, 9, doi:10.1007/S13679-011-0005-4.

128. Johnston, J.D.; Ordovás, J.M.; Scheer, F.A.; Turek, F.W. Circadian Rhythms, Metabolism, and Chrononutrition in Rodents and Humans. *Advances in Nutrition* **2016**, *7*, 399, doi:10.3945/AN.115.010777.

129. Engin, A. Circadian Rhythms in Diet-Induced Obesity. *Advances in Experimental Medicine and Biology* **2017**, *960*, 19–52, doi:10.1007/978-3-319-48382-5_2.

130. McHill, A.W.; Wright, K.P. Role of Sleep and Circadian Disruption on Energy Expenditure and in Metabolic Predisposition to Human Obesity and Metabolic Disease. *Obesity Reviews* **2017**, *18*, 15–24, doi:10.1111/OBR.12503.

131. Baron, K.G.; Reid, K.J. Circadian Misalignment and Health. *Int Rev Psychiatry* **2014**, *26*, 139, doi:10.3109/09540261.2014.911149.

132. Bray, M.S.; Young, M.E. Circadian Rhythms in the Development of Obesity: Potential Role for the Circadian Clock within the Adipocyte. *Obesity Reviews* **2007**, *8*, 169–181, doi:10.1111/J.1467-789X.2006.00277.X.

133. Pendergast, J.S.; Branecky, K.L.; Yang, W.; Ellacott, K.L.J.; Niswender, K.D.; Yamazaki, S. High-Fat Diet Acutely Affects Circadian Organization and Eating Behavior. *Eur J Neurosci* **2013**, *37*, 1350, doi:10.1111/EJN.12133.

134. Kohsaka, A.; Laposky, A.D.; Ramsey, K.M.; Estrada, C.; Joshu, C.; Kobayashi, Y.; Turek, F.W.; Bass, J. High-Fat Diet Disrupts Behavioral and Molecular Circadian Rhythms in Mice. *Cell Metab* **2007**, *6*, 414–421, doi:10.1016/J.CMET.2007.09.006.

135. Thaiss, C.A.; Zeevi, D.; Levy, M.; Zilberman-Schapira, G.; Suez, J.; Tengeler, A.C.; Abramson, L.; Katz, M.N.; Korem, T.; Zmora, N.; et al. Transkingdom Control of Microbiota Diurnal Oscillations Promotes Metabolic Homeostasis. *Cell* **2014**, *159*, 514–529, doi:10.1016/J.CELL.2014.09.048.

136. Yasumoto, Y.; Hashimoto, C.; Nakao, R.; Yamazaki, H.; Hiroyama, H.; Nemoto, T.; Yamamoto, S.; Sakurai, M.; Oike, H.; Wada, N.; et al. Short-Term Feeding at the Wrong Time Is Sufficient to Desynchronize Peripheral Clocks and Induce Obesity with Hyperphagia, Physical Inactivity and Metabolic Disorders in Mice. *Metabolism - Clinical and Experimental* **2016**, *65*, 714–727, doi:10.1016/J.METABOL.2016.02.003.

137. Arble, D.M.; Bass, J.; Laposky, A.D.; Vitaterna, M.H.; Turek, F.W. Circadian Timing of Food Intake Contributes to Weight Gain. *Obesity (Silver Spring)* **2009**, *17*, 2100, doi:10.1038/OBY.2009.264.

138. Scheer, F.A.J.L.; Hilton, M.F.; Mantzoros, C.S.; Shea, S.A. Adverse Metabolic and Cardiovascular Consequences of Circadian Misalignment. *Proc Natl Acad Sci U S A* **2009**, *106*, 4453–4458, doi:10.1073/PNAS.0808180106/SUPPL_FILE/0808180106SI.PDF.

139. Shi, S.Q.; Ansari, T.S.; McGuinness, O.P.; Wasserman, D.H.; Johnson, C.H. Circadian Disruption Leads to Insulin Resistance and Obesity. *Curr Biol* **2013**, *23*, 372–381, doi:10.1016/J.CUB.2013.01.048.

140. Shimba, S.; Ogawa, T.; Hitosugi, S.; Ichihashi, Y.; Nakadaira, Y.; Kobayashi, M.; Tezuka, M.; Kosuge, Y.; Ishige, K.; Ito, Y.; et al. Deficient of a Clock Gene, Brain and Muscle Arnt-Like Protein-1 (BMAL1), Induces Dyslipidemia and Ectopic Fat Formation. *PLOS ONE* **2011**, *6*, e25231, doi:10.1371/JOURNAL.PONE.0025231.

141. Turek, F.W.; Joshu, C.; Kohsaka, A.; Lin, E.; Ivanova, G.; McDearmon, E.; Laposky, A.; Losee-Olson, S.; Easton, A.; Jensen, D.R.; et al. Obesity and Metabolic Syndrome in Circadian Clock Mutant Mice. *Science* **2005**, *308*, 1043–1045, doi:10.1126/SCIENCE.1108750.

142. Shimba, S.; Ishii, N.; Ohta, Y.; Ohno, T.; Watabe, Y.; Hayashi, M.; Wada, T.; Aoyagi, T.; Tezuka, M. Brain and Muscle Arnt-like Protein-1 (BMAL1), a Component of the Molecular Clock, Regulates Adipogenesis. *Proc Natl Acad Sci U S A* **2005**, *102*, 12071–12076, doi:10.1073/PNAS.0502383102/SUPPL_FILE/02383FIG11.PDF.

143. Marcheva, B.; Ramsey, K.M.; Buhr, E.D.; Kobayashi, Y.; Su, H.; Ko, C.H.; Ivanova, G.; Omura, C.; Mo, S.; Vitaterna, M.H.; et al. Disruption of the Clock

Components CLOCK and BMAL1 Leads to Hypoinsulinemia and Diabetes. *Nature* **2010**, *466*, 627, doi:10.1038/NATURE09253.

144. de Bacquer, D.; van Risseghem, M.; Clays, E.; Kittel, F.; de Backer, G.; Braeckman, L. Rotating Shift Work and the Metabolic Syndrome: A Prospective Study. *Int J Epidemiol* **2009**, *38*, 848–854, doi:10.1093/IJE/DYN360.

145. Wang, X.S.; Armstrong, M.E.G.; Cairns, B.J.; Key, T.J.; Travis, R.C. Shift Work and Chronic Disease: The Epidemiological Evidence. *Occup Med (Lond)* **2011**, *61*, 78–89, doi:10.1093/OCCMED/KQR001.

146. Kim, K.Y.; Yun, J.M. Analysis of the Association between Health-Related and Work-Related Factors among Workers and Metabolic Syndrome Using Data from the Korean National Health and Nutrition Examination Survey (2016). *Nutrition Research and Practice* **2019**, *13*, 444, doi:10.4162/NRP.2019.13.5.444.

147. Canuto, R.; Garcez, A.S.; Olinto, M.T.A. Metabolic Syndrome and Shift Work: A Systematic Review. *Sleep Medicine Reviews* **2013**, *17*, 425–431, doi:10.1016/J.SMRV.2012.10.004.

148. Stoner, L.; Castro, N.; Signal, L.; Skidmore, P.; Faulkner, J.; Lark, S.; Williams, M.A.; Muller, Di.; Harrex, H. Sleep and Adiposity in Preadolescent Children: The Importance of Social Jetlag. *Childhood Obesity* **2018**, *14*, 158–164, doi:10.1089/CHI.2017.0272/ASSET/IMAGES/LARGE/FIGURE1.JPEG.

149. Stoner, L.; Beets, M.W.; Brazendale, K.; Moore, J.B.; Weaver, R.G. Social Jetlag Is Associated With Adiposity in Children. *Global Pediatric Health* **2018**, *5*, doi:10.1177/2333794X18816921.

150. Roenneberg, T.; Allebrandt, K. v.; Merrow, M.; Vetter, C. Social Jetlag and Obesity. *Curr Biol* **2012**, *22*, 939–943, doi:10.1016/J.CUB.2012.03.038.

151. Moreno, J.P.; Crowley, S.J.; Alfano, C.A.; Hannay, K.M.; Thompson, D.; Baranowski, T. Potential Circadian and Circannual Rhythm Contributions to the Obesity Epidemic in Elementary School Age Children. *International Journal of Behavioral Nutrition and Physical Activity* **2019**, *16*, 1–10, doi:10.1186/S12966-019-0784-7/FIGURES/1.

152. Zhu, B.; Chan, S.L.; Li, J.; Li, K.; Wu, H.; Cui, K.; Chen, H. Non-Alcoholic Steatohepatitis Pathogenesis, Diagnosis, and Treatment. *Frontiers in Cardiovascular Medicine* **2021**, *8*, doi:10.3389/FCVM.2021.742382/FULL.

153. Jorge-Galarza, E.; Medina-Urrutia, A.; Posadas-Sánchez, R.; Posadas-Romero, C.; Cardoso-Saldaña, G.; Vargas-Alarcón, G.; Caracas-Portilla, N.; González-Salazar, C.; Torres-Tamayo, M.; Juárez-Rojas, J.G. Adipose Tissue Dysfunction Increases Fatty Liver Association with Pre Diabetes and Newly Diagnosed Type 2 Diabetes Mellitus. *Diabetology and Metabolic Syndrome* **2016**, *8*, 1–8, doi:10.1186/S13098-016-0189-6/TABLES/3.

154. Li, L.; Liu, D.W.; Yan, H.Y.; Wang, Z.Y.; Zhao, S.H.; Wang, B. Obesity Is an Independent Risk Factor for Non-Alcoholic Fatty Liver Disease: Evidence from a Meta-Analysis of 21 Cohort Studies. *Obesity Reviews* **2016**, *17*, 510–519, doi:10.1111/OBR.12407.

155. Yilmaz, Y. NAFLD in the Absence of Metabolic Syndrome: Different Epidemiology, Pathogenetic Mechanisms, Risk Factors for Disease Progression? *Seminars in Liver Disease* **2012**, *32*, 14–21, doi:10.1055/S-0032-1306422/ID/JR00634-44.

156. Mendez-Sanchez, N.; Cruz-Ramon, V.C.; Ramirez-Perez, O.L.; Hwang, J.P.; Barranco-Fragoso, B.; Cordova-Gallardo, J. New Aspects of Lipotoxicity in Nonalcoholic Steatohepatitis. *International Journal of Molecular Sciences* **2018**, *19*, doi:10.3390/IJMS19072034.

157. Day, C.P.; James, O.F.W. Steatohepatitis: A Tale of Two "Hits"? *Gastroenterology* **1998**, *114*, 842–845, doi:10.1016/S0016-5085(98)70599-2.

158. Shoelson, S.E.; Lee, J.; Goldfine, A.B. Inflammation and Insulin Resistance. *The Journal of Clinical Investigation* **2006**, *116*, 1793–1801, doi:10.1172/JCI29069.

159. Postic, C.; Girard, J. Contribution of de Novo Fatty Acid Synthesis to Hepatic Steatosis and Insulin Resistance: Lessons from Genetically Engineered Mice. *J Clin Invest* **2008**, *118*, 829–838, doi:10.1172/JCI34275.

160. Lettéron, P.; Sutton, A.; Mansouri, A.; Fromenty, B.; Pessayre, D. Inhibition of Microsomal Triglyceride Transfer Protein: Another Mechanism for Drug-Induced Steatosis in Mice. *Hepatology* **2003**, *38*, 133–140, doi:10.1053/JHEP.2003.50309.

161. Buzzetti, E.; Pinzani, M.; Tsochatzis, E.A. The Multiple-Hit Pathogenesis of Non-Alcoholic Fatty Liver Disease (NAFLD). *Metabolism - Clinical and Experimental* **2016**, *65*, 1038–1048, doi:10.1016/J.METABOL.2015.12.012.

162. Wellen, K.E.; Hotamisligil, G.S. Inflammation, Stress, and Diabetes. *The Journal of Clinical Investigation* **2005**, *115*, 1111–1119, doi:10.1172/JCI25102.

163. Hotamisligil, G.S. Inflammation and Metabolic Disorders. *Nature 2006 444:7121* **2006**, *444*, 860–867, doi:10.1038/nature05485.

164. Cohen, J.C.; Horton, J.D.; Hobbs, H.H. Human Fatty Liver Disease: Old Questions and New Insights. *Science (1979)* **2011**, *332*, 1519–1523, doi:10.1126/SCIENCE.1204265.

165. Shetty, A.; Hsu, J.W.; Manka, P.P.; Syn, W.K. Role of the Circadian Clock in the Metabolic Syndrome and Nonalcoholic Fatty Liver Disease. *Digestive Diseases and Sciences* **2018**, *63*, 3187–3206, doi:10.1007/S10620-018-5242-X/FIGURES/2.

166. Zhang, D.; Tong, X.; Nelson, B.B.; Jin, E.; Sit, J.; Charney, N.; Yang, M.; Omary, M.B.; Yin, L. The Hepatic BMAL1/AKT/Lipogenesis Axis Protects against Alcoholic Liver Disease in Mice via Promoting PPARα Pathway. *Hepatology* **2018**, *68*, 883–896, doi:10.1002/HEP.29878/SUPPINFO.

167. Bugge, A.; Feng, D.; Everett, L.J.; Briggs, E.R.; Mullican, S.E.; Wang, F.; Jager, J.; Lazar, M.A. Rev-Erbα and Rev-Erbβ Coordinately Protect the Circadian Clock and Normal Metabolic Function. *Genes & Development* **2012**, *26*, 657–667, doi:10.1101/GAD.186858.112.

168. Chaix, A.; Lin, T.; Le, H.D.; Chang, M.W.; Panda, S. Time-Restricted Feeding Prevents Obesity and Metabolic Syndrome in Mice Lacking a Circadian Clock. *Cell Metabolism* **2019**, *29*, 303-319.e4, doi:10.1016/J.CMET.2018.08.004.

169. Montagner, A.; Polizzi, A.; Fouché, E.; Ducheix, S.; Lippi, Y.; Lasserre, F.; Barquissau, V.; Régnier, M.; Lukowicz, C.; Benhamed, F.; et al. Liver PPARα Is Crucial for Whole-Body Fatty Acid Homeostasis and Is Protective against NAFLD. *Gut* **2016**, *65*, 1202–1214, doi:10.1136/GUTJNL-2015-310798.

170. Ip, E.; Farrell, G.C.; Robertson, G.; Hall, P.; Kirsch, R.; Leclercq, I. Central Role of PPARalpha-Dependent Hepatic Lipid Turnover in Dietary Steatohepatitis in Mice. *Hepatology* **2003**, *38*, 123–132, doi:10.1053/JHEP.2003.50307.

171. Hsieh, M.C.; Yang, S.C.; Tseng, H.L.; Hwang, L.L.; Chen, C.T.; Shieh, K.R. Abnormal Expressions of Circadian-Clock and Circadian Clock-Controlled Genes in the Livers and Kidneys of Long-Term, High-Fat-Diet-Treated Mice. *Int J Obes (Lond)* **2010**, *34*, 227–239, doi:10.1038/IJO.2009.228.

172. Pagliassotti, M.J. Endoplasmic Reticulum Stress in Nonalcoholic Fatty Liver Disease. *http://dx.doi.org/10.1146/annurev-nutr-071811-150644* **2012**, *32*, 17–33, doi:10.1146/ANNUREV-NUTR-071811-150644.

173. Dara, L.; Ji, C.; Kaplowitz, N. The Contribution of Endoplasmic Reticulum Stress to Liver Diseases. *Hepatology* **2011**, *53*, 1752–1763, doi:10.1002/HEP.24279.

174. Kapoor, A.; Sanyal, A.J. Endoplasmic Reticulum Stress and the Unfolded Protein Response. *Clin Liver Dis* **2009**, *13*, 581–590, doi:10.1016/J.CLD.2009.07.004.

175. Schattenberg, J.M.; Singh, R.; Wang, Y.; Lefkowitch, J.H.; Rigoli, R.M.; Scherer, P.E.; Czaja, M.J. JNK1 but Not JNK2 Promotes the Development of Steatohepatitis in Mice. *Hepatology* **2006**, *43*, 163–172, doi:10.1002/HEP.20999.

176. Hetz, C. The Unfolded Protein Response: Controlling Cell Fate Decisions under ER Stress and Beyond. *Nature Reviews Molecular Cell Biology 2012 13:2* **2012**, *13*, 89–102, doi:10.1038/nrm3270.

177. Gonen, N.; Sabath, N.; Burge, C.B.; Shalgi, R. Widespread PERK-Dependent Repression of ER Targets in Response to ER Stress. *Scientific Reports 2019 9:1* **2019**, *9*, 1–12, doi:10.1038/s41598-019-38705-5.

178. Bartoszewska, S.; Collawn, J.F. Unfolded Protein Response (UPR) Integrated Signaling Networks Determine Cell Fate during Hypoxia. *Cellular & Molecular Biology Letters 2020 25:1* **2020**, *25*, 1–20, doi:10.1186/S11658-020-00212-1.

179. Li, M.; Baumeister, P.; Roy, B.; Phan, T.; Foti, D.; Luo, S.; Lee, A.S. ATF6 as a Transcription Activator of the Endoplasmic Reticulum Stress Element: Thapsigargin Stress-Induced Changes and Synergistic Interactions with NF-Y and YY1. *Molecular and Cellular Biology* **2000**, *20*, 5096, doi:10.1128/MCB.20.14.5096-5106.2000.

180. Johnston, B.P.; McCormick, C. Herpesviruses and the Unfolded Protein Response. *Viruses 2020, Vol. 12, Page 17* **2019**, *12*, 17, doi:10.3390/V12010017.

181. Cretenet, G.; le Clech, M.; Gachon, F. Circadian Clock-Coordinated 12 Hr Period Rhythmic Activation of the IRE1α Pathway Controls Lipid Metabolism in Mouse Liver. *Cell Metabolism* **2010**, *11*, 47–57, doi:10.1016/J.CMET.2009.11.002/ATTACHMENT/9214E6C7-B91F-4D88-954C-9CE8C6BA95E7/MMC1.PDF.

182. Senft, D.; Ronai, Z.A. UPR, Autophagy, and Mitochondria Crosstalk Underlies the ER Stress Response. *Trends in Biochemical Sciences* **2015**, *40*, 141–148, doi:10.1016/J.TIBS.2015.01.002.

183. Saini, R.K.; Keum, Y.S. Omega-3 and Omega-6 Polyunsaturated Fatty Acids: Dietary Sources, Metabolism, and Significance — A Review. *Life Sciences* **2018**, *203*, 255–267, doi:10.1016/J.LFS.2018.04.049.

184. Bril, F.; Cusi, K. Management of Nonalcoholic Fatty Liver Disease in Patients With Type 2 Diabetes: A Call to Action. *Diabetes Care* **2017**, *40*, 419–430, doi:10.2337/DC16-1787.

185. Vasam, G.; Reid, K.; Burelle, Y.; Menzies, K.J. Nutritional Regulation of Mitochondrial Function. *Mitochondria in Obesity and Type 2 Diabetes: Comprehensive Review on Mitochondrial Functioning and Involvement in Metabolic Diseases* **2019**, 93–126, doi:10.1016/B978-0-12-811752-1.00004-3.

186. Nassir, F.; Ibdah, J.A. Role of Mitochondria in Nonalcoholic Fatty Liver Disease. *International Journal of Molecular Sciences* **2014**, *15*, 8713, doi:10.3390/IJMS15058713.

187. Putti, R.; Sica, R.; Migliaccio, V.; Lionetti, L. Diet Impact on Mitochondrial Bioenergetics and Dynamics. *Frontiers in Physiology* **2015**, *6*, 109, doi:10.3389/FPHYS.2015.00109/BIBTEX.

188. Waldhart, A.N.; Muhire, B.; Johnson, B.; Pettinga, D.; Madaj, Z.B.; Wolfrum, E.; Dykstra, H.; Wegert, V.; Pospisilik, J.A.; Han, X.; et al. Excess Dietary Carbohydrate Affects Mitochondrial Integrity as Observed in Brown Adipose Tissue. *Cell Rep* **2021**, *36*, 109488, doi:10.1016/J.CELREP.2021.109488.

189. Longo, M.; Meroni, M.; Paolini, E.; Macchi, C.; Dongiovanni, P. Mitochondrial Dynamics and Nonalcoholic Fatty Liver Disease (NAFLD): New Perspectives for a Fairy-Tale Ending? *Metabolism - Clinical and Experimental* **2021**, *117*, doi:10.1016/J.METABOL.2021.154708.

190. Zhang, Z.; Li, T.E.; Chen, M.; Xu, D.; Zhu, Y.; Hu, B.Y.; Lin, Z.F.; Pan, J.J.; Wang, X.; Wu, C.; et al. MFN1-Dependent Alteration of Mitochondrial Dynamics Drives Hepatocellular Carcinoma Metastasis by Glucose Metabolic Reprogramming. *British Journal of Cancer 2019 122:2* **2019**, *122*, 209–220, doi:10.1038/s41416-019-0658-4.

191. Manach, C.; Scalbert, A.; Morand, C.; Rémésy, C.; Jiménez, L. Polyphenols: Food Sources and Bioavailability. *The American Journal of Clinical Nutrition* **2004**, *79*, 727–747, doi:10.1093/AJCN/79.5.727.

192. Ebel, J.; Hahlbrock, K. Biosynthesis BT - The Flavonoids: Advances in Research. *The Flavonoids* **1982**, 641–679.

193. Han, X.; Shen, T.; Lou, H. Dietary Polyphenols and Their Biological Significance. *International Journal of Molecular Sciences 2007, Vol. 8, Pages 950-988* **2007**, *8*, 950–988, doi:10.3390/I8090950.

194. del Rio, D.; Rodriguez-Mateos, A.; Spencer, J.P.E.; Tognolini, M.; Borges, G.; Crozier, A. Dietary (Poly)Phenolics in Human Health: Structures, Bioavailability, and Evidence of Protective Effects against Chronic Diseases. *Antioxidants and Redox Signaling* **2013**, *18*, 1818–1892, doi:10.1089/ARS.2012.4581/ASSET/IMAGES/LARGE/FIGURE41.JPEG.

195. Pereira, D.M.; Valentão, P.; Pereira, J.A.; Andrade, P.B. Phenolics: From Chemistry to Biology. *Molecules* **2009**, *14*, 2202, doi:10.3390/MOLECULES14062202.

196. Rauf, A.; Imran, M.; Abu-Izneid, T.; Iahtisham-Ul-Haq; Patel, S.; Pan, X.; Naz, S.; Sanches Silva, A.; Saeed, F.; Rasul Suleria, H.A. Proanthocyanidins: A Comprehensive Review. *Biomedicine & pharmacotherapy = Biomedecine & pharmacotherapie* **2019**, *116*, doi:10.1016/J.BIOPHA.2019.108999.

197. Manach, C.; Scalbert, A.; Morand, C.; Rémésy, C.; Jiménez, L. Polyphenols: Food Sources and Bioavailability. *Am J Clin Nutr* **2004**, *79*, 727–747, doi:10.1093/AJCN/79.5.727.

198. Aron, P.M.; Kennedy, J.A. Flavan-3-Ols: Nature, Occurrence and Biological Activity. *Molecular Nutrition & Food Research* **2008**, *52*, 79–104, doi:10.1002/MNFR.200700137.

199. Cory, H.; Passarelli, S.; Szeto, J.; Tamez, M.; Mattei, J. The Role of Polyphenols in Human Health and Food Systems: A Mini-Review. *Frontiers in Nutrition* **2018**, *5*, 87, doi:10.3389/FNUT.2018.00087.

200. Manchope, M.F.; Ferraz, C.R.; Borghi, S.M.; Rasquel-Oliveira, F.S.; Franciosi, A.; Bagatim-Souza, J.; Dionisio, A.M.; Casagrande, R.; Verri, W.A. Therapeutic Role of Naringenin to Alleviate Inflammatory Pain. *Treatments, Mechanisms, and Adverse Reactions of Anesthetics and Analgesics* **2022**, 443–455, doi:10.1016/B978-0-12-820237-1.00038-7.

201. Hertog, M.G.L.; Hollman, P.C.H.; Hertog, M.G.L.; Katan, M.B. Content of Potentially Anticarcinogenic Flavonoids of 28 Vegetables and 9 Fruits Commonly Consumed in the Netherlands. *Journal of Agricultural and Food Chemistry* **1992**, *40*, 2379–2383, doi:10.1021/JF00024A011/ASSET/JF00024A011.FP.PNG_V03.

202. Hertog, M.G.L.; Hollman, P.C.H.; van de Putte, B. Content of Potentially Anticarcinogenic Flavonoids of Tea Infusions, Wines, and Fruit Juices. *Journal of Agricultural and Food Chemistry* **1993**, *41*, 1242–1246, doi:10.1021/JF00032A015/ASSET/JF00032A015.FP.PNG_V03.

203. Jiang, N.; Doseff, A.I.; Grotewold, E. Flavones: From Biosynthesis to Health Benefits. *Plants* **2016**, *5*, 1–1256, doi:10.3390/PLANTS5020027.

204. Setchell, K.D.R.; Brown, N.M.; Lydeking-Olsen, E. The Clinical Importance of the Metabolite Equol—A Clue to the Effectiveness of Soy and Its

Isoflavones. *The Journal of Nutrition* **2002**, *132*, 3577–3584, doi:10.1093/JN/132.12.3577.

205. Prior, R.L.; Wu, X. Anthocyanins: Structural Characteristics That Result in Unique Metabolic Patterns and Biological Activities. *http://dx.doi.org/10.1080/10715760600758522* **2009**, *40*, 1014–1028, doi:10.1080/10715760600758522.

206. Ignat, I.; Volf, I.; Popa, V.I. A Critical Review of Methods for Characterisation of Polyphenolic Compounds in Fruits and Vegetables. *Food Chemistry* **2011**, *126*, 1821–1835, doi:10.1016/J.FOODCHEM.2010.12.026.

207. Berman, A.Y.; Motechin, R.A.; Wiesenfeld, M.Y.; Holz, M.K. The Therapeutic Potential of Resveratrol: A Review of Clinical Trials. *npj Precision Oncology 2017 1:1* **2017**, *1*, 1–9, doi:10.1038/s41698-017-0038-6.

208. Durazzo, A.; Lucarini, M.; Souto, E.B.; Cicala, C.; Caiazzo, E.; Izzo, A.A.; Novellino, E.; Santini, A. Polyphenols: A Concise Overview on the Chemistry, Occurrence, and Human Health. *Phytotherapy Research* **2019**, *33*, 2221–2243, doi:10.1002/PTR.6419.

209. Gutierrez-Orozco, F.; Failla, M.L. Biological Activities and Bioavailability of Mangosteen Xanthones: A Critical Review of the Current Evidence. *Nutrients* **2013**, *5*, 3163–3183, doi:10.3390/NU5083163.

210. Favero, A.; Parpinel, M.; Franceschi, S. Diet and Risk of Breast Cancer: Major Findings from an Italian Case-Control Study. *Biomedicine & Pharmacotherapy* **1998**, *52*, 109–115, doi:10.1016/S0753-3322(98)80088-7.

211. Russell, W.R.; Labat, A.; Scobbie, L.; Duncan, S.H. Availability of Blueberry Phenolics for Microbial Metabolism in the Colon and the Potential Inflammatory Implications. *Molecular Nutrition & Food Research* **2007**, *51*, 726–731, doi:10.1002/MNFR.200700022.

212. Bolling, B.W.; Chen, C.Y.O.; McKay, D.L.; Blumberg, J.B. Tree Nut Phytochemicals: Composition, Antioxidant Capacity, Bioactivity, Impact Factors. A Systematic Review of Almonds, Brazils, Cashews, Hazelnuts, Macadamias, Pecans, Pine Nuts, Pistachios and Walnuts. *Nutrition Research Reviews* **2011**, *24*, 244–275, doi:10.1017/S095442241100014X.

213. Buijsse, B.; Weikert, C.; Drogan, D.; Bergmann, M.; Boeing, H. Chocolate Consumption in Relation to Blood Pressure and Risk of Cardiovascular Disease in German Adults. *European Heart Journal* **2010**, *31*, 1616–1623, doi:10.1093/EURHEARTJ/EHQ068.

214. He, F.J.; Nowson, C.A.; Lucas, M.; MacGregor, G.A. Increased Consumption of Fruit and Vegetables Is Related to a Reduced Risk of Coronary Heart Disease: Meta-Analysis of Cohort Studies. *Journal of Human Hypertension 2007 21:9* **2007**, *21*, 717–728, doi:10.1038/sj.jhh.1002212.

215. Dauchet, L.; Amouyel, P.; Hercberg, S.; Dallongeville, J. Fruit and Vegetable Consumption and Risk of Coronary Heart Disease: A Meta-Analysis of Cohort Studies. *J Nutr* **2006**, *136*, 2588–2593, doi:10.1093/JN/136.10.2588.

216. Dai, Q.; Borenstein, A.R.; Wu, Y.; Jackson, J.C.; Larson, E.B. Fruit and Vegetable Juices and Alzheimer's Disease: The Kame Project. *The American Journal of Medicine* **2006**, *119*, 751–759, doi:10.1016/J.AMJMED.2006.03.045.

217. Letenneur, L.; Proust-Lima, C.; le Gouge, A.; Dartigues, J.F.; Barberger-Gateau, P. Flavonoid Intake and Cognitive Decline over a 10-Year Period. *American Journal of Epidemiology* **2007**, *165*, 1364–1371, doi:10.1093/AJE/KWM036.

218. Anhê, F.F.; Desjardins, Y.; Pilon, G.; Dudonné, S.; Genovese, M.I.; Lajolo, F.M.; Marette, A. Polyphenols and Type 2 Diabetes: A Prospective Review. *PharmaNutrition* **2013**, *1*, 105–114, doi:10.1016/J.PHANU.2013.07.004.

219. Suliga, E.; Kozieł, D.; Cieśla, E.; Rębak, D.; Głuszek, S. Coffee Consumption and the Occurrence and Intensity of Metabolic Syndrome: A Cross-Sectional Study. *http://dx.doi.org/10.1080/09637486.2016.1256381* **2016**, *68*, 507–513, doi:10.1080/09637486.2016.1256381.

220. Yamagata, K. Metabolic Syndrome: Preventive Effects of Dietary Flavonoids. *Studies in Natural Products Chemistry* **2019**, *60*, 1–28, doi:10.1016/B978-0-444-64181-6.00001-2.

221. Neri-Numa, I.A.; Cazarin, C.B.B.; Ruiz, A.L.T.G.; Paulino, B.N.; Molina, G.; Pastore, G.M. Targeting Flavonoids on Modulation of Metabolic Syndrome. *Journal of Functional Foods* **2020**, *73*, doi:10.1016/J.JFF.2020.104132.

222. Fujii, K.; Ota, Y.; Nishiyama, K.; Kunitake, H.; Yamasaki, Y.; Tari, H.; Araki, K.; Arakawa, T.; Yamasaki, M. Blueberry Leaf Polyphenols Prevent Body Fat Accumulation in Mice Fed High-Fat, High-Sucrose Diet. *Journal of Oleo Science* **2019**, *68*, 471–479, doi:10.5650/JOS.ESS18226.

223. Gil-Cardoso, K.; Ginés, I.; Pinent, M.; Ardévol, A.; Arola, L.; Blay, M.; Terra, X. Chronic Supplementation with Dietary Proanthocyanidins Protects from Diet-Induced Intestinal Alterations in Obese Rats. *Molecular Nutrition and Food Research* **2017**, *61*, doi:10.1002/MNFR.201601039.

224. Bas, J.M. del; Ricketts, M.L.; Vaqué, M.; Sala, E.; Quesada, H.; Ardevol, A.; Salvadó, M.J.; Blay, M.; Arola, L.; Moore, D.D.; et al. Dietary Procyanidins Enhance Transcriptional Activity of Bile Acid-Activated FXR in Vitro and Reduce Triglyceridemia in Vivo in a FXR-Dependent Manner. *Molecular Nutrition and Food Research* **2009**, *53*, 805–814, doi:10.1002/MNFR.200800364.

225. Gonzalez-Abuin, N.; Pinent, M.; Casanova-Marti, A.; Arola, L.; Blay, M.; Ardevol, A. Procyanidins and Their Healthy Protective Effects Against Type 2 Diabetes. *Current Medicinal Chemistry* **2014**, *22*, 39–50, doi:10.2174/0929867321666140916115519.

226. Bertoia, M.L.; Rimm, E.B.; Mukamal, K.J.; Hu, F.B.; Willett, W.C.; Cassidy, A. Dietary Flavonoid Intake and Weight Maintenance: Three Prospective Cohorts of 124 086 US Men and Women Followed for up to 24 Years. *BMJ* **2016**, *352*, doi:10.1136/BMJ.I17.

227. Marranzano, M.; Ray, S.; Godos, J.; Galvano, F. Association between Dietary Flavonoids Intake and Obesity in a Cohort of Adults Living in the Mediterranean Area. *International Journal of Food Sciences and Nutrition*

2018, *69*, 1020–1029, doi:10.1080/09637486.2018.1452900/SUPPL_FILE/IIJF_A_1452900_SM6769.PDF.

228. Rufino, A.T.; Costa, V.M.; Carvalho, F.; Fernandes, E. Flavonoids as Antiobesity Agents: A Review. *Medicinal Research Reviews* **2021**, *41*, 556–585, doi:10.1002/MED.21740.

229. Tokunaga, S.; White, I.R.; Frost, C.; Tanaka, K.; Kono, S.; Tokudome, S.; Akamatsu, T.; Moriyama, T.; Zakouji, H. Green Tea Consumption and Serum Lipids and Lipoproteins in a Population of Healthy Workers in Japan. *Annals of Epidemiology* **2002**, *12*, 157–165, doi:10.1016/S1047-2797(01)00307-6.

230. Li, G.; Zhu, Y.; Zhang, Y.; Lang, J.; Chen, Y.; Ling, W. Estimated Daily Flavonoid and Stilbene Intake from Fruits, Vegetables, and Nuts and Associations with Lipid Profiles in Chinese Adults. *J Acad Nutr Diet* **2013**, *113*, 786–794, doi:10.1016/J.JAND.2013.01.018.

231. Aviram, M. Flavonoids-Rich Nutrients with Potent Antioxidant Activity Prevent Atherosclerosis Development: The Licorice Example. *International Congress Series* **2004**, *1262*, 320–327, doi:10.1016/S0531-5131(03)01453-5.

232. Bondonno, N.P.; Murray, K.; Bondonno, C.P.; Lewis, J.R.; Croft, K.D.; Kyrø, C.; Gislason, G.; Tjønneland, A.; Scalbert, A.; Cassidy, A.; et al. Flavonoid Intake and Its Association with Atrial Fibrillation. *Clinical Nutrition* **2020**, *39*, 3821–3828, doi:10.1016/J.CLNU.2020.04.025.

233. Perez-Vizcaino, F.; Fraga, C.G. Research Trends in Flavonoids and Health. *Archives of Biochemistry and Biophysics* **2018**, *646*, 107–112, doi:10.1016/J.ABB.2018.03.022.

234. Fraga, C.G.; Croft, K.D.; Kennedy, D.O.; Tomás-Barberán, F.A. The Effects of Polyphenols and Other Bioactives on Human Health. *Food & Function* **2019**, *10*, 514–528, doi:10.1039/C8FO01997E.

235. Cassidy, A.; O'Reilly, É.J.; Kay, C.; Sampson, L.; Franz, M.; Forman, J.P.; Curhan, G.; Rimm, E.B. Habitual Intake of Flavonoid Subclasses and Incident Hypertension in Adults. *The American Journal of Clinical Nutrition* **2011**, *93*, 338–347, doi:10.3945/AJCN.110.006783.

236. Testai, L.; Piragine, E.; Piano, I.; Flori, L.; da Pozzo, E.; Miragliotta, V.; Pirone, A.; Citi, V.; di Cesare Mannelli, L.; Brogi, S.; et al. The Citrus Flavonoid Naringenin Protects the Myocardium from Ageing-Dependent Dysfunction: Potential Role of SIRT1. *Oxidative Medicine and Cellular Longevity* **2020**, *2020*, doi:10.1155/2020/4650207.

237. Novotny, J.A.; Baer, D.J.; Khoo, C.; Gebauer, S.K.; Charron, C.S. Cranberry Juice Consumption Lowers Markers of Cardiometabolic Risk, Including Blood Pressure and Circulating C-Reactive Protein, Triglyceride, and Glucose Concentrations in Adults. *The Journal of Nutrition* **2015**, *145*, 1185–1193, doi:10.3945/JN.114.203190.

238. Johnson, S.A.; Navaei, N.; Pourafshar, S.; Jaime, S.J.; Akhavan, N.S.; Alvarez-Alvarado, S.; Proaño, G. v.; Litwin, N.S.; Clark, E.A.; Foley, E.M.; et al. Effects of Montmorency Tart Cherry Juice Consumption on Cardiometabolic

Biomarkers in Adults with Metabolic Syndrome: A Randomized Controlled Pilot Trial. *https://home.liebertpub.com/jmf* **2020**, *23*, 1238–1247, doi:10.1089/JMF.2019.0240.

239. Saeedi, P.; Petersohn, I.; Salpea, P.; Malanda, B.; Karuranga, S.; Unwin, N.; Colagiuri, S.; Guariguata, L.; Motala, A.A.; Ogurtsova, K.; et al. Global and Regional Diabetes Prevalence Estimates for 2019 and Projections for 2030 and 2045: Results from the International Diabetes Federation Diabetes Atlas, 9 Th Edition. *Diabetes Res Clin Pract* **2019**, *157*, doi:10.1016/J.DIABRES.2019.107843.

240. Ahmed, A.; Lager, A.; Fredlund, P.; Elinder, L.S. fer Consumption of Fruit and Vegetables and the Risk of Type 2 Diabetes: A 4-Year Longitudinal Study among Swedish Adults. *Journal of Nutritional Science* **2020**, *9*, doi:10.1017/JNS.2020.7.

241. Alperet, D.J.; Butler, L.M.; Koh, W.P.; Yuan, J.M.; van Dam, R.M. Influence of Temperate, Subtropical, and Tropical Fruit Consumption on Risk of Type 2 Diabetes in an Asian Population. *The American Journal of Clinical Nutrition* **2017**, *105*, 736–745, doi:10.3945/AJCN.116.147090.

242. Alkhalidy, H.; Wang, Y.; Liu, D. Dietary Flavonoids in the Prevention of T2D: An Overview. *Nutrients* **2018**, *10*, doi:10.3390/NU10040438.

243. Barik, S.K.; Russell, W.R.; Moar, K.M.; Cruickshank, M.; Scobbie, L.; Duncan, G.; Hoggard, N. The Anthocyanins in Black Currants Regulate Postprandial Hyperglycaemia Primarily by Inhibiting α-Glucosidase While Other Phenolics Modulate Salivary α-Amylase, Glucose Uptake and Sugar Transporters. *The Journal of Nutritional Biochemistry* **2020**, *78*, 108325, doi:10.1016/J.JNUTBIO.2019.108325.

244. Chen, Z.; Li, W.; Guo, Q.; Xu, L.; Santhanam, R.K.; Gao, X.; Chen, Y.; Wang, C.; Panichayupakaranant, P.; Chen, H. Anthocyanins from Dietary Black Soybean Potentiate Glucose Uptake in L6 Rat Skeletal Muscle Cells via Up-Regulating Phosphorylated Akt and GLUT4. *Journal of Functional Foods* **2019**, *52*, 663–669, doi:10.1016/J.JFF.2018.11.049.

245. Choi, K.H.; Lee, H.A.; Park, M.H.; Han, J.S. Cyanidin-3-Rutinoside Increases Glucose Uptake by Activating the PI3K/Akt Pathway in 3T3-L1 Adipocytes. *Environmental Toxicology and Pharmacology* **2017**, *54*, 1–6, doi:10.1016/J.ETAP.2017.06.007.

246. Parhiz, H.; Roohbakhsh, A.; Soltani, F.; Rezaee, R.; Iranshahi, M. Antioxidant and Anti-Inflammatory Properties of the Citrus Flavonoids Hesperidin and Hesperetin: An Updated Review of Their Molecular Mechanisms and Experimental Models. *Phytotherapy Research* **2015**, *29*, 323–331, doi:10.1002/PTR.5256.

247. Barth, S.W.; Koch, T.C.L.; Watzl, B.; Dietrich, H.; Will, F.; Bub, A. Moderate Effects of Apple Juice Consumption on Obesity-Related Markers in Obese Men: Impact of Diet-Gene Interaction on Body Fat Content. *European Journal of Nutrition* **2012**, *51*, 841–850, doi:10.1007/S00394-011-0264-6/FIGURES/2.

248. Quesada, H.; del Bas, J.M.; Pajuelo, D.; Díaz, S.; Fernandez-Larrea, J.; Pinent, M.; Arola, L.; Salvadó, M.J.; Bladé, C. Grape Seed Proanthocyanidins Correct

Dyslipidemia Associated with a High-Fat Diet in Rats and Repress Genes Controlling Lipogenesis and VLDL Assembling in Liver. *International Journal of Obesity 2009 33:9* **2009**, *33*, 1007–1012, doi:10.1038/ijo.2009.136.

249. Castell-Auví, A.; Cedó, L.; Pallarès, V.; Blay, M.; Pinent, M.; Ardévol, A. Grape Seed Procyanidins Improve β-Cell Functionality under Lipotoxic Conditions Due to Their Lipid-Lowering Effect. *The Journal of Nutritional Biochemistry* **2013**, *24*, 948–953, doi:10.1016/J.JNUTBIO.2012.06.015.

250. Baselga-Escudero, L.; Arola-Arnal, A.; Pascual-Serrano, A.; Ribas-Latre, A.; Casanova, E.; Salvadó, M.J.; Arola, L.; Blade, C. Chronic Administration of Proanthocyanidins or Docosahexaenoic Acid Reversess the Increase of MiR-33a and MiR-122 in Dyslipidemic Obese Rats. *PLOS ONE* **2013**, *8*, e69817, doi:10.1371/JOURNAL.PONE.0069817.

251. Baselga-Escudero, L.; Bladé, C.; Ribas-Latre, A.; Casanova, E.; Salvadó, M.J.; Arola, L.; Arola-Arnal, A. Grape Seed Proanthocyanidins Repress the Hepatic Lipid Regulators MiR-33 and MiR-122 in Rats. *Molecular Nutrition and Food Research* **2012**, *56*, 1636–1646, doi:10.1002/MNFR.201200237.

252. Baselga-Escudero, L.; Blade, C.; Ribas-Latre, A.; Casanova, E.; Salvadó, M.J.; Arola, L.; Arola-Arnal, A. Chronic Supplementation of Proanthocyanidins Reduces Postprandial Lipemia and Liver MiR-33a and MiR-122 Levels in a Dose-Dependent Manner in Healthy Rats. *Journal of Nutritional Biochemistry* **2014**, *25*, 151–156, doi:10.1016/J.JNUTBIO.2013.09.014.

253. Pons, Z.; Margalef, M.; Bravo, F.I.; Arola-Arnal, A.; Muguerza, B. Chronic Administration of Grape-Seed Polyphenols Attenuates the Development of Hypertension and Improves Other Cardiometabolic Risk Factors Associated with the Metabolic Syndrome in Cafeteria Diet-Fed Rats. *British Journal of Nutrition* **2017**, *117*, 200–208, doi:10.1017/S0007114516004426.

254. Pinent, M.; Cedó, L.; Montagut, G.; Blay, M.; Ardévol, A. Procyanidins Improve Some Disrupted Glucose Homoeostatic Situations: An Analysis of Doses and Treatments According to Different Animal Models. *http://dx.doi.org/10.1080/10408398.2010.501533* **2012**, *52*, 569–584, doi:10.1080/10408398.2010.501533.

255. Yamashita, Y.; Okabe, M.; Natsume, M.; Ashida, H. Prevention Mechanisms of Glucose Intolerance and Obesity by Cacao Liquor Procyanidin Extract in High-Fat Diet-Fed C57BL/6 Mice. *Archives of Biochemistry and Biophysics* **2012**, *527*, 95–104, doi:10.1016/J.ABB.2012.03.018.

256. Kanamoto, Y.; Yamashita, Y.; Nanba, F.; Yoshida, T.; Tsuda, T.; Fukuda, I.; Nakamura-Tsuruta, S.; Ashida, H. A Black Soybean Seed Coat Extract Prevents Obesity and Glucose Intolerance by Up-Regulating Uncoupling Proteins and Down-Regulating Inflammatory Cytokines in High-Fat Diet-Fed Mice. *Journal of Agricultural and Food Chemistry* **2011**, *59*, 8985–8993, doi:10.1021/JF201471P.

257. Pascual-Serrano, A.; Bladé, C.; Suárez, M.; Arola-Arnal, A. Grape Seed Proanthocyanidins Improve White Adipose Tissue Expansion during Diet-Induced Obesity Development in Rats. *International Journal of Molecular*

Sciences 2018, Vol. 19, Page 2632 **2018**, *19*, 2632, doi:10.3390/IJMS19092632.

258. Colom-Pellicer, M.; Rodríguez, R.M.; Navarro-Masip, È.; Bravo, F.I.; Mulero, M.; Arola, L.; Aragonès, G. Time-of-Day Dependent Effect of Proanthocyanidins on Adipose Tissue Metabolism in Rats with Diet-Induced Obesity. *Int J Obes (Lond)* **2022**, doi:10.1038/S41366-022-01132-0.

259. Casanova, E.; Baselga-Escudero, L.; Ribas-Latre, A.; Arola-Arnal, A.; Bladé, C.; Arola, L.; Salvadó, M.J. Omega-3 Polyunsaturated Fatty Acids and Proanthocyanidins Improve Postprandial Metabolic Flexibility in Rat. *BioFactors* **2014**, *40*, 146–156, doi:10.1002/BIOF.1129.

260. Terra, X.; Montagut, G.; Bustos, M.; Llopiz, N.; Ardèvol, A.; Bladé, C.; Fernández-Larrea, J.; Pujadas, G.; Salvadó, J.; Arola, L.; et al. Grape-Seed Procyanidins Prevent Low-Grade Inflammation by Modulating Cytokine Expression in Rats Fed a High-Fat Diet. *The Journal of Nutritional Biochemistry* **2009**, *20*, 210–218, doi:10.1016/J.JNUTBIO.2008.02.005.

261. Foretz, M.; Even, P.C.; Viollet, B. AMPK Activation Reduces Hepatic Lipid Content by Increasing Fat Oxidation In Vivo. *International Journal of Molecular Sciences 2018, Vol. 19, Page 2826* **2018**, *19*, 2826, doi:10.3390/IJMS19092826.

262. Casanova, E.; Baselga-Escudero, L.; Ribas-Latre, A.; Cedó, L.; Arola-Arnal, A.; Pinent, M.; Bladé, C.; Arola, L.; Salvadó, M.J. Chronic Intake of Proanthocyanidins and Docosahexaenoic Acid Improves Skeletal Muscle Oxidative Capacity in Diet-Obese Rats. *The Journal of Nutritional Biochemistry* **2014**, *25*, 1003–1010, doi:10.1016/J.JNUTBIO.2014.05.003.

263. Ribas-Latre, A.; del Bas, J.M.; Baselga-Escudero, L.; Casanova, E.; Arola-Arnal, A.; Salvadó, M.J.; Arola, L.; Bladé, C. Dietary Proanthocyanidins Modulate Melatonin Levels in Plasma and the Expression Pattern of Clock Genes in the Hypothalamus of Rats. *Molecular Nutrition & Food Research* **2015**, *59*, 865–878, doi:10.1002/MNFR.201400571.

264. Ribas-Latre, A.; del Bas, J.M.; Baselga-Escudero, L.; Casanova, E.; Arola-Arnal, A.; Salvadó, M.J.; Bladé, C.; Arola, L. Dietary Proanthocyanidins Modulate the Rhythm of BMAL1 Expression and Induce RORα Transactivation in HepG2 Cells. *Journal of Functional Foods* **2015**, *13*, 336–344, doi:10.1016/j.jff.2015.01.017.

265. Ribas-Latre, A.; Baselga-Escudero, L.; Casanova, E.; Arola-Arnal, A.; Salvadó, M.-J.; Bladé, C.; Arola, L. Dietary Proanthocyanidins Modulate BMAL1 Acetylation, Nampt Expression and NAD Levels in Rat Liver OPEN. *Nature Publishing Group* **2015**, *5*, 10954, doi:10.1038/srep10954.

266. Ribas-Latre, A.; Baselga-Escudero, L.; Casanova, E.; Arola-Arnal, A.; Salvadó, M.J.; Arola, L.; Bladé, C. Chronic Consumption of Dietary Proanthocyanidins Modulates Peripheral Clocks in Healthy and Obese Rats. *The Journal of Nutritional Biochemistry* **2015**, *26*, 112–119, doi:10.1016/J.JNUTBIO.2014.09.006.

II. HYPOTHESIS AND OBJECTIVES

UNIVERSITAT ROVIRA I VIRGILI
THE INFLUENCE OF BIOLOGICAL RHYTHMS ON THE BENEFICIAL EFFECTS OF GRAPE SEED PROANTHOCYANIDIN EXTRACT (GSPE) ON LIVER METABOLISM IN HEALTH AND DISEASE
Romina Mariel Rodriguez

HYPOTHESIS AND OBJECTIVES

Metabolic syndrome (MS) is a cluster of metabolic related diseases that include dyslipidemia, hypertension, insulin resistance and obesity. In addition to all the metabolic disorders associated with obesity, excessive energy intake hugely contributes to the development of nonalcoholic fatty liver disease (NAFLD), a condition in which excess fat accumulates in the liver.

Growing evidence has demonstrated the strong relationship between nutrition and circadian rhythms, and its association with health and disease. The main function of circadian clocks is to allow organisms to anticipate daily changes in their environment in a way that the body foresees the sleep and activity periods; nevertheless, clocks can be also helpful in organizing internal metabolic processes. In this regard, peripheral clocks are known to be responsible for daily rhythm of metabolism. As the liver is a central organ in metabolic control, the hepatic clock is a main regulator of liver glucose and lipid metabolism. The generation and maintenance of these rhythms largely depends on the interaction between the circadian clock and external cues, such as light and food (feeding time and meal quality). In modern times, several human behaviors and activities often interfere with these metabolic rhythms. Disruptions in the circadian system can lead to disturbances in metabolism and energy homeostasis that contribute to or worsen the development of different pathologies such as MS and NAFLD.

In recent decades, polyphenols, and especially flavonoids, have been investigated as a tool for fighting against obesity-related diseases. Proanthocyanidins are the most widely consumed flavonoid class due to their ubiquity in foodstuffs. In particular, grape seed procyanidin extract (GSPE) has proven to exert anti-obesity properties mitigating inflammatory responses, improving dyslipidemia and insulin resistance, among other effects. Furthermore, mitochondria also appear to play a crucial role in

mediating the health effects of this compound. Additionally, mitochondrial function and dynamics are strongly influenced by the circadian clock. In this sense, GSPE may act as a possible modulator of circadian rhythms, improving the obesity-related clock disruption, helping to ameliorate the quality of life of overweight subjects.

Thus, considering all the previous information, the work gathered in this doctoral thesis, which has been carried out in the Nutrigenomics Research Group, is mainly focused on studying the interactions of the circadian and seasonal rhythms with the effectiveness of bioactive compounds related to health. In this regard, **we hypothesize that biological rhythms can modulate the potential beneficial effects of dietary consumption of proanthocyanidins, and more precisely GSPE, on the glucose and lipid liver metabolism.** In other words, dietary consumption of GSPE, will produce different hepatic metabolic responses depending on the time-of-day and time-of-year administration.

Therefore, **the main objective of this thesis was to assess whether there is a time of day-dependent and season-dependent beneficial effect of GSPE consumption on liver metabolism, particularly in an NAFLD context.**

To achieve this general purpose, specific objectives were proposed:

1. **To determine the impact of the timing of GSPE administration on the hepatic circadian clock in relationship with mitochondrial function in an obesogenic context (Manuscript 1).**

To fulfill this first objective and determine whether GSPE effectiveness in the liver is impacted by the timing of administration we designed an experimental animal study in which rats were fed with standard chow (STD) or cafeteria (CAF) diet for 9 weeks and were treated with vehicle (VH) or GSPE at the beginning of the light period (ZT0) or at the beginning of the dark period (ZT12). Rats were sacrificed at different times of the day (ZT1, ZT7, ZT13 and ZT19) in order to generate the circadian profile. We carried

out analysis of hepatic clock genes and mitochondrial dynamic gene expressions together with the evaluation of mitochondrial respiratory complex activities and metabolites involved in Krebs cycle.

2. **To determine how an obesity-inducing diet affects the rhythm of hepatic lipid and carbohydrate metabolism and to observe whether there is any time-dependent restorative effect of GSPE administration (Manuscript 2).**

To develop this objective, we used the same experimental design explained above, but focused our study on the rhythms of key metabolic genes together with the evaluation of lipid liver profile and metabolomic analysis by focusing on main liver metabolic pathways that play a pivotal role in NAFLD development.

3. **To determine the role of (+)-catechin and (-)-epicatechin, two of the main phenolic components of GSPE, on its hepatic clock-synchronizing and metabolic improvement effects against NAFLD (Manuscript 2).**

To achieve this objective, we used a hepatocyte derived AML12 cell line that has been stably transfected by a luciferase gene driven by the *Bmal1* promoter and treated the cells with palmitic acid (NALFD *in vitro* model) and (+)-catechin and (-)-epicatechin. We measured the circadian rhythm luminescence expression driven by *Bmal1* using the LumiCycle luminometer equipment. In addition, we analyzed mRNA expression of genes related to lipid and glucose metabolism.

4. **To determine the impact of seasonal variations on GSPE consumption over the hepatic circadian clock and liver metabolism of healthy rats (Manuscript 3).**

To fulfill this objective, photoperiod-sensitive rats were subjected to STD diet and chronically exposed to three photoperiods (L12, L18 and L6) to mimic the day length of different seasons. Rats were treated either with

GSPE or VH and we further carried out biochemical, mRNA, protein, metabolomic and hepatic lipids assays to assess whether seasonal adaptations can influence GSPE molecular effect on liver metabolism in heathy rats.

5. **To determine the influence of seasonal variations on the beneficial effects of GSPE consumption in obesity and NAFLD (Manuscript 4).**

To develop this objective, photoperiod-sensitive rats were chronically exposed to three photoperiods (L12, L18 and L6) to mimic the day length of different seasons, were fed a CAF diet to induce obesity and were either treated with GSPE or VH. Rats fed a STD diet and treated with VH were used as a normal-weight control in each photoperiod. We determined the biochemical and liver lipid profile, we carried out serum and liver metabolomic assays, and hepatic clock and metabolic mRNA gene expression analysis to evaluate any seasonal-dependent effects of GSPE consumption on liver and whole-body metabolism in obese rats.

III. RESULTS

UNIVERSITAT ROVIRA I VIRGILI
THE INFLUENCE OF BIOLOGICAL RHYTHMS ON THE BENEFICIAL EFFECTS OF GRAPE SEED PROANTHOCYANIDIN EXTRACT (GSPE) ON LIVER METABOLISM IN HEALTH AND DISEASE
Romina Mariel Rodriguez

CHAPTER I

OBJECTIVE 1

To determine the impact of the timing of GSPE administration on the hepatic circadian clock in relationship with mitochondrial function in an obesogenic context.

UNIVERSITAT ROVIRA I VIRGILI
THE INFLUENCE OF BIOLOGICAL RHYTHMS ON THE BENEFICIAL EFFECTS OF GRAPE SEED PROANTHOCYANIDIN EXTRACT (GSPE) ON LIVER METABOLISM IN HEALTH AND DISEASE
Romina Mariel Rodriguez

MANUSCRIPT 1

Time-of-Day Circadian Modulation of Grape-Seed Procyanidin Extract (GSPE) in Hepatic Mitochondrial Dynamics in Cafeteria-Diet-Induced Obese Rats

Romina M Rodríguez [1], Antonio J. Cortés-Espinar [1], Jorge R. Soliz-Rueda [1], Christine Feillet-Coudray [2], François Casas [2], Marina Colom-Pellicer [1], Javier Avila-Román [3], Begoña Muguerza [1], Gerard Aragonès [1], Miquel Mulero [1*] and Maria Josepa Salvadó [1]

[1] Nutrigenomics Research Group, Department of Biochemistry and Biotechnology, Campus Sescelades, Universitat Rovira i Virgili (URV), 43007 Tarragona, Spain.

[2] Muscle Dynamics and Metabolism (DMEM), National Research Institute for Agriculture, Food and Environment (INRAE), EMN, UMR 866, Université de Montpellier, 34090 Montpellier, France

[3] Molecular and Applied Pharmacology Group (FARMOLAP), Department of Pharmacology, Faculty of Pharmacy, Reina Mercedes Campus, Universidad de Sevilla, 41012 Sevilla, Spain

* Correspondence: miquel.mulero@urv.cat; Tel.: +34 977559565

Published

Nutrients **2022, *14*(4), 774; https://doi.org/10.3390/nu14040774**

UNIVERSITAT ROVIRA I VIRGILI
THE INFLUENCE OF BIOLOGICAL RHYTHMS ON THE BENEFICIAL EFFECTS OF GRAPE SEED PROANTHOCYANIDIN EXTRACT (GSPE) ON LIVER METABOLISM IN HEALTH AND DISEASE
Romina Mariel Rodriguez

nutrients

MDPI

Article

Time-of-Day Circadian Modulation of Grape-Seed Procyanidin Extract (GSPE) in Hepatic Mitochondrial Dynamics in Cafeteria-Diet-Induced Obese Rats

Romina M. Rodríguez [1], Antonio J. Cortés-Espinar [1], Jorge R. Soliz-Rueda [1], Christine Feillet-Coudray [2], François Casas [2], Marina Colom-Pellicer [1], Gerard Aragonès [1], Javier Avila-Román [3], Begoña Muguerza [1], Miquel Mulero [1,*] and Maria Josepa Salvadó [1]

[1] Nutrigenomics Research Group, Department of Biochemistry and Biotechnology, Campus Sescelades, Universitat Rovira i Virgili, 43007 Tarragona, Spain; rominamariel.rodriguez@urv.cat (R.M.R.); antoniojesus.cortes@urv.cat (A.J.C.-E.); jorgericardo.soliz@urv.cat (J.R.S.-R.); marina.colom@urv.cat (M.C.-P.); gerard.aragones@urv.cat (G.A.); begona.muguerza@urv.cat (B.M.); mariajosepa.salvado@urv.cat (M.J.S.)
[2] Muscle Dynamics and Metabolism (DMEM), National Research Institute for Agriculture, Food and Environment (INRAE), EMN, UMR 866, Université de Montpellier, 34090 Montpellier, France; christine.coudray@inrae.fr (C.F.-C.); francois.casas@inrae.fr (F.C.)
[3] Molecular and Applied Pharmacology Group (FARMOLAP), Department of Pharmacology, Faculty of Pharmacy, Reina Mercedes Campus, Universidad de Sevilla, 41012 Sevilla, Spain; javieravila@us.es
* Correspondence: miquel.mulero@urv.cat; Tel.: +34-9-77-559-565

check for updates

Citation: Rodríguez, R.M.; Cortés-Espinar, A.J.; Soliz-Rueda, J.R.; Feillet-Coudray, C.; Casas, F.; Colom-Pellicer, M.; Aragonès, G.; Avila-Román, J.; Muguerza, B.; Mulero, M.; et al. Time-of-Day Circadian Modulation of Grape-Seed Procyanidin Extract (GSPE) in Hepatic Mitochondrial Dynamics in Cafeteria-Diet-Induced Obese Rats. *Nutrients* **2022**, *14*, 774. https://doi.org/10.3390/nu14040774

Academic Editor: Andrew W. McHill

Received: 25 December 2021
Accepted: 8 February 2022
Published: 12 February 2022

Publisher's Note: MDPI stays neutral with regard to jurisdictional claims in published maps and institutional affiliations.

Abstract: Major susceptibility to alterations in liver function (e.g., hepatic steatosis) in a prone environment due to circadian misalignments represents a common consequence of recent sociobiological behavior (i.e., food excess and sleep deprivation). Natural compounds and, more concisely, polyphenols have been shown as an interesting tool for fighting against metabolic syndrome and related consequences. Furthermore, mitochondria have been identified as an important target for mediation of the health effects of these compounds. Additionally, mitochondrial function and dynamics are strongly regulated in a circadian way. Thus, we wondered whether some of the beneficial effects of grape-seed procyanidin extract (GSPE) on metabolic syndrome could be mediated by a circadian modulation of mitochondrial homeostasis. For this purpose, rats were subjected to "standard", "cafeteria" and "cafeteria diet + GSPE" treatments (n = 4/group) for 9 weeks (the last 4 weeks, GSPE/vehicle) of treatment, administering the extract/vehicle at diurnal or nocturnal times (ZT0 or ZT12). For circadian assessment, one hour after turning the light on (ZT1), animals were sacrificed every 6 h (ZT1, ZT7, ZT13 and ZT19). Interestingly, GSPE was able to restore the rhythm on clock hepatic genes (*Bmal1*, *Per2*, *Cry1*, *Rorα*), as this correction was more evident in nocturnal treatment. Additionally, during nocturnal treatment, an increase in hepatic fusion genes and a decrease in fission genes were observed. Regarding mitochondrial complex activity, there was a strong effect of cafeteria diet at nearly all ZTs, and GSPE was able to restore activity at discrete ZTs, mainly in the diurnal treatment (ZT0). Furthermore, a differential behavior was observed in tricarboxylic acid (TCA) metabolites between GSPE diurnal and nocturnal administration times. Therefore, GSPE may serve as a nutritional preventive strategy in the recovery of hepatic-related metabolic disease by modulating mitochondrial dynamics, which is concomitant to the restoration of the hepatic circadian machinery.

Keywords: grape-seed procyanidin extract; circadian rhythms; clock genes; Zeitgebers; obesity; nutrition; hepatic metabolism; mitochondrial dynamics

1. Introduction

The typical role of mitochondria is oxidative phosphorylation, which provides adenosine triphosphate (ATP) as a primary energy source for most biochemical and physiological processes. However, these intracellular double-membrane-bound structures also play a

pivotal role in ion homeostasis, apoptosis, reactive oxygen species (ROS) production, and in several metabolic pathways since they host fatty acid β-oxidation, as well as urea and Krebs cycles [1,2]. Although these organelles were originally considered static cellular powerhouses, it is now known that they also connect and exchange materials with other cellular organelles, including the nucleus and the endoplasmic reticulum [3,4]. In this sense, mitochondrial organelles are now seen as dynamic structures that actively "evolve" in response to the energy demand and supply. Hence, a nutrient-abundant environment is associated with a fragmented mitochondrial network. Meanwhile, a calorie-restricted state tends to elongate mitochondria [5]. These morphological changes exhibit a high plasticity and influence the capacity and efficiency of ATP production in response to changes in energy balance. Thus, in the case of starvation, mitochondrial fusion is needed in order to sustain ATP production and to preserve cell viability [6]. In contrast, mitochondrial fission is related to a decrease in ATP production, an increase in mitochondrial uncoupling and nutrient storage to avoid waste of energy and the deleterious effect of food excess [7]. In mammals, fusion depends on three GTPases: mitofusins 1 and 2 (*Mfn1* and *Mfn2*) for the fusion of the outer mitochondrial membrane (OMM) [8]; and the inner-mitochondrial-membrane (IMM)-located protein optic atrophy 1 (Opa1), which is responsible for IMM fusion [9]. On the other hand, the GTPase dynamin-related protein 1 (*Drp1*), together with OMM-located mitochondrial fission 1 protein (*Fis1*), conducts the fission events. These processes constantly counteract one another; therefore, the inactivation of fission activates fusion and vice-versa [10].

On the other hand, several studies have clearly shown the central role of mitochondrial dysfunction in metabolic diseases, specifically in type 2 diabetes mellitus, obesity, dyslipidemia and nonalcoholic fatty liver disease (NAFLD), as well as in the aging process [11–13]. Thus, improper function of mitochondria causes oxidative stress and impaired cellular functions, which could lead to insulin resistance and other metabolic changes typical of metabolic syndrome. Furthermore, it has been described that the reduction in proteins involved in mitochondrial fusion, as well as the increase in proteins in mitochondrial fission, are also characteristic of insulin-resistant states [7,14–16]. Additionally, it is well known that the liver plays a central role in glucose homeostasis and is essential for maintaining the body's overall energetic metabolism. Moreover, it is one of the richest organs regarding density and number of mitochondria. In this sense, most chronic liver diseases are related to mitochondrial malfunction and to the accumulation of damaged mitochondria [17].

Furthermore, metabolism follows circadian rhythms, which are driven by peripheral clocks. The molecular machinery of circadian clock consists of transcriptional and translational feedback loops. The heterodimer formed by circadian locomotor output cycles kaput (CLOCK), and brain and muscle aryl hydrocarbon receptor nuclear translocator-like 1 (*Bmal1*) is the main player in the circadian clock. The CLOCK-*Bmal1* heterodimer binds to E-box, and period (*Per*) and cryptochrome (*Cry*) genes are transcribed. PER and CRY*Per* and *Cry* proteins can heterodimerize to repress the CLOCK-*Bmal1* gene-associated translation. Casein kinase 1 (Ck1) phosphorylates both proteins, PERand CRY, and this step is required to start the repression. Nevertheless, protein phosphatase 1 (Pp1) catalyzes the opposite reaction: the dephosphorylation of these proteins. Post-transcriptional and post-translational processes are able to regulate the PER-CRY repression. CLOCK-*Bmal1* also transcribes retinoid-related orphan receptor (*Ror*) and nuclear receptor subfamily 1 group D (*Rev-Erb*). Both products activate and repress respectively, *Bmal1* gene expression [18–21].

Experimental data support the idea that mitochondrial function is closely related to the clock machinery. In this sense, it has been previously identified that several genes involved in mitochondrial dynamics and mitochondrial respiration are expressed in a daily manner in mouse liver and that these daily oscillations are lost in *Bmal1* liver-specific knockout mice [4]. Moreover, in the absence of *Bmal1*, mitochondria are more vulnerable to damage caused by oxidative stress; additionally, levels of *Mfn1* and *Opa1* fusion proteins are decreased [22]. Using an electron microscope, Uchiyama and collaborators observed

significant changes in the shape and volume of mitochondria between the light and dark cycle in hepatocytes of Wistar rats [23].

Additionally, mitochondrial dynamics might also influence circadian rhythms. Studies carried out using *Drp1*-deficient mice showed an important loss of *Bmal1* and *Per1/2* circadian oscillations, as well as a loss of circadian ATP production. This evidence suggest that circadian activation of *Drp1* plays an important role in connecting circadian and mitochondrial metabolic cycles [24].

A high-fat diet induces a delay in the liver circadian-clock machinery, which promotes the activation of hepatic stellate cells and damage in hepatocytes, causing hepatic steatosis, in some cases leading to cell death. All these events result in a disruption of the normal circadian rhythm and a decrease in the amplitude of circadian-clock oscillations [25–27].

Polyphenols are secondary compounds widely distributed in the plant kingdom. There is evidence that phenolic substances act as antioxidants by preventing the oxidation of low-density lipoprotein (LDL), platelet aggregation, and damage of red blood cells [28]. Additionally, phenolics act as (i) metal chelators, (ii) antimutagens and anticarcinogens, (iii) antimicrobial agents and (iv) anti-inflammatory agents [29].

Interestingly, polyphenols have been shown to restore specific disruptions in the circadian clock due to nutrient overload [30–32]. In this regard, it has been found that dietary tea polyphenols ameliorate metabolic syndrome via circadian-clock-related mechanisms [33]. Interestingly, it has also been shown that polyphenol pretreatment ameliorated hydrogen-peroxide (H_2O_2)-elicited mitochondria impairment in a *Bmal1*-dependent manner and that such a *Bmal1*-dependent effect was involved in tea polyphenol-stimulated *Nrf2/Are/Ho-1* and *Akt/Creb/Bsnf* signaling pathway [34]. Additionally, Pajuelo and collaborators [35,36] demonstrated the beneficial effects of supplementation of a grape-seed proanthocyanidin extract (GSPE) on mitochondrial dysfunction of brown adipose tissue and skeletal muscle caused by an obesity-induced diet in rats.

Considering these previous considerations, the aim of the present study was to evaluate the possible misalignment of hepatic circadian rhythm in relationship with mitochondrial function caused by an obesity-induced cafeteria diet and to assess whether GSPE supplementation in these obese rats could mitigate expected detrimental effects.

2. Materials and Methods

2.1. Experimental Procedure in Animals

Ninety-six 12-week-old male Fischer 344 rats (Charles River Laboratories, Barcelona, Spain) were used in this experiment. Rats were housed in pairs at 22 °C, 55% humidity and under a standard photoperiod of 12 h of light and 12 of darkness. A 4-day adaptation period was carried out where rats were fed with a standard diet (STD) ad libitum. The STD composition was 20% protein, 8% fat and 72% carbohydrates (Panlab, Barcelona, Spain). Rats were randomly divided into 2 groups, depending on the diet; 32 rats were fed with STD, and 64 rats were fed a cafeteria diet (CAF) during a 5-week pre-treatment. CAF consisted of biscuits with cheese and pâté, bacon, coiled puff pastry from Mallorca (Hacendado, Spain), feed, carrots and sweetened milk (22% sucrose w/v). CAF composition was 14% protein, 35% fat and 76% carbohydrates. The treatment period started at the 5th week and lasted for 4 weeks. Rats continued with the diet they were fed during the pre-treatment period. The administration of treatments was performed at two time points: 48 rats were treated at the beginning of the light phase (8 a.m., ZT0), and 48 rats were treated at the beginning of the dusk phase (8 p.m., ZT12). All STD-fed rats were treated with condensed milk or vehicle (VH). CAF-feed rats were divided into two groups; 32 were treated with the VH, and 32 with 25 mg/kg GSPE (Les Dérivés Résiniques et Terpéniques, Dax, France) diluted 1/5 in condensed milk. GSPE was composed of catechin (58 µmol/g), dimeric procyanidins (250 µmol/g), epicatechin (52 µmol/g), epigallocatechin (5.50 µmol/g), epicatechin gallate (89 µmol/g), epigallocatechin gallate (1.40 µmol/g), hexameric procyanidins (0.38 µmol/g), pentameric procyanidins (0.73 µmol/g), tetrameric procyanidins (8.8 µmol/g) and trimeric procyanidins (1568 µmol/g) [37]. The treatment was orally administered daily using a

syringe. During both the pre-treatment and treatment, body weight and food intake were recorded weekly. The rats were fasted for 3 h, then sacrificed by decapitation. Each diet-treatment group was divided into 4 sub-groups of 4 rats, depending on the time of sacrifice (9 a.m. (ZT1), 3 p.m. (ZT7), 9 p.m. (ZT13) or 3 a.m. (ZT19)). Blood was collected to obtain serum after a 15-min centrifugation (12,000× *g* and 4 °C) and stored at −80 °C. The liver was collected and stored at −80 °C for further analysis. All animal care and experimental protocols with animals were approved by the Ethics Review Committee for Animal Experimentation of the Universitat Rovira i Virgili (reference number 9495, 18 September 2019) and were carried out in accordance with Directive 86/609EEC of the Council of the European Union and the procedure established by the Departament d'Agricultura, Ramaderia i Pesca of the Generalitat de Catalunya.

2.2. RNA Extraction

A liver-tissue portion (20–30 mg) was mixed with Trizol® reagent (Thermo Fisher, Madrid, Spain) and homogenized by Tissue Lyser LT (Qiagen, Madrid, Spain). After a 10-min centrifugation (12,000× *g* and 4 °C), the homogenate was placed into a new eppendorf tube, and 120 µL of chloroform was added. Two phases were separated after a 15-min centrifugation (12,000× *g* and 4 °C). The aqueous phase was transferred into a new eppendorf tube, and 300 µL of isopropanol was added. After an overnight incubation at −20 °C, samples were centrifugated at 4 °C and 12,000×*g* for 10 min. The supernatant was discarded, and the pellet was cleaned twice with 500 µL and centrifuged for 5 min (8000× *g* and 4 °C). The supernatant was discarded again, and the washed pellet was resuspended with 60 µL of nuclease-free water (Thermo Fisher, Madrid, Spain). RNA concentration (ng/µL) and purity were measured by a Nanodrop ND-1000 spectrophotometer (Thermo Fisher, Madrid, Spain).

2.3. Gene-Expression Analysis

Complementary deoxyribonucleic acid (cDNA) was obtained by a reverse transcription of the RNA extracted using a high-capacity complementary DNA reverse-transcription kit (Thermo Fisher, Madrid, Spain). Quantitative polymerase chain reactions (qPCRs) were performed in 384-well plates in a 7900HT fast real-time PCR (Thermo Fisher, Madrid, Spain) using iTaq™ Universal SYBR® Green Supermix (Bio-Rad, Barcelona, Spain). The thermal-cycle program used in all qPCRs was 30 s at 90 °C, 40 cycles of 15 s at 95 °C and 1 min at 60 °C. The analyzed liver genes were normalized by the housekeeping gene peptidylprolyl isomerase A (Ppia). The primers used for each gene were obtained from Biomers (Ulm, Germany) and can be found in Table 1. The relative expression of each gene was calculated using the $2^{-\Delta\Delta Ct}$ method, as reported by Schmittgen and Livak [38].

Table 1. Nucleotide sequences of primers used for real-time quantitative PCR.

Gene	Forward Primer (5′ to 3′)	Reverse Primer (5′ to 3′)
Bmal1	GTAGATCAGAGGGCGACGGCTA	CTTGTCTGTAAAACTTGCCTGTGAC
Cry1	TGGAAGGTATGCGTGTCCTC	TCCAGGAGAACCTCCTCACG
Drp1	CCAGGAATGACCAAGGTCCC	CCTCGTCCATCAGGTCCAAC
Fis1	GCACGCAGTTTGAATACGCC	CTGCTCCTCTTTGCTACCTTTGG
Mfn1	CCTTGTACATCGATTCCTGGGTTC	CCTGGGCTGCATTATCTGGTG
Mfn2	GATGTCACCACGGAGCTGGA	AGAGACGCTCACTCACTTTG
Nampt	CTCTTCACAAGAGACTGCCG	TTCATGGTCTTTCCCCCACG
Nr1d1	ACAGCTGACACCACCCAGATC	CATGGGCATAGGTGAAGATTTCT
Pcg1α	AGAGTCACCAAATGACCCCAAG	TTGGCTTTATGAGGAGGAGTCG
Per2	CGGACCTGGCTTCAGTTCAT	AGGATCCAAGAACGGCACAG
Ppia	CCAAACACAAATGGTTCCCAGT	ATTCCTGGACCCAAAACGCT
Rorα	CCCGATGTCTTCAAATCCTTAGG	TCAGTCAGATGCATAGAACACAAACTC

2.4. Serum Analysis

Enzymatic colorimetric assays were used for the analysis of glucose, total cholesterol (TC), triglycerides (TAG) (QCA, Amposta, Tarragona, Spain) and non-esterified free fatty acids (NEFAs) (WAKO, Neuss, Germany) according to the manufacturer's instructions.

2.5. Extraction and Measurement of Concentrations of Lipids in Liver

Liver lipids were extracted following the Bligh–Dyer method [39], and levels of hepatic cholesterol, TAG and total lipid liver content were measured using a colorimetric kit assay (QCA, Barcelona, Spain).

2.6. Determination of Liver Mitochondrial Enzymatic Activities

Liver samples were homogenized in a cold phosphate buffer (50 mM, pH 7) in the following proportion: 0.5 g of liver tissue for 4.5 mL buffer using a Polytron homogenizer (Kinematica, Switzerland). Then, homogenates were centrifuged at 1000× *g* for 10 min at 4 °C, and supernatants were collected for enzymatic analysis. Citrate synthase (CS) activity was determined as described by Srere [40]: the deacetylation of acetyl coenzyme A (Acetyl-CoA) in the presence of oxalacetate and 5,5′-dithiobis-2-nitrobenzoic acid (DNTB) produced by CS can be followed spectrophotometrically at 412 nm for 30 s due to the formation of 5-thio-2-nitrobenzoic acid (TNB). Complex I (CI) activity was determined as described by Janssen et al. [41], spectrophotometrically measuring, at 600 nm for 30 s, the reduction of 2,6-dichloroindophenol (DCPIP) produced by the electrons accepted from decylubiquinol, reduced by complex I in a previous step. The activity of Complex II (CII) and complex II + III (CII + III) was measured according to Rustin et al. [42], spectrophotometrically following the reduction of DCPIP by the succinate at 600 nm for 1 min for CII and the oxidation of cytochrome c at 550 nm for 1 min for CII + III. Cytochrome c oxidase (COX) activity was determined as described by Wharton and Tzagoloff [43], spectrophotometrically measuring oxidation of cytochrome c reduced at 550 nm for 30 s.

2.7. Metabolomic Analysis

Metabolomic analysis of the 96 rat liver samples was performed at the Centre for Omic Sciences (COS, Tarragona, Spain) using gas chromatography coupled with quadrupole time-of-flight mass spectrometry (GC-qTOF model 7200, Agilent, Santa Clara, CA, USA). The extraction was performed by adding 400 µL of methanol:water (8:2)-containing internal standard mixture to liver samples (approx. 10—20 mg). Then, the samples were mixed and homogenized on a bullet blender using a stainless-steel ball, incubated at 4 °C for 10 min and centrifuged at 19,000× *g* rpm; supernatant was evaporated to dryness before compound derivatization (methoximation and silylation). The derivatized compounds were analyzed by GC-qTOF. Chromatographic separation was based on the Fiehn Method, [44] using a J&W Scientific HP5-MS film capillary column (30 m × 0.25 mm × 0.25 µm, Agilent, Santa Clara, CA, USA) and helium as carrier gas with an oven program from 60 to 325 °C. Ionization was done by electronic impact (EI), with electron energy of 70 eV and operating in full-scan mode. Identification of metabolites was performed using commercial standards and by matching their EI mass spectrum and retention time to a metabolomic Fiehn library (from Agilent, Santa Clara, CA, USA), which contains more than 1400 metabolites. After putative identification of metabolites, they were semi-quantified in terms of internal standard response ratio.

2.8. Circadian-Rhythm Analysis

To analyze the circadian rhythms of the different clock genes, we used a cosinor-based rhythmometry method. We considered the presence of circadian rhythm when the model of each gene expressions fit the cosine curves ($p < 0.05$). For this, a script was developed by J.R. S.-R. using PyCharm software (v. 2018.2.4, JetBrains s.r.o., Prague, Czech Republic) with Python Software Foundation version 3.7.4 (Wilmington, DE, USA), and circadian-rhythm estimates were plotted using CosinorPy package (v. 1.1) (Ljubljana, Slovenia) [45].

2.9. Statistical Analysis

Data are reported as mean ± standard error of the mean (SEM). Biometric parameters, liver mitochondrial enzymatic activity, liver weight and liver gene expression were subjected to Student's t test, as well as one- and two-way analysis of variance (ANOVA) with the least significant difference test (LDS) for post hoc comparisons using the computer program SPSS version 25 (SPSS Inc., Chicago, IL, USA). Graphics were done by GraphPad Prism 8 software (San Diego, CA, USA). For all analyses, a probability (p) value of <0.05 was considered statistically significant.

Heatmaps of metabolites were performed after data normalization and autoscaling using MetaboAnalyst 5.0 software (Edmonton, Alberta, Canada; https://www.metaboanalyst.ca/, accessed on 20 December 2021) [46].

3. Results

3.1. Animal Body-Weight Gain Corroborates the Obesogenic Effect of the Cafeteria Diet

The final body-weight gain of animals fed with CAF diet was significantly higher than that of animals fed an STD diet ($p = 0.0001$) (Figure 1A,B). After demonstrating the efficacy of the CAF diet in the experimental animals, the different treatments were analyzed. In this sense, Figure 1C,D shows the comparison of body-weight gain between the two treatments—VH or GSPE—in the morning (ZT0) and at night (ZT12) in rats fed a CAF diet. Interestingly, animals treated with GSPE at night (ZT12) showed a reduction in body-weight gain when compared to the control CAF-fed group ($p = 0.005$). This result points out a first differential effect of GSPE depending on the time of administration. Furthermore, globally, this result is in agreement with previous studies that showed GSPE efficiency for treating metabolic syndrome and, more specifically, body weight [47–49]. During the ZT12 treatment, rats treated with GSPE consumed fewer kilojoules (kJ) than rats treated with VH (732.5 ± 22.38 vs. 674.9 ± 14.77 kJ; $p = 0.03$). These results are in concordance with the inhibition effects of GSPE over food intake described by Serrano and colleagues [50]. Nevertheless, these differences were not seen in the ZT0 treatment.

3.2. Intake of Obesogenic Diet Alters Circulating Levels of Glucose, TAG and TC

Fasting serum glucose, TC, TAG and NEFAs levels were measured after animals were sacrificed at four different circadian time points (ZT1 to ZT19). On the one hand, regarding morning treatments (ZT0), glucose levels in the STD-VH group remained constant at almost all circadian points, except for the last one (ZT19), where its concentration was decreased (Table 2). Moreover, it could also be observed that glucose levels of the CAF-VH group were significantly higher than those of the control group at the ZT7 ($p = 0.007$) and ZT13 ($p = 0.021$) time points, possibly due to the hyperglycemic state associated with obesity. When comparing between the CAF-VH and CAF-GSPE groups, no significant differences in glucose levels were observed. However, GSPE supplementation in the CAF diet tended to improve glucose levels compared to the CAF-VH group at ZT13 ($p = 0.08$). It is noteworthy that at this time point, the CAF-GSPE group reached a similar glucose level to that of the control group. On the other hand, regarding night treatment (ZT12), glucose levels of the STD-VH group remained constant from ZT1 to ZT19, and CAF promoted a homeostatic disruption by increasing glucose levels around 40 percent at all time points. Even though no significant differences were observed between CAF-VH and GSPE groups, serum levels of animals treated with GSPE at ZT13 and ZT19 tended to decrease.

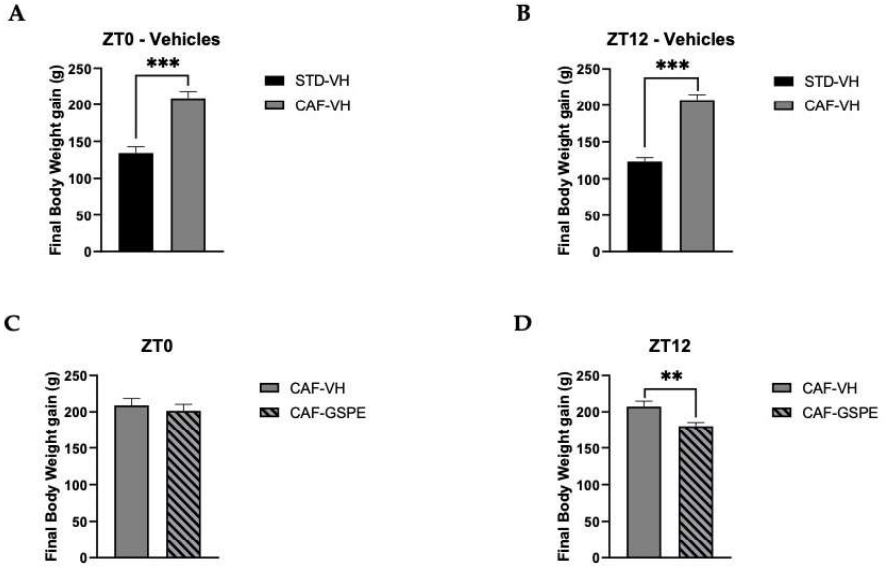

Figure 1. Body-weight gain (g). (**A**) Body-weight gain in grams of ZT0-vehicle rats (standard diet-vehicle (STD-VH) and cafeteria-diet-vehicle rats (CAF-VH) in the nine weeks of the experiment. (**B**) Body-weight gain in grams of ZT12-vehicle rats (STD-VH and CAF-VH) in the nine weeks of the experiment. (**C**) Body-weight gain in grams of ZT0-CAF-VH and cafeteria diet–grape-seed proanthocyanidin extract (CAF-GSPE) groups in the nine weeks of the experiment. (**D**) Body-weight gain in grams of ZT12 CAF-VH and CAF-GSPE groups in the nine weeks of the experiment. *** Indicates significant differences using repeatedly measured ANOVA followed by Student's *t* test between VH groups (STD-VH vs. CAF-VH) ($p \leq 0.001$); ** indicates significant differences within CAF groups (CAF-VH vs. CAF-GSPE) ($p \leq 0.01$).

The serum lipid profile was analyzed by TAG and TC levels in all rats after sacrifice and is presented in Table 2 for each time of death. Among the treatments, the CAF-VH showed the highest levels of TAG at each time of death. In the case of diurnal treatment (ZT0), the CAF-GSPE group presented a slight decrease in TAG levels at all time points compared to CAF-VH-treated rats, showing the highest reductions of, 12 and 33%, at ZT7 and ZT13, respectively. These differences were not observed at ZT12, where the levels of TAG in CAF-VH and GSPE groups were similar. The cholesterol levels did not show such an apparent oscillatory pattern as was present for TAG. However, there was a peak in its level at ZT7 in the CAF-VH group treated in the morning (ZT0) and at ZT19 in the CAF-VH nocturnally treated animals, increasing 33 and 44 percent in comparison with the STD-VH group. Regarding NEFA plasmatic levels, no significant differences were found in any experimental group comparison (STD-VH versus CAF-VH and CAF-VH versus CAF-GSPE).

Table 2. Biochemical parameters of rats fed with STD or CAF diet supplemented with vehicle or GSPE.

			Glucose (mg/dL)	Cholesterol (mg/dL)	Triglycerides (mg/dL)	NEFA (mg/dL)
ZT0	ZT1	STD-VH	90.11 ± 2.68	90.96 ± 13.33	64.07 ± 5.81	21.93 ± 3.84
		CAF-VH	96.22 ± 5.25	95.99 ± 7.07	108.5 ± 6.17 **	24.71 ± 2.46
		CAF-GSPE	101.72 ± 7.7	100.55 ± 8.53	107.41 ± 19.36	21.12 ± 1.23
	ZT7	STD-VH	89.45 ± 3.38	101.17 ± 4.2	118.11 ± 14.71	32.4 ± 2.23
		CAF-VH	110.84 ± 4.22 **	134.24 ± 14.32 *	319.19 ± 15.87 ***	31.15 ± 2.2
		CAF-GSPE	114.6 ± 6.01	142.02 ± 13.78	280.27 ± 42.88	33.17 ± 1.51
	ZT13	STD-VH	89.6 ± 3.67	87.6 ± 6.68	53.13 ± 9.52	25.38 ± 6.2
		CAF-VH	111.29 ± 6 *	112.86 ± 22.76	204.94 ± 57.47 *	32.62 ± 3.96
		CAF-GSPE	96.13 ± 3.89 #	79.6 ± 7.44	136.11 ± 32.03	35.5 ± 1.05
	ZT19	STD-VH	79.62 ± 4.25	85.75 ± 9.53	50.22 ± 6.36	22.23 ± 3.02
		CAF-VH	96.2 ± 6.8	97.05 ± 4.44	133.68 ± 18 **	28.66 ± 2.04
		CAF-GSPE	97.38 ± 11.51	82.53 ± 9.56	118.93 ± 11.97	31.92 ± 2.97
ZT12	ZT1	STD-VH	85.7 ± 4.92	119.64 ± 17.95	84.23 ± 19.56	31.46 ± 10.85
		CAF-VH	103.82 ± 4.64 *	88.39 ± 10.1	122.92 ± 10.74	26.58 ± 2.58
		CAF-GSPE	108.95 ± 8.27	92.68 ± 7.49	181.82 ± 27.14	30.66 ± 7.37
	ZT7	STD-VH	87.28 ± 8.97	134.24 ± 14.51	163.51 ± 19.99	30.14 ± 2.47
		CAF-VH	116.33 ± 6.05 *	122.37 ± 17.35	320.27 ± 48.57 *	32.74 ± 2.73
		CAF-GSPE	125.87 ± 7.78	151.36 ± 13.35	366.76 ± 45.42	34.47 ± 3.99
	ZT13	STD-VH	85.49 ± 4.15	100.51 ± 14.49	49.84 ± 3.83	27.29 ± 2.74
		CAF-VH	124.13 ± 10.98 *	119.27 ± 13.91	189.03 ± 39.51 *	33.28 ± 4.73
		CAF-GSPE	112.93 ± 9.55	118.23 ± 17.02	183.64 ± 55.82	34.24 ± 3.52
	ZT19	STD-VH	81.01 ± 7.4	93.55 ± 6.9	65.25 ± 6.78	31.02 ± 2.14
		CAF-VH	125.05 ± 10.89 *	134.03 ± 19.23 *	213.53 ± 51.16 *	30.18 ± 2.07
		CAF-GSPE	106.35 ± 14.1	128.44 ± 30.01	179.87 ± 44.01	32.26 ± 8.15

Serum parameters of rats fed with standard diet (STD) or cafeteria diet (CAF) for 9 weeks and supplemented with vehicle or grape-seed proanthocyanidin extract (GSPE) for the last 4 weeks. Values are expressed as the mean ± standard error of the mean (SEM) (n = 4). * The effect of diet within vehicle groups (Student's t test, * $p \leq 0.05$, ** $p \leq 0.01$, *** $p \leq 0.001$); # indicates tendency between cafeteria-diet–vehicle (CAF-VH) and cafeteria-diet–grape-seed proanthocyanidin extract (CAF-GSPE) using Student's t test (p = 0.1–0.051).

3.3. GSPE Restores CAF Diet-Related Disruption of Circadian Rhythm of Liver Core-Clock Genes

To evaluate the effects of diet and GSPE treatments on circadian rhythm of the peripheral-clock genes in the liver, we used the cosinor method to model the oscillation of these genes in a 24 h period. This method allowed for the assessment of different circadian parameters, such as amplitude, acrophase and midline estimating statistic of rhythm (MESOR), as well as the comparison of these oscillations and parameters between the different treatment groups (Supplementary Materials, Table S1).

Interestingly, it was observed that the expression of clock genes presented a clear and robust circadian rhythm in practically all the experimental groups (Figures 2 and 3). However, a clear disruption caused by CAF diet was detected in some parameters, such as amplitude (p = 0.047) and acrophase (p = 0.033) of N1rd1 gene expression in the groups treated in the morning (ZT0) (Figure 2G,H). In this case, a significant displacement of the acrophase was observed, occurring before the moment of the greatest expression of this gene regarding the standard group. In addition, an increase in its expression was observed at that time point compared to its STD-diet group, increasing the amplitude of oscillation (Figure 2H). Another gene affected by CAF diet was *Rorα*; in this case, a strong displacement of the acrophase in the CAF group in comparison to the control-diet group was clearly observed (p = 0.022) (Figure 2K,L). GSPE treatment was able to reverse this acrophase shift in *Rorα*, returning the time point of the highest expression of this gene to

similar values as those of the control group. For these groups treated in the morning (ZT0), no other significant difference was detected.

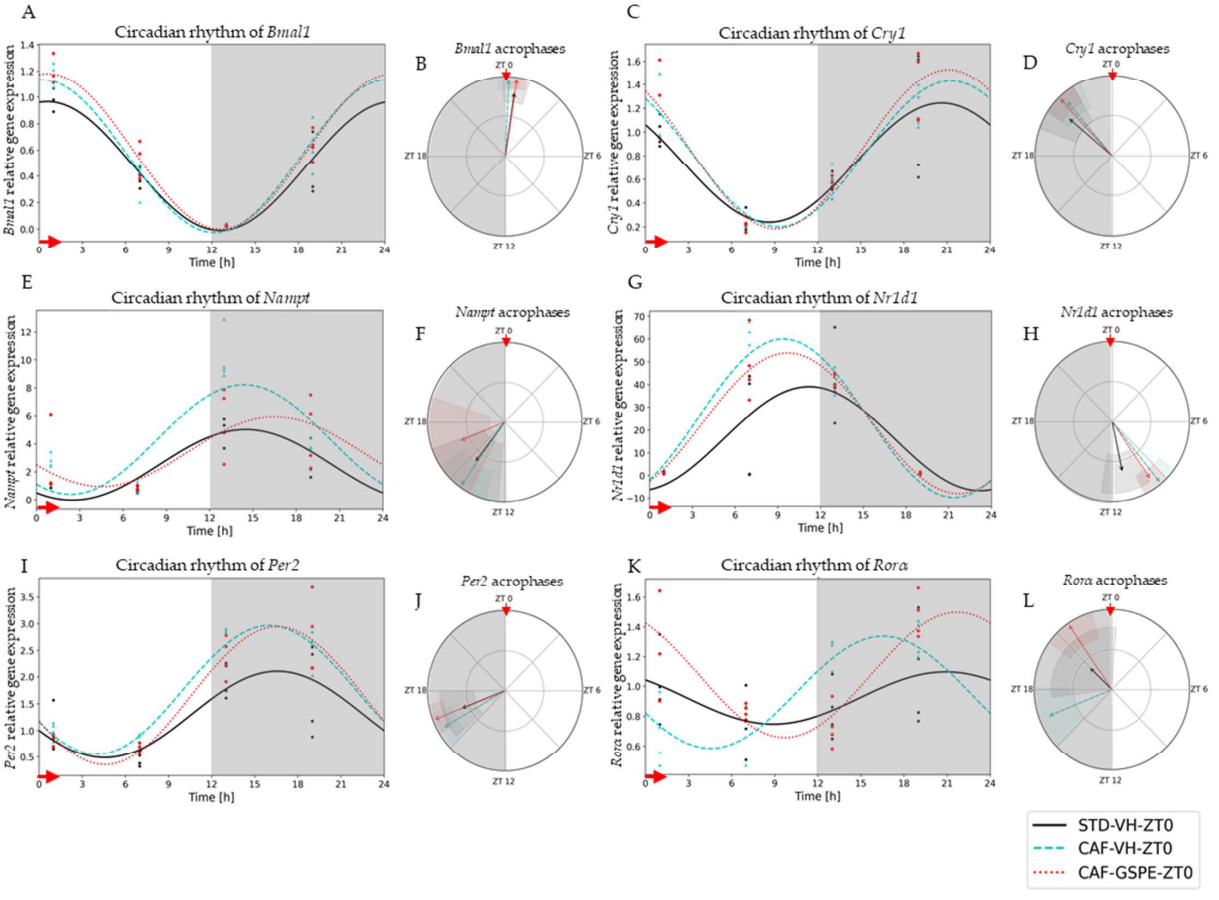

Figure 2. Estimated circadian rhythms (relative gene expression) of groups treated in the morning (ZT0). (**A**) Estimated circadian rhythms and (**B**) acrophases with their amplitudes represented of *Bmal1* for ZT0-vehicle and treatments groups (STD-VH, CAF-VH and CAF-GSPE). (**C**) Estimated circadian rhythms and (**D**) acrophases with their amplitudes represented of *Cry1* for ZT0-vehicles and treatments groups (STD-VH, CAF-VH and CAF-GSPE). (**E**) Estimated circadian rhythms and (**F**) acrophases with their amplitudes represented of *Nampt* for ZT0-vehicle and treatments groups (STD-VH, CAF-VH and CAF-GSPE). (**G**) Estimated circadian rhythms and (**H**) acrophases with their amplitudes represented of Nr1d1 for ZT0-vehicle and treatments groups (STD-VH, CAF-VH and CAF-GSPE). (**I**) Estimated circadian rhythms and (**J**) acrophases with their amplitudes represented of *Per2* for ZT0-vehicle and treatments groups (STD-VH, CAF-VH and CAF-GSPE). (**K**) Estimated circadian rhythms and (**L**) acrophases with their amplitudes represented of *Rorα* for ZT0-vehicles and treatments groups (STD-VH, CAF-VH and CAF-GSPE).

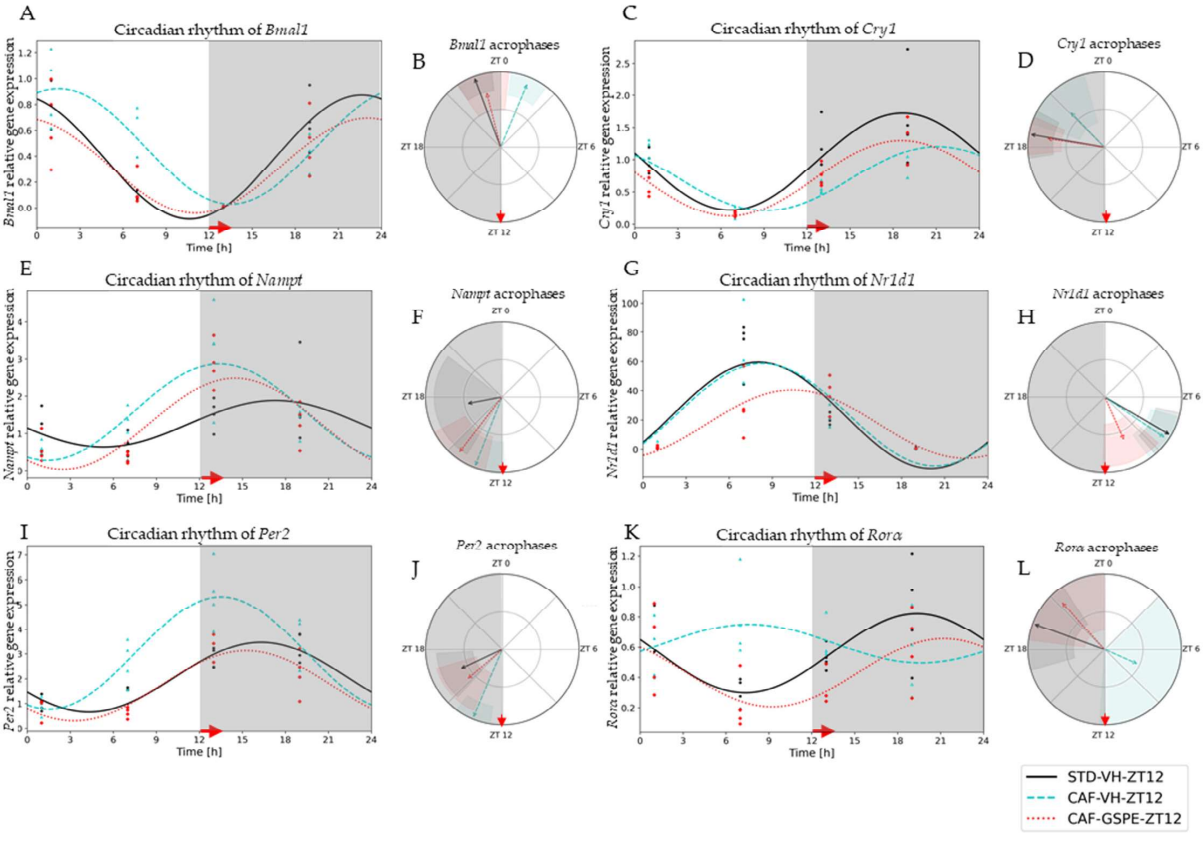

Figure 3. Estimated circadian rhythms (relative gene expression) of groups treated at night (ZT12). (**A**) Estimated circadian rhythms and (**B**) acrophases with their amplitudes represented of *Bmal1* for ZT12-Vehicles and Treatments Groups (STD-VH, CAF-VH and CAF-GSPE). (**C**) Estimated circadian rhythms and (**D**) acrophases with their amplitudes represented of *Cry1* for ZT12-Vehicles and Treatments Groups (STD-VH, CAF-VH and CAF-GSPE). (**E**) Estimated circadian rhythms and (**F**) acrophases with their amplitudes represented of *Nampt* for ZT12-Vehicles and Treatments Groups (STD-VH, CAF-VH and CAF-GSPE). (**G**) Estimated circadian rhythms and (**H**) acrophases with their amplitudes represented of Nr1d1 for ZT12-Vehicles and Treatments Groups (STD-VH, CAF-VH and CAF-GSPE). (**I**) Estimated circadian rhythms and (**J**) acrophases with their amplitudes represented of *Per2* for ZT12-Vehicles and Treatments Groups (STD-VH, CAF-VH and CAF-GSPE). (**K**) Estimated circadian rhythms and (**L**) acrophases with their amplitudes represented of *Rorα* for ZT12-Vehicles and Treatments Groups (STD-VH, CAF-VH and CAF-GSPE).

Regarding the night-treated groups (ZT12), CAF-diet effects were detected in genes such as *Bmal1*, *Per2*, *Cry1*, *Rorα* and *Nampt*. The CAF-diet effect on *Bmal1* expression resulted in an acrophase displacement in comparison to the STD-diet group ($p = 0.0001$) (Figure 3A,B). This displacement was significantly restored by GSPE treatment ($p = 0.0001$) (Supplementary Materials, Table S2). Another gene also altered by CAF diet was *Per2* (Figure 3I,J). A similar situation was detected for *Cry1* gene expression; its acrophase was displaced with the CAF diet ($p = 0.036$) and restored with the GSPE treatment at ZT12 ($p = 0.001$) (Figure 3C,D). In this case, a significant displacement of acrophase and an increase in amplitude with CAF diet was observed; nevertheless, the administration of GSPE restored both circadian parameters. Interestingly, the most altered gene was *Rorα*, the circadian rhythmic expression of which was fully disrupted ($p = 0.037$) by the CAF diet (Figure 3K,L). This total disruption of rhythmicity was significantly restored by GSPE

treatment (p = 0.046), and both circadian parameters (acrophase and amplitude) were reestablished to similar values as those in the STD-diet group (p = 0.000). Finally, circadian rhythm of *Nampt* expression was also altered by the CAF diet, shifting its acrophase (p = 0.033). Intriguingly, in this case, GSPE treatment was not able to restore its circadian disruption.

3.4. GSPE Modulates Changes in Mitochondrial Dynamics and Biogenesis Induced by Cafeteria Diet

Several studies suggest that mitochondrial dysfunction plays a critical role in initiating or propagating events in fatty liver disfunction and NAFLD [51]. Moreover, mitochondrial dysfunction and obesity are tightly connected, as these organelles embrace fatty acid oxidation. It should be noted that β-oxidation depends on organelle activity and number to efficiently synthesize ATP from oxidation of metabolic fuels [52]. Therefore, to evaluate mitochondrial dynamics and biogenesis in the liver, gene-expression assessment of mitochondrial fusion (*Mfn1* and *Mfn2*), fission (*Drp1* and *Fis1*) and biogenesis (*Pgc1a*) at each time of death condition (ZT1 to ZT19) was performed (Figures 4–6).

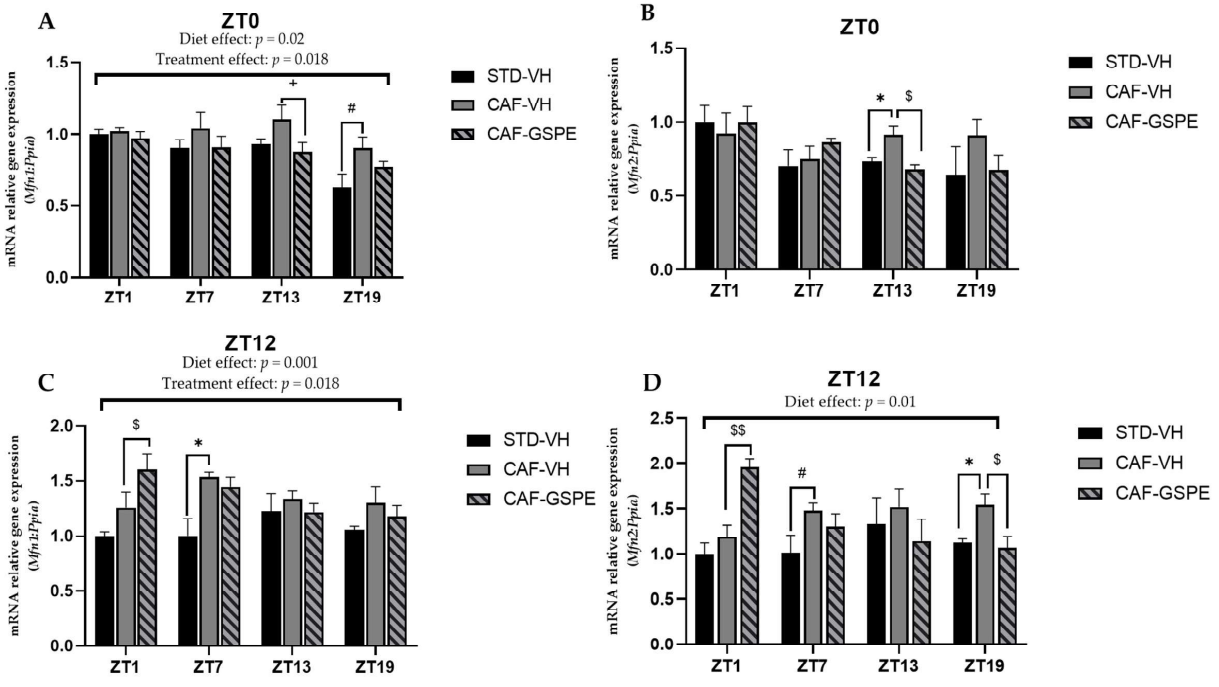

Figure 4. Relative gene expression of mitochondrial fusion genes in the liver. Rats were fed an STD or CAF diet and received a daily dosage of vehicle or GSPE in the morning (ZT0) (**A**,**B**) or at night (ZT12) (**C**,**D**). After 9 weeks, the rats were sacrificed at 9 a.m. (ZT1), 3 p.m. (ZT7), 9 p.m. (ZT13) or 3 a.m. (ZT19), and mRNA levels of *Mfn1* and *Mfn2* were determined. The values are the mean ± SEM (n = 4). * The effect of diet within vehicle groups (Student's t test or DMS post hoc test, $p < 0.05$); $ the effect of GSPE consumption within CAF groups (Student's t test or DMS post hoc test, $ $p \leq 0.05$, $$ $p \leq 0.01$); # indicates tendency between STD-VH and CAF-VH using Student's t test (p = 0.1–0.051); + indicates tendency between CAF-VH and CAF-GSPE using Student's t test (p = 0.1–0.051).

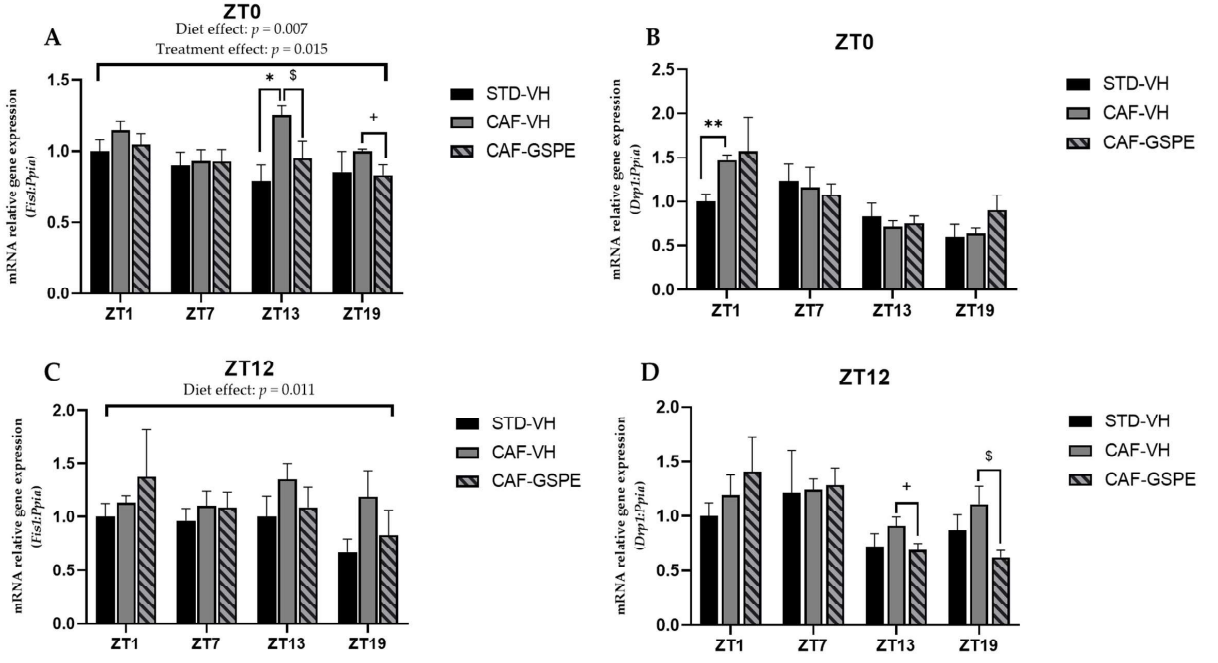

Figure 5. Relative gene expression of mitochondrial fission genes in the liver. Rats were fed an STD or CAF diet and received a daily dosage of vehicle or GSPE in the morning (ZT0) (**A**,**B**) or at night (ZT12) (**C**,**D**). After 9, weeks the rats were sacrificed at 9 a.m. (ZT1), 3 p.m. (ZT7), 9 p.m. (ZT13) or 3 a.m. (ZT19), and mRNA levels of *Fis1* and *Drp1* were determined. The values are the mean ± SEM ($n = 4$). * The effect of diet within vehicle groups (Student's *t* test or DMS post hoc test, * $p \leq 0.05$, ** $p \leq 0.01$); $ the effect of GSPE consumption within CAF groups (Student's *t* test or DMS post hoc test, $p < 0.05$; + indicates tendency between CAF-VH and CAF-GSPE using Student's *t* test ($p = 0.1$–0.051).

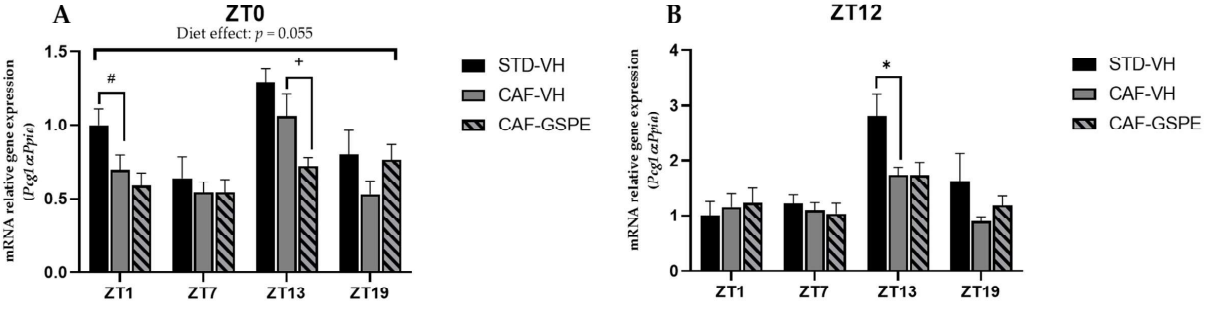

Figure 6. Relative gene expression of mitochondrial biogenesis gen in the liver. Rats were fed an STD or CAF diet and received a daily dosage of vehicle or GSPE in the morning (ZT0) (**A**) or at night (ZT12) (**B**). After 9 weeks, the rats were sacrificed at 9 a.m. (ZT1), 3 p.m. (ZT7), 9 p.m. (ZT13) or 3 a.m. (ZT19), and mRNA levels of *Pgc1α* were determined. The values are the mean ± SEM ($n = 4$). * The effect of diet within vehicle groups (Student's *t* test or DMS post-hoc test, $p < 0.05$); # indicates tendency between STD-VH and CAF-VH using Student's *t* test ($p = 0.1$–0.051); + indicates tendency between CAF-VH and CAF-GSPE using Student's *t* test ($p = 0.1$–0.051).

As shown in Figure 4, at ZT13 and ZT19, there is a slight effect of GSPE in the morning treatment (ZT0) on *Mfn1* ($p = 0.96$) (Figure 4A) and *Mfn2* ($p = 0.01$) (Figure 4B), avoiding the increase in these gene expressions induced by cafeteria treatment. This effect is also evident in Mnf2 expression in the nocturnal treatment (ZT12) at the ZT19 death time

($p = 0.03$) (Figure 4D). Thus, in relation to mitofusin expression, and except for this last ZT19 condition, the night GSPE treatment behaves completely differently than for the rest of ZTs in comparison with the day GSPE treatment. The most remarkable result is that there is a clear overexpression in both *Mnf1* and *Mfn2*, a 27 and 65% increment, respectively, in the GSPE group in the night treatment (ZT12) compared with the CAF-VH group. Altogether, these results could suggest that the effect of GSPE inducing the fusion of mitochondria seems to be more relevant with night treatment and shortly after GSPE ingestion (ZT1) in cafeteria-fed animals.

Regarding fission genes, when comparing VH groups (CAF vs. STD) treated in the morning (ZT0), it can be seen that CAF-fed animals exhibit significantly higher expression levels of *Drp1* and *Fis1* at ZT1 ($p = 0.011$) and ZT13 ($p = 0.004$), respectively. These differences were not observed between STD-VH and CAF-GSPE groups (Figure 5A–B). Regarding the GSPE effect, a decrease of almost 30 percent in *Fis1* gene expression is observed in the ZT13 condition. As some of these effects were also observed for the fusion genes, it seems that morning GSPE treatment promotes a relatively mild effect and prompts an equilibrium between the fusion and fission events, suggesting that there could be a balance in the morphology of the mitochondrial population.

On the other hand, concerning the expression of the fission genes in the GSPE night treatment (Figure 5C–D), we found significant effects at ZT13 ($p = 0.069$) and ZT19 ($p = 0.032$) in *Drp1* gene expression (between CAF-VH and CAF-GSPE group). In consequence, it seems that in the night treatment, mitochondria could be more present in an elongated/fussed form due to both the induction of fusion genes and the inhibition of fission genes induced by GSPE.

Mitochondrial biogenesis is regulated by transcription factor *Pgc1α*. As shown in Figure 6A,B, *Pgc1α* expression of STD-VH animals is three-fold higher at ZT13 in both diurnal and nocturnal treatments, as well as at ZT1 in the morning treatment (ZT0) ($p = 0.090$). Interestingly, there is a subtle effect (tendency) of GSPE to decrease biogenesis in the morning treatment at ZT13 ($p = 0.076$). Nevertheless, it seems that GSPE is more capable of modulating the fission and fusion events than biogenesis events. It should be noted that while mitochondrial dynamics are highly regulated by a few genes (*Mfn1/2*, *Drp1*, and *Fis1*), mitochondrial biogenesis involves more factors, which is why, perhaps, no effect of GSPE treatment on the master regulator *Pgc1-α* is observed. Thus, it is likely that other genes, such as *Tfam*, could be also acting.

3.5. Mitochondrial Respiratory Activity Is Highly Altered Due to CAF Diet but Partially Ameliorated by GSPE

As it is well known, mitochondrial activity dysfunction is highly related to steatosis and steatohepatitis, as well as fibrosis [53]. For this reason, we measured the activity of the complexes that form part of the respiratory chain. In this sense, as can be seen in Figure 7, a clear alteration produced by CAF diet regarding mitochondrial complexes was observed. Particularly, the activity of mitochondrial complexes I, II and II + III were altered at different times of day.

Regarding complex I, there was a disruption in its activity due to the CAF diet when CAF-VH groups were compared with STD-VH groups, as shown in Figure 7A,B. In addition, these differences were increased when the activity of complex I was measured at ZT7, regardless of the treatment time ($p = 0.0007$ at ZT0 and $p = 0.012$ at ZT12). However, when GSPE was supplied in the morning (ZT0), there was an improvement of the activity at ZT7 ($p = 0.013$) and at ZT13 ($p = 0.010$), with values like those of the STD group. Furthermore, diurnal GSPE-treated animals (ZT0) showed a tendency to increase complex I activity ($p = 0.054$) when compared to treated and non-treated CAF groups (Figure 7A).

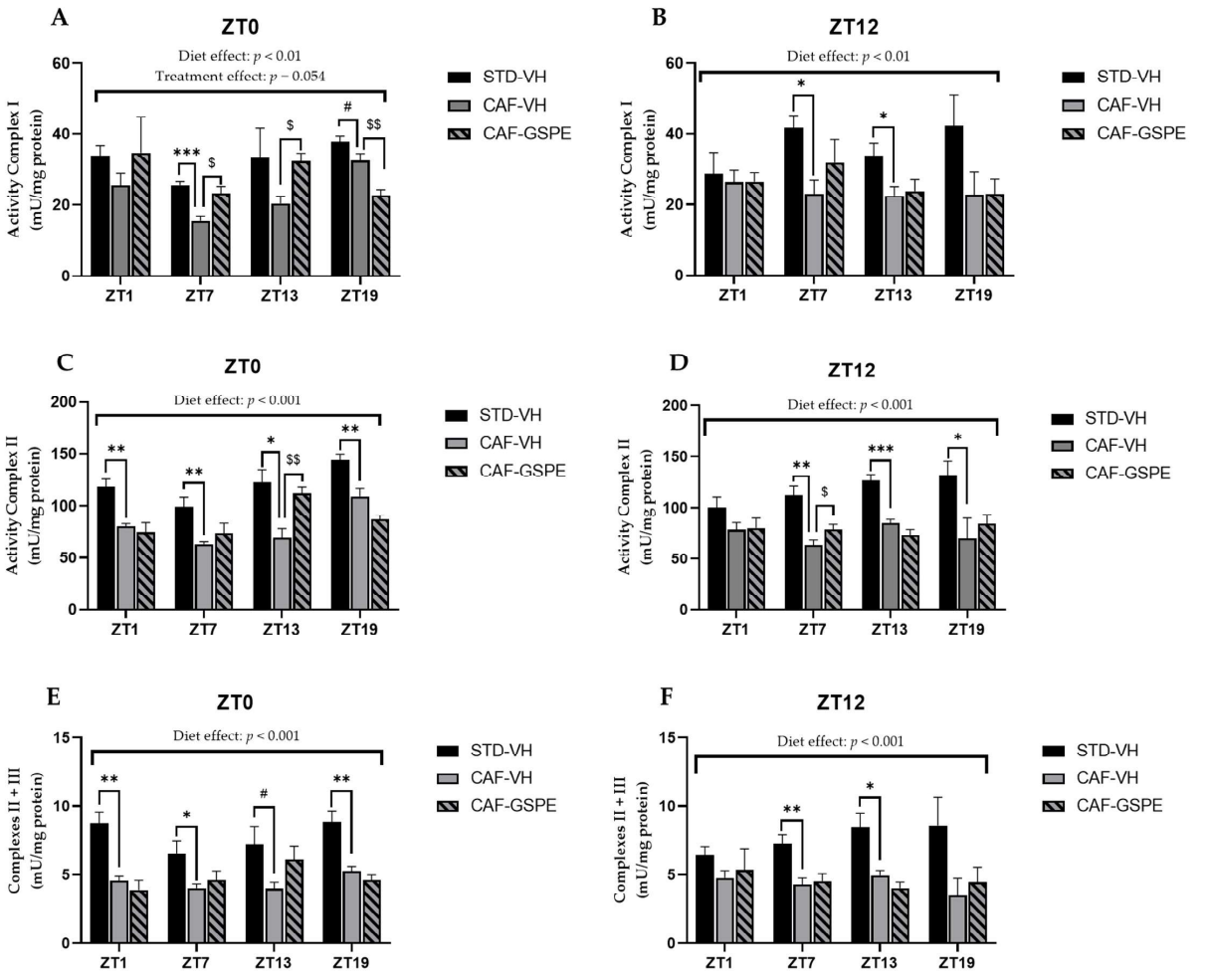

Figure 7. Mitochondrial respiratory activity in the liver. Rats were fed an STD or CAF diet and received a daily dosage of vehicle or GSPE in the morning (ZT0) (**A**,**C**,**E**) or at night (ZT12) (**B**,**D**,**F**). After 9 weeks, the rats were sacrificed at 9 a.m. (ZT1), 3 p.m. (ZT7), 9 p.m. (ZT13) or 3 a.m. (ZT19), and the activity of mitochondrial complexes I, II and III was determined. The values are the mean ± SEM (n = 4). * The effect of diet within vehicle groups (Student's t test or DMS post hoc test, * $p \leq 0.05$, ** $p \leq 0.01$, *** $p \leq 0.001$); $ the effect of GSPE consumption within CAF groups (Student's t test or DMS post hoc test, $ $p \leq 0.05$, $$ $p \leq 0.01$); # indicates tendency between STD-VH and CAF-VH using Student's t test (p = 0.1–0.051).

With respect to complex II, the activity of the complex was extremely altered due to the CAF diet, as shown in Figure 7C,D, with activity disruptions at all measured times, except for ZT1, when treated at night (ZT12). Nevertheless, when GSPE treatment was supplied in the morning (ZT0), there was an amelioration of the activity of this complex at ZT13 (p = 0.007), showing an activity similar to that in the STD-fed group, which could suggest that GSPE improved the state of this complex.

As expected, the activity of complexes II + III was also highly altered due to the CAF diet, showing a decrease in activity of almost 50% in some of the cases compared to the STD-fed group, as shown in Figure 7E,F. In addition, this decrease in activity was accentuated at ZT1 when VH was supplied in the morning (ZT0) (p = 0.003). However,

regarding the activity of complexes II + III, no significant differences were found due to treatment with GSPE.

Concerning the last complex of the respiratory chain, complex IV or COX, not enough differences were found due to CAF or GSPE treatment. In this case, the activity of the complex was constant in all conditions and at all measured times. Finally, we also measured the activity of citrate synthase, which is considered a marker for mitochondrial activity. Despite the fact that there were no differences due to the CAF diet or GSPE treatment, there was a significant increase in the activity of this enzyme at ZT13 in rats treated diurnally with GSPE (ZT0), even exceeding the activity of the STD group ($p = 0.001$) (Supplementary Materials, Table S3).

Altogether, these subtle results of mitochondrial complex activity suggest that there is a strong effect of the cafeteria diet at nearly all ZTs and that GSPE is able to restore them at discrete ZTs above all in the diurnal treatment. Additionally, it seems that the dynamics processes (fission and fusion) are more easily modulated, at certain ZTs, by GSPE than mitochondrial biogenesis.

3.6. GSPE Treatment Strongly Increases Concentrations of Metabolites of Tricarboxylic Acid Cycles in CAF-Fed Rats

As a key regulator of metabolic pathways, mitochondria produce metabolites that are necessary for energy homeostasis, cell survival and proliferation. Therefore, six metabolites involved in one of the most important mitochondrial pathways, TCA cycle, were studied. When analyzing diurnal treatment (ZT0), Figure 8A shows that GSPE-treated animals exhibited a higher concentration of fumaric ($p = 0.039$), a-ketoglutaric ($p = 0.013$), malic ($p = 0.047$) and pyruvic acid ($p = 0.024$) metabolites at ZT1 than the STD and/or CAF-VH groups.

On the other hand, in the CAF-VH group at the same time point, a decrease in the concentration of these metabolites was observed. At ZT7 in the CAF-GSPE group, the concentration of the metabolites mentioned above remained high, whereas succinic acid levels began to rise ($p = 0.047$). On the other hand, 13 h after dosage, at ZT13, GSPE-treated animals displayed an important decrease in the concentration of metabolites, which continued in the same way at ZT19. CAF-VH animals showed lower concentrations of pyruvic acid than STD-VH animals at ZT13 ($p = 0.040$), as well as lower concentration of a-ketoglutaric acid than CAF-GSPE animals at ZT19 ($p = 0.046$). The lowest concentration was seen in STD animals at ZT19, where some metabolites values were two-fold lower than in CAF-GSPE animals (Supplementary Materials, Table S4.1).

This could mean that the cafeteria treatment depletes TCA metabolites due to the rich ATP environment arresting TCA and re-orienting these metabolites through anabolic purposes, i.e., lipid synthesis. On the other hand, GSPE could be partially restore this metabolic pathway. This is in agreement with the fact that the major restoration respiratory complexes induced by GSPE were also seen at several ZTs but always in the morning treatment.

Regarding nocturnal treatment (ZT12), fumaric, a-ketoglutaric, malic and citric acid metabolites exhibit a higher concentration from ZT1 to ZT7 in VH-, CAF- and STD-diet animals; whereas in the case of GSPE-treated rats, higher amounts of these compounds were seen from ZT19 to ZT1, 6 h earlier than in the vehicles. What is more, lower concentrations of the aforementioned metabolites were seen from ZT13 to ZT19 in CAF-VH and STD-VH groups, while for CAF-GSPE animals, the lowest amount of these compounds was observed from ZT7 to ZT13 (Figure 8B). Succinic acid was significantly increased at ZT13 when treated with GSPE ($p = 0.005$), whereas pyruvic acid exhibited a significant decrease ($p = 0.008$) compared to CAF and STD VH, respectively (Supplementary Materials, Table S4.2). In this case, the fact that the rats were active in the nocturnal phase could explain the indistinctive results among treatments due to the fact that in this period, the ATP requirements increased, promoting TCA activity in all experimental groups. Nevertheless, we must also take into account that cafeteria treatment decreased complex activity.

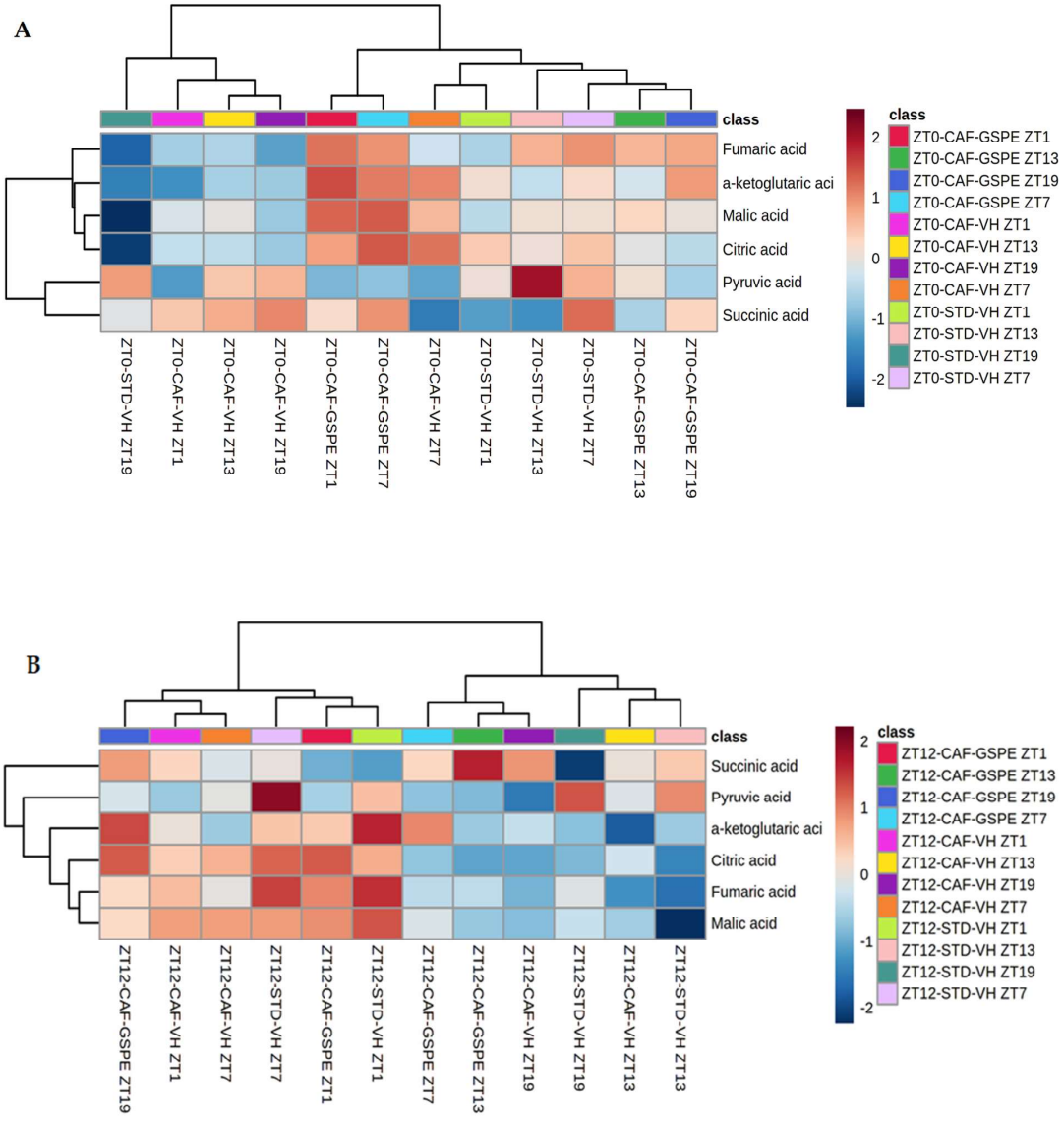

Figure 8. Heatmaps of TCA cycle metabolites in the liver. Rats were fed an STD or CAF diet and received a daily dosage of vehicle or GSPE in the morning (ZT0) (**A**) or at night (ZT12) (**B**). After 9 weeks, the rats were sacrificed at 9 a.m. (ZT1), 3 p.m. (ZT7), 9 p.m. (ZT13) or 3 a.m. (ZT19).

4. Discussion

It is well known that polyphenols can mitigate the detrimental effects of a CAF diet by decreasing body weight, blood pressure and blood glucose, as well as by improving lipid metabolism [31]. In this sense, our results show that GSPE is able to decrease body-weight gain and improve blood glucose levels of obese rats.

Furthermore, it has been previously shown that a dose of 25 mg GSPE/kg body weight per day administered for 30 days improved the homeostasis model assessment-insulin resistance index (HOMA-index). This was accompanied by downregulation of Pparg2, Glut4 and Irs1 in mesenteric white adipose tissue. Similarly, a chronic GSPE treatment of insulin-resistant 3T3-L1 adipocytes downregulated the mRNA levels of those adipocyte markers, although cells were still able to respond to the acute stimulation of glucose uptake.

This indicates that the 25 mg/kg body weight per day GSPE treatment has a positive long-term effect on glucose homeostasis [48].

On the other hand, a limitation of our study is the number of animals used per group, although similar experiments on circadian rhythms [54–57] also used a low number of animals (around four) for each experimental time point.

Several lines of evidence suggest that the consumption of a high-fat diet causes misalignment of the liver molecular clock [58]. In this regard, our results indicate that a CAF diet causes a disruption in hepatic circadian-clock genes, as acrophases are shifted and rhythmicity of some core-clock genes are lost. Ribas-Latre and collaborators [59] studied the effect of GSPE on the clock system in HepG2 cells. According to their study, *Bmal1* was found to be the most GSPE-sensitive gene, since GSPE treatment strongly increased *Bmal1* expression. It is noteworthy that GSPE was also found to enhance the transcriptional activity of *Rorα*, which is an activator of *Bmal1* expression, suggesting that it might be responsible for the modulation of *Bmal1* by GSPE. This is in agreement with our results, as GSPE treatment is capable of restoring hepatic circadian misalignment of *Rorα* in both diurnal and nocturnal treatments, as well as of *Bmal1*, *Cry1* and *Per2* in animals treated at night (ZT12). Interestingly, Ribas-Latre et. al. [59] conducted another study where they administered GSPE in the morning (ZT0) or at night (ZT12) to healthy rats.

When analyzing the expression of clock genes in the liver, they observed that the effect of GSPE on *Bmal1* only occurred in night-treated animals (ZT12) [60]. Hence, they postulated that GSPE could act as an adaptive element in the liver, enhancing the energy profile of rats and improving mitochondrial function and oxidation at night, during the active phase, as rats are nocturnal animals. Interestingly, we also found a major corrective effect on the misalignment of the circadian rhythm induced by a cafeteria diet in the nocturnal treatment (ZT12) in comparison to the diurnal treatment (ZT0). Additionally, this correlates with the increase in parameters suggestive of a fussed morphology at night. In this sense, it was observed that the morphology of the mitochondrial network shows circadian rhythmicity in cultured fibroblast, shifting from a tubular mitochondrial network at 16 h after synchronization to a greatly fragmented network 28 h after, coinciding with the rhythmicity of ATP content and oxidative phosphorylation. Moreover, *Per1*/*Per2* mutant mice lack these rhythms, and therefore, ATP levels are not cyclic, and the mitochondrial network remains fragmented at all time points [24]. Likewise, liver-specific *Bmal1* mutant mice exhibit swollen mitochondria, parallel with reduced levels of mitophagy proteins *Fis1* and *Pink1*, in addition to the inability to adapt to different nutritional conditions [22]. Furthermore, as has already been exposed, levels of mitochondrial fusion proteins *Mfn1* and *Opa1* are reduced in *Bmal1* knockout mice [4].

On the other hand, the recovery of mitochondrial complexes at ZT13 of diurnal GSPE administration are in agreement with changes in mitochondrial morphology (*Mfn1*, *Mfn2* and *Fis1*). In this regard, it has been shown that structural remodeling can act as a compensatory mechanism for inefficient mitochondrial ATP synthesis [61].

NAFLD is considered the hepatic manifestation of metabolic syndrome [62], where oxidative stress is the main mechanism of liver injury, leading to hepatic inflammation and fibrosis. As the major contributor to oxidative stress, mitochondrial dysfunction plays a significant role in this pathogenesis [63]. Thus, improper functioning of mitochondria could lead to the development of metabolic diseases, such as obesity, type 2 diabetes mellitus and NAFLD. Moreover, a large number of liver diseases are characterized by mitochondrial alterations [52]. Our results demonstrate that a CAF diet promotes a significant alteration in hepatic mitochondrial function, with three of the electron-transport-chain (ETC) components (complex I, II and III) exhibiting a decrease in activity. The ETC is the main site of ATP generation; therefore, we demonstrated that mitochondrial respiratory activity is hugely altered in rats consuming a CAF diet. Moreover, our results suggest that GSPE treatment could reduce, at least partially, the negative effect of the CAF diet over mitochondrial function. This last finding is in agreement with previously published studies about the

beneficial effect of chronic supplementation with proanthocyanidins over mitochondrial activity and functionality in brown adipose tissue and skeletal muscle of obese rats [35,36].

To maintain healthy mitochondria, mitochondria are continuously formed and removed through dynamic processes called mitochondrial fission, fusion, mitophagy and biogenesis [64].Our results showed a differential effect on expression of fusion genes *Mfn1* and *Mfn2*, depending on the time of treatment administration. While in the morning treatment (ZT0), CAF was able to increase the expression of these genes and GSPE maintained similar expression levels as in healthy rats, in nocturnal treatment (ZT12), an increase in fusion gene expression was observed in GSPE-treated animals at ZT1. An excess of caloric intake causes an increase in glucose levels, which triggers the production of ROS, thereby generating mitochondrial oxidative stress [16]. It has been previously shown that mitochondrial oxidative stress causes mitochondrial fragmentation via differential modulation of mitochondrial fission–fusion proteins. On one side, some authors suggest overexpression of *Mfn1* and/or *Mfn2* causes mitochondrial dysfunction and cell death [65]. However, other authors demonstrate that overexpression of *Mfn2* improves liver fibrosis in hepatic stellate cells of mice [66]. In this regard, our results suggest that GSPE could enhance fusion expression when administrated at night (ZT12) to alleviate stress caused by a CAF-diet, thereby combining contents of partially damaged mitochondria as a form of complementation. Fission is necessary to create new mitochondria but also contributes to quality control by enabling the deletion of damaged mitochondria and could promote apoptosis during high levels of cellular stress. However, disruption of fission machinery is implicated in the development of neurodegenerative and metabolic diseases [67]. Our results show that the expression levels of fission genes in GSPE-treated rats were similar to those of STD-diet rats, whereas CAF-VH rats exhibited an increase in expression of these genes at most death time points. These findings are in accordance with several studies in which high-fat-diet-induced obesity mice showed overexpression of mitochondrial fission genes *Drp1* and *Fis1*, whereas inhibition or disruption of these genes led to an improvement in insulin resistance and mitochondrial dysfunction in skeletal muscle [7]. Furthermore, a decrease in mitochondrial fission has also been found to ameliorate hepatic steatosis and to protect the liver against metabolic deterioration in a murine model of NAFLD [68,69].

Food-derived fatty acids, carbohydrates and proteins are oxidized inside mitochondria via β-oxidation and TCA cycle [63]. Thereby, TCA cycle, also known as Krebs cycle, plays an important role as an energy supply for metabolism. Moreover, it produces important intermediates involved in gluconeogenesis, lipolysis and neurotransmitter synthesis, among others. It is also known that TCA cycle and the ETC are intimately related, since byproduct generation of 3 nicotinamide adenine dinucleotide (NADH) and 1 flavin adenine dinucleotide (FADH2) by TCA cycle feeds ETC complex I (NADH dehydrogenase) and complex II succinate dehydrogenase (SDH), respectively. Furthermore, oxidation of the aforementioned byproducts in complexes I and II is necessary to maintain the proper functioning of the TCA cycle [70]. For these reasons, we evaluated the concentration of the TCA cycle metabolites in the liver and observed higher concentrations of these metabolites in morning GSPE-treated animals (ZT0). It is possible that a correlation exists between this result and the tendency to increase complex I activity when GSPE was supplied in the morning at ZT0. Moreover, not only are concentrations of these metabolites strongly deceased in CAF-fed animals in both diurnal and nocturnal treatments, but mitochondrial respiratory activity is also hugely altered. This could be partially attributed to the accumulation of NADH due to malfunctioning of ETC. The regulatory enzymes of the TCA cycle are inhibited by NADH. Therefore, we suggest that the TCA cycle turns off in CAF-fed animals as a consequence of ETC dysfunction. Interestingly, we observed that as expression of *Fis1* and/or *Drp1* in CAF-VH group decreases, concentrations of TCA metabolites increase at the same time of death. In the same way, an enhancement of fission gene expression in CAF-VH animals correlates with a decrease in TCA metabolite concentrations. Considering the significant role of mitochondrial dynamics and respiratory-chain activity in mitochondrial and cellular functions, it could be suggested that obesity and excessive caloric intake cause an

imbalance of these processes, leading to mitochondrial dysfunction and contributing to the development of hepatic metabolic impairment.

Several studies go along with the idea that maintaining circadian rhythm is essential, as it plays a pivotal role in hepatic metabolism and mitochondrial function [20]. In this sense, Kim and collaborators [71] demonstrated liver-specific inhibition of *Rorα* induced abnormal mitochondrial function, thus worsening NAFLD in mice with a high-fat diet. They evidenced *Rorα* that increased the rate of oxygen consumption and the expression of genes involved in mitochondrial quality control [71]. Moreover, Jacobi and colleges revealed circadian control of *Bmal1* over expression of mitochondrial-dynamics-related genes. Their study exposed that the hepatic deletion of *Bmal1* causes oxidative stress and damages mitochondria [22]. In this sense, our results show that circadian oscillations of *Rorα* and *Bmal1* were disrupted in the CAF-diet group and that GSPE was able to restore this disruption of both clock genes when treated at night (ZT12). Therefore, we can suggest that chronic consumption of GSPE could be useful to ameliorate obesity-induced mitochondrial dysfunction by improving the disturbance of circadian rhythm.

Finally, in this experiment, GSPE was administered at 25 mg of GSPE/ kg of body weight. This dose, using a translation of animal to human doses [72] and estimating the daily intake for a 70 kg human, corresponds to an intake of 284 mg of GSPE/day. This GSPE intake can be achieved in humans with a polyphenol-rich diet. For example, in Spanish adults, the mean dietary flavonoid intake is 313.26 mg/day, with proanthocyanidins comprising 60.1% [73]. Although experimental data obtained in rats cannot be directly extrapolated to humans, the fact that GSPE is able to restore the rhythm of clock hepatic genes (given this correction more evident on the nocturnal treatment), as well as other mitochondrial parameters and TCA-related metabolites, suggests that the inclusion of proanthocyanidin-rich foods in the diets of obese humans could be a good strategy to improve their hepatic circadian and mitochondrial alterations.

5. Conclusions

In summary, dietary supplementation with GSPE caused a decrease in body-weight gain in animals fed a CAF diet. Moreover, other significant metabolic conditions associated with metabolic syndrome were also improved after GSPE administration. In particular, an improvement in serum glucose levels was observed compared to CAF non-treated animals. Furthermore, GSPE was able to restore the rhythmicity of some core-clock genes in the liver that were totally disrupted by a CAF diet. In addition, our results demonstrate significant alteration in hepatic mitochondrial function caused by an obesogenic diet intake, such as a decrease in mitochondrial complex I, II and II + III activities; an increase in the expression of mitochondrial fission genes, which can result in fragmented mitochondria that are susceptible to apoptosis; and a strong decease in the concentrations of TCA cycle metabolites. In this sense, our results suggest that GSPE treatment could ameliorate the effect of the CAF diet over mitochondrial function. Notably, the major improvements in GSPE supplementations were seen at the ZT12 dosage. This may be partially explained by the fact that GSPE enhances the energy profile of rats and improves mitochondrial function and oxidation in the liver at night, during the active phase when rats are metabolically more active, as rats are nocturnal animals. Nevertheless, further studies are needed to elucidate the molecular mechanisms involved in these events.

Supplementary Materials: The following are available online at https://www.mdpi.com/article/10.3390/nu14040774/s1, Table S1: Circadian parameters of liver clock genes, Table S2: Comparison of circadian parameters of liver clock genes between groups, Table S3: Measurement of ETC components in the liver, Table S4.1: Metabolites of the TCA cycle in the liver at ZT0, Table S4.2: Metabolites of the TCA cycle in the liver at ZT12.

Author Contributions: Conceptualization, M.M., M.J.S. and B.M.; methodology, R.M.R., A.J.C.-E., J.R.S.-R., M.C.-P., G.A., J.A.-R., B.M. and M.J.S.; software, R.M.R. and J.R.S.-R.; validation, M.M., C.F.-C. and F.C.; formal analysis, M.M.; investigation, R.M.R., A.J.C.-E. and J.R.S.-R.; resources, M.M., B.M., C.F.-C. and F.C.; data curation, A.J.C.-E. and M.M.; writing—original draft preparation R.M.R., A.J.C.-E., J.R.S.-R. and M.M.; writing—review and editing, R.M.R., A.J.C.-E., J.R.S.-R. and M.M.; visualization, M.M., B.M., C.F.-C. and F.C.; supervision, M.M.; project administration, M.M. and B.M.; funding acquisition, A.J.C.-E., M.M., B.M. and M.J.S. All authors have read and agreed to the published version of the manuscript.

Funding: This research was funded by the Spanish Ministry of Economy and Competitiveness (MINECO), AGL2016-77105-R (CHRONOFOOD project). R.M.R. is recipient of a predoctoral fellowship from Universitat Rovira i Virgili—Martí i Franquès, grant number 2018PMF-PIPF-11. A.J.C.E. is recipient of a predoctoral fellowship from Universitat Rovira i Virgili—Martí i Franquès. M.C.P. is recipient of a predoctoral fellowship from the Catalan Government, grant number 2021FI_B2 00150. J.S.R. is supported by the Ministry of Science and Innovation (MICINN) and the European Social Fund (ESF), grant number: BES-2017-080919. M.M. is a Serra-Hunter fellow.

Institutional Review Board Statement: All animal care and experimental protocols involving animals were approved by the Ethics Review Committee for Animal Experimentation of the Universitat Rovira i Virgili (reference number 9495, 18 September 2019) and were carried out in accordance with Directive 86/609EEC of the Council of the European Union and the procedure established by the Departament d'Agricultura, Ramaderia i Pesca of the Generalitat de Catalunya.

Informed Consent Statement: Not applicable.

Data Availability Statement: The data presented in this study are available on request from the corresponding author. The data are not publicly available due to lack of platform to publish them.

Acknowledgments: The authors would like to thank to Niurka Llópiz and Rosa Pastor (Tarragona), as well as Beatrice Bonafos (Montpellier), for their help and technical assistance. The authors would also like to thank to the OPEN2021 program of the Univeristat Rovira i Virgili.

Conflicts of Interest: The authors declare no conflict of interest. The funders had no role in the design of the study; in the collection, analyses, or interpretation of data; in the writing of the manuscript, or in the decision to publish the results.

References

1. Hüttemann, M.; Helling, S.; Sanderson, T.H.; Sinkler, C.; Samavati, L.; Mahapatra, G.; Varughese, A.; Lu, G.; Liu, J.; Ramzan, R.; et al. Regulation of Mitochondrial Respiration and Apoptosis through Cell Signaling: Cytochrome c Oxidase and Cytochrome c in Ischemia/Reperfusion Injury and Inflammation. *Biochim. Biophys. Acta Bioenerg.* **2012**, *1817*, 598–609. [CrossRef] [PubMed]
2. Brand, M.D.; Orr, A.L.; Perevoshchikova, I.V.; Quinlan, C.L. The Role of Mitochondrial Function and Cellular Bioenergetics in Ageing and Disease. *Br. J. Dermatol.* **2013**, *169*, 1–8. [CrossRef]
3. Schrepfer, E.; Scorrano, L. Mitofusins, from Mitochondria to Metabolism. *Mol. Cell* **2016**, *61*, 683–694. [CrossRef] [PubMed]
4. Kohsaka, A.; Das, P.; Hashimoto, I.; Nakao, T.; Deguchi, Y.; Gouraud, S.S.; Waki, H.; Muragaki, Y.; Maeda, M. The Circadian Clock Maintains Cardiac Function by Regulating Mitochondrial Metabolism in Mice. *PLoS ONE* **2014**, *9*, e112811. [CrossRef] [PubMed]
5. Molina, A.J.A.; Wikstrom, J.D.; Stiles, L.; Las, G.; Mohamed, H.; Elorza, A.; Walzer, G.; Twig, G.; Katz, S.; Corkey, B.E.; et al. Mitochondrial Networking Protects β-Cells from Nutrient-Induced Apoptosis. *Diabetes* **2009**, *58*, 2303–2315. [CrossRef] [PubMed]
6. Gomes, L.C.; Di Benedetto, G.; Scorrano, L. During Autophagy Mitochondria Elongate, Are Spared from Degradation and Sustain Cell Viability. *Nat. Cell Biol.* **2011**, *13*, 589–598. [CrossRef] [PubMed]
7. Jheng, H.-F.; Tsai, P.-J.; Guo, S.-M.; Kuo, L.-H.; Chang, C.-S.; Su, I.-J.; Chang, C.-R.; Tsai, Y.-S. Mitochondrial Fission Contributes to Mitochondrial Dysfunction and Insulin Resistance in Skeletal Muscle. *Mol. Cell. Biol.* **2012**, *32*, 309–319. [CrossRef]
8. Eura, Y.; Ishihara, N.; Yokota, S.; Mihara, K. Two Mitofusin Proteins, Mammalian Homologues of FZO, with Distinct Functions Are Both Required for Mitochondrial Fusion. *J. Biochem.* **2003**, *134*, 333–344. [CrossRef]
9. Olichon, A.; Emorine, L.J.; Descoins, E.; Pelloquin, L.; Brichese, L.; Gas, N.; Guillou, E.; Delettre, C.; Valette, A.; Hamel, C.P.; et al. The Human Dynamin-Related Protein OPA1 Is Anchored to the Mitochondrial Inner Membrane Facing the Inter-Membrane Space. *FEBS Lett.* **2002**, *523*, 171–176. [CrossRef]
10. Scorrano, L. Keeping Mitochondria in Shape: A Matter of Life and Death. *European J. Clin. Investig.* **2013**, *43*, 886–893. [CrossRef]
11. Simmons, R.A.; Suponitsky-Kroyter, I.; Selak, M.A. Progressive Accumulation of Mitochondrial DNA Mutations and Decline in Mitochondrial Function Lead to β-Cell Failure. *J. Biol. Chem.* **2005**, *280*, 28785–28791. [CrossRef]

12. Price, N.L.; Gomes, A.P.; Ling, A.J.Y.; Duarte, F.V.; Martin-Montalvo, A.; North, B.J.; Agarwal, B.; Ye, L.; Ramadori, G.; Teodoro, J.S.; et al. SIRT1 Is Required for AMPK Activation and the Beneficial Effects of Resveratrol on Mitochondrial Function. *Cell Metab.* **2012**, *15*, 675–690. [CrossRef]
13. Dey, A.; Swaminathan, K. Hyperglycemia-Induced Mitochondrial Alterations in Liver. *Life Sci.* **2010**, *87*, 197–214. [CrossRef] [PubMed]
14. Civitarese, A.E.; Ravussin, E. Minireview: Mitochondrial Energetics and Insulin Resistance. *Endocrinology* **2008**, *149*, 950–954. [CrossRef] [PubMed]
15. Szendroedi, J.; Phielix, E.; Roden, M. The Role of Mitochondria in Insulin Resistance and Type 2 Diabetes Mellitus. *Nat. Rev. Endocrinol.* **2012**, *8*, 92–103. [CrossRef] [PubMed]
16. Rovira-Llopis, S.; Bañuls, C.; Diaz-Morales, N.; Hernandez-Mijares, A.; Rocha, M.; Victor, V.M. Mitochondrial Dynamics in Type 2 Diabetes: Pathophysiological Implications. *Redox Biol.* **2017**, *11*, 637–645. [CrossRef] [PubMed]
17. Degli Esposti, D.; Hamelin, J.; Bosselut, N.; Saffroy, R.; Sebagh, M.; Pommier, A.; Martel, C.; Lemoine, A. Mitochondrial Roles and Cytoprotection in Chronic Liver Injury. *Biochem. Res. Int.* **2012**, *2012*, 387626. [CrossRef] [PubMed]
18. Tahara, Y.; Shibata, S. Circadian Rhythms of Liver Physiology and Disease: Experimental and Clinical Evidence. *Nat. Rev. Gastroenterol. Hepatol.* **2016**, *13*, 217–226. [CrossRef] [PubMed]
19. Shetty, A.; Hsu, J.W.; Manka, P.P.; Syn, W.K. Role of the Circadian Clock in the Metabolic Syndrome and Nonalcoholic Fatty Liver Disease. *Dig. Dis. Sci.* **2018**, *63*, 3187–3206. [CrossRef] [PubMed]
20. Reinke, H.; Asher, G. Circadian Clock Control of Liver Metabolic Functions. *Gastroenterology* **2016**, *150*, 574–580. [CrossRef] [PubMed]
21. Sardon Puig, L.; Valera-Alberni, M.; Cantó, C.; Pillon, N.J. Circadian Rhythms and Mitochondria: Connecting the Dots. *Front. Genet.* **2018**, *9*, 452. [CrossRef] [PubMed]
22. Jacobi, D.; Liu, S.; Burkewitz, K.; Kory, N.; Knudsen, N.H.; Alexander, R.K.; Unluturk, U.; Li, X.; Kong, X.; Hyde, A.L.; et al. Hepatic Bmal1 Regulates Rhythmic Mitochondrial Dynamics and Promotes Metabolic Fitness. *Cell Metab.* **2015**, *22*, 709–720. [CrossRef] [PubMed]
23. Uchiyama, Y. Circadian Alterations in Tubular Structures on the Outer Mitochondrial Membrane of Rat Hepatocytes. *Cell Tissue Res.* **1981**, *214*, 519–527. [CrossRef] [PubMed]
24. Schmitt, K.; Grimm, A.; Dallmann, R.; Oettinghaus, B.; Restelli, L.M.; Witzig, M.; Ishihara, N.; Mihara, K.; Ripperger, J.A.; Albrecht, U.; et al. Circadian Control of DRP1 Activity Regulates Mitochondrial Dynamics and Bioenergetics. *Cell Metab.* **2018**, *27*, 657–666.e5. [CrossRef]
25. Zhou, D.; Wang, Y.; Chen, L.; Jia, L.; Yuan, J.; Sun, M.; Zhang, W.; Wang, P.; Zuo, J.; Xu, Z.; et al. Evolving Roles of Circadian Rhythms in Liver Homeostasis and Pathology. *Oncotarget* **2016**, *7*, 8625–8639. [CrossRef] [PubMed]
26. Mukherji, A.; Bailey, S.M.; Staels, B.; Baumert, T.F. The Circadian Clock and Liver Function in Health and Disease. *J. Hepatol.* **2019**, *71*, 200–211. [CrossRef] [PubMed]
27. Mazzoccoli, G.; De Cosmo, S.; Mazza, T. The Biological Clock: A Pivotal Hub in Non-Alcoholic Fatty Liver Disease Pathogenesis. *Front. Physiol.* **2018**, *9*, 193. [CrossRef] [PubMed]
28. Cheynier, V. Polyphenols in Foods Are More Complex than Often Thought. *Am. J. Clin. Nutr.* **2005**, *81*, 223S–229S. [CrossRef]
29. Fraga, C.G.; Croft, K.D.; Kennedy, D.O.; Tomás-Barberán, F.A. The Effects of Polyphenols and Other Bioactives on Human Health. *Food Funct.* **2019**, *10*, 514–528. [CrossRef] [PubMed]
30. Mi, Y.; Qi, G.; Fan, R.; Ji, X.; Liu, Z.; Liu, X. EGCG Ameliorates Diet-Induced Metabolic Syndrome Associating with the Circadian Clock. *Biochim. Biophys. Acta Mol. Basis Dis.* **2017**, *1863*, 1575–1589. [CrossRef]
31. Chiva-Blanch, G.; Badimon, L. Effects of Polyphenol Intake on Metabolic Syndrome: Current Evidences from Human Trials. *Oxidative Med. Cell. Longev.* **2017**, *2017*, 5812401. [CrossRef]
32. Sun, L.; Wang, Y.; Song, Y.; Cheng, X.R.; Xia, S.; Rahman, M.R.T.; Shi, Y.; Le, G. Resveratrol Restores the Circadian Rhythmic Disorder of Lipid Metabolism Induced by High-Fat Diet in Mice. *Biochem. Biophys. Res. Commun.* **2015**, *458*, 86–91. [CrossRef]
33. Qi, G.; Mi, Y.; Liu, Z.; Fan, R.; Qiao, Q.; Sun, Y.; Ren, B.; Liu, X. Dietary Tea Polyphenols Ameliorate Metabolic Syndrome and Memory Impairment via Circadian Clock Related Mechanisms. *J. Funct. Foods* **2017**, *34*, 168–180. [CrossRef]
34. Qi, G.; Mi, Y.; Fan, R.; Zhao, B.; Ren, B.; Liu, X. Tea Polyphenols Ameliorates Neural Redox Imbalance and Mitochondrial Dysfunction via Mechanisms Linking the Key Circadian Regular Bmal1. *Food Chem. Toxicol.* **2017**, *110*, 189–199. [CrossRef] [PubMed]
35. Pajuelo, D.; Fernández-Iglesias, A.; Díaz, S.; Quesada, H.; Arola-Arnal, A.; Bladé, C.; Salvadó, J.; Arola, L. Improvement of Mitochondrial Function in Muscle of Genetically Obese Rats after Chronic Supplementation with Proanthocyanidins. *J. Agric. Food Chem.* **2011**, *59*, 8491–8498. [CrossRef] [PubMed]
36. Pajuelo, D.; Quesada, H.; Díaz, S.; Fernández-Iglesias, A.; Arola-Arnal, A.; Bladé, C.; Salvadó, J.; Arola, L. Chronic Dietary Supplementation of Proanthocyanidins Corrects the Mitochondrial Dysfunction of Brown Adipose Tissue Caused by Diet-Induced Obesity in Wistar Rats. *Br. J. Nutr.* **2012**, *107*, 170–178. [CrossRef]
37. Serra, A.; MacI, A.; Romero, M.P.; Valls, J.; Bladé, C.; Arola, L.; Motilva, M.J. Bioavailability of Procyanidin Dimers and Trimers and Matrix Food Effects in in Vitro and in Vivo Models. *Br. J. Nutr.* **2010**, *103*, 944–952. [CrossRef] [PubMed]
38. Livak, K.J.; Schmittgen, T.D. Analysis of Relative Gene Expression Data Using Real-Time Quantitative PCR and the 2(-Delta Delta C(T)) Method. *Methods* **2001**, *25*, 402–408. [CrossRef]

39. Bligh, E.G.; Dyer, W.J. A rapid method of total lipid extraction and purification. *Can. J. Biochem. Physiol.* **1959**, *37*, 911–917. [CrossRef] [PubMed]
40. Srere, P.A. Citrate Synthase. EC 4.1.3.7. Citrate Oxaloacetate-Lyase (CoA-Acetylating)]. *Methods Enzymol.* **1969**, *13*, 3–11. [CrossRef]
41. Janssen, A.J.M.; Trijbels, F.J.M.; Sengers, R.C.A.; Smeitink, J.A.M.; Van Den Heuvel, L.P.; Wintjes, L.T.M.; Stoltenborg-Hogenkamp, B.J.M.; Rodenburg, R.J.T. Spectrophotometric Assay for Complex I of the Respiratory Chain in Tissue Samples and Cultured Fibroblasts. *Clin. Chem.* **2007**, *53*, 729–734. [CrossRef] [PubMed]
42. Rustin, P.; Chretien, D.; Bourgeron, T.; Gérard, B.; Rötig, A.; Saudubray, J.M.; Munnich, A. Biochemical and Molecular Investigations in Respiratory Chain Deficiencies. *Clin. Chim. Acta* **1994**, *228*, 35–51. [CrossRef]
43. Wharton, D.C.; Tzagoloff, A. Cytochrome Oxidase from Beef Heart Mitochondria. *Methods Enzymol.* **1967**, *10*, 245–250. [CrossRef]
44. Cajka, T.; Fiehn, O. Toward Merging Untargeted and Targeted Methods in Mass Spectrometry-Based Metabolomics and Lipidomics. *Anal. Chem.* **2016**, *88*, 524–545. [CrossRef]
45. Moškon, M. CosinorPy: A Python Package for Cosinor-Based Rhythmometry. *BMC Bioinform.* **2020**, *21*, 485. [CrossRef] [PubMed]
46. Xia, J.; Psychogios, N.; Young, N.; Wishart, D.S. MetaboAnalyst: A Web Server for Metabolomic Data Analysis and Interpretation. *Nucleic Acids Res.* **2009**, *37*, W652–W660. [CrossRef]
47. Pons, Z.; Margalef, M.; Bravo, F.I.; Arola-Arnal, A.; Muguerza, B. Acute Administration of Single Oral Dose of Grape Seed Polyphenols Restores Blood Pressure in a Rat Model of Metabolic Syndrome: Role of Nitric Oxide and Prostacyclin. *Eur. J. Nutr.* **2016**, *55*, 749–758. [CrossRef]
48. Montagut, G.; Bladé, C.; Blay, M.; Fernández-Larrea, J.; Pujadas, G.; Salvadó, M.J.; Arola, L.; Pinent, M.; Ardévol, A. Effects of a Grapeseed Procyanidin Extract (GSPE) on Insulin Resistance. *J. Nutr. Biochem.* **2010**, *21*, 961–967. [CrossRef] [PubMed]
49. Pons, Z.; Margalef, M.; Bravo, F.I.; Arola-Arnal, A.; Muguerza, B. Chronic Administration of Grape-Seed Polyphenols Attenuates the Development of Hypertension and Improves Other Cardiometabolic Risk Factors Associated with the Metabolic Syndrome in Cafeteria Diet-Fed Rats. *Br. J. Nutr.* **2017**, *117*, 200–208. [CrossRef] [PubMed]
50. Serrano, J.; Casanova-Martí, À.; Blay, M.; Terra, X.; Ardévol, A.; Pinent, M. Defining Conditions for Optimal Inhibition of Food Intake in Rats by a Grape-Seed Derived Proanthocyanidin Extract. *Nutrients* **2016**, *8*, 652. [CrossRef]
51. Wei, Y.; Rector, R.S.; Thyfault, J.P.; Ibdah, J.A. Nonalcoholic Fatty Liver Disease and Mitochondrial Dysfunction. *World J. Gastroenterol.* **2008**, *14*, 193–199. [CrossRef] [PubMed]
52. Crescenzo, R.; Bianco, F.; Mazzoli, A.; Giacco, A.; Liverini, G.; Iossa, S. A Possible Link between Hepatic Mitochondrial Dysfunction and Diet-Induced Insulin Resistance. *Eur. J. Nutr.* **2016**, *55*, 1–6. [CrossRef] [PubMed]
53. Prasun, P.; Ginevic, I.; Oishi, K. Mitochondrial Dysfunction in Nonalcoholic Fatty Liver Disease and Alcohol Related Liver Disease. *Transl. Gastroenterol. Hepatol.* **2021**, *6*, 4. [CrossRef] [PubMed]
54. Murakami, M.; Tognini, P.; Liu, Y.; Eckel-Mahan, K.L.; Baldi, P.; Sassone-Corsi, P. Gut Microbiota Directs PPARγ-Driven Reprogramming of the Liver Circadian Clock by Nutritional Challenge. *EMBO Rep.* **2016**, *17*, 1292–1303. [CrossRef] [PubMed]
55. Dyar, K.A.; Lutter, D.; Artati, A.; Ceglia, N.J.; Liu, Y.; Armenta, D.; Jastroch, M.; Schneider, S.; de Mateo, S.; Cervantes, M.; et al. Atlas of Circadian Metabolism Reveals System-Wide Coordination and Communication between Clocks. *Cell* **2018**, *174*, 1571. [CrossRef]
56. Ribas-Latre, A.; Santos, R.B.; Fekry, B.; Tamim, Y.M.; Shivshankar, S.; Mohamed, A.M.T.; Baumgartner, C.; Kwok, C.; Gebhardt, C.; Rivera, A.; et al. Cellular and Physiological Circadian Mechanisms Drive Diurnal Cell Proliferation and Expansion of White Adipose Tissue. *Nat. Commun.* **2021**, *12*, 3482. [CrossRef] [PubMed]
57. Greco, C.M.; Koronowski, K.B.; Smith, J.G.; Shi, J.; Kunderfranco, P.; Carriero, R.; Chen, S.; Samad, M.; Welz, P.S.; Zinna, V.M.; et al. Integration of Feeding Behavior by the Liver Circadian Clock Reveals Network Dependency of Metabolic Rhythms. *Sci. Adv.* **2021**, *7*, eabi7828. [CrossRef] [PubMed]
58. Branecky, K.L.; Niswender, K.D.; Pendergast, J.S. Disruption of Daily Rhythms by High-Fat Diet Is Reversible. *PLoS ONE* **2015**, *10*, e0137970. [CrossRef] [PubMed]
59. Ribas-Latre, A.; Del Bas, J.M.; Baselga-Escudero, L.; Casanova, E.; Arola-Arnal, A.; Salvadó, M.J.; Bladé, C.; Arola, L. Dietary Proanthocyanidins Modulate the Rhythm of BMAL1 Expression and Induce RORα Transactivation in HepG2 Cells. *J. Funct. Foods* **2015**, *13*, 336–344. [CrossRef]
60. Ribas-Latre, A.; Baselga-Escudero, L.; Casanova, E.; Arola-Arnal, A.; Salvadó, M.-J.; Bladé, C.; Arola, L. Dietary Proanthocyanidins Modulate BMAL1 Acetylation, Nampt Expression and NAD Levels in Rat Liver. *Sci. Rep.* **2015**, *5*, 10954. [CrossRef] [PubMed]
61. Jarosz, J.; Ghosh, S.; Delbridge, L.M.D.; Petzer, A.; Hickey, A.J.R.; Crampin, E.J.; Hanssen, E.; Rajagopal, V. Changes in Mitochondrial Morphology and Organization Can Enhance Energy Supply from Mitochondrial Oxidative Phosphorylation in Diabetic Cardiomyopathy. *Am. J. Physiol. Cell Physiol.* **2017**, *312*, C190–C197. [CrossRef] [PubMed]
62. Farrell, G.C.; Larter, C.Z. Nonalcoholic Fatty Liver Disease: From Steatosis to Cirrhosis. *Hepatology* **2006**, *43*, S99–S112. [CrossRef] [PubMed]
63. García-Ruiz, C.; Fernández-Checa, J.C. Mitochondrial Oxidative Stress and Antioxidants Balance in Fatty Liver Disease. *Hepatol. Commun.* **2018**, *2*, 1425–1439. [CrossRef] [PubMed]
64. Detmer, S.A.; Chan, D.C. Functions and Dysfunctions of Mitochondrial Dynamics. *Nat. Rev. Mol. Cell Biol.* **2007**, *8*, 870–879. [CrossRef]

65. Huang, P.; Yu, T.; Yoon, Y. Mitochondrial Clustering Induced by Overexpression of the Mitochondrial Fusion Protein Mfn2 Causes Mitochondrial Dysfunction and Cell Death. *Eur. J. Cell Biol.* **2007**, *86*, 289–302. [CrossRef]
66. Zhu, H.; Shan, Y.; Ge, K.; Lu, J.; Kong, W.; Jia, C. Specific Overexpression of Mitofusin-2 in Hepatic Stellate Cells Ameliorates Liver Fibrosis in Mice Model. *Hum. Gene Ther.* **2020**, *31*, 103–109. [CrossRef]
67. Youle, R.J.; Van Der Bliek, A.M. Mitochondrial Fission, Fusion, and Stress. *Science* **2012**, *337*, 1062–1065. [CrossRef]
68. Galloway, C.A.; Lee, H.; Brookes, P.S.; Yoon, Y. Decreasing Mitochondrial Fission Alleviates Hepatic Steatosis in a Murine Model of Nonalcoholic Fatty Liver Disease. *Am. J. Physiol. Gastrointest. Liver Physiol.* **2014**, *307*, G632–G641. [CrossRef]
69. Wang, L.; Ishihara, T.; Ibayashi, Y.; Tatsushima, K.; Setoyama, D.; Hanada, Y.; Takeichi, Y.; Sakamoto, S.; Yokota, S.; Mihara, K.; et al. Disruption of Mitochondrial Fission in the Liver Protects Mice from Diet-Induced Obesity and Metabolic Deterioration. *Diabetologia* **2015**, *58*, 2371–2380. [CrossRef]
70. Martínez-reyes, I.; Chandel, N.S. Mitochondrial TCA Cycle Metabolites Control. *Nat. Commun.* **2020**, *11*, 102. [CrossRef] [PubMed]
71. Kim, H.J.; Han, Y.H.; Na, H.; Kim, J.Y.; Kim, T.; Kim, H.J.; Shin, C.; Lee, J.W.; Lee, M.O. Liver-Specific Deletion of RORα Aggravates Diet-Induced Nonalcoholic Steatohepatitis by Inducing Mitochondrial Dysfunction. *Sci. Rep.* **2017**, *7*, 13392. [CrossRef] [PubMed]
72. Reagan-Shaw, S.; Nihal, M.; Ahmad, N. Dose Translation from Animal to Human Studies Revisited. *FASEB J.* **2008**, *22*, 659–661. [CrossRef] [PubMed]
73. Zamora-Ros, R.; Forouhi, N.G.; Sharp, S.J.; González, C.A.; Buijsse, B.; Guevara, M.; van der Schouw, Y.T.; Amiano, P.; Boeing, H.; Bredsdorff, L.; et al. Dietary Intakes of Individual Flavanols and Flavonols Are Inversely Associated with Incident Type 2 Diabetes in European Populations. *J. Nutr.* **2014**, *144*, 335–343. [CrossRef] [PubMed]

Table S1. Circadian parameters of liver clock genes.

			p	amplitude	*p*(amplitude)	acrophase (h)	*p*(acrophase)	MESOR
Bmal1	ZT0	STD-VH	**0.000**	0.488	**0.000**	0.566	**0.011**	0.478
		CAF-VH	**0.000**	0.579	**0.000**	0.187	**0.000**	0.553
		CAF-GSPE	**0.000**	0.591	**0.000**	0.59	0.518	0.59
	ZT12	STD-VH	**0.000**	0.479	**0.000**	22.638	**0.007**	0.394
		CAF-VH	**0.000**	0.446	**0.000**	1.51	0.111	0.477
		CAF-GSPE	**0.001**	0.369	**0.000**	23.055	**0.000**	0.326
Cry1	ZT0	STD-VH	**0.001**	0.503	**0.000**	20.629	**0.000**	0.742
		CAF-VH	**0.000**	0.615	**0.000**	21.272	**0.000**	0.816
		CAF-GSPE	**0.000**	0.672	**0.000**	21.1	**0.000**	0.856
	ZT12	STD-VH	**0.001**	0.753	**0.000**	18.664	**0.000**	0.969
		CAF-VH	**0.000**	0.497	**0.000**	21.09	**0.000**	0.705
		CAF-GSPE	**0.000**	0.753	**0.000**	18.577	**0.000**	0.71
Per2	ZT0	STD-VH	**0.003**	0.807	**0.000**	16.58	**0.000**	1.295
		CAF-VH	**0.000**	1.205	**0.000**	16.017	**0.000**	1.762
		CAF-GSPE	**0.000**	1.293	**0.000**	16.58	**0.000**	1.651
	ZT12	STD-VH	**0.000**	1.407	**0.000**	16.304	**0.000**	2.067
		CAF-VH	**0.000**	2.264	**0.000**	13.519	**0.000**	3.035
		CAF-GSPE	**0.000**	1.408	**0.000**	15.271	**0.000**	1.719
Nr1d1	ZT0	STD-VH	**0.004**	22.855	**0.000**	11.207	**0.000**	16.15
		CAF-VH	**0.000**	34.868	**0.000**	9.386	**0.000**	25.125
		CAF-GSPE	**0.000**	30.889	**0.000**	9.692	**0.000**	22.919
	ZT12	STD-VH	**0.000**	36.283	**0.000**	8.038	**0.000**	23.206
		CAF-VH	**0.001**	34.974	**0.000**	8.312	**0.000**	23.648
		CAF-GSPE	**0.000**	23.224	**0.000**	10.424	**0.000**	17.181
Ror-α	ZT0	STD-VH	0.184	0.174	**0.049**	20.905	**0.000**	0.921
		CAF-VH	**0.000**	0.376	**0.000**	16.541	**0.000**	0.961
		CAF-GSPE	**0.000**	0.42	**0.000**	21.71	**0.000**	1.078
	ZT12	STD-VH	**0.020**	0.261	**0.001**	19.361	**0.000**	0.56
		CAF-VH	0.307	0.128	0.107	7.621	**0.001**	0.623
		CAF-GSPE	**0.046**	0.225	**0.005**	21.231	**0.000**	0.431
Nampt	ZT0	STD-VH	**0.001**	2.523	**0.000**	14.497	**0.000**	2.495
		CAF-VH	**0.003**	3.915	**0.000**	14.361	**0.000**	4.3
		CAF-GSPE	**0.031**	2.493	**0.002**	16.522	**0.000**	3.437
	ZT12	STD-VH	0.062	0.624	**0.008**	17.284	**0.000**	1.26
		CAF-VH	**0.003**	1.295	**0.000**	13.401	**0.000**	1.576
		CAF-GSPE	**0.001**	1.224	**0.000**	14.488	**0.000**	1.26

Rats fed with standard diet (STD) or cafeteria diet (CAF) were daily dosage with vehicle or grape seed procyanidins extract (GSPE) in the morning (ZT0) or at night (ZT12) and after 9 weeks were sacrificed at 9 a.m. (ZT1), 3 p.m. (ZT7), 9 p.m. (ZT13) or 3 a.m. (ZT19). Acrophase is the time at which the peak of a rhythm occurs (h); Amplitude is the difference between the peak and the mean value of a wave; MESOR is a circadian rhythm-adjusted mean. The values are the estimation of circadian parameters obtained by Cosinor method. The statistically significant p-values ($p < 0.05$) are highlighted in bold.

Table S2. Comparison of circadian parameters of liver clock genes between groups.

			p	d_amplitude	*p*(d_amplitude)	d_acrophase	*p*(d_acrophase)
Bmal1	ZT0	STD-VH vs. CAF-VH	**0.000**	0.091	0.149	0.099	0.406
		CAF-VH vs. CAF-GSPE	**0.000**	0.012	0.845	−0.106	0.278
	ZT12	STD-VH vs. CAF-VH	**0.000**	−0.033	0.689	5.531	**0.000**
		CAF-VH vs. CAF-GSPE	**0.000**	−0.077	0.419	−5.64	**0.000**
Cry1	ZT0	STD-VH vs. CAF-VH	**0.000**	0.113	0.369	−0.168	0.459
		CAF-VH vs. CAF-GSPE	**0.000**	0.057	0.598	0.045	0.793
	ZT12	STD-VH vs. CAF-VH	**0.000**	−0.256	0.149	−0.635	**0.036**
		CAF-VH vs. CAF-GSPE	**0.000**	0.09	0.424	0.658	**0.001**
Per2	ZT0	STD-VH vs. CAF-VH	**0.000**	0.398	0.055	0.148	0.499
		CAF-VH vs. CAF-GSPE	**0.000**	0.089	0.615	−0.148	0.301
	ZT12	STD-VH vs. CAF-VH	**0.000**	0.857	**0.027**	0.729	**0.001**
		CAF-VH vs. CAF-GSPE	**0.000**	−0.856	**0.048**	−0.458	0.071
Nr1d1	ZT0	STD-VH vs. CAF-VH	**0.000**	12.013	**0.047**	0.477	**0.033**
		CAF-VH vs. CAF-GSPE	**0.000**	−3.979	0.308	−0.08	0.506
	ZT12	STD-VH vs. CAF-VH	**0.000**	−1.308	0.881	−0.072	0.763
		CAF-VH vs. CAF-GSPE	**0.000**	−11.75	0.122	−0.553	**0.040**
Ror-α	ZT0	STD-VH vs. CAF-VH	**0.001**	0.203	0.068	1.143	**0.022**
		CAF-VH vs. CAF-GSPE	**0.000**	0.044	0.662	−1.353	**0.000**
	ZT12	STD-VH vs. CAF-VH	**0.037**	−0.133	0.235	3.074	**0.000**
		CAF-VH vs. CAF-GSPE	**0.024**	0.097	0.387	−3.563	**0.000**
Nampt	ZT0	STD-VH vs. CAF-VH	**0.000**	1.392	0.181	0.036	0.918
		CAF-VH vs. CAF-GSPE	**0.001**	−1.422	0.248	−0.566	0.180
	ZT12	STD-VH vs. CAF-VH	**0.001**	0.671	0.077	1.017	**0.033**
		CAF-VH vs. CAF-GSPE	**0.000**	−0.071	0.852	−0.285	0.345

Rats fed with STD or CAF were daily dosage with vehicle or GSPE in the morning (ZT0) or at night (ZT12) and after 9 weeks were sacrificed at 9 a.m. (ZT1), 3 p.m. (ZT7), 9 p.m. (ZT13) or 3 a.m. (ZT19). Acrophase is the time at which the peak of a rhythm occurs ([h], hours); Amplitude is the difference between the peak and the mean value of a wave; MESOR is a circadian rhythm-adjusted mean. The first column (*p*) indicates if there are significant differences between two circadian rhythms. The circadian parameter values are the differences between two groups of each circadian parameter. The statistically significant p-values ($p < 0.05$) are highlighted in bold.

Table S3. Measurement of ETC components in the liver.

			Citrate synthase mU/mg protein	Complex I mU/mg protein	Complex II mU/mg protein	Complex II + II mU/mg protein	COX mU/mg protein
ZT0	ZT1	STD-VH	62.55 ± 6.08	33.95 ± 5.68	118.40 ± 15.08	8.74 ± 1.67	71.69 ± 6.08
		CAF-VH	64.81 ± 6.52	25.54 ± 6.79	80.07 ± 5.57 **	4.55 ± 0.66 **	66.92 ± 10.38
		CAF-GSPE	56.91 ± 3.04	34.86 ± 17.53	74.46 ± 15.99	3.86 ± 1.25	62.51 ± 24.41
	ZT7	STD-VH	60.23 ± 9.33	25.62 ± 1.85	99.40 ± 19.49	6.53 ± 1.86	69.85 ± 18.45
		CAF-VH	60.05 ± 6.28	15.52 ± 2.66 ***	63.28 ± 4.12 **	4.02 ± 0.58 *	66.76 ± 11.18
		CAF-GSPE	59.88 ± 8.09	23.38 ± 3.59 $	73.66 ± 19.14	4.59 ± 1.34	67.68 ± 15.91
	ZT13	STD-VH	70.28 ± 9.0	33.24 ± 16.81	122.42 ± 25.57	7.22 ± 2.58	58.71 ± 12.70
		CAF-VH	64.31 ± 2.44	20.33 ± 4.51	69.25 ± 17.96 *	3.98 ± 0.94 #	54.83 ± 5.00
		CAF-GSPE	74.67 ± 2.57 $$	32.33 ± 4.71 $	112.02 ± 12.16 $$	60.8 ± 1.99 +	56.46 ± 4.48
	ZT19	STD-VH	69.49 ± 7.01	37.74 ± 3.34	144.27 ± 11.08	8.82 ± 1.64	58.21 ± 11.96
		CAF-VH	72.49 ± 4.64	32.53 ± 4.06 $	108.75 ± 16.10 **	5.24 ± 0.70 **	51.22 ± 11.64
		CAF-GSPE	70.23 ± 8.78	22.88 ± 3.00 $$	86.97 ± 8.35 +	4.61 ± 0.75	57.59 ± 11.44
ZT12	ZT1	STD-VH	65.02 ± 7.97	28.71 ± 12.08	100.19 ± 19.64	6.41 ± 1.28	65.95 ± 9.85
		CAF-VH	60.97 ± 4.69	26.26 ± 6.81	78.31 ± 13.99	4.75 ± 1.06 #	57.39 ± 12.80
		CAF-GSPE	63.93 ± 6.21	26.41 ± 5.10	79.91 ± 19.67	5.33 ± 3.11	54.90 ± 4.42
	ZT7	STD-VH	59.72 ± 4.06	41.60 ± 7.40	112.19 ± 17.75	7.25 ± 1.29	56.98 ± 10.80
		CAF-VH	59.32 ± 3.77	23.12 ± 7.33 *	63.43 ± 9.66 **	4.28 ± 0.94 **	54.85 ± 6.49
		CAF-GSPE	57.36 ± 2.32	31.85 ± 12.93	78.61 ± 9.95 +	4.53 ± 1.07	57.65 ± 2.35
	ZT13	STD-VH	68.75 ± 8.66	33.91 ± 6.82	126.38 ±12.90	8.46 ± 2.03	56.22 ± 10.17
		CAF-VH	64.66 ± 5.09	22.63 ± 4.91 *	84.67 ± 7.61 ***	4.94 ± 0.70 *	47.79 ± 6.68
		CAF-GSPE	58.93 ± 3.03	23.86 ± 6.35	72.84 ± 11.18	4.02 ± 0.86	43.98 ± 5.64
	ZT19	STD-VH	69.00 ± 5.11	42.16 ± 17.59	132.48 ± 26.19	8.59 ± 4.10	56.59 ± 11.18
		CAF-VH	63.16 ± 6.68	22.95 ± 12.47	69.47 ± 40.41 *	3.49 ±2.50 +	55.52 ± 19.91
		CAF-GSPE	61.66 ± 8.12	23.06 ± 8.14	84.00 ±18.94	4.45 ± 2.16	45.36 ± 11.36

Rats fed with STD or CAF were daily dosage with vehicle or GSPE in the morning (ZT0) or at night (ZT12) and after 9 weeks were sacrificed at 9 a.m. (ZT1), 3 p.m. (ZT7), 9 p.m. (ZT13) or 3 a.m. (ZT19). The values are the mean ± standard error of the mean (SEM). (n = 4). * The effect of diet within vehicle groups (Student's t test, $p < 0.05$); $ The effect of GSPE consumption within CAF groups (Student's t test, $p < 0.05$); + Indicates tendency between CAF-VH and CAF-GSPE using Student´s t test (p = 0.1–0.051). COX Cytochrome c oxidase.

Table S4.1 Metabolites of the TCA cycle in the liver.

ZT	Metabolite	ZT0-STD-VH vs. ZT0-CAF-VH				ZT0-CAF-VH vs. ZT0-CAF-GSPE				ZT0-STD-VH vs. ZT0-CAF-GSPE			
		ZT0-STD-VH	ZT0-CAF-VH	*p*-value	FC	ZT0-CAF-VH	ZT0-CAF-GSPE	*p*-value	FC	ZT0-STD-VH	ZT0-CAF-GSPE	*p*-value	FC
ZT1	Pyruvic acid	0.46 ± 0.03	0.32 ± 0.06	0.068	0.7	0.32 ± 0.06	0.34 ± 0.02	0.816	1.1	0.46 ± 0.03	0.34 ± 0.02	**0.024**	0.7
	Succinic acid	0.75 ± 0.08	1.1 ± 0.2	0.155	1.5	1.1 ± 0.2	1.06 ± 0.25	0.886	1	0.75 ± 0.08	1.06 ± 0.25	0.242	1.4
	Fumaric acid	6.37 ± 0.69	6.54 ± 1.13	0.905	1	6.54 ± 1.13	9.41 ± 0.87	0.118	1.4	6.37 ± 0.69	9.41 ± 0.87	**0.039**	1.5
	Malic acid	2.61 ± 0.37	2.86 ± 0.54	0.709	1.1	2.86 ± 0.54	3.79 ± 0.11	0.212	1.3	2.61 ± 0.37	3.79 ± 0.11	**0.047**	1.5
	α-ketoglutaric acid	0.04 ± 0.01	0.02 ± 0	0.150	0.5	0.02 ± 0	0.05 ± 0.01	**0.013**	2.5	0.04 ± 0.01	0.05 ± 0.01	0.245	1.3
	Citric acid	0.37 ± 0.08	0.26 ± 0.07	0.332	0.7	0.26 ± 0.07	0.43 ± 0.06	0.128	1.7	0.37 ± 0.08	0.43 ± 0.06	0.600	1.2
ZT7	Pyruvic acid	0.56 ± 0.06	0.32 ± 0.01	**0.005**	0.6	0.32 ± 0.01	0.36 ± 0.03	0.349	1.1	0.56 ± 0.06	0.36 ± 0.03	**0.019**	0.6
	Succinic acid	1.27 ± 0.15	0.73 ± 0.14	**0.038**	0.6	0.73 ± 0.14	1.18 ± 0.12	**0.047**	1.6	1.27 ± 0.15	1.18 ± 0.12	0.658	0.9
	Fumaric acid	9.17 ± 1.48	7.15 ± 1.37	0.356	0.8	7.15 ± 1.37	8.98 ± 0.99	0.322	1.3	9.17 ± 1.48	8.98 ± 0.99	0.918	1
	Malic acid	3 ± 0.51	3.56 ± 0.84	0.593	1.2	3.56 ± 0.84	3.98 ± 0.56	0.688	1.1	3 ± 0.51	3.98 ± 0.56	0.242	1.3
	α-ketoglutaric acid	0.04 ± 0.01	0.05 ± 0.01	0.307	1.3	0.05 ± 0.01	0.05 ± 0.01	0.944	1	0.04 ± 0.01	0.05 ± 0.01	0.263	1.3
	Citric acid	0.42 ± 0.16	0.52 ± 0.04	0.586	1.2	0.52 ± 0.04	0.6 ± 0.12	0.508	1.2	0.42 ± 0.16	0.6 ± 0.12	0.392	1.4
ZT13	Pyruvic acid	0.86 ± 0.1	0.54 ± 0.07	**0.040**	0.6	0.54 ± 0.07	0.47 ± 0.03	0.376	0.9	0.86 ± 0.1	0.47 ± 0.03	**0.010**	0.5
	Succinic acid	0.73 ± 0.08	1.16 ± 0.19	0.083	1.6	1.16 ± 0.19	0.88 ± 0.16	0.311	0.8	0.73 ± 0.08	0.88 ± 0.16	0.436	1.2
	Fumaric acid	8.4 ± 0.73	6.38 ± 0.61	0.079	0.8	6.38 ± 0.61	8.4 ± 0.86	0.104	1.3	8.4 ± 0.73	8.4 ± 0.86	0.999	1
	Malic acid	2.91 ± 0.27	2.81 ± 0.25	0.793	1	2.81 ± 0.25	3.11 ± 0.48	0.597	1.1	2.91 ± 0.27	3.11 ± 0.48	0.726	1.1
	α-ketoglutaric acid	0.03 ± 0.01	0.03 ± 0	0.674	1	0.03 ± 0	0.03 ± 0	0.495	1	0.03 ± 0.01	0.03 ± 0	0.883	1
	Citric acid	0.3 ± 0.05	0.22 ± 0.02	0.209	0.7	0.22 ± 0.02	0.29 ± 0.06	0.334	1.3	0.3 ± 0.05	0.29 ± 0.06	0.893	1
ZT19	Pyruvic acid	0.62 ± 0.11	0.55 ± 0.03	0.568	0.9	0.55 ± 0.03	0.39 ± 0.06	0.053	0.7	0.62 ± 0.11	0.39 ± 0.06	0.112	0.6
	Succinic acid	1.02 ± 0.21	1.23 ± 0.16	0.464	1.2	1.23 ± 0.16	1.08 ± 0.2	0.589	0.9	1.02 ± 0.21	1.08 ± 0.2	0.843	1.1
	Fumaric acid	4.74 ± 0.52	5.56 ± 0.63	0.352	1.2	5.56 ± 0.63	8.79 ± 1.26	0.061	1.6	4.74 ± 0.52	8.79 ± 1.26	**0.025**	1.9
	Malic acid	1.63 ± 0.18	2.43 ± 0.3	0.061	1.5	2.43 ± 0.3	3.02 ± 0.63	0.427	1.2	1.63 ± 0.18	3.02 ± 0.63	0.076	1.9
	α-ketoglutaric acid	0.02 ± 0	0.03 ± 0	0.083	1.5	0.03 ± 0	0.04 ± 0.01	**0.046**	1.3	0.02 ± 0	0.04 ± 0.01	**0.008**	2
	Citric acid	0.09 ± 0.02	0.2 ± 0.04	**0.042**	2.2	0.2 ± 0.04	0.23 ± 0.04	0.660	1.2	0.09 ± 0.02	0.23 ± 0.04	**0.022**	2.6

Metabolites of the tricarboxylic acid (TCA) cycle in the liver of rats fed with STD or CAF diet were daily dosage with vehicle or GSPE in the morning (ZT0) and after 9 weeks were sacrificed at 9 a.m. (ZT1), 3 p.m. (ZT7), 9 p.m. (ZT13) or 3 a.m. (ZT19). The statistically significant p-values ($p < 0.05$) are highlighted in bold.

Table S4.2 Metabolites of the TCA cycle in the liver.

ZT	Metabolite	ZT12-STD-VH vs. ZT12-CAF-VH				ZT12-CAF-VH vs. ZT12-CAF-GSPE				ZT12-STD-VH vs. ZT12-CAF-GSPE			
		ZT12-STD-VH	ZT12-CAF-VH	*p*-value	FC	ZT12-CAF-VH	ZT12-CAF-GSPE	p-value	FC	ZT12-STD-VH	ZT12-CAF-GSPE	*p*-value	FC
ZT1	Pyruvic acid	0.46 ± 0.04	0.37 ± 0.04	0.128	0.8	0.37 ± 0.04	0.39 ± 0.06	0.808	1.1	0.46 ± 0.04	0.39 ± 0.06	0.343	0.8
	Succinic acid	0.9 ± 0.24	1.13 ± 0.17	0.470	1.3	1.13 ± 0.17	0.98 ± 0.35	0.724	0.9	0.9 ± 0.24	0.98 ± 0.35	0.846	1.1
	Fumaric acid	13.34 ± 2.3	9.71 ± 0.81	0.186	0.7	9.71 ± 0.81	11.19 ± 1.74	0.468	1.2	13.34 ± 2.3	11.19 ± 1.74	0.484	0.8
	Malic acid	4.55 ± 0.66	3.76 ± 0.23	0.301	0.8	3.76 ± 0.23	3.99 ± 0.5	0.696	1.1	4.55 ± 0.66	3.99 ± 0.5	0.525	0.9
	α-ketoglutaric acid	0.04 ± 0.01	0.03 ± 0.01	0.482	0.8	0.03 ± 0.01	0.04 ± 0.01	0.804	1.3	0.04 ± 0.01	0.04 ± 0.01	0.650	1
	Citric acid	0.31 ± 0.06	0.32 ± 0.11	0.933	1	0.32 ± 0.11	0.41 ± 0.15	0.637	1.3	0.31 ± 0.06	0.41 ± 0.15	0.548	1.3
ZT7	Pyruvic acid	0.62 ± 0.07	0.42 ± 0.05	**0.045**	0.7	0.42 ± 0.05	0.36 ± 0.03	0.344	0.9	0.62 ± 0.07	0.36 ± 0.03	**0.012**	0.6
	Succinic acid	1.05 ± 0.14	1.02 ± 0.14	0.874	1	1.02 ± 0.14	1.13 ± 0.17	0.652	1.1	1.05 ± 0.14	1.13 ± 0.17	0.754	1.1
	Fumaric acid	12.51 ± 1.53	8.5 ± 1.14	0.081	0.7	8.5 ± 1.14	7.94 ± 1.71	0.796	0.9	12.51 ± 1.53	7.94 ± 1.71	0.094	0.6
	Malic acid	3.9 ± 0.55	3.81 ± 0.39	0.892	1	3.81 ± 0.39	3.01 ± 0.63	0.325	0.8	3.9 ± 0.55	3.01 ± 0.63	0.329	0.8
	α-ketoglutaric acid	0.03 ± 0	0.03 ± 0.01	0.568	1	0.03 ± 0.01	0.04 ± 0	0.355	1.3	0.03 ± 0	0.04 ± 0	0.667	1.3
	Citric acid	0.37 ± 0.1	0.3 ± 0.05	0.580	0.8	0.3 ± 0.05	0.22 ± 0.06	0.365	0.7	0.37 ± 0.1	0.22 ± 0.06	0.273	0.6
ZT13	Pyruvic acid	0.5 ± 0.03	0.41 ± 0.05	0.188	0.8	0.41 ± 0.05	0.35 ± 0.03	0.341	0.9	0.5 ± 0.03	0.35 ± 0.03	**0.008**	0.7
	Succinic acid	1.13 ± 0.09	1.04 ± 0.08	0.487	0.9	1.04 ± 0.08	1.45 ± 0.05	**0.005**	1.4	1.13 ± 0.09	1.45 ± 0.05	**0.021**	1.3
	Fumaric acid	5.55 ± 0.64	6.11 ± 0.67	0.570	1.1	6.11 ± 0.67	7.69 ± 0.98	0.233	1.3	5.55 ± 0.64	7.69 ± 0.98	0.118	1.4
	Malic acid	1.57 ± 0.22	2.51 ± 0.21	**0.023**	1.6	2.51 ± 0.21	2.48 ± 0.31	0.946	1	1.57 ± 0.22	2.48 ± 0.31	0.053	1.6
	α-ketoglutaric acid	0.03 ± 0	0.02 ± 0	0.315	0.7	0.02 ± 0	0.03 ± 0.01	0.356	1.5	0.03 ± 0	0.03 ± 0.01	0.942	1
	Citric acid	0.18 ± 0.03	0.24 ± 0.04	0.240	1.3	0.24 ± 0.04	0.21 ± 0.05	0.690	0.9	0.18 ± 0.03	0.21 ± 0.05	0.614	1.2
ZT19	Pyruvic acid	0.54 ± 0.03	0.31 ± 0.03	**0.001**	0.6	0.31 ± 0.03	0.42 ± 0.07	0.205	1.4	0.54 ± 0.03	0.42 ± 0.07	0.151	0.8
	Succinic acid	0.68 ± 0.09	1.29 ± 0.25	0.063	1.9	1.29 ± 0.25	1.24 ± 0.16	0.879	1	0.68 ± 0.09	1.24 ± 0.16	**0.022**	1.8
	Fumaric acid	8.46 ± 1.43	6.79 ± 1.09	0.388	0.8	6.79 ± 1.09	8.95 ± 0.68	0.143	1.3	8.46 ± 1.43	8.95 ± 0.68	0.769	1.1
	Malic acid	2.8 ± 0.44	2.44 ± 0.45	0.583	0.9	2.44 ± 0.45	3.21 ± 0.25	0.181	1.3	2.8 ± 0.44	3.21 ± 0.25	0.447	1.1
	α-ketoglutaric acid	0.03 ± 0.01	0.03 ± 0.01	0.888	1	0.03 ± 0.01	0.04 ± 0.01	0.406	1.3	0.03 ± 0.01	0.04 ± 0.01	0.370	1.3
	Citric acid	0.21 ± 0.06	0.22 ± 0.08	0.915	1	0.22 ± 0.08	0.38 ± 0.11	0.295	1.7	0.21 ± 0.06	0.38 ± 0.11	0.237	1.8

Metabolites of the TCA cycle in the liver of rats fed with STD or CAF diet were daily dosage with vehicle or GSPE at night (ZT12) and after 9 weeks were sacrificed at 9 a.m. (ZT1), 3 p.m. (ZT7), 9 p.m. (ZT13) or 3 a.m. (ZT19). The statistically significant p-values ($p < 0.05$) are highlighted in bold.

CHAPTER II

OBJECTIVE 2

To determine how an obesity-inducing diet affects the rhythm of hepatic lipid and carbohydrate metabolism and to observe whether there is any time-dependent restorative effect of GSPE administration.

OBJECTIVE 3

To determine the role of (+)-catechin and (-)-epicatechin, two of the main phenolic components of GSPE, on its hepatic clock-synchronizing and metabolic improvement effects against NAFLD.

UNIVERSITAT ROVIRA I VIRGILI
THE INFLUENCE OF BIOLOGICAL RHYTHMS ON THE BENEFICIAL EFFECTS OF GRAPE SEED PROANTHOCYANIDIN EXTRACT (GSPE) ON LIVER METABOLISM IN HEALTH AND DISEASE
Romina Mariel Rodriguez

MANUSCRIPT 2

Grape-seed proanthocyanidin extract (GSPE) modulates diurnal oscillations of key hepatic metabolic genes and metabolites alleviating hepatic lipid deposition in cafeteria-fed obese rats in a time-of-day-dependent manner

Romina M Rodríguez [1], Leonardo Vinícius Monteiro de Assis [2], Marina Colom-Pellicer [1], Sergio Quesada-Vázquez [3], Álvaro Cruz-Carrión [4], Xavier Escoté [3], Henrik Oster [2], Gerard Aragonès [1] and Miquel Mulero [1*]

[1] Nutrigenomics Research Group, Department of Biochemistry and Biotechnology, Campus Sescelades, Universitat Rovira i Virgili (URV), 43007 Tarragona, Spain.

[2] Institute of Neurobiology, Center of Brain, Behavior and Metabolism, University of Lübeck, Marie Curie Street, 23562 Lübeck, Germany.

[3] Eurecat, Technology Centre of Catalunya, Nutrition and Health Unit, 43204 Reus, Spain.

[4] United States Department of Agriculture and The Agricultural Research Service (USDA-ARS), Arkansas Children's Nutrition Center and Department of Pediatrics, University of Arkansas for Medical Science, AR 72202, Little Rock, USA.

* Correspondence: miquel.mulero@urv.cat; Tel.: +34 977559565

Prepared for submission to Molecular Metabolism

UNIVERSITAT ROVIRA I VIRGILI
THE INFLUENCE OF BIOLOGICAL RHYTHMS ON THE BENEFICIAL EFFECTS OF GRAPE SEED PROANTHOCYANIDIN EXTRACT (GSPE) ON LIVER METABOLISM IN HEALTH AND DISEASE
Romina Mariel Rodriguez

Abstract

Metabolic syndrome (MS) and its related diseases, including obesity and non-alcoholic fatty liver disease (NAFLD), have become a public health issue due to their increasing prevalence. Polyphenols, such as grape seed proanthocyanidin extract (GSPE), are bioactive compounds present in fruits and vegetables that show promise for MS treatment. We have previously demonstrated that the efficacy of this phenolic extract in the modulation of liver circadian clocks was affected by the time of the day at which it was ingested. Thus, we wondered if the beneficial effects of GSPE consumption in NAFLD could be mediated by diurnal modulation of hepatic lipid and glucose metabolism and whether GSPE effects on liver metabolism are impacted by the timing of administration. Results from hepatic lipid profiling, expression rhythm analysis of metabolic genes together with liver metabolomics in rats revealed that the CAF diet impaired glucose homeostasis and enhanced lipogenesis in the liver, leading to the generation of hepatosteatosis. Chronic consumption of GSPE at the onset of the active phase was able to restore the daily oscillation of liver mass and of key lipogenic and glycogenic genes, along with the reestablishment of liver metabolite rhythms, demonstrating hepatoprotective properties by decreasing triglyceride accumulation and lipid droplet formation in the liver, thus mitigating the development of CAF-induced NAFLD. Furthermore, in vitro data suggest that catechin, one of the main phenolic compounds found in the GSPE extract, may be involved in the ameliorating effects of GSPE against NAFLD.

Key words: circadian rhythms; liver metabolism; proanthocyanidins; NAFLD

1 INTRODUCTION

In modern times, as a consequence of the rising prevalence of obesity, the metabolic syndrome (MS) has become a common metabolic disorder [1]. It is comprised of several metabolic abnormalities, such as increased visceral

adiposity, dyslipidemia, hyperglycemia, and hypertension. MS is also characterized by elevated levels of circulating triglycerides, lower levels of high-density lipoprotein cholesterol, and impaired fasting blood glucose concentrations [2]. Consequently, these changes increase the risk of developing type 2 diabetes and cardiovascular disease [3]. In the liver, MS manifests as nonalcoholic fatty liver disease (NAFLD), which includes a disease spectrum varying from simple steatosis to non-alcoholic steatohepatitis (NASH) and cirrhosis, with insulin resistance as an important pathogenetic hallmark [4]. Nowadays, excess of food intake and lack of physical activity are the main basis of the growing worldwide epidemic of metabolic disorders and NAFLD [5]. Moreover artificial light at night and late-time work together with sleep deprivation are principal features of the industrialized world contributing to the pathogenesis of MS [6]. Particularly, it has been suggested that these changes cause circadian rhythm disturbances with a resulting upregulation of appetite leading to alterations in lipid and glucose metabolism[6–8]. Additionally, there is now increasing evidence connecting alterations of circadian rhythms with the key components of MS [9–11], suggesting that the circadian system is one of the main regulators of metabolism [12,13].

As a major metabolic organ, the liver is responsible for glucose and lipid homeostasis, where opposite metabolic processes such as glycolysis/gluconeogenesis, and lipogenesis/fatty acid oxidation take place, requiring the need for temporal separation [14]. Therefore, hepatic function, besides being under control of the insulin-glucagon signaling network, is tightly regulated by circadian clocks [15]. It has been described that not only transcripts, but also enzymes and proteins, which are important regulators of metabolic processes, undergo circadian oscillation in the liver [16,17]. Moreover, it is known that many hepatic metabolites oscillate in a daily manner [18].

The master circadian pacemaker, the suprachiasmatic nucleus (SCN) located in the hypothalamus, is influenced primarily by light, while

peripheral circadian clocks located in tissues including the liver can be also regulated by the time of feeding and type of diet [19]. It has been demonstrated in mice that the intake of a high-fat diet (HFD) generates a profound reorganization of the liver clock reprogramming, in consequence, the oscillation of metabolic and transcriptional liver pathways. Diurnal rhythms of transcripts and metabolites involved in insulin signaling pathways, fatty acid and primary bile acid biosynthesis were found altered due to HFD [20]. Furthermore, it has been shown that the reset of the liver clock was specifically due to the nutritional challenge (HFD), and not due to the development of obesity. Of note, such dietary effects on the circadian clock are reversible [20].

Polyphenols, and specifically proanthocyanidins, are naturally occurring secondary plant metabolites that can be found in many fruits and vegetables, mostly in apples, cinnamon, grape seed and skin [21,22]. Proanthocyanidins are known to possess antioxidant, antimicrobial, anti-inflammatory, antiallergic, anti-obesity and vasodilatory properties [23,24]. Epidemiological evidence has linked the consumption of proanthocyanidins to a reduced risk of chronic diseases, including certain types of cancer and cardiovascular disease, as well as NAFLD [25]. Moreover, it has been shown that grape seed proanthocyanidin extract (GSPE) exhibits hepatoprotective effects in animal models of diet-induced obesity, helping to prevent the progression of steatosis and NAFLD [26–28]. Growing evidence suggests that polyphenols may also affect circadian rhythms by acting on the SCN and peripheral tissue circadian clock gene expression [29–32]. Among other issues, the bioavailability and the timing of administration arise as important features when studying the polyphenols effect on metabolic dysfunctions like MS [33]. The main constituents of GSPE are flavan-3-ol monomeric, dimeric, and trimeric procyanidins, with relatively low proportions of larger polymers [34]. In this regard, based on its low molecular weight procyanidin composition, GSPE has been considered to be

highly bioavailable [35]. However, most studies do not consider the timing of administration, leaving this variable largely unexplored.

Taking into consideration the above explained factors and based on our previous results, in which we demonstrate that GSPE was able to restore hepatic circadian clock synchrony in cafeteria diet (CAF) fed rats [36], we further investigated the implications of obesity and MS in the close relationship between the hepatic molecular clock metabolic function, and energy regulation. Therefore, the aim of the present study was to investigate how an obesogenic diet intake affects the rhythm of hepatic lipid and glucose metabolism of rats and to determine whether. GSPE's restorative effects on liver rhythms are impacted by the timing of administration. To achieve this, rats were fed with standard chow (STD) or cafeteria (CAF) diet for 9 weeks. During the last 4 weeks they were treated in the morning (ZT0) or at night (ZT12) with vehicle (VH) or 25 mg/kg of GSPE. Animals were sacrificed one hour after turning the light on (ZT1) and every 6 hours (ZT1, ZT7, ZT13 and ZT19) to assess diurnal transcript and metabolite profiles. Our data suggest a vital role for the circadian clock machinery and key metabolic gene rhythms in the generation and propagation of NAFLD, and a time-of-day dependent effect of GSPE in the amelioration of hepatic steatosis.

2 MATERIALS AND METHODS

2.1 Grape seed proanthocyanidin extract

Grape seed proanthocyanidin extract (GSPE) was obtained from Les Dérives Résiniques et Terpéniques (Dax, France). GSPE was directly analyzed by LC-MS/MS (Agilent Technologies, Palo Alto, CA, USA). A ZORBAX SE-aq column (150 mm×2.1 mm i.d., 3.5 µm particle size, Aglient Technologies) was used. The mobile phase consisted of (A) 0.2 % acetic acid in water and (B) acetonitrile. The gradient mode was as follows: initial conditions, 5 % B; 0-10 min, 5-55 % B; 10-12 min, 55-88 % B; 12-15 min, 80 % B isocratic, and 15-16 min, 80-85 % B. A post-run of 10 min was required for column re-

equilibration. The flow rate was set at 0.4 mL/min, and the injection volume was 2.5 µL for all runs. Electrospray ionization (ESI) was conducted at 350 °C, the flow rate was 12 L/min with a nebulizer gas pressure of 45 psi, and the capillary voltage was 4,000 V. The mass spectrometer was operated in negative mode, and the MS/MS data were acquired in multiple reaction monitoring (MRM) mode. MRM conditions for the analysis of the phenolic compounds studied using HPLC-ESI-MS/MS were conducted as previously described [37]. The total polyphenol content, the individual flavanols and the phenolic acids comprising the extract are detailed in Table 1.

2.2 Animal handling

All procedures involving the use and care of animals were reviewed and approved by the Animal Ethics Committee of the Universitat Rovira i Virgili (permit number 9495, 18th of September 2019). All experiments were performed in accordance with relevant guidelines and regulations of the Council of the European Union and the procedure established by the Departament d'Agricultura, Ramaderia i Pesca of the Generalitat de Catalunya.

Ninety-six 12-week-old male Fischer 344 rats were purchased from Charles River (Barcelona, Spain). The animals were housed in pairs in a 12-h/12-h light-dark cycle at 22 °C, 55 % humidity, and were provided a standard chow diet (STD) and tap water *ad libitum*. The STD diet composition was 20 % protein, 8 % fat and 72 % carbohydrates (Panlab, Barcelona, Spain). After a 4-day adaptation period, the animals were randomly divided into two groups depending on the diet; 32 rats were fed with STD, and 64 rats were fed a cafeteria diet (CAF) during a 5-week pre-treatment. CAF consisted of biscuits with cheese and pâté, bacon, coiled puff pastry from Mallorca (Hacendado, Spain), feed, carrots, and sweetened milk (22 % sucrose w/v). CAF composition was 14 % protein, 35 % fat and 76 % carbohydrates. After the pre-treatment period, rats were divided into two groups according to the Zeitgeber time (ZT) when the treatment was administered: 48 rats were treated at the beginning of the light phase (8 a.m., ZT0), and 48 rats were

treated at the beginning of the dark phase (8 p.m., ZT12). The treatment period started in the 5th week and lasted for 4 weeks. Rats continued with the diet they were fed during the pre-treatment period. All STD-fed rats were treated with commercial sweetened skim condensed milk (Nestle; 100 g: 8.9 g protein, 0.4 g fat, 60.5 g carbohydrates, 1175 kJ) as vehicle (VH). CAF-fed rats were divided into two groups; 32 were treated with VH, and 32 with 25 mg/kg GSPE diluted 1/5 in condensed milk. The treatment was orally administered daily using a syringe. The rats were fasted for 3 h, then sacrificed by decapitation under anesthesia (sodium pentobarbital, 50 mg/kg per body weight). Each diet-treatment group was divided into 4 sub-groups (n=4), depending on the time of sacrifice (9 a.m. (ZT1), 3 p.m. (ZT7), 9 p.m. (ZT13) or 3 a.m. (ZT19)). Part of the liver was fixed with 10 % formalin, the rest of the liver tissue was quickly frozen in liquid nitrogen and then stored at −80 °C for further analysis.

2.3 RNA extraction

A liver tissue portion (20–30 mg) was mixed with TRIzol reagent (Thermo Fisher, Madrid, Spain) and homogenized by Tissue Lyser LT (Qiagen, Madrid, Spain). After a 10-min centrifugation (12,000 × g and 4 °C), the homogenate was placed into a new Eppendorf tube, and 120 µL of chloroform was added. Two phases were separated after a 15-min centrifugation (12,000 × g and 4 °C). The aqueous phase was transferred into a new Eppendorf tube, and 300 µL of isopropanol was added. After an overnight incubation at −20 °C, samples were centrifugated at 4 °C and 12,000 × g for 10 min. The supernatant was discarded, and the pellet was cleaned twice with 500 µL of ethanol 70 % and centrifuged for 5 min (8,000 × g and 4 °C). The supernatant was discarded again, and the washed pellet was resuspended with 60 µL of nuclease-free water (Thermo Fisher, Madrid, Spain). RNA concentration (ng/µL) and purity were measured by a Nanodrop ND-1000 spectrophotometer (Thermo Fisher, Madrid, Spain).

For AML12 *Bmal1-luc* cells, 750 µL TRIzol reagent (Thermo Fisher, Germany) were added to each 35-mm well and, after a 5 min incubation on

ice, cells were collected, placed into Eppendorf tubes and 150 µL of chloroform was added. Two phases were separated after a 15-min centrifugation (12,000 × g and 4 °C). The aqueous phase was transferred into a new Eppendorf tube, and 375 µL of isopropanol was added. After an overnight incubation at −20 °C, samples were centrifugated at 4 °C and 12,000 × g for 40 min. The supernatant was discarded, and the pellet was cleaned twice with 350 µL of ethanol 70 % and centrifuged for 15 min (12,000 × g and 4 °C). The supernatant was discarded again, and the washed pellet was resuspended with 15 µL of nuclease-free water (Thermo Fisher, Madrid, Spain). RNA concentration (ng/µL) and purity were measured by a Nanodrop spectrophotometer (Thermo Fisher, Germany).

2.4 Gene-expression analysis

Complementary deoxyribonucleic acid (cDNA) was obtained by reverse transcription of the RNA extracted using a high-capacity complementary DNA reverse-transcription kit (Thermo Fisher, Madrid, Spain). Quantitative polymerase chain reactions (qPCRs) were performed in 384-well plates in a 7900HT fast real-time PCR (Thermo Fisher, Madrid, Spain) using iTaq Universal SYBR Green Supermix (Bio-Rad, Barcelona, Spain). The cycle program used in all qPCRs was 30 s at 90 °C, 40 cycles of 15 s at 95 °C and 1 min at 60 °C. The analyzed liver genes were normalized by the housekeeping gene peptidylprolyl isomerase A (*Ppia*) and the cell samples were normalized by the housekeeping gene Eukaryotic translation elongation factor 1 alpha (*eEf1a*). No marked changes in cycle thresholds (Cts) of the housekeeping genes were seen across the different times of sacrifice among the groups or cells samples. The primers used for each gene were obtained from Biomers (Ulm, Germany) and can be found in Supplementary Tables (ST) 1 and ST2. The relative expression of each gene was calculated using the $2^{-\Delta\Delta Ct}$ method, as reported by Schmittgen and Livak [38].

2.5 Liver lipid profiling

Liver lipids were extracted following the Bligh–Dyer method [39], and levels of hepatic cholesterol, TAG and total lipid liver content were measured using a colorimetric kit assay (QCA, Barcelona, Spain).

2.6 Liver histology

Liver portions fixed in buffered formalin (4% formaldehyde, 4 g/L NaH_2PO_4, 6.5 g/L Na_2HPO_4; pH 6.8) were cut at a thickness of 3.5 µm and stained with hematoxylin & eosin (H&E). Liver images (magnification 40X) were taken with a microscope (ECLIPSE Ti; Nikon, Tokyo, Japan) coupled to a digital sight camera (DS-Ri1, Nikon) and analyzed using ImageJ NDPI software (National Institutes of Health, Bethesda, MD, USA; https://imagej.nih.gov/ij, version 1.52a). To avoid any bias in the analysis, the study had a double-blind design, preventing the reviewers from knowing any data from the rats during the histopathological analysis. A general NAFLD scoring system was established to diagnose rats with NAFLD/NASH. The key features of NAFLD and NASH were categorized as follows: steatosis was assessed by analyzing macrovesicular (0–3) and microvesicular steatosis (0–3) separately, followed by hepatocellular hypertrophy (0–3), which evaluates abnormal cellular enlargement, and finally giving a total score of 9 points of steatosis state. Inflammation was scored by counting cell aggregates (inflammatory foci). The score 0 to 3 depends on the grade of the feature. It is categorized as 0 (66 %), and this scoring is used in each feature of steatosis and then added to the total steatosis score [40]. Ballooning was not included in the scoring system, because only quantitative measures were considered for the rodent NAFLD score. It is important to highlight that hypertrophy is not a sign of cellular injury and slightly refers to an anomalous enlargement of the cells without recognizing the source of this enlargement [40].

2.7 Metabolomic analysis

Metabolomic analysis of the 96 rat liver samples was performed at the Centre for Omic Sciences (COS, Tarragona, Spain) using gas chromatography

coupled with quadrupole time-of-flight mass spectrometry (GC-qTOF model 7200, Agilent, Santa Clara, CA, USA). The extraction was performed by adding 400 µL of methanol:water (8:2)-containing internal standard mixture to liver samples (approx. 10—20 mg). Then, the samples were mixed and homogenized on a bullet blender using a stainless-steel ball, incubated at 4 °C for 10 min and centrifuged at 19.000× *g* rpm; supernatant was evaporated to dryness before compound derivatization (methoximation and silylation). The derivatized compounds were analyzed by GC-qTOF. Chromatographic separation was based on the Fiehn Method [41] using a J&W Scientific HP5-MS film capillary column (30 m × 0.25 mm × 0.25 µm, Agilent, Santa Clara, CA, USA) and helium as carrier gas with an oven program from 60 to 325 °C. Ionization was done by electronic impact (EI) with an electron energy of 70 eV and operating in full-scan mode. Identification of metabolites was performed using commercial standards and by matching their EI mass spectrum and retention time to a metabolomic Fiehn library (from Agilent, Santa Clara, CA, USA) which contains more than 1,400 metabolites. After putative identification of metabolites they were semi-quantified in terms of internal standard response ratio.

2.8 Alpha mouse liver 12 (AML-12) *Bmal1-luc* maintenance

AML-12 wild-type cells were originally obtained from ATCC biobank (cat number CRL-2254) and grown in DMEM/F12 media containing 15 mM of HEPES, 1 % of penicillin-streptomycin (10,000 units/mL and 10,000 µg/mL, respectively), 1 % of insulin-transferrin-selenium (ITS), 10 % of non-heat inactived serum (all items from Thermo Fisher, Germany). Dexamethasone at 10 nM (Sigma-Aldirch, USA) was supplemented for regular culture maintenance.

To generate *Bmal1-luc* cells, HEK 293 cells were transfected using $CaCl_2$ solution containing *Bmal1-luc* plasmid (17.5 µg, pABpuro-Bluf [42]) together with packing plasmids psPax and pMD2G (12.5 and 7.5 µg, respectively). Supernatant containing virus was collected 48 h later and 10-

X concentrated using Lenti-X Concentrator (Takara Bio, Germany). AML-12 wild-type cells were transduced using concentrated virus and selected using 3 μg/mL of puromycin. From the heterogenous cell culture, single clones were identified and isolated. AML-12 *Bmal1-luc* clone 4 was selected and used for subsequent assays.

2.9 In vitro model of NAFLD by supplementing palmitate

AML-12 *Bmal1-luc* cells were grown in the above-mentioned media without phenol red and dexamethasone. Serum was replaced for charcoal-dextran treated serum that has a significant reduction in endogenous bovine hormones (HyClone, USA). Cells were pre-treated with (+)-catechin or (-)-epicatechin 10 μM or 100 μM for 72 h, using dimethylsulfoxide (DMSO) as a solvent 0.01 % (v/v) or 0.1% (v/v), respectively. $2x10^5$ cells were then spited and seeded in 35 mm dishes containing medium with (+)-catechin or (-)-epicatechin 10 μM or 100 μM. Twenty-four h later, cells were synchronized using 200 nM of dexamethasone for 2 h. Cells were washed with PBS and loaded with media containing (+)-catechin or (-)-epicatechin 10uM or 100uM. To mimic a high-fat scenario *in vitro*, cells were loaded with sterile bovine serum albumin (BSA) conjugated with palmitate (0.25 mM) or with serum albumin (0.04 mM) as control, both with 0.1 % (v/v) DMSO. In all conditions, stocks solutions were highly concentrated and underwent serial dilution to remove organic solvents. Stock solution of 5 mM palmitate:0.8 mM BSA was acquired from Cayman, USA and filtered using a 0.22-μm filter. Luciferin (200 μM) was added to each dish, which were covered with round glass lids, and sealed with parafilm. All dishes were transferred to the Lumicycle and bioluminescence was measured every 10 minutes (Actimetrics, USA) at 32.5 °C for 4 days. Bioluminescence measurements were collected, and the raw data were imported to the Lumicycle software. Baseline subtracted bioluminescence, calculated by 24-hour running-average subtraction, was used for rhythm evaluation.

2.10 Rhythm analysis

Rhythmic analyzes were performed using CircaCompare algorithm [43]. Rhythmic parameters were compared in a pairwise fashion using CircaCompare. Presence of rhythmicity was considered when p-value < 0.05 was achieved. Comparison between amplitude and MESOR was performed for genes or metabolites, regardless of rhythmicity status. Phase estimation was performed only on gene or metabolites that showed significant rhythms in both groups.

For bioluminescence data, rhythmicity was assessed using the Circasingle algorithm as previously described [44] using the normalized bioluminescent data per hour. CircaSingle algorithm was set to consider amplitude a decay factor and period was not pre-established. Rhythmicity was confirmed when p-value < 0.05.

2.11 Statistical analysis

All data, except for bioluminescence data, were log2 transformed. The data displayed in all figures and tables represents mean ± standard error of the mean (SEM). Hepatic lipids, metabolites and gene expression oscillations were analyzed as described above. Global metabolomics analysis was performed using one-way ANOVA, followed by Tukey's post-test in R environment. PCA analyzes were performed using the factoextra package and Hartigan-Wong, Lloyd, and Forgy MacQueen algorithms (version 1.0.7) in R. Liver lipid profiles were subjected to Student's t test and one-way ANOVA followed by Turkey's multiple-range post-hoc test using IBM SPSS Statistics (version 25) software. Graphics were done in GraphPad Prism 9 software (San Diego, CA, USA) and R using ggplot package. For all analyses, a probability (p) value of < 0.05 was considered to reflect a statistically significant difference.

3 RESULTS

3.1 Hematoxylin & eosin staining demonstrates that CAF diet induces NAFLD and a time dependent effectiveness of GSPE treatment

H & E staining was performed to study the pathological consequences of CAF diet intake on the liver tissue. As is shown in Figure 1 A-B compared to STD liver tissue, lipid droplets were visible in the liver and many hepatocytes had swelling and injury in CAF-VH groups, in both ZT0 and ZT12 treatments. Analysis of H & E staining showed that there was a significant difference in the histopathology and lipid accumulation between STD diet liver tissues and liver tissues of CAF diet animals. Interestingly, GSPE treatment was able to reduce the numbers of lipid droplets when it was administered at ZT12 ($p = 0.01$) but not at ZT0, lowering the level of inflammation from 0.75 to 0.44 and steatosis score from 3.17 to 2.67 changing the NASH status to NAFLD only at ZT12 (Figure 1 C, Table 2).

3.2 GSPE restores CAF-diet disrupted daily oscillations in liver weight

To obtain a temporal representation of the diurnal changes in liver lipid abundance, we measured levels of triglycerides (TAGs), total cholesterol, total lipid content and liver weight at 6-hour intervals across the day. Results from circadian analysis, including rhythmometric parameters can be found on ST3 and group comparisons in ST4 [43].

In the morning treatment (ZT0), cholesterol levels and total lipid content showed rhythmicity in STD-VH ($p = 0.04$ and 0.001, respectively) but not in CAF-VH and CAF-GSPE animals. On the other hand, no rhythmic pattern was found for hepatic triglycerides in any of the groups. Interestingly, diurnal oscillations in liver weight were observed in all groups. While liver weight in STD-VH and CAF-GSPE groups peaked around ZT10, CAF-VH animals livers showed maximum weight at ZT16, causing a phase delay of 6 hours ($p = 0.001$) (Figure 2 A-D).

After GSPE night (ZT12) treatment (Figure 2 E-H), non-rhythmic expression was observed for total lipid content in all groups, whereas total cholesterol

showed rhythmicity only in the STD-VH group (p = 0.03). Although hepatic triglycerides did not show a significant circadian oscillation neither in STD-VH nor in CAFs groups; a tendency of decreasing the overall expression (MESOR) was observed in CAF-GSPE compared to CAF-VH group (p = 0.058). This result indicates that GSPE tends to reduce hepatic triglyceride accumulation. Interestingly, animals subjected to ZT12 GSPE treatment showed lower hepatic triglycerides levels compared to CAF-VH when considering all ZTs together (p = 0.04). In addition, the CAF diet disrupted circadian oscillations of liver weight, but animals treated with GSPE recovered the pattern of rhythmic expression with a slight phase delay (p = 0.01). It is worth to mention that MESOR was higher in CAF fed animals (VH and GSPE) when compared to STD-VH rats for all hepatic lipid parameters, which might reflect the differences in fat and carbohydrate content of both diets.

3.3 Daily oscillations of lipid metabolism related genes are lost in CAF but reestablished by GSPE treatment

To investigate how the CAF diet affects liver lipid metabolism by influencing the circadian system, we analyzed oscillations in the expression levels of genes that play crucial roles in regulating lipid metabolism in the liver. All rhythm analysis results such as phases, amplitudes and MESOR are shown in ST5 and group comparisons in ST6.

SREBP-1c (sterol regulatory element binding protein 1c) is one of the main transcription factors controlling the expression of lipid metabolism related genes downstream of the core clock machinery. Amongst others it regulates rate-limiting enzymes of fatty acid biosynthesis [45]. In the morning treatment (ZT0), the mRNA levels of SREBP-1c showed a clear daily oscillation in the STD group (p = 0.009), which was lost in CAF-VH animals and re-established when rats were treated with GSPE (p = 0.001). *Acaca* (acetyl-CoA carboxylase alpha) and *Cd36* (cluster of differentiation 36), also known as fatty acid translocase, involved in fatty acid biosynthesis and transport [46], did not show rhythmic expression patterns neither in the

STD-VH nor in the CAF-VH group, but they followed a circadian oscillation in CAF-GSPE treated animals (p = 0.002 and 0.01, respectively). A rhythmic expression of FATP5 (fatty acid transport protein 5) was observed in CAF-VH and CAF-GSPE with no differences between these two groups. For *Fasn* (fatty acid synthase), which contributes to *de novo* lipogenesis [47], our results showed a loss of rhythmicity caused by the CAF diet, and a restoration of its circadian oscillation when CAF rats were also treated with GSPE (p = 0.009). These animals also displayed a decrease in *Fasn* MESOR expression when compared to STD group (p = 0.001) (Figure 3-E). *Pparα* (peroxisome proliferator-activated receptor α) is a nuclear receptor that also connects the clock genes with lipid metabolism [48]. As is shown in figure 3-F all groups displayed diurnal rhythms for *Pparα*, although both CAF groups (VH and GSPE) showed an increase of the MESOR compared to the STD-VH (p < 0.001 and p = 0.002, respectively) and the GSPE group exhibited a phase delay of 4 hours compared to STD (p = 0.03). *Cyp7a1* (cytochrome P450 family 7 subfamily A member 1 also known as Cholesterol 7α-hydroxylase), is a gene that encodes for a protein involved in bile acid biosynthesis. It catalyzes the first reaction in the cholesterol catabolic pathway in the liver, which converts cholesterol to bile acids [49]. Non-rhythmic expression of *Cyp7a1* was seen in the STD group, but when comparing both CAF groups that showed a rhythmic pattern, CAF-VH exhibited a higher MESOR than GSPE (p = 0.04).

In the case of night (ZT12) treatment (Figure 3 H-N), when compared to STD-VH, both CAF-VH and CAF-GSPE showed higher MESOR levels of SREBP-1c (p = 0.001 and 0.004, respectively). Its downstream target, *Acaca*, exhibited a 3-hour phase advance in the CAF-VH compared to CAF-GSPE group (p = 0.047), whereas non rhythmic expression for this gene was found in the STD group. Moreover, the amplitude of its mRNA oscillation was increased in rats treated with GSPE compared to the STD group (p = 0.048). Interestingly, CAF-GSPE rats were the only group that showed a circadian rhythm (p = 0.01) for *Cd36,* but for FATP5 only STD-VH showed rhythmic

oscillation (p = 0.01). In the case of *Fasn* shifted phases induced by the CAF diet were seen - 5 h of phase shift when comparing STD-VH to CAF-VH (p = 0.009) and 4 h of phase shift if STD-VH and CAF-GSPE groups were compared (p= 0.05). *Pparα* showed diurnal rhythms in STD-VH (p = 0.001), CAF-VH (p = 0.002), and CAF-GSPE (p = 0.001) groups, although a reduction in the amplitude was seen in the CAF-GSPE group compared to STD-VH (p = 0.001). *Cyp7a1* mRNA expression displayed diurnal rhythmic variations in all groups, although a 3-hour phase advance was caused by CAF diet and was not re-adjusted by GSPE treatment. Additionally, amplitude was lower in CAF-GSPE than CAF-VH group (p = 0.04) for this gene.

3.4 Diurnal rhythms of glucose metabolic genes are disrupted by CAF-diet intake and restored by GSPE

To further explore the impact of CAF diet on hepatic glucose metabolism, we analyzed diurnal expression profiles of genes that are key regulators of glucose metabolism in the liver. All rhythmic analysis results (phases, amplitudes and MESOR) are shown in ST7 and group comparisons in ST8.

G6PC (glucose-6-phosphatase) is a key enzyme in glucose homeostasis, functioning in gluconeogenesis and glycogenolysis [50]. All experimental groups exhibited circadian oscillations for mRNA of its catalytic subunit (*G6pc*), however CAF-VH and GSPE showed a decrease in MESOR compared to STD-VH (p = 0.023 and 0.020, respectively) (Figure 4-A). *Slc2a2* (solute carrier family 2 member 2) encodes for the main liver glucose transporter, GLUT2 [51]. Although its mRNA levels exhibited rhythmicity in all groups, CAF-VH showed an increase in the MESOR compared to STD-VH (p = 0.02) and CAF-GSPE (p = 0.006). Expression of the mRNA of G6PD (glucose-6-phosphate dehydrogenase) which catalyzes the first rate-limiting step in the pentose phosphate pathway [52], showed a loss of its rhythmic expression under CAF diet, meanwhile GSPE treatment was able to restore this rhythm, albeit a decrease in MESOR compared to the STD group (p = 0.001). A major regulator of hepatic gluconeogenesis is Peroxisome proliferator-activated receptor gamma coactivator 1-alpha (encoded by *Ppargc1α*), which induces

the transcription of gluconeogenic genes [53]. Only GSPE treated group exhibited rhythmicity of this gene (p = 0.04). Finally, when analyzing *Sirt1* (sirtuin 1), a nicotinamide adenosine dinucleotide (NAD)-dependent deacetylase that regulates glycogen synthesis and gluconeogenesis [54], non-significant rhythm was seen in STD group, but CAF-VH and CAF-GSPE groups showed a rhythmic expression (p = 0.02 and 0.04, respectively).

Regarding the night treatment (ZT12), mRNA levels of *G6pc* showed a clear diurnal oscillation in the three experimental groups, but a decrease of MESOR was found between the STD and both CAF groups (VH and GSPE; p = 0.02). For *Slc2a2*, a phase delay caused by the CAF diet was observed (p = 0.004) compared to STD group, whereas in GSPE treated animals this phase shift was not detected. In addition, a 2-fold decreased amplitude in CAF-GSPE rats compared to the CAF-VH group was observed. Intriguingly, circadian oscillation of G6PD was totally disrupted in CAF fed animals and restored by GSPE treatment (p = 0.01; Figure 4-H). *Ppargc1α* showed a clear diurnal rhythmicity in the STD group while CAF diet had a tendency to decrease its MESOR (p = 0.07) and amplitude (p = 0.09). Although there were no significant differences in phase between STD and CAF-VH groups, animals treated with GSPE peaked at the same time as the STD group (ZT13), whereas CAF-VH rats peaked at ZT11, i.e., 2-hour phase delay. *Sirt1* showed a rhythmic expression in STD animals (p = 0.01) but not in the two CAF diet groups.

3.5 Global analysis of hepatic metabolomic assay reveals GSPE increased key metabolites concentrations decreased due to CAF diet affecting several metabolic pathways

To gain direct insights into the effects of obesogenic diet intake on hepatic metabolism, we conducted a metabolomic analysis on liver tissue. 61 metabolites were identified and quantified in the liver of all experimental groups.

Principal component analyzes (PCA) showed a clear differentiation between the groups when treated at ZT0 and ZT12, thus arguing for a time-

dependent effect of GSPE treatment (Supplementary Figure 1). As a first step, we conducted a global analysis without considering sacrifice time points (ZTs), to have a general view of metabolite concentrations. They are plotted in Figures 5 and 6 where statistically significant differences between groups are shown.

In the morning treatment ZT0 (Figure 5), CAF diet lowered the levels of pyruvic acid, sarcosine, urea, myo-inositol, and cholesterol when compared to the STD-VH group, whereas CAF-GSPE did not significantly reduce the levels of sarcosine, myo-inositol and cholesterol but instead showed a reduction on the levels of oxoproline, taurine and palmitoleic acid in addition to pyruvic acid and urea when compared to the STD-VH group. Levels of serine, threonine, glutamic acid, and oleic acid iso1 were higher in both CAF groups when compared to STD-VH. Meanwhile GSPE treatment increased concentration of fumaric acid with respect to CAF-VH, malic acid compared to STD-VH and α-ketoglutaric acid relative to STD and CAF-VH groups.

Analysis of metabolites in the night treatment (ZT12) showed that the CAF groups (VH and GSPE) had lower levels of pyruvic acid, sarcosine, urea, methionine, myo-inositol, oleic acid iso2, and cholesterol than the STD-VH group (Figure 6). Interestingly, nicotinamide levels were decreased in CAF-VH ($p = 0.046$) but not in animals treated with GSPE compared to STD-VH. In addition, the concentrations of serine in CAF-GSPE rats were sharply increased when compared to CAF ($p = 0.023$) and STD VH ($p = 0.001$). Meanwhile, oleic acid iso1 was the only metabolite increased in both CAF groups.

3.6 Rhythmicity of liver metabolites is disrupted by CAF diet and partially restored by GSPE

Since the coordinated oscillations of metabolites are critical for the optimal functioning of liver metabolism, we analyzed the diurnal expression of the 61 quantified hepatic metabolites using the CircaCompare algorithm [43] (ST9 and ST10).

A Venn Diagram was created only with those metabolites that displayed statistically significant rhythms (Figure 7). Among them, we selected those that showed an exclusive rhythmic expression in each group as it was reported that a HFD causes an unexpected genesis of *de novo* oscillating metabolites, that lead to a reprogramming of the metabolic liver pathways [20]. In addition, an enrichment analysis was performed to identify the pathways in which these metabolites were involved (Figure 8). In STD-VH animals treated at ZT0 rhythmic metabolites showed enrichment for urea cycle, mitochondrial transport chain, and arginine and proline metabolism. On the other hand, in CAF-VH treated animals rhythmic metabolites showed an enrichment for lactose and galactose metabolism, while malate-aspartate shuttle, glucose-alanine cycle and alanine metabolism were found enriched in CAF-GSPE group (Figure 8A; ST11). Upon animals treated at ZT12, pathways that were enriched in STD-VH group were mainly associated with thiamine, riboflavin, and alanine metabolism, among others. While glycine and serine metabolism, malate-aspartate shuttle, glucose-alanine cycle, and glutathione metabolism were the metabolic pathways that were observed to be enriched in CAF-VH group. In the case of CAF-GSPE group no significant enriched pathway was found among its exclusive rhythmic metabolites. (Figure 8B; ST11).

In addition, we focused on the metabolites that lost rhythmicity in the CAF-VH group compared to STD-VH and observed that in the morning treatment (ZT0) oscillations of several metabolites were affected due to CAF diet: urea, glycine, fumaric acid, serine, threonine, malic acid, oxoproline, 4-hydroxyproline, glycerol 1-phosphate, ornithine, adenosine, and adenosine-5-mono- (AMP), -di- (ADP), and -triphosphate (ATP). Interestingly, GSPE treatment restored diurnal oscillations of urea, glycine, threonine, and AMP, ADP, and ATP (Figure 9 A-D). A phase delay was observed in lactic acid, alanine, proline, nicotinamide, d-galactitol, myo-inositol, sedoheptulose, and pyruvic acid (tendency $p = 0.055$) metabolites in CAF-VH animals, whereas CAF-GSPE rats exhibit a phase delay only in proline, nicotinamide

and glycine - both compared to STD-VH. Moreover, compared to CAF-VH animals treated with GSPE showed a 6-hour phase advance in α-ketoglutaric acid, an increase of MESOR for sarcosine, fumaric acid, α-ketoglutaric acid and d-glucuronic acid, and a MESOR decrease for oxoproline, taurine, fructose 6-phosphate and glucose 6-phosphate.

In the case of the night treatment CAF diet caused loss of circadian oscillations in several metabolites including 2-hydroxybutyric acid, glycerol, succinic acid, serine, methionine, oxoproline, aspartic acid, taurine, citric acid, hydroxyphenyllactic acid, d-glucose, d-sorbitol, xanthosine, and inosine 5-monophosphate. Treatment with GSPE restored the rhythmic expression of 2-hydroxybutyric acid, glycerol, aspartic acid, and xanthosine (Figure 9 E-H) and tended to do the same for succinic, citric acid ($p = 0.08$), d-glucose ($p = 0.055$) and hydroxyphenyllactic acid ($p=0.06$). Moreover, the last-mentioned metabolite had a lower amplitude in CAF-VH but not in CAF-GSPE compared to STD-VH animals. When comparing CAF-VH and CAF-GSPE groups, animals that were treated with GSPE showed an increase in serine MESOR ($p = 0.03$) and a trend to increase in glycine MESOR ($p = 0.05$), a phase advance in adenine and malic acid, and higher amplitude in d-xylitol.

3.7 (+)-Catechin is one of the main GSPE phenolic components involved in its hepatoprotective effect against NAFLD

Predominant phenolic compounds in GSPE as determined by HPLC analysis included (+)-catechin and (-)-epicatechin. On the background of GSPE treatment's restorative effect on mRNA and metabolite rhythms in liver, we decided to explore the capacity of these two polyphenols to affect circadian rhythm regulation in an *in vitro* model of NAFLD [55]. AML12 cells stably expressing a circadian *Bmal1-Luc* reporter were cultivated with 0.25 mM palmitate (to induce steatosis) or BSA and then treated at different concentrations (10 and 100 μM) with catechin or epicatechin. Circadian rhythms were determined by real-time luminescence measurements and responses to treatment analyzed for effects on rhythm parameters, i.e., phase, amplitude, period and dampening

Results showed a reduction of the amplitude in AML12 *Bmal1-luc* cells when cultured with palmitate compared to BSA cultured control cells ($p < 0.001$; Figure 10 A-B). Whereas treatment with (-)- epicatechin could not improve this reduction in *Bmal1* amplitude caused by palmitate, cells treated with (+)-catechin exhibit a restoration of the amplitude, with an amelioration of the decreasing amplitude produced by palmitate treatment. Similar results were seen in acrophase, as only (+)-catechin treatments could restore the phase delay caused by palmitate (Figure 10 C). A lengthening of the period was observed in palmitate and (-)-epicatechin treated-cells ($p < 0.001$) but not in cells treated with (+)-catechin (Figure 10 D). Based on these results, we analyzed the expression of glucose and lipid metabolism associated genes as mediators of the circadian regulation of metabolic control. The first step of glycolysis is catalyzed by glucokinase (enconded by *Gk).* As is shown in Figure 10 F an increase of *Gk* expression was observed in cells treated with (+)-catechin (100 μM) compared to palmitate and with cells treated with (-)-epicatechin (100 μM). Moreover, expression of *Gys2* (glycogen synthase 2), which encodes the rate-limiting enzyme of glycogen storage in the liver, was downregulated due to palmitate, whereas treatment with (+)-catechin 100 μM reverted this decrease in *Gys2* expression (Figure 10 G). A downregulation of *G6pc* expression in palmitate-treated cells was observed, whereas this was not seen in cells treated with polyphenol extracts at the highest concentration (100 μM) (Figure 10 H). Regarding genes involved in lipid metabolism, a decrease in *Acaca* expression as well as in *Fasn* was observed in palmitate-treated cells, whereas cells treated with (+)-catechin did not show this downregulation in *Acaca* expression (Figure 10 I-J). Non-significant differences were seen for *Pfkl* (phosphofructokinase) and *Pck1* (phosphoenolpyruvate carboxykinase 1) (Figure 10 K-L).

4 DISCUSSION

The liver circadian clock plays an important role in regulating glucose, lipid, and bile acid metabolism, by controlling the expression of key metabolic genes implicated in these pathways. In fact, the pathophysiology of NAFLD

involves dysfunction of these regulatory pathways. Moreover, genes that control the circadian clock have been implicated with the progression of NAFLD [56]. Therefore, the aim of the present study was to investigate the hepatic diurnal rhythm of lipid and glucose metabolism in cafeteria diet induced obese rats and to observe the effects of GSPE administration considering the timing of administration. Furthermore, we wanted to investigate the role of (+)-catechin and (-)-epicatechin, as principal polyphenols' components of GSPE, in its hepatic metabolic circadian regulation.

CLOCK-BMAL1 heterodimer contributes to modulate daily lipid metabolism in the liver by influencing SREBP-1c, and its downstream targets such as *Fasn* and *Acaca* [57]. Moreover, several studies involving liver specific depletion of clock genes have demonstrated the influence of circadian rhythms on liver energy metabolism [58]. By knocking out *Rorα* in the liver of mice, Zhang and collaborators demonstrated that this clock gene controls lipid metabolism by regulating expression of *Fasn, Elovl6, Acaca*, and SREBP-1c [59]. *Per2* knockout mice developed hepatic fibrosis with activation of hepatic stellate cells in the carbon tetrachloride-induced hepatitis model [60]. In addition, *Per* or *Cry* knockout mice can develop hepatocellular carcinoma [61]. In this sense, we have previously reported that CAF diet impairs the rhythmic expression pattern of hepatic core-clock genes, including *Bmal1, Per2, Cry1*, and *Rorα*, and that treatment with GSPE can restore the circadian oscillation of these clock genes mainly by correcting the phase shift caused by the CAF diet, with more emphasis at ZT12 treatment [36]. Remarkably our present results show that many genes encoding components of the lipogenic pathway, including *Acaca, Fasn,* SREBP-1c and *Cd36* display impaired or lost circadian expression rhythms in animals fed a CAF diet. However, when GSPE treatment was administered rats showed a robust diurnal expression pattern of these genes, conceivably improving lipid metabolism in the liver by restoring clock genes diurnal oscillations. The present study confirmed that the CAF diet induced

misalignment of the oscillations of lipid metabolism–related genes, which could lead to enhance the *de novo* lipogenesis. This correlates with studies of liver-specific *Bmal1* and *Rorα* knock-out mice which exhibit increased liver triglyceride accumulation [59,62]. Our results showed that CAF animals that were administered with GSPE at ZT12 had lower levels of hepatic triglycerides and decreased lipid droplets than those who were administered with the VH at the same ZT. Moreover, our *in vitro* results point to (+)-catechin as one of the main GSPE components involved in hepatic clock regulation, increasing amplitude of *Bmal1*, restoring the phase delay and period lengthening, and improving expression of glucose and lipid related metabolic genes in cells exposed to palmitate treatment. Antioxidant and anti-inflammatory properties of (+)-catechin treatment have been evidenced by *in vitro* studies as it influences gene expression of Nrf2 and NF-kB inflammatory pathways and regulates key enzymes involved in oxidative stress, showing hepatoprotective effects against liver injury [63–65]. It was also shown that (+)-catechin exerts anti-obesogenic properties in 3T3-L1 adipocytes by inhibiting 3T3-L1 preadipocyte differentiation via modulating the C/EBP/PPARγ/SREBP-1c pathway. Moreover, (+)-catechin stimulated lipid degradation of mature adipocytes through cAMP/PKA pathways thereby exerting anti-adipogenic effects [66].

Sinturel and collaborators observed diurnal oscillations in liver mass and hepatocyte size in mice, the amplitude of which depends on both feeding-fasting and light-dark cycles [67]. They discover that ribosome number, and protein content follow a daily rhythm, and that rRNA polyadenylation cycles are antiphasic to ribosomal protein synthesis oscillations. In this regard, in the present study animals treated at ZT0 showed a robust daily oscillation of liver mass in all groups, nonetheless CAF-VH animals exhibit a 6-hour phase delay compared to STD-VH. It is remarkable that treatment with GSPE is able to restore this phase shift caused by the CAF diet. Moreover, in animals treated at ZT12, CAF-VH rats completely lost rhythmicity of liver weight compared to STD, while treatment with GSPE restores hepatic mass

oscillation albeit with a phase delay. Since the liver is crucial for metabolism and xenobiotic detoxification, an accurate mass oscillation is needed to ensure the proper execution of these processes.

Several recent studies have demonstrated a close relationship between metabolites and the circadian clock machinery [68]. Results from transcriptome and metabolome studies suggest circadian clocks in peripheral tissues have a major role in the temporal coordination of food processing [69,70]. In this sense, our study identified several metabolites that were significantly different in diet-induced obese rats compared to the control lean group. One of the most strongly affected metabolites was urea together with some urea cycle intermediates which include ornithine and aspartic acid. Several studies demonstrated an association between liver injury in NAFLD and impairment of urea biosynthesis [71–73]. In this sense, all these studies exhibit a downregulation of the urea cycle components altering the functional capacity for ureagenesis. Our results showed not only a decrease in urea levels in animals fed a CAF diet but a loss of rhythmicity on hepatic urea, ornithine, and aspartic acid. Treatment with GSPE was able to restore the diurnal oscillation of urea in ZT0 and of aspartic acid in ZT12. In addition, it has been shown that alterations in metabolites of the urea cycle act as a sensor of hepatocyte mitochondrial damage [74]. We have previously reported that the CAF diet causes dysfunction of mitochondrial dynamics by enhancing mitochondrial fission [36]. In addition, diurnal oscillations of intermediates of the TCA cycle such as pyruvic acid, succinic acid, fumaric acid, malic acid, a-ketoglutaric acid, and citric acid were lost or phase shifted in CAF fed animals. The partial restoration of TCA cycle circadian rhythmicity by GSPE supplementation may have beneficial effects on hepatic metabolic homeostasis, as mitochondria play a key role in energy metabolism. Moreover, it is known that glycine, serine and threonine can enter into and promote TCA cycle activity by converting into acetyl-CoA [75]. In this sense, our results show that glycine and its precursor threonine lose their diurnal rhythms in CAF fed rats while GSPE treatment can

reestablish a daily oscillation despite a delay in phase when compared to STD-VH group in the morning treatment (ZT0). Moreover, reduced concentration of these two glucogenic amino acids, glycine and serine, have been observed in diabetic mice [76].

In insulin-resistant cells, glucose uptake is impaired, triggering hepatic gluconeogenesis and consuming these glucogenic amino acids to initiate the production of the glucose precursors pyruvate and 3-phosphoglycerate [77]. This evidence goes in line with our results as we observed a decrease in MESOR of glycine and serine in ZT12-CAF-VH animals compared to CAF-GSPE rats. In addition, concentrations of serine were significantly increased in animals treated with GSPE at ZT12, although rhythmicity of this amino acid could not be restored by GSPE treatment. However, GSPE treatment at ZT12 showed the greatest ability to restore the rhythm of metabolites affected by the CAF diet. In this sense diurnal changes of glycerol, of 2-hydroxybutyric acid, aspartic acid, and xanthosine were restored with no differences in phase or amplitude regarding the STD-VH group. It has been shown that NAFLD disrupts glycerol metabolism affecting the insulin resistant state [78]. Moreover, liver steatosis was linked to increased glycerol metabolism via pathways intersecting with the TCA cycle and delayed gluconeogenesis from glycerol [79]. Therefore, glycerol is a pivotal substrate for hepatic glucose synthesis. Besides, a trend to reestablish d-glucose oscillations is seen in rats treated with GSPE at ZT12. This result correlates with mRNA circadian expression of *Slc2a2* which codifies the glucose transporter GLUT2, a crucial protein for glucose flux in hepatocytes. *Slc2a2* mRNA was phase delayed in CAF-VH but not in CAF-GSPE animals after ZT12 dosage. 2-hydroxybutyric acid has been reported as an early biomarker of insulin resistance and impaired glucose balance [80]. Furthermore, it was identified as an exercise-induced metabolite that may reflect the cytosolic redox state and energy stress at a systemic level. Another study supports this concept showing that elevated levels of this metabolite are associated with excess glutathione demand and disrupted

mitochondrial energy metabolism, leading to increased oxidative stress in insulin resistance associated states [81]. Furthermore, aspartic acid also plays a role in energy production in the body as an intermediate in the urea cycle and is involved in gluconeogenesis [82]. In this sense, there is a close relationship between ureagenesis and gluconeogenesis [83] and both processes have been seen to be affected by the obesogenic CAF diet intake. Moreover, glutathione metabolism was also observed to be compromised in CAF-VH groups by the metabolic pathway enrichment analysis. In addition to energy dysregulation, the levels of metabolites involved in purine metabolism, including xanthine and its precursor xanthosine are upregulated in NAFLD subjects, human patients, and rats, which might accumulate reactive oxygen species (ROS) in the liver promoting hepatic steatosis [84–86], showing a correlation with the histological results. The mechanism underlying may involve stimulation of superoxide radical production through the hypoxanthine-xanthine oxidase system associated with various ROS-related diseases [87,88]. Hydroxyphenyllactic acid, which is a derivative of tyrosine, can enhance oxidative stress by promoting the production of ROS in the mitochondria [89]. Indeed, a dysregulation in circadian oscillation and amplitude of hydroxyphenyllactic acid was observed in CAF-VH fed rats but not in animals treated with GSPE at ZT12.

Energy for lipogenesis is provided by NADPH, which is primarily produced by the pentose phosphate pathway (PPP). A loss of G6PD rhythmic expression due to CAF diet was observed in both day and night treatment groups. This gene encodes for a cytosolic enzyme that catalyzes the rate-limiting step of the oxidative PPP and whose principal function is to provide NADPH and pentose phosphates for fatty acid and nucleic acid synthesis [51]. In this sense, GSPE treatment at ZT0 and ZT12 is able to restore these circadian disruptions, although a decrease in MESOR was observed in the morning treatment compared to STD group. Moreover, in our previous study we had observed that circadian oscillations of nicotinamide phosphoribosyltransferase (*Nampt*), which encodes for rate limiting

component in the mammalian NAD biosynthesis pathway, exhibit a 3-hour phase advance in CAF-VH group in comparison to STD, meanwhile this difference had not been seen when CAF animals were treated with GSPE at ZT12 [36]. Remarkably, also at night treatment nicotinamide levels were lower in CAF-VH but not in CAF-GSPE animals compared to STD-VH rats. This suggests that energy production through NAD-related metabolism and enzymes may be impaired in CAF diet obese rats, resulting in the accumulation of TAGs in the liver and a dysregulation of energy balance. These findings are consistent with previous studies in the field of proanthocyanidins treatment. An acute dose of 250 mg/kg of GSPE, ten times the dose used in the present study, was found to increase hepatic *Nampt* expression and NAD levels in the dark phase while the effect was the opposite when it was administered in the light phase in healthy rats [90]. Furthermore, a significant increase of hepatic NAD content was observed after a chronic treatment with GSPE in healthy rats [91]. GSPE treatment was shown to modulate hepatic concentrations of the major NAD precursors and mRNA levels of genes encoding enzymes involved in NAD metabolism together with the upregulation of *Sirt1* gene expression in a dose-dependent manner. In addition, the authors suggested that this increase in NAD concentrations and *Sirt1* mRNA levels is significantly associated with improved protection against hepatic TAG accumulation [91]. It is known that SIRT1 acts in the liver as a master metabolic regulator controlling the expression of downstream metabolic targets [92]. It forms a complex with the CLOCK-BMAL1 heterodimer binding to E-box elements promoting the expression of *Nampt*. Nevertheless, no effect on circadian oscillations with GSPE treatment were observed for *Sirt1*; but a clear rhythmic expression was seen in *Ppargc1α* after ZT0 and ZT12 GSPE treatments. In the night treatment cohort, *Ppargc1α* circadian oscillations in CAF-VH animals peaked at ZT11 whereas in STD-VH and CAF-GSPE animals the peak was at ZT13. It has been described that SIRT1 induces gluconeogenic genes and hepatic glucose output through PGC-1α [93]. Therefore, the intake of an obesogenic diet causes a dysregulation of glucose

and lipid homeostasis in the liver, while a low dose of GSPE during the active phase (ZT12) ameliorates this disruption in a clock-related manner. The integrative results from hepatic lipid profiles, circadian gene expression of core clock and metabolic genes together with the metabolomic studies suggest that, in CAF diet rat livers, glucose metabolism is disrupted, and lipogenesis is enhanced, promoting fatty liver development. By restoring the oscillations of hepatic circadian clocks, liver mass, key lipogenic and glucogenic gene expression, and liver metabolites, ZT12-GSPE supplementation has liver-protecting properties and counteracts NAFLD development.

5 CONCLUSIONS

Our chrono-nutritional approach, in a rat model, showed that an intake of a CAF diet disturbed the hepatic circadian clock, lipid and glucose-related metabolic genes, as well as concentrations and oscillations of liver metabolites, ultimately promoting the development of NAFLD. Supplementation with GSPE ameliorates and partially corrects this disruption, with a stronger effect when administration is timed to the active phase (ZT12 treatment). This indicates that modulation of metabolic rhythms by proanthocyanidins is highly dependent on the time of administration. Furthermore, our *in vitro* results suggest (+)-catechin, one of the main phenolic compounds found in the GSPE extract, may be involved in the ameliorating effects of GSPE on NAFLD development. Our findings underline the importance of taking diurnal rhythms into account in the interpretation of metabolic studies and suggest that they should more generally be considered for therapeutic intervention targeting liver metabolism. In this sense, a better understanding of circadian metabolism can help the design of new drugs or natural compounds to be administered in a way that maximizes benefits, possibly enabling lower dosages and fewer administrations to reach a therapeutic dose.

CONFLICTS OF INTEREST

Nothing to declare.

ACKNOWLEDGMENTS

This research was funded by the Spanish Ministry of Economy and Competitiveness (MINECO), AGL2016-77105-R (CHRONOFOOD project), and by grants from the German Research Foundation (DFG): HO353-10/1, HO353-11/1 and CRC-296 (TP13). The authors would like to thank to Niurka Llópiz and Rosa Pastor (Tarragona), for their help and technical assistance.

REFERENCES

1. Eckel, R.H.; Grundy, S.M.; Zimmet, P.Z. The Metabolic Syndrome. *The Lancet* **2005**, *365*, 1415–1428, doi:10.1016/S0140-6736(05)66378-7.
2. Grundy, S.M.; Brewer, H.B.; Cleeman, J.I.; Smith, S.C.; Lenfant, C. Definition of Metabolic Syndrome: Report of the National Heart, Lung, and Blood Institute/American Heart Association Conference on Scientific Issues Related to Definition. *Circulation* **2004**, *109*, 433–438, doi:10.1161/01.CIR.0000111245.75752.C6.
3. Zimmet, P.; Alberti, K.G.M.M.; Stern, N.; Bilu, C.; El-Osta, A.; Einat, H.; Kronfeld-Schor, N. The Circadian Syndrome: Is the Metabolic Syndrome and Much More! *Journal of Internal Medicine* **2019**, *286*, 181–191, doi:10.1111/JOIM.12924.
4. Vanni, E.; Bugianesi, E.; Kotronen, A.; de Minicis, S.; Yki-Järvinen, H.; Svegliati-Baroni, G. From the Metabolic Syndrome to NAFLD or Vice Versa? *Digestive and Liver Disease* **2010**, *42*, 320–330, doi:10.1016/J.DLD.2010.01.016.
5. Maury, E.; Ramsey, K.M.; Bass, J. Circadian Rhythms and Metabolic Syndrome: From Experimental Genetics to Human Disease. *Circulation Research* **2010**, *106*, 447–462, doi:10.1161/CIRCRESAHA.109.208355.
6. Knutson, K.L.; Spiegel, K.; Penev, P.; van Cauter, E. The Metabolic Consequences of Sleep Deprivation. *Sleep Medicine Reviews* **2007**, *11*, 163–178, doi:10.1016/J.SMRV.2007.01.002.
7. Briones, B.; Adams, N.; Strauss, M.; Rosenberg, C.; Whalen, C.; Carskadon, M.; Roebuck, T.; Winters, M.; Redline, S. Relationship Between Sleepiness and General Health Status. *Sleep* **1996**, *19*, 583–588, doi:10.1093/SLEEP/19.7.583.
8. Qian, J.; Caputo, R.; Morris, C.J.; Wang, W.; Scheer, F.A. 0041 Circadian Misalignment Increases The Desire For Food Intake In Chronic Shift Workers. *Sleep* **2018**, *41*, A17–A17, doi:10.1093/SLEEP/ZSY061.040.

9. Kumar Jha, P.; Challet, E.; Kalsbeek, A. Circadian Rhythms in Glucose and Lipid Metabolism in Nocturnal and Diurnal Mammals. *Molecular and Cellular Endocrinology* **2015**, *418*, 74–88, doi:10.1016/J.MCE.2015.01.024.

10. Qian, J.; Scheer, F.A.J.L. Circadian System and Glucose Metabolism: Implications for Physiology and Disease. *Trends Endocrinol Metab* **2016**, *27*, 282, doi:10.1016/J.TEM.2016.03.005.

11. Ruger, M.; Scheer, F.A.J.L. Effects of Circadian Disruption on the Cardiometabolic System. *Reviews in Endocrine and Metabolic Disorders* **2009**, *10*, 245–260, doi:10.1007/S11154-009-9122-8/FIGURES/1.

12. Li, M.D.; Li, C.M.; Wang, Z. The Role of Circadian Clocks in Metabolic Disease. *The Yale Journal of Biology and Medicine* **2012**, *85*, 387.

13. de Assis, L.V.M.; Oster, H. The Circadian Clock and Metabolic Homeostasis: Entangled Networks. *Cell Mol Life Sci* **2021**, *78*, 4563–4587, doi:10.1007/S00018-021-03800-2.

14. Rutter, J.; Reick, M.; McKnight, S.L. Metabolism and the Control of Circadian Rhythms. *Annu Rev Biochem* **2002**, *71*, 307–331, doi:10.1146/ANNUREV.BIOCHEM.71.090501.142857.

15. Schwabe, R.F.; Wiley, J.W.; Reinke, H.; Asher, G. Circadian Clock Control of Liver Metabolic Functions. *Gastroenterology* **2016**, *150*, 574–580, doi:10.1053/J.GASTRO.2015.11.043.

16. Panda, S.; Antoch, M.P.; Miller, B.H.; Su, A.I.; Schook, A.B.; Straume, M.; Schultz, P.G.; Kay, S.A.; Takahashi, J.S.; Hogenesch, J.B. Coordinated Transcription of Key Pathways in the Mouse by the Circadian Clock. *Cell* **2002**, *109*, 307–320, doi:10.1016/S0092-8674(02)00722-5.

17. Panda, S. Circadian Physiology of Metabolism. *Science* **2016**, *354*, 1008, doi:10.1126/SCIENCE.AAH4967.

18. Eckel-Mahan, K.L.; Patel, V.R.; Mohney, R.P.; Vignola, K.S.; Baldi, P.; Sassone-Corsi, P. Coordination of the Transcriptome and Metabolome by the Circadian Clock. *Proc Natl Acad Sci U S A* **2012**, *109*, 5541–5546, doi:10.1073/PNAS.1118726109/SUPPL_FILE/SD04.XLSX.

19. Asher, G.; Sassone-Corsi, P. Time for Food: The Intimate Interplay between Nutrition, Metabolism, and the Circadian Clock. *Cell* **2015**, *161*, 84–92, doi:10.1016/J.CELL.2015.03.015.

20. Eckel-Mahan, K.L.; Patel, V.R.; de Mateo, S.; Orozco-Solis, R.; Ceglia, N.J.; Sahar, S.; Dilag-Penilla, S.A.; Dyar, K.A.; Baldi, P.; Sassone-Corsi, P. Reprogramming of the Circadian Clock by Nutritional Challenge. *Cell* **2013**, *155*, 1464–1478, doi:10.1016/J.CELL.2013.11.034/ATTACHMENT/E7850CFC-CB5D-4BBC-800E-A44448444E38/MMC4.XLSX.

21. Gu, L.; Kelm, M.A.; Hammerstone, J.F.; Beecher, G.; Holden, J.; Haytowitz, D.; Prior, R.L. Screening of Foods Containing Proanthocyanidins and Their Structural Characterization Using LC-MS/MS and Thiolytic Degradation. *Journal of Agricultural and Food Chemistry* **2003**, *51*, 7513–7521, doi:10.1021/JF034815D/SUPPL_FILE/JF034815DSI20030924_021717.PDF.

22. Gu, L.; Kelm, M.A.; Hammerstone, J.F.; Beecher, G.; Holden, J.; Haytowitz, D.; Gebhardt, S.; Prior, R.L. Concentrations of Proanthocyanidins in Common Foods and Estimations of Normal Consumption. *J Nutr* **2004**, *134*, 613–617, doi:10.1093/JN/134.3.613.

23. de La Iglesia, R.; Milagro, F.I.; Campión, J.; Boqué, N.; Martínez, J.A. Healthy Properties of Proanthocyanidins. *BioFactors* **2010**, *36*, 159–168, doi:10.1002/BIOF.79.

24. Chen, Z.Y.; Chan, P.T.; Ho, K.Y.; Fung, K.P.; Wang, J. Antioxidant Activity of Natural Flavonoids Is Governed by Number and Location of Their Aromatic Hydroxyl Groups. *Chemistry and Physics of Lipids* **1996**, *79*, 157–163, doi:10.1016/0009-3084(96)02523-6.

25. Yang, J.; Xiao, Y.Y. Grape Phytochemicals and Associated Health Benefits. *http://dx.doi.org/10.1080/10408398.2012.692408* **2013**, *53*, 1202–1225, doi:10.1080/10408398.2012.692408.

26. Baselga-Escudero, L.; Arola-Arnal, A.; Pascual-Serrano, A.; Ribas-Latre, A.; Casanova, E.; Salvadó, M.J.; Arola, L.; Blade, C. Chronic Administration of Proanthocyanidins or Docosahexaenoic Acid Reversess the Increase of MiR-33a and MiR-122 in Dyslipidemic Obese Rats. *PLoS ONE* **2013**, *8*, doi:10.1371/JOURNAL.PONE.0069817.

27. Baselga-Escudero, L.; Pascual-Serrano, A.; Ribas-Latre, A.; Casanova, E.; Salvadó, M.J.; Arola, L.; Arola-Arnal, A.; Bladé, C. Long-Term Supplementation with a Low Dose of Proanthocyanidins Normalized Liver MiR-33a and MiR-122 Levels in High-Fat Diet–Induced Obese Rats. *Nutrition Research* **2015**, *35*, 337–345, doi:10.1016/J.NUTRES.2015.02.008.

28. Hussein, S.A.; Abou Zaid, O.A.R.; Azab, M.A.; Mohamed, S.K. Therapeutic Potential and Hepatoprotective Activity of Proanthocyanidin and Clopidogrel in Non-Alcoholic Fatty Liver Disease-Induced Rats. *Benha Veterinary Medical Journal* **2021**, *40*, 104–108, doi:10.21608/BVMJ.2021.65036.1346.

29. Cui, Y.; Yin, Y.; Li, S.; Xie, Y.; Wu, Z.; Yang, H.; Qian, Q.; Li, X. Apple Polyphenol Extract Targets Circadian Rhythms to Improve Liver Biological Clock and Lipid Homeostasis in C57BL/6 Male Mice with Mistimed High-Fat Diet Feeding. *Journal of Functional Foods* **2022**, *92*, 105051, doi:10.1016/J.JFF.2022.105051.

30. Zhang, Y.; Cheng, L.; Liu, Y.; Zhang, R.; Wu, Z.; Cheng, K.; Zhang, X. Omics Analyses of Intestinal Microbiota and Hypothalamus Clock Genes in Circadian Disturbance Model Mice Fed with Green Tea Polyphenols. *Journal of Agricultural and Food Chemistry* **2022**, *70*, 1890–1901, doi:10.1021/ACS.JAFC.1C07594/SUPPL_FILE/JF1C07594_SI_001.PDF.

31. Qi, G.; Mi, Y.; Liu, Z.; Fan, R.; Qiao, Q.; Sun, Y.; Ren, B.; Liu, X. Dietary Tea Polyphenols Ameliorate Metabolic Syndrome and Memory Impairment via Circadian Clock Related Mechanisms. *Journal of Functional Foods* **2017**, *34*, 168–180, doi:10.1016/J.JFF.2017.04.031.

32. Miranda, J.; Portillo, M.P.; Madrid, J.A.; Arias, N.; Macarulla, M.T.; Garaulet, M. Effects of Resveratrol on Changes Induced by High-Fat Feeding on Clock Genes in Rats. *British Journal of Nutrition* **2013**, *110*, 1421–1428, doi:10.1017/S0007114513000755.

33. Man, A.W.C.; Ning Xia, |; Daiber, A.; Li, H. The Roles of Gut Microbiota and Circadian Rhythm in the Cardiovascular Protective Effects of Polyphenols. **2019**, doi:10.1111/bph.v177.6/issuetoc.

34. Quiñones, M.; Guerrero, L.; Suarez, M.; Pons, Z.; Aleixandre, A.; Arola, L.; Muguerza, B. Low-Molecular Procyanidin Rich Grape Seed Extract Exerts Antihypertensive Effect in Males Spontaneously Hypertensive Rats. *Food Research International* **2013**, *2*, 587–595, doi:10.1016/J.FOODRES.2013.01.023.

35. Ricketts, M.-L.; Ferguson, B.S. Polyphenols: Novel Signaling Pathways. *Current Pharmaceutical Design* **2018**, *24*, 158–170, doi:10.2174/1381612824666171129204054.

36. Rodríguez, R.M.; Cortés-Espinar, A.J.; Soliz-Rueda, J.R.; Feillet-Coudray, C.; Casas, F.; Colom-Pellicer, M.; Aragonès, G.; Avila-Román, J.; Muguerza, B.; Mulero, M.; et al. Time-of-Day Circadian Modulation of Grape-Seed Procyanidin Extract (GSPE) in Hepatic Mitochondrial Dynamics in Cafeteria-Diet-Induced Obese Rats. *Nutrients 2022, Vol. 14, Page 774* **2022**, *14*, 774, doi:10.3390/NU14040774.

37. Margalef, M.; Iglesias-Carres, L.; Pons, Z.; Bravo, F.I.; Muguerza, B.; Arola-Arnal, A. Age Related Differences in the Plasma Kinetics of Flavanols in Rats. *The Journal of Nutritional Biochemistry* **2016**, *29*, 90–96, doi:10.1016/J.JNUTBIO.2015.11.007.

38. Livak, K.J.; Schmittgen, T.D. Analysis of Relative Gene Expression Data Using Real-Time Quantitative PCR and the 2(-Delta Delta C(T)) Method. *Methods* **2001**, *25*, 402–408, doi:10.1006/meth.2001.1262.

39. *Canadian Journal of Biochemistry and Physiology Issued by THE NATIONAL RESEARCH COUNCIL OF CANADA A RAPID METHOD OF TOTAL LIPID EXTRACTION AND PURIFICATION1*;

40. Liang, W.; Menke, A.L.; Driessen, A.; Koek, G.H.; Lindeman, J.H.; Stoop, R.; Havekes, L.M.; Kleemann., R.; van den Hoek, A.M. Establishment of a General NAFLD Scoring System for Rodent Models and Comparison to Human Liver Pathology. *PLOS ONE* **2014**, *9*, e115922, doi:10.1371/JOURNAL.PONE.0115922.

41. Cajka, T.; Fiehn, O. Toward Merging Untargeted and Targeted Methods in Mass Spectrometry-Based Metabolomics and Lipidomics. **2015**, doi:10.1021/acs.analchem.5b04491.

42. Brown, S.A.; Fleury-Olela, F.; Nagoshi, E.; Hauser, C.; Juge, C.; Meier, C.A.; Chicheportiche, R.; Dayer, J.M.; Albrecht, U.; Schibler, U. The Period Length of Fibroblast Circadian Gene Expression Varies Widely among Human Individuals. *PLOS Biology* **2005**, *3*, e338, doi:10.1371/JOURNAL.PBIO.0030338.

43. Parsons, R.; Parsons, R.; Garner, N.; Oster, H.; Rawashdeh, O. CircaCompare: A Method to Estimate and Statistically Support Differences in Mesor, Amplitude and Phase, between Circadian Rhythms. *Bioinformatics* **2020**, *36*, 1208–1212, doi:10.1093/BIOINFORMATICS/BTZ730.

44. Ungefroren, H.; Thürling, I.; Färber, B.; Kowalke, T.; Fischer, T.; Vinícius, L.; de Assis, M.; Braun, R.; Castven, D.; Oster, H.; et al. The Quasimesenchymal

Pancreatic Ductal Epithelial Cell Line PANC-1—A Useful Model to Study Clonal Heterogeneity and EMT Subtype Shifting. *Cancers 2022, Vol. 14, Page 2057* **2022**, *14*, 2057, doi:10.3390/CANCERS14092057.

45. le Martelot, G.; Claudel, T.; Gatfield, D.; Schaad, O.; Kornmann, B.; lo Sasso, G.; Moschetta, A.; Schibler, U. REV-ERBα Participates in Circadian SREBP Signaling and Bile Acid Homeostasis. *PLOS Biology* **2009**, *7*, e1000181, doi:10.1371/JOURNAL.PBIO.1000181.

46. Nishikawa, S.; Doi, K.; Nakayama, H.; Uetsuka, K. The Effect of Fasting on Hepatic Lipid Accumulation and Transcriptional Regulation of Lipid Metabolism Differs between C57BL/6J and BALB/cA Mice Fed a High-Fat Diet. *Toxicologic Pathology* **2008**, *36*, 850–857, doi:10.1177/0192623308323920.

47. Jensen-Urstad, A.P.L.; Semenkovich, C.F. Fatty Acid Synthase and Liver Triglyceride Metabolism: Housekeeper or Messenger? *Biochimica et Biophysica Acta (BBA) - Molecular and Cell Biology of Lipids* **2012**, *1821*, 747–753, doi:10.1016/J.BBALIP.2011.09.017.

48. Oishi, K.; Uchida, D.; Ishida, N. Circadian Expression of FGF21 Is Induced by PPARα Activation in the Mouse Liver. *FEBS Letters* **2008**, *582*, 3639–3642, doi:10.1016/J.FEBSLET.2008.09.046.

49. Hatting, M.; Tavares, C.D.J.; Sharabi, K.; Rines, A.K.; Puigserver, P. Insulin Regulation of Gluconeogenesis. *Ann N Y Acad Sci* **2018**, *1411*, 21–35, doi:10.1111/NYAS.13435.

50. Lizák, B.; Szarka, A.; Kim, Y.; Choi, K.S.; Németh, C.E.; Marcolongo, P.; Benedetti, A.; Bánhegyi, G.; Margittai, É. Glucose Transport and Transporters in the Endomembranes. *International Journal of Molecular Sciences 2019, Vol. 20, Page 5898* **2019**, *20*, 5898, doi:10.3390/IJMS20235898.

51. Tian, W.N.; Braunstein, L.D.; Pang, J.; Stuhlmeier, K.M.; Xi, Q.C.; Tian, X.; Stanton, R.C. Importance of Glucose-6-Phosphate Dehydrogenase Activity for Cell Growth. *J Biol Chem* **1998**, *273*, 10609–10617, doi:10.1074/JBC.273.17.10609.

52. Qi, Y.; Jiang, C.; Cheng, J.; Krausz, K.W.; Li, T.; Ferrell, J.M.; Gonzalez, F.J.; Chiang, J.Y.L. Bile Acid Signaling in Lipid Metabolism: Metabolomic and Lipidomic Analysis of Lipid and Bile Acid Markers Linked to Anti-Obesity and Anti-Diabetes in Mice. *Biochimica et Biophysica Acta (BBA) - Molecular and Cell Biology of Lipids* **2015**, *1851*, 19–29, doi:10.1016/J.BBALIP.2014.04.008.

53. Puigserver, P.; Rhee, J.; Donovan, J.; Walkey, C.J.; Yoon, J.C.; Oriente, F.; Kitamura, Y.; Altomonte, J.; Dong, H.; Accili, D.; et al. Insulin-Regulated Hepatic Gluconeogenesis through FOXO1-PGC-1alpha Interaction. *Nature* **2003**, *423*, 550–555, doi:10.1038/NATURE01667.

54. Rahman, S.; Islam, R. Mammalian Sirt1: Insights on Its Biological Functions. *Cell Communication and Signaling : CCS* **2011**, *9*, 11, doi:10.1186/1478-811X-9-11.

55. Ogawa, Y.; Imajo, K.; Honda, Y.; Kessoku, T.; Tomeno, W.; Kato, S.; Fujita, K.; Yoneda, M.; Saito, S.; Saigusa, Y.; et al. Palmitate-Induced Lipotoxicity Is Crucial for the Pathogenesis of Nonalcoholic Fatty Liver Disease in

Cooperation with Gut-Derived Endotoxin. *Scientific Reports 2018 8:1* **2018**, *8*, 1–14, doi:10.1038/s41598-018-29735-6.

56. Froy, O. Circadian Rhythms, Nutrition and Implications for Longevity in Urban Environments. *Proc Nutr Soc* **2018**, *77*, 216–222, doi:10.1017/S0029665117003962.

57. Friedrichs, M.; Kolbe, I.; Seemann, J.; Tsang, A.H.; Cherradi, L.; Klein, J.; Oster, H. Circadian Clock Rhythms in Different Adipose Tissue Model Systems. *https://doi.org/10.1080/07420528.2018.1494603* **2018**, *35*, 1543–1552, doi:10.1080/07420528.2018.1494603.

58. Froy, O. Metabolism and Circadian Rhythms—Implications for Obesity. *Endocrine Reviews* **2010**, *31*, 1–24, doi:10.1210/ER.2009-0014.

59. Zhang, Y.; Papazyan, R.; Damle, M.; Fang, B.; Jager, J.; Feng, D.; Peed, L.C.; Guan, D.; Sun, Z.; Lazar, M.A. The Hepatic Circadian Clock Fine-Tunes the Lipogenic Response to Feeding through RORα/γ. *Genes Dev* **2017**, *31*, 1202–1211, doi:10.1101/GAD.302323.117.

60. Chen, P.; Han, Z.; Yang, P.; Zhu, L.; Hua, Z.; Zhang, J. Loss of Clock Gene MPer2 Promotes Liver Fibrosis Induced by Carbon Tetrachloride. *Hepatology Research* **2010**, *40*, 1117–1127, doi:10.1111/J.1872-034X.2010.00695.X.

61. Kettner, N.M.; Voicu, H.; Finegold, M.J.; Coarfa, C.; Sreekumar, A.; Putluri, N.; Katchy, C.A.; Lee, C.; Moore, D.D.; Fu, L. Circadian Homeostasis of Liver Metabolism Suppresses Hepatocarcinogenesis. *Cancer Cell* **2016**, *30*, 909–924, doi:10.1016/J.CCELL.2016.10.007.

62. Pan, X.; Bradfield, C.A.; Hussain, M.M. Global and Hepatocyte-Specific Ablation of Bmal1 Induces Hyperlipidaemia and Enhances Atherosclerosis. *Nature Communications 2016 7:1* **2016**, *7*, 1–15, doi:10.1038/ncomms13011.

63. Kalender, Y.; Yel, M.; Kalender, S. Doxorubicin Hepatotoxicity and Hepatic Free Radical Metabolism in Rats: The Effects of Vitamin E and Catechin. *Toxicology* **2005**, *209*, 39–45, doi:10.1016/J.TOX.2004.12.003.

64. Baranwal, A.; Aggarwal, P.; Rai, A.; Kumar, N. Pharmacological Actions and Underlying Mechanisms of Catechin: A Review. *Mini-Reviews in Medicinal Chemistry* **2021**, *22*, 821–833, doi:10.2174/1389557521666210902162120.

65. Kobayashi, H.; Tanaka, Y.; Asagiri, K.; Asakawa, T.; Tanikawa, K.; Kage, M.; Yagi, M. The Antioxidant Effect of Green Tea Catechin Ameliorates Experimental Liver Injury. *Phytomedicine* **2010**, *17*, 197–202, doi:10.1016/J.PHYMED.2009.12.006.

66. Jiang, Y.; Ding, S.; Li, F.; Zhang, C.; Sun-Waterhouse, D.; Chen, Y.; Li, D. Effects of (+)-Catechin on the Differentiation and Lipid Metabolism of 3T3-L1 Adipocytes. *Journal of Functional Foods* **2019**, *62*, 103558, doi:10.1016/J.JFF.2019.103558.

67. Sinturel, F.; Gerber, A.; Mauvoisin, D.; Wang, J.; Gatfield, D.; Stubblefield, J.J.; Green, C.B.; Gachon, F.; Schibler, U. Diurnal Oscillations in Liver Mass and Cell Size Accompany Ribosome Assembly Cycles. *Cell* **2017**, *169*, 651-663.e14, doi:10.1016/J.CELL.2017.04.015/ATTACHMENT/C0BF0EEE-43F1-400B-A84A-FA2B40FA2E17/MMC1.DOCX.

68. Asher, G.; Schibler, U. Crosstalk between Components of Circadian and Metabolic Cycles in Mammals. *Cell Metabolism* **2011**, *13*, 125–137, doi:10.1016/J.CMET.2011.01.006.

69. Marcheva, B.; Ramsey, K.M.; Peek, C.B.; Affinati, A.; Maury, E.; Bass, J. Circadian Clocks and Metabolism. *Handb Exp Pharmacol* **2013**, *217*, 127, doi:10.1007/978-3-642-25950-0_6.

70. Dibner, C.; Schibler, U. Circadian Timing of Metabolism in Animal Models and Humans. *Journal of Internal Medicine* **2015**, *277*, 513–527, doi:10.1111/JOIM.12347.

71. Gallego-Durán, R.; Ampuero, J.; Pastor-Ramírez, H.; Álvarez-Amor, L.; Antonio Del Campo, J.; Maya-Miles, D.; Montero-Vallejo, R.; Cárdenas-García, A.; Jesús Pareja, M.; Gato-Zambrano, S.; et al. Liver Injury in Non-Alcoholic Fatty Liver Disease Is Associated with Urea Cycle Enzyme Dysregulation. *Scientific Reports 2022 12:1* **2022**, *12*, 1–11, doi:10.1038/s41598-022-06614-9.

72. de Chiara, F.; Heebøll, S.; Marrone, G.; Montoliu, C.; Hamilton-Dutoit, S.; Ferrandez, A.; Andreola, F.; Rombouts, K.; Grønbæk, H.; Felipo, V.; et al. Urea Cycle Dysregulation in Non-Alcoholic Fatty Liver Disease. *Journal of Hepatology* **2018**, *69*, 905–915, doi:10.1016/J.JHEP.2018.06.023.

73. Eriksen, P.L.; Vilstrup, H.; Rigbolt, K.; Suppli, M.P.; Sørensen, M.; Heebøll, S.; Veidal, S.S.; Knop, F.K.; Thomsen, K.L. Non-Alcoholic Fatty Liver Disease Alters Expression of Genes Governing Hepatic Nitrogen Conversion. *Liver International* **2019**, *39*, 2094–2101, doi:10.1111/LIV.14205.

74. Ajaz, S.; McPhail, M.J.; Gnudi, L.; Trovato, F.M.; Mujib, S.; Napoli, S.; Carey, I.; Agarwal, K. Mitochondrial Dysfunction as a Mechanistic Biomarker in Patients with Non-Alcoholic Fatty Liver Disease (NAFLD). *Mitochondrion* **2021**, *57*, 119–130, doi:10.1016/J.MITO.2020.12.010.

75. Zhang, Y.; Zhou, X.; Li, C.; Wu, J.; Kuo, J.E.; Wang, C. Assessment of Early Triage for Acute Radiation Injury in Rat Model Based on Urinary Amino Acid Target Analysis †. *Mol. BioSyst* **2014**, *10*, 1441, doi:10.1039/c3mb70526a.

76. Altmaier, E.; Ramsay, S.L.; Graber, A.; Mewes, H.W.; Weinberger, K.M.; Suhre, K. Bioinformatics Analysis of Targeted Metabolomics—Uncovering Old and New Tales of Diabetic Mice under Medication. *Endocrinology* **2008**, *149*, 3478–3489, doi:10.1210/EN.2007-1747.

77. Magnusson, I.; Rothman, D.L.; Katz, L.D.; Shulman, R.G.; Shulman, G.I. Increased Rate of Gluconeogenesis in Type II Diabetes Mellitus. A 13C Nuclear Magnetic Resonance Study. *J Clin Invest* **1992**, *90*, 1323–1327, doi:10.1172/JCI115997.

78. Samuel, V.T.; Shulman, G.I. Nonalcoholic Fatty Liver Disease as a Nexus of Metabolic and Hepatic Diseases. *Cell Metabolism* **2018**, *27*, 22–41, doi:10.1016/J.CMET.2017.08.002.

79. Jin, E.S.; Browning, J.D.; Murphy, R.E.; Malloy, C.R. Fatty Liver Disrupts Glycerol Metabolism in Gluconeogenic and Lipogenic Pathways in Humans. *Journal of Lipid Research* **2018**, *59*, 1685, doi:10.1194/JLR.M086405.

80. Sousa, A.P.; Cunha, D.M.; Franco, C.; Teixeira, C.; Gojon, F.; Baylina, P.; Fernandes, R. Which Role Plays 2-Hydroxybutyric Acid on Insulin Resistance? *Metabolites* **2021**, *11*, doi:10.3390/METABO11120835.

81. Gall, W.E.; Beebe, K.; Lawton, K.A.; Adam, K.P.; Mitchell, M.W.; Nakhle, P.J.; Ryals, J.A.; Milburn, M. v.; Nannipieri, M.; Camastra, S.; et al. α-Hydroxybutyrate Is an Early Biomarker of Insulin Resistance and Glucose Intolerance in a Nondiabetic Population. *PLOS ONE* **2010**, *5*, e10883, doi:10.1371/JOURNAL.PONE.0010883.

82. Xie, Z.; Li, H.; Wang, K.; Lin, J.; Wang, Q.; Zhao, G.; Jia, W.; Zhang, Q. Analysis of Transcriptome and Metabolome Profiles Alterations in Fatty Liver Induced by High-Fat Diet in Rat. *Metabolism - Clinical and Experimental* **2010**, *59*, 554–560, doi:10.1016/J.METABOL.2009.08.022.

83. Ipata, P.L.; Pesi, R. Understanding the Interrelationship between the Synthesis of Urea and Gluconeogenesis by Formulating an Overall Balanced Equation. *Adv Physiol Educ* **2017**, *41*, 286–290, doi:10.1152/ADVAN.00180.2016/ASSET/IMAGES/LARGE/ZU100217310 40001.JPEG.

84. Dong, S.; Zhan, Z.Y.; Cao, H.Y.; Wu, C.; Bian, Y.Q.; Li, J.Y.; Cheng, G.H.; Liu, P.; Sun, M.Y. Urinary Metabolomics Analysis Identifies Key Biomarkers of Different Stages of Nonalcoholic Fatty Liver Disease. *World Journal of Gastroenterology* **2017**, *23*, 2771–2784, doi:10.3748/wjg.v23.i15.2771.

85. Safaei, A.; Oskouie, A.A.; Mohebbi, S.R.; Rezaei-Tavirani, M.; Mahboubi, M.; Peyvandi, M.; Okhovatian, F.; Zamanian-Azodi, M. Metabolomic Analysis of Human Cirrhosis, Hepatocellular Carcinoma, Non-Alcoholic Fatty Liver Disease and Non-Alcoholic Steatohepatitis Diseases. *Gastroenterology and Hepatology from Bed to Bench* **2016**, *9*, 158–173, doi:10.22037/GHFBB.V0I0.952.

86. Son, N.; Hur, H.J.; Sung, M.J.; Kim, M.S.; Hwang, J.T.; Park, J.H.; Yang, H.J.; Kwon, D.Y.; Yoon, S.H.; Chung, H.Y.; et al. Liquid Chromatography-Mass Spectrometry-Based Metabolomic Analysis of Livers from Aged Rats. *Journal of Proteome Research* **2012**, *11*, 2551–2558, doi:10.1021/PR201263Q/ASSET/IMAGES/PR201263Q.SOCIAL.JPEG_V03.

87. Willems, L.; Garnham, B.; Headrick, J.P. Aging-Related Changes in Myocardial Purine Metabolism and Ischemic Tolerance. *Experimental Gerontology* **2003**, *38*, 1169–1177, doi:10.1016/J.EXGER.2003.08.003.

88. Tsedensodnom, O.; Sadler, K.C. ROS: Redux and Paradox in Fatty Liver Disease. *Hepatology* **2013**, *58*, 1210–1212, doi:10.1002/HEP.26497.

89. Levchuk, A.A.; Faron, R.A.; Khrustalev, S.A.; Raushenbakh, M.O. Effect of the Carcinogenic Tyrosin Metabolite, p-Hydroxyphenyllactic Acid, on Ascorbic Acid Levels in Mouse Organs and Blood. *Bulletin of Experimental Biology and Medicine 1987 102:4* **1986**, *102*, 1417–1418, doi:10.1007/BF00851066.

90. Ribas-Latre, A.; Baselga-Escudero, L.; Casanova, E.; Arola-Arnal, A.; Salvadó, M.-J.; Bladé, C.; Arola, L. Dietary Proanthocyanidins Modulate BMAL1 Acetylation, Nampt Expression and NAD Levels in Rat Liver OPEN. *Nature Publishing Group* **2015**, *5*, 10954, doi:10.1038/srep10954.

91. Aragonès, G.; Suárez, M.; Ardid-Ruiz, A.; Vinaixa, M.; Rodríguez, M.A.; Correig, X.; Arola, L.; Bladé, C. Dietary Proanthocyanidins Boost Hepatic NAD + Metabolism and SIRT1 Expression and Activity in a Dose-Dependent Manner in Healthy Rats. *Nature Publishing Group* **2016**, doi:10.1038/srep24977.

92. Saran, A.R.; Dave, S.; Zarrinpar, A. Circadian Rhythms in the Pathogenesis and Treatment of Fatty Liver Disease. *Gastroenterology* **2020**, *158*, 1948, doi:10.1053/J.GASTRO.2020.01.050.

93. Rodgers, J.T.; Lerin, C.; Haas, W.; Gygi, S.P.; Spiegelman, B.M.; Puigserver, P. Nutrient Control of Glucose Homeostasis through a Complex of PGC-1α and SIRT1. *Nature 2005 434:7029* **2005**, *434*, 113–118, doi:10.1038/nature03354.

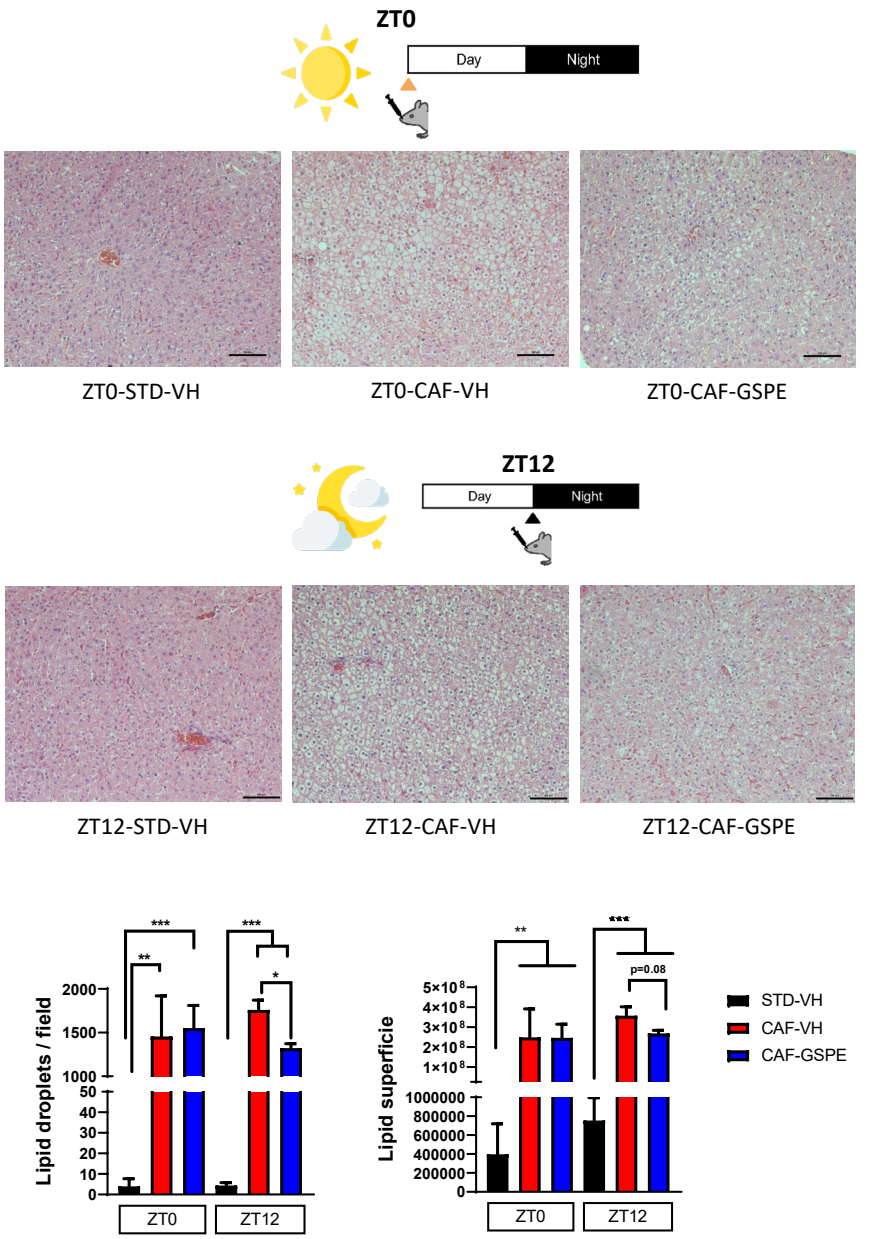

Figure 1. Representative pictures of H&E-stained liver sections. Scale bar, 100 µm. Rats were fed a STD or CAF diet and received a daily dosage of vehicle or GSPE at the beginning of the light phase (ZT0) **(A)** or at the beginning of the dark phase (ZT12) **(B)**. **C** Quantitative analysis of lipid droplets in liver samples per microscopic field (100×). * Indicates significant differences (Student's t test, *p<0.05, **p<0.01, ***p<0.001). Shown are means ± SEM (n=4/group at each time point).

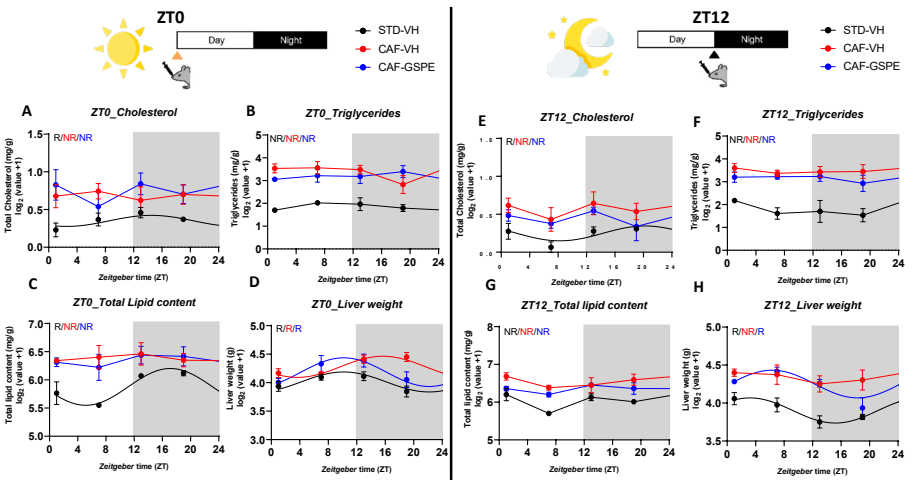

Figure 2. Diurnal rhythms of liver lipid levels and liver weight. Rats were fed a STD or CAF diet and received a daily dosage of vehicle or GSPE at the beginning of the light phase (ZT0) **(A-D)** or at the beginning of the dark phase (ZT12) **(E-H).** Rhythm parameter determination and comparison were performed using CircaCompare. R/NR indicates significant/non-significant rhythmicity ($p < 0.05$). Shown are means ± SEM (n=4/group at each time point).

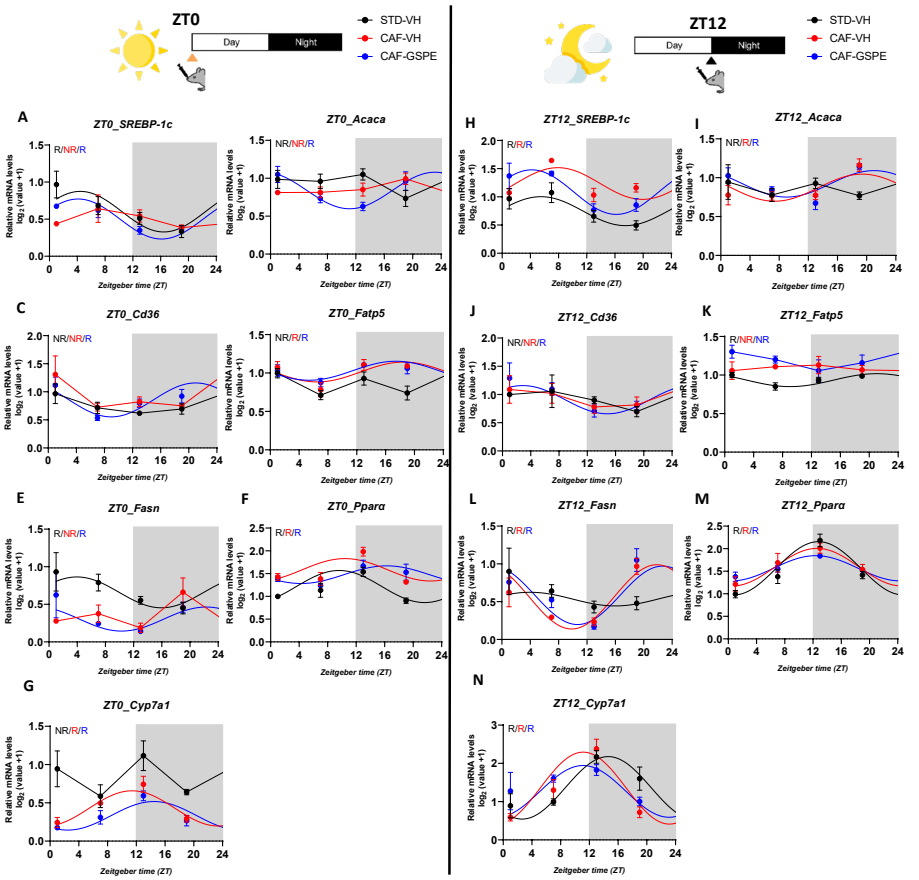

Figure 3. Diurnal mRNA profiles of key genes involved in lipid and bile acid metabolism. Rats were fed a STD or CAF diet and received a daily dosage of vehicle or GSPE at the beginning of the light phase (ZT0) **(A-G)** or at the beginning of the dark phase (ZT12) **(H-N).** Rhythm parameter determination and comparison were performed using CircaCompare. R/NR indicates significant/non-significant rhythmicity ($p < 0.05$). Shown are means ± SEM (n=4/group at each time point).

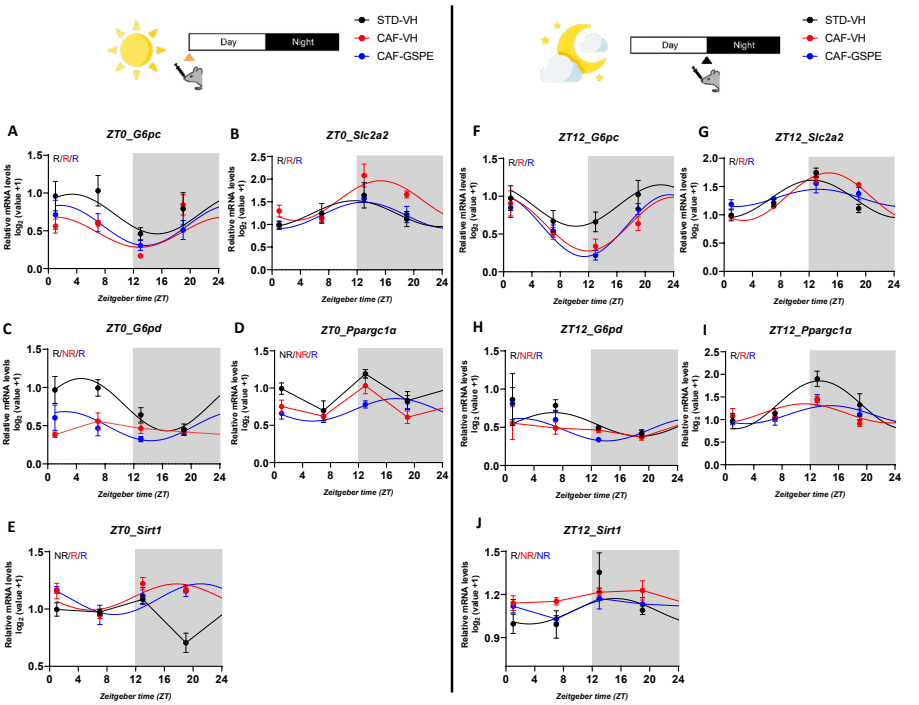

Figure 4. Diurnal mRNA profiles of key genes involved in glucose metabolism. Rats were fed a STD or CAF diet and received a daily dosage of vehicle or GSPE at the beginning of the light phase (ZT0) **(A-E)** or at the beginning of the dark phase (ZT12) **(F-J).** Rhythm parameter determination and comparison were performed using CircaCompare. R/NR indicates significant/non-significant rhythmicity ($p < 0.05$). Shown are means ± SEM (n=4/group at each time point).

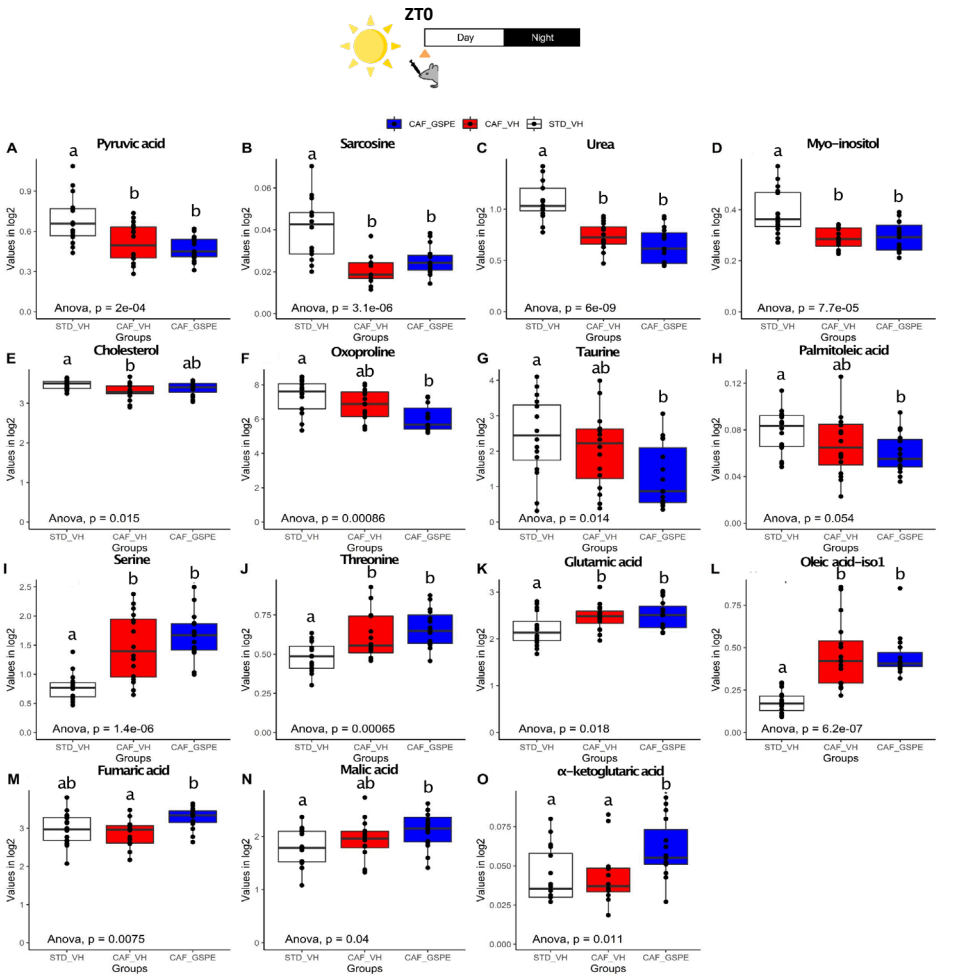

Figure 5. Box plots of metabolite levels in the liver of rats treated at ZT0. Rats were fed a STD or CAF diet and received a daily dosage of vehicle or GSPE at the beginning of the light phase (ZT0). One-way ANOVA followed by Tukey post-test were performed to compare the values between groups. Significant differences ($p \leq 0.05$) are represented by different letters (a-c). Shown are means ± SEM (n=16/group).

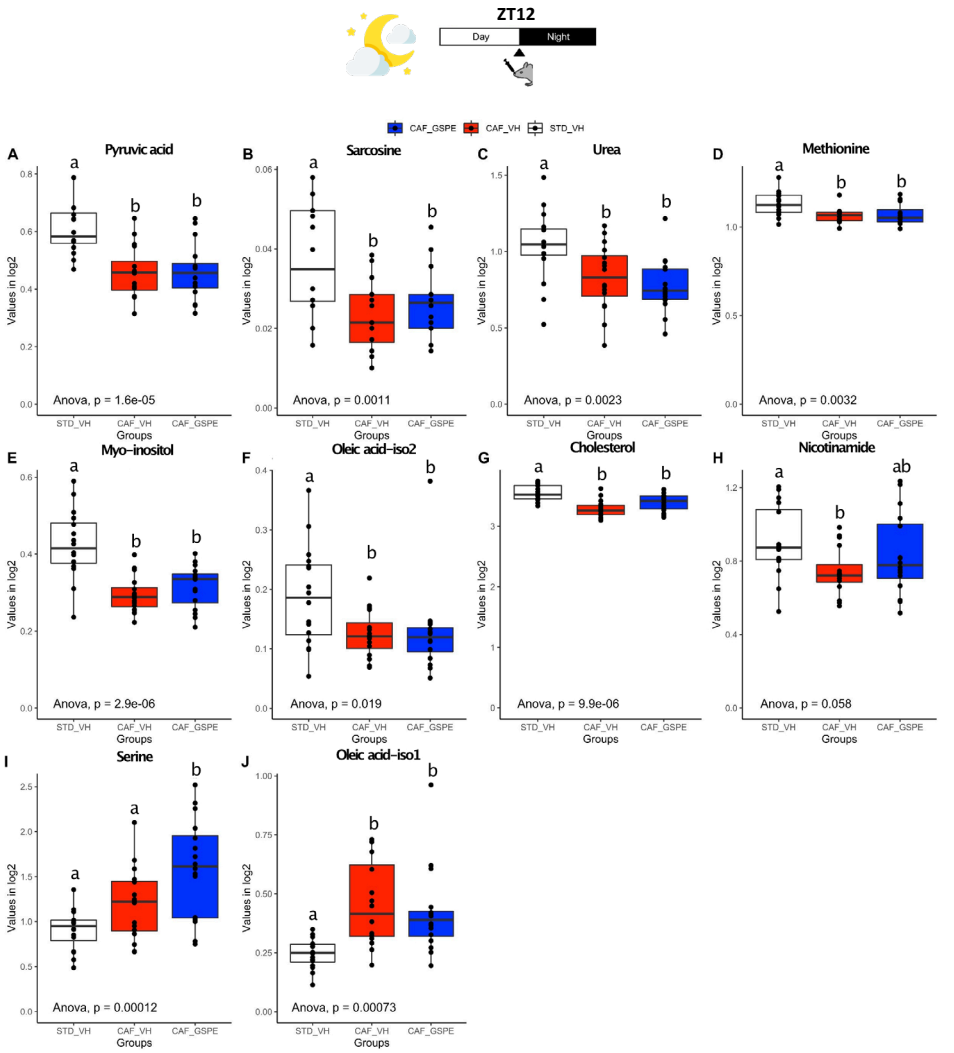

Figure 6. Box plots of metabolite levels in the liver of rats treated at ZT12. Rats were fed a STD or CAF diet and received a daily dosage of vehicle or GSPE at the beginning of the light phase (ZT12). One-way ANOVA followed by Tukey post-test were performed to compare the values between groups. Significant differences ($p \leq 0.05$) are represented by different letters (a-c). Shown are means ± SEM (n=16/group).

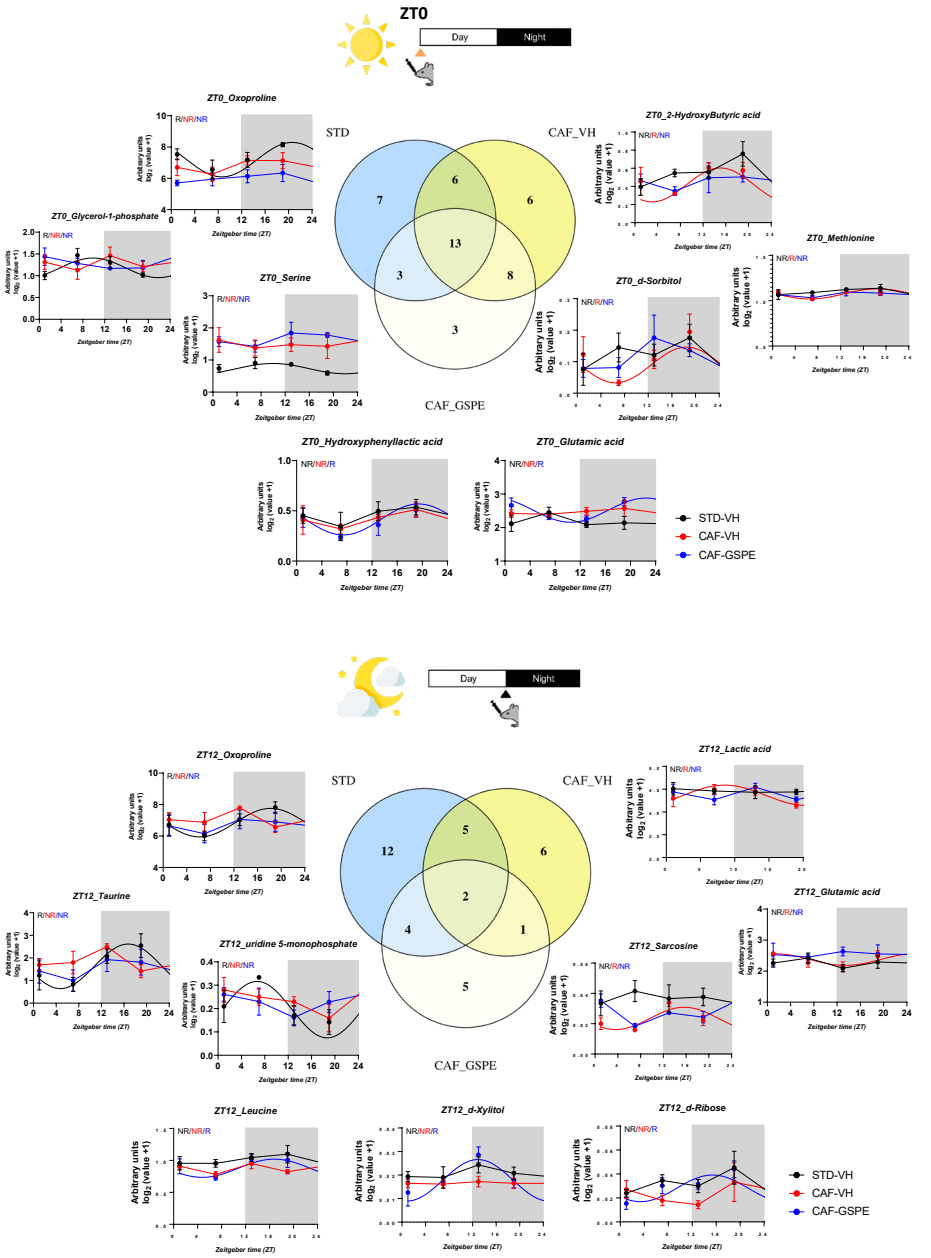

Figure 7. Metabolite rhythms under different diet/GSPE conditions. Rats were fed a STD or CAF diet and received a daily dosage of vehicle or GSPE at the beginning of the light phase (ZT0) **(A)** or at the beginning of the dark phase (ZT12) **(B)**. Venn diagrams depict numbers of rhythmic metabolites under each condition. Profiles show exemplary metabolites. Rhythm parameter determination and comparison were performed using CircaCompare. R/NR indicates significant/non-significant rhythmicity ($p < 0.05$). Shown are means ± SEM (n=4/group at each time point).

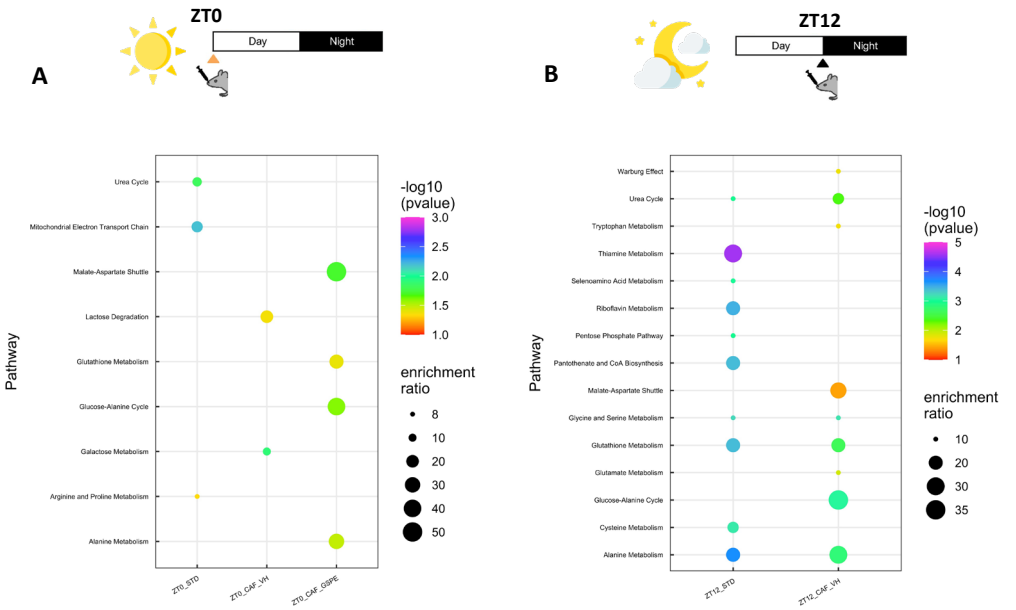

Figure 8. Metabolic pathways enrichment analysis of metabolites that showed an exclusive rhythmic expression in each group. Rats were fed a STD or CAF diet and received a daily dosage of vehicle or GSPE at the beginning of the light phase (ZT0) **(A)** or at the beginning of the dark phase (ZT12) **(B)**. The analysis was performed using MetaboAnalyst (Version 5.0, URL: http://www.metaboanalyst.ca).

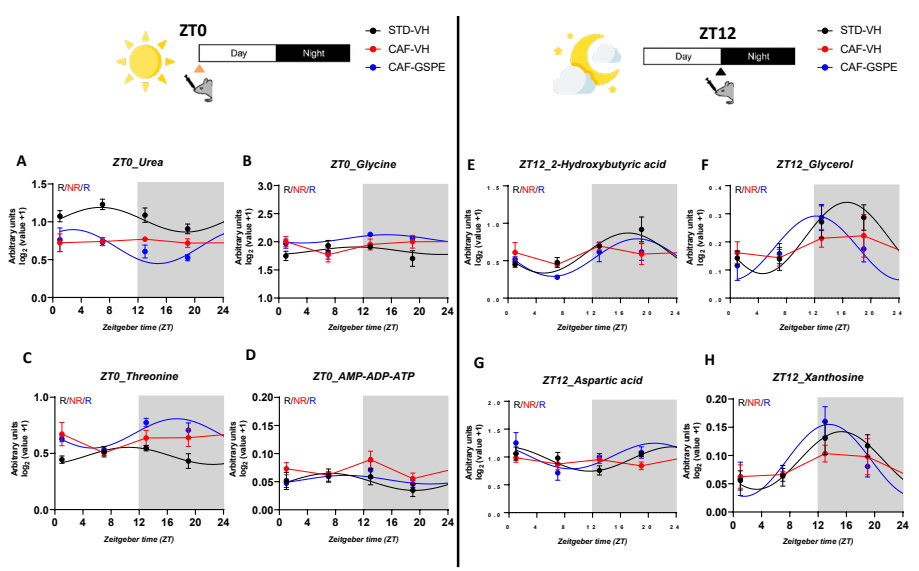

Figure 9. Restored diurnal oscillations of liver metabolites after chronic GSPE treatment. Rats were fed a STD or CAF diet and received a daily dosage of vehicle or GSPE at the beginning of the light phase (ZT0) **(A-D)** or at the beginning of the dark

phase (ZT12) **(E-H)**. Rhythm parameter determination and comparison were performed using CircaCompare. R/NR indicates significant/non-significant rhythmicity ($p < 0.05$). Shown are means ± SEM (n=4/group at each time point).

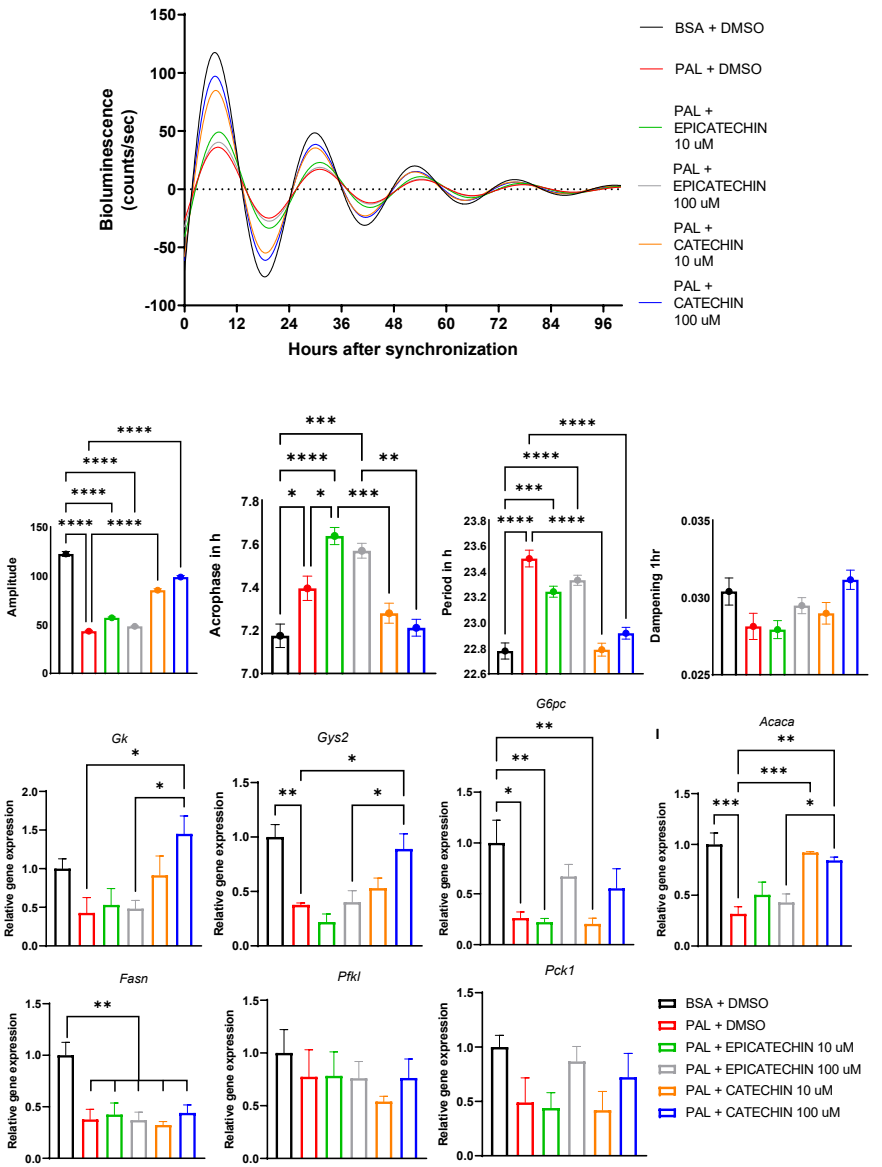

Figure 10. Effects of palmitate/GSPE treatment on circadian clock rhythms in hepatocytes in vitro. **(A)** Luminescence rhythms in synchronized AML12 hepatocytes stably expressing *Bmal1-luc* reporter and after treatment with GSPE. Representative dampened sine curve fits on normalized bioluminescence data are shown. **(B-E)** Circadian rhythm parameters of AML12 *Bmal1-luc* cells (amplitude,

acrophase, period, and dampening) in response to palmitate/GSPE treatment. Cells were treated with catechin or epicatechin (10 μM or 100 μM) for 96 h and cultured with sterile bovine serum albumin (BSA) conjugated with palmitate (PAL) (0.25 mM) with 0.1 % (v/v) DMSO. Cells cultured in BSA (0.04 mM) with 0.1 % (v/v) DMSO were used as control. Bioluminescence was measured using LumiCycle incubator in 10-min intervals. Rhythm parameters were assessed on normalized bioluminescence data using CircaSingle algorithm. **(F-L)** mRNA expression levels of metabolic genes in AML12/*Bmal1-luc* cells treated with catechin or epicatechin (10 μM or 100 μM) for 96 h and cultured with sterile bovine serum albumin (BSA) conjugated with palmitate (PAL) (0.25 mM) with 0.1 % (v/v) DMSO. Cells cultured in BSA (0.04 mM) with 0.1 % (v/v) DMSO were used as control. Data are means ± SEM (n = 4). One-way ANOVA followed by Tukey's post-test was performed to compare values between groups (*p<0.05, **p<0.01, ***p<0.001).

Table 1. Main phenolic compounds (flavanols and phenolic acids) of the grape seed proanthocyanidin extract (GSPE) used in this study, analyzed by HPLC-MS/MS.

Phenolic compound	(M-H)-	Calibration curve	Total amount (mg/g)	SD
Protocatechuic acid (PCA)	153.0187	y = 1E+06x	1.40	0.25
Catechin	289.0712	y = 1E+06x	51.88	5.56
Epicatechin	289.0712	y = 935152x	62.86	8.32
Gallic acid	169.0136	y = 287040x	44.66	7.76
Kaempferol-3-glucoside	447.0927	y = 1E+06x	0.50	0.02
Naringenin-7-glucoside	433.1135	y = 3E+06x	0.64	0.08
p-Coumaric acid	163.0395	y = 2E+06x	0.09	0.01
Quercetin	301.0348	y = 2E+06x	0.05	0.01
Quercetin-3-O-galactoside	463.0877	y = 2E+06x	0.43	0.05
Vanillic acid	167.0342	y = 1E+06x	0.09	0.01
Procyanidin dimer	577.1346	y = 664077x	76.84	15.76
Procyanidin trimer	865.1979	y = 664077x	13.04	0.64
Procyanidin tetramer	1153.2613	y = 664077x	5.14	0.28
Dimer gallate	729.1455	y = 1E+06x	15.22	2.72
Epicatechin gallate	441.0821	y = 1E+06x	14.24	2.76
Epigallocatechin gallate	457.077	y = 1E+06x	0.06	0.01

Table 2. Analysis of liver hematoxylin & eosin staining of rats that were fed a STD or CAF diet and received a daily dosage of vehicle or GSPE at the beginning of the light phase (ZT0) or at the beginning of the dark phase (ZT12).

	ZT0			ZT12		
	STD-VH	**CAF-VH**	**CAF-GSPE**	**STD-VH**	**CAF-VH**	**CAF-GSPE**
Macrovesicular st. (0-3)	0.000	0.167	0.111	0.000	0.000	0.000
Microvesicular st.(0-3)	0.000	1.750	1.667	0.000	2.167	2.000
Hypertrophy (0-3)	0.000	0.667	0.333	0.000	1.000	0.667
Steatosis score (0-9)	0.000	2.583	2.111	0.000	3.167	2.667
Inflammation	0.417	0.500	0.500	0.250	0.750	0.444
Diagnosis	No NAFLD	NASH	NASH	No NAFLD	NASH	NAFLD
Lipid droplets number	3.9	1175.7	1590.7	4.4	1397.7	1323.5
Total volum ($pixels^3$)	1485.3	792289.4	970609.2	2883.8	1135575.0	1070155.1
Total surface ($pixels^2$)	396872.7	195104404.3	251846625.1	754340.5	277785713.8	268128385.0
Average surface area ($pixels^2$)	74895.3	133774.2	176223.3	93125.2	189227.5	204359.4

SUPPLEMENTARY MATERIAL

Supplementary Figure 1. Principal component analysis (PCA) of liver metabolome analysis. Rats were fed a STD or CAF diet and received a daily dosage of vehicle or GSPE at the beginning of the light phase (ZT0) **(A)** or at the beginning of the dark phase (ZT12) **(B).** Analyzes were performed using the factoextra package and Hartigan-Wong, Lloyd, and Forgy MacQueen algorithms (version 1.0.7) in R.

Supplementary Table 1. Nucleotide sequences of primers used for real-time quantitative PCR in liver tissue.

Gene	Forward primer (5' to 3')	Reverse primer (5' to 3')
Acacα	TGCAGGTATCCCCACTCTTC	TTCTGATTCCCTTCCCTCCT
Cd36	GTCCTGGCTGTGTTTGGA	GCTCAAAGATGGCTCCATTG
Cyp7a1	CACTTGTTCAAGACCGCACA	TGCTTGAGATGCCCAGAGAA
Fasn	TAAGCGGTCTGGAAAGCTGA	CACCAGTGTTTGTTCCTCGG
Fatp5	CCTGCCAAGCTTCGTGCTAAT	GCTCATGTGATAGGATGGCTGG
G6pc	ATTCCGGTGCTTGAATGTCG	TGGAGGCTGGCATTGTAGAT
G6pd	ACCAGGCATTCAAAACGCAT	CAGTCTCAGGGAAGTGTGGT
Gk	CTGTGAAAGCGTGTCCACTC	GCCCTCCTCTGATTCGATGA
Ppargc1α	AGAGTCACCAAATGACCCCAAG	TTGGCTTTATGAGGAGGAGTCG
Pparα	CGGCGTTGAAAACAAGGAGG	TTGGGTTCCATGATGTCGCA
Ppia	CCAAACACAAATGGTTCCCAGT	ATTCCTGGACCCAAAACGCT
Sirt1	TTGGCACCGATCCTCGAA	ACAGAAACCCCAGCTCCA
Slc2a2	AGTCACACCAGCACATACGA	TGGCTTTGATCCTTCCGAGT
Srebp1c	CCCACCCCCTTACACACC	GCCTGCGGTCTTCATTGT

Supplementary Table 2. Nucleotide sequences of primers used for real-time quantitative PCR in cells.

Gene	Forward primer (5' to 3')	Reverse primer (5' to 3')
Acacα	GTCCCCAGGGATGAACCAATA	GCCATGCTCAACCAAAGTAGC
eEf1a	TGCCCCAGGACACAGAGACTTCA	AATTCACCAACACCAGCAGCAA
Fasn	GGAGGTGGTGATAGCCGGTAT	TGGGTAATCCATAGAGCCCAG
G6pc	CGACTCGCTATCTCCAAGTGA	GTTGAACCAGTCTCCGACCA
Gk	AGACCTGGGAGGAACCAACT	TTTGTCTTCACGCTCCACTG
Gys2	GCTCTCCAGACGTTCTTGCA	GTGCGGTTCCTCTGAATGATC
Pck1	AAGCATTCAACGCCAGGTTC	GGGCGAGTCTGTCAGTTCAAT
Pfkl	GAACTACGCACACTTGACCAT	CTCCAAAACAAAGGTCCTCTGG

Supplementary Table 3. Rhythmic parameters of lipid liver profile

Parameter	ZT	Groups	*p*	MESOR	Amplitude	Acrophase [h]
Cholesterol	ZT0	STD-VH	0.038	1.191	0.064	12.996
		CAF-VH	0.734	1.388	0.021	3.527
		CAF-GSPE	0.515	1.411	0.049	17.921
	ZT12	STD-VH	0.034	1.123	0.064	19.007
		CAF-VH	0.589	1.310	0.031	17.746
		CAF-GSPE	0.681	1.238	0.019	11.628
Triglycerides	ZT0	STD-VH	0.152	2.226	0.140	10.409
		CAF-VH	0.085	3.497	0.324	6.704
		CAF-GSPE	0.626	3.382	0.085	17.860
	ZT12	STD-VH	0.455	2.141	0.148	1.642
		CAF-VH	0.541	3.592	0.088	23.201
		CAF-GSPE	0.422	3.307	0.123	7.382
Total lipid liver content	ZT0	STD-VH	0.001	5.898	0.314	17.173
		CAF-VH	0.572	6.404	0.067	11.436
		CAF-GSPE	0.342	6.364	0.117	16.686
	ZT12	STD-VH	0.105	6.034	0.156	19.857
		CAF-VH	0.091	6.541	0.159	22.295
		CAF-GSPE	0.221	6.357	0.088	17.305
Liver weight	ZT0	STD-VH	0.016	4.086	0.145	9.360
		CAF-VH	0.001	4.370	0.181	16.309
		CAF-GSPE	0.019	4.271	0.225	10.607
	ZT12	STD-VH	0.005	3.995	0.162	2.833
		CAF-VH	0.289	4.403	0.078	2.726
		CAF-GSPE	0.001	4.301	0.229	6.826

Rats were fed a STD or CAF diet and were treated with vehicle or GSPE at the beginning of the light phase (ZT0) or at the beginning of the dark phase (ZT12). The $p < 0.05$ indicates significant rhythmic expression. MESOR is a mean adjusted to the circadian rhythm. Amplitude is the difference between the peak and the mean value of a sine wave. Acrophase is the time at which the peak of a rhythm occurs in hours.

Supplementary Table 4. Comparison of rhythmic parameters of lipid liver profile between groups.

Parameter	ZT	Comparison	d_MESOR	*p*(d_MESOR)	d_amplitude	*p*(d_amplitude)	d_phase	*p*(d_phase)
Cholesterol	ZT0	STD-VH vs. CAF-VH	0.197	0.000	-0.043	0.520	-9.469	0.302
		CAF-VH vs. CAF-GSPE	0.023	0.740	0.028	0.768	-9.606	0.478
		STD-VH vs. CAF-GSPE	0.220	0.001	-0.015	0.847	4.925	0.383
	ZT12	STD-VH vs. CAF-VH	0.188	0.000	-0.033	0.600	-1.261	0.836
		CAF-VH vs. CAF-GSPE	-0.072	0.167	-0.012	0.865	-6.118	0.616
		STD-VH vs. CAF-GSPE	0.116	0.004	-0.045	0.394	-7.379	0.355
Triglycerides	ZT0	STD-VH vs. CAF-VH	1.271	0.000	0.184	0.359	-3.705	0.379
		CAF-VH vs. CAF-GSPE	-0.115	0.528	-0.239	0.337	11.156	0.236
		STD-VH vs. CAF-GSPE	1.156	0.000	-0.055	0.773	7.451	0.348
	ZT12	STD-VH vs. CAF-VH	1.452	0.000	-0.059	0.802	-2.440	0.765
		CAF-VH vs. CAF-GSPE	-0.285	0.059	0.035	0.867	8.181	0.297
		STD-VH vs. CAF-GSPE	1.167	0.000	-0.025	0.918	5.740	0.394
Total lipid liver content	ZT0	STD-VH vs. CAF-VH	0.506	0.000	-0.248	0.082	-5.737	0.307
		CAF-VH vs. CAF-GSPE	-0.040	0.731	0.051	0.763	5.250	0.493
		STD-VH vs. CAF-GSPE	0.466	0.000	-0.197	0.173	-0.487	0.892
	ZT12	STD-VH vs. CAF-VH	0.507	0.000	0.003	0.982	2.439	0.426
		CAF-VH vs. CAF-GSPE	-0.185	0.027	-0.071	0.524	-4.990	0.218
		STD-VH vs. CAF-GSPE	0.323	0.001	-0.068	0.554	-2.552	0.545
Liver weight	ZT0	STD-VH vs. CAF-VH	0.284	0.000	0.036	0.600	6.949	0.000
		CAF-VH vs. CAF-GSPE	-0.099	0.137	0.045	0.631	-5.701	0.003
		STD-VH vs. CAF-GSPE	0.185	0.011	0.081	0.410	1.247	0.559

	ZT12	STD-VH vs. CAF-VH	0.408	0.000	-0.084	0.332	-0.107	0.974
		CAF-VH vs. CAF-GSPE	-0.102	0.110	0.151	0.097	4.100	0.213
		STD-VH vs. CAF-GSPE	0.306	0.000	0.067	0.352	3.993	0.010

Rats were fed a STD or CAF diet and were treated with vehicle or GSPE at the beginning of the light phase (ZT0) or at the beginning of the dark phase (ZT12). d_MESOR represents the difference in MESOR values between the groups. d_amplitude represents the difference in amplitude values between the groups. d_phase represents the difference in acrophase values between the groups. The $p < 0.05$ indicates significant differences between groups at each rhythmic parameter.

Supplementary Table 5. Rhythmic parameters of hepatic lipid metabolic genes.

Gene	ZT	Groups	*p*	MESOR	Amplitude	Acrophase [h]
Acaca	ZT0	STD-VH	0.146	0.933	0.117	8.075
		CAF-VH	0.085	0.868	0.091	18.192
		CAF-GSPE	0.002	0.844	0.240	23.118
	ZT12	STD-VH	0.919	0.854	0.009	2.741
		CAF-VH	0.012	0.869	0.198	19.014
		CAF-GSPE	0.001	0.921	0.231	22.324
Fasn	ZT0	STD-VH	0.040	0.686	0.248	3.677
		CAF-VH	0.143	0.376	0.150	20.176
		CAF-GSPE	0.010	0.366	0.262	23.384
	ZT12	STD-VH	0.053	0.613	0.249	2.267
		CAF-VH	0.001	0.530	0.389	21.007
		CAF-GSPE	0.002	0.626	0.394	22.216
Cd36	ZT0	STD-VH	0.060	0.745	0.180	1.224
		CAF-VH	0.094	0.902	0.244	0.805
		CAF-GSPE	0.011	0.834	0.241	21.407
	ZT12	STD-VH	0.101	0.913	0.188	5.970
		CAF-VH	0.141	0.926	0.186	3.233
		CAF-GSPE	0.010	0.976	0.326	2.774
Fatp5	ZT0	STD-VH	0.605	0.844	0.037	23.531
		CAF-VH	0.017	1.013	0.155	18.612
		CAF-GSPE	0.047	1.011	0.100	17.570
	ZT12	STD-VH	0.011	0.944	0.074	20.654
		CAF-VH	0.486	1.090	0.042	11.010
		CAF-GSPE	0.259	1.206	0.074	2.086
SREBP-1c	ZT0	STD-VH	0.010	0.623	0.288	3.502
		CAF-VH	0.072	0.502	0.139	8.485
		CAF-GSPE	0.001	0.502	0.203	3.507
	ZT12	STD-VH	0.005	0.797	0.329	5.121
		CAF-VH	0.017	1.228	0.244	6.684
		CAF-GSPE	0.001	1.102	0.411	3.849
Ppara	ZT0	STD-VH	0.004	1.145	0.293	11.474
		CAF-VH	0.011	1.527	0.280	12.529
		CAF-GSPE	0.047	1.449	0.210	15.968
	ZT12	STD-VH	0.000	1.493	0.595	13.118
		CAF-VH	0.002	1.613	0.407	12.296
		CAF-GSPE	0.000	1.574	0.230	12.746
Cyp7a1	ZT0	STD-VH	0.538	0.822	0.090	14.157

		CAF-VH	0.000	0.443	0.270	11.531
		CAF-GSPE	0.002	0.332	0.216	12.615
	ZT12	STD-VH	0.001	1.413	0.708	14.700
		CAF-VH	0.000	1.249	0.939	11.799
		CAF-GSPE	0.048	1.426	0.406	9.842

Rats were fed a STD or CAF diet and were treated with vehicle or GSPE at the beginning of the light phase (ZT0) or at the beginning of the dark phase (ZT12). The $p < 0.05$ indicates significant rhythmic expression. MESOR is a mean adjusted to the circadian rhythm. Amplitude is the difference between the peak and the mean value of a sine wave. Acrophase is the time at which the peak of a rhythm occurs in hours.

Supplementary Table 6. Comparison of rhythmic parameters of hepatic lipid metabolic genes between groups.

Gene	ZT	Comparison	d_MESOR	p(d_MESOR)	d_amplitude	p(d_amplitude)	d_phase	p(d_phase)
Acaca	ZT0	STD-VH vs. CAF-VH	-0.065	0.317	-0.026	0.773	10.117	0.006
		CAF-VH vs. CAF-GSPE	-0.024	0.668	0.149	0.067	4.926	0.051
		STD-VH vs. CAF-GSPE	-0.089	0.212	0.123	0.225	-8.957	0.001
	ZT12	STD-VH vs. CAF-VH	0.015	0.854	0.189	0.110	-7.727	0.814
		CAF-VH vs. CAF-GSPE	0.052	0.416	0.033	0.712	3.310	0.047
		STD-VH vs. CAF-GSPE	0.067	0.387	0.222	0.049	-4.417	0.887
Fasn	ZT0	STD-VH vs. CAF-VH	-0.309	0.006	-0.098	0.503	-7.501	0.020
		CAF-VH vs. CAF-GSPE	-0.011	0.909	0.112	0.398	3.208	0.233
		STD-VH vs. CAF-GSPE	-0.320	0.003	0.014	0.921	-4.293	0.046
	ZT12	STD-VH vs. CAF-VH	-0.083	0.428	0.140	0.345	-5.260	0.009
		CAF-VH vs. CAF-GSPE	0.097	0.311	0.005	0.972	1.208	0.358
		STD-VH vs. CAF-GSPE	0.014	0.901	0.145	0.356	-4.051	0.051
Cd36	ZT0	STD-VH vs. CAF-VH	0.157	0.181	0.064	0.702	-0.419	0.888
		CAF-VH vs. CAF-GSPE	-0.069	0.550	-0.004	0.982	-3.398	0.194
		STD-VH vs. CAF-GSPE	0.089	0.293	0.060	0.614	-3.818	0.087
	ZT12	STD-VH vs. CAF-VH	0.013	0.907	-0.002	0.991	-2.736	0.408
		CAF-VH vs. CAF-GSPE	0.050	0.667	0.140	0.392	-0.459	0.866
		STD-VH vs. CAF-GSPE	0.063	0.563	0.138	0.371	-3.195	0.217
Fatp5	ZT0	STD-VH vs. CAF-VH	0.169	0.013	0.118	0.197	-4.919	0.475
		CAF-VH vs. CAF-GSPE	-0.001	0.979	-0.055	0.461	-1.042	0.687

		STD-VH vs. CAF-GSPE	0.167	0.011	0.063	0.457	-5.961	0.379
	ZT12	STD-VH vs. CAF-VH	0.146	0.003	-0.032	0.619	-9.644	0.051
		CAF-VH vs. CAF-GSPE	0.116	0.065	0.032	0.711	-8.924	0.158
		STD-VH vs. CAF-GSPE	0.262	0.000	0.000	1.000	5.432	0.107
SREBP-1c	ZT0	STD-VH vs. CAF-VH	-0.121	0.162	-0.149	0.219	4.983	0.062
		CAF-VH vs. CAF-GSPE	0.000	0.994	0.064	0.457	-4.978	0.019
		STD-VH vs. CAF-GSPE	-0.121	0.123	-0.085	0.439	0.005	0.998
	ZT12	STD-VH vs. CAF-VH	0.431	0.000	-0.085	0.522	1.563	0.396
		CAF-VH vs. CAF-GSPE	-0.126	0.182	0.168	0.209	-2.835	0.103
		STD-VH vs. CAF-GSPE	0.305	0.004	0.083	0.547	-1.272	0.381
Ppara	ZT0	STD-VH vs. CAF-VH	0.383	0.000	-0.013	0.922	1.056	0.535
		CAF-VH vs. CAF-GSPE	-0.078	0.420	-0.071	0.605	3.439	0.126
		STD-VH vs. CAF-GSPE	0.305	0.002	-0.083	0.514	4.495	0.033
	ZT12	STD-VH vs. CAF-VH	0.120	0.228	-0.189	0.183	-0.822	0.464
		CAF-VH vs. CAF-GSPE	-0.040	0.634	-0.176	0.141	0.450	0.776
		STD-VH vs. CAF-GSPE	0.081	0.272	-0.365	0.001	-0.372	0.773
Cyp7a1	ZT0	STD-VH vs. CAF-VH	-0.379	0.001	0.180	0.241	-2.627	0.586
		CAF-VH vs. CAF-GSPE	-0.111	0.037	-0.054	0.466	1.084	0.342
		STD-VH vs. CAF-GSPE	-0.490	0.000	0.126	0.432	-1.542	0.759
	ZT12	STD-VH vs. CAF-VH	-0.164	0.337	0.231	0.340	-2.901	0.017
		CAF-VH vs. CAF-GSPE	0.178	0.325	-0.533	0.043	-1.958	0.291
		STD-VH vs. CAF-GSPE	0.013	0.941	-0.302	0.240	-4.858	0.018

Supplementary Table 7. Rhythmic parameters of genes related to hepatic glucose metabolism.

Gene	ZT	Groups	*p*	MESOR	Amplitude	Acrophase [h]
G6pc	ZT0	STD-VH	0.052	0.810	0.276	2.718
		CAF-VH	0.023	0.543	0.232	22.878
		CAF-GSPE	0.032	0.536	0.213	1.868
	ZT12	STD-VH	0.046	0.832	0.236	21.769
		CAF-VH	0.002	0.597	0.290	0.153
		CAF-GSPE	0.000	0.610	0.348	23.346
G6pd	ZT0	STD-VH	0.002	0.763	0.318	4.938
		CAF-VH	0.121	0.456	0.082	9.043
		CAF-GSPE	0.040	0.451	0.140	1.729
	ZT12	STD-VH	0.051	0.641	0.260	3.993
		CAF-VH	0.374	0.470	0.075	4.536
		CAF-GSPE	0.011	0.540	0.253	2.432
Slc2a2	ZT0	STD-VH	0.035	1.245	0.320	12.255
		CAF-VH	0.002	1.544	0.472	15.258
		CAF-GSPE	0.002	1.229	0.305	13.562
	ZT12	STD-VH	0.000	1.265	0.381	12.511
		CAF-VH	0.000	1.332	0.397	14.920
		CAF-GSPE	0.026	1.351	0.189	13.884
Ppargc1α	ZT0	STD-VH	0.229	0.928	0.119	15.293
		CAF-VH	0.106	0.754	0.139	12.805
		CAF-GSPE	0.045	0.718	0.113	16.884
	ZT12	STD-VH	0.003	1.333	0.476	13.748
		CAF-VH	0.048	1.125	0.200	11.573
		CAF-GSPE	0.015	1.126	0.251	13.819
Sirt1	ZT0	STD-VH	0.280	0.952	0.070	9.612
		CAF-VH	0.017	1.124	0.114	17.910
		CAF-GSPE	0.042	1.094	0.107	19.720
	ZT12	STD-VH	0.018	1.103	0.176	14.092
		CAF-VH	0.107	1.184	0.054	16.010
		CAF-GSPE	0.123	1.111	0.061	16.911

Rats were fed a STD or CAF diet and were treated with vehicle or GSPE at the beginning of the light phase (ZT0) or at the beginning of the dark phase (ZT12). The $p < 0.05$ indicates significant rhythmic expression. MESOR is a mean adjusted to the circadian rhythm. Amplitude is the difference between the peak and the mean value of a sine wave. Acrophase is the time at which the peak of a rhythm occurs in hours.

Supplementary Table 8. Comparison of rhythmic parameters of genes related to hepatic glucose metabolism between groups.

Gene	ZT	Comparison	d_MESOR	p(d_MESOR)	d_amplitude	p(d_amplitude)	d_phase	p(d_phase)
G6pc	ZT0	STD-VH vs. CAF-VH	-0.267	0.024	-0.045	0.779	-3.840	0.121
		CAF-VH vs. CAF-GSPE	-0.007	0.937	-0.019	0.882	2.990	0.168
		STD-VH vs. CAF-GSPE	-0.274	0.021	-0.064	0.694	-0.850	0.734
	ZT12	STD-VH vs. CAF-VH	-0.235	0.018	0.053	0.689	2.384	0.232
		CAF-VH vs. CAF-GSPE	0.013	0.859	0.058	0.579	-0.807	0.525
		STD-VH vs. CAF-GSPE	-0.222	0.020	0.111	0.388	1.577	0.377
G6pd	ZT0	STD-VH vs. CAF-VH	-0.307	0.000	-0.236	0.021	4.106	0.222
		CAF-VH vs. CAF-GSPE	-0.005	0.924	0.059	0.455	-7.314	0.017
		STD-VH vs. CAF-GSPE	-0.312	0.000	-0.177	0.102	-3.209	0.144
	ZT12	STD-VH vs. CAF-VH	-0.171	0.109	-0.185	0.216	0.543	0.922
		CAF-VH vs. CAF-GSPE	0.070	0.409	0.178	0.143	-2.104	0.640
		STD-VH vs. CAF-GSPE	-0.101	0.345	-0.006	0.966	-1.561	0.485
Slc2a2	ZT0	STD-VH vs. CAF-VH	0.299	0.024	0.152	0.405	3.003	0.102
		CAF-VH vs. CAF-GSPE	-0.315	0.006	-0.167	0.266	-1.696	0.292
		STD-VH vs. CAF-GSPE	-0.016	0.884	-0.015	0.924	1.308	0.486
	ZT12	STD-VH vs. CAF-VH	0.067	0.234	0.016	0.838	2.409	0.004
		CAF-VH vs. CAF-GSPE	0.019	0.759	-0.208	0.021	-1.036	0.445
		STD-VH vs. CAF-GSPE	0.086	0.242	-0.192	0.070	1.373	0.402

Ppargc1α	ZT0	STD-VH vs. CAF-VH	-0.174	0.057	0.020	0.871	-2.489	0.506
		CAF-VH vs. CAF-GSPE	-0.036	0.606	-0.026	0.787	4.080	0.189
		STD-VH vs. CAF-GSPE	-0.210	0.012	-0.006	0.958	1.591	0.667
	ZT12	STD-VH vs. CAF-VH	-0.208	0.076	-0.276	0.094	-2.175	0.359
		CAF-VH vs. CAF-GSPE	0.001	0.991	0.051	0.694	2.246	0.304
		STD-VH vs. CAF-GSPE	-0.207	0.076	-0.225	0.174	0.071	0.970
Sirt1	ZT0	STD-VH vs. CAF-VH	0.172	0.003	0.044	0.560	8.298	0.021
		CAF-VH vs. CAF-GSPE	-0.030	0.513	-0.007	0.911	1.810	0.430
		STD-VH vs. CAF-GSPE	0.142	0.018	0.037	0.639	10.108	0.011
	ZT12	STD-VH vs. CAF-VH	0.081	0.106	-0.122	0.091	1.918	0.591
		CAF-VH vs. CAF-GSPE	-0.073	0.042	0.007	0.884	0.901	0.784
		STD-VH vs. CAF-GSPE	0.008	0.878	-0.115	0.130	2.819	0.424

Rats were fed a STD or CAF diet and were treated with vehicle or GSPE at the beginning of the light phase (ZT0) or at the beginning of the dark phase (ZT12). d_MESOR represents the difference in MESOR values between the groups. d_amplitude represents the difference in amplitude values between the groups. d_phase represents the difference in acrophase values between the groups. The $p < 0.05$ indicates significant differences between groups at each rhythmic parameter.

Supplementary Table 9. Rhythmic parameters of genes related to hepatic glucose metabolism.

Metabolite	ZT	Groups	*p*	MESOR	Amplitude	Acrophase [h]
Pyruvic acid	ZT0	STD-VH	0.003	0.692	0.172	13.488
		CAF-VH	0.000	0.511	0.162	16.145
		CAF-GSPE	0.041	0.469	0.071	13.902
	ZT12	STD-VH	0.239	0.612	0.041	8.852
		CAF-VH	0.062	0.458	0.060	8.479
		CAF-GSPE	0.396	0.460	0.032	20.971
Lactic acid	ZT0	STD-VH	0.004	4.372	0.341	10.959
		CAF-VH	0.003	4.356	0.288	16.364
		CAF-GSPE	0.202	4.324	0.092	13.599
	ZT12	STD-VH	0.571	4.461	0.042	1.999
		CAF-VH	0.035	4.349	0.192	8.512
		CAF-GSPE	0.562	4.381	0.053	13.207
Alanine	ZT0	STD-VH	0.015	3.057	0.263	9.393
		CAF-VH	0.021	3.157	0.224	17.446
		CAF-GSPE	0.178	3.164	0.098	17.709
	ZT12	STD-VH	0.115	3.189	0.108	4.834
		CAF-VH	0.033	3.195	0.123	8.499
		CAF-GSPE	0.292	3.256	0.084	13.816
2-HydroxyButyric acid	ZT0	STD-VH	0.082	0.565	0.133	16.497
		CAF-VH	0.040	0.490	0.150	16.996
		CAF-GSPE	0.255	0.451	0.081	18.054
	ZT12	STD-VH	0.002	0.635	0.253	17.041
		CAF-VH	0.282	0.586	0.082	16.885
		CAF-GSPE	0.017	0.508	0.177	17.928
Sarcosine	ZT0	STD-VH	0.211	0.040	0.007	21.291
		CAF-VH	0.013	0.021	0.006	18.877
		CAF-GSPE	0.017	0.025	0.006	19.362
	ZT12	STD-VH	0.644	0.037	0.002	9.624
		CAF-VH	0.010	0.023	0.008	14.656
		CAF-GSPE	0.101	0.026	0.005	22.555
Valine	ZT0	STD-VH	0.166	0.842	0.070	11.575
		CAF-VH	0.011	0.781	0.121	17.247
		CAF-GSPE	0.012	0.798	0.109	17.878

	ZT12	STD-VH	0.323	0.915	0.061	15.606
		CAF-VH	0.694	0.791	0.015	14.399
		CAF-GSPE	0.064	0.829	0.123	17.229
Urea	ZT0	STD-VH	0.008	1.075	0.162	7.176
		CAF-VH	0.602	0.739	0.026	11.482
		CAF-GSPE	0.046	0.654	0.126	4.634
	ZT12	STD-VH	0.054	1.037	0.162	6.406
		CAF-VH	0.001	0.829	0.223	6.691
		CAF-GSPE	0.398	0.774	0.057	2.770
Leucine	ZT0	STD-VH	0.113	0.914	0.084	12.337
		CAF-VH	0.007	0.870	0.148	17.400
		CAF-GSPE	0.005	0.891	0.140	17.412
	ZT12	STD-VH	0.221	1.014	0.084	16.882
		CAF-VH	0.528	0.867	0.029	15.995
		CAF-GSPE	0.040	0.918	0.148	17.461
Phosphoric acid	ZT0	STD-VH	0.025	5.512	0.112	14.572
		CAF-VH	0.001	5.476	0.200	18.197
		CAF-GSPE	0.009	5.431	0.167	15.418
	ZT12	STD-VH	0.068	5.534	0.099	15.606
		CAF-VH	0.662	5.455	0.025	11.603
		CAF-GSPE	0.037	5.479	0.089	13.006
Glycerol	ZT0	STD-VH	0.048	0.177	0.065	15.971
		CAF-VH	0.009	0.165	0.098	19.306
		CAF-GSPE	0.033	0.172	0.074	16.456
	ZT12	STD-VH	0.006	0.210	0.098	16.264
		CAF-VH	0.174	0.185	0.047	16.791
		CAF-GSPE	0.017	0.184	0.086	13.378
Isoleucine	ZT0	STD-VH	0.249	0.531	0.042	12.182
		CAF-VH	0.007	0.503	0.091	17.201
		CAF-GSPE	0.006	0.513	0.082	17.787
	ZT12	STD-VH	0.248	0.585	0.051	16.539
		CAF-VH	0.479	0.500	0.020	16.393
		CAF-GSPE	0.053	0.529	0.091	17.421
Proline	ZT0	STD-VH	0.035	1.711	0.182	11.939
		CAF-VH	0.006	1.625	0.249	17.698
		CAF-GSPE	0.040	1.690	0.171	17.300
	ZT12	STD-VH	0.076	1.801	0.184	16.341

		CAF-VH	0.175	1.627	0.107	16.346
		CAF-GSPE	0.058	1.705	0.188	17.206
Glycine	ZT0	STD-VH	0.046	1.824	0.142	9.331
		CAF-VH	0.141	1.931	0.118	19.809
		CAF-GSPE	0.017	1.989	0.155	16.641
	ZT12	STD-VH	0.178	1.928	0.095	12.556
		CAF-VH	0.212	1.843	0.115	19.551
		CAF-GSPE	0.204	1.999	0.085	14.985
Succinic acid	ZT0	STD-VH	0.316	0.938	0.095	6.651
		CAF-VH	0.051	1.016	0.186	18.591
		CAF-GSPE	0.386	1.023	0.082	3.130
	ZT12	STD-VH	0.043	0.937	0.173	9.294
		CAF-VH	0.280	1.068	0.085	20.087
		CAF-GSPE	0.072	1.111	0.184	13.813
Fumaric acid	ZT0	STD-VH	0.001	2.970	0.438	8.601
		CAF-VH	0.368	2.844	0.130	7.186
		CAF-GSPE	0.496	3.281	0.081	2.149
	ZT12	STD-VH	0.001	3.345	0.603	2.750
		CAF-VH	0.009	3.088	0.336	2.751
		CAF-GSPE	0.078	3.261	0.257	23.355
Serine	ZT0	STD-VH	0.046	0.775	0.168	8.481
		CAF-VH	0.726	1.476	0.077	23.708
		CAF-GSPE	0.149	1.650	0.228	16.390
	ZT12	STD-VH	0.004	0.906	0.215	3.640
		CAF-VH	0.477	1.191	0.110	6.121
		CAF-GSPE	0.362	1.592	0.191	4.562
Threonine	ZT0	STD-VH	0.051	0.485	0.066	10.395
		CAF-VH	0.214	0.613	0.069	19.970
		CAF-GSPE	0.005	0.658	0.117	16.188
	ZT12	STD-VH	0.367	0.547	0.041	4.267
		CAF-VH	0.495	0.568	0.033	8.151
		CAF-GSPE	0.721	0.659	0.025	9.631
Nicotinamide	ZT0	STD-VH	0.010	0.809	0.121	12.772
		CAF-VH	0.007	0.702	0.181	18.413
		CAF-GSPE	0.029	0.736	0.160	18.195
	ZT12	STD-VH	0.148	0.904	0.104	19.604
		CAF-VH	0.268	0.742	0.054	19.344

		CAF-GSPE	0.135	0.834	0.123	15.977
Malic acid	ZT0	STD-VH	0.014	1.783	0.299	7.852
		CAF-VH	0.215	1.923	0.174	7.185
		CAF-GSPE	0.109	2.128	0.207	4.573
	ZT12	STD-VH	0.000	1.987	0.574	2.228
		CAF-VH	0.001	2.012	0.335	4.223
		CAF-GSPE	0.025	2.025	0.262	0.190
Methionine	ZT0	STD-VH	0.147	1.105	0.037	15.725
		CAF-VH	0.035	1.076	0.039	18.866
		CAF-GSPE	0.172	1.069	0.031	16.791
	ZT12	STD-VH	0.047	1.131	0.048	17.113
		CAF-VH	0.226	1.064	0.019	15.529
		CAF-GSPE	0.145	1.073	0.031	17.480
Oxoproline	ZT0	STD-VH	0.015	7.358	0.813	19.836
		CAF-VH	0.143	6.812	0.487	17.191
		CAF-GSPE	0.380	6.042	0.277	16.008
	ZT12	STD-VH	0.011	6.895	0.912	18.343
		CAF-VH	0.222	7.067	0.409	11.499
		CAF-GSPE	0.324	6.688	0.432	17.107
Aspartic acid	ZT0	STD-VH	0.136	0.916	0.096	7.102
		CAF-VH	0.114	1.015	0.123	6.896
		CAF-GSPE	0.577	1.017	0.038	1.730
	ZT12	STD-VH	0.033	0.963	0.155	0.120
		CAF-VH	0.703	0.914	0.023	4.064
		CAF-GSPE	0.042	1.011	0.223	21.327
4-Hydroxyproline	ZT0	STD-VH	0.013	0.226	0.079	8.401
		CAF-VH	0.057	0.216	0.084	16.300
		CAF-GSPE	0.062	0.193	0.048	0.754
	ZT12	STD-VH	0.074	0.227	0.031	7.081
		CAF-VH	0.880	0.226	0.005	2.136
		CAF-GSPE	0.135	0.257	0.066	22.283
a-ketoglutaric acid	ZT0	STD-VH	0.055	0.044	0.012	5.489
		CAF-VH	0.018	0.043	0.014	8.077
		CAF-GSPE	0.027	0.062	0.016	1.463
	ZT12	STD-VH	0.118	0.047	0.010	2.272
		CAF-VH	0.232	0.041	0.007	0.366
		CAF-GSPE	0.401	0.050	0.007	22.689

Glutamic acid	ZT0	STD-VH	0.241	2.197	0.154	6.645
		CAF-VH	0.382	2.470	0.092	17.568
		CAF-GSPE	0.006	2.512	0.301	21.895
	ZT12	STD-VH	0.366	2.268	0.105	3.484
		CAF-VH	0.027	2.366	0.236	23.209
		CAF-GSPE	0.682	2.545	0.071	16.056
Phenylalanine	ZT0	STD-VH	0.204	0.449	0.041	12.041
		CAF-VH	0.015	0.444	0.084	16.916
		CAF-GSPE	0.007	0.441	0.068	17.157
	ZT12	STD-VH	0.240	0.509	0.040	14.278
		CAF-VH	0.714	0.437	0.008	19.355
		CAF-GSPE	0.072	0.452	0.075	16.997
Taurine	ZT0	STD-VH	0.034	2.437	0.854	18.933
		CAF-VH	0.043	2.037	0.769	16.408
		CAF-GSPE	0.544	1.302	0.211	17.536
	ZT12	STD-VH	0.010	1.672	0.956	17.236
		CAF-VH	0.087	1.853	0.444	11.308
		CAF-GSPE	0.212	1.540	0.479	16.909
d-Ribose	ZT0	STD-VH	0.550	0.020	0.001	12.523
		CAF-VH	0.427	0.044	0.008	17.342
		CAF-GSPE	0.198	0.041	0.021	10.664
	ZT12	STD-VH	0.323	0.033	0.006	17.049
		CAF-VH	0.145	0.023	0.010	21.650
		CAF-GSPE	0.046	0.030	0.011	15.708
d-Xylitol	ZT0	STD-VH	0.053	0.019	0.006	9.296
		CAF-VH	0.001	0.016	0.008	18.328
		CAF-GSPE	0.165	0.016	0.003	14.707
	ZT12	STD-VH	0.268	0.021	0.003	14.323
		CAF-VH	0.778	0.017	0.000	14.766
		CAF-GSPE	0.010	0.019	0.008	13.167
Glycerol-1-phosphate	ZT0	STD-VH	0.005	1.199	0.272	9.235
		CAF-VH	0.516	1.277	0.085	14.949
		CAF-GSPE	0.176	1.264	0.140	2.473
	ZT12	STD-VH	0.141	1.312	0.153	3.823
		CAF-VH	0.354	1.308	0.086	3.906
		CAF-GSPE	0.084	1.426	0.216	18.479
	ZT0	STD-VH	0.013	0.132	0.042	15.275

Hypoxanthine		CAF-VH	0.007	0.122	0.058	18.918
		CAF-GSPE	0.004	0.139	0.065	16.641
	ZT12	STD-VH	0.129	0.201	0.068	21.512
		CAF-VH	0.696	0.126	0.010	9.644
		CAF-GSPE	0.459	0.161	0.026	15.530
Ornithine	ZT0	STD-VH	0.015	0.110	0.049	8.181
		CAF-VH	0.408	0.102	0.010	0.914
		CAF-GSPE	0.244	0.109	0.014	14.520
	ZT12	STD-VH	0.076	0.147	0.058	3.645
		CAF-VH	0.290	0.105	0.010	9.524
		CAF-GSPE	0.720	0.128	0.007	4.592
Citric acid	ZT0	STD-VH	0.014	0.355	0.184	6.240
		CAF-VH	0.002	0.369	0.168	6.603
		CAF-GSPE	0.002	0.460	0.203	5.450
	ZT12	STD-VH	0.040	0.333	0.111	4.183
		CAF-VH	0.278	0.337	0.061	4.238
		CAF-GSPE	0.081	0.369	0.132	22.324
Adenine	ZT0	STD-VH	0.798	0.034	0.001	4.051
		CAF-VH	0.091	0.033	0.007	16.566
		CAF-GSPE	0.322	0.030	0.003	8.821
	ZT12	STD-VH	0.818	0.037	0.001	23.940
		CAF-VH	0.034	0.030	0.007	0.893
		CAF-GSPE	0.028	0.033	0.010	14.455
Hydroxyphenyllactic acid	ZT0	STD-VH	0.176	0.457	0.098	18.165
		CAF-VH	0.113	0.419	0.098	18.516
		CAF-GSPE	0.021	0.384	0.138	19.955
	ZT12	STD-VH	0.005	0.481	0.268	16.828
		CAF-VH	0.800	0.474	0.015	22.610
		CAF-GSPE	0.062	0.469	0.184	18.586
d-Glucose	ZT0	STD-VH	0.222	7.260	0.023	10.526
		CAF-VH	0.032	7.269	0.049	18.564
		CAF-GSPE	0.196	7.273	0.025	18.076
	ZT12	STD-VH	0.040	7.219	0.045	13.824
		CAF-VH	0.362	7.226	0.019	13.526
		CAF-GSPE	0.056	7.252	0.055	15.437
d-Mannonic acid	ZT0	STD-VH	0.010	0.037	0.008	15.821
		CAF-VH	0.001	0.032	0.012	17.969

		CAF-GSPE	0.023	0.033	0.010	16.605
	ZT12	STD-VH	0.340	0.035	0.006	9.724
		CAF-VH	0.002	0.033	0.010	13.877
		CAF-GSPE	0.082	0.040	0.008	15.607
d-Sorbitol	ZT0	STD-VH	0.410	0.130	0.027	15.293
		CAF-VH	0.015	0.115	0.081	19.357
		CAF-GSPE	0.095	0.117	0.057	14.921
	ZT12	STD-VH	0.011	0.156	0.093	16.249
		CAF-VH	0.075	0.118	0.052	17.136
		CAF-GSPE	0.166	0.280	0.303	8.028
d-Galactitol	ZT0	STD-VH	0.003	0.025	0.009	10.118
		CAF-VH	0.010	0.029	0.010	16.555
		CAF-GSPE	0.095	0.029	0.006	13.115
	ZT12	STD-VH	0.114	0.020	0.002	11.369
		CAF-VH	0.362	0.021	0.001	11.226
		CAF-GSPE	0.018	0.023	0.006	14.471
d-Gluconic acid	ZT0	STD-VH	0.075	0.090	0.039	16.473
		CAF-VH	0.005	0.069	0.042	18.533
		CAF-GSPE	0.032	0.083	0.045	16.154
	ZT12	STD-VH	0.014	0.110	0.059	16.429
		CAF-VH	0.030	0.079	0.041	15.859
		CAF-GSPE	0.065	0.086	0.032	14.240
Palmitoleic acid	ZT0	STD-VH	0.186	0.079	0.009	7.219
		CAF-VH	0.309	0.067	0.010	14.997
		CAF-GSPE	0.065	0.060	0.012	10.043
	ZT12	STD-VH	0.033	0.078	0.018	7.711
		CAF-VH	0.020	0.059	0.011	10.039
		CAF-GSPE	0.377	0.068	0.013	19.253
Xanthine	ZT0	STD-VH	0.086	0.093	0.043	14.284
		CAF-VH	0.011	0.112	0.074	18.593
		CAF-GSPE	0.020	0.130	0.086	15.513
	ZT12	STD-VH	0.137	0.158	0.068	16.350
		CAF-VH	0.176	0.108	0.050	16.252
		CAF-GSPE	0.056	0.140	0.076	13.330
d-Glucuronic acid	ZT0	STD-VH	0.047	0.004	0.001	14.451
		CAF-VH	0.004	0.004	0.001	17.937
		CAF-GSPE	0.009	0.004	0.001	17.821

	ZT12	STD-VH	0.031	0.005	0.002	16.001
		CAF-VH	0.018	0.003	0.001	16.936
		CAF-GSPE	0.033	0.004	0.001	13.936
myo-Inositol	ZT0	STD-VH	0.033	0.390	0.067	11.979
		CAF-VH	0.024	0.290	0.033	17.778
		CAF-GSPE	0.112	0.293	0.034	18.277
	ZT12	STD-VH	0.740	0.424	0.012	12.917
		CAF-VH	0.745	0.295	0.006	13.357
		CAF-GSPE	0.104	0.315	0.033	19.004
Ribose 5-phosphate	ZT0	STD-VH	0.137	0.030	0.006	4.863
		CAF-VH	0.674	0.051	0.005	15.347
		CAF-GSPE	0.189	0.048	0.022	9.668
	ZT12	STD-VH	0.434	0.043	0.005	6.218
		CAF-VH	0.197	0.030	0.010	23.659
		CAF-GSPE	0.255	0.036	0.005	16.715
Sedoheptulose	ZT0	STD-VH	0.023	0.022	0.006	7.635
		CAF-VH	0.011	0.019	0.005	16.618
		CAF-GSPE	0.668	0.017	0.001	5.918
	ZT12	STD-VH	0.128	0.025	0.005	4.922
		CAF-VH	0.056	0.020	0.005	3.316
		CAF-GSPE	0.293	0.022	0.003	16.727
Oleic acid-iso1	ZT0	STD-VH	0.270	0.180	0.027	10.525
		CAF-VH	0.161	0.465	0.104	12.454
		CAF-GSPE	0.633	0.448	0.025	11.551
	ZT12	STD-VH	0.136	0.247	0.035	0.754
		CAF-VH	0.665	0.456	0.030	10.894
		CAF-GSPE	0.390	0.420	0.060	18.820
Oleic acid-iso2	ZT0	STD-VH	0.078	0.180	0.051	13.536
		CAF-VH	0.075	0.151	0.058	12.917
		CAF-GSPE	0.563	0.117	0.010	17.437
	ZT12	STD-VH	0.554	0.188	0.019	9.257
		CAF-VH	0.967	0.126	0.001	22.417
		CAF-GSPE	0.165	0.127	0.038	18.239
Stearic acid	ZT0	STD-VH	0.161	3.904	0.138	9.770
		CAF-VH	0.033	3.957	0.121	13.517
		CAF-GSPE	0.124	4.082	0.204	8.096
	ZT12	STD-VH	0.715	3.982	0.023	3.536

		CAF-VH	0.634	3.959	0.035	16.576
		CAF-GSPE	0.450	4.074	0.073	13.470
Fructose 6-phosphate	ZT0	STD-VH	0.023	0.030	0.022	5.558
		CAF-VH	0.003	0.030	0.017	8.433
		CAF-GSPE	0.000	0.020	0.010	6.427
	ZT12	STD-VH	0.004	0.026	0.018	5.037
		CAF-VH	0.033	0.022	0.012	5.319
		CAF-GSPE	0.113	0.024	0.006	4.223
Glucose 6-phosphate	ZT0	STD-VH	0.022	0.067	0.057	5.497
		CAF-VH	0.003	0.069	0.047	8.624
		CAF-GSPE	0.000	0.045	0.024	5.622
	ZT12	STD-VH	0.003	0.055	0.040	5.008
		CAF-VH	0.039	0.047	0.027	5.634
		CAF-GSPE	0.112	0.052	0.015	4.275
Arachidic acid	ZT0	STD-VH	0.109	0.078	0.014	7.789
		CAF-VH	0.347	0.074	0.003	14.030
		CAF-GSPE	0.095	0.089	0.022	7.955
	ZT12	STD-VH	0.352	0.081	0.005	16.309
		CAF-VH	0.307	0.077	0.005	20.994
		CAF-GSPE	0.398	0.087	0.006	11.474
Inosine	ZT0	STD-VH	0.018	0.498	0.135	15.896
		CAF-VH	0.012	0.492	0.218	17.017
		CAF-GSPE	0.050	0.474	0.154	16.444
	ZT12	STD-VH	0.125	0.666	0.183	21.206
		CAF-VH	0.597	0.473	0.045	5.099
		CAF-GSPE	0.271	0.565	0.135	16.291
Adenosine	ZT0	STD-VH	0.070	0.134	0.038	7.149
		CAF-VH	0.814	0.132	0.004	15.166
		CAF-GSPE	0.120	0.160	0.032	22.586
	ZT12	STD-VH	0.236	0.177	0.059	11.201
		CAF-VH	0.536	0.164	0.016	20.849
		CAF-GSPE	0.152	0.186	0.044	14.415
Xanthosine	ZT0	STD-VH	0.034	0.075	0.030	15.094
		CAF-VH	0.004	0.077	0.041	17.330
		CAF-GSPE	0.017	0.073	0.038	15.270
	ZT12	STD-VH	0.008	0.092	0.046	15.359
		CAF-VH	0.089	0.083	0.026	15.524

		CAF-GSPE	0.010	0.091	0.051	13.556
d-Maltose	ZT0	STD-VH	0.849	0.201	0.011	15.463
		CAF-VH	0.123	0.200	0.113	18.511
		CAF-GSPE	0.483	0.221	0.048	3.121
	ZT12	STD-VH	0.097	0.266	0.165	23.838
		CAF-VH	0.828	0.364	0.024	1.560
		CAF-GSPE	0.495	0.313	0.064	9.917
Lignoceric acid	ZT0	STD-VH	0.772	0.305	0.022	14.670
		CAF-VH	0.119	0.302	0.154	18.412
		CAF-GSPE	0.625	0.323	0.043	3.808
	ZT12	STD-VH	0.080	0.374	0.206	23.691
		CAF-VH	0.853	0.534	0.030	0.598
		CAF-GSPE	0.413	0.461	0.106	9.798
uridine 5-monophosphate	ZT0	STD-VH	0.113	0.246	0.072	4.716
		CAF-VH	0.182	0.244	0.035	7.838
		CAF-GSPE	0.057	0.201	0.051	3.142
	ZT12	STD-VH	0.014	0.214	0.098	6.217
		CAF-VH	0.127	0.229	0.052	5.064
		CAF-GSPE	0.111	0.220	0.049	1.068
inosine 5-monophosphate	ZT0	STD-VH	0.160	0.052	0.014	8.043
		CAF-VH	0.328	0.070	0.009	11.585
		CAF-GSPE	0.076	0.056	0.014	11.078
	ZT12	STD-VH	0.001	0.053	0.033	8.097
		CAF-VH	0.056	0.049	0.015	5.169
		CAF-GSPE	0.390	0.057	0.009	6.153
adenosine-5-monophosphate_diphosphate_triphosphate	ZT0	STD-VH	0.035	0.630	0.171	5.845
		CAF-VH	0.055	0.651	0.081	7.287
		CAF-GSPE	0.005	0.597	0.121	4.289
	ZT12	STD-VH	0.008	0.595	0.187	6.913
		CAF-VH	0.244	0.590	0.087	6.289
		CAF-GSPE	0.108	0.601	0.102	23.934
Cholesterol	ZT0	STD-VH	0.143	3.478	0.067	11.149
		CAF-VH	0.067	3.295	0.136	18.585
		CAF-GSPE	0.283	3.369	0.076	12.257
	ZT12	STD-VH	0.103	3.546	0.077	10.035
		CAF-VH	0.607	3.283	0.028	22.088
		CAF-GSPE	0.180	3.388	0.069	9.826

Supplementary Table 10. Comparison of rhythmic parameters of liver metabolites between groups.

Metabolite	ZT	Comparison	d_MESOR	p(d_MESOR)	d_amplitude	p(d_amplitude)	d_phase	p(d_phase)
Pyruvic acid	ZT0	STD-VH vs. CAF-VH	-0.181	0.000	-0.010	0.862	2.657	0.056
		CAF-VH vs. CAF-GSPE	-0.043	0.185	-0.090	0.057	-2.244	0.226
		STD-VH vs. CAF-GSPE	-0.223	0.000	-0.100	0.100	0.414	0.861
	ZT12	STD-VH vs. CAF-VH	-0.154	0.000	0.019	0.670	-0.373	0.917
		CAF-VH vs. CAF-GSPE	0.002	0.957	-0.029	0.543	-11.508	0.017
		STD-VH vs. CAF-GSPE	-0.152	0.000	-0.010	0.847	-11.881	0.033
Lactic acid	ZT0	STD-VH vs. CAF-VH	-0.016	0.859	-0.052	0.683	5.405	0.002
		CAF-VH vs. CAF-GSPE	-0.032	0.673	-0.196	0.079	-2.765	0.395
		STD-VH vs. CAF-GSPE	-0.048	0.576	-0.249	0.051	2.641	0.467
	ZT12	STD-VH vs. CAF-VH	-0.111	0.159	0.150	0.179	6.513	0.373
		CAF-VH vs. CAF-GSPE	0.031	0.714	-0.139	0.258	4.695	0.469
		STD-VH vs. CAF-GSPE	-0.080	0.330	0.011	0.924	11.208	0.244
Alanine	ZT0	STD-VH vs. CAF-VH	0.100	0.275	-0.040	0.755	8.053	0.000
		CAF-VH vs. CAF-GSPE	0.007	0.927	-0.126	0.262	0.262	0.940
		STD-VH vs. CAF-GSPE	0.107	0.213	-0.166	0.168	8.316	0.030
	ZT12	STD-VH vs. CAF-VH	0.006	0.918	0.014	0.865	3.665	0.192
		CAF-VH vs. CAF-GSPE	0.062	0.352	-0.039	0.675	5.317	0.151
		STD-VH vs. CAF-GSPE	0.068	0.346	-0.025	0.805	8.982	0.036

2-HydroxyButyric acid	ZT0	STD-VH vs. CAF-VH	-0.075	0.283	0.016	0.867	0.499	0.850
		CAF-VH vs. CAF-GSPE	-0.039	0.569	-0.069	0.473	1.059	0.781
		STD-VH vs. CAF-GSPE	-0.114	0.119	-0.052	0.598	1.557	0.701
	ZT12	STD-VH vs. CAF-VH	-0.049	0.491	-0.171	0.098	-0.156	0.964
		CAF-VH vs. CAF-GSPE	-0.078	0.267	0.094	0.343	1.043	0.770
		STD-VH vs. CAF-GSPE	-0.127	0.063	-0.077	0.416	0.887	0.613
Sarcosine	ZT0	STD-VH vs. CAF-VH	-0.020	0.000	-0.001	0.838	-2.414	0.488
		CAF-VH vs. CAF-GSPE	0.005	0.028	0.000	0.948	0.485	0.809
		STD-VH vs. CAF-GSPE	-0.015	0.001	-0.001	0.868	-1.929	0.596
	ZT12	STD-VH vs. CAF-VH	-0.014	0.002	0.005	0.387	5.032	0.456
		CAF-VH vs. CAF-GSPE	0.003	0.233	-0.003	0.506	7.899	0.003
		STD-VH vs. CAF-GSPE	-0.011	0.015	0.003	0.672	-11.069	0.139
Valine	ZT0	STD-VH vs. CAF-VH	-0.061	0.181	0.050	0.430	5.672	0.053
		CAF-VH vs. CAF-GSPE	0.017	0.674	-0.012	0.832	0.632	0.742
		STD-VH vs. CAF-GSPE	-0.044	0.321	0.039	0.531	6.303	0.035
	ZT12	STD-VH vs. CAF-VH	-0.123	0.019	-0.046	0.514	-1.208	0.927
		CAF-VH vs. CAF-GSPE	0.038	0.458	0.108	0.139	2.830	0.830
		STD-VH vs. CAF-GSPE	-0.085	0.165	0.062	0.470	1.622	0.702
Urea	ZT0	STD-VH vs. CAF-VH	-0.336	0.000	-0.135	0.070	4.306	0.568
		CAF-VH vs. CAF-GSPE	-0.084	0.126	0.099	0.195	-6.848	0.385
		STD-VH vs. CAF-GSPE	-0.420	0.000	-0.036	0.642	-2.542	0.243

	ZT12	STD-VH vs. CAF-VH	-0.208	0.004	0.061	0.524	0.285	0.885
		CAF-VH vs. CAF-GSPE	-0.055	0.367	-0.166	0.061	-3.921	0.357
		STD-VH vs. CAF-GSPE	-0.264	0.001	-0.105	0.303	-3.636	0.479
Leucine	ZT0	STD-VH vs. CAF-VH	-0.044	0.362	0.064	0.349	5.063	0.053
		CAF-VH vs. CAF-GSPE	0.021	0.642	-0.007	0.908	0.013	0.994
		STD-VH vs. CAF-GSPE	-0.023	0.613	0.057	0.382	5.076	0.047
	ZT12	STD-VH vs. CAF-VH	-0.147	0.015	-0.055	0.492	-0.887	0.911
		CAF-VH vs. CAF-GSPE	0.051	0.372	0.119	0.143	1.467	0.847
		STD-VH vs. CAF-GSPE	-0.096	0.155	0.064	0.495	0.580	0.866
Phosphoric acid	ZT0	STD-VH vs. CAF-VH	-0.036	0.436	0.088	0.188	3.626	0.054
		CAF-VH vs. CAF-GSPE	-0.045	0.380	-0.033	0.652	-2.780	0.075
		STD-VH vs. CAF-GSPE	-0.081	0.109	0.055	0.436	0.846	0.674
	ZT12	STD-VH vs. CAF-VH	-0.079	0.143	-0.075	0.323	-4.003	0.638
		CAF-VH vs. CAF-GSPE	0.024	0.622	0.065	0.342	1.402	0.856
		STD-VH vs. CAF-GSPE	-0.055	0.224	-0.010	0.878	-2.601	0.319
Glycerol	ZT0	STD-VH vs. CAF-VH	-0.012	0.689	0.033	0.457	3.335	0.138
		CAF-VH vs. CAF-GSPE	0.008	0.809	-0.023	0.602	-2.850	0.178
		STD-VH vs. CAF-GSPE	-0.005	0.877	0.009	0.827	0.485	0.840
	ZT12	STD-VH vs. CAF-VH	-0.025	0.430	-0.051	0.255	0.527	0.853
		CAF-VH vs. CAF-GSPE	-0.001	0.974	0.039	0.393	-3.413	0.263
		STD-VH vs. CAF-GSPE	-0.026	0.404	-0.012	0.788	-2.886	0.122

Isoleucine	ZT0	STD-VH vs. CAF-VH	-0.028	0.388	0.048	0.296	5.019	0.127
		CAF-VH vs. CAF-GSPE	0.010	0.713	-0.009	0.806	0.586	0.738
		STD-VH vs. CAF-GSPE	-0.018	0.564	0.039	0.373	5.605	0.085
	ZT12	STD-VH vs. CAF-VH	-0.085	0.026	-0.031	0.550	-0.146	0.984
		CAF-VH vs. CAF-GSPE	0.029	0.437	0.071	0.178	1.029	0.883
		STD-VH vs. CAF-GSPE	-0.056	0.200	0.040	0.510	0.882	0.810
Proline	ZT0	STD-VH vs. CAF-VH	-0.085	0.273	0.068	0.535	5.760	0.007
		CAF-VH vs. CAF-GSPE	0.065	0.399	-0.079	0.465	-0.398	0.851
		STD-VH vs. CAF-GSPE	-0.020	0.793	-0.011	0.920	5.361	0.034
	ZT12	STD-VH vs. CAF-VH	-0.174	0.053	-0.078	0.528	0.005	0.999
		CAF-VH vs. CAF-GSPE	0.079	0.350	0.082	0.493	0.861	0.803
		STD-VH vs. CAF-GSPE	-0.095	0.317	0.004	0.976	0.866	0.751
Glycine	ZT0	STD-VH vs. CAF-VH	0.107	0.140	-0.023	0.816	10.478	0.001
		CAF-VH vs. CAF-GSPE	0.058	0.396	0.037	0.701	-3.167	0.259
		STD-VH vs. CAF-GSPE	0.165	0.012	0.014	0.875	7.311	0.003
	ZT12	STD-VH vs. CAF-VH	-0.085	0.285	0.020	0.856	6.995	0.097
		CAF-VH vs. CAF-GSPE	0.156	0.051	-0.030	0.782	-4.566	0.296
		STD-VH vs. CAF-GSPE	0.071	0.285	-0.010	0.913	2.429	0.542
Succinic acid	ZT0	STD-VH vs. CAF-VH	0.078	0.387	0.091	0.475	11.940	0.006
		CAF-VH vs. CAF-GSPE	0.006	0.942	-0.104	0.413	8.540	0.068
		STD-VH vs. CAF-GSPE	0.085	0.359	-0.013	0.918	-3.521	0.531

	ZT12	STD-VH vs. CAF-VH	0.131	0.096	-0.088	0.422	10.794	0.009
		CAF-VH vs. CAF-GSPE	0.043	0.620	0.099	0.417	-6.275	0.149
		STD-VH vs. CAF-GSPE	0.174	0.053	0.012	0.925	4.519	0.095
Fumaric acid	ZT0	STD-VH vs. CAF-VH	-0.127	0.322	-0.307	0.095	-1.415	0.715
		CAF-VH vs. CAF-GSPE	0.438	0.002	-0.049	0.790	-5.037	0.479
		STD-VH vs. CAF-GSPE	0.311	0.009	-0.357	0.034	-6.452	0.230
	ZT12	STD-VH vs. CAF-VH	-0.257	0.060	-0.267	0.160	0.001	1.000
		CAF-VH vs. CAF-GSPE	0.173	0.171	-0.078	0.656	-3.396	0.151
		STD-VH vs. CAF-GSPE	-0.084	0.558	-0.345	0.097	-3.395	0.150
Serine	ZT0	STD-VH vs. CAF-VH	0.701	0.000	-0.090	0.697	-8.773	0.329
		CAF-VH vs. CAF-GSPE	0.174	0.365	0.151	0.575	-7.318	0.457
		STD-VH vs. CAF-GSPE	0.875	0.000	0.060	0.714	7.909	0.023
	ZT12	STD-VH vs. CAF-VH	0.285	0.019	-0.105	0.519	2.481	0.583
		CAF-VH vs. CAF-GSPE	0.401	0.033	0.082	0.748	-1.559	0.829
		STD-VH vs. CAF-GSPE	0.685	0.000	-0.024	0.911	0.922	0.819
Threonine	ZT0	STD-VH vs. CAF-VH	0.129	0.006	0.003	0.959	9.575	0.010
		CAF-VH vs. CAF-GSPE	0.045	0.333	0.048	0.461	-3.782	0.200
		STD-VH vs. CAF-GSPE	0.173	0.000	0.051	0.273	5.793	0.011
	ZT12	STD-VH vs. CAF-VH	0.021	0.641	-0.008	0.907	3.884	0.570
		CAF-VH vs. CAF-GSPE	0.091	0.131	-0.009	0.917	1.480	0.896
		STD-VH vs. CAF-GSPE	0.112	0.059	-0.016	0.840	5.364	0.607

Nicotinamide	ZT0	STD-VH vs. CAF-VH	-0.107	0.039	0.060	0.395	5.641	0.005
		CAF-VH vs. CAF-GSPE	0.034	0.587	-0.021	0.804	-0.217	0.914
		STD-VH vs. CAF-GSPE	-0.073	0.190	0.039	0.612	5.423	0.019
	ZT12	STD-VH vs. CAF-VH	-0.162	0.010	-0.050	0.550	-0.260	0.956
		CAF-VH vs. CAF-GSPE	0.092	0.163	0.069	0.455	-3.368	0.499
		STD-VH vs. CAF-GSPE	-0.070	0.344	0.019	0.859	-3.627	0.308
Malic acid	ZT0	STD-VH vs. CAF-VH	0.140	0.255	-0.125	0.470	-0.667	0.829
		CAF-VH vs. CAF-GSPE	0.205	0.124	0.033	0.856	-2.612	0.484
		STD-VH vs. CAF-GSPE	0.345	0.005	-0.092	0.570	-3.279	0.213
	ZT12	STD-VH vs. CAF-VH	0.025	0.807	-0.238	0.109	1.995	0.148
		CAF-VH vs. CAF-GSPE	0.013	0.890	-0.073	0.585	-4.033	0.028
		STD-VH vs. CAF-GSPE	0.038	0.734	-0.311	0.058	-2.037	0.262
Methionine	ZT0	STD-VH vs. CAF-VH	-0.029	0.177	0.002	0.946	3.141	0.294
		CAF-VH vs. CAF-GSPE	-0.007	0.701	-0.008	0.758	-2.075	0.503
		STD-VH vs. CAF-GSPE	-0.036	0.128	-0.006	0.845	1.066	0.778
	ZT12	STD-VH vs. CAF-VH	-0.066	0.001	-0.029	0.287	-1.584	0.697
		CAF-VH vs. CAF-GSPE	0.009	0.635	0.012	0.631	1.951	0.644
		STD-VH vs. CAF-GSPE	-0.058	0.010	-0.016	0.583	0.367	0.905
Oxoproline	ZT0	STD-VH vs. CAF-VH	-0.546	0.082	-0.326	0.453	-2.645	0.347
		CAF-VH vs. CAF-GSPE	-0.770	0.020	-0.211	0.634	-1.183	0.813
		STD-VH vs. CAF-GSPE	-1.316	0.000	-0.537	0.214	-3.827	0.393

	ZT12	STD-VH vs. CAF-VH	0.172	0.587	-0.503	0.267	-6.844	0.043
		CAF-VH vs. CAF-GSPE	-0.379	0.319	0.023	0.965	5.608	0.254
		STD-VH vs. CAF-GSPE	-0.207	0.580	-0.480	0.366	-1.236	0.735
Aspartic acid	ZT0	STD-VH vs. CAF-VH	0.098	0.153	0.027	0.780	-0.206	0.952
		CAF-VH vs. CAF-GSPE	0.002	0.971	-0.084	0.403	-5.166	0.474
		STD-VH vs. CAF-GSPE	0.101	0.119	-0.058	0.526	-5.372	0.424
	ZT12	STD-VH vs. CAF-VH	-0.050	0.436	-0.132	0.148	3.944	0.707
		CAF-VH vs. CAF-GSPE	0.097	0.243	0.199	0.095	-6.738	0.621
		STD-VH vs. CAF-GSPE	0.048	0.572	0.067	0.574	-2.793	0.275
4-Hydroxyproline	ZT0	STD-VH vs. CAF-VH	-0.010	0.763	0.004	0.932	7.899	0.002
		CAF-VH vs. CAF-GSPE	-0.023	0.494	-0.036	0.458	8.454	0.009
		STD-VH vs. CAF-GSPE	-0.033	0.197	-0.032	0.392	-7.647	0.003
	ZT12	STD-VH vs. CAF-VH	-0.001	0.965	-0.026	0.499	-4.944	0.803
		CAF-VH vs. CAF-GSPE	0.031	0.425	0.061	0.266	-3.854	0.891
		STD-VH vs. CAF-GSPE	0.029	0.356	0.035	0.435	-8.798	0.050
a-ketoglutaric acid	ZT0	STD-VH vs. CAF-VH	0.000	0.950	0.002	0.819	2.588	0.267
		CAF-VH vs. CAF-GSPE	0.019	0.002	0.002	0.826	-6.614	0.003
		STD-VH vs. CAF-GSPE	0.018	0.004	0.004	0.677	-4.026	0.092
	ZT12	STD-VH vs. CAF-VH	-0.006	0.333	-0.003	0.740	-1.907	0.623
		CAF-VH vs. CAF-GSPE	0.009	0.176	-0.001	0.927	-1.677	0.753
		STD-VH vs. CAF-GSPE	0.003	0.618	-0.004	0.703	-3.583	0.458

Glutamic acid	ZT0	STD-VH vs. CAF-VH	0.273	0.024	-0.062	0.705	10.924	0.058
		CAF-VH vs. CAF-GSPE	0.043	0.663	0.209	0.138	4.326	0.304
		STD-VH vs. CAF-GSPE	0.315	0.009	0.147	0.354	-8.750	0.008
	ZT12	STD-VH vs. CAF-VH	0.098	0.353	0.130	0.383	-4.275	0.310
		CAF-VH vs. CAF-GSPE	0.179	0.206	-0.164	0.407	-7.153	0.362
		STD-VH vs. CAF-GSPE	0.277	0.066	-0.034	0.869	-11.428	0.232
Phenylalanine	ZT0	STD-VH vs. CAF-VH	-0.006	0.853	0.043	0.327	4.875	0.133
		CAF-VH vs. CAF-GSPE	-0.003	0.917	-0.016	0.669	0.241	0.902
		STD-VH vs. CAF-GSPE	-0.009	0.755	0.027	0.480	5.116	0.090
	ZT12	STD-VH vs. CAF-VH	-0.072	0.015	-0.031	0.432	5.077	0.698
		CAF-VH vs. CAF-GSPE	0.016	0.622	0.066	0.146	-2.358	0.870
		STD-VH vs. CAF-GSPE	-0.057	0.119	0.035	0.494	2.719	0.485
Taurine	ZT0	STD-VH vs. CAF-VH	-0.400	0.266	-0.085	0.866	-2.525	0.293
		CAF-VH vs. CAF-GSPE	-0.735	0.043	-0.559	0.257	1.128	0.869
		STD-VH vs. CAF-GSPE	-1.135	0.004	-0.644	0.206	-1.397	0.841
	ZT12	STD-VH vs. CAF-VH	0.181	0.528	-0.512	0.211	-5.928	0.036
		CAF-VH vs. CAF-GSPE	-0.313	0.320	0.035	0.936	5.601	0.134
		STD-VH vs. CAF-GSPE	-0.132	0.703	-0.477	0.334	-0.327	0.916
d-Ribose	ZT0	STD-VH vs. CAF-VH	0.024	0.004	0.007	0.513	4.819	0.813
		CAF-VH vs. CAF-GSPE	-0.003	0.814	0.012	0.504	-6.678	0.285
		STD-VH vs. CAF-GSPE	0.021	0.056	0.019	0.203	-1.859	0.946

	ZT12	STD-VH vs. CAF-VH	-0.010	0.109	0.004	0.665	4.601	0.320
		CAF-VH vs. CAF-GSPE	0.007	0.220	0.001	0.945	-5.942	0.057
		STD-VH vs. CAF-GSPE	-0.003	0.564	0.004	0.571	-1.341	0.733
d-Xylitol	ZT0	STD-VH vs. CAF-VH	-0.003	0.190	0.002	0.532	9.032	0.000
		CAF-VH vs. CAF-GSPE	0.001	0.782	-0.005	0.105	-3.620	0.158
		STD-VH vs. CAF-GSPE	-0.003	0.312	-0.003	0.466	5.412	0.118
	ZT12	STD-VH vs. CAF-VH	-0.004	0.032	-0.002	0.408	0.442	0.981
		CAF-VH vs. CAF-GSPE	0.002	0.253	0.008	0.017	-1.598	0.938
		STD-VH vs. CAF-GSPE	-0.002	0.475	0.005	0.136	-1.156	0.762
Glycerol-1-phosphate	ZT0	STD-VH vs. CAF-VH	0.077	0.474	-0.187	0.226	5.714	0.265
		CAF-VH vs. CAF-GSPE	-0.013	0.913	0.055	0.738	11.524	0.061
		STD-VH vs. CAF-GSPE	0.065	0.467	-0.132	0.303	-6.761	0.018
	ZT12	STD-VH vs. CAF-VH	-0.004	0.964	-0.067	0.618	0.083	0.986
		CAF-VH vs. CAF-GSPE	0.118	0.262	0.130	0.382	-9.428	0.067
		STD-VH vs. CAF-GSPE	0.114	0.295	0.063	0.679	-9.345	0.008
Hypoxanthine	ZT0	STD-VH vs. CAF-VH	-0.009	0.574	0.016	0.505	3.643	0.060
		CAF-VH vs. CAF-GSPE	0.016	0.382	0.008	0.771	-2.277	0.175
		STD-VH vs. CAF-GSPE	0.007	0.677	0.023	0.328	1.366	0.453
	ZT12	STD-VH vs. CAF-VH	-0.075	0.040	-0.058	0.250	-11.867	0.374
		CAF-VH vs. CAF-GSPE	0.035	0.267	0.016	0.710	5.885	0.633
		STD-VH vs. CAF-GSPE	-0.041	0.298	-0.042	0.450	-5.982	0.325

Ornithine	ZT0	STD-VH vs. CAF-VH	-0.008	0.581	-0.039	0.082	-7.267	0.209
		CAF-VH vs. CAF-GSPE	0.008	0.528	0.004	0.822	-10.393	0.061
		STD-VH vs. CAF-GSPE	-0.001	0.956	-0.035	0.118	6.339	0.138
	ZT12	STD-VH vs. CAF-VH	-0.043	0.065	-0.047	0.143	5.879	0.487
		CAF-VH vs. CAF-GSPE	0.024	0.147	-0.003	0.897	-4.932	0.626
		STD-VH vs. CAF-GSPE	-0.019	0.460	-0.050	0.176	0.947	0.944
Citric acid	ZT0	STD-VH vs. CAF-VH	0.013	0.808	-0.016	0.836	0.363	0.831
		CAF-VH vs. CAF-GSPE	0.091	0.067	0.035	0.602	-1.154	0.425
		STD-VH vs. CAF-GSPE	0.105	0.090	0.019	0.820	-0.790	0.643
	ZT12	STD-VH vs. CAF-VH	0.004	0.932	-0.050	0.495	0.055	0.988
		CAF-VH vs. CAF-GSPE	0.032	0.612	0.071	0.426	-5.914	0.180
		STD-VH vs. CAF-GSPE	0.037	0.550	0.021	0.807	-5.859	0.039
Adenine	ZT0	STD-VH vs. CAF-VH	-0.001	0.748	0.006	0.371	-11.484	0.396
		CAF-VH vs. CAF-GSPE	-0.003	0.361	-0.004	0.395	-7.745	0.139
		STD-VH vs. CAF-GSPE	-0.004	0.273	0.002	0.787	4.770	0.721
	ZT12	STD-VH vs. CAF-VH	-0.007	0.125	0.005	0.418	0.953	0.942
		CAF-VH vs. CAF-GSPE	0.003	0.349	0.004	0.450	-10.438	0.000
		STD-VH vs. CAF-GSPE	-0.004	0.469	0.009	0.211	-9.485	0.518
Hydroxyphenyllactic acid	ZT0	STD-VH vs. CAF-VH	-0.038	0.553	0.000	0.996	0.351	0.921
		CAF-VH vs. CAF-GSPE	-0.035	0.540	0.040	0.613	1.440	0.597
		STD-VH vs. CAF-GSPE	-0.073	0.254	0.039	0.653	1.790	0.555

	ZT12	STD-VH vs. CAF-VH	-0.007	0.923	-0.254	0.016	5.782	0.755
		CAF-VH vs. CAF-GSPE	-0.005	0.949	0.169	0.123	-4.024	0.841
		STD-VH vs. CAF-GSPE	-0.012	0.893	-0.084	0.490	1.757	0.422
d-Glucose	ZT0	STD-VH vs. CAF-VH	0.009	0.627	0.026	0.348	8.037	0.031
		CAF-VH vs. CAF-GSPE	0.003	0.861	-0.024	0.385	-0.488	0.891
		STD-VH vs. CAF-GSPE	0.013	0.488	0.002	0.945	7.550	0.085
	ZT12	STD-VH vs. CAF-VH	0.008	0.708	-0.026	0.364	-0.298	0.946
		CAF-VH vs. CAF-GSPE	0.026	0.274	0.036	0.289	1.911	0.702
		STD-VH vs. CAF-GSPE	0.033	0.159	0.010	0.772	1.613	0.530
d-Mannonic acid	ZT0	STD-VH vs. CAF-VH	-0.004	0.146	0.004	0.385	2.148	0.187
		CAF-VH vs. CAF-GSPE	0.000	0.924	-0.002	0.697	-1.364	0.434
		STD-VH vs. CAF-GSPE	-0.004	0.252	0.002	0.728	0.784	0.697
	ZT12	STD-VH vs. CAF-VH	-0.002	0.669	0.005	0.469	4.153	0.237
		CAF-VH vs. CAF-GSPE	0.007	0.079	-0.002	0.736	1.730	0.430
		STD-VH vs. CAF-GSPE	0.005	0.355	0.003	0.700	5.883	0.170
d-Sorbitol	ZT0	STD-VH vs. CAF-VH	-0.015	0.630	0.054	0.227	4.065	0.376
		CAF-VH vs. CAF-GSPE	0.003	0.928	-0.024	0.581	-4.436	0.080
		STD-VH vs. CAF-GSPE	-0.012	0.703	0.030	0.516	-0.371	0.939
	ZT12	STD-VH vs. CAF-VH	-0.038	0.211	-0.041	0.333	0.887	0.721
		CAF-VH vs. CAF-GSPE	0.161	0.283	0.250	0.239	-9.107	0.410
		STD-VH vs. CAF-GSPE	0.123	0.410	0.209	0.325	-8.220	0.204

d-Galactitol	ZT0	STD-VH vs. CAF-VH	0.004	0.155	0.001	0.766	6.436	0.001
		CAF-VH vs. CAF-GSPE	0.000	0.972	-0.004	0.450	-3.440	0.154
		STD-VH vs. CAF-GSPE	0.004	0.146	-0.002	0.565	2.996	0.173
	ZT12	STD-VH vs. CAF-VH	0.001	0.627	-0.001	0.597	-0.142	0.976
		CAF-VH vs. CAF-GSPE	0.002	0.299	0.005	0.067	3.244	0.592
		STD-VH vs. CAF-GSPE	0.003	0.174	0.004	0.136	3.102	0.377
d-Gluconic acid	ZT0	STD-VH vs. CAF-VH	-0.020	0.230	0.003	0.890	2.060	0.367
		CAF-VH vs. CAF-GSPE	0.013	0.399	0.003	0.888	-2.379	0.235
		STD-VH vs. CAF-GSPE	-0.007	0.720	0.006	0.816	-0.319	0.900
	ZT12	STD-VH vs. CAF-VH	-0.031	0.117	-0.018	0.505	-0.570	0.793
		CAF-VH vs. CAF-GSPE	0.007	0.673	-0.009	0.705	-1.620	0.518
		STD-VH vs. CAF-GSPE	-0.024	0.212	-0.027	0.314	-2.189	0.393
Palmitoleic acid	ZT0	STD-VH vs. CAF-VH	-0.012	0.165	0.001	0.946	7.778	0.102
		CAF-VH vs. CAF-GSPE	-0.007	0.360	0.002	0.883	-4.954	0.226
		STD-VH vs. CAF-GSPE	-0.019	0.005	0.002	0.782	2.824	0.396
	ZT12	STD-VH vs. CAF-VH	-0.019	0.004	-0.007	0.413	2.327	0.361
		CAF-VH vs. CAF-GSPE	0.009	0.394	0.002	0.874	9.214	0.068
		STD-VH vs. CAF-GSPE	-0.010	0.390	-0.005	0.774	11.542	0.010
Xanthine	ZT0	STD-VH vs. CAF-VH	0.019	0.438	0.032	0.363	4.309	0.094
		CAF-VH vs. CAF-GSPE	0.018	0.530	0.012	0.776	-3.080	0.120
		STD-VH vs. CAF-GSPE	0.037	0.190	0.043	0.279	1.229	0.652

	ZT12	STD-VH vs. CAF-VH	-0.050	0.214	-0.018	0.746	-0.098	0.979
		CAF-VH vs. CAF-GSPE	0.032	0.382	0.026	0.613	-2.922	0.377
		STD-VH vs. CAF-GSPE	-0.018	0.650	0.008	0.893	-3.020	0.322
d-Glucuronic acid	ZT0	STD-VH vs. CAF-VH	0.000	0.391	0.000	0.565	3.486	0.097
		CAF-VH vs. CAF-GSPE	0.001	0.042	0.000	0.984	-0.116	0.946
		STD-VH vs. CAF-GSPE	0.001	0.250	0.000	0.571	3.370	0.132
	ZT12	STD-VH vs. CAF-VH	-0.001	0.024	0.000	0.525	0.935	0.689
		CAF-VH vs. CAF-GSPE	0.001	0.095	0.000	0.559	-2.999	0.206
		STD-VH vs. CAF-GSPE	0.000	0.571	0.000	0.962	-2.065	0.367
myo-Inositol	ZT0	STD-VH vs. CAF-VH	-0.100	0.000	-0.034	0.282	5.799	0.050
		CAF-VH vs. CAF-GSPE	0.003	0.865	0.001	0.957	0.499	0.859
		STD-VH vs. CAF-GSPE	-0.097	0.001	-0.032	0.356	6.298	0.063
	ZT12	STD-VH vs. CAF-VH	-0.129	0.000	-0.006	0.886	0.440	0.982
		CAF-VH vs. CAF-GSPE	0.020	0.284	0.028	0.303	5.648	0.644
		STD-VH vs. CAF-GSPE	-0.109	0.001	0.022	0.577	6.088	0.534
Ribose 5--phosphate	ZT0	STD-VH vs. CAF-VH	0.021	0.021	-0.001	0.954	10.484	0.242
		CAF-VH vs. CAF-GSPE	-0.003	0.817	0.017	0.384	-5.679	0.602
		STD-VH vs. CAF-GSPE	0.018	0.128	0.016	0.305	4.805	0.539
	ZT12	STD-VH vs. CAF-VH	-0.013	0.077	0.004	0.653	-6.559	0.254
		CAF-VH vs. CAF-GSPE	0.006	0.347	-0.004	0.604	-6.944	0.167
		STD-VH vs. CAF-GSPE	-0.007	0.227	0.000	0.999	10.498	0.078

Sedoheptulose	ZT0	STD-VH vs. CAF-VH	-0.003	0.149	-0.001	0.752	8.983	0.000
		CAF-VH vs. CAF-GSPE	-0.002	0.407	-0.004	0.173	-10.700	0.202
		STD-VH vs. CAF-GSPE	-0.005	0.055	-0.005	0.145	-1.717	0.855
	ZT12	STD-VH vs. CAF-VH	-0.005	0.119	0.000	0.962	-1.606	0.595
		CAF-VH vs. CAF-GSPE	0.001	0.599	-0.002	0.641	-10.588	0.009
		STD-VH vs. CAF-GSPE	-0.003	0.319	-0.002	0.652	11.806	0.011
Oleic acid-iso1	ZT0	STD-VH vs. CAF-VH	0.285	0.000	0.078	0.304	1.929	0.804
		CAF-VH vs. CAF-GSPE	-0.017	0.789	-0.079	0.381	-0.903	0.925
		STD-VH vs. CAF-GSPE	0.268	0.000	-0.002	0.977	1.026	0.897
	ZT12	STD-VH vs. CAF-VH	0.209	0.000	-0.004	0.952	10.140	0.244
		CAF-VH vs. CAF-GSPE	-0.036	0.599	0.030	0.761	7.926	0.416
		STD-VH vs. CAF-GSPE	0.173	0.002	0.025	0.724	-5.934	0.360
Oleic acid-iso2	ZT0	STD-VH vs. CAF-VH	-0.030	0.304	0.007	0.866	-0.620	0.828
		CAF-VH vs. CAF-GSPE	-0.034	0.180	-0.048	0.173	4.520	0.667
		STD-VH vs. CAF-GSPE	-0.064	0.009	-0.041	0.201	3.900	0.686
	ZT12	STD-VH vs. CAF-VH	-0.063	0.018	-0.019	0.602	-10.840	0.941
		CAF-VH vs. CAF-GSPE	0.001	0.954	0.038	0.225	-4.181	0.974
		STD-VH vs. CAF-GSPE	-0.061	0.044	0.019	0.645	8.981	0.175
Stearic acid	ZT0	STD-VH vs. CAF-VH	0.053	0.482	-0.017	0.871	3.746	0.244
		CAF-VH vs. CAF-GSPE	0.125	0.195	0.083	0.533	-5.420	0.129
		STD-VH vs. CAF-GSPE	0.179	0.117	0.065	0.673	-1.674	0.654

	ZT12	STD-VH vs. CAF-VH	-0.022	0.743	0.012	0.903	-10.960	0.416
		CAF-VH vs. CAF-GSPE	0.115	0.182	0.038	0.750	-3.105	0.761
		STD-VH vs. CAF-GSPE	0.092	0.258	0.050	0.663	9.934	0.475
Fructose 6-phosphate	ZT0	STD-VH vs. CAF-VH	0.000	0.992	-0.005	0.612	2.875	0.154
		CAF-VH vs. CAF-GSPE	-0.009	0.017	-0.008	0.152	-2.006	0.255
		STD-VH vs. CAF-GSPE	-0.009	0.165	-0.013	0.175	0.869	0.768
	ZT12	STD-VH vs. CAF-VH	-0.004	0.464	-0.006	0.407	0.282	0.886
		CAF-VH vs. CAF-GSPE	0.002	0.637	-0.005	0.398	-1.096	0.715
		STD-VH vs. CAF-GSPE	-0.002	0.720	-0.011	0.086	-0.814	0.776
Glucose 6-phosphate	ZT0	STD-VH vs. CAF-VH	0.002	0.907	-0.010	0.707	3.127	0.111
		CAF-VH vs. CAF-GSPE	-0.025	0.022	-0.023	0.119	-3.002	0.124
		STD-VH vs. CAF-GSPE	-0.023	0.177	-0.033	0.165	0.125	0.966
	ZT12	STD-VH vs. CAF-VH	-0.008	0.503	-0.013	0.443	0.626	0.750
		CAF-VH vs. CAF-GSPE	0.004	0.683	-0.012	0.410	-1.359	0.659
		STD-VH vs. CAF-GSPE	-0.003	0.731	-0.025	0.087	-0.733	0.789
Arachidic acid	ZT0	STD-VH vs. CAF-VH	-0.003	0.619	-0.011	0.226	6.241	0.425
		CAF-VH vs. CAF-GSPE	0.015	0.108	0.019	0.139	-6.075	0.570
		STD-VH vs. CAF-GSPE	0.012	0.277	0.008	0.594	0.166	0.961
	ZT12	STD-VH vs. CAF-VH	-0.004	0.352	0.000	0.975	4.685	0.390
		CAF-VH vs. CAF-GSPE	0.010	0.110	0.002	0.842	-9.520	0.131
		STD-VH vs. CAF-GSPE	0.005	0.391	0.001	0.868	-4.836	0.441

Inosine	ZT0	STD-VH vs. CAF-VH	-0.006	0.927	0.082	0.367	1.121	0.598
		CAF-VH vs. CAF-GSPE	-0.018	0.806	-0.064	0.542	-0.573	0.800
		STD-VH vs. CAF-GSPE	-0.024	0.698	0.019	0.830	0.548	0.813
	ZT12	STD-VH vs. CAF-VH	-0.193	0.060	-0.138	0.329	7.893	0.368
		CAF-VH vs. CAF-GSPE	0.093	0.371	0.090	0.536	11.192	0.230
		STD-VH vs. CAF-GSPE	-0.101	0.388	-0.048	0.769	-4.915	0.233
Adenosine	ZT0	STD-VH vs. CAF-VH	-0.003	0.875	-0.034	0.167	8.017	0.670
		CAF-VH vs. CAF-GSPE	0.028	0.104	0.028	0.246	7.420	0.683
		STD-VH vs. CAF-GSPE	0.026	0.191	-0.006	0.826	-8.563	0.008
	ZT12	STD-VH vs. CAF-VH	-0.013	0.733	-0.043	0.435	9.648	0.309
		CAF-VH vs. CAF-GSPE	0.023	0.413	0.028	0.480	-6.434	0.355
		STD-VH vs. CAF-GSPE	0.010	0.811	-0.015	0.786	3.214	0.458
Xanthosine	ZT0	STD-VH vs. CAF-VH	0.002	0.865	0.012	0.506	2.236	0.261
		CAF-VH vs. CAF-GSPE	-0.004	0.750	-0.003	0.853	-2.060	0.245
		STD-VH vs. CAF-GSPE	-0.002	0.880	0.008	0.657	0.176	0.934
	ZT12	STD-VH vs. CAF-VH	-0.009	0.515	-0.020	0.331	0.165	0.947
		CAF-VH vs. CAF-GSPE	0.009	0.576	0.025	0.256	-1.968	0.451
		STD-VH vs. CAF-GSPE	-0.001	0.966	0.005	0.811	-1.803	0.317
d-Maltose	ZT0	STD-VH vs. CAF-VH	-0.001	0.982	0.102	0.261	3.048	0.891
		CAF-VH vs. CAF-GSPE	0.021	0.754	-0.065	0.501	8.610	0.151
		STD-VH vs. CAF-GSPE	0.020	0.747	0.037	0.674	11.658	0.589

	ZT12	STD-VH vs. CAF-VH	0.099	0.340	-0.141	0.335	1.722	0.916
		CAF-VH vs. CAF-GSPE	-0.051	0.615	0.040	0.782	8.358	0.627
		STD-VH vs. CAF-GSPE	0.047	0.613	-0.101	0.445	10.079	0.098
Lignoceric acid	ZT0	STD-VH vs. CAF-VH	-0.003	0.973	0.132	0.279	3.742	0.800
		CAF-VH vs. CAF-GSPE	0.021	0.814	-0.112	0.387	9.396	0.272
		STD-VH vs. CAF-GSPE	0.018	0.821	0.021	0.858	-10.862	0.484
	ZT12	STD-VH vs. CAF-VH	0.160	0.252	-0.176	0.372	0.907	0.959
		CAF-VH vs. CAF-GSPE	-0.073	0.616	0.075	0.713	9.200	0.630
		STD-VH vs. CAF-GSPE	0.087	0.463	-0.100	0.550	10.107	0.043
uridine 5-monophosphate	ZT0	STD-VH vs. CAF-VH	-0.002	0.945	-0.037	0.455	3.122	0.467
		CAF-VH vs. CAF-GSPE	-0.043	0.087	0.017	0.638	-4.696	0.155
		STD-VH vs. CAF-GSPE	-0.046	0.204	-0.021	0.684	-1.574	0.627
	ZT12	STD-VH vs. CAF-VH	0.016	0.640	-0.046	0.336	-1.153	0.680
		CAF-VH vs. CAF-GSPE	-0.009	0.768	-0.002	0.955	-3.996	0.229
		STD-VH vs. CAF-GSPE	0.007	0.837	-0.048	0.291	-5.149	0.073
inosine 5-monophosphate	ZT0	STD-VH vs. CAF-VH	0.018	0.048	-0.005	0.701	3.541	0.449
		CAF-VH vs. CAF-GSPE	-0.014	0.083	0.005	0.644	-0.506	0.901
		STD-VH vs. CAF-GSPE	0.004	0.629	0.000	0.970	3.035	0.352
	ZT12	STD-VH vs. CAF-VH	-0.004	0.630	-0.018	0.096	-2.929	0.178
		CAF-VH vs. CAF-GSPE	0.008	0.330	-0.006	0.616	0.984	0.823
		STD-VH vs. CAF-GSPE	0.005	0.594	-0.024	0.063	-1.945	0.634

adenosine-5-monophosphate_adenosine-5-diphosphate_adenosine-5-triphosphate	ZT0	STD-VH vs. CAF-VH	0.020	0.728	-0.090	0.284	1.443	0.637
		CAF-VH vs. CAF-GSPE	-0.054	0.162	0.040	0.456	-2.999	0.167
		STD-VH vs. CAF-GSPE	-0.033	0.573	-0.050	0.551	-1.556	0.502
	ZT12	STD-VH vs. CAF-VH	-0.005	0.944	-0.100	0.291	-0.624	0.846
		CAF-VH vs. CAF-GSPE	0.010	0.874	0.016	0.867	-6.355	0.105
		STD-VH vs. CAF-GSPE	0.006	0.924	-0.085	0.325	-6.979	0.011
Cholesterol	ZT0	STD-VH vs. CAF-VH	-0.183	0.003	0.069	0.398	7.435	0.050
		CAF-VH vs. CAF-GSPE	0.074	0.282	-0.059	0.544	-6.328	0.107
		STD-VH vs. CAF-GSPE	-0.110	0.055	0.010	0.904	1.107	0.788
	ZT12	STD-VH vs. CAF-VH	-0.263	0.000	-0.049	0.488	-11.947	0.102
		CAF-VH vs. CAF-GSPE	0.105	0.051	0.041	0.577	11.739	0.129
		STD-VH vs. CAF-GSPE	-0.158	0.002	-0.008	0.906	-0.209	0.952

Rats were fed a STD or CAF diet and were treated with vehicle or GSPE at the beginning of the light phase (ZT0) or at the beginning of the dark phase (ZT12). d_MESOR represents the difference in MESOR values between the groups. d_amplitude represents the difference in amplitude values between the groups. d_phase represents the difference in acrophase values between the groups. The $p < 0.05$ indicates significant differences between groups at each rhythmic parameter.

Supplementary Table 11. Enrichment analysis of group-exclusive rhythmic liver metabolites.

	Rhythmic metabolites enriched pathways	Hits	Expect	P value	Holm P	FDR	Enrichment Ratio
ZT0 STD-VH	Mitochondrial Electron Transport Chain	19	2	0.13	0.00648	0.635	16
	Urea Cycle	29	2	0.198	0.0149	1	12
	Arginine and Proline Metabolism	53	2	0.362	0.0467	1	8
	De Novo Triacylglycerol Biosynthesis	9	1	0.0615	0.0601	1	16
	Malate-Aspartate Shuttle	10	1	0.0684	0.0666	1	12
	Glycerol Phosphate Shuttle	11	1	0.0752	0.073	1	12
	Cardiolipin Biosynthesis	11	1	0.0752	0.073	1	12
	Spermidine and Spermine Biosynthesis	18	1	0.123	0.117	1	8
	Glutathione Metabolism	21	1	0.144	0.135	1	8
	Glycerolipid Metabolism	25	1	0.171	0.159	1	8
	Phenylalanine and Tyrosine Metabolism	28	1	0.191	0.177	1	8
	Phospholipid Biosynthesis	29	1	0.198	0.183	1	8
	Citric Acid Cycle	32	1	0.219	0.2	1	8
	Aspartate Metabolism	35	1	0.239	0.217	1	8
	Gluconeogenesis	35	1	0.239	0.217	1	8
	Warburg Effect	58	1	0.396	0.336	1	4
	Glycine and Serine Metabolism	59	1	0.403	0.341	1	4
	Tyrosine Metabolism	72	1	0.492	0.401	1	2

	Purine Metabolism	74	1	0.506	0.409	1	2
ZT0-CAF-VH	Galactose Metabolism	38	2	0.186	0.0125	1	10
	Lactose Degradation	9	1	0.0439	0.0433	1	20
	Glucose-Alanine Cycle	13	1	0.0635	0.062	1	15
	Spermidine and Spermine Biosynthesis	18	1	0.0879	0.085	1	10
	Lactose Synthesis	20	1	0.0977	0.0941	1	10
	Betaine Metabolism	21	1	0.103	0.0986	1	10
	Transfer of Acetyl Groups into Mitochondria	22	1	0.107	0.103	1	10
	Glycolysis	25	1	0.122	0.116	1	10
	Plasmalogen Synthesis	26	1	0.127	0.121	1	10
	Mitochondrial Beta-Oxidation of Long Chain Saturated Fatty Acids	28	1	0.137	0.13	1	10
	Fructose and Mannose Degradation	32	1	0.156	0.147	1	5
	Gluconeogenesis	35	1	0.171	0.16	1	5
	Sphingolipid Metabolism	40	1	0.195	0.181	1	5
	Propanoate Metabolism	42	1	0.205	0.189	1	5
	Methionine Metabolism	43	1	0.21	0.193	1	5
	Warburg Effect	58	1	0.283	0.253	1	2
	Glycine and Serine Metabolism	59	1	0.288	0.257	1	2
ZT0-CAF-GSPE	Malate-Aspartate Shuttle	10	1	0.0195	0.0194	1	50
	Glucose-Alanine Cycle	13	1	0.0254	0.0252	1	40
	Alanine Metabolism	17	1	0.0332	0.0329	1	30

	Glutathione Metabolism	21	1	0.041	0.0406	1	25
	Cysteine Metabolism	26	1	0.0508	0.0502	1	20
	Phenylalanine and Tyrosine Metabolism	28	1	0.0547	0.054	1	20
	Folate Metabolism	29	1	0.0566	0.0559	1	20
	Urea Cycle	29	1	0.0566	0.0559	1	20
	Lysine Degradation	30	1	0.0586	0.0578	1	20
	Ammonia Recycling	32	1	0.0625	0.0616	1	20
	Amino Sugar Metabolism	33	1	0.0645	0.0634	1	20
	Beta-Alanine Metabolism	34	1	0.0664	0.0653	1	20
	Aspartate Metabolism	35	1	0.0684	0.0672	1	20
	Nicotinate and Nicotinamide Metabolism	37	1	0.0723	0.071	1	20
	Propanoate Metabolism	42	1	0.082	0.0804	1	10
	Histidine Metabolism	43	1	0.084	0.0823	1	10
	Glutamate Metabolism	49	1	0.0957	0.0935	1	10
	Arginine and Proline Metabolism	53	1	0.104	0.101	1	10
	Warburg Effect	58	1	0.113	0.11	1	10
	Glycine and Serine Metabolism	59	1	0.115	0.112	1	10
	Valine, Leucine and Isoleucine Degradation	60	1	0.117	0.114	1	10
	Tryptophan Metabolism	60	1	0.117	0.114	1	10
	Arachidonic Acid Metabolism	69	1	0.135	0.13	1	10
	Tyrosine Metabolism	72	1	0.141	0.136	1	5

	Purine Metabolism	74	1	0.145	0.139	1	5
ZT12-STD-VH	Thiamine Metabolism	9	3	0.0703	0.0000258	0.00253	30
	Alanine Metabolism	17	3	0.133	0.000203	0.0197	20
	Riboflavin Metabolism	20	3	0.156	0.000336	0.0323	20
	Glutathione Metabolism	21	3	0.164	0.000391	0.0371	20
	Pantothenate and CoA Biosynthesis	21	3	0.164	0.000391	0.0371	20
	Glycine and Serine Metabolism	59	4	0.461	0.000587	0.0546	10
	Cysteine Metabolism	26	3	0.203	0.000749	0.0689	15
	Selenoamino Acid Metabolism	28	3	0.219	0.000937	0.0853	10
	Pentose Phosphate Pathway	29	3	0.227	0.00104	0.0937	10
	Urea Cycle	29	3	0.227	0.00104	0.0937	10
	Ammonia Recycling	32	3	0.25	0.0014	0.123	10
	Fructose and Mannose Degradation	32	3	0.25	0.0014	0.123	10
	Phenylacetate Metabolism	9	2	0.0703	0.00187	0.161	25
	Lactose Degradation	9	2	0.0703	0.00187	0.161	25
	Nicotinate and Nicotinamide Metabolism	37	3	0.289	0.00215	0.181	10
	Galactose Metabolism	38	3	0.297	0.00232	0.193	10
	Trehalose Degradation	11	2	0.0859	0.00284	0.233	20
	Propanoate Metabolism	42	3	0.328	0.00312	0.252	10
	Methionine Metabolism	43	3	0.336	0.00334	0.267	10
	Histidine Metabolism	43	3	0.336	0.00334	0.267	10

	Phosphatidylethanolamine Biosynthesis	12	2	0.0938	0.00339	0.267	15
	Pyruvate Metabolism	48	3	0.375	0.00459	0.353	15
	Phosphatidylcholine Biosynthesis	14	2	0.109	0.00464	0.353	15
	Glutamate Metabolism	49	3	0.383	0.00487	0.365	15
	Arginine and Proline Metabolism	53	3	0.414	0.0061	0.452	15
	Beta Oxidation of Very Long Chain Fatty Acids	17	2	0.133	0.00685	0.5	15
	Phosphatidylinositol Phosphate Metabolism	17	2	0.133	0.00685	0.5	10
	Spermidine and Spermine Biosynthesis	18	2	0.141	0.00768	0.545	10
	Butyrate Metabolism	19	2	0.148	0.00855	0.599	10
	Mitochondrial Electron Transport Chain	19	2	0.148	0.00855	0.599	10
	Ethanol Degradation	19	2	0.148	0.00855	0.599	10
	Nucleotide Sugars Metabolism	20	2	0.156	0.00946	0.634	10
	Lactose Synthesis	20	2	0.156	0.00946	0.634	10
	Threonine and 2-Oxobutanoate Degradation	20	2	0.156	0.00946	0.634	10
	Betaine Metabolism	21	2	0.164	0.0104	0.667	5
	Bile Acid Biosynthesis	65	3	0.508	0.0109	0.685	5
	Sulfate/Sulfite Metabolism	22	2	0.172	0.0114	0.708	5
	Transfer of Acetyl Groups into Mitochondria	22	2	0.172	0.0114	0.708	5
	Glycerolipid Metabolism	25	2	0.195	0.0147	0.879	5
	Glycolysis	25	2	0.195	0.0147	0.879	5
	Purine Metabolism	74	3	0.578	0.0156	0.904	5

	Oxidation of Branched Chain Fatty Acids	26	2	0.203	0.0158	0.904	5
	Phytanic Acid Peroxisomal Oxidation	26	2	0.203	0.0158	0.904	5
	Inositol Phosphate Metabolism	26	2	0.203	0.0158	0.904	5
	Mitochondrial Beta-Oxidation of Short Chain Saturated Fatty Acids	27	2	0.211	0.017	0.918	5
	Mitochondrial Beta-Oxidation of Medium Chain Saturated Fatty Acids	27	2	0.211	0.017	0.918	5
	Phenylalanine and Tyrosine Metabolism	28	2	0.219	0.0182	0.949	2
	Mitochondrial Beta-Oxidation of Long Chain Saturated Fatty Acids	28	2	0.219	0.0182	0.949	2
	Folate Metabolism	29	2	0.227	0.0195	0.976	2
	Starch and Sucrose Metabolism	31	2	0.242	0.0222	1	2
	Citric Acid Cycle	32	2	0.25	0.0236	1	2
	Inositol Metabolism	33	2	0.258	0.025	1	2
	Amino Sugar Metabolism	33	2	0.258	0.025	1	2
	Aspartate Metabolism	35	2	0.273	0.0279	1	2
	Gluconeogenesis	35	2	0.273	0.0279	1	2
	Sphingolipid Metabolism	40	2	0.312	0.0359	1	2
	Fatty acid Metabolism	43	2	0.336	0.0411	1	2
	Steroid Biosynthesis	48	2	0.375	0.0503	1	2
	Biotin Metabolism	8	1	0.0625	0.061	1	2
	Warburg Effect	58	2	0.453	0.0708	1	2
	Pyrimidine Metabolism	59	2	0.461	0.073	1	2
	Valine, Leucine and Isoleucine Degradation	60	2	0.469	0.0753	1	2

	Taurine and Hypotaurine Metabolism	12	1	0.0938	0.0903	1	2
	Tryptophan Metabolism	60	1	0.469	0.384	1	2
ZT12-CAF-VH	Glycine and Serine Metabolism	59	3	0.23	0.000699	0.0685	10
	Glucose-Alanine Cycle	13	2	0.0508	0.000881	0.0854	35
	Alanine Metabolism	17	2	0.0664	0.00153	0.147	30
	Glutathione Metabolism	21	2	0.082	0.00235	0.223	20
	Urea Cycle	29	2	0.113	0.00449	0.422	15
	Glutamate Metabolism	49	2	0.191	0.0127	1	10
	Warburg Effect	58	2	0.227	0.0176	1	10
	Tryptophan Metabolism	60	2	0.234	0.0188	1	10
	Malate-Aspartate Shuttle	10	1	0.0391	0.0385	1	25
	Cysteine Metabolism	26	1	0.102	0.0979	1	10
	Phenylalanine and Tyrosine Metabolism	28	1	0.109	0.105	1	10
	Selenoamino Acid Metabolism	28	1	0.109	0.105	1	10
	Folate Metabolism	29	1	0.113	0.109	1	10
	Lysine Degradation	30	1	0.117	0.112	1	10
	Ammonia Recycling	32	1	0.125	0.119	1	10
	Amino Sugar Metabolism	33	1	0.129	0.123	1	10
	Beta-Alanine Metabolism	34	1	0.133	0.127	1	10
	Aspartate Metabolism	35	1	0.137	0.13	1	10
	Gluconeogenesis	35	1	0.137	0.13	1	10

	Nicotinate and Nicotinamide Metabolism	37	1	0.145	0.137	1	10
	Propanoate Metabolism	42	1	0.164	0.154	1	5
	Methionine Metabolism	43	1	0.168	0.158	1	5
	Histidine Metabolism	43	1	0.168	0.158	1	5
	Pyruvate Metabolism	48	1	0.188	0.175	1	5
	Arginine and Proline Metabolism	53	1	0.207	0.192	1	5
	Valine, Leucine and Isoleucine Degradation	60	1	0.234	0.215	1	5
	Arachidonic Acid Metabolism	69	1	0.27	0.244	1	5
	Tyrosine Metabolism	72	1	0.281	0.253	1	2
	Purine Metabolism	74	1	0.289	0.26	1	2
ZT12-CAF-GSPE	Pentose Phosphate Pathway	29	1	0.085	0.0827	1	10
	Valine, Leucine and Isoleucine Degradation	60	1	0.176	0.166	1	6

Group-exclusive rhythmic metabolites enriched pathways of rats that were fed a STD or CAF diet and were treated with vehicle or GSPE at the beginning of the light phase (ZT0) or at the beginning of the dark phase (ZT12). Metabolic pathways enrichment analysis was performed in MetaboAnalyst (Version 5.0, URL: http://www.metaboanalyst.ca) using the metabolites that were rhythmic exclusively in each group.

CHAPTER III

OBJECTIVE 4

To determine the impact of seasonal variations on GSPE consumption over the hepatic circadian clock and liver metabolism of healthy rats.

UNIVERSITAT ROVIRA I VIRGILI
THE INFLUENCE OF BIOLOGICAL RHYTHMS ON THE BENEFICIAL EFFECTS OF GRAPE SEED PROANTHOCYANIDIN EXTRACT (GSPE) ON LIVER METABOLISM IN HEALTH AND DISEASE
Romina Mariel Rodriguez

MANUSCRIPT 3

Grape-Seed Procyanidin Extract (GSPE) seasonal-dependent modulation of glucose and lipid metabolism in the liver of healthy F344 rats

Romina M Rodríguez [1], Marina Colom-Pellicer [1], Jordi Blanco [2], Enrique Calvo [1], Gerard Aragonès [1] and Miquel Mulero [1*]

[1] Nutrigenomics Research Group, Department of Biochemistry and Biotechnology, Campus Sescelades, Universitat Rovira i Virgili (URV), 43007 Tarragona, Spain.

[2] Research in Neurobehavior and Health (NEUROLAB), Laboratory of Toxicology and Environmental Health, Physiology Unit, Institute of Health Research Pere Virgili (IISPV), School of Medicine, Universitat Rovira i Virgili (URV), 43202 Tarragona, Spain.

* Correspondence: miquel.mulero@urv.cat; Tel.: +34 977559565

Published

Biomolecules **2022, *12*(6), 839.**

https://doi.org/10.3390/biom12060839

UNIVERSITAT ROVIRA I VIRGILI
THE INFLUENCE OF BIOLOGICAL RHYTHMS ON THE BENEFICIAL EFFECTS OF GRAPE SEED PROANTHOCYANIDIN EXTRACT (GSPE) ON LIVER METABOLISM IN HEALTH AND DISEASE
Romina Mariel Rodriguez

biomolecules

MDPI

Article

Grape-Seed Procyanidin Extract (GSPE) Seasonal-Dependent Modulation of Glucose and Lipid Metabolism in the Liver of Healthy F344 Rats

Romina M. Rodríguez [1], Marina Colom-Pellicer [1], Jordi Blanco [2], Enrique Calvo [1], Gerard Aragonès [1] and Miquel Mulero [1,*]

[1] Nutrigenomics Research Group, Department of Biochemistry and Biotechnology, Campus Sescelades, Universitat Rovira i Virgili (URV), 43007 Tarragona, Spain; rominamariel.rodriguez@urv.cat (R.M.R.); marina.colom@urv.cat (M.C.-P.); enrique.calvo@urv.cat (E.C.); gerard.aragones@urv.cat (G.A.)
[2] Research in Neurobehavior and Health (NEUROLAB), Laboratory of Toxicology and Environmental Health, Physiology Unit, Institute of Health Research Pere Virgili (IISPV), School of Medicine, Universitat Rovira i Virgili (URV), 43202 Tarragona, Spain; jordi.blanco@urv.cat
* Correspondence: miquel.mulero@urv.cat; Tel.: +34-977559565

Abstract: Seasonality is gaining attention in the modulation of some physiological and metabolic functions in mammals. Furthermore, the consumption of natural compounds, such as GSPE, is steadily increasing. Consequently, in order to study the interaction of seasonal variations in day length over natural compounds' molecular effects, we carried out an animal study using photosensitive rats which were chronically exposed for 9 weeks to three photoperiods (L6, L18, and L12) in order to mimic the day length of different seasons (winter/summer/and autumn-spring). In parallel, animals were also treated either with GSPE 25 (mg/kg) or vehicle (VH) for 4 weeks. Interestingly, a seasonal-dependent GSPE modulation on the hepatic glucose and lipid metabolism was observed. For example, some metabolic genes from the liver (SREBP-1c, *Gk*, *Acacα*) changed their expression due to seasonality. Furthermore, the metabolomic results also indicated a seasonal influence on the GSPE effects associated with glucose-6-phosphate, D-glucose, and D-ribose, among others. These differential effects, which were also reflected in some plasmatic parameters (i.e., glucose and triglycerides) and hormones (corticosterone and melatonin), were also associated with significant changes in the expression of several hepatic circadian clock genes (*Bmal1*, *Cry1*, and *Nr1d1*) and ER stress genes (*Atf6*, *Grp78*, and *Chop*). Our results point out the importance of circannual rhythms in regulating metabolic homeostasis and suggest that seasonal variations (long or short photoperiods) affect hepatic metabolism in rats. Furthermore, they suggest that procyanidin consumption could be useful for the modulation of the photoperiod-dependent changes on glucose and lipid metabolism, whose alterations could be related to metabolic diseases (e.g., diabetes, obesity, and cardiovascular disease). Furthermore, even though the GSPE effect is not restricted to a specific photoperiod, our results suggest a more significant effect in the L18 condition.

Keywords: photoperiod; seasonal; GSPE; AMPK; clock genes; liver

Citation: Rodríguez, R.M.; Colom-Pellicer, M.; Blanco, J.; Calvo, E.; Aragonès, G.; Mulero, M. Grape-Seed Procyanidin Extract (GSPE) Seasonal-Dependent Modulation of Glucose and Lipid Metabolism in the Liver of Healthy F344 Rats. *Biomolecules* **2022**, *12*, 839. https://doi.org/10.3390/biom12060839

Academic Editors: Randy J. Nelson and James C. Walton

Received: 15 May 2022
Accepted: 15 June 2022
Published: 17 June 2022

1. Introduction

Apart from Earth's rotation around its axis, at the same time, the Earth is moving around the Sun creating circannual periods, which define the day length variations and the seasons. Related to this, animals have been adapted to circannual rhythms by a physiological process that depends on an innate long-term timer which is synchronized with the annual environmental cycle (photoperiodic entrainment) [1]. In mammals, this information is received via photoreceptor cells in the retina, which are connected through the retinohypothalamic tract to pineal gland, which converts the photic information through the neurohormone melatonin. Therefore, photoperiodism relies on the way that the pineal

gland transduces a photoperiod into a twenty-four-hour melatonin signal, and how its duration is decoded in melatonin-sensitive tissues that control specific aspects of seasonal physiology and behavior [2]. Thus, melatonin codes for day length as it is excreted at night, playing a pivotal role in the control of seasonal and daily changes [3].

In consequence, the study of seasonal adaptations of mammals is important for understanding the underlying regulatory mechanisms implicated, which has great potential for translational research as there is increasing evidence indicating an impact of seasonal timing on several biological processes (e.g., immunity). For example, it has been shown that more than 4000 protein-coding mRNAs in human white blood cells and adipose tissue have seasonal expression profiles, with inverted patterns observed between Europe and Oceania. This shows a seasonal component as part of human immunity and physiology [4]. Furthermore, regarding hepatic lipid metabolism, it has been shown that the fish *Oryzias latipes* showed a greater accumulation of fatty acids in the liver under the short-day condition than under the long-day condition [5]. Additionally, Togo and colleagues demonstrated that the photoperiod regulates feeding and energy metabolism in young growing Fischer 344 rats. These rats preferred a diet with high carbohydrate content compared to one with less carbohydrates under the long-day condition, while no preference for diets was observed under the short-day condition. Moreover, rats under the long-day condition showed an increase in body weight, epididymal fat mass, and plasma leptin levels compared to animals under short-day condition regardless of dietary composition [6]. On the other hand, another season-dependent biological parameter is ROS. In this regard, it has been shown that seasonal changes in the antioxidant defenses enable species to maintain their correct levels of ROS to carry out physiological functions in response to changing physical environmental parameters [7]. Interestingly, Cruz-Carrión and colleagues demonstrated that photoperiods modulate the oxidative stress response to the consumption of local and non-local sweet cherries in rats [8].

This evidence has led, in the last years, to an increasing scientific interest in the study of the influence of circannual rhythmicity in the development of metabolic diseases, and how the addition of bioactive compounds to the diet may help to attenuate these disorders. For this purpose, Fisher 344 rats are known to be a species sensitive to photoperiods, and therefore an excellent model for studying seasonal variation [6].

On the other hand, polyphenols, which are organic compounds found in plants, have become a new field of research in nutrition in recent decades. Among them, proanthocyanidins are powerful naturally derived antioxidants, which have been proven to exhibit anticarcinogenic, anti-inflammatory, antiallergic, antibacterial, antiviral, antidiabetic, immuno-stimulating, neuroprotective, and cardioprotective effects [9,10], as well as to extend the lifespan of animals, apparently by mimicking the beneficial effects of caloric restriction through the increase of SIRT1 expression, which has been recognized as an essential factor for lifespan extension [11,12] In addition, these polyphenolic compounds are able to dampen inflammatory signaling, induce selective apoptosis of senescent cells, and modulate nutrient-sensing pathways. These are biological processes that become dysfunctional with age and are relevant in the pathogenesis of age-related syndrome [13,14]. Interestingly, several in vivo and in vitro experiments demonstrated that supplementation with grape seed procyanidin extract (GSPE) alleviated oxidative stress through the inhibition of lipid peroxidation [15], mitigated endoplasmic reticulum (ER) stress [16], improved mitochondrial function [17], and reduced liver glutathione alteration in obese rat models [18]. Furthermore, GSPE was able to increase normal insulin content and to decrease the number of apoptotic cells in diabetic pancreatic islets [19]. Consequently, these experiments have demonstrated that GSPE is nontoxic, highly bioavailable, and provides significant multiorgan protection. Additionally, GSPE intake in rats has also been shown to produce behavioral changes, such as decreased locomotor activity and decreased food consumption, and modulations on energy expenditure, which could be related to changes observed on mechanisms subjected to seasonal control, such as dopaminergic and somatostatinergic systems [20–22]. Consequently, these experiments have demonstrated

that polyphenols provide significant multiorgan protection and could modulate seasonal rhythms by acting not only at a central level but also in peripheral tissues, such as liver and adipose tissue, exerting an impact on systemic metabolism. However, little is known about the influence of seasonal variations on the beneficial effects of polyphenols, which may condition their administration schedule. Therefore, the aim of this study was to investigate the hypothetical differential effect of GSPE supplementation on hepatic glucose and lipid metabolism in Fischer 344 rats under different photoperiod conditions.

2. Materials and Methods

2.1. Grape Seed Proanthocyanidin-Rich Extract

The GSPE was kindly provided by Les Dérivés Résiniques et Terpéniques (Dax, France). According to the manufacturer, the GSPE composition used in this study contained monomers (21.3%), dimers (17.4%), trimers (16.3%), tetramers (13.3%), and oligomers (5–13 units; 31.7%) of proanthocyanidins. The exact phenolic composition of GSPE was determined by HPLC-MS/MS and consisted of catechin (58 μmol/g), dimeric procyanidins (250 μmol/g), epicatechin (52 μmol/g), epigallocatechin (5.50 μmol/g), epicatechin gallate (89 μmol/g), epigallocatechin gallate (1.40 μmol/g), hexameric procyanidins (0.38 μmol/g), pentameric procyanidins (0.73 μmol/g), tetrameric procyanidins (8.8 μmol/g), and trimericprocyanidins (1568 μmol/g) [23].

2.2. Experimental Design

A total of 48 12-week-old male Fischer 344 (F344) rats (Charles River Laboratories, Barcelona, Spain) were housed in pairs (in cages) at 22 °C, 55% humidity, and subjected to three different light schedules for 9 weeks to mimic seasonal day lengths: short day photoperiod L6 (n = 16, 6 h light and 18 h darkness), normal day or standard photoperiod L12 (n = 16, 12 h light and 12 h darkness), and long day photoperiod L18 (n = 16, 18 h light and 6 h darkness). Animals were fed with a standard diet (STD) ad libitum. The STD composition was 20% protein, 8% fat, and 72% carbohydrates (Panlab, Barcelona, Spain). Within each photoperiod group, rats were randomly divided into two groups depending on the treatment: 8 STD-fed rats were treated with condensed milk, vehicle (VH), and 8 STD-fed rats were treated with 25 mg/kg GSPE. The treatment lasted four weeks and was orally administered daily using a syringe. During the entire study, rats had free access to water, and body weight and food intake were weekly recorded. After 9 weeks, animals were kept from food for 3 h and then sacrificed by decapitation at 9 am (one hour after light was turned on; ZT1) under anesthesia (sodium pentobarbital, 50 mg/kg per body weight). Blood was collected and serum was obtained by centrifugation (15,000× g, 10 min, 4 °C) and stored at −80 °C until analysis. The liver was rapidly weighed, frozen in liquid nitrogen, and stored at −80 °C for further analysis. The Animal Ethics Committee of the Universitat Rovira i Virgili (Tarragona, Spain) approved all procedures (reference number 9495, 18 September 2019) and they were carried out in accordance with Directive 86/609EEC of the Council of the European Union and the procedure established by the Departament d'Agricultura, Ramaderia i Pesca of the Generalitat de Catalunya.

2.3. Serum Analysis

Circulating levels of glucose, total cholesterol, HDL and LDL cholesterol and triglycerides (QCA, Barcelona, Spain), were analyzed by colorimetric enzymatic assay kits according to the manufacturer's instructions.

2.4. RNA Extraction

Approximately 20–30 mg of liver tissue was mixed with Trizol® reagent (Thermo Fisher, Madrid, Spain) and homogenized by Tissue Lyser LT (Qiagen, Madrid, Spain). After a 10-min centrifugation (12,000× g and 4 °C), the homogenate was placed into a new Eppendorf tube and 120 μL of chloroform was added. Two phases were separated after a 15-min centrifugation (12,000× g and 4 °C). The aqueous phase was transferred into a

new Eppendorf and 300 µL of isopropanol was added. An overnight incubation (−20 °C) was carried out to extract the microRNA (miRNA). The supernatant was discarded after a 10-min centrifugation (12,000× *g* and 4 °C). The pellet was cleaned twice with 5-min centrifugation (8000× *g* and 4 °C) with 500 µL of ethanol 70%. The supernatant was discarded, and the cleaned pellet was resuspended with 60 µL of nuclease-free water (Thermo Fisher, Madrid, Spain). The RNA concentration (ng/µL) and the purity were measured in Nanodrop ND-1000 spectrophotometer (Thermo Fisher, Madrid, Spain).

2.5. Gene Expression Analysis

The cDNA was obtained by a reverse transcription of the RNA extracted using a High-Capacity Complementary DNA Reverse Transcription Kit (Thermo Fisher, Madrid, Spain). The quantitative polymerase chain reactions (qPCRs) were performed in 384-well plates in a 7900HT Fast Real-Time PCR (Thermo Fisher, Madrid, Spain) using iTaq™ Universal SYBR® Green Supermix (Bio-Rad, Barcelona, Spain). The thermal cycle used in all qPCRs was 30 s at 90 °C and 40 cycles of 15 s at 95 °C and 1 min at 60 °C. All liver genes were normalized by the housekeeping gene peptidylprolyl Isomerase A (*Ppia).* The primers used for each gene were obtained from Biomers (Ulm, Germany) (Table 1). The relative expression of each gene was calculated according to the Pfaffl method (2001) and normalized by the control group L12-STD-VH.

Table 1. Nucleotide sequences of primers used for real-time quantitative PCR.

Gene	Forward Primer (5′ to 3′)	Reverse Primer (5′ to 3′)
Acacα	TGCAGGTATCCCCACTCTTC	TTCTGATTCCCTTCCCTCCT
Atf4	TATGGATGGGTTGGTCAGTG	CTCATCTGGCATGGTTTCC
Atf6	GACTGGGAGTCCACGTTGTT	GAACAGGAGTCTGTGGACCG
Bmal1	GTAGATCAGAGGGCGACGGCTA	CTTGTCTGTAAAACTTGCCTGTGAC
Cd36	GTCCTGGCTGTGTTTGGA	GCTCAAAGATGGCTCCATTG
Chop	AAGATGAGCGGGTGGCAGCG	CCGGTTTCTGCTTTCAGGTGTGGT
Cry1	TGGAAGGTATGCGTGTCCTC	TCCAGGAGAACCTCCTCACG
Fatp5	CCTGCCAAGCTTCGTGCTAAT	GCTCATGTGATAGGATGGCTGG
G6pdh	ACCAGGCATTCAAAACGCAT	CAGTCTCAGGGAAGTGTGGT
Gk	CTGTGAAAGCGTGTCCACTC	GCCCTCCTCTGATTCGATGA
Grp78	CTACGAAGGTGAACGACCCC	ATTTCTTCAGGGGTCAGGCG
Nampt	CTCTTCACAAGAGACTGCCG	TTCATGGTCTTTCCCCCACG
Nr1d1	ACAGCTGACACCACCCAGATC	CATGGGCATAGGTGAAGATTTCT
Per2	CGGACCTGGCTTCAGTTCAT	AGGATCCAAGAACGGCACAG
Pparα	CGGCGTTGAAAACAAGGAGG	TTGGGTTCCATGATGTCGCA
Ppia	CCAAACACAAATGGTTCCCAGT	ATTCCTGGACCCAAAACGCT
Rorα	CCCGATGTCTTCAAATCCTTAGG	TCAGTCAGATGCATAGAACACAAACTC
Srebp1c	CCCACCCCCTTACACACC	GCCTGCGGTCTTCATTGT
s-Xbp1	AAACAGAGTAGCAGCACAGACTGC	TCCTTCTGGGTAGACCTCTGGGAG

2.6. Extraction and Measurement of Concentrations of Lipids in Liver

Liver lipids were extracted following the Bligh and Dyer method [24] and levels of hepatic cholesterol, triglycerides, and phospholipids were measured using a colorimetric kit assay (QCA, Barcelona, Spain).

2.7. Protein Extraction

A liver tissue portion (20 mg) was mixed with 500 µL of radioimmunoprecipitation assay (RIPA) buffer containing phosphatase inhibitor cocktail 2 and 3, protease inhibitor cocktail, and phenylmethylsulphonyl fluoride. The Eppendorf tube content was homogenized by Tissue Lyser LT (Qiagen, Madrid, Spain). The samples were shaken 30 min at 4 °C and the tube content was placed into a new Eppendorf tube. After a 15-min centrifugation (12,000× *g* and 4 °C), the supernatant was transferred into a new Eppendorf tube. The protein quantification was carried out using a colorimetric bicinchoninic acid (BCA) assay kit (Thermo Fisher, Madrid, Spain) according to the manufacturer instructions.

2.8. Determination of Serum Hormones

The analytes melatonin (≥98%), corticosterone (≥98%), 3,3′,5-triiodo-L-thyronine (T3) (≥95%), L-thyroxine (T4) (≥98%) were obtained from Sigma-Aldrich (St. Louis, MO, USA). The internal standards L-thyroxine-D4 (≥98%) and 3,3′,5-triiodo-L-thyronine (≥98%) were purchased from Sigma-Aldrich (St. Louis, MO, USA); melatonin-D4 (≥98%)) was purchased from Cluzeau Info Labo (Sainte-Foy-la-Grande, France); and corticosterone-D8 (≥98%) was obtained from NeoChema (Bodenheim, Germany). Formic acid and ethyl acetate were obtained from Sigma-Aldrich (Madrid, Spain) and methanol from MERK (Madrid, Spain). All solvents and reagents used in the present study were HPLC grade. HPLC grade water was obtained by ultrafiltration (Millipore Milli Q system, Bedford, MA, USA). The standard stock (1 mg/mL) and internal standard (100 µg/mL) solutions were prepared in methanol. The working and calibration solutions were prepared in a water–methanol solution (1:1, v/v).

For determination of melatonin, corticosterone, triiodothyronine (T3), and thyroxine (T4) levels, serum samples were thawed at 4 °C. Then, 50 µL of serum was mixed with 250 µL of methanol containing the internal standard (2 ng/mL). Then, the mixture was vortexed and centrifuged for 5 min at 4 °C and 15,000 rpm. The supernatant was transferred to a new tube and mixed with 700 µL of 0.1% formic acid in water. The sample was loaded to an SPE tube previously conditioned with methanol and 0.1% formic acid in water. The cartridge was washed with 0.1% formic acid in water and dried under high vacuum. The compounds were eluted with 500 µL of methanol. Samples were evaporated in a SpeedVac at 45 °C and reconstituted with 50 µL of water:methanol (60:40, v/v) and transferred to a glass vial for analysis. Simultaneous detection and quantification of hormones levels were achieved using liquid chromatography coupled to triple quadrupole mass spectrometry (LC-QqQ).

2.9. Metabolomic Analysis

Metabolomic analysis of the 48 rat liver samples was performed at the Centre for Omic Sciences (COS, Tarragona, Spain) using gas chromatography coupled with quadrupole time-of-flight mass spectrometry (GC-qTOF model 7200, Agilent, Santa Clara, CA, USA). The extraction was performed by adding 400 µL of methanol:water (8:2)-containing internal standard mixture to liver samples (approximately 10–20 mg). Then, the samples were mixed and homogenized on a bullet blender using a stainless-steel ball, incubated at 4 °C for 10 min, and centrifuged at 19,000× g; supernatant was evaporated to dryness before compound derivatization (methoximation and silylation). The derivatized compounds were analyzed by GC-qTOF. Chromatographic separation was based on the Fiehn Method [25] using a J&W Scientific HP5-MS film capillary column (30 m × 0.25 mm × 0.25 µm, Agilent, Santa Clara, CA, USA) and helium as carrier gas with an oven program from 60 to 325 °C. Ionization was done by electronic impact (EI), with electron energy of 70 eV and operating in full-scan mode. Identification of metabolites was performed using commercial standards and by matching their EI mass spectrum and retention time to a metabolomic Fiehn library (from Agilent, Santa Clara, CA, USA), which contains more than 1400 metabolites. After putative identification of metabolites, they were semi-quantified in terms of internal standard response ratio.

2.10. Statistical Analysis

Data are reported as mean ± standard error of the mean (SEM). Serum and liver biochemical profile, liver weight, glucose-related hepatic metabolites, and liver gene expression were subjected to Student's t test and one- and two-way analysis of variance (ANOVA) with the least significant difference test (LDS) for post hoc comparisons using the computer program SPSS version 25 (SPSS Inc., Chicago, IL, USA). Graphics were done by GraphPad Prism 8 software (San Diego, CA, USA). For all analyses, a probability (p) value of <0.05 was considered statistically significant.

3. Results

3.1. Photoperiod Strongly Influences Body Weight Gain of F344 Rats

As shown in Figure 1, irrespective of treatment, rats exposed to a short photoperiod showed significantly higher body weight gain than animals subjected to the standard photoperiod (L12-VH vs. L6-VH; $p = 0.045$) (L12-GSPE vs. L6-GSPE; $p = 0.0049$). No differences were observed between the L12 and L18 groups or between L18 and L6 in relation to body weight gain. Regarding food intake, we observed no differences among the groups (Supplementary Figure S1).

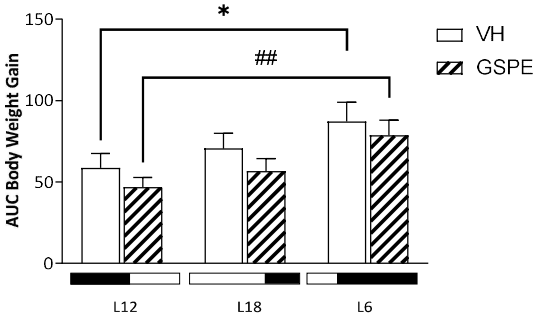

Figure 1. Body weight gain as area under the curve (AUC) of Fischer 344 rats treated with VH or GSPE exposed to standard (12 h light:12 h dark), long (18 h light:6 h dark), or short (6 h light:18 h dark) photoperiods fed with STD diet ($n = 8$). The results are presented as the mean ± SEM. * indicates significant differences within VH groups (Student's *t* test, * $p < 0.05$); # indicates significant differences within GSPE groups (Student's *t* test, ## $p < 0.01$).

3.2. The Effect of GSPE on Serum Parameters Depends on Photoperiod

As shown in Table 2, serum triglycerides levels of L12-GSPE animals tend to decrease compared to L12-VH ($p = 0.07$), whereas an increase in L6-GSPE animals compared to L12-GSPE group is observed ($p = 0.01$). Serum glucose values are elevated in L18-GSPE animals compared to L12 counterparts ($p = 0.001$), showing clear interaction between treatment and photoperiod. In addition, L6 photoperiod showed even higher values of serum glucose when compared to other VH groups, L12 vs. L6 ($p = 0.004$) and L18 vs. L6 ($p = 0.001$). Interestingly, L6-GSPE rats showed the highest serum glucose levels, raising its value around 15 percent compared to its VH, and showed a significant increase of total serum cholesterol compared to its control ($p = 0.006$). Additionally, a photoperiod effect is seen in HDL levels as animals exposed to short photoperiod exhibit lower values; on the other hand, LDL levels are affected not only by photoperiod but also by treatment showing a decrease in LDL values only on L18-GSPE rats.

Table 2. Concentration of serum parameters in response to different photoperiod exposure and GSPE treatment in animals fed a STD diet for 9 weeks.

Serum Parameters	L12		L18		L6		2wA
	STD-VH	STD-GSPE	STD-VH	STD-GSPE	STD-VH	STD-GSPE	
Glucose (mg/dL)	110.96 ± 4.67 ^{a}	102.72 ± 2.63 ^{a}	110.34 ± 2.86 ^{a}	141.81 ± 3.06 ^{b}	136.34 ± 5.82 ^{b}	154.49 ± 6.65 ^{c}	T, P, T*P
Cholesterol (mg/dL)	98.53 ± 5.30 ^{a}	104.54 ± 6.98 ^{ab}	107.15 ± 7.06 ^{ab}	108.36 ± 4.84 ^{ab}	98.60 ± 3.61 ^{a}	117.47 ± 4.15 ^{b}	T
Triglycerides (mg/dL)	56.13 ± 4.08 ^{ab}	46.73 ± 2.02 ^{b}	58.72 ± 4.69 ^{ab}	60.71 ± 5.84 ^{ab,*}	52.90 ± 3.25 ^{ab}	64.73 ± 6.93 ^{a}	
HDL (mg/dL)	35.33 ± 1.43 ^{a}	32.11 ± 2.28 ^{ab}	28.57 ± 2.25 ^{bc}	31.38 ± 1.13 ^{abd}	25.44 ± 1.27 ^{c}	26.93 ± 2.49 ^{cd}	P
LDL (mg/dL)	30.55 ± 3.20 ^{a}	34.79 ± 2.59 ^{a}	32.47 ± 3.33 ^{a}	20.80 ± 1.94 ^{b}	19.45 ± 1.47 ^{b}	19.43 ± 2.08 ^{b}	P, T*P

Serum parameters of Fischer 344 rats fed a STD diet and exposed to three different photoperiods for 9 weeks, supplemented with vehicle or GSPE for the last 4 weeks. Data are given as mean ± SEM. ($n = 8$). One- and two-way ANOVA following by LSD post hoc tests were performed to compare the values between groups and significant differences ($p \leq 0.05$) were represented with different letters (a, b, c, d). * Indicates tendency between L12-STD-GSPE and L18-STD-GSPE groups ($p = 0.052$). P, photoperiod effect. T, treatment effect. T*P, interaction between photoperiod and treatment. Abbreviations: HDL, high-density lipoprotein; LDL, low-density lipoprotein.

3.3. The Exposure to Different Photoperiods Altered the Expression of Circadian Rhythm-Related Genes in the Liver of GSPE-Treated Rats

We analyzed the hepatic mRNA expression of key clock genes to try to find correlations with the changes in serum parameters under different photoperiods in response to GSPE treatment. The gene expression of the brain and muscle Arnt-like protein-1 (*Bmal1*) gene was higher in L18 and L6-GSPE rats compered to L12-treated ones ($p = 0.006$ and 0.04, respectively), whereas expression levels of Period circadian clock 2 (*Per2*) only showed changes in VH groups with an increase in L18 compared to L12 and L6 photoperiods ($p = 0.02$ and 0.03, respectively) (Figure 2). Additionally, GSPE lowers mRNA relative levels of hepatic Cryptochrome circadian clock 1 (*Cry1*) gene in L18 ($p = 0.002$), which is highly upregulated in L18-VH. The *Bmal1* activator RAR-related orphan receptor alpha (*Rorα)* gene expression is lower in L6-GSPE compared to L6-VH animals ($p = 0.048$), while L6-VH rats exhibit a higher expression level than L12-VH ($p = 0.03$). Expression of nuclear receptor subfamily 1 group D member 1 gene (*Nr1d1*), a *Bmal1* repressor, is modulated by light showing a totally repressed expression in animals exposed to a long photoperiod while GSPE treatment slightly increased its expression ($p = 0.04$). Regarding Nicotinamide phosphoribosyltransferase (*Nampt*) gene expression, it decreased with GSPE treatment in L12 ($p = 0.008$) and increased when compared with L6-GSPE rats ($p = 0.046$).

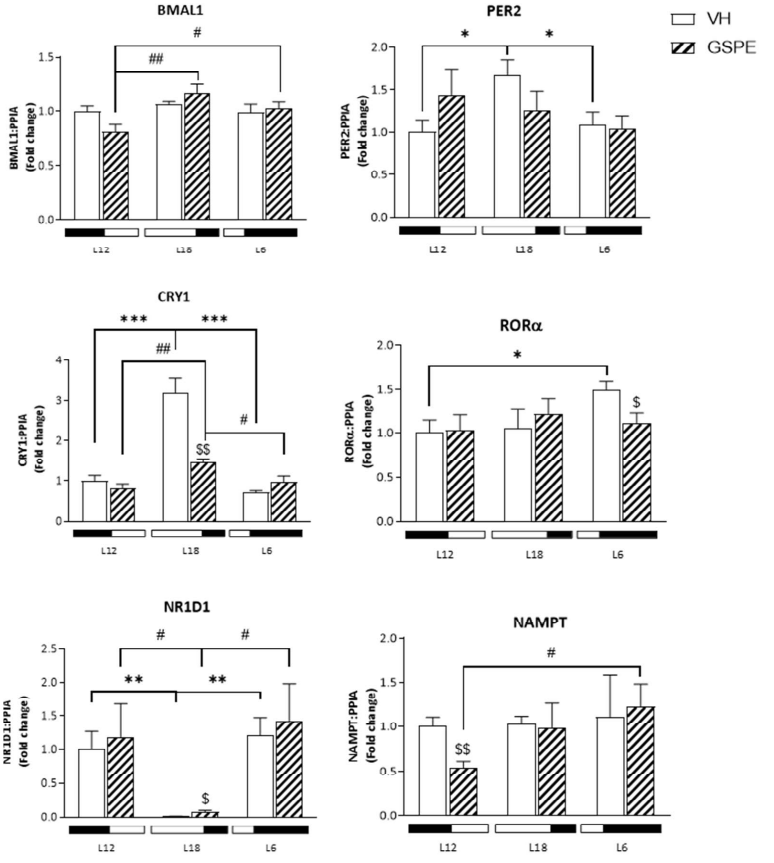

Figure 2. mRNA expression levels of clock genes in the liver of Fischer 344 rats treated with VH or GSPE exposed to standard (12 h light:12 h dark), long (18 h light:6 h dark), or short (6 h light:18 h dark) photoperiods fed with STD diet ($n = 8$). The results are presented as the mean ± SEM. * indicates significant differences within VH groups (Student's *t* test, * $p < 0.05$, ** $p < 0.01$, *** $p < 0.001$); # indicates significant differences within GSPE groups (Student's *t* test, # $p < 0.05$, ## $p < 0.01$); $ indicates significant differences between treatments (VH vs. GSPE) (Student's *t* test, $ $p < 0.05$, $$ $p < 0.01$).

3.4. Melatonin and Hormones from the Hypothalamus Pituitary Adrenal (HPA) Axes Have a Seasonal Variation which Is Affected by GSPE Consumption

Serum levels of corticosterone, T3 and T4, together with melatonin were analyzed. In this sense, Figure 3 shows significant increase of corticosterone levels in L6-GSPE animals ($p = 0.01$ vs. L6-VH, $p = 0.004$ vs. L12-GSPE, and $p = 0.002$ vs. L18-GSPE), whereas the L18 non-treated group shows an increase compared to the standard photoperiod ($p = 0.05$). In the case of melatonin, GSPE raised the levels of this hormone in the L18 photoperiod ($p = 0.05$); meanwhile, non-significant differences were found in T3 and T4 levels.

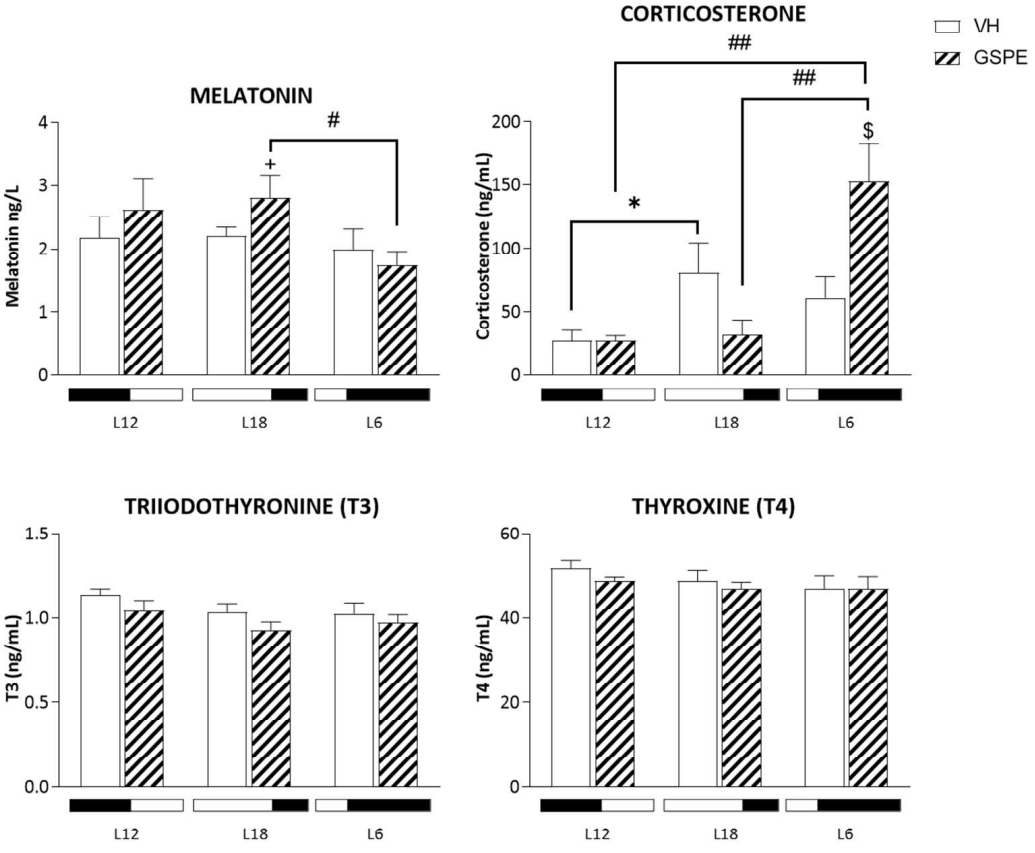

Figure 3. Concentration of serum hormones in response to different photoperiod exposure and GSPE treatment in animals fed a STD for 9 weeks. Fischer 344 rats fed a STD diet were treated with VH or GSPE and exposed to standard (12 h light:12 h dark), long (18 h light:6 h dark), or short (6 h light:18 h dark) photoperiods ($n = 8$). The results are presented as the mean ± SEM. * indicates significant differences within VH groups (Student's *t* test, * $p < 0.05$); # indicates significant differences within GSPE groups (Student's *t* test, # $p < 0.05$, ## $p < 0.01$); $ indicates significant differences between treatments (VH vs. GSPE) (Student's *t* test, $ $p < 0.05$). + indicates tendency between VH and GSPE treatment in L18 using Student's *t* test (+ $p = 0.050$).

3.5. Lipid Liver Profile

A clear photoperiod effect is seen in the levels of liver triglycerides, with an increase in L6 compared to standard photoperiod ($p = 0.007$). In addition, GSPE rats subjected to short photoperiod present higher values than L18 ($p = 0.02$) and L12 GSPE animals ($p = 0.001$) (Table 3). Total cholesterol, phospholipids, and liver weight showed no significant differences among groups.

Table 3. Liver lipids parameters in response to different photoperiod exposure and GSPE treatment in animals fed a STD for 9 weeks.

Parameters	L12		L18		L6		2wA
	STD-VH	STD-GSPE	STD-VH	STD-GSPE	STD-VH	STD-GSPE	
Cholesterol (mg/g)	1.19 ± 0.06^{ab}	1.27 ± 0.08^{a}	1.04 ± 0.07^{b}	1.09 ± 0.07^{ab}	1.14 ± 0.05^{ab}	1.12 ± 0.06^{ab}	
Triglycerides (mg/g)	2.62 ± 0.17^{b}	2.98 ± 0.10^{ab}	3.44 ± 0.35^{abc}	3.34 ± 0.13^{a}	3.68 ± 0.29^{ac}	3.84 ± 0.15^{c}	P
Phospholipids (mg/g)	6.82 ± 0.27^{a}	6.86 ± 0.36^{a}	6.3 ± 0.34^{a}	6.32 ± 0.26^{a}	6.92 ± 0.34^{a}	7.05 ± 0.42 a	
Liver weight (g)	14.78 ± 0.5^{a}	15.25 ± 0.6^{a}	15.21 ± 0.7^{a}	15.13 ± 0.61^{a}	15.6 ± 0.47^{a}	14.68 ± 0.61^{a}	

Lipid parameters in the liver of Fischer 344 rats fed a STD diet and exposed to three different photoperiods for 9 weeks, supplemented with vehicle or GSPE for the last 4 weeks. Data are given as mean ± SEM. ($n = 8$). One- and two-way ANOVA following by LSD post hoc tests were performed to compare the values between groups and significant differences ($p \leq 0.05$) were represented with different letters (a, b, c). P, photoperiod effect.

3.6. mRNA Levels of Key Hepatic Lipid and Glucose-Metabolic Regulators Varies due to Photoperiod and GSPE Treatment

In order to assess the effect of GSPE treatment on liver lipid and glucose metabolism. mRNA levels of genes implicated in both processes were analyzed. As shown in Figure 4. mRNA levels of SREBP-1c in L6-GSPE rats are higher compared to L12 ones ($p = 0.001$). Moreover. *Acacα* mRNA levels are also increased in L6-GSPE animals ($p = 0.03$). whereas GSPE treatment decreases the expression of this gene in a long photoperiod ($p = 0.04$). Sirtuin 1 (*Sirt1*) gene expression is higher in L6-VH compared to L18-VH animals showing a clear photoperiod effect ($p = 0.024$). Curiously. this expression is decreased when treated with GSPE in L6 ($p = 0.023$). Glucokinase (*Gk*) showed an 85 percent increase in its expression in L18-VH animals compared to other photoperiods ($p = 0.019$ vs. L12-VH and $p = 0.017$ vs. L6-VH). whereas GSPE treatment decreased by 62 percent *Gk* mRNA levels in L18 ($p = 0.004$). Other metabolic genes were analyzed such as *Pparα. Cd36. Fatp5.* and *G6pdh.* although no significant differences were found among groups.

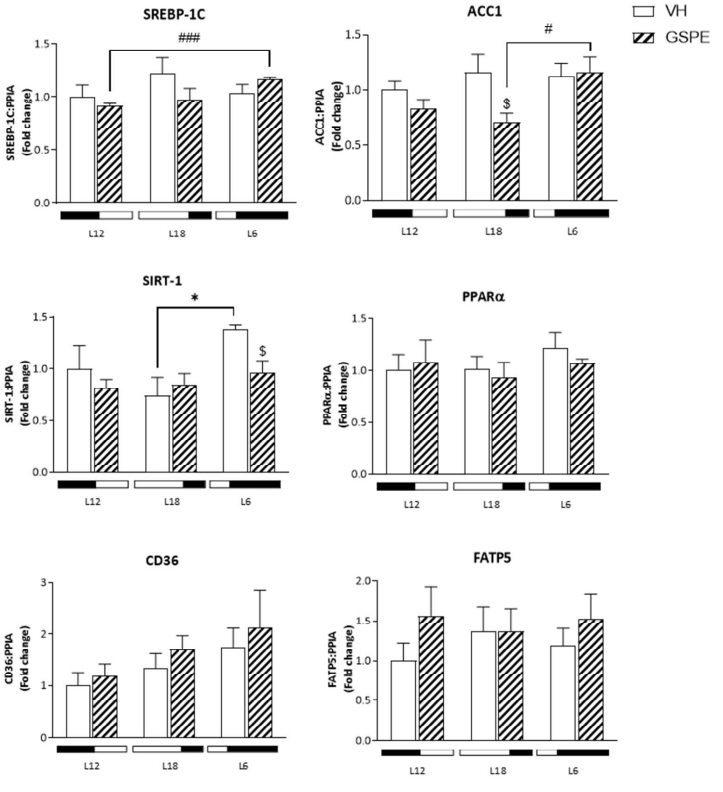

Figure 4. *Cont.*

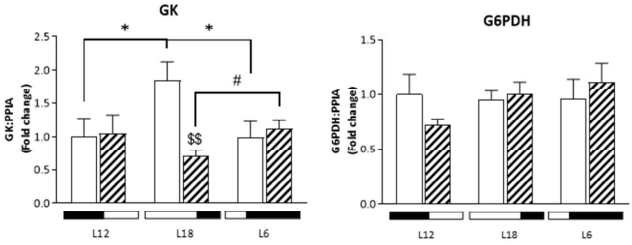

Figure 4. mRNA expression levels of liver lipid and glucose metabolism of Fischer 344 rats treated with VH or GSPE exposed to standard (12 h light:12 h dark), long (18 h light:6 h dark) or short (6 h light:18 h dark) photoperiods fed with STD diet (n = 8). The results are presented as the mean ± SEM. * indicates significant differences within VH groups (Student's t test, * $p < 0.05$); # indicates significant differences within GSPE groups (Student's t test, # $p < 0.05$, ### $p < 0.001$); $ indicates significant differences between treatments (VH vs. GSPE) (Student's t test, $ $p < 0.05$, $$ $p < 0.01$).

3.7. Analysis of Glucose-Related Metabolites Reveals Photoperiod Influence over GSPE Effect

Liver metabolites related to glucose pathways were studied and plotted in boxplots to visualize their concentrations in and between photoperiods and GSPE treatment. As it is seen in Figure 5, levels of D-glucose are lower in L18-GSPE animals compared to its VH (p = 0.027), as well as for D-ribose which shows a decrease in L18-GSPE animals but is increased in L18-VH when compared to L12-VH (p = 0.043). In the case of ribose-5-phosphate, L18-GSPE rats show lower levels than L6-GSPE animals (p = 0.034). Glucose-6-phosphate and fructose-6-phosphate show a similar pattern, with higher concentration levels in non-treated L12 animals (VH vs. GSPE) (p = 0.033 and 0.018, respectively). When compared between GSPE groups, L12 rats exhibit lower levels of these metabolites than in L18 animals (p = 0.043 in the case of glucose-6-phosphate and p = 0.028 in fructose-6-phosphate), whereas there is a tendency of increasing levels of fructose-6-phosphate in L6-GSPE rats compared to L12 counterparts (p = 0.055) (Supplementary Tables S1 and S2).

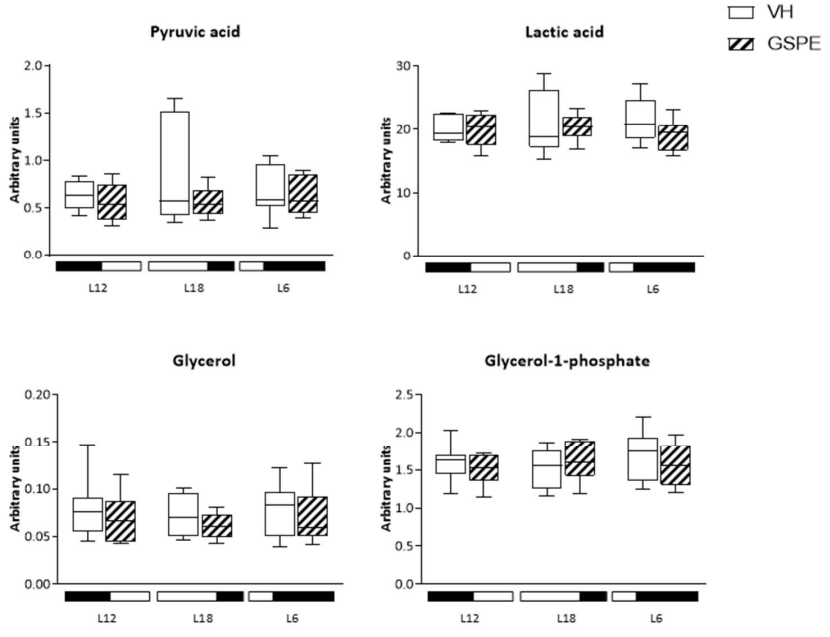

Figure 5. *Cont.*

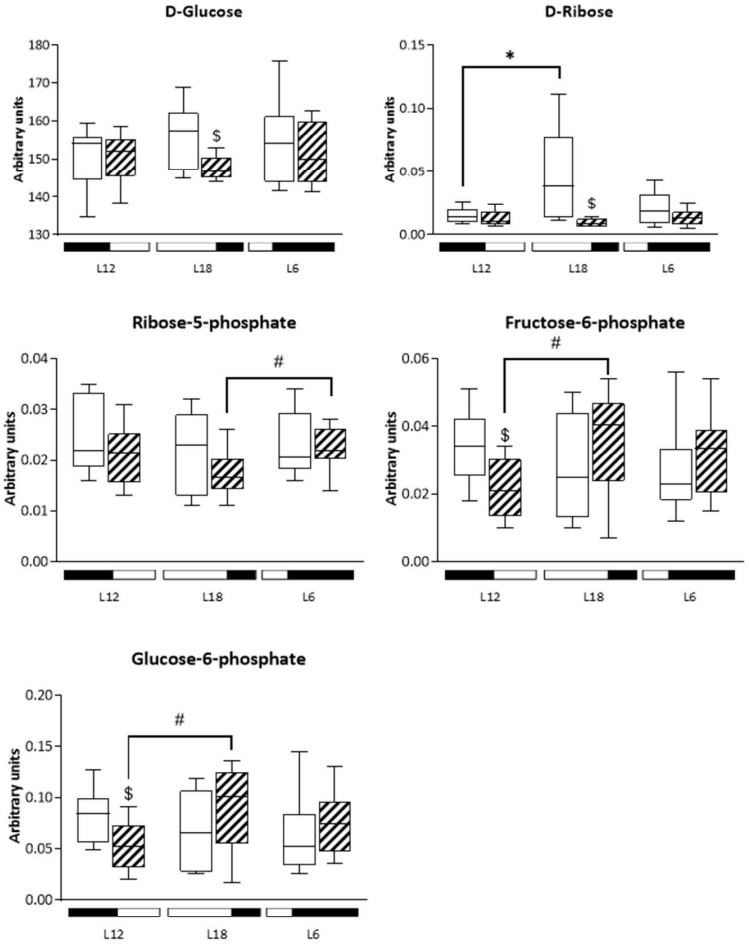

Figure 5. Metabolites related to hepatic glucose metabolism. Metabolites of glucose metabolism in the liver of Fischer 344 rats treated with VH or GSPE exposed to standard (12 h light:12 h dark), long (18 h light:6 h dark), or short (6 h light:18 h dark) photoperiods fed with STD diet (n = 8). The results are presented as the mean ± SEM. * indicates significant differences within VH groups (Student's t test, * $p < 0.05$); # indicates significant differences within GSPE groups (Student's t test, # $p < 0.05$); $ indicates significant differences between treatments (VH vs. GSPE) (Student's t test, $ $p < 0.05$).

3.8. Photoperiod Affects the GSPE Effect on ER Stress Genes

We measured the relative gene expression of the following key ER stress genes: *Atf4*. *Atf6*. *Grp78*. *s-Xbp1*. and *Chop*.

As shown in Figure 6. the relative gene expression of *Grp78* in L6 GSPE animals is the highest of all treatments (p = 0.001 vs. L6-VH and vs. L18-GSPE. p = 0.037 vs. L12-GSPE). whereas L18 GSPE-treated animals showed the lowest expression of this gene. Similar results are seen in the *Atf6* gene expression for L18 GSPE group (p = 0.002 vs. L18-VH. p = 0.005 vs. L12-GSPE. p = 0.001 vs. L6-GSPE). and it is also seen an increase in the expression of this gene in L6 GSPE animals compared to its control group (p = 0.03). In the same line. *Chop* gene expression is decreased in L18 GSPE-treated animals (p = 0.005 vs. L18-VH) and increased in L6 GSPE group (p = 0.013 vs. L6-VH).

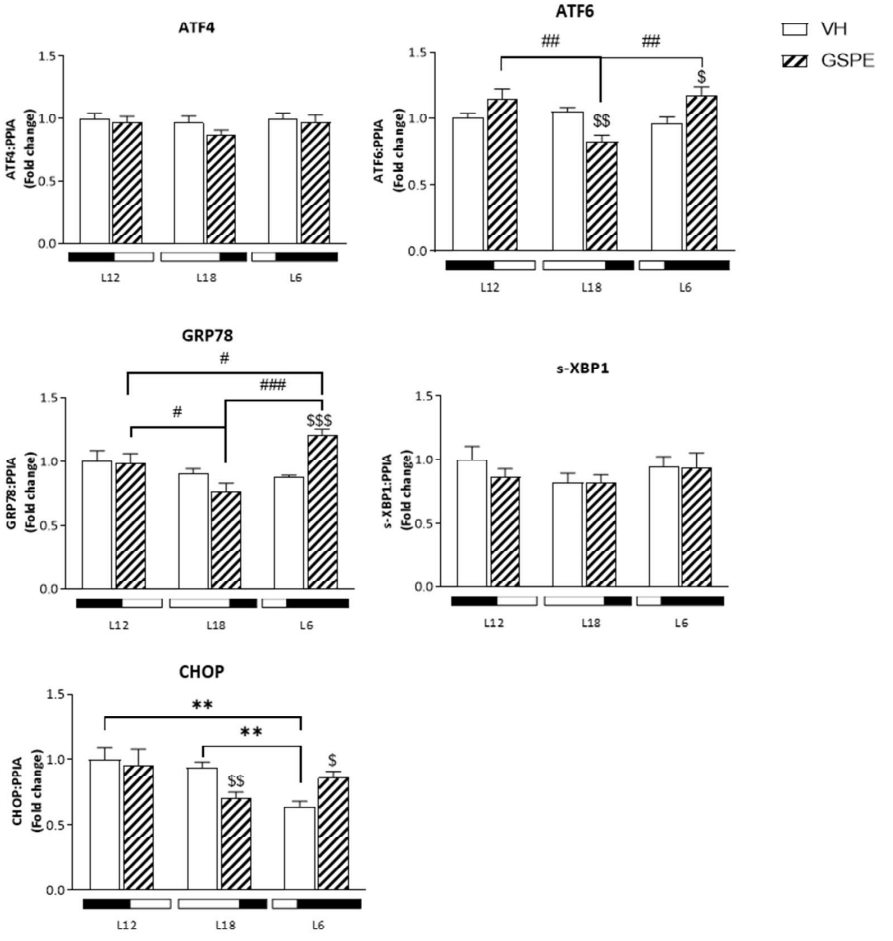

Figure 6. mRNA expression levels of ER stress genes of Fischer 344 rats treated with VH or GSPE exposed to standard (12 h light:12 h dark), long (18 h light:6 h dark), or short (6 h light:18 h dark) photoperiods fed with STD diet (n = 8). The results are presented as the mean ± S.E.M. * indicates significant differences within VH groups (Student's t test, ** $p < 0.01$); # indicates significant differences within GSPE groups (Student's t test, # $p < 0.05$, ## $p < 0.01$, ### $p < 0.001$); $ indicates significant differences between treatments (VH vs. GSPE) (Student's t test, $ $p < 0.05$, $$ $p < 0.01$, $$$ $p < 0.001$).

4. Discussion

Intrinsically synchronized with the natural year, circannual rhythms are responsible for scheduling seasonal activities in relation to the outer environmental cues. These rhythms function as a sensor to adjust the physiology and behavior of an organism to the periodically changing conditions [26].

Polyphenols have been widely described as compounds able to regulate metabolic syndrome-associated disorders which can also interact with the biological rhythms by affecting the expression of clock genes [27]. Consequently, the season of the year in which polyphenols are consumed could likely modify their ability to restore metabolic disorders. The current study aims to investigate whether these adaptative mechanisms can also modulate the effect on liver metabolism of a specific polyphenol extract.

The first conclusion that we can draw from our results is the slight alteration on metabolic health due to short photoperiod exposure (L6) in rats (discussed below). This result strongly correlates with previous findings in which L6 rats exhibited markedly altered glucose homeostasis and fatty acid uptake and oxidation when compared to animals

exposed to longer photoperiods [28]. More precisely, depending on the light schedules, we observed variations in hepatic triglycerides levels, some serum parameters (i.e., glucose and triglycerides), hormones (corticosterone and melatonin), and hepatic glucose metabolites, which could be linked to changes in the expression of several hepatic circadian clock genes such as *Bmal1*, *Cry1*, and *Nr1d1*, as well as lipogenic (SREBP-1c, *Acacα*) and ER stress (*Atf6*, *Grp78*, and *Chop*) genes.

Numerous studies have documented that the exposure to different day length schedules has an impact on physiology, behavior, and reproduction in animals that are exposed to different photoperiods. In fact, many of these studies have been carried out using photoperiod-sensitive F344 rats. In the present study, we observed no changes in food intake between the different photoperiods, which was in agreement with previous studies using F344 rats subjected to STD diet [28]. On the other hand, we observed differences in body weight gain which was increased in rats exposed to the short photoperiod compared to the standard, and this effect was independent of the treatment. This could be attributed to the hours of sleep L6 animals had, as it has been reported that short sleep duration could be an independent risk factor for weight gain [29]. These results, however, clearly differed from other studies using the F344 strain, in which the exposure to a short photoperiod reduced body mass compared to long-day photoperiods. These could be explained by the differences in age and reproductive status of the animals used and the duration of the experiments [30–32] Nevertheless, human studies have shown that lower levels of melatonin secretion in the autumn-winter period can increase appetite and lead to weight gain [33]. These results are in agreement with our present results, regarding the lower melatonin levels in the L6 photoperiod and the weight gain.

Regarding the effect of GSPE administration, our results clearly showed a differential GSPE modulation on the hepatic glucose and lipid metabolism in a seasonal-dependent manner.

The liver, the main organ involved in cholesterol homeostasis, synthesizes very low-density lipoproteins (VLDL) to transport triacylglycerol from the hepatocyte to peripheral tissues. A remnant is formed after this particle is metabolized in extrahepatic tissues, and part of this remnant is converted into LDL. It is known that one of the most important risk factors of atherosclerotic disease is the concentration of cholesterol carried in LDL [34], both parameters also being closely related to the prevalence of non-alcoholic fatty liver disease [35]. Humans show total cholesterol and LDL levels higher in winter than in summer [36,37], partly due to seasonal variations in food intake and physical activity which lead to an increase of body weight in winter [38]. Accordingly with these observations in humans, in our study, rats exposed to the short photoperiod (L6) showed the highest levels of serum cholesterol, which GSPE was unable to reduce, contrary to the anticholesterolemic activity showed by GSPE on rats exposed to a long photoperiod (L18). Nevertheless, we have to keep in mind that such cholesterol levels are not associated, in this case, with any pathological state.

Our results also showed different responses regarding the maintenance of glucose homeostasis between the experimental groups. In high glycemic conditions, glucose is phosphorylated to glucose-6-phosphate by GK in the hepatocyte. Glucose-6 phosphate serves as a metabolic link connecting glycolysis with the pentose phosphate pathway, de novo lipogenesis, and glycogen synthesis by inducing glycogen synthase activation in hepatocytes [39–41]. These findings agree with our results in which L18-GSPE animals display the highest levels of glucose-6-phosphate, consistent with the elevated blood glucose levels showed in this group, meanwhile L6-GSPE animals did not show this increase in glucose-6-phosphate concentrations despite their elevated bloodstream glucose.

In addition, it is important to note that in conditions of ribose 5-phosphate requirements, the cells transform glucose 6-phosphate into fructose 6-phosphate and glyceraldehyde 3-phosphate through the glycolytic pathway. These molecules are then converted into ribose 5-phosphate via the reverse steps of the nonoxidative phase. When NADPH is needed, the cell firstly undergoes oxidative reactions followed by non-oxidative reactions and finally gluconeogenesis. As a result, ribose 5-phosphate is recycled back into

glucose 6-phosphate, which is used to synthesize NADPH molecules. A cell that needs ATP and NADPH undergoes both oxidative and non-oxidative phases, thereby synthesizing NADPH and transforming the ribose 5-phosphate into glycolytic intermediates that can be used to synthesize ATP [42,43]. Our results showed levels of fructose-6-phosphate also higher in L18-GSPE animals whereas L6-GSPE rats showed elevated levels of ribose-5-phosphate. Therefore, based on these results, it is possible to suggest that L18-GSPE rats have enhanced the glycolytic metabolic pathway, whereas L6-GSPE animals display stimulated gluconeogenesis. This observation in L6-GSPE rats may be partly explained by the variation of corticosterone circulating levels between the experimental groups. It is known that glucocorticoids increase fat storage and glucose production in the liver [44,45] and L6-GSPE rats showed corticosterone levels five times higher than the others GSPE groups.

We also analyzed the levels of melatonin based on its activity as scavenger of free radicals, thus increasing the activity of antioxidant enzymes (i.e., glutathione peroxidase, superoxide dismutase and catalase), which are crucial for maintaining liver function and determining the protective role of melatonin on liver damage [46–51]. We observed differences in melatonin levels between L18 and L6 that can be attributed to the different hours of light exposure. As melatonin is released during the dark phase, animals exposed to long photoperiod have fewer hours of darkness than animals exposed to short photoperiod. As they were sacrificed at the same time, the peak of melatonin will be more pronounced in L18 than in L6 rats because the dark phase of L18 animals is closer to the sacrifice time point, meanwhile in short photoperiods, melatonin is released 12 h earlier, at the beginning of their dark phase. In addition to light exposure, it is known that GSPE can modulate melatonin levels in plasma [52]. In accordance with other parameters that seem to confer beneficial properties to the L18-GSPE group, our results showed a more evident increase in melatonin levels in such animals.

Past research has demonstrated an association between ER stress and hepatic lipogenesis, as ER plays an important role not only in protein folding but also in lipid synthesis and metabolism [53]. Interestingly, prior studies have shown that ER stress can activate SREBPs, resulting in the upregulation of lipogenic genes such as *Fasn* and *Acacα*, as well as of transcription factors and proteins involved in hepatic cholesterol and in triglyceride synthesis [54,55]. Moreover, another study demonstrated that activation of SREBP-1 by ER stress induces hepatic triglyceride accumulation in mice [56]. In addition, it was found that culture liver cells with saturated fatty acids or with triglyceride-rich particles disrupt ER homeostasis and activates the expression of ER stress genes and proteins [57,58]. These findings are consistent with those obtained in our study as a downregulation in the expression of *Atf6* and *Chop*, genes involved in ER stress, in L18-GSPE rats, has been observed together with the decrease in the expression of lipogenic genes and liver triglycerides. In contrast, L6-GSPE rats, those with a more adverse lipid profile, overexpressed *Grp78, Atf6*, and *Chop*. Therefore, ER stress activation may play an early and critical role in the cellular response to fatty acid overload. In concordance with these results, levels of *Sirt1* were found to be downregulated in L6-GSPE animals. It is known that *Sirt1* is essential for the regulation of liver lipid metabolism and gluconeogenesis [59]. In more detail, it has been shown that *Sirt1* negatively regulates the expression of genes involved in glycolysis, triglyceride synthesis, and lipid metabolism [60]. This result strongly agrees with another study which demonstrated that hepatic lipid concentrations negatively correlated with *Sirt1* mRNA levels in animals supplemented with GSPE [61]. In addition, it has been demonstrated that SREBP-1c is necessary for *Gk* expression in hepatocytes [62], as well as the requirement of GK for the expression of lipogenic genes such as *Fasn* and *Acacα* [63]. Thus, glucose phosphorylation by hepatic GK is not only a crucial event for glucose metabolism but also for lipid metabolism in the liver. Accordingly, in our results, the decrease of lipogenic genes expression in L18-GSPE rats was also accompanied by a dramatic reduction in *Gk* liver expression. In this regard, a summary table of the main metabolic changes due to the GSPE treatment in each photoperiod has been added in Supplementary Table S3.

Finally, one of the duties of the mammalian circadian clock is to measure photoperiodic time, acting as an accurate natural predictor of annual phases, making it possible to adapt to seasonal changes [64]. We detected changes at both photoperiod and treatment comparisons, as differences between treatments were observed in L12 (*Nampt*) as well as in L18 (*Cry1, Nr1d1*) and in L6 (*Rorα).* According to these results, it is likely that a circadian rhythm mismatch in L18-VH animals and GSPE treatment is able to recover from this disturbance in these animals exposed to a long photoperiod. It has been shown that clock-core genes contribute to the regulation of glucose and lipid metabolism in the liver [65]. In this regard, it is plausible to suggest that regulation seen on L18-GSPE animals on lipogenic genes may have a relationship with the restoration of circadian mismatch seen on animals exposed to L18 photoperiod. However, one limitation is that we were able to measure the expression of circadian rhythm-related genes only at a single time point (ZT 1). Therefore, an analysis conducted over a 24-h period at different daily time points would be necessary to confirm this hypothesis. Nevertheless, our results correlate with previous studies showing that the exposure to short and long photoperiods caused a disruption in the expression of hepatic circadian clock impairing lipid and glucose metabolism in the liver [66]. Furthermore, in order to depict the global metabolic scenario regarding our experimental approach, it will be also important to carry out proteomics and epigenomics approaches to investigate further into the physiological outcomes of photoperiods and treatments.

5. Conclusions

The present study highlights the importance of circannual rhythms in regulating metabolic homeostasis and suggests that seasonal variations (long or short photoperiods) affect hepatic metabolism. Furthermore, our findings suggest that GSPE effects vary among photoperiods and could improve the consequences related to a change in photoperiod (e.g., partial disruption in the circadian rhythmicity of clock genes, slight alterations on lipid and glucose metabolism) which could be associated with obesity promotion. Finally, our results suggest that the GSPE effect, although not restricted to any specific photoperiod, is especially relevant in the L18 photoperiod under physiological conditions.

Supplementary Materials: The following are available online at https://www.mdpi.com/article/10.3390/biom12060839/s1, Table S1. Treatment comparison between metabolites related to hepatic glucose metabolism; Table S2. Photoperiod comparison between metabolites related to hepatic glucose metabolism; Table S3. Summary of the main metabolic changes due to the GSPE treatment in each photoperiod compared to its respective VH control; Figure S1. Average of weekly food intake (kJ) of different photoperiods.

Author Contributions: Conceptualization, M.M., G.A. and E.C.; methodology, R.M.R., M.C.-P. and J.B.; software, R.M.R.; validation, R.M.R., M.M. and G.A.; formal analysis R.M.R., M.C.-P. and J.B.; resources, M.M., G.A. and E.C.; data curation, R.M.R. and M.M.; writing—original draft preparation R.M.R. and M.M.; writing—review and editing R.M.R. and M.M.; visualization, M.M, G.A. and E.C.; supervision, M.M.; project administration, M.M. and G.A.; funding acquisition, M.M., G.A. and E.C. All authors have read and agreed to the published version of the manuscript.

Funding: This research was funded by the Spanish Ministry of Economy and Competitiveness (MINECO), AGL2016-77105-R (CHRONOFOOD project). R.M.R. is recipient of a predoctoral fellowship from Universitat Rovira i Virgili—Martí i Franquès, grant number 2018PMF-PIPF-11. M.C.P. is recipient of a predoctoral fellowship from the Catalan Government, grant number 2021FI_B2 00150. J.B., G.A. and M.M. are Serra-Hunter fellows.

Institutional Review Board Statement: All animal care and experimental protocols involving animals were approved by the Ethics Review Committee for Animal Experimentation of the Universitat Rovira i Virgili (reference number 9495, 18 September 2019) and were carried out in accordance with Directive 86/609EEC of the Council of the European Union and the procedure established by the Departament d'Agricultura, Ramaderia i Pesca of the Generalitat de Catalunya.

Informed Consent Statement: Not applicable.

Data Availability Statement: The data presented in this study are available on request from the corresponding author. The data are not publicly available due to lack of platform to publish them.

Acknowledgments: The authors would like to thank Niurka Llópiz and Rosa Pastor (Tarragona) for their help and technical assistance. We thank Antoni del Pino from the Metabolomics facility of the Centre for Omic Sciences (COS) Joint Unit of the Universitat Rovira i Virgili-Eurecat for their contribution to mass spectrometry analysis. The authors would also like to thank the OPEN2022 program of the Univeristat Rovira i Virgili.

Conflicts of Interest: The authors declare no conflict of interest. The funders had no role in the design of the study; in the collection, analyses, or interpretation of data; in the writing of the manuscript, or in the decision to publish the results.

References

1. Wood, S.; Loudon, A.; Wood, S.; Loudon, A. Clocks for All Seasons: Unwinding the Roles and Mechanisms of Circadian and Interval Timers in the Hypothalamus and Pituitary. *J. Endocrinol.* **2014**, *222*, R39–R59. [CrossRef] [PubMed]
2. Lincoln, G.A.; Anderson, H.; Loudon, A. Clock Genes in Calendar Cells as the Basis of Annual Timekeeping in Mammals—A Unifying Hypothesis. *J. Endocrinol.* **2003**, *179*, 1–13. [CrossRef] [PubMed]
3. Arendt, J. Melatonin, Circadian Rhythms, and Sleep. *N. Engl. J. Med.* **2000**, *343*, 1114–1116. [CrossRef] [PubMed]
4. Dopico, X.C.; Evangelou, M.; Ferreira, R.C.; Guo, H.; Pekalski, M.L.; Smyth, D.J.; Cooper, N.; Burren, O.S.; Fulford, A.J.; Hennig, B.J.; et al. Widespread Seasonal Gene Expression Reveals Annual Differences in Human Immunity and Physiology. *Nat. Commun.* **2015**, *6*, 1–13. [CrossRef] [PubMed]
5. Fujisawa, K.; Takami, T.; Shintani, H.; Sasai, N.; Matsumoto, T.; Yamamoto, N.; Sakaida, I. Seasonal Variations in Photoperiod Affect Hepatic Metabolism of Medaka (Oryzias Latipes). *FEBS Open Bio* **2021**, *11*, 1029–1040. [CrossRef]
6. Togo, Y.; Otsuka, T.; Goto, M.; Furuse, M.; Yasuo, S. Photoperiod Regulates Dietary Preferences and Energy Metabolism in Young Developing Fischer 344 Rats but Not in Same-Age Wistar Rats. *Am. J. Physiol. Endocrinol. Metab.* **2012**, *303*, 777–786. [CrossRef] [PubMed]
7. Chainy, G.B.N.; Paital, B.; Dandapat, J. An Overview of Seasonal Changes in Oxidative Stress and Antioxidant Defence Parameters in Some Invertebrate and Vertebrate Species. *Scientifica* **2016**, *2016*, 6126570. [CrossRef]
8. Cruz-Carrión, Á.; de Azua, M.J.R.; Mulero, M.; Arola-Arnal, A.; Suárez, M. Oxidative Stress in Rats Is Modulated by Seasonal Consumption of Sweet Cherries from Different Geographical Origins: Local vs. Non-Local. *Nutrients* **2020**, *12*, 2854. [CrossRef]
9. Rauf, A.; Imran, M.; Abu-Izneid, T.; Iahtisham-Ul-Haq; Patel, S.; Pan, X.; Naz, S.; Sanches Silva, A.; Saeed, F.; Rasul Suleria, H.A. Proanthocyanidins: A Comprehensive Review. *Biomed. Pharmacother.* **2019**, *116*, 108999. [CrossRef]
10. Cos, P.; Bruyne, T.; Hermans, N.; Apers, S.; Berghe, D.; Vlietinck, A. Proanthocyanidins in Health Care: Current and New Trends. *Curr. Med. Chem.* **2012**, *11*, 1345–1359. [CrossRef]
11. Baur, J.A.; Sinclair, D.A. What Is Xenohormesis? *Am. J. Pharmacol. Toxicol.* **2008**, *3*, 149–156. [CrossRef] [PubMed]
12. Yokozawa, T.; Lee1, Y.A.; Cho, E.J.; Matsumoto, K.; Park, C.H.; Shibahara, N. Anti-Aging Effects of Oligomeric Proanthocyanidins Isolated from Persimmon Fruits. *Drug Discov.* **2011**, *5*, 109–118. [CrossRef] [PubMed]
13. Höhn, A.; Weber, D.; Jung, T.; Ott, C.; Hugo, M.; Kochlik, B.; Kehm, R.; König, J.; Grune, T.; Castro, J.P. Happily (n)Ever after: Aging in the Context of Oxidative Stress, Proteostasis Loss and Cellular Senescence. *Redox Biol.* **2017**, *11*, 482–501. [CrossRef] [PubMed]
14. Barbosa, M.C.; Grosso, R.A.; Fader, C.M. Hallmarks of Aging: An Autophagic Perspective. *Front. Endocrinol.* **2019**, *10*, 790. [CrossRef]
15. Okudan, N.; Barışkaner, H.; Gökbel, H.; Şahin, A.S.; Belviranlı, M.; Baysal, H. The Effect of Supplementation of Grape Seed Proanthocyanidin Extract on Vascular Dysfunction in Experimental Diabetes. *J. Med. Food* **2011**, *14*, 1298–1302. [CrossRef]
16. Ding, Y.; Dai, X.; Jiang, Y.; Zhang, Z.; Bao, L.; Li, Y.; Zhang, F.; Ma, X.; Cai, X.; Jing, L.; et al. Grape Seed Proanthocyanidin Extracts Alleviate Oxidative Stress and ER Stress in Skeletal Muscle of Low-Dose Streptozotocin- and High-Carbohydrate/High-Fat Diet-Induced Diabetic Rats. *Mol. Nutr. Food Res.* **2013**, *57*, 365–369. [CrossRef] [PubMed]
17. Pajuelo, D.; Quesada, H.; Díaz, S.; Fernández-Iglesias, A.; Arola-Arnal, A.; Bladé, C.; Salvadó, J.; Arola, L. Chronic Dietary Supplementation of Proanthocyanidins Corrects the Mitochondrial Dysfunction of Brown Adipose Tissue Caused by Diet-Induced Obesity in Wistar Rats. *Br. J. Nutr.* **2012**, *107*, 170–178. [CrossRef]
18. Fernández-Iglesias, A.; Pajuelo, D.; Quesada, H.; Díaz, S.; Bladé, C.; Arola, L.; Salvadó, M.J.; Mulero, M. Grape Seed Proanthocyanidin Extract Improves the Hepatic Glutathione Metabolism in Obese Zucker Rats. *Mol. Nutr. Food Res.* **2014**, *58*, 727–737. [CrossRef]
19. Li, Y.; Ding, Y.; Zhang, Z.; Dai, X.; Jiang, Y.; Bao, L.; Li, Y. Grape Seed Proanthocyanidins Ameliorate Pancreatic Beta-Cell Dysfunction and Death in Low-Dose Streptozotocin- and High-Carbohydrate/High-Fat Diet-Induced Diabetic Rats Partially by Regulating Endoplasmic Reticulum Stress. *Nutr. Metab.* **2013**, *10*, 51. [CrossRef]
20. Ibars, M.; Ardid-Ruiz, A.; Suárez, M.; Muguerza, B.; Bladé, C.; Aragonès, G. Proanthocyanidins Potentiate Hypothalamic Leptin/STAT3 Signalling and Pomc Gene Expression in Rats with Diet-Induced Obesity. *Int. J. Obes.* **2016**, *41*, 129–136. [CrossRef]

21. Serrano, J.; Casanova-Martí, À.; Gual, A.; Maria Pérez-Vendrell, A.; Teresa Blay, M.; Terra, X.; Ardévol, A.; Pinent, M. A Specific Dose of Grape Seed-Derived Proanthocyanidins to Inhibit Body Weight Gain Limits Food Intake and Increases Energy Expenditure in Rats. *Eur. J. Nutr.* **2017**, *56*, 1629–1636. [CrossRef] [PubMed]
22. Kim, K.S.; Yoon, Y.R.; Lee, H.J.; Yoon, S.; Kim, S.Y.; Shin, S.W.; An, J.J.; Kim, M.S.; Choi, S.Y.; Sun, W.; et al. Enhanced Hypothalamic Leptin Signaling in Mice Lacking Dopamine D2 Receptors. *J. Biol. Chem.* **2010**, *285*, 8905–8917. [CrossRef] [PubMed]
23. Serra, A.; MacI, A.; Romero, M.P.; Valls, J.; Bladé, C.; Arola, L.; Motilva, M.J. Bioavailability of Procyanidin Dimers and Trimers and Matrix Food Effects in in Vitro and in Vivo Models. *Br. J. Nutr.* **2010**, *103*, 944–952. [CrossRef] [PubMed]
24. Smedes, F.; Thomasen, T.K. Evaluation of the Bligh & Dyer Lipid Determination Method. *Mar. Pollut. Bull.* **1996**, *32*, 681–688. [CrossRef]
25. Cajka, T.; Fiehn, O. Toward Merging Untargeted and Targeted Methods in Mass Spectrometry-Based Metabolomics and Lipidomics. *Anal. Chem.* **2015**, *88*, 524–545. [CrossRef]
26. Visser, M.E.; Caro, S.P.; van Oers, K.; Schaper, S.V.; Helm, B. Phenology, Seasonal Timing and Circannual Rhythms: Towards a Unified Framework. *Philos. Trans. R. Soc. B Biol. Sci.* **2010**, *365*, 3113–3127. [CrossRef] [PubMed]
27. Ávila-Román, J.; Soliz-Rueda, J.R.; Bravo, F.I.; Aragonès, G.; Suárez, M.; Arola-Arnal, A.; Mulero, M.; Salvadó, M.J.; Arola, L.; Torres-Fuentes, C.; et al. Phenolic Compounds and Biological Rhythms: Who Takes the Lead? *Trends Food Sci. Technol.* **2021**, *113*, 77–85. [CrossRef]
28. Mariné-Casadó, R.; Domenech-Coca, C.; del Bas, J.M.; Bladé, C.; Arola, L.; Caimari, A. The Exposure to Different Photoperiods Strongly Modulates the Glucose and Lipid Metabolisms of Normoweight Fischer 344 Rats. *Front. Physiol.* **2018**, *9*, 416. [CrossRef]
29. Patel, S.R.; Hu, F.B. Short Sleep Duration and Weight Gain: A Systematic Review. *Obesity* **2008**, *16*, 643–653. [CrossRef]
30. Heideman, P.D.; Sylvester, C.J. Reproductive Photoresponsiveness in Unmanipulated Male Fischer 344 Laboratory Rats. *Biol. Reprod.* **1997**, *57*, 134–138. [CrossRef]
31. Tavolaro, F.M.; Thomson, L.M.; Ross, A.W.; Morgan, P.J.; Helfer, G. Photoperiodic Effects on Seasonal Physiology, Reproductive Status and Hypothalamic Gene Expression in Young Male F344 Rats. *J. Neuroendocrinol.* **2015**, *27*, 79–87. [CrossRef] [PubMed]
32. Ross, A.W.; Helfer, G.; Russell, L.; Darras, V.M.; Morgan, P.J. Thyroid Hormone Signalling Genes Are Regulated by Photoperiod in the Hypothalamus of F344 Rats. *PLoS ONE* **2011**, *6*, e21351. [CrossRef] [PubMed]
33. Sato, M.; Kanikowska, D.; Iwase, S.; Shimizu, Y.; Nishimura, N.; Inukai, Y.; Sato, M.; Sugenoya, J. Seasonal Differences in Melatonin Concentrations and Heart Rates during Sleep in Obese Subjects in Japan. *Int. J. Biometeorol.* **2013**, *57*, 743–748. [CrossRef]
34. Spady, D.K.; Woollett, L.A.; Dietschy, J.M. Regulation of Plasma LDL-Cholesterol Levels by Dietary Cholesterol and Fatty Acids. *Annu. Rev. Nutr.* **1993**, *13*, 355–381. [CrossRef] [PubMed]
35. Sun, D.-Q.; Liu, W.-Y.; Wu, S.-J.; Zhu, G.-Q.; Braddock, M.; Zhang, D.-C.; Shi, K.-Q.; Song, D.; Zheng, M.-H.; Sun, D.-Q.; et al. Increased Levels of Low-Density Lipoprotein Cholesterol within the Normal Range as a Risk Factor for Nonalcoholic Fatty Liver Disease. *Oncotarget* **2015**, *7*, 5728–5737. [CrossRef]
36. Sasaki, J.; Kumagae, G.; Sata, T.; Ikeda, M.; Tsutsumi, S.; Arakawa, K. Seasonal Variation of Serum High Density Lipoprotein Cholesterol Levels in Men. *Atherosclerosis* **1983**, *48*, 167–172. [CrossRef]
37. Fager, G.; Wiklund, O.; Olofsson, S.O.; Bondjers, G. Seasonal Variations in Serum Lipid and Apolipoprotein Levels Evaluated by Periodic Regression Analyses. *J. Chronic Dis.* **1982**, *35*, 643–648. [CrossRef]
38. Ma, Y.; Olendzki, B.C.; Li, W.; Hafner, A.R.; Chiriboga, D.; Hebert, J.R.; Campbell, M.; Sarnie, M.; Ockene, I.S. Seasonal Variation in Food Intake, Physical Activity, and Body Weight in a Predominantly Overweight Population. *Eur. J. Clin. Nutr.* **2006**, *60*, 519–528. [CrossRef]
39. Carabaza, A.; Ciudad, C.J.; Baqué, S.; Guinovart, J.J. Glucose Has to Be Phosphorylated to Activate Glycogen Synthase, but Not to Inactivate Glycogen Phosphorylase in Hepatocytes. *FEBS Lett.* **1992**, *296*, 211–214. [CrossRef]
40. Nakamura, T.; Kato, S.; Ichihara, A. Glucagon and Glucose as Major Regulators of Glycogen Metabolism in Primary Cultured Rat Hepatocytes. *J. Biochem.* **1984**, *95*, 1691–1696. [CrossRef]
41. Stalmans, W.; de Wulf, H.; Hue, L.; Hers, H.-G. The Sequential Inactivation of Glycogen Phosphorylase and Activation of Glycogen Synthetase in Liver after the Administration of Glucose to Mice and Rats. The Mechanism of the Hepatic Threshold to Glucose. *Eur. J. Biochem.* **1974**, *41*, 127–134. [CrossRef] [PubMed]
42. Gumaa, K.A.; MacLeod, R.M.; McLean, P. The Pentose Phosphate Pathway of Glucose Metabolism. Influence of a Growth-Hormone-Secreting Pituitary Tumour on the Oxidative and Non-Oxidative Reactions of the Cycle in Liver. *Biochem. J.* **1969**, *113*, 215–220. [CrossRef] [PubMed]
43. Jin, E.S.; Sherry, A.D.; Malloy, C.R. Interaction between the Pentose Phosphate Pathway and Gluconeogenesis from Glycerol in the Liver. *J. Biol. Chem.* **2014**, *289*, 32593–32603. [CrossRef] [PubMed]
44. Rockall, A.G.; Sohaib, S.A.; Evans, D.; Kaltsas, G.; Isidori, A.M.; Monson, J.P.; Besser, G.M.; Grossman, A.B.; Reznek, R.H. Hepatic Steatosis in Cushing's Syndrome: A Radiological Assessment Using Computed Tomography. *Eur. J. Endocrinol.* **2003**, *149*, 543–548. [CrossRef] [PubMed]
45. Amatruda, J.M.; Livingston, J.N.; Lockwood, D.H. Cellular Mechanisms in Selected States of Insulin Resistance: Human Obesity, Glucocorticoid Excess, and Chronic Renal Failure. *Diabetes/Metab. Rev.* **1985**, *1*, 293–317. [CrossRef]
46. Oleshchuk, O.; Ivankiv, Y.; Falfushynska, H.; Mudra, A.; Lisnychuk, N. Hepatoprotective Effect of Melatonin in Toxic Liver Injury in Rats. *Medicina* **2019**, *55*, 304. [CrossRef]

47. Bonomini, F.; Borsani, E.; Favero, G.; Rodella, L.F.; Rezzani, R. Dietary Melatonin Supplementation Could Be a Promising Preventing/Therapeutic Approach for a Variety of Liver Diseases. *Nutrients* **2018**, *10*, 1135. [CrossRef]
48. Zhang, J.-J.; Meng, X.; Li, Y.; Zhou, Y.; Xu, D.-P.; Li, S.; Li, H.-B. Molecular Sciences Effects of Melatonin on Liver Injuries and Diseases. *Int. J. Mol. Sci.* **2017**, *18*, 673. [CrossRef]
49. Ohta, Y.; Kongo, M.; Sasaki, E.; Nishida, K.; Ishiguro, I. Therapeutic Effect of Melatonin on Carbon Tetrachloride-Induced Acute Liver Injury in Rats. *J. Pineal Res.* **2000**, *28*, 119–126. [CrossRef]
50. Tahan, G.; Akin, H.; Aydogan, F.; Ramadan, S.S.; Yapicier, O.; Tarcin, O.; Uzun, H.; Tahan, V.; Zengin, K. Melatonin Ameliorates Liver Fibrosis Induced by Bile-Duct Ligation in Rats. *Can. J. Surg.* **2010**, *53*, 313.
51. Chojnacki, C.; Walecka-Kapica, E.; Romanowski, M.; Chojnacki, J.; Klupinska, G. Protective Role of Melatonin in Liver Damage. *Curr. Pharm. Des.* **2014**, *20*, 4828–4833. [CrossRef] [PubMed]
52. Ribas-Latre, A.; del Bas, J.M.; Baselga-Escudero, L.; Casanova, E.; Arola-Arnal, A.; Salvadó, M.J.; Arola, L.; Bladé, C. Dietary Proanthocyanidins Modulate Melatonin Levels in Plasma and the Expression Pattern of Clock Genes in the Hypothalamus of Rats. *Mol. Nutr. Food Res.* **2015**, *59*, 865–878. [CrossRef] [PubMed]
53. Basseri, S.; Austin, R.C. ER Stress and Lipogenesis: A Slippery Slope toward Hepatic Steatosis. *Dev. Cell* **2008**, *15*, 795–796. [CrossRef] [PubMed]
54. Colgan, S.M.; Tang, D.; Werstuck, G.H.; Austin, R.C. Endoplasmic Reticulum Stress Causes the Activation of Sterol Regulatory Element Binding Protein-2. *Int. J. Biochem. Cell Biol.* **2007**, *39*, 1843–1851. [CrossRef] [PubMed]
55. Lee, J.N.; Ye, J. Proteolytic Activation of Sterol Regulatory Element-Binding Protein Induced by Cellular Stress through Depletion of Insig-1. *J. Biol. Chem.* **2004**, *279*, 45257–45265. [CrossRef]
56. Kim, Y.R.; Lee, E.J.; Shin, K.O.; Kim, M.H.; Pewzner-Jung, Y.; Lee, Y.M.; Park, J.W.; Futerman, A.H.; Park, W.J. Hepatic Triglyceride Accumulation via Endoplasmic Reticulum Stress-Induced SREBP-1 Activation Is Regulated by Ceramide Synthases. *Exp. Mol. Med.* **2019**, *51*, 1–16. [CrossRef]
57. Kim, D.S.; Jeong, S.K.; Kim, H.R.; Kim, D.S.; Chae, S.W.; Chae, H.J. Effects of Triglyceride on ER Stress and Insulin Resistance. *Biochem. Biophys. Res. Commun.* **2007**, *363*, 140–145. [CrossRef]
58. Wei, Y.; Wang, D.; Topczewski, F.; Pagliassotti, M.J. Saturated Fatty Acids Induce Endoplasmic Reticulum Stress and Apoptosis Independently of Ceramide in Liver Cells. *Am. J. Physiol. Endocrinol. Metab.* **2006**, *291*, 275–281. [CrossRef]
59. Ding, R.-B.; Bao, J.; Deng, C.-X. Emerging Roles of SIRT1 in Fatty Liver Diseases. *Int. J. Biol. Sci* **2017**, *13*, 852–867. [CrossRef]
60. Kim, H.S.; Xiao, C.; Wang, R.H.; Lahusen, T.; Xu, X.; Vassilopoulos, A.; Vazquez-Ortiz, G.; Jeong, W.-I.; Park, O.; Ki, S.H.; et al. Hepatic Specific Disruption of SIRT6 in Mice Results in Fatty Liver Formation Due to Enhanced Glycolysis and Triglyceride Synthesis. *Cell Metab.* **2010**, *12*, 224. [CrossRef]
61. Aragonès, G.; Suárez, M.; Ardid-Ruiz, A.; Vinaixa, M.; Rodríguez, M.A.; Correig, X.; Arola, L.; Bladé, C. Dietary Proanthocyanidins Boost Hepatic NAD + Metabolism and SIRT1 Expression and Activity in a Dose-Dependent Manner in Healthy Rats. *Sci. Rep.* **2016**, *6*, 24977. [CrossRef] [PubMed]
62. Foretz, M.; Guichard, C.; Ferré, P.; Foufelle, F. Sterol Regulatory Element Binding Protein-1c Is a Major Mediator of Insulin Action on the Hepatic Expression of Glucokinase and Lipogenesis-Related Genes. *Proc. Natl. Acad. Sci. USA* **1999**, *96*, 12737–12742. [CrossRef] [PubMed]
63. Dentin, R.; Pé, J.-P.; Benhamed, F.; Foufelle, F.; Ferré, P.; Ronique Fauveau, V.; Magnuson, M.A.; Girard, J.; Postic, C. Hepatic Glucokinase Is Required for the Synergistic Action of ChREBP and SREBP-1c on Glycolytic and Lipogenic Gene Expression. *J. Biol. Chem.* **2004**, *279*, 20314–20326. [CrossRef] [PubMed]
64. Ikegami, K.; Iigo, M.; Yoshimura, T. Circadian Clock Gene Per2 Is Not Necessary for the Photoperiodic Response in Mice. *PLoS ONE* **2013**, *8*, 58482. [CrossRef]
65. Lamia, K.A.; Storch, K.-F.; Weitz, C.J. Physiological Significance of a Peripheral Tissue Circadian Clock. *Proc. Natl. Acad. Sci. USA* **2008**, *105*, 15172–15177. [CrossRef]
66. Xie, X.; Zhao, B.; Huang, L.; Shen, Q.; Ma, L.; Chen, Y.; Wu, T.; Fu, Z. Effects of Altered Photoperiod on Circadian Clock and Lipid Metabolism in Rats. *Chronobiol. Int.* **2017**, *34*, 1094–1104. [CrossRef]

Table S1. Treatment comparation between metabolites related to hepatic glucose metabolism. Metabolites of glucose metabolism in the liver of Fischer 344 rats fed a STD diet and exposed to three different photoperiods for 9 weeks, supplemented with vehicle or GSPE for the last 4 weeks. The statistically significant p-values ($p < 0.05$) are highlighted in bold.

Metabolites	L12				L18				L6			
	STD-VH	STD-GSPE	p-value	FC	STD-VH	STD-GSPE	p-value	FC	STD-VH	STD-GSPE	p-value	FC
Pyruvic acid	0.62 ± 0.05	0.55 ± 0.07	0.424	0.9	0.87 ± 0.19	0.56 ± 0.05	0.144	0.6	0.68 ± 0.09	0.62 ± 0.07	0.661	0.9
Lactic acid	20.07 ± 0.74	20.01 ± 0.89	0.957	1	20.66 ± 1.78	20.34 ± 0.7	0.871	1	21.52 ± 1.21	19.21 ± 0.86	0.141	0.9
Glycerol	0.08 ± 0.01	0.07 ± 0.01	0.407	0.8	0.07 ± 0.01	0.06 ± 0	0.218	0.8	0.08 ± 0.01	0.07 ± 0.01	0.568	0.9
Glycerol-1-phosphate	1.6 ± 0.09	1.51 ± 0.08	0.421	0.9	1.53 ± 0.09	1.62 ± 0.09	0.492	1.1	1.69 ± 0.12	1.56 ± 0.1	0.404	0.9
d-Glucose	150.4 ± 2.92	150.72 ± 2.33	0.933	1	156.07 ± 2.94	147.73 ± 1.19	**0.027**	0.9	154.73 ± 4.04	151.43 ± 2.78	0.511	1
d-Ribose	0.02 ± 0	0.01 ± 0	0.582	0.9	0.05 ± 0.02	0.01 ± 0	**0.027**	0.2	0.02 ± 0	0.01 ± 0	0.187	0.7
Ribose-5-phosphate	0.62 ± 0.05	0.55 ± 0.07	0.424	0.9	0.87 ± 0.19	0.56 ± 0.05	0.144	0.6	0.68 ± 0.09	0.62 ± 0.07	0.661	0.9
Fructose-6-phosphate	0.03 ± 0	0.02 ± 0	**0.018**	0.6	0.03 ± 0.01	0.04 ± 0.01	0.37	1.3	0.03 ± 0	0.03 ± 0	0.418	1.2
Glucose-6-phosphate	0.08 ± 0.01	0.05 ± 0.01	**0.033**	0.6	0.07 ± 0.01	0.09 ± 0.01	0.318	1.3	0.06 ± 0.01	0.08 ± 0.01	0.44	1.2

Table S2. Photoperiod comparation between metabolites related to hepatic glucose metabolism. Metabolites of glucose metabolism in the liver of Fischer 344 rats fed a STD diet and exposed to three different photoperiods for 9 weeks, supplemented with vehicle or GSPE for the last 4 weeks. The statistically significant p-values ($p < 0.05$) are highlighted in bold.

Metabolites	L12-VH vs. L18-VH		L12- VH vs. L6-VH		L18-VH vs. L6-VH		L12-GSPE vs. L18-GSPE		L12-GSPE vs. L6-GSPE		L18-GSPE vs. L6-GSPE	
	p-value	FC	p-value	FC	p-value	FC	p-value	FC	p-value	FC	p-value	FC
Pyruvic acid	0.241	1.4	0.639	1.1	0.381	0.8	0.931	1	0.472	1.1	0.47	1.1
Lactic acid	0.766	1	0.323	1.1	0.692	1	0.775	1	0.527	1	0.325	0.9
Glycerol	0.564	0.9	0.876	1	0.652	1.1	0.469	0.9	0.899	1	0.417	1.2
Glycerol-1-phosphate	0.576	1	0.549	1.1	0.298	1.1	0.356	1.1	0.664	1	0.655	1
d-Glucose	0.193	1	0.399	1	0.793	1	0.295	1	0.848	1	0.267	1
d-Ribose	**0.043**	3.1	0.308	1.4	0.102	0.4	0.159	0.7	0.947	1	0.12	1.5
Ribose-5-phosphate	0.241	1.4	0.639	1.1	0.381	0.8	0.931	1	0.472	1.1	0.47	1.1
Fructose-6-phosphate	0.411	0.8	0.266	0.8	0.87	1	**0.038**	1.7	0.055	1.5	0.661	0.9
Glucose-6-phosphate	0.432	0.8	0.269	0.8	0.791	0.9	0.043	1.7	0.095	1.5	0.506	0.9

Table S3: Summary of the main metabolic changes due to the GSPE treatment in each photoperiod compared to its respective VH control.

pathway/treatment	GSPE L12	GSPE L18	GSPE L6
GLUCONEOGENESIS	equal	equal	increased
GLUCOLISIS	equal	increased	equal
LIPOLISIS	equal	equal	equal
LIPOGENESIS	equal	decreased	equal

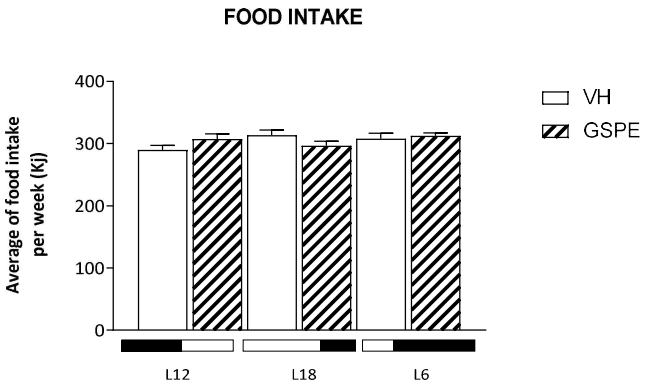

Figure S1: Average of weekly food intake (kJ) of different photoperiods

UNIVERSITAT ROVIRA I VIRGILI
THE INFLUENCE OF BIOLOGICAL RHYTHMS ON THE BENEFICIAL EFFECTS OF GRAPE SEED PROANTHOCYANIDIN EXTRACT (GSPE) ON LIVER METABOLISM IN HEALTH AND DISEASE
Romina Mariel Rodriguez

CHAPTER IV

OBJECTIVE 5

To determine the influence of seasonal variations on the beneficial effects of GSPE consumption in obesity and NAFLD.

UNIVERSITAT ROVIRA I VIRGILI
THE INFLUENCE OF BIOLOGICAL RHYTHMS ON THE BENEFICIAL EFFECTS OF GRAPE SEED PROANTHOCYANIDIN EXTRACT (GSPE) ON LIVER METABOLISM IN HEALTH AND DISEASE
Romina Mariel Rodriguez

MANUSCRIPT 4

Photoperiod modulates the metabolic beneficial effect of Grape-seed proanthocyanidin extract (GSPE) in cafeteria-fed obese rats

Romina M Rodríguez [1], Marina Colom-Pellicer [1], Julia Hernandez-Baixauli [2] Sergio Quesada-Vázquez [2], Gerard Aragonès [1] and Miquel Mulero [1*]

[1] Nutrigenomics Research Group, Department of Biochemistry and Biotechnology, Campus Sescelades, Universitat Rovira i Virgili (URV), 43007 Tarragona, Spain.

[2] Eurecat, Technology Centre of Catalunya, Nutrition and Health Unit, 43204 Reus, Spain.

* Correspondence: miquel.mulero@urv.cat; Tel.: +34 977559565

Prepared for submission to Journal of Photochemistry and Photobiology

UNIVERSITAT ROVIRA I VIRGILI
THE INFLUENCE OF BIOLOGICAL RHYTHMS ON THE BENEFICIAL EFFECTS OF GRAPE SEED PROANTHOCYANIDIN EXTRACT (GSPE) ON LIVER METABOLISM IN HEALTH AND DISEASE
Romina Mariel Rodriguez

Abstract

Biological rhythms allow the timing optimization of fundamental behavioral and biological processes to the 24-hr day-night cycle and 365-day seasonal cycle. Disruption of these rhythms due to excessive caloric intake has been shown to promote metabolic disorders. Proanthocyanidins, such as grape seed proanthocyanidin extract (GSPE), are natural compounds with beneficial effects for human health. Moreover, it has been demonstrated that GSPE is able to modulate both central and peripheral clocks, thus influencing the circadian rhythm. However, the influence of seasonal variations in day length (i.e., photoperiod) over the beneficial effects of GSPE consumption on Metabolic Syndrome (MS) and non-alcoholic fatty liver disease (NAFLD) has not yet been fully examined. Therefore, the aim of this study was to assess whether photoperiod could influence GSPE effects on hepatic circadian clock and liver metabolism of obese rats. To achieve this purpose, photoperiod-sensitive rats were fed a cafeteria (CAF) diet and chronically exposed to three different photoperiods to mimic the day length of different seasons: standard (12 h light/day, L12), long (18 h light/day, L18) or short (6 h light/day, L6), and were treated either with 25 mg/kg GSPE or vehicle (VH). Rats fed a STD diet and treated with VH were used as a normal-weight control in each photoperiod. The results demonstrate that chronic administration of GSPE in animals fed a CAF-diet triggered different responses according to the photoperiod. In L12 condition, GSPE reduced body weight gain, lowered serum levels of total cholesterol and triglycerides, increased hepatic expression of *Nampt*, *Sirt1*, *Cd36* and *Fatp5*, and restored the concentrations of serum and liver metabolites. In L18 photoperiod, treatment with GSPE tended to decrease body weight gain and to increase testosterone levels, reduced liver weight, restored the alterations in expression levels of hepatic lipogenic genes SREBP-1c and *Acacα*, and, remarkably, reversed the decrease in serum levels of critical amino acids. Whereas in L6 photoperiod, GSPE treatment showed an improvement in serum glucose and triglyceride levels and

produced changes in serum and hepatic metabolite levels that were modified by the consumption of the CAF diet. Therefore, the greatest beneficial effects of GSPE consumption against MS-associated diseases were observed in rats under the standard 12 h light-12 h dark photoperiod. Although the impact of these findings on human physiology and health deserves further research, this study evidence the influence of day length variations on the beneficial effects of GSPE consumption and highlights the importance of considering biological rhythms in the search for therapeutic strategies against metabolic diseases.

Key words: photoperiod, circannual rhythms, obesity, liver metabolism, GSPE.

1 INTRODUCTION

Evolution has conserved biological rhythms across taxa, allowing physiological and behavioral responses to cyclic environmental changes [1,2]. Thus, adaptations to the 24 h day-night cycle (circadian rhythm) and to the 365-day seasonal cycle (circannual rhythm) allows the timing optimization of fundamental cellular and physiological processes and behaviors [3,4]. In this sense, processes such as body temperature, hormone secretion, blood pressure and immune and metabolic functions show periodic oscillations and are regulated, in part, by an innate timing system, the so-called circadian clock [5]. In mammals, the circadian timing system comprises a central pacemaker located in the suprachiasmatic nucleus of the hypothalamus, which receives the photic information captured by cells in the retina via the retinohypothalamic tract, and is able to generate, adjust and sustain rhythms affecting whole-body physiology [6]. In addition to the central oscillator, there are peripheral clocks located in nearly every tissue and organ of the human body which can be regulated by the master clock but also show an independent physiological control in synchrony with the environment [7].

The circadian clock regulates the sleep-wake and feeding-fasting cycles by responding to light changes in our environment [8]. In fact, changes in

photoperiod, resembling seasonal day length variations, have been shown to alter circadian rhythmic expression and to impair lipid metabolism in rats [9]. In addition, a photoperiod-dependent response in terms of body weight gain, eating behaviors, and lipid and glucose metabolism has been demonstrated in healthy and obese photoperiod-sensitive Fischer (F344) rats [10–12].

Moreover, several studies have demonstrated that human patterns of natality, mortality and illness could be influenced by the seasons [13]. Additionally, circulating levels of triglycerides, cholesterol, glucose, and insulin were found to be elevated in winter, together with a higher accumulation of body fat than in summer, contributing to an increase in cardiometabolic diseases, especially during winter season [14–18].

Not only light but also food has been shown to entrain the molecular clock machinery, especially the clocks located in metabolic organs, such as the liver [19]. Therefore, metabolism and circadian rhythms are intimately and reciprocally linked [20,21]. There is increasing evidence showing that an excessive caloric intake causes disturbances in the circadian system and consequently a disruption of metabolic circadian synchrony, increasing the risk of developing metabolic disorders, including obesity, type 2 diabetes mellitus (T2DM), Metabolic Syndrome (MS) and Non-alcoholic fatty liver disease (NAFLD) [22–25]. Due to the increasing rise of metabolic diseases, mainly caused by modern human lifestyle with constant food availability, increased intake of the Western diet, sleep deprivation and sedentary behaviors; the discovery of new strategies to mitigate these metabolic disorders have been intensified in the last years. In this regard, polyphenols, and in particular proanthocyanidins, have emerged as promising natural plant-based compounds capable of ameliorating metabolic alterations associated with MS and related diseases. Several studies have evidenced the health benefits of its consumption protecting against cardiovascular disease, obesity, dyslipidemia, hyperglycemia, and liver damage [26]. Moreover, it has been demonstrated that grape seed proanthocyanidin

extract (GSPE) is able to modulate both central and peripheral clocks not only in healthy but also in diet-induced obesity animals [27,28], suggesting a possible mechanism involved in its beneficial effects, allowing the restoration of the circadian misalignment caused by the obesogenic diet [29]. Additionally, it has been recently reported that GSPE was able to attenuate the alterations in feeding patters, locomotor activity and serum hormones caused by an abrupt change of photoperiod in healthy and obese rats [30].

We have previously reported a seasonal modulation of the effects of GSPE on glucose and lipid metabolism in the liver of healthy rats [31]. Hence, this study aims to evaluate the influence of seasonal variations in day length (i.e., photoperiod) on the effects of GSPE consumption over the hepatic circadian clock and metabolism of obese rats. To achieve this purpose, photoperiod-sensitive rats (F344) were fed a cafeteria (CAF) diet and chronically exposed to three different photoperiods (L12, L18 and L6) to mimic the day length of different seasons and were treated either with GSPE or vehicle (VH). Rats fed a standard (STD) diet and treated with VH were used as a normal-weight control in each photoperiod. We further conducted biochemical, gene expression, serum and liver metabolomics and hepatic lipid characterization assays to assess whether changes in photoperiod exposure can influence the molecular effect of GSPE on lipid and glucose metabolism in obese rats.

2 MATERIALS AND METHODS

2.1 Animal handling

Seventy two 12-week-old male F344 rats (Charles River Laboratories, Barcelona, Spain) were housed in pairs in cages at 22 °C, 55% of humidity and subjected to three different light schedules during 9 weeks to mimic seasonal day lengths: normal day or standard photoperiod L12 (n = 24, 12 h light and 12 h darkness), long day photoperiod L18 (n = 24, 18 h and 6 h darkness) and short day photoperiod L6 (n = 24, 6 h light and 18 h

darkness). A 4-day adaptation period was carried out where rats were fed with STD diet *ad libitum.* The STD composition was 20% protein, 8% fat and 72% carbohydrates (Panlab, Barcelona, Spain). Within each photoperiod rats were randomly divided into 2 groups depending on the diet, 8 rats were fed with STD and 16 rats with CAF diet during a 5-week pre-treatment. CAF consisted of biscuits with cheese and pâté, bacon, coiled puff pastry from Mallorca (Spain), feed, carrots and sweetened milk (22% sucrose w/v). CAF composition was 14% protein, 35% fat and 76% carbohydrates. The treatment period started at 5th week, lasted four weeks and was daily orally administered at ZT0 using a syringe. Rats continued with the diet they were fed during the pre-treatment period. All STD-fed rats were treated with condensed milk, named vehicle (VH). Within each photoperiod CAF-feed rats were divided into two groups, 8 were treated with the VH, and 8 with 25 mg/kg GSPE (Les Dérivés Résiniques et Terpéniques, Dax, France) diluted 1/5 in condensed milk. GSPE was composed of catechin (58 μmol/g), dimeric procyanidins (250 μmol/g), epicatechin (52 μmol/g), epigallocatechin (5.50 μmol/g), epicatechin gallate (89 μmol/g), epigallocatechin gallate (1.40 μmol/g), hexameric procyanidins (0.38 μmol/g), pentameric procyanidins (0.73 μmol/g), tetrameric procyanidins (8.8 μmol/g) and trimeric procyanidins (1568 μmol/g) [32]. During the entire study, rats had free access to water, and body weight was weekly recorded. After 9 weeks, animals were fasted for 3 h and then sacrificed by decapitation at 9 am (one hour after light was turned on; ZT1) under anesthesia (sodium pentobarbital, 50 mg/kg per body weight). Blood was collected, and serum was obtained by centrifugation (15.000X *g*, 10 min, 4 °C) and stored at -80 °C until analysis. The liver was rapidly weighed, frozen in liquid nitrogen, and stored at -80 °C for further analysis.

The Animal Ethics Committee of the Universitat Rovira i Virgili (Tarragona, Spain) approved all procedures (reference number 9495 by Generalitat de Catalunya). All the above-mentioned experiments were performed as authorized by the European Directive 86/609/CEE and Royal Decree

223/1988 of the Spanish Ministry of Agriculture, Fisheries and Food, Madrid, Spain.

2.2 Serum Analysis

Circulating levels of glucose, total cholesterol, triglycerides (QCA, Barcelona, Spain) were analyzed by colorimetric enzymatic assay kits according to the manufacturer's instructions. Serum levels of insulin were measured using mouse/rat-specific immunometric sandwich enzyme-linked immunosorbent assay (ELISA) kit purchased from Millipore Ibérica (Madrid, Spain). Homeostasis model assessment-estimated insulin resistance (HOMA-IR) index was calculated from insulin and glucose serum levels.

2.3 Gene Expression Analysis

Total RNA from liver was extracted and quantified as previously described [33]. The cDNA was obtained by a reverse transcription of the RNA extracted using a High-Capacity Complementary DNA Reverse Transcription Kit (Thermo Fisher, Madrid, Spain). The quantitative polymerase chain reactions (qPCRs) were performed in 384-well plates in a 7900HT Fast Real-Time PCR (Thermo Fisher, Madrid, Spain) using iTaq™ Universal SYBR® Green Supermix (Bio-Rad, Barcelona, Spain). The thermal cycle used in all qPCRs was 30 seconds at 90 ºC and 40 cycles of 15 seconds at 95 ºC and 1 minute at 60 ºC. All liver genes were normalized by the housekeeping gene peptidylprolyl Isomerase A (Ppia). The primers used for each gene were obtained from Biomers (Ulm, Germany) (Supplementary Table 1). The relative expression of each gene was calculated according to the Pfaffl method (2001) [34] and normalized by the control group L12-STD-VH.

2.4 Lipid Liver Profile

Extractions of lipids from liver tissue were carried out following the Bligh & Dyer method (1959) [35] and levels of hepatic cholesterol, triglycerides and

phospholipids were measured using a colorimetric kit assay (QCA, Barcelona, Spain).

2.5 Serum Hormones Quantification

For determination of melatonin, testosterone and corticosterone levels, serum samples were thawed at 4 °C. 50 µL of serum were mixed with 250 µL of methanol containing the internal standard (2 ng/mL). Then, the mixture was vortexed and centrifuged for 5 minutes at 4 ºC and 15000 rpm. The supernatant was transferred to a new tube and mixed with 700 µL of 0,1 % formic acid in water. The sample was loaded to an SPE tube previously conditioned with methanol and 0,1 % formic acid in water. The cartridge was washed with 0,1 % formic acid in water and dried under high vacuum. The compounds were eluted with 500 µL of methanol. Samples were evaporated in a SpeedVac at 45 ºC and reconstituted with 50 µL of water:methanol (60:40, v/v) and transferred to a glass vial for analysis. Simultaneous detection and quantification of hormones levels were achieved using liquid chromatography coupled to triple quadrupole mass spectrometry (LC-QqQ).

2.6 Metabolome analysis by GC-MS in rat serum and liver samples

Metabolomic analysis of 72 rat serum and liver samples was performed at the Centre for Omic Sciences (COS, Tarragona, Spain) using gas chromatography coupled with quad-rupole time-of-flight mass spectrometry (GC-qTOF model 7200, Agilent, Santa Clara, CA, USA). For serum samples a protein precipitation extraction was performed by adding eight volumes of methanol:water (8:2) containing internal standard mixture to serum samples. For liver samples the extraction was performed by adding 400 µL of methanol:water (8:2)-containing internal standard mixture to liver samples (approx. 10—20 mg). Then, liver samples were homogenized on a bullet blender using a stainless-steel ball. Serum and liver samples were mixed and incubated at 4 °C for 10 min and centrifuged at 19,000× g, supernatant was evaporated to dryness before compound derivatization (methoximation and silylation). The derivatized compounds

were analyzed by GC-qTOF. Chromatographic separation was based on the Fiehn Method, [33] using a J&W Scientific HP5-MS film capillary column (30 m × 0.25 mm × 0.25 µm, Agilent, Santa Clara, CA, USA) and helium as carrier gas with an oven program from 60 to 325 °C. Ionization was done by electronic impact (EI), with electron energy of 70 eV and operating in full-scan mode. Identification of metabolites was performed using commercial standards and by matching their EI mass spectrum and retention time to a metabolomic Fiehn library (from Agilent, Santa Clara, CA, USA), which contains more than 1,400 metabolites. After putative identification of metabolites, they were semi-quantified in terms of internal standard response ratio.

2.7 Statistical Analysis of Serum and Liver Metabolomic Assays

The results were expressed as the mean ± SEM. Individual comparisons between metabolites were determined by the Kruskal-Wallis H-test, a non-parametric version of ANOVA, due to the variables follow the assumption of a non-parametric test. The p-value adjustment for multiple comparisons was carried out according to the Benjamin-Hochberg (BH) correction method with a false discovery rate (FDR) of 5%, and a Post-hoc Dunn. In parallel, a predictive analysis was done to evaluate the prediction power of the oxidative stress model. On the one hand, principal component analysis (PCA), an unsupervised multivariate data projection method, was performed to explore the native variance of the samples. On the other hand, partial least squares discriminant analysis (PLS-DA) was performed to determine the prediction power that supervised multivariate data projection method explores, possible relationships between the observable variables (X) and the predicted variables or target (Y) by regression extensions. The predictive performance of the test set was estimated by the Q2Y parameter calculated through cross-validation. The values of $Q2 < 0$ suggests a model with no predictive ability, $0 < Q2 < 0.5$ suggests some predictive character and $Q2 > 0.5$ indicates good predictive ability [36]. The feature importance was calculated through the variable importance in

projection (VIP), which reflects both the loading weights for each component and the variability of the response explained by the component.

2.8 General Statistical Analysis

All data are reported as mean ± standard error of the mean (SEM). Body weight gain, serum and liver biochemical profile, liver weight, and liver gene expression were subjected to Student´s *t* test, one and two-way analysis of variance (ANOVA) with the least significant difference test (LDS) for post hoc comparisons using the computer program SPSS version 25 (SPSS Inc., Chicago, IL, USA). Graphics were done by GraphPad Prism 8 software (San Diego, CA, USA). For all analyses, a probability (p) value of < 0.05 was considered statistically significant.

3 RESULTS

3.1 The effect of GSPE on body weight gain in CAF-fed rats differs according to the photoperiod

The intake of an obesogenic diet is reflected in the body weight gain of the animals subjected to CAF diet as it was significantly increased in rats exposed to L12 and L18, but not in L6-CAF-VH animals compared to their STD diet controls (Figure 1). This was corroborated with results of 2-way ANOVA that showed an interaction between diet and photoperiod ($p = 0.0019$). The chronic consumption of GSPE reduced body weight gain in L12 animals ($p = 0.020$) and tended to lower the body weight of animals exposed to long photoperiod (L18) ($p = 0.059$) compared to its respectively CAF-VH, whereas this effect was not observed in L6-CAF-GSPE rats.

3.2 The effect of GSPE on Serum Parameters is influence by photoperiod in CAF-fed rats

As is shown in Figure 2 the serum levels of glucose were significantly higher in all CAF-VH groups compared to their STD, whereas effect of GSPE treatment was only observed in L12 photoperiod with a tendency of decreasing serum glucose levels compared to L12-CAF-VH animals ($p = 0.053$). Moreover, L12-GSPE animals also showed a significant decrease of

total serum cholesterol in comparison to its CAF-VH (p = 0.001). Regarding serum triglycerides levels, a clear interaction between treatment and photoperiod was observed (p = 0.003), since triglycerides values were elevated in all CAF-VH groups but could only be lowered by GSPE treatment in animals subjected to L12 (p = 0.003) and L6 (p = 0.006) photoperiods. Insulin levels also showed an interaction between diet and photoperiod (p = 0.024) where CAF-VH increased or tended to increase its values in L12 (p = 0.023) and L6 (p = 0.054) photoperiods, but not in L18. Similar results were observed for HOMA-IR.

3.3 Photoperiod has a major impact on levels of lipids in the liver of obese rats

As is shown in Table 1, liver cholesterol values were increased due to CAF-diet intake compared to the STD lean control independently of the photoperiod but were higher in L18-CAF-VH rats compared to L12 counterparts (p = 0.024). Furthermore, a strong influence of photoperiod was also observed in triglycerides levels (p = 0.001), as they raised in all CAF-VH groups compared to STD groups, but triglycerides levels of CAF-fed animals subjected to long or short photoperiod were even higher compared to L12 CAF-fed rats. Similar results were observed on phospholipids content with a tendency of increasing values on CAF-VH groups in the L18 condition (p = 0.064) and L6 condition (p = 0.52) compared to L12 rats; and even a higher level in L6-CAF-GSPE compared to L12-CAF-GSPE group (p = 0.013). The effect of the obesogenic diet was also observed on the liver weight as all CAF-VH groups showed an increase of the weight this organ compared to their lean controls. Moreover, animals subjected to long photoperiod (L18) and treated with GSPE showed a decrease in liver weight compared to its CAF-VH group (p = 0.01).

3.4 Effects of GSPE on serum hormones of obese rats are strongly influenced by photoperiod

Serum levels of melatonin, corticosterone and testosterone were analyzed and plotted in figure 3. In this regard, melatonin levels were found to be

affected by photoperiod (p = 0.048) and diet (p = 0.046) showing an increase in L18 and L6 CAF-fed animals. Testosterone levels were also strongly influenced by photoperiod (p = 0.003), and animals treated with GSPE under long day conditions had higher testosterone levels compared to the lean control group (p = 0.001) and tended to increase compared to CAF-VH rats (p = 0.055). Similar results were observed in L12 conditions for serum corticosterone levels, where GSPE treatment increased or tended to increase corticosterone values compared to STD-VH (p = 0.001) and CAF-VH (p = 0.054) groups.

3.5 The Exposure to Long or Short Photoperiod Alters the Expression Clock-Genes in the Liver of obese rats

The hepatic mRNA expressions of clock genes were analyzed as it is well known that metabolism is regulated not only but largely by circadian rhythms [37]. As is shown in Figure 3, on the one hand, apart from the effect of GSPE consumption in increasing Nicotinamide phosphoribosyl transferase (*Nampt*) gene expression, no further changes in clock genes expressions were seen between groups exposed to L12 photoperiod. On the other hand, CAF-fed animals exposed to long or short photoperiods showed differences in the expression of some clock genes compared to their STD-VH controls. In this regard, expression of the Brain and muscle Arnt-like protein-1 (*Bmal1*) gene was higher in L18-CAF-VH (p = 0.001), but not in L18-CAF-GSPE rats compared to L18-STD-VH. In animals exposed to short photoperiod CAF diet caused a strong downregulation of the expression of this gene that could not be restored by GSPE treatment. No differences were seen in the expression of Cryptochrome circadian clock 1 (*Cry1*) gene between groups within each photoperiod, but animals exposed to L18 exhibited a two hundred percent increase in its expression compared to animals exposed to L12 and L6. Regarding expression levels of Period circadian clock 2 (*Per2*) significant differences were seen only in animals exposed to L6 with a significant rise in CAF-VH (p = 0.008) but not in CAF-GSPE compared to their STD-VH control. Expression of nuclear receptor

subfamily 1 group D member 1 gene (*Nr1d1*) was totally repressed in animals exposed to long photoperiod (L18). Under short day conditions CAF diet caused an upregulation in the expression of this gene compared to its lean STD control ($p = 0.001$), while treatment with GSPE was able to reduce these levels compared to CAF-VH ($p = 0.025$). *Bmal1* activator, the RAR-related orphan receptor alpha (*Rorα)* gene expression was downregulated in both CAF-fed animals subjected to short photoperiod (L6) compared to L6-STD-VH control.

3.6 CAF dietary intake and chronic exposure to different photoperiods influence the effect of GSPE on the expression of lipid- and glucose-related genes in the liver

The mRNA levels of key genes involved in lipid and glucose metabolism were analyzed to evaluate the impact of GSPE treatment on liver metabolism under different photoperiods (Figure 4). In this regard, GSPE showed a trend to increase mRNA levels of Sirtuin 1 (*Sirt1*) compared to CAF-VH group in animals subjected to standard photoperiod (L12) ($p = 0.061$). The transcription factor sterol regulatory element binding protein-1c (SREBP-1c) primarily regulates the expression of genes involved in de *novo* lipogenesis and triglyceride synthesis, including acetyl-CoA carboxylase (*Acacα*). The mRNA levels of SREBP-1c varied according to diet and photoperiod, since the intake of CAF diet increased it expression in L12-CAF-VH but not in L12-GSPE rats compared to its control ($p = 0.04$), whereas tended to decrease its levels in L18-CAF-VH but not in L18-CAF-GSPE animals compared to L18-STD-VH control ($p = 0.056$). Similar results were observed in L18-CAF-VH animals with a significant downregulation of *Acacα* gene expression compared to its lean control group ($p = 0.004$). Moreover, GSPE consumption was able to reverse this downregulation in the expression of *Acacα* gene in these animals that were exposed to long photoperiod compared to L18-CAF-VH ($p = 0.001$). mRNA levels of fatty acid translocase cluster of differentiation 36 (*Cd36)* and fatty acid transport protein 5 (*Fatp5*) were increased in animals treated with GSPE under L12 photoperiod compared to L12-CAF-VH rats ($p = 0.021$ and 0.030,

respectively). An effect of photoperiod on the expression of the glucokinase (*Gk*) gene was observed, since its levels were higher in L18 VHs animals compared to L12 and L6 VHs rats. Regarding glucose-6-phosphate dehydrogenase (*G6pd*) a strong downregulation caused by CAF diet was observed in the expression of this gene that GSPE was not able to revert in any of the three photoperiods. Any differential expression of peroxisome proliferator-activated receptor alpha (*PPARα*) was observed among groups within each photoperiod.

3.7 Impact of diet and photoperiod on GSPE treatment on the serum metabolome

66 metabolites were evaluated for different photoperiods to study the effect on the serum metabolome of diet (STD and CAF) and treatment (VH and GSPE). The results of the serum metabolome were obtained using GC-qTOP approaches.

Table 2 summarizes the statistical and predictive analysis of the serum metabolome for L12 groups. Regarding diet effect, 21 out of 66 metabolites were significant altered between STD-VH and CAF-VH groups after the adjustment of the statistical test. Regarding treatment effect, 4 metabolites were significantly different between CAF-VH and CAF-GSPE groups (proline, 2-hydroxyisobutyric acid, 4-hydroxyproline and 3-Phosphoglyceric acid). In the case of proline, 4-hydroxyproline and 3-Phosphoglyceric acid, GSPE counteracted the increase produced by the CAF diet to levels similar to those of the STD diet group.

Focusing on the effect of diet in the L18 condition, 24 out of 66 metabolites were significant altered between STD-VH and CAF-VH groups after the adjustment of the statistical test (Table 3). While CAF-VH and CAF-GSPE animals presented differences in 4 metabolites (leucine, isoleucine, valine and methionine). These altered amino acids suggest some effect of GSPE in the long day period.

Regarding L6 photoperiod, Table 4 summarises the statistical and predictive analysis of the serum metabolome for L6 groups. 16 out of 66 metabolites were significant altered between STD-VH and CAF-VH groups after the adjustment of the statistical test. The effect of treatment was observed between CAF-VH and CAF-GSPE animals which presented differences in 8 metabolites (d-fructose, 3-hydroxisovaleric acid, 3-hydroxytutiric acid, glycolytic acid, oxalic acid, hippuric acid, aspartic and 2-hydroxybutyric acid).

The predictive analysis, despite the low clustering in the PCA (Figure S1; S3; S5), presented differences in the PLS-DA model allowing the differentiation among groups (Figure S2; S4; S6).

3.8 Influence of diet and photoperiod on GSPE treatment on the liver metabolome

61 metabolites were evaluated for different photoperiods to study the effect on the liver metabolome of diet (STD and CAF) and treatment (VH and GSPE). The results of the liver metabolome were obtained using GC-qTOP approaches.

As is shown in Table 5, 4 metabolites were significant altered between STD-VH and CAF-VH groups after the adjustment of the statistical test. When comparing CAF-VH and CAF-GSPE, 4 metabolites presented significant differences between these two groups (d-galactitol, adenine, citric acid, and d-glucose).

Table 6 summarises the statistical and predictive analysis of the liver metabolome for L18 photoperiod. 14 out of 61 metabolites were significant altered between STD-VH and CAF-VH groups after the adjustment of the statistical test. CAF diet groups that received VH or GSPE presented differences in adenine and citric acid, which were also discriminative in L12 liver metabolome

Regarding L6, Table 7 summarises the statistical and predictive analysis of the liver metabolome. 14 out of 61 metabolites were significant altered

between STD-VH and CAF-VH groups, while CAF-VH and CAF-GSPE animals presented differences in glucose 6-phosphate, d-xylitol, and glycerol.

The predictive analysis, despite the low group clustering in the PCA (Figure S7; S9; S11), presented differences in the PLS-DA model allowing the discrimination among groups (Figure S8; S10; S12).

4 DISCUSSION

Obesity is primarily caused by the combination of an excessive caloric intake and lack of physical activity. This imbalance between caloric consumption and energy expenditure leads to ectopic fat accumulation in organs such as the liver, pancreas, skeletal muscle, and heart; causing severe metabolic disorders including MS and NAFLD. In addition, several studies suggest that changes in the photoperiod may contribute to increased risk factors of obesity and related metabolic disturbances [38,39]. In this sense these studies reveal an increase in body weight and disruption of lipid and glucose metabolism in animals exposed to long and especially short photoperiod. On the other hand, increasing evidence has demonstrated the health benefits associated with obesity of polyphenols, and particularly, GSPE consumption. However, the influence of seasonal variations in day length on the beneficial effects of GSPE consumption on MS and NAFLD has not yet been examined. In this regard, to the best of our knowledge this study demonstrates for the first time how changes in photoperiod significantly influence the molecular effects of GSPE on metabolic homeostasis, and especially on lipid and glucose metabolism in the liver of obese rats.

The beneficial GSPE effects was initially evidenced by the significant reduction in body weight gain of CAF-fed rats due to GSPE treatment only in the L12 conditions, showing a trend in L18, but no body weight reduction effect was observed in the L6 condition. In agreement with these results, rats fed CAF diet and subjected to L12 showed an improvement in the serum profile in terms of glucose, cholesterol and triglyceride parameters when

treated with GSPE. Despite the absence of any weight loss effect in the L6 photoperiod, GSPE treatment was also able to reduce the levels of triglycerides and to attenuate the increase in glucose levels due to the CAF diet. Conversely, the tendency of lowering weight with GSPE treatment at L18 was not reflected in any amelioration of the previous serum parameters. This could be likely related to the increase of testosterone levels in L18-CAF-GSPE animals as it has been shown that this hormone has a major influence on body fat composition; and its deficiency has been associated with increased central adiposity [40]. Our results are consistent with previous studies showing an improvement in serum lipid and glycemic profile due to GSPE treatment. Interestingly, these experiments were carried out under standard conditions 12 h light-12 h darkness, where a better response to GSPE treatment in these parameters was also observed [41–44].

The liver plays a key role in controlling lipid homeostasis [45]. Interestingly, our study showed that liver lipid levels of CAF-fed rats were greatly influenced by the photoperiod exposure. In this sense, exposure to long photoperiod increased levels of cholesterol, whereas triglycerides and phospholipids levels were raised in both long and short photoperiods compared to their L12 counterparts. Therefore, these findings confirm previous results showing a strong regulation of lipids levels by photoperiod, increasing its levels in animals fed an obesogenic diet and exposed to long and short photoperiod [46], which can be related to changes in energy expenditure in response to photoperiod. It was also observed that animals fed a CAF diet and exposed to L12 photoperiod showed an increased energy expenditure compared to STD counterparts, which was lost when they were switched to L18 or L6 photoperiods [30].

Although no differences in the amount of lipids between CAF-VH and CAF-GSPE were observed, chronic consumption of GSPE was able to reduce liver weight of rats exposed to L18, which could be related with the increase in

testosterone levels observed in L18-CAF-GSPE animals, as lower levels of this hormone have been associated with NAFLD [47,48].

The bidirectional crosstalk between circadian rhythms and metabolism is evident in the generation of metabolic output pathways by the clock's transcriptional network, as well as in the mutual ways in which metabolic pathways reprogram the clock [49]. In this regard, L12-GSPE animals showed increased expression of the clock-controlled gene *Nampt* which was correlated with the increase in the expression of *Sirt1* by GSPE in these animals. *Nampt* plays a pivotal role in the regulation of energy homeostasis as it encodes the rate-limiting enzyme responsible for NAD+ biosynthesis, whose intracellular levels determine the expression of *Sirt1* [50]. The NAD+-dependent deacetylase *Sirt1* is a key metabolic gene involved in the regulation of various metabolic processes such as gluconeogenesis, glycolysis, insulin sensitivity, fatty acid oxidation, and cholesterol metabolism in the liver [51]. It has been suggested that the activation of *Sirt1* by polyphenols is beneficial for regulation of metabolism [52]. In this regard, Aragonés and colleagues reported that GSPE consumption was able to modulate NAD+ levels in the liver and showed that levels of *Sirt1* were increased due to GSPE treatment [53]. Therefore, the modulation of NAD+ homeostasis by GSPE consumption enables these natural compounds to regulate many metabolic processes in the liver. Nevertheless, based on our present results such modulation appears to be influenced by photoperiod exposure as it was only observed under standard conditions (L12). Furthermore, several studies highlight *Sirt1* and NAD+ levels as promising targets for treating metabolic and cardiovascular diseases [54–56].

Furthermore, a human clinical trial in which patients were chronically administered a combined treatment of niacin, a NAD+ precursor, and clofibrate, a *PPPARα* inductor, showed improved levels of serum cholesterol and triglycerides [57]. Another study observed similar results regarding the improvement on serum lipids by niacin treatment [58]. This supports our finding as we observed lower levels of triglycerides and cholesterol in L12-

CAF-GSPE rats. In addition, it has been reported that mice with Sirt1 catalytic activity ablation that were fed a high fat diet (HFD) exhibited an increased in SREBP-1c levels and a decreased phosphorylation of AMPK in the liver promoting NAFLD [59], which is consistent with the results obtained for SREBP-1c in L12-CAF fed rats.

L12-CAF-GSPE rats also showed an increase in the expression of *Cd36* and *Fatp5*. It has been demonstrated that hepatic overexpression of *Cd36* in the liver improves glycogen homeostasis and alleviates liver steatosis induced by a HFD in mice [60]. Moreover, expression of *Fatp5* in the liver of NAFLD patients was found inversely correlated with the hallmarks of histological progression, such as ballooning and fibrosis [61]. Therefore, *Cd36* and *Fatp5* may act as hepatic "metabolic gatekeepers" protecting the liver under lipid overload and metabolic stress.

On the other hand, the exposure to short or long photoperiods in CAF-fed rats clearly altered clock genes expressions in the liver at a single time point. In this sense, L6-CAF-VH rats exhibited a downregulation of mRNA levels of *Bmal1* and its activator *Rorα*, compared to the healthy control. In addition, the CAF diet increased the expression of the clock genes *Per2* and *Nr1d1*, also known as *Rev-erbα*, while GSPE treated animals not only did not show any significant increase in *Per2* expression compared to the lean control, but also decreased the mRNA levels of *Nr1d1. Rev-erbα* has been suggested as an integrator of circadian rhythms and metabolism [62]. Indeed, it has been shown that liver-specific overexpression of *Rev-erbα* disrupts the molecular clock of the liver dampening hepatic circadian transcriptional variation to a large extent (nearly 90%) [63]. In addition, *Rev-erbα* is involved in lipid and bile acid homeostasis and mice lacking this clock gene displays dyslipidemia characterized by increased triglyceride levels [64,65]. This goes in line with our results as we observed a decrease of serum triglycerides levels in L6-GSPE treated rats.

Regarding animals subjected to long photoperiod CAF-diet upregulated *Bmal1* expression whereas this significant increment was not observed in L18-CAF-GSPE animals compared to the lean control group. It has been demonstrated that *Bmal1* is required for *de novo* synthesis of lipids in the liver through the activation of AKT [66]. Moreover, liver-specific *Bmal1* knockout ethanol-fed mice exhibit simultaneous inhibition of *de novo* lipogenesis and fatty acid oxidation pathways, leading to hepatic steatosis, which was rescued by the administration of synthetic PPARα ligands [67]. In line with these results, we observed a downregulation of the mRNA levels of lipogenic genes such as SREBP-1c and its direct target *Acacα,* which encodes for the rate-limiting enzyme in *de novo* fatty acid synthesis, in L18-CAF-VH compared to its control. While GSPE consumption is able to reverse the impaired expression in these animals subjected to long photoperiod. Furthermore, although levels of *PPARα* were not significantly increased in L18-CAF-GSPE rats, it seemed that the GSPE treatment tended to enhance its expression.

Since the last decade, 24-hour rhythms have been described in circulating and tissue metabolites levels varying in concentration in a daily-manner [68–72]. Therefore, metabolites are also expected to vary throughout the year, in a season-dependent manner [73–76]. Alterations in the rhythmic expression of serum metabolites was reported due to shift work[69], and disturbances in daily rhythms of hepatic metabolites have been observed in CAF-fed rats [77]. In this sense, we found significant alterations of several serum and hepatic metabolites in CAF-fed obese rats, which vary depending on the photoperiod, as well as the effects of GSPE on these metabolites. In L12 CAF-fed animals GSPE was able to counteract the increase on serum proline, 4-hydroxyproline and 3-Phosphoglyceric acid (3PG) caused by the obesogenic diet intake. Proline and 4-hydroxyproline (produced by hydroxylation of the amino acid proline), play a key role in whole-body homeostasis being essential for metabolism as they are involved in the synthesis and structure of proteins, arginine and glutamate

synthesis, collagen production, as well as in antioxidant reactions, wound healing, and immune responses [78]. 3PG is the acid conjugate of glycerate 3-phosphate. Glycerate is a biochemically important metabolic intermediate in glycolysis. 3PG is also involved in gluconeogenesis, glycerol, lipid metabolism, glycine, serine, and threonine metabolism, playing a key role in several metabolic pathways [79–82].

One of the most remarkable effects of GSPE was the increase in serum levels of methionine and the three essential branched-chain amino acids (BCAAs) leucine, isoleucine, and valine, which were decreased due to CAF-diet intake. Methionine is an essential amino acid involved in anabolic metabolism and the reduction of free radicals and has been found to be decreased in MS patients [83] and in obese children [84]. Moreover, disorders of BCAAs have a huge impact on metabolism, as they have been found to be associated with several metabolic diseases [85]. The largest differences in serum metabolites concentrations were observed between CAF-VH and CAF-GSPE in rats subjected to short photoperiod (L6). Among them, 2-hydroxybutyric acid, also known as alpha-hydroxybutyrate (α-HB), displayed a 1.6-fold change increase in CAF-GSPE animals compared to CAF-VH. It has been observed that α-HB could act as a potential functional metabolite reversing HFD-induced metabolic changes as for example the reduction of serum triglyceride levels, which is consistent with the results obtained in L6-CAF-GSPE and suggest that this metabolite could be involved, at least partially, in this reduction [86]. Similar results have been observed regarding the levels of 3-Hydroxybutyric acid, also named beta-hydroxybutyrate (β-HB), and of 3-hydroxyisovaleric which have been reported as biomarkers in the diagnosis of diabetic ketoacidosis, a complication of diabetes mellitus [87–89]. In addition, lower levels of β-HB have been observed in plasma of obese patients [90]. GSPE also raised levels of oxalic acid which has been suggested as a novel treatment for obesity, since it proved to be a highly active lipase inhibitor [91].

Increased fructose concentrations in blood of patients with T2DM has also been observed [92]. Remarkably, GSPE was able to reduce serum D-fructose levels in L6 CAF-fed animals, restoring them to values like those observed in the healthy control.

The liver metabolome analysis showed lower levels of hepatic citric acid, a key metabolite involved in Krebs cycle, in L12 and L18-CAF-VH rats compared to L12 and L18 animals that were chronic supplemented with GSPE, while the contrary was observed for adenine, which was higher in CAF-VH animals in L12 and L18, respectively. In this sense, changes in the total concentration of adenine in rat liver mitochondria have been associated to the inhibition of adenine nucleotide translocase and impairs the activation of ATP hydrolysis [93]. High blood glucose concentrations lead to increased intracellular levels of glucose-6-phosphate in the liver [94]. In this regard we observed reduced hepatic levels of glucose-6-phosphate in L6-CAF-GSPE, together with values of blood glucose that were not statistically different between the lean control L6-STD-VH and L6-CAF-GSPE, as it was in the case of L6-CAF-VH. In addition, GSPE chronic consumption in L6 rats increased the hepatic levels of glycerol and D-xylitol, both implicated in important metabolic pathways. In this sense, alterations on glycerol metabolism were observed due to fatty liver, which were prevented by dietary administration of glycerol [95]. Moreover, the supplementation of xylitol in the diet helps to reduce obesity and to treat lipid metabolism disorders [96]. The singular photoperiod-dependent effects of GSPE consumption in obese rats suggest that adaptations to seasonal variations in day length along with the metabolic challenges of the obesogenic diet might be driving these effects.

5 CONCLUSIONS

This study demonstrates that seasonal variations in day length (photoperiods) influence the effects of GSPE consumption on liver and whole-body metabolism in obese rats. Thus, chronic administration of GSPE in animals fed a CAF-diet triggered different responses according to the

photoperiod. CAF-fed rats exposed to standard 12 h daylight condition and treated with GSPE showed a reduction on body weight gain, lower levels of total cholesterol and triglycerides in serum, increased hepatic expression of crucial metabolic genes *Nampt*, *Sirt1*, *Cd36* and *Fatp5*, together with a restorative effect in the concentrations of serum and liver metabolites such as proline, 4-hydroxyproline and 3-Phosphoglyceric, adenine and citric acid that were altered due to CAF-diet intake. When CAF-fed rats were exposed to long -day conditions (L18), treatment with GSPE tended to decrease body weight gain and to increase testosterone levels, reduced liver weight, restored the alterations in expression levels of hepatic lipogenic genes SREBP-1c and *Acacα*, and, remarkably, reversed the decrease in serum levels of critical amino acids (methionine and BCAAs) due to the intake of the obesogenic diet. Under short-day conditions (L6) GSPE treatment in obese rats showed an improvement in serum glucose and triglyceride levels, decreased the expression of the hepatic clock gene *Nr1d1,* and produced changes in serum and hepatic metabolite levels that were modified by the consumption of the CAF diet. These distinctive photoperiod-dependent effects of GSPE consumption suggest a contribution of adaptation to seasonal variations. In conclusion, although GSPE was able to mitigate some metabolic disturbances caused by the intake of an obesogenic diet in the three different photoperiods, it appears to be more effective under standard 12 h light - 12 h darkness condition, evidencing the influence of day length variations on its metabolic effects. These findings should be further investigated considering their implications for human health and physiology.

REFERENCES

1. Cretenet, G.; le Clech, M.; Gachon, F. Circadian Clock-Coordinated 12 Hr Period Rhythmic Activation of the IRE1α Pathway Controls Lipid Metabolism in Mouse Liver. *Cell Metabolism* **2010**, *11*, 47–57, doi:10.1016/J.CMET.2009.11.002/ATTACHMENT/9214E6C7-B91F-4D88-954C-9CE8C6BA95E7/MMC1.PDF.
2. Karatsoreos, I.N.; Bhagat, S.; Bloss, E.B.; Morrison, J.H.; McEwen, B.S. Disruption of Circadian Clocks Has Ramifications for Metabolism, Brain,

and Behavior. *Proc Natl Acad Sci U S A* **2011**, *108*, 1657–1662, doi:10.1073/PNAS.1018375108/SUPPL_FILE/PNAS.201018375SI.PDF.

3. Ayyar, V.S.; Sukumaran, S. Circadian Rhythms: Influence on Physiology, Pharmacology, and Therapeutic Interventions. *Journal of Pharmacokinetics and Pharmacodynamics 2021 48:3* **2021**, *48*, 321–338, doi:10.1007/S10928-021-09751-2.

4. Kumar, V.; Mishra, I. Circannual Rhythms. *Encyclopedia of Reproduction* **2018**, 442–450, doi:10.1016/B978-0-12-801238-3.64613-5.

5. Challet, E. Circadian Clocks, Food Intake, and Metabolism. *Progress in Molecular Biology and Translational Science* **2013**, *119*, 105–135, doi:10.1016/B978-0-12-396971-2.00005-1.

6. Albrecht, U.; Eichele, G. The Mammalian Circadian Clock. *Current Opinion in Genetics & Development* **2003**, *13*, 271–277, doi:10.1016/S0959-437X(03)00055-8.

7. Brown, A.J.; Pendergast, J.S.; Yamazaki, S. Peripheral Circadian Oscillators: Interesting Mechanisms and Powerful Tools. *Ann N Y Acad Sci* **2008**, *1129*, 327–335, doi:10.1196/ANNALS.1417.005.

8. Roenneberg, T.; Kumar, C.J.; Merrow, M. The Human Circadian Clock Entrains to Sun Time. *Curr Biol* **2007**, *17*, doi:10.1016/J.CUB.2006.12.011.

9. Xie, X.; Zhao, B.; Huang, L.; Shen, Q.; Ma, L.; Chen, Y.; Wu, T.; Fu, Z. Effects of Altered Photoperiod on Circadian Clock and Lipid Metabolism in Rats. *Chronobiology International* **2017**, *34*, 1094–1104, doi:10.1080/07420528.2017.1341906.

10. Mariné-Casadó, R.; Domenech-Coca, C.; del Bas, J.M.; Bladé, C.; Arola, L.; Caimari, A. Intake of an Obesogenic Cafeteria Diet Affects Body Weight, Feeding Behavior, and Glucose and Lipid Metabolism in a Photoperiod-Dependent Manner in F344 Rats. *Frontiers in Physiology* **2018**, *9*, 1639, doi:10.3389/FPHYS.2018.01639/BIBTEX.

11. Mariné-Casadó, R.; Domenech-Coca, C.; del Bas, J.M.; Bladé, C.; Arola, L.; Caimari, A. The Exposure to Different Photoperiods Strongly Modulates the Glucose and Lipid Metabolisms of Normoweight Fischer 344 Rats. *Frontiers in Physiology* **2018**, *9*, 416, doi:10.3389/FPHYS.2018.00416/BIBTEX.

12. Tsai, L.L.; Tsai, Y.C.; Hwang, K.; Huang, Y.W.; Tzeng, J.E. Repeated Light-Dark Shifts Speed up Body Weight Gain in Male F344 Rats. *American Journal of Physiology - Endocrinology and Metabolism* **2005**, *289*, 212–217, doi:10.1152/AJPENDO.00603.2004/ASSET/IMAGES/LARGE/ZH10080521880007.JPEG.

13. Foster, R.G.; Roenneberg, T. Human Responses to the Geophysical Daily, Annual and Lunar Cycles. *Current Biology* **2008**, *18*, R784–R794, doi:10.1016/J.CUB.2008.07.003.

14. Kanikowska, D.; Sato, M.; Witowski, J. Contribution of Daily and Seasonal Biorhythms to Obesity in Humans. *International Journal of Biometeorology* **2015**, *59*, 377–384, doi:10.1007/S00484-014-0871-Z/FIGURES/2.

15. Pell, J.P.; Cobbe, S.M. Seasonal Variations in Coronary Heart Disease. *QJM: An International Journal of Medicine* **1999**, *92*, 689–696, doi:10.1093/QJMED/92.12.689.

16. Reilly, T.; Peiser, B. Seasonal Variations in Health-Related Human Physical Activity. *Sports Medicine* **2006**, *36*, 473–485, doi:10.2165/00007256-200636060-00002/FIGURES/TAB2.

17. Haus, E. Chronobiology in the Endocrine System. *Advanced Drug Delivery Reviews* **2007**, *59*, 985–1014, doi:10.1016/J.ADDR.2007.01.001.

18. Wen, W.L. Seasonal Changes in Preprandial Glucose, A1C, and Blood Pressure in Diabetic Patients. *Diabetes Care* **2007**, *30*, 2501–2502, doi:10.2337/DC07-0597.

19. Asher, G.; Sassone-Corsi, P. Time for Food: The Intimate Interplay between Nutrition, Metabolism, and the Circadian Clock. *Cell* **2015**, *161*, 84–92, doi:10.1016/J.CELL.2015.03.015.

20. Guan, D.; Lazar, M.A. Interconnections between Circadian Clocks and Metabolism. *The Journal of Clinical Investigation* **2021**, *131*, doi:10.1172/JCI148278.

21. Johnston, J.D.; Ordovás, J.M.; Scheer, F.A.; Turek, F.W. Circadian Rhythms, Metabolism, and Chrononutrition in Rodents and Humans. *Advances in Nutrition* **2016**, *7*, 399, doi:10.3945/AN.115.010777.

22. Eckel-Mahan, K.L.; Patel, V.R.; de Mateo, S.; Orozco-Solis, R.; Ceglia, N.J.; Sahar, S.; Dilag-Penilla, S.A.; Dyar, K.A.; Baldi, P.; Sassone-Corsi, P. Reprogramming of the Circadian Clock by Nutritional Challenge. *Cell* **2013**, *155*, 1464–1478, doi:10.1016/J.CELL.2013.11.034/ATTACHMENT/E7850CFC-CB5D-4BBC-800E-A44448444E38/MMC4.XLSX.

23. Hsieh, M.C.; Yang, S.C.; Tseng, H.L.; Hwang, L.L.; Chen, C.T.; Shieh, K.R. Abnormal Expressions of Circadian-Clock and Circadian Clock-Controlled Genes in the Livers and Kidneys of Long-Term, High-Fat-Diet-Treated Mice. *International Journal of Obesity 2010 34:2* **2009**, *34*, 227–239, doi:10.1038/ijo.2009.228.

24. Shetty, A.; Hsu, J.W.; Manka, P.P.; Syn, W.K. Role of the Circadian Clock in the Metabolic Syndrome and Nonalcoholic Fatty Liver Disease. *Digestive Diseases and Sciences* **2018**, *63*, 3187–3206, doi:10.1007/S10620-018-5242-X/FIGURES/2.

25. Shi, D.; Chen, J.; Wang, J.; Yao, J.; Huang, Y.; Zhang, G.; Bao, Z. Circadian Clock Genes in the Metabolism of Non-Alcoholic Fatty Liver Disease. *Frontiers in Physiology* **2019**, *10*, 423, doi:10.3389/FPHYS.2019.00423/BIBTEX.

26. Rasmussen, S.E.; Frederiksen, H.; Krogholm, K.S.; Poulsen, L. Dietary Proanthocyanidins: Occurrence, Dietary Intake, Bioavailability, and Protection against Cardiovascular Disease. *Molecular Nutrition & Food Research* **2005**, *49*, 159–174, doi:10.1002/MNFR.200400082.

27. Ribas-Latre, A.; Baselga-Escudero, L.; Casanova, E.; Arola-Arnal, A.; Salvadó, M.J.; Arola, L.; Bladé, C. Chronic Consumption of Dietary Proanthocyanidins Modulates Peripheral Clocks in Healthy and Obese Rats. *The Journal of*

Nutritional Biochemistry **2015**, *26*, 112–119, doi:10.1016/J.JNUTBIO.2014.09.006.

28. Ribas-Latre, A.; del Bas, J.M.; Baselga-Escudero, L.; Casanova, E.; Arola-Arnal, A.; Salvadó, M.J.; Arola, L.; Bladé, C. Dietary Proanthocyanidins Modulate Melatonin Levels in Plasma and the Expression Pattern of Clock Genes in the Hypothalamus of Rats. *Molecular Nutrition & Food Research* **2015**, *59*, 865–878, doi:10.1002/MNFR.201400571.

29. Ávila-Román, J.; Soliz-Rueda, J.R.; Bravo, F.I.; Aragonès, G.; Suárez, M.; Arola-Arnal, A.; Mulero, M.; Salvadó, M.J.; Arola, L.; Torres-Fuentes, C.; et al. Phenolic Compounds and Biological Rhythms: Who Takes the Lead? *Trends in Food Science & Technology* **2021**, *113*, 77–85, doi:10.1016/J.TIFS.2021.04.050.

30. Soliz-Rueda, J.R.; López-Fernández-Sobrino, R.; Bravo, F.I.; Aragonès, G.; Suarez, M.; Muguerza, B. Grape Seed Proanthocyanidins Mitigate the Disturbances Caused by an Abrupt Photoperiod Change in Healthy and Obese Rats. *Nutrients 2022, Vol. 14, Page 1834* **2022**, *14*, 1834, doi:10.3390/NU14091834.

31. Walton, J.C.; Rodríguez, R.M.; Colom-Pellicer, M.; Blanco, J.; Calvo, E.; Aragonès, G.; Mulero, M. Grape-Seed Procyanidin Extract (GSPE) Seasonal-Dependent Modulation of Glucose and Lipid Metabolism in the Liver of Healthy F344 Rats. *Biomolecules 2022, Vol. 12, Page 839* **2022**, *12*, 839, doi:10.3390/BIOM12060839.

32. Serra, A.; MacI, A.; Romero, M.P.; Valls, J.; Bladé, C.; Arola, L.; Motilva, M.J. Bioavailability of Procyanidin Dimers and Trimers and Matrix Food Effects in in Vitro and in Vivo Models. *British Journal of Nutrition* **2010**, *103*, 944–952, doi:10.1017/S0007114509992741.

33. Rodríguez, R.M.; Cortés-Espinar, A.J.; Soliz-Rueda, J.R.; Feillet-Coudray, C.; Casas, F.; Colom-Pellicer, M.; Aragonès, G.; Avila-Román, J.; Muguerza, B.; Mulero, M.; et al. Time-of-Day Circadian Modulation of Grape-Seed Procyanidin Extract (GSPE) in Hepatic Mitochondrial Dynamics in Cafeteria-Diet-Induced Obese Rats. *Nutrients 2022, Vol. 14, Page 774* **2022**, *14*, 774, doi:10.3390/NU14040774.

34. Pfaffl, M.W. A New Mathematical Model for Relative Quantification in Real-Time RT–PCR. *Nucleic Acids Research* **2001**, *29*, e45–e45, doi:10.1093/NAR/29.9.E45.

35. Smedes, F.; Thomasen, T.K. Evaluation of the Bligh & Dyer Lipid Determination Method. *Marine Pollution Bulletin* **1996**, *32*, 681–688, doi:10.1016/0025-326X(96)00079-3.

36. Llorach-Asunción, R.; Jauregui, O.; Urpi-Sarda, M.; Andres-Lacueva, C. Methodological Aspects for Metabolome Visualization and Characterization: A Metabolomic Evaluation of the 24 h Evolution of Human Urine after Cocoa Powder Consumption. *Journal of Pharmaceutical and Biomedical Analysis* **2010**, *51*, 373–381, doi:10.1016/J.JPBA.2009.06.033.

37. Sahar, S.; Sassone-Corsi, P. Regulation of Metabolism: The Circadian Clock Dictates the Time. *Trends in Endocrinology and Metabolism* **2012**, *23*, 1, doi:10.1016/J.TEM.2011.10.005.

38. Xie, X.; Zhao, B.; Huang, L.; Shen, Q.; Ma, L.; Chen, Y.; Wu, T.; Fu, Z. Effects of Altered Photoperiod on Circadian Clock and Lipid Metabolism in Rats. *http://dx.doi.org/10.1080/07420528.2017.1341906* **2017**, *34*, 1094–1104, doi:10.1080/07420528.2017.1341906.

39. Gibert-Ramos, A.; Crescenti, A.; Salvadó, M.J. Consumption of Cherry out of Season Changes White Adipose Tissue Gene Expression and Morphology to a Phenotype Prone to Fat Accumulation., doi:10.3390/nu10081102.

40. Kelly, D.M.; Jones, T.H. Testosterone: A Metabolic Hormone in Health and Disease. *Journal of Endocrinology* **2013**, *217*, R25–R45, doi:10.1530/JOE-12-0455.

41. Serrano, J.; Casanova-Martí, À.; Gual, A.; Maria Pérez-Vendrell, A.; Teresa Blay, M.; Terra, X.; Ardévol, A.; Pinent, M. A Specific Dose of Grape Seed-Derived Proanthocyanidins to Inhibit Body Weight Gain Limits Food Intake and Increases Energy Expenditure in Rats. *Eur J Nutr* **2017**, *56*, 1629–1636, doi:10.1007/s00394-016-1209-x.

42. Pascual-Serrano, A.; Arola-Arnal, A.; Suárez-García, S.; Bravo, F.I.; Suárez, M.; Arola, L.; Bladé, C. Grape Seed Proanthocyanidin Supplementation Reduces Adipocyte Size and Increases Adipocyte Number in Obese Rats. *International Journal of Obesity 2017 41:8* **2017**, *41*, 1246–1255, doi:10.1038/ijo.2017.90.

43. Pascual-Serrano, A.; Bladé, C.; Suárez, M.; Arola-Arnal, A. Grape Seed Proanthocyanidins Improve White Adipose Tissue Expansion during Diet-Induced Obesity Development in Rats. *International Journal of Molecular Sciences 2018, Vol. 19, Page 2632* **2018**, *19*, 2632, doi:10.3390/IJMS19092632.

44. Pons, Z.; Margalef, M.; Bravo, F.I.; Arola-Arnal, A.; Muguerza, B. Chronic Administration of Grape-Seed Polyphenols Attenuates the Development of Hypertension and Improves Other Cardiometabolic Risk Factors Associated with the Metabolic Syndrome in Cafeteria Diet-Fed Rats. *British Journal of Nutrition* **2017**, *117*, 200–208, doi:10.1017/S0007114516004426.

45. Postic, C.; Dentin, R.; Girard, J. Role of the Liver in the Control of Carbohydrate and Lipid Homeostasis. *Diabetes & Metabolism* **2004**, *30*, 398–408, doi:10.1016/S1262-3636(07)70133-7.

46. Ross, A.W.; Russell, L.; Helfer, G.; Thomson, L.M.; Dalby, M.J.; Morgan, P.J. Photoperiod Regulates Lean Mass Accretion, but Not Adiposity, in Growing F344 Rats Fed a High Fat Diet. **2015**, doi:10.1371/journal.pone.0119763.

47. Mody, A.; Whitec, D.; Kanwal, F.; Garcia, J.M. Relevance of Low Testosterone to Non-Alcoholic Fatty Liver Disease. *Cardiovasc Endocrinol* **2015**, *4*, 83–89, doi:10.1097/XCE.0000000000000057.

48. Kim, S.; Kwon, H.; Park, J.H.; Cho, B.; Kim, D.; Oh, S.W.; Lee, C.M.; Choi, H.C. A Low Level of Serum Total Testosterone Is Independently Associated with Nonalcoholic Fatty Liver Disease. *BMC Gastroenterology* **2012**, *12*, 1–8, doi:10.1186/1471-230X-12-69/TABLES/2.

49. Kim, Y.H.; Lazar, M.A. Transcriptional Control of Circadian Rhythms and Metabolism: A Matter of Time and Space. *Endocrine Reviews* **2020**, *41*, 707–732, doi:10.1210/ENDREV/BNAA014.

50. Yamaguchi, S.; Franczyk, M.P.; Chondronikola, M.; Qi, N.; Gunawardana, S.C.; Stromsdorfer, K.L.; Porter, L.C.; Wozniak, D.F.; Sasaki, Y.; Rensing, N.; et al. Adipose Tissue NAD+ Biosynthesis Is Required for Regulating Adaptive Thermogenesis and Whole-Body Energy Homeostasis in Mice. *Proc Natl Acad Sci U S A* **2019**, *116*, 23822–23828, doi:10.1073/PNAS.1909917116.

51. Li, X. SIRT1 and Energy Metabolism. *Acta Biochimica et Biophysica Sinica* **2013**, *45*, 51, doi:10.1093/ABBS/GMS108.

52. Chung, S.; Yao, H.; Caito, S.; Hwang, J. woong; Arunachalam, G.; Rahman, I. Regulation of SIRT1 in Cellular Functions: Role of Polyphenols. *Arch Biochem Biophys* **2010**, *501*, 79, doi:10.1016/J.ABB.2010.05.003.

53. Aragonès, G.; Suárez, M.; Ardid-Ruiz, A.; Vinaixa, M.; Rodríguez, M.A.; Correig, X.; Arola, L.; Bladé, C. Dietary Proanthocyanidins Boost Hepatic NAD + Metabolism and SIRT1 Expression and Activity in a Dose-Dependent Manner in Healthy Rats. *Nature Publishing Group* **2016**, doi:10.1038/srep24977.

54. Kane, A.E.; Sinclair, D.A. Sirtuins and NAD+ in the Development and Treatment of Metabolic and Cardiovascular Diseases. *Circulation Research* **2018**, *123*, 868–885, doi:10.1161/CIRCRESAHA.118.312498.

55. Cantó, C.; Auwerx, J. Targeting SIRT1 to Improve Metabolism: All You Need Is NAD + ?, doi:10.1124/pr.110.003905.

56. Buonvicino, D.; Ranieri, G.; Pittelli, M.; Lapucci, A.; Bragliola, S.; Chiarugi, A. SIRT1-Dependent Restoration of NAD+ Homeostasis after Increased Extracellular NAD+ Exposure. *Journal of Biological Chemistry* **2021**, *297*, 100855–100856, doi:10.1016/J.JBC.2021.100855/ATTACHMENT/476CDF80-38B9-4979-8546-2972EC1FDC37/MMC1.DOCX.

57. Carlson, L.A.; ROSENHAMER, G. Reduction of Mortality in the Stockholm Ischaemic Heart Disease Secondary Prevention Study by Combined Treatment with Clofibrate and Nicotinic Acid. *Acta Medica Scandinavica* **1988**, *223*, 405–418, doi:10.1111/J.0954-6820.1988.TB15891.X.

58. Taylor, A.J.; Sullenberger, L.E.; Lee, H.J.; Lee, J.K.; Grace, K.A. Arterial Biology for the Investigation of the Treatment Effects of Reducing Cholesterol (ARBITER) 2: A Double-Blind, Placebo-Controlled Study of Extended-Release Niacin on Atherosclerosis Progression in Secondary Prevention Patients Treated with Statins. *Circulation* **2004**, *110*, 3512–3517, doi:10.1161/01.CIR.0000148955.19792.8D.

59. Cheng, J.; Liu, C.; Hu, K.; Greenberg, A.; Wu, D.; Ausman, L.M.; McBurney, M.W.; Wang, X.D. Ablation of Systemic SIRT1 Activity Promotes Nonalcoholic Fatty Liver Disease by Affecting Liver-Mesenteric Adipose Tissue Fatty Acid Mobilization. *Biochimica et Biophysica Acta (BBA) - Molecular Basis of Disease* **2017**, *1863*, 2783–2790, doi:10.1016/J.BBADIS.2017.08.004.

60. Garbacz, W.G.; Lu, P.; Miller, T.M.; Poloyac, S.M.; Eyre, N.S.; Mayrhofer, G.; Xu, M.; Ren, S.; Xie, W. Hepatic Overexpression of CD36 Improves Glycogen Homeostasis and Attenuates High-Fat Diet-Induced Hepatic Steatosis and Insulin Resistance. *Molecular and Cellular Biology* **2016**, *36*, 2715–2727, doi:10.1128/MCB.00138-16/ASSET/881F280B-A2F4-4C5C-8996-A74C0CB54D83/ASSETS/GRAPHIC/ZMB9991013350007.JPEG.

61. Enooku, K.; Tsutsumi, T.; Kondo, M.; Fujiwara, N.; Sasako, T.; Shibahara, J.; Kado, A.; Okushin, K.; Fujinaga, H.; Nakagomi, R.; et al. Hepatic FATP5 Expression Is Associated with Histological Progression and Loss of Hepatic Fat in NAFLD Patients. *Journal of Gastroenterology* **2020**, *55*, 227–243, doi:10.1007/S00535-019-01633-2/TABLES/5.

62. Duez, H.; Staels, B. Rev-Erb-α: An Integrator of Circadian Rhythms and Metabolism. *Journal of Applied Physiology* **2009**, *107*, 1972–1980, doi:10.1152/JAPPLPHYSIOL.00570.2009/ASSET/IMAGES/LARGE/ZDG01 20987720003.JPEG.

63. Kornmann, B.; Schaad, O.; Bujard, H.; Takahashi, J.S.; Schibler, U. System-Driven and Oscillator-Dependent Circadian Transcription in Mice with a Conditionally Active Liver Clock. *PLOS Biology* **2007**, *5*, e34, doi:10.1371/JOURNAL.PBIO.0050034.

64. Duez, H.; van der Veen, J.N.; Duhem, C.; Pourcet, B.; Touvier, T.; Fontaine, C.; Derudas, B.; Baugé, E.; Havinga, R.; Bloks, V.W.; et al. Regulation of Bile Acid Synthesis by the Nuclear Receptor Rev-Erbα. *Gastroenterology* **2008**, *135*, 689-698.e5, doi:10.1053/J.GASTRO.2008.05.035.

65. Raspé, E.; Duez, H.; Mansén, A.; Fontaine, C.; Fiévet, C.; Fruchart, J.C.; Vennström, B.; Staels, B. Identification of Rev-Erbα as a Physiological Repressor of ApoC-III Gene Transcription. *Journal of Lipid Research* **2002**, *43*, 2172–2179, doi:10.1194/JLR.M200386-JLR200.

66. Zhang, D.; Tong, X.; Arthurs, B.; Guha, A.; Rui, L.; Kamath, A.; Inoki, K.; Yin, L. Liver Clock Protein BMAL1 Promotes de Novo Lipogenesis through Insulin-MTORC2-AKT Signaling. *Journal of Biological Chemistry* **2014**, *289*, 25925–25935, doi:10.1074/JBC.M114.567628.

67. Zhang, D.; Tong, X.; Nelson, B.B.; Jin, E.; Sit, J.; Charney, N.; Yang, M.; Omary, M.B.; Yin, L. The Hepatic BMAL1/AKT/Lipogenesis Axis Protects against Alcoholic Liver Disease in Mice via Promoting PPARα Pathway. *Hepatology* **2018**, *68*, 883–896, doi:10.1002/HEP.29878/SUPPINFO.

68. Isherwood, C.M.; van der Veen, D.R.; Johnston, J.D.; Skene, D.J. Twenty-Four-Hour Rhythmicity of Circulating Metabolites: Effect of Body Mass and Type 2 Diabetes. *The FASEB Journal* **2017**, *31*, 5557–5567, doi:10.1096/FJ.201700323R.

69. Skene, D.J.; Skornyakov, E.; Chowdhury, N.R.; Gajula, R.P.; Middleton, B.; Satterfield, B.C.; Porter, K.I.; van Dongen, H.P.A.; Gaddameedhi, S. Separation of Circadian- and Behavior-Driven Metabolite Rhythms in Humans Provides a Window on Peripheral Oscillators and Metabolism. *Proc Natl Acad Sci U S A* **2018**, *115*, 7825–7830, doi:10.1073/PNAS.1801183115/-/DCSUPPLEMENTAL.

70. Dallmann, R.; Viola, A.U.; Tarokh, L.; Cajochen, C.; Brown, S.A. The Human Circadian Metabolome. *Proc Natl Acad Sci U S A* **2012**, *109*, 2625–2629, doi:10.1073/PNAS.1114410109/SUPPL_FILE/ST05.DOCX.

71. Eckel-Mahan, K.L.; Patel, V.R.; Mohney, R.P.; Vignola, K.S.; Baldi, P.; Sassone-Corsi, P. Coordination of the Transcriptome and Metabolome by the Circadian Clock. *Proc Natl Acad Sci U S A* **2012**, *109*, 5541–5546, doi:10.1073/PNAS.1118726109/SUPPL_FILE/SD04.XLSX.

72. Colom-Pellicer, M.; Rodríguez, R.M.; Soliz-Rueda, J.R.; Vinícius, L.; de Assis, M.; Navarro-Masip, È.; Quesada-Vázquez, S.; Escoté, X.; Oster, H.; Mulero, M.; et al. Proanthocyanidins Restore the Metabolic Diurnal Rhythm of Subcutaneous White Adipose Tissue According to Time-Of-Day Consumption. *Nutrients 2022, Vol. 14, Page 2246* **2022**, *14*, 2246, doi:10.3390/NU14112246.

73. Losonczy, M.F.; Mohs, R.C.; Davis, K.L. Seasonal Variations of Human Lumbar CSF Neurotransmitter Metabolite Concentrations. *Psychiatry Research* **1984**, *12*, 79–87, doi:10.1016/0165-1781(84)90140-9.

74. Nicolai, A.; Filser, J.; Lenz, R.; Bertrand, C.; Charrier, M. Adjustment of Metabolite Composition in the Haemolymph to Seasonal Variations in the Land Snail Helix Pomatia. *Journal of Comparative Physiology B: Biochemical, Systemic, and Environmental Physiology* **2011**, *181*, 457–466, doi:10.1007/S00360-010-0539-X/FIGURES/3.

75. Vesala, L.; Salminen, T.S.; Kostál, V.; Zahradníčková, H.; Hoikkala, A. Myo-Inositol as a Main Metabolite in Overwintering Flies: Seasonal Metabolomic Profiles and Cold Stress Tolerance in a Northern Drosophilid Fly. *Journal of Experimental Biology* **2012**, *215*, 2891–2897, doi:10.1242/JEB.069948.

76. do Nascimento, T.G.; dos Santos Arruda, R.E.; da Cruz Almeida, E.T.; dos Santos Oliveira, J.M.; Basílio-Júnior, I.D.; Celerino de Moraes Porto, I.C.; Rodrigues Sabino, A.; Tonholo, J.; Gray, A.; Ebel, R.A.E.; et al. Comprehensive Multivariate Correlations between Climatic Effect, Metabolite-Profile, Antioxidant Capacity and Antibacterial Activity of Brazilian Red Propolis Metabolites during Seasonal Study. *Scientific Reports 2019 9:1* **2019**, *9*, 1–16, doi:10.1038/s41598-019-54591-3.

77. Palacios-Jordan, H.; Martín-González, M.Z.; Suárez, M.; Aragonès, G.; Mugureza, B.; Rodríguez, M.A.; Bladé, C. The Disruption of Liver Metabolic Circadian Rhythms by a Cafeteria Diet Is Sex-Dependent in Fischer 344 Rats. *Nutrients 2020, Vol. 12, Page 1085* **2020**, *12*, 1085, doi:10.3390/NU12041085.

78. Wu, G.; Bazer, F.W.; Burghardt, R.C.; Johnson, G.A.; Kim, S.W.; Knabe, D.A.; Li, P.; Li, X.; McKnight, J.R.; Satterfield, M.C.; et al. Proline and Hydroxyproline Metabolism: Implications for Animal and Human Nutrition. *Amino Acids* **2011**, *40*, 1053, doi:10.1007/S00726-010-0715-Z.

79. Arutyunov, D.Y.; Muronetz, V.I. The Activation of Glycolysis Performed by the Nonphosphorylating Glyceraldehyde-3-Phosphate Dehydrogenase in the Model System q.

80. Toews, C.J.; Lowy, C.; Ruderman, N.B. The Regulation of Gluconeogenesis: THE EFFECT OF PENT-4-ENOIC ACID ON GLUCONEOGENESIS AND ON

THE GLUCONEOGENIC METABOLITE CONCENTRATIONS OF ISOLATED PERFUSED RAT LIVER. *Journal of Biological Chemistry* **1970**, *245*, 818–824, doi:10.1016/S0021-9258(18)63338-1.

81. Ray, P.D.; Hanson, R.L.; Lardy, H.A. Inhibition by Hydrazine of Gluconeogenesis in the Rat. *THE JOURNAL cm BIOLOGICAL CHEMISTRY* **1970**, *245*, 690, doi:10.1016/S0021-9258(18)63317-4.

82. Harkness, D.R.; Ponce, J.; Grayson, V. A Comparative Study on the Phosphoglyceric Acid Cycle in Mammalian Erythrocytes. *Comparative Biochemistry and Physiology* **1969**, *28*, 129–138, doi:10.1016/0010-406X(69)91327-9.

83. Reddy, P.; Leong, J.; Jialal, I. Amino Acid Levels in Nascent Metabolic Syndrome: A Contributor to the pro-Inflammatory Burden. *Journal of Diabetes and its Complications* **2018**, *32*, 465–469, doi:10.1016/J.JDIACOMP.2018.02.005.

84. Wahl, S.; Yu, Z.; Kleber, M.; Singmann, P.; Holzapfel, C.; He, Y.; Mittelstrass, K.; Polonikov, A.; Prehn, C.; Römisch-Margl, W.; et al. Childhood Obesity Is Associated with Changes in the Serum Metabolite Profile. *Obesity Facts* **2012**, *5*, 660–670, doi:10.1159/000343204.

85. Holeček, M. Branched-Chain Amino Acids in Health and Disease: Metabolism, Alterations in Blood Plasma, and as Supplements. *Nutrition and Metabolism* **2018**, *15*, 1–12, doi:10.1186/S12986-018-0271-1/FIGURES/5.

86. Li, B.; Hong, Y.; Gu, Y.; Ye, S.; Hu, K.; Yao, J.; Ding, K.; Zhao, A.; Jia, W.; Li, H. Functional Metabolomics Reveals That Astragalus Polysaccharides Improve Lipids Metabolism through Microbial Metabolite 2-Hydroxybutyric Acid in Obese Mice. *Engineering* **2022**, *9*, 111–122, doi:10.1016/J.ENG.2020.05.023.

87. Stojanovic, V.; Ihle, S. Role of Beta-Hydroxybutyric Acid in Diabetic Ketoacidosis: A Review. *The Canadian Veterinary Journal* **2011**, *52*, 426.

88. Sheikh-Ali, M.; Karon, B.S.; Basu, A.; Kudva, Y.C.; Muller, L.A.; Xu, J.; Schwenk, W.F.; Miles, J.M. Can Serum Beta-Hydroxybutyrate Be Used to Diagnose Diabetic Ketoacidosis? *Diabetes Care* **2008**, *31*, 643–647, doi:10.2337/DC07-1683.

89. Landaas, S. Accumulation of 3-Hydroxyisobutyric Acid, 2-Methyl-3-Hydroxybutyric Acid and 3-Hydroxyisovaleric Acid in Ketoacidosis. *Clinica Chimica Acta* **1975**, *64*, 143–154, doi:10.1016/0009-8981(75)90196-5.

90. Vice, E.; Privette, J.D.; Hickner, R.C.; Barakat, H.A. Ketone Body Metabolism in Lean and Obese Women. *Metabolism - Clinical and Experimental* **2005**, *54*, 1542–1545, doi:10.1016/J.METABOL.2005.05.023.

91. Liu, T.T.; He, X.R.; Xu, R.X.; Wu, X.B.; Qi, Y.X.; Huang, J.Z.; Chen, Q.H.; Chen, Q.X. Inhibitory Mechanism and Molecular Analysis of Furoic Acid and Oxalic Acid on Lipase. *International Journal of Biological Macromolecules* **2018**, *120*, 1925–1934, doi:10.1016/J.IJBIOMAC.2018.09.150.

92. Kawasaki, T.; Akanuma, H.; Yamanouchi, T. Increased Fructose Concentrations in Blood and Urine in Patients with Diabetes. *Diabetes Care* **2002**, *25*, 353–357, doi:10.2337/DIACARE.25.2.353.

93. Cardoso, C.M.P.; Moreno, A.J.M.; Almeida, L.M.; Custódio, J.B.A. Comparison of the Changes in Adenine Nucleotides of Rat Liver Mitochondria Induced by Tamoxifen and 4-Hydroxytamoxifen. *Toxicology in Vitro* **2003**, *17*, 663–670, doi:10.1016/S0887-2333(03)00106-1.

94. Viijlar-Palasí, C.; Guinovart, J.J. The Role of Glucose 6-Phosphate in the Control of Glycogen Synthase. *The FASEB Journal* **1997**, *11*, 544–558, doi:10.1096/FASEBJ.11.7.9212078.

95. Rao, G.A.; Riley, D.E.; Larkin, E.C. Fatty Liver Caused by Chronic Alcohol Ingestion Is Prevented by Dietary Supplementation with Pyruvate or Glycerol. *Lipids* **1984**, *19*, 583–588, doi:10.1007/BF02534715.

96. Ur-Rehman, S.; Mushtaq, Z.; Zahoor, T.; Jamil, A.; Murtaza, M.A. Xylitol: A Review on Bioproduction, Application, Health Benefits, and Related Safety Issues. *https://doi.org/10.1080/10408398.2012.702288* **2015**, *55*, 1514–1528, doi:10.1080/10408398.2012.702288.

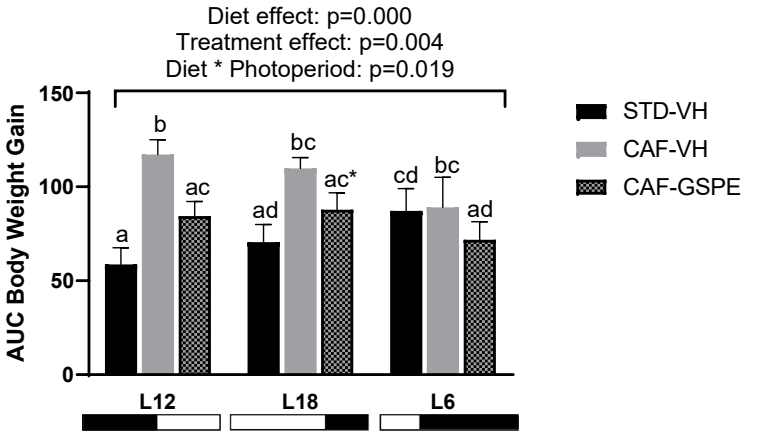

Figure 1. Body weight gain as area under the curve (AUC) in Fischer 344 STD and CAF-fed rats exposed to standard (12 h light:12 h dark), long (18 h light:6 h dark) or short (6 h light:18 h dark) photoperiods (n=8). The results are presented as the mean ± S.E.M. One- and two-way ANOVA following by LSD post hoc tests were performed to compare the values between groups and significant differences ($p \leq 0.05$) were represented with different letters (a, b, c, d). * Indicates tendency between L18-CAF-VH and L18-CAF-GSPE groups ($p = 0.059$).

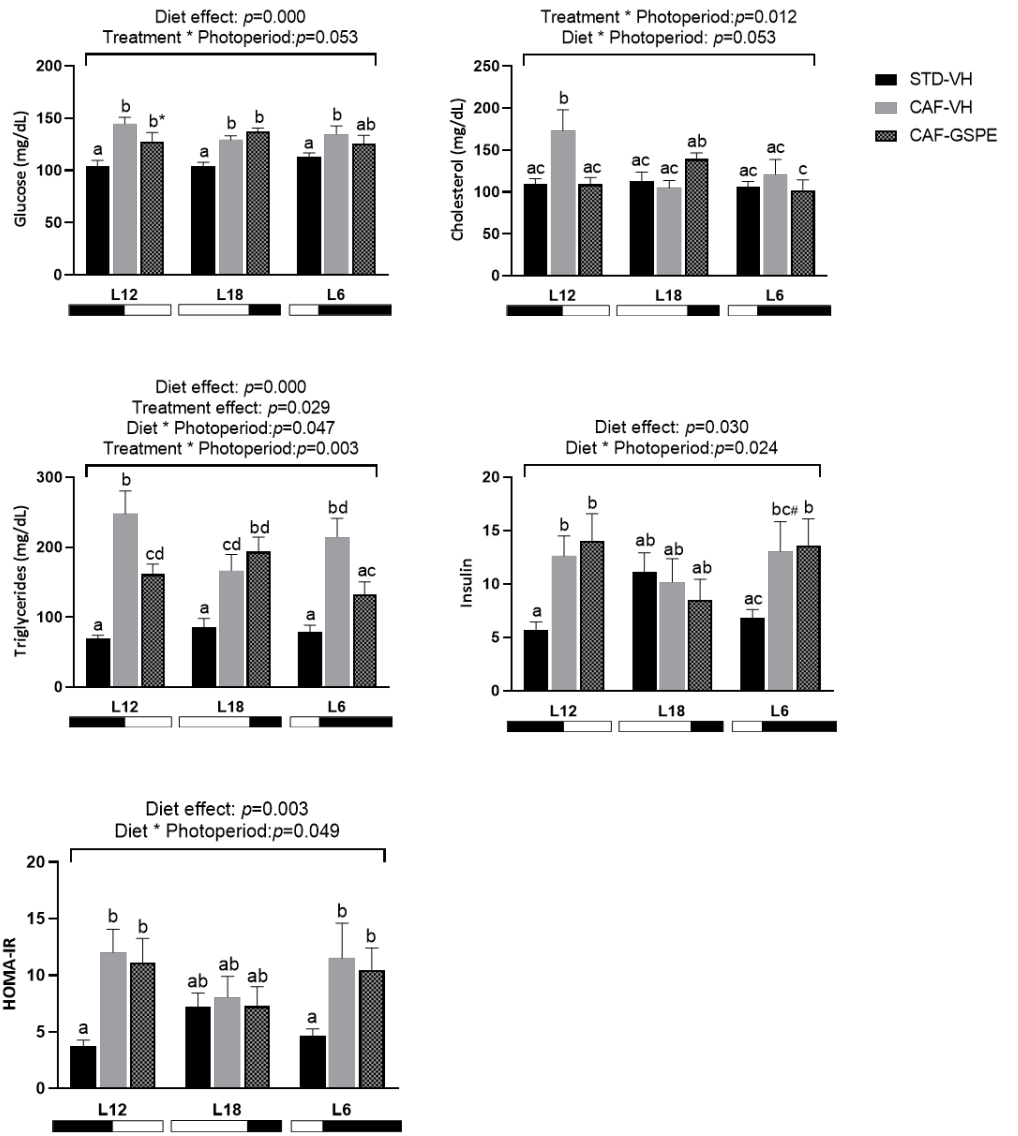

Figure 2. Serum parameters of Fischer 344 STD and CAF-fed rats exposed to L12, L18 or L6 photoperiods (n=8). The results are presented as the mean ± S.E.M. One- and two-way ANOVA following by LSD post hoc tests were performed to compare the values between groups and significant differences ($p \leq 0.05$) were represented with different letters (a, b, c, d). *Indicates tendency between L12-CAF-VH and L12-CAF-GSPE groups ($p = 0.053$). #Indicates tendency between L6-STD-VH and L6-CAF-VH groups ($p = 0.054$).

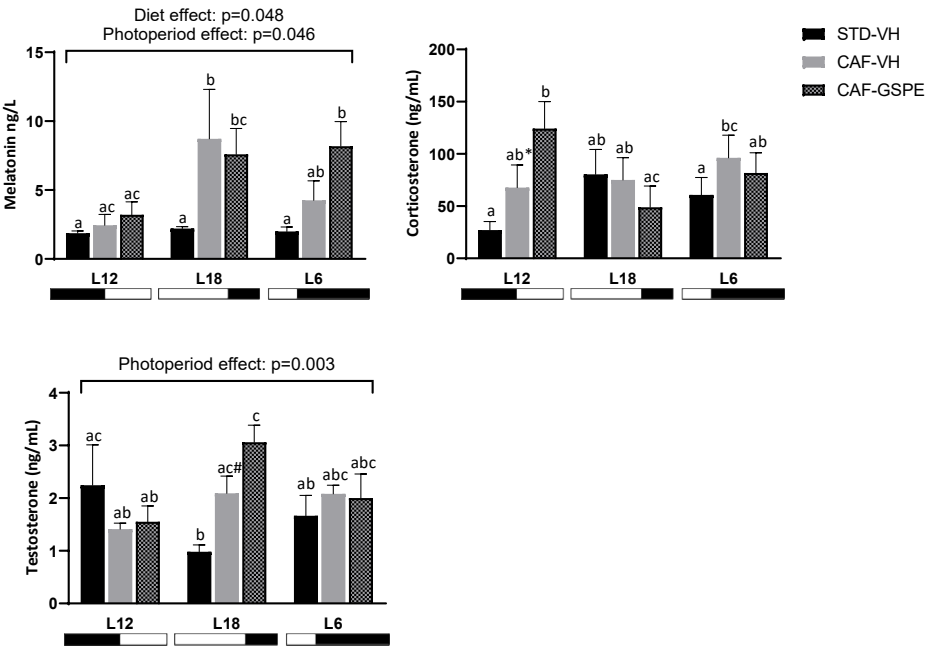

Figure 3. Serum hormones of Fischer 344 STD and CAF-fed rats exposed to L12, L18 or L6 photoperiods (n=8). The results are presented as the mean ± S.E.M. One- and two-way ANOVA following by LSD post hoc tests were performed to compare the values between groups and significant differences ($p \leq 0.05$) were represented with different letters (a, b, c). *Indicates tendency between L12-CAF-VH and L12-CAF-GSPE groups ($p = 0.054$). #Indicates tendency between L18-CAF-VH and L18-CAF-GSPE groups ($p = 0.055$).

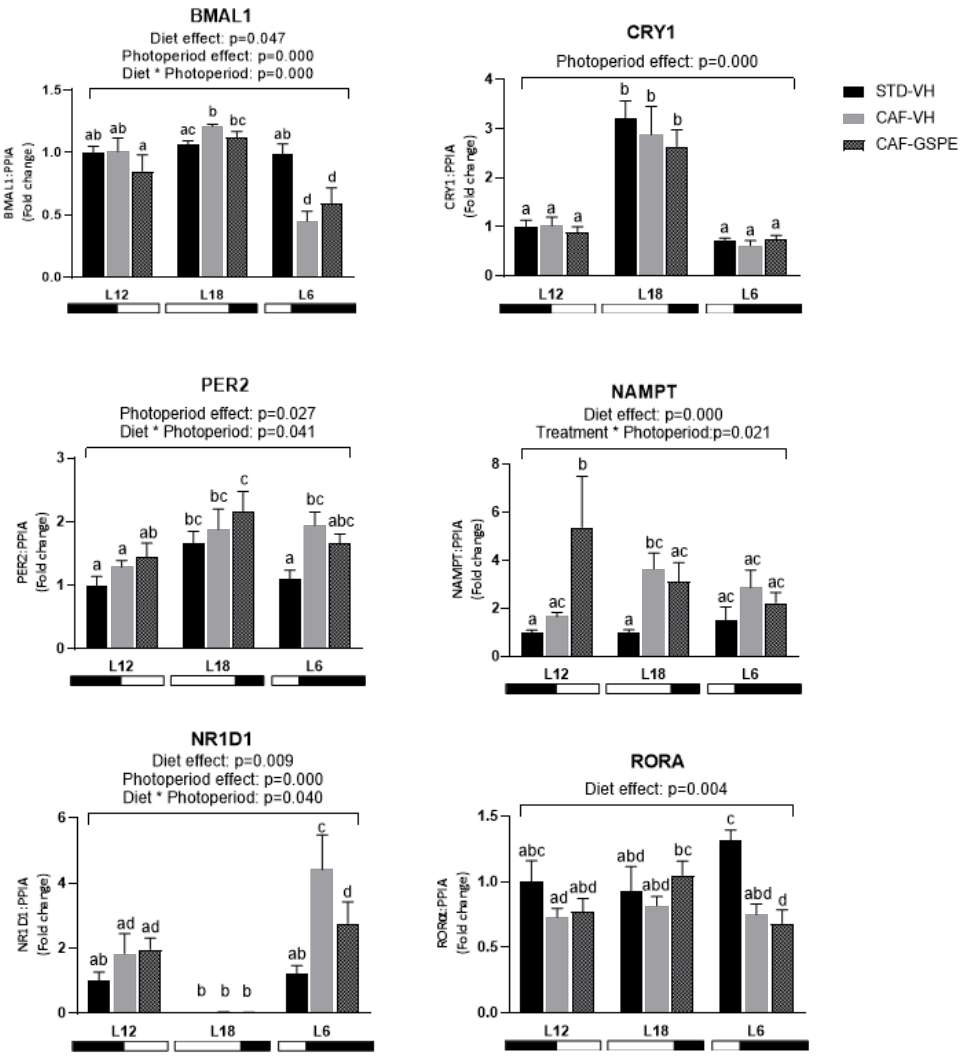

Figure 4. mRNA expression levels of clock genes in the liver of Fischer 344 STD and CAF-fed rats exposed to L12, L18 or L6 photoperiods (n=8). The results are presented as the mean ± S.E.M. One- and two-way ANOVA following by LSD post hoc tests were performed to compare the values between groups and significant differences ($p \leq 0.05$) were represented with different letters (a, b, c, d).

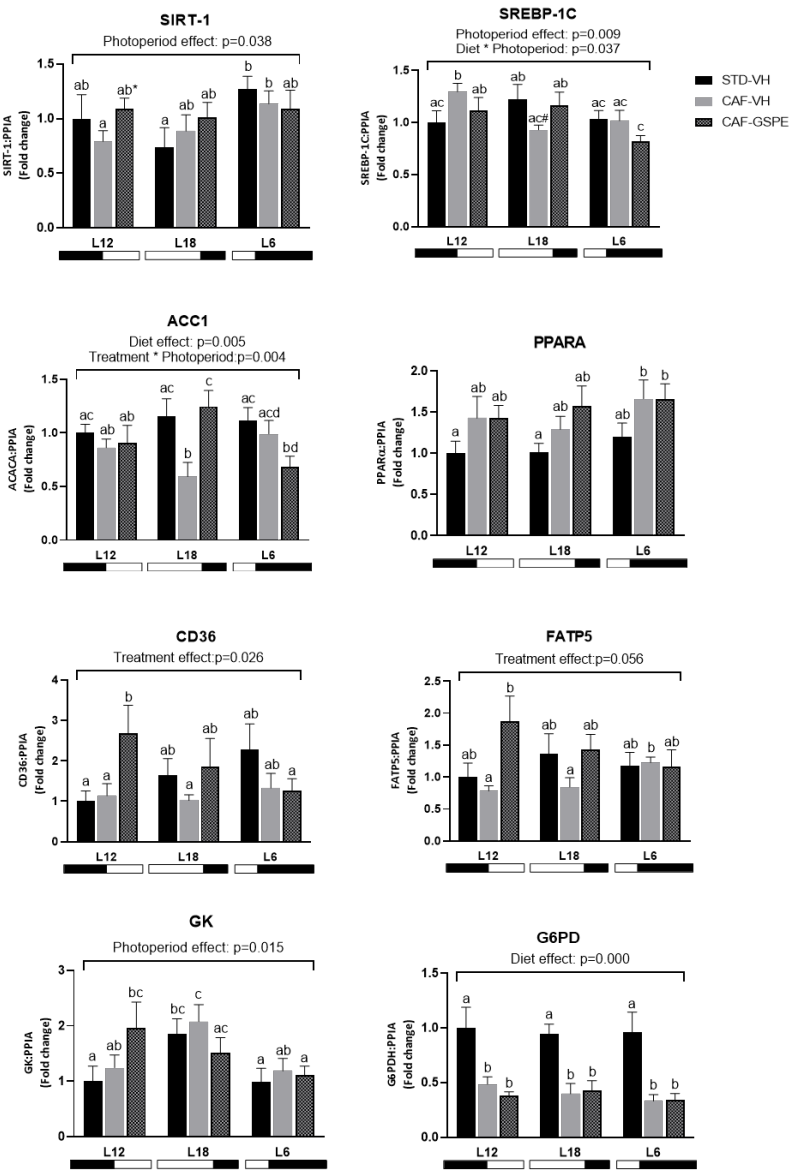

Figure 5. mRNA expression levels of liver lipid and glucose metabolism of Fischer 344 STD and CAF-fed rats exposed to L12, L18 or L6 photoperiods (n=8). The results are presented as the mean ± S.E.M. One- and two-way ANOVA following by LSD post hoc tests were performed to compare the values between groups and significant differences ($p \leq 0.05$) were represented with different letters (a, b, c, d). *Indicates tendency between L12-CAF-VH and L12-CAF-GSPE groups ($p = 0.061$). #Indicates tendency between L18-STD-VH and L18-CAF-VH groups ($p = 0.056$).

Parameters	L12			L18			L6			2wA
	STD-VH	CAF-VH	CAF-GSPE	STD-VH	CAF-VH	CAF-GSPE	STD-VH	CAF-VH	CAF-GSPE	
Cholesterol (mg/g)	1,19 ± 0,1 a	1,63 ± 0,1 b	1,84 ± 0,1 bc	1,04 ± 0,1 a	2,05 ± 0,1 c	2,05 ± 0,2 c	1,14 ± 0,1 a	1,78 ± 0,1 bc	2,01 ± 0,3 bc	*D, D*P*
Triglycerides (mg/g)	2,62 ± 0,2 a	5,18 ± 0,4 b	4,84 ± 0,4 b	3,44 ± 0,3 a	6,75 ± 0,4 c	6,93 ± 0,4 c	3,68 ± 0,3 a	6,9 ± 0,5 c	6,92 ± 0,7 c	*D, P*
Phospholipids (mg/g)	6,82 ± 0,3 ab	5,94 ± 0,3 a	6,36 ± 0,4 a	6,3 ± 0,3 a	7,06 ± 0,4 ab*	7,06 ± 0,3 ab	6,92 ± 0,3 ab	7,16 ± 0,7 ab#	7,89 ± 0,6 b	*P*
Liver weight (g)	14,78 ± 0,5 a	20,3 ± 1,4 bc	18,64 ± 0,6 bc	15,21 ± 0,7 a	20,01 ± 0,5 c	17,53 ± 0,7 b	15,6 ± 0,5 ad	19,23 ± 1,5 bc	17,91 ± 1,3 bcd	*D*

Table 1. Lipid parameters in the liver of Fischer 344 STD and CAF-fed rats exposed to L12, L18 or L6 photoperiods (n=8). The results are presented as the mean ± S.E.M. One- and two-way ANOVA following by LSD post hoc tests were performed to compare the values between groups and significant differences ($p \leq 0.05$) were represented with different letters (a, b, c, d). *Indicates tendency between L12-CAF-VH and L18-CAF-VH groups ($p = 0.064$). #Indicates tendency between L12-CAF-VH and L6-CAF-VH groups ($p = 0.052$). P, photoperiod effect. D, diet effect. D*P, interaction between photoperiod and diet.

Metabolite	STD-VH	CAF-VH	CAF-GSPE	*p*-value	STD-VH vs CAF-VH	STD-VH vs CAF-GSPE	CAF-VH vs CAF-GSPE	VIP
2-Hydroxyisobutyric acid	1.83 ± 0.11	2.49 ± 0.08	3.09 ± 0.17	**<0.001	*0.016	**<0.001	*0.039	1.78
Oleic acid	2.2 ± 0.32	9.61 ± 1.13	6.9 ± 0.67	**<0.001	**<0.001	*0.005	0.129	1.76
Indole-3-propanoic acid	1.7 ± 0.17	0.76 ± 0.18	0.33 ± 0.09	*0.001	*0.012	**<0.001	0.074	1.68
Dodecanoic acid	0.16 ± 0.01	0.32 ± 0.01	0.32 ± 0.03	*0.001	*0.001	*0.001	0.375	1.59
Glycine	5.32 ± 0.13	4.75 ± 0.09	4.6 ± 0.11	*0.001	*0.006	*0.001	0.170	1.41
Serine	10.01 ± 0.32	12.89 ± 0.36	12.63 ± 0.42	*0.001	*0.001	*0.002	0.458	1.57
2-HydroxyButyric acid	0.6 ± 0.04	1.34 ± 0.36	2.08 ± 0.42	*0.001	*0.013	*0.001	0.115	1.34
Hippuric acid	0.43 ± 0.09	0.09 ± 0.02	0.1 ± 0.03	*0.002	*0.002	*0.003	0.500	1.43
Pipecolic acid	0.11 ± 0.01	0.07 ± 0.01	0.06 ± 0.01	*0.003	*0.005	*0.003	0.349	1.45
Heptanoic	0.23 ± 0.01	0.28 ± 0.01	0.32 ± 0.02	*0.004	*0.023	*0.002	0.137	1.37
Glycolic acid	0.1 ± 0.01	0.13 ± 0.00	0.13 ± 0.00	*0.006	*0.013	*0.004	0.251	1.38
Threonic acid	0.82 ± 0.09	1.27 ± 0.13	1.39 ± 0.13	*0.009	*0.010	*0.007	0.362	1.20
Glycerol	0.9 ± 0.16	1.52 ± 0.08	1.44 ± 0.15	*0.014	*0.009	*0.019	0.298	1.28

3-Hydroxyisovaleric acid	0.37 ± 0.02	0.44 ± 0.03	0.49 ± 0.03	*0.016	0.050	*0.007	0.161	1.27
Proline	23.86 ± 3.30	33.98 ± 2.12	26.32 ± 1.58	*0.019	*0.018	0.444	*0.013	1.18
3-hydroxybutyric acid	8.78 ± 0.69	13.41 ± 1.17	15.42 ± 2.37	*0.019	*0.011	*0.022	0.500	1.10
3-Phosphoglyceric acid	0.02 ± 0.01	0.05 ± 0.00	0.03 ± 0.00	*0.024	*0.011	0.179	0.050	1.36
Valine	10.23 ± 0.35	9.71 ± 0.31	9 ± 0.30	*0.039	0.122	*0.016	0.126	1.14
Glucose	29.87 ± 1.18	31.52 ± 1.4	34.74 ± 1.18	*0.044	0.179	*0.020	0.090	1.14

Table 2. Summary analysis of the serum metabolome at L12 photoperiod for STD-VH, CAF-VH and CAF-GSPE groups (n = 8). Relative abundances (AU) of metabolites are presented by the mean ± SEM. The p-value adjustment for multiple comparisons was carried out according to the Benjamin-Hochberg (BH) correction method with a false discovery rate (FDR) of 5%, and a Post-hoc Dunn. The multivariate analysis is represented by the variable importance in projection (VIP) value of PLS-DA. * Denotes $p < 0.05$ (statistically significant) and ** $p < 0.001$ (statistically highly significant).

Metabolite	STD-VH	CAF-VH	CAF-GSPE	*p*-value	STD-VH vs CAF-VH	STD-VH vs CAF-GSPE	CAF-VH vs CAF-GSPE	VIP
2-HydroxyButyric acid	0.52 ± 0.02	2.07 ± 0.28	1.23 ± 0.15	**<0.001	**<0.001	*0.006	0.069	1.73
Glycolic acid	0.09 ± 0.00	0.13 ± 0.01	0.12 ± 0.01	**<0.001	**<0.001	*0.003	0.161	1.51
d-Sucrose	0.04 ± 0.01	0.37 ± 0.11	0.66 ± 0.17	*0.001	*0.005	**<0.001	0.153	1.31
Dodecanoic acid	0.17 ± 0.00	0.29 ± 0.04	0.35 ± 0.04	*0.001	*0.003	*0.001	0.274	1.23
Oleic acid	3.15 ± 0.35	6.92 ± 1.06	8.91 ± 0.87	*0.001	*0.007	**<0.001	0.137	1.44
Glycerol	1.07 ± 0.08	1.67 ± 0.11	1.64 ± 0.11	*0.001	*0.001	*0.002	0.336	1.34
Threonic acid	0.68 ± 0.06	1.47 ± 0.24	1.53 ± 0.19	*0.001	*0.002	*0.001	0.336	1.22
Serine	10.17 ± 0.23	13.34 ± 0.70	13.9 ± 0.33	*0.001	*0.007	*0.001	0.161	1.47
2-Hydroxyisobutyric acid	1.78 ± 0.16	3.05 ± 0.19	2.65 ± 0.25	*0.002	*0.001	*0.010	0.161	1.39
Hippuric acid	0.53 ± 0.09	0.1 ± 0.02	0.12 ± 0.03	*0.002	*0.003	*0.003	0.402	1.45
Indole-3-propanoic acid	1.49 ± 0.25	0.38 ± 0.08	0.71 ± 0.31	*0.005	*0.004	*0.007	0.323	1.15
Pyruvic acid	17.86 ± 1.19	24.24 ± 0.80	23.07 ± 1.65	*0.006	*0.003	*0.021	0.179	1.22
Fumaric acid	1.19 ± 0.11	2.22 ± 0.35	2.86 ± 0.53	*0.007	*0.016	*0.004	0.240	1.17
Pipecolic acid	0.11 ± 0.01	0.07 ± 0.01	0.06 ± 0.01	*0.010	*0.015	*0.006	0.298	1.23
Leucine	7.82 ± 0.14	6.94 ± 0.26	8.18 ± 0.30	*0.011	0.054	0.122	*0.005	1.66
3-Hydroxyisovaleric acid	0.34 ± 0.02	0.42 ± 0.01	0.41 ± 0.02	*0.013	*0.006	*0.033	0.198	1.11
Methionine	3.73 ± 0.09	3.32 ± 0.10	3.61 ± 0.05	*0.013	*0.006	0.198	*0.033	1.48
Malic acid	0.98 ± 0.11	1.49 ± 0.22	2.02 ± 0.33	*0.014	0.058	*0.006	0.129	1.18
4-hydroxyPhenyllactic acid	23.56 ± 5.77	38.09 ± 5.54	52.31 ± 7.62	*0.014	0.058	*0.006	0.129	1.22
Valine	9.65 ± 0.22	8.46 ± 0.26	9.67 ± 0.42	*0.016	*0.010	0.486	*0.018	1.41
Oxoproline	122.6 ± 4.81	138.36 ± 4.8	147.59 ± 7.23	*0.024	*0.042	*0.012	0.229	1.10
3-hydroxybutyric acid	10.25 ± 0.86	18.3 ± 2.32	13.99 ± 2.11	*0.027	*0.011	0.108	0.110	1.18

Isoleucine	5.12 ± 0.13	4.72 ± 0.22	5.6 ± 0.24	*0.035	0.129	0.110	*0.015	1.48
Phenylalanine	4.25 ± 0.09	3.75 ± 0.12	4.02 ± 0.10	*0.038	*0.016	0.145	0.103	1.31

Table 3. Summary analysis of the serum metabolome at L18 photoperiod for STD-VH, CAF-VH and CAF-GSPE groups (n = 8 animals per group). Relative abundances (AU) of metabolites are presented by the mean ± SEM. The p-value adjustment for multiple comparisons was carried out according to the Benjamin-Hochberg (BH) correction method with a false discovery rate (FDR) of 5%, and a Post-hoc Dunn. The multivariate analysis is represented by the variable importance in projection (VIP) value of PLS-DA. * Denotes $p < 0.05$ (statistically significant) and ** $p < 0.001$ (statistically highly significant).

Metabolite	STD-VH	CAF-VH	CAF-GSPE	*p*-value	STD-VH vs CAF-VH	STD-VH vs CAF-GSPE	CAF-VH vs CAF-GSPE	VIP
Oleic acid	2.34 ± 0.38	7.92 ± 0.90	5.5 ± 0.47	*0.001	**<0.001	*0.005	0.116	1.77
2-HydroxyButyric acid	0.59 ± 0.04	1.32 ± 0.23	2.16 ± 0.28	*0.001	0.297	**<0.001	*0.046	1.57
Glycolic acid	0.1 ± 0.00	0.11 ± 0.00	0.13 ± 0.00	*0.001	*0.042	**<0.001	*0.037	1.64
d-Sucrose	0.02 ± 0	0.4 ± 0.14	0.41 ± 0.17	*0.001	*0.002	*0.001	0.406	1.09
d-Fructose	0.05 ± 0.00	0.13 ± 0.05	0.05 ± 0.00	*0.002	*0.001	0.290	*0.003	1.21
Dodecanoic acid	0.16 ± 0.01	0.27 ± 0.02	0.25 ± 0.01	*0.002	*0.001	*0.005	0.204	1.48
Hippuric acid	0.42 ± 0.08	0.09 ± 0.01	0.05 ± 0.01	*0.002	*0.050	*0.001	*0.045	1.61
Serine	9.87 ± 0.34	13.27 ± 0.69	13.4 ± 0.8	*0.002	*0.002	*0.003	0.487	1.43
Pipecolic acid	0.1 ± 0.01	0.07 ± 0.00	0.05 ± 0.01	*0.003	*0.013	*0.002	0.208	1.52
Glycerol	0.81 ± 0.07	1.58 ± 0.16	1.37 ± 0.14	*0.006	*0.004	*0.011	0.243	1.43
Glutamine	0.18 ± 0.02	0.31 ± 0.07	0.39 ± 0.04	*0.011	0.096	*0.004	0.076	1.20
3-Hydroxyisovaleric acid	0.4 ± 0.03	0.41 ± 0.03	0.51 ± 0.02	*0.011	0.484	*0.014	*0.008	1.40

Indole-3-propanoic acid	1.33 ± 0.25	0.76 ± 0.15	0.44 ± 0.14	*0.013	0.063	*0.005	0.125	1.28
Glucose	29.83 ± 1.11	34.28 ± 0.95	36.23 ± 2.74	*0.014	*0.016	*0.008	0.464	1.01
Heptanoic	0.24 ± 0.01	0.29 ± 0.02	0.33 ± 0.02	*0.016	*0.033	*0.008	0.238	1.23
3-hydroxybutyric acid	9.75 ± 0.97	11.73 ± 3.25	17.06 ± 1.50	*0.020	0.467	*0.022	*0.014	1.27
Threonine	8.23 ± 0.26	10.06 ± 0.56	9.66 ± 0.55	*0.026	*0.016	*0.028	0.289	1.13
Lactic acid	64.93 ± 2.27	74.75 ± 2.12	81.25 ± 6.33	*0.036	*0.027	*0.027	0.420	1.06
Methionine	3.67 ± 0.10	3.52 ± 0.06	3.34 ± 0.07	*0.038	0.183	*0.018	0.086	1.13

Table 4. Summary analysis of the serum metabolome at L6 photoperiod for STD-VH, CAF-VH and CAF-GSPE groups (n = 8 animals per group). Relative abundances (AU) of metabolites are presented by the mean ± SEM. The p-value adjustment for multiple comparisons was carried out according to the Benjamin-Hochberg (BH) correction method with a false discovery rate (FDR) of 5%, and a Post-hoc Dunn. The multivariate analysis is represented by the variable importance in projection (VIP) value of PLS-DA. * Denotes $p < 0.05$ (statistically significant) and ** $p < 0.001$ (statistically highly significant).

SUPPLEMENTARY MATERIAL

Supplementary Table 1. Nucleotide sequences of primers used for real-time quantitative PCR

Gene	Forward primer (5' to 3')	Reverse primer (5' to 3')
Acacα	TGCAGGTATCCCCACTCTTC	TTCTGATTCCCTTCCCTCCT
Bmal1	GTAGATCAGAGGGCGACGGCTA	CTTGTCTGTAAAACTTGCCTGTGAC
Cd36	GTCCTGGCTGTGTTTGGA	GCTCAAAGATGGCTCCATTG
Cry1	TGGAAGGTATGCGTGTCCTC	TCCAGGAGAACCTCCTCACG
Fatp5	CCTGCCAAGCTTCGTGCTAAT	GCTCATGTGATAGGATGGCTGG
G6pd	ACCAGGCATTCAAAACGCAT	CAGTCTCAGGGAAGTGTGGT
Gk	CTGTGAAAGCGTGTCCACTC	GCCCTCCTCTGATTCGATGA
Nampt	CTCTTCACAAGAGACTGCCG	TTCATGGTCTTTCCCCCACG
Nr1d1	ACAGCTGACACCACCCAGATC	CATGGGCATAGGTGAAGATTTCT
Per2	CGGACCTGGCTTCAGTTCAT	AGGATCCAAGAACGGCACAG
Pparα	CGGCGTTGAAAACAAGGAGG	TTGGGTTCCATGATGTCGCA
Ppia	CCAAACACAAATGGTTCCCAGT	ATTCCTGGACCCAAAACGCT
Rorα	CCCGATGTCTTCAAATCCTTAGG	TCAGTCAGATGCATAGAACACAAACTC
Sirt1	TTGGCACCGATCCTCGAA	ACAGAAACCCCAGCTCCA
Srebp1c	CCCACCCCCTTACACACC	GCCTGCGGTCTTCATTGT

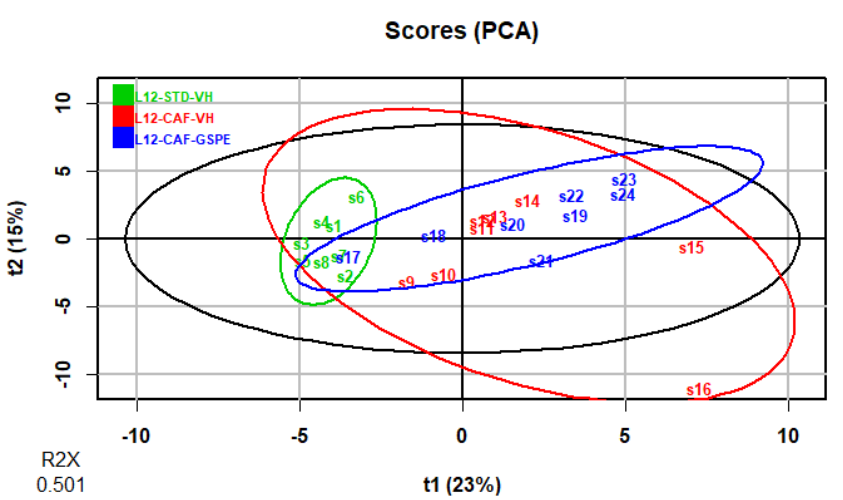

Supplementary figure 1. PCA score plot coloured according to groups at L12 photoperiod (serum metabolome).

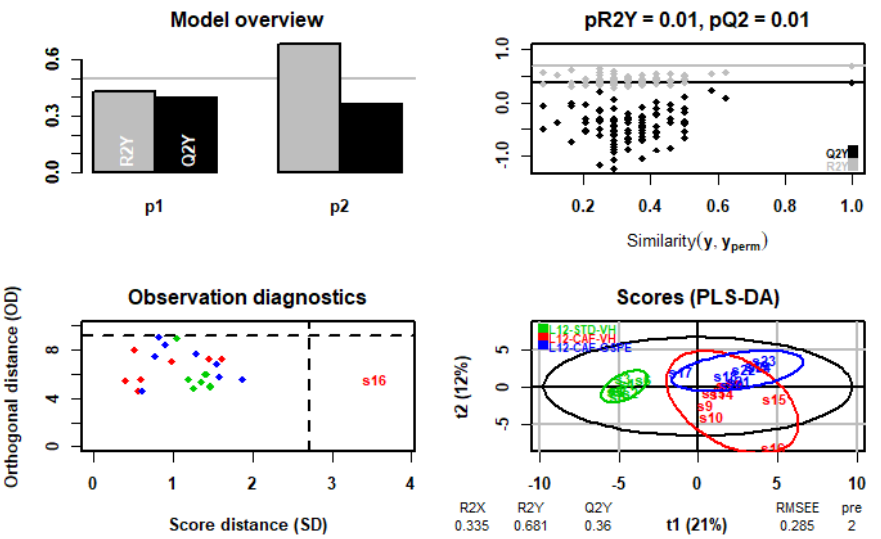

Supplementary figure 2. PLS-DA model of the L12 photoperiod (serum metabolome). Top left: inertia barplot: the graphic here suggests that 2 components may be sufficient to capture most of the inertia; Top right: significance diagnostic: the R2Y and Q2Y of the model are compared with the corresponding values obtained after random permutation of the y response; Bottom left: outlier diagnostics; Bottom right: x-score plot: the number of components and the cumulative R2X, R2Y and Q2Y are indicated below the plot.

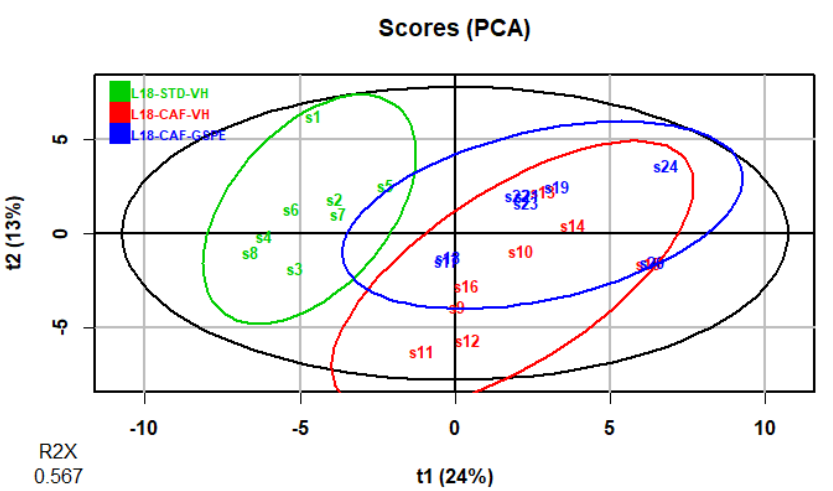

Supplementary figure 3. PCA score plot coloured according to groups at L18 photoperiod (serum metabolome).

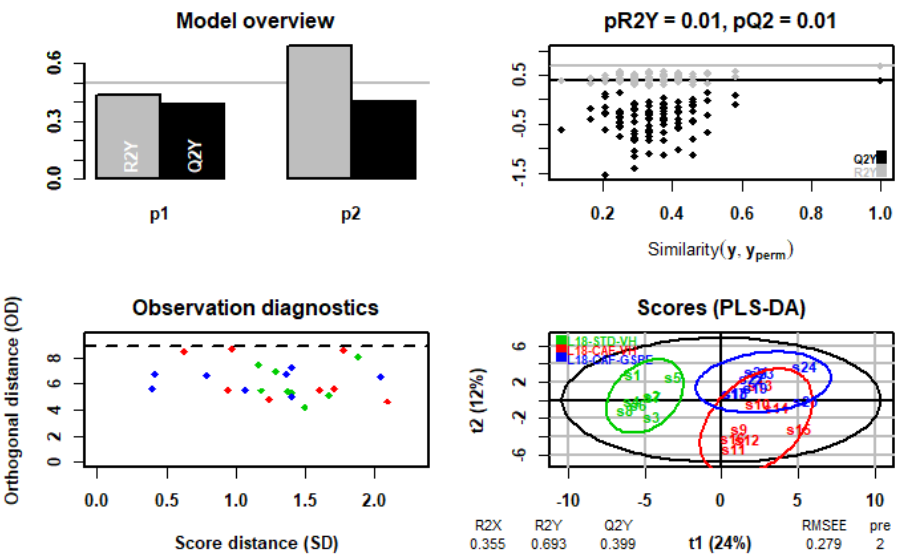

Supplementary figure 4. PLS-DA model of the L18 photoperiod (serum metabolome). Top left: inertia barplot: the graphic here suggests that 2 components may be sufficient to capture most of the inertia; Top right: significance diagnostic: the R2Y and Q2Y of the model are compared with the corresponding values obtained after random permutation of the y response; Bottom left: outlier diagnostics; Bottom right: x-score plot: the number of components and the cumulative R2X, R2Y and Q2Y are indicated below the plot.

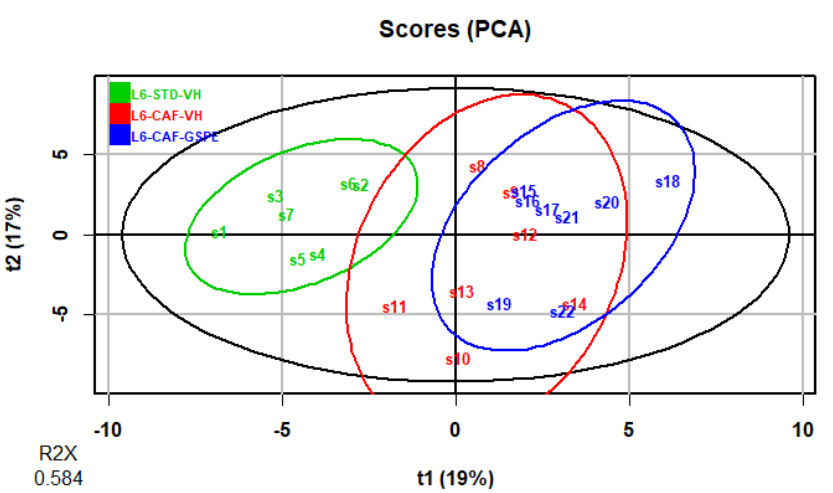

Supplementary figure 5. PCA score plot coloured according to groups at L6 photoperiod (serum metabolome).

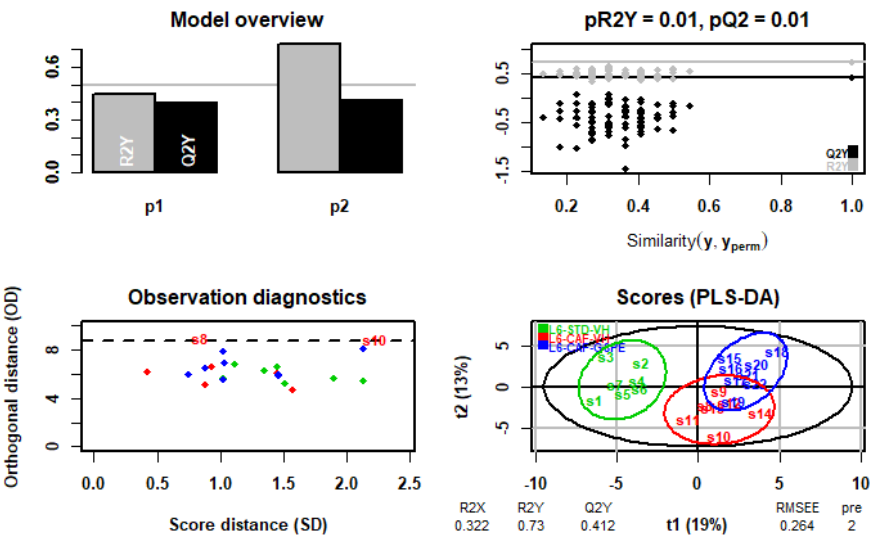

Supplementary figure 6. PLS-DA model of the L6 photoperiod (serum metabolome). Top left: inertia barplot: the graphic here suggests that 2 components may be sufficient to capture most of the inertia; Top right: significance diagnostic: the R2Y and Q2Y of the model are compared with the corresponding values obtained after random permutation of the y response; Bottom left: outlier diagnostics; Bottom right: x-score plot: the number of components and the cumulative R2X, R2Y and Q2Y are indicated below the plot.

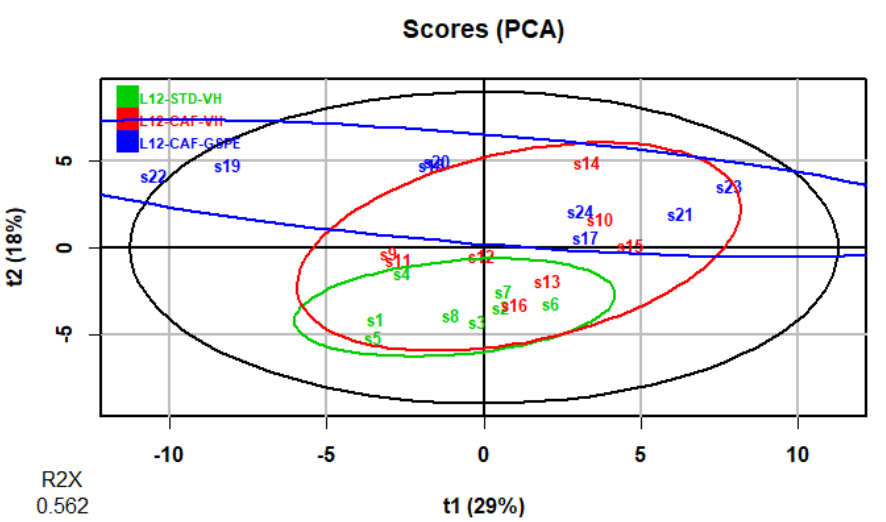

Supplementary figure 7. PCA score plot coloured according to groups at L12 photoperiod (liver metabolome).

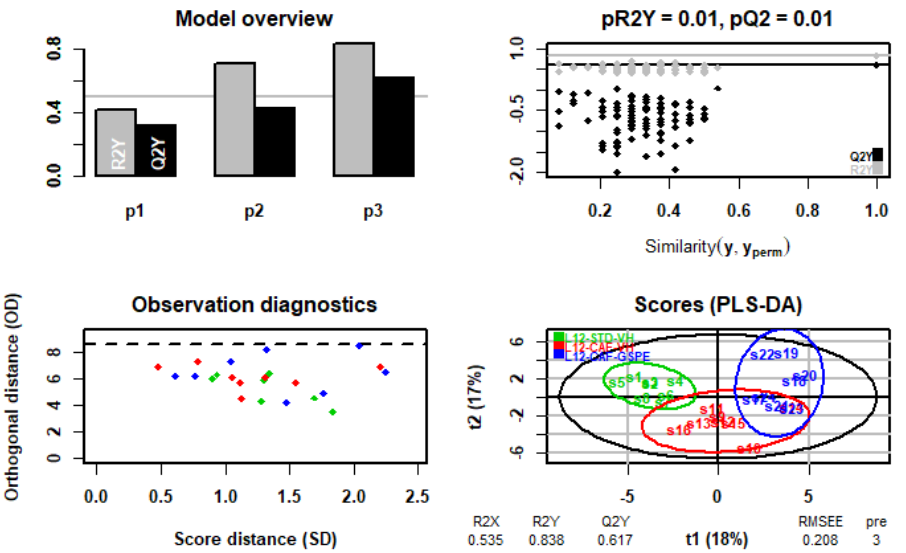

Supplementary figure 8. PLS-DA model of the L12 photoperiod (liver metabolome). Top left: inertia barplot: the graphic here suggests that 3 components may be sufficient to capture most of the inertia; Top right: significance diagnostic: the R2Y and Q2Y of the model are compared with the corresponding values obtained after random permutation of the y response; Bottom left: outlier diagnostics; Bottom right: x-score plot: the number of components and the cumulative R2X, R2Y and Q2Y are indicated below the plot.

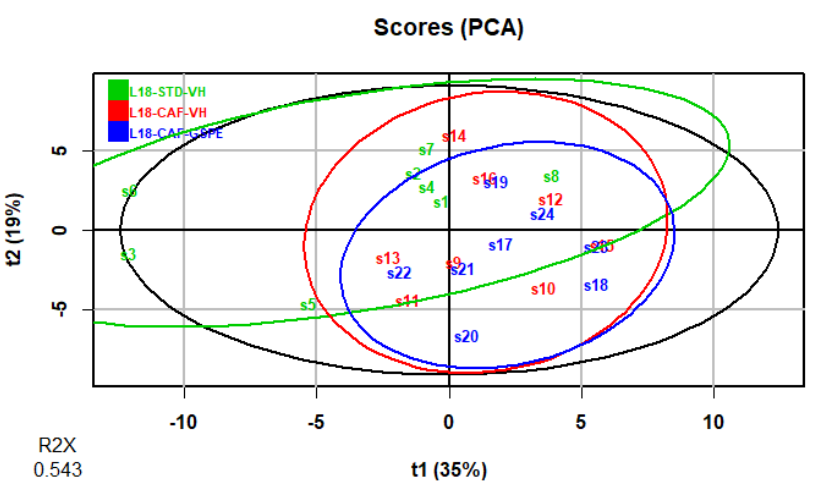

Supplementary figure 9. PCA score plot coloured according to groups at L18 photoperiod (liver metabolome).

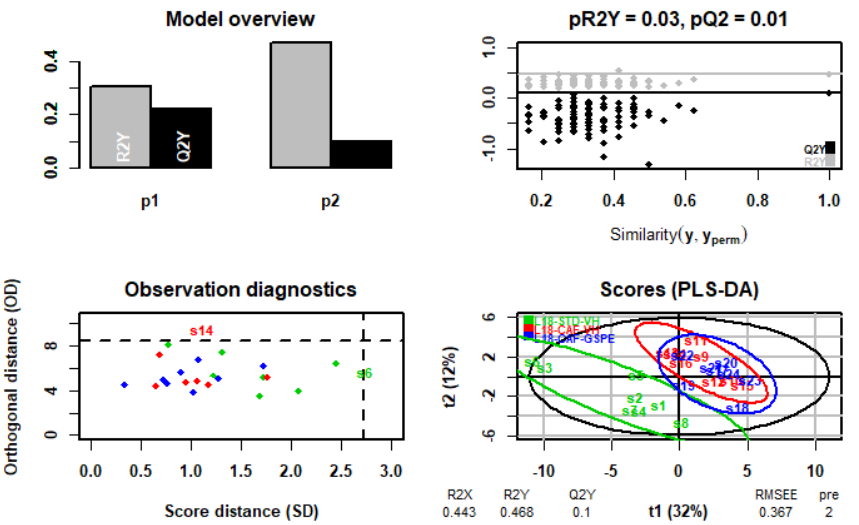

Supplementary figure 10. PLS-DA model of the L18 photoperiod (liver metabolome). Top left: inertia barplot: the graphic here suggests that 2 components may be sufficient to capture most of the inertia; Top right: significance diagnostic: the R2Y and Q2Y of the model are compared with the corresponding values obtained after random permutation of the y response; Bottom left: outlier diagnostics; Bottom right: x-score plot: the number of components and the cumulative R2X, R2Y and Q2Y are indicated below the plot.

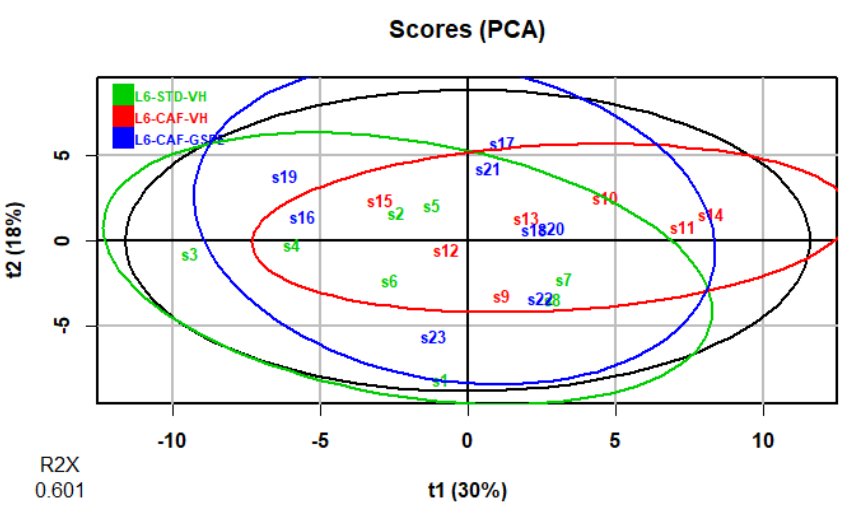

Supplementary figure 11. PCA score plot coloured according to groups at L6 photoperiod (liver metabolome).

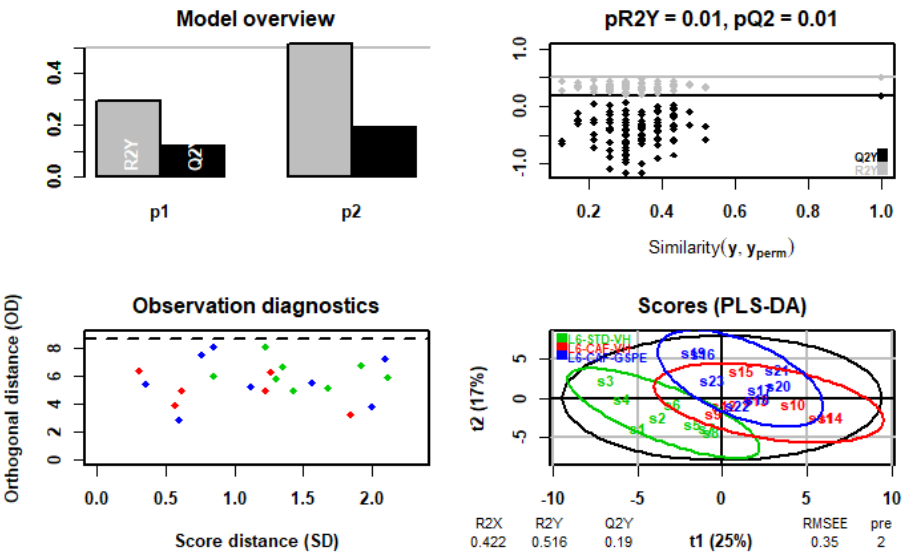

Supplementary figure 12. PLS-DA model of the L6 photoperiod (liver metabolome). Top left: inertia barplot: the graphic here suggests that 2 components may be sufficient to capture most of the inertia; Top right: significance diagnostic: the R2Y and Q2Y of the model are compared with the corresponding values obtained after random permutation of the y response; Bottom left: outlier diagnostics; Bottom right: x-score plot: the number of components and the cumulative R2X, R2Y and Q2Y are indicated below the plot.

IV. GENERAL DISCUSSION

UNIVERSITAT ROVIRA I VIRGILI
THE INFLUENCE OF BIOLOGICAL RHYTHMS ON THE BENEFICIAL EFFECTS OF GRAPE SEED PROANTHOCYANIDIN EXTRACT (GSPE) ON LIVER METABOLISM IN HEALTH AND DISEASE
Romina Mariel Rodriguez

GENERAL DISCUSSION

Biological rhythms are universal phenomena present in almost all living organisms, ranging from bacteria to humans. These biological rhythms synchronize various behavioral, biochemical, and physiological processes with changes in environmental factors thus allowing the organism to effectively adapt, anticipate, and respond to external changes. Mainly modulated by the light and dark cycle, the persistent daily oscillations of all these functions are known as circadian rhythms [1–4]. Circadian rhythms are therefore 24-h endogenous oscillations observed in virtually all aspects of mammalian function from gene expression to complex physiological and biological processes [5]. In this sense, circadian clocks optimize the timing of metabolic processes such as glucose production and insulin secretion due to coordination of behavior and physiology with daily environmental cycles. Such circadian regulation of metabolism provides an adaptive advantage in diverse organisms [6]. Previous studies have reported an association between dysregulation of circadian rhythms and metabolic dysfunction as both metabolites [7] and metabolic gene expression [8,9] broadly exhibit circadian oscillations. In humans, circadian misalignments are associated with metabolic disturbances including obesity, hyperlipidemia, diabetes, and metabolic syndrome (MS) [10,11]. Moreover, metabolism and food intake also feedback the circadian system in order to modulate its response. A wide range of studies show that excessive fat and carbohydrate intake induces a disruption of circadian regulation of metabolic pathways, playing a crucial role in the development and progression of metabolic diseases such as MS and its hepatic manifestation named non-alcoholic fatty liver disease (NAFLD) [12]. In addition, dietary composition has a significant impact on mitochondrial health, as nutrients provide the building blocks for cellular energy production in the form of ATP, thereby affecting essential cellular functions and processes [13]. As MS and its related metabolic disorders are wide-spreading, there is increasing public interest in studying

these metabolic abnormalities in an attempt to find strategies to fight against their development and their detrimental consequences on metabolism. In this regard, polyphenols, natural occurring compounds found in plant-based food or drinks, have been identified as powerful agents for the prevention and treatment of MS and NAFLD [14]. In particular, grape seed proanthocyanidin extract (GSPE) has demonstrated its ability to decrease body weight, blood pressure and blood glucose, improve insulin resistance and ameliorate dyslipidemia in diet-induced obese rats [15–19]. Additionally, improvement of mitochondrial function on skeletal muscle and brown adipose tissue has been observed after GSPE chronic supplementation in obese rats [20,21]. Furthermore, GSPE has also been able to modulate gene expression of peripheral clocks, including liver, gut and adipose tissue, in lean and obese rats [22]. Moreover, Ribas-Latre and collaborators observed a time-dependent effect of acute administration of GSPE on the modulation of hepatic clock genes in healthy rats, exerting a stronger effect when it was administered at the beginning of the dark period (ZT12).

However, little is known about: (a) the influence of the light-dark cycle on the effects of chronic GSPE consumption on the hepatic clock molecular components, and (b) the effect of GSPE on liver mitochondrial function in obesity and NAFLD. Therefore, our first objective was **to assess the impact of GSPE chronic administration timing on the hepatic circadian clock and mitochondrial function in obese rats** (Manuscript 1). For this purpose, we chronically administered 25 mg/kg of GSPE to rats with cafeteria-diet-induced obesity at two different times of the day: at the beginning of the light period (ZT0), or at the beginning of the dark period (ZT12). The results of our study validate the beneficial effects of GSPE consumption on body weight gain but highlights the first time-of-day-dependent effect of GSPE consumption as an important factor, because only rats that were treated at ZT12 showed this body weight reduction effect. As it is well described in literature, the intake of a high-fat diet can impair daily

rhythms of the central clock in the SNC and in peripheral tissues such as the liver [23,24]. In this sense, we observed not only a loss in *Rorα* rhythmic expression caused by CAF-diet but also phase shifts of several clock genes including *Bmal1, Cry1, Per2, Nr1d1*, and the clock-controlled gene *Nampt.* When analyzing GSPE effects over these clock liver disruptions, we observed that GSPE was able to restore the CAF-diet disturbances on the hepatic clock rhythms showing better results in the night treatment (ZT12). In this regard, GSPE is capable of restoring hepatic circadian misalignment of *Bmal1, Cry1, Per2* at ZT12, and of *Rorα* at both ZT0 and ZT12. These results are in agreement with those observed by Ribas-Latre in the GSPE acute treatment in healthy rats [25], and also demonstrate the effect of timing of administration on the modulation of liver clock genes by GSPE.

Several studies have demonstrated the interplay between hepatic circadian clock and mitochondrial function. In this sense, Kim and collaborators observed that liver-specific ablation of *Rorα,* a promoter of *Bmal1* expression, induces altered mitochondrial function, thereby exacerbating NAFLD in high-fat diet feeding mice. Moreover, liver specific *Bmal1* knockout mice exhibit abnormal mitochondrial morphology which increases oxidative damage and impairs hepatic metabolic flexibility [26]. In addition, it was observed a decrease in the expression of genes related to the mitochondrial respiratory chain, together with a downregulation of *Mfn1* and *Opa1* fusion genes in mice with heart-specific deletion of *Bmal1*. All these results suggest that *Bmal1* is the main clock component involved in the circadian control of mitochondrial dynamics and respiration. In line with these results, we observed an impaired expression of genes involved in mitochondrial dynamics, a significant decrease of the mitochondrial respiratory activity at both ZT0 and ZT12 treatments in CAF-fed rats, which exhibit disrupted hepatic *Bmal1* rhythm. As it was mentioned, GSPE could only restore *Bmal1* disruption when it was administered at ZT12, and this action was accompanied by an increase in the expression of mitochondrial fusion genes and a decrease of mitochondrial fission genes expression in

ZT12-GSPE animals. In addition, GSPE was also able to counteract CAF-diet disturbances in the activity of mitochondrial complexes that form part of the respiratory chain not only at ZT12, but also at ZT0 treatment. We obtained similar results regarding the influence of GSPE on TCA cycle metabolites. In each time of sacrifice we observed a depletion of some of these metabolites due to CAF-diet intake. This could mean that because of the ATP-rich environment, TCA metabolites are being redirected to anabolic pathways, e.g., lipid synthesis. When treated with GSPE, we observed higher concentrations of these metabolites mainly in ZT0-GSPE-treated rats. This could be related to the major restoration of the respiratory complexes induced by GSPE at ZT0, as they are closely linked to TCA cycle metabolites. In this sense, the by-products of the TCA cycle feed the complexes of the electron transport chain and, likewise, the oxidation of these by-products in the complexes is required for the proper functioning of the TCA cycle [27]. Hence, we demonstrated that a chronic consumption of GSPE could alleviate the effect of the CAF diet over mitochondrial function. In summary, rats that were treated at ZT12 exhibit not only improvements in the rhythmicity of clock genes in the liver that were disrupted by the CAF diet, but also an amelioration of mitochondrial dynamics with a balance between fusion and fission processes, an improvement of respiratory complex II activity, and a reduction in body weight. In consequence, we could suggest that there is a time-dependent effect of GSPE consumption; however, little is known about the influence of the light-dark cycle on the molecular effects of GSPE on liver metabolism.

Therefore, once we had demonstrated that the restoration of the liver clock by GSPE consumption was time-dependent, it was essential to study whether this clock-enhancing effect was also reflected in changes in the rhythms of lipid and glucose metabolism. In this regard our second objective was to **evaluate the impact of GSPE chronic administration timing on the lipid and carbohydrate metabolism in obese rats** (Manuscript 2). The role of circadian control on liver metabolic pathways have been

demonstrated in experiments using transgenic animal models [28]. Liver-specific *Rorα* knockout animals fed a HFD diet exhibit an upregulation of SREBP-1c lipogenic gene expression under feeding conditions [29]. Moreover, mice with liver-specific deletion of *Bmal1* display impaired glucose homeostasis with a loss of rhythmic expression of hepatic glucose regulatory genes such as GLUT2 [30], and hyperlipidemia with an increase accumulation of triglyceride and cholesterol in the liver [31]. In this sense, we observed an impaired or lost rhythmicity of key metabolic genes involved in fatty acid and carbohydrate metabolism in CAF-diet-induced obese rats. Furthermore, GSPE improved this diet-induced effect by the reestablishment of the rhythmic expression of the glucogenic and lipogenic genes at both ZT0 and ZT12 treatments. This last effect seems reasonable since GPSE was able to restore *Rorα* rhythmic expression independently of the time of administration, and also the expression of *Bmal1* at ZT12, consequently improving the rhythm oscillations of genes related with glucose and lipid metabolism including SREBP-1c, *Acaca*, *Fasn*, *Cd36*, GLUT2, and *G6pd* [32]. When analyzing the lipid liver profile, we discovered that the diurnal oscillations in liver mass, which has been previously reported by Sinture *et al*. in mice [33], were altered or lost by the CAF-diet intake. Since the liver plays a key role in metabolism and xenobiotic detoxification, the accuracy of its mass oscillation is critical. In this sense, GSPE successfully recovered these hepatic mass diurnal oscillations at both ZT0 and ZT12 treatment. However, we observed a decreased hepatic triglyceride accumulation in rats subjected to ZT12-GSPE chronic consumption but not in ZT0-GSPE treated rats. In addition, we found a reduction of lipid droplets formation in the liver of rats treated with GSPE at ZT12 while this effect was not observed at ZT0 treatment. As discussed, liver function is under intricate temporal control by the hepatic circadian clock. Therefore, appropriate oscillations of metabolites involved in the liver's metabolic pathways are necessary for the precise functioning of whole-body metabolism. In this regard, we observed that CAF-diet impaired not only the rhythmic oscillations but also the concentrations of metabolites

related to the urea cycle, whereas treatment with GSPE restored the diurnal oscillation of urea at ZT0 and of aspartic acid, an intermediate in the urea cycle, at ZT12. Urea and TCA cycle are intimately related as intermediates generated by TCA cycle can directly or indirectly affect the urea pathway [34]. Moreover, disturbances in urea cycle metabolites have been shown to act as a sensor of liver mitochondrial dysfunction [35]. Therefore, our results are in concordance with the exposed previous evidence, as we observed an improvement in mitochondrial function (manuscript 1), together with a boost of TCA and urea cycle metabolites in CAF-fed rats treated with GSPE, at both ZT0 and ZT12 treatments. Interestingly, Zhuo and co-workers observed that chronic consumption of green tea polyphenols improve energy conversion by enhancing the mitochondrial TCA cycle and the urea cycle of the gut microbiota in rats [36]. Furthermore, the rhythmicity of metabolites that are known to promote the TCA cycle, such as glycine and its precursor threonine, were disrupted in CAF diet-induced obese animals and partially recovered with chronic GSPE consumption at ZT0, albeit with a phase delay compared to the lean control. It is, however, the treatment at ZT12 that most effectively restored the metabolites' rhythms in CAF diet rats. In this regard, diurnal oscillations of glycerol, of 2-hydroxyButyric acid, aspartic acid, and xanthosine were totally restored with no differences in phase or amplitude compared to the lean control group. These metabolites are related to energy homeostasis and production of reactive oxygen species (ROS) in the liver, which could trigger lipid accumulation promoting hepatic steatosis. Thus, GSPE influences the gluconeogenic and lipogenic pathways in the liver by restoring proper oscillations of these metabolites on ZT12 treatment. These results also corroborate the antioxidant properties of GSPE in the liver and other tissues, protecting against oxidative damage [37–40].

Ribas-Latre and collaborators demonstrated that an acute treatment of GSPE in healthy rats modulated the expression pattern of hepatic clock genes and clock-controlled genes, such as *Nampt*, when administered at

ZT12 but not at ZT0. Additionally, they observed a significant increase in NAD levels with the acute GSPE administration only at ZT12. In line with these results, we observed a decrease in the levels of NAD in the CAF-diet-induced obesity animals compared to the control lean group, whereas this reduction was not observed in rats that chronically consumed GSPE at ZT12. Thus, besides *Bmal1*; *Nampt* and NAD emerge as molecular targets of GSPE in the liver due to their role in metabolism [41,42]. It is interesting to consider NAD levels being modulated by GSPE to explain some of its metabolic effects. In this sense, the enhancement of the hepatic NAD metabolism is associated with improved protection against triglycerides accumulation in the liver [43] which corroborates the histological and lipid profile results, as we observed lower levels of triglycerides and a decrease in lipid droplets formation in ZT12-GSPE treated rats.

Altogether, our results clearly show that the ability of GSPE to entrain diurnal rhythms of the core clock and clock-controlled genes in the liver of obese rats depends on the time of administration (Manuscript 1). By influencing the liver clock molecular machinery, GSPE is able to modulate the rhythmic expression of lipid and glucose related metabolic genes and metabolites that play a critical role in the maintenance of fat and energy homeostasis and the hepatic function (Manuscript 2). Furthermore, GSPE is also capable of improving mitochondrial function by regulating expression of genes involved in mitochondrial dynamics and recovering mitochondrial respiratory activity (Manuscript 1). All these beneficial effects of GSPE against obesity and NAFLD (lowering body weight and reducing lipid accumulation in the liver) are most effective when GSPE is consumed at the beginning of the dark phase (ZT12), which corresponds to the beginning of the active phase in rats, as they are nocturnal animals.

In order to assess the total polyphenol content of the GSPE extract used in the animal experiment, it was essential to perform its phenolic characterization by HPLC-ESI-MS/MS. The results of this technique showed that (+)-catechin and (-)-epicatechin were among the most predominant

phenolic compounds contained in the GSPE extract. Therefore, our third objective was **to determine the role of (+)-catechin and (-)-epicatechin in the clock-synchronizing and metabolic-enhancing effects of GSPE in NAFLD.** We addressed this goal by using an *in vitro* model consisting of a hepatocyte derived AML12 cell line that has been stably transfected by a luciferase gene which is transcriptionally driven by the *Bmal1* promoter. By measuring luminescence rhythms mediated by *Bmal1* 5' untranslated region with a special equipment (LumiCycle incubator), we were able to study the influence of these two phenolic compounds on the liver circadian clock in an obesogenic environment (by using palmitic acid). After co-culturing the cells with palmitate and (+)-catechin or (-)-epicatechin (10 or 100 uM) and not observing any significant impact on the circadian expression of *Bmal1-luc*, which could be related to the limitations of an *in vitro* study, we decided to pre-treat the cells with the phenolic compounds before exposing them to palmitate. Results from this work showed a decrease in *Bmal1-luc* amplitude caused by palmitate treatment. Surprisingly, only cells that were pre-treated with (+)-catechin showed a restoration of amplitude, with an improvement from the decreasing amplitude produced by palmitate treatment. Moreover, (+)-catechin pre-treatment also corrected the phase delay and the increasing of the period observed in the palmitate-treated cells. To further determine the effects of these phenolic compounds on liver metabolism, we analyzed the expression of glucose and lipid related metabolic genes of AML12 *Bmal1::Luc* hepatocyte-derived cells. In the same line as the bioluminescence assay, we observed that only (+)-catechin treatment was able to mitigate the effects of palmitate over the expression of *Gk*, *Gys2*, *G6pc* and *Acaca*, key enzymes in gluconeogenesis and lipogenesis pathways, whereas an ameliorative effect of (-)-epicatechin was only observed in *G6pc* expression.

There are several *in vitro* studies demonstrating the antioxidant and anti-inflammatory properties of (+)-catechin treatment, as it is capable of inducing changes in major enzymes that participates in oxidative stress, and

also of influencing gene expression of Nrf2 and NF-kB inflammatory pathways thereby exerting hepatoprotective effects against liver damages [44–46]. Moreover, (+)-catechin has also been shown to exert anti-obesity properties in 3T3-L1 adipocytes, as it strongly inhibited differentiation of 3T3-L1 preadipocytes via regulating the C/EBPs/PPARγ/SREBP1C pathway. In addition, (+) catechin was shown to promote the lipid decomposition of mature adipocytes by regulating the cAMP/PKA pathways, demonstrating anti-adipogenesis effects [47]. Thus, it is possible to suggest that the effect of GSPE in rescuing the hepatic clock rhythmicity disturbances caused by an obesogenic diet, can be attributed to (+)-catechin molecular impact on *Bmal1* driven circadian expression, thereby controlling the transcription of genes involved in crucial metabolic pathways.

As the Earth rotates on its axis, which in turn causes day and night, it also orbits the sun. It takes about 365 days for the Earth to make one complete circle around the sun, generating the seasons. In order to cope with predictable seasonal changes in their environments, almost all living organisms have genetically evolved by acquiring timing adaptation mechanisms. These mechanisms control the seasonal cycles in physiology and behavior, optimizing survival and reproduction, and are known as circannual rhythms [48]. In this regard, our fourth objective was **to determine the impact of seasonal variations in day length on the effects of GSPE consumption over the hepatic clock and the lipid and carbohydrate metabolism of healthy rats** (Manuscript 3). To achieve this goal, STD diet fed-rats were chronically exposed during 9 weeks to three different photoperiods to mimic the day length of different seasons: standard photoperiod (L12, 12 h light/12 h darkness), long photoperiod (L18, 18 h light/6 h darkness), and short photoperiod (L6, 6 h light/18 h darkness), and were treated either with GSPE or VH during the last 4 weeks.

Several studies have shown that exposure to different day length schedules has an impact on the physiology, on body weight gain as rats exposed to short photoperiod increased their body mass compared to the standard

behavior, and reproduction of animals [49–51]. In this regard, we observed a clear photoperiod effect photoperiod group, independently of the treatment, which could be related to a short sleep duration due to photoperiod exposure in L6 animals, as sleep deprivation has been linked to increasing risk of weight gain [52].

In addition, our results showed a season-dependent modulation of GSPE on lipid and glucose metabolism in healthy rats, as the effect of GSPE on the expression of liver clock genes and genes involved in crucial metabolic pathways, hepatic triglycerides levels, serum parameters, as well as on hormone and hepatic metabolites levels, were strongly influenced by the exposure to different photoperiods. In this sense, we observed a downregulation in the expression of *Acaca* in L18-GSPE rats, which was not observed in L6-GSPE animals. This could be linked to the increase in corticosterone levels in L6-GSPE rats as it has been demonstrated that glucocorticoids increase fat accumulation and glucose production in the liver [53,54]. In line with this result, GSPE-treated rats exposed to L6 photoperiod exhibited higher hepatic triglycerides levels compared to its L12 and L18 counterparts and showed a decrease in *Sirt1* expression compared to its control. In this regard, according to another study, hepatic lipid concentrations negatively correlated with *Sirt1* transcript levels in animals supplemented with GSPE [43]. Interestingly, another result where the season-dependent differential effect of GSPE was evidenced involved cholesterol and LDL levels. Thus, GSPE was not able to reduce the serum cholesterol levels in rats exposed to the short photoperiod, whereas anticholesterolemic activity was evident in rats exposed to the long photoperiod reducing LDL cholesterol levels. Furthermore, L18-GSPE rats showed reduced *Gk* gene expression, consistent with the downregulation of genes involved in lipogenesis, as it was demonstrated that *Gk* expression is needed for the expression of lipogenic genes [55]. Moreover, we observed a decreased expression of ER stress genes in L18-GSPE animals, while the opposite effect was found in L6-GSPE rats, evidencing the role of ER stress

activation in lipid metabolism as it was reported to induce hepatic triglyceride accumulation in mice through activation of SREBP-1c [56]. In addition, concentrations of glucose-related metabolites, including glucose-6-phosphate, fructose-6-phosphate, D-glucose, and D-ribose, might suggest that GSPE is enhancing glycolytic metabolic pathways in animals exposed to the long photoperiod (L18).

Ribas-Latre and collaborators showed that GSPE can modulate melatonin levels in plasma [57]. In this sense, our results showed an increase in melatonin levels only in animals treated with GSPE in L18 compared to its control. This increase of melatonin levels in these rats (L18-GSPE) could also be responsible for the more favorable metabolic landscape in L18-GSPE compared to L6-GSPE animals; which is in agreement with many studies that have shown the protective and ameliorative role of melatonin on liver damage [58–62].

As it has been previously exposed, the molecular clock machinery plays a key role in the regulation of hepatic metabolism. We observed an improvement of *Cry1* and *Nr1d1* gene expression in L18-GSPE rats compared to its control, which could be linked to the downregulation in the expression of lipogenic genes in these rats, thereby regulating metabolic homeostasis. However, our study was limited by the fact that we could only measure the expression of clock genes at one time point (ZT1). Therefore, to confirm this hypothesis, a 24-hour analysis at several different daily time points would be necessary. Thus, under physiological conditions, it seems that the GSPE effect, although not limited to any specific photoperiod, is particularly relevant under L18 conditions. Based on the results, we demonstrate that the season of the year in which GSPE is consumed could likely modify its ability to modulate hepatic lipid and glucose metabolism, and consequently, its capacity to restore metabolic disorders.

Once we demonstrated that photoperiod could influence the molecular effects of GSPE on liver metabolism, our last objective was **to determine**

how an obesogenic diet intake affects GSPE metabolic responses to seasonal variations. To achieve this, rats were chronically exposed to three different photoperiods (L12, L18 and L6), were fed with CAF diet and were treated either with GSPE or VH. The results demonstrate significant alterations on biochemical and liver lipid profile, on hepatic clock and metabolic genes expression and on levels of serum and liver metabolites due to CAF-diet intake, which vary according to the photoperiod, thus influencing the beneficial effects of GSPE consumption against obesity and fatty liver.

In this sense, we observed profound changes in serum parameters of CAF-fed animals subjected to L12 photoperiod, with increased glucose, total cholesterol, and triglycerides levels, that were improved by the chronic administration of GSPE. Furthermore, procyanidins also decreased body weight gain in these animals. These results agree with previous studies showing an improvement in serum biochemical parameters and reduction of body weight gain by GSPE treatment in obese rats under standard 12 h light/12 h dark cycle [63–66]. In addition, we observed higher lipid accumulation in the liver of CAF-fed rats exposed to L18 and L6 compared to L12 photoperiod, which demonstrates the influence of photoperiod in the hepatic lipid levels of obese rats. Interestingly, similar results were observed in L6 normal-weight rats (Manuscript 3), as well as in HFD-fed rats [67].

The effects of chronic GSPE administration in the mRNA expression levels of clock/clock-controlled genes in the liver as well as of hepatic metabolic genes seems to be photoperiod-responsive in obese rats, which is consistent with what has been previously observed in STD diet-fed rats (Manuscript 3). It has been reported that GSPE is able to modulate hepatic *Nampt* gene expression, thus regulating intracellular NAD+ levels [25] and *Sirt1* gene expression [43]. Remarkably, this GSPE effect was only observed under L12 conditions, playing an important role in the improvements seen in the levels of serum triglycerides and total cholesterol. Additionally, *Cd36* and *Fatp5*

expression levels, which are thought to protect liver cells from metabolic stress and lipid overload [68,69], were both significantly elevated only in L12-CAF-GSPE rats.

A strong interaction between photoperiod and CAF-diet was observed in the expressions of *Bmal1*, *Per2* and *Nr1d1* genes. In this sense, *Bmal1* was found downregulated in L6-CAF-VH animals but upregulated in L18-CAF-VH rats compared to their respective lean controls. CAF-diet also increased the levels of *Per2* and *Nr1d1*, but only in animals exposed to short photoperiod. Alterations in the circadian clock machinery have been shown to be associated with the development and worsening of metabolic diseases [70]. Interestingly, it has been shown that *Nr1d1* serves as a link between circadian system and metabolism, as it is involved in lipid and bile acid homeostasis [71]. In this regard, GSPE treatment was able to decrease expression of this gene in L6-CAF-GSPE animals, thus improving lipid metabolism, which was reflected by the decrease in serum triglyceride levels in these animals. The upregulation of *Bmal1* expression found in CAF-VH animals under L18 conditions was not observed in L18 animals treated with GSPE compared to the lean control group. Since *Bmal1* is involved in *de novo* lipid synthesis in the liver [72], these results correlate with the downregulation of expression levels of lipogenic genes such as SREBP-1c and its direct target *Acaca,* which mediate the rate-limiting step of fatty acid synthesis, in L18-CAF-VH compared to its healthy control.

The influence of photoperiod and CAF-diet was also evidenced in the concentrations of serum metabolites. Altered levels of some of these metabolites due to CAF-diet intake were found to vary photoperiodically, thus influencing the restorative effects of GSPE in a photoperiod-dependent manner. In L12 condition, GSPE reduced the increase of serum proline, 4-hydroxyproline and 3-Phosphoglyceric acid, metabolites involved in key metabolic pathways such as gluconeogenesis, glycine, serine and threonine metabolism, protein synthesis and structure and antioxidative reactions [73–77]. In L18 photoperiod, GSPE was able to restore the levels of

branched-chain amino acids (BCAAs) leucine, isoleucine, and valine as well as of methionine, all essential amino acid that play a critical role in the regulation of energy homeostasis, lipid metabolism, oxidative stress, gut health, immunity, and metabolic diseases [78,79]. On the other hand, in L6 photoperiod, GSPE increased the levels of metabolites reported to exert anti-obesity effects, such as oxalic acid, which inhibited lipase activity *in vitro* [80], and 2-hydroxybutyric acid, which reduced serum triglyceride levels in HFD rats [81]. This fact is consistent with the results observed in serum levels of L6-CAF-GSPE rats. Furthermore, GSPE treatment was effective in decreasing serum d-fructose levels, restoring them to values comparable to those of healthy controls.

Remarkably, the results of liver metabolome showed two common discriminative metabolites in L12 and L18 CAF-GSPE animals compared to their respective CAF-VH counterparts. On the one hand, concentration of citric acid, a critical metabolite for TCA cycle, was found to increase in animals treated with GSPE. On the other hand, hepatic adenine was decreased in these animals suggesting a possible alteration in mitochondrial function due to CAF-diet intake [82]. In L6 CAF-GSPE animals, a decrease in the hepatic metabolite glucose 6-phosphate was observed compared to CAF-VH rats, which was consistent with the results of significant higher blood glucose levels in the CAF-VH group compared to the STD-VH group, that was not observed in CAF-GSPE animals. Additionally, increased hepatic levels of glycerol and d-xylitol were observed in L6-CAF-GSPE animals. Interestingly, these metabolites are involved in important metabolic pathways and their supplementation has been shown to mitigate the detrimental effects of obesity and fatty liver [83,84]. Therefore, based on the distinct photoperiod-dependent effects of GSPE consumption, it could be suggested that seasonal changes in day length and obesity-induced metabolic deficiencies could be driving these effects. Hence, it appears that the beneficial effects of GSPE on MS and obesity are most effective under a 12 h light-12 h dark cycle.

Overall, the results obtained demonstrate that the effects of GSPE consumption on liver metabolism are strongly influenced by diurnal and seasonal rhythms and suggest that biological rhythms should be taken into consideration when studying the therapeutic actions of bioactive compounds in MS-associated diseases.

REFERENCES

1. Dibner, C.; Schibler, U.; Albrecht, U. The Mammalian Circadian Timing System: Organization and Coordination of Central and Peripheral Clocks. *http://dx.doi.org/10.1146/annurev-physiol-021909-135821* **2010**, *72*, 517–549, doi:10.1146/ANNUREV-PHYSIOL-021909-135821.
2. Sahar, S.; Sassone-Corsi, P. Regulation of Metabolism: The Circadian Clock Dictates the Time. *Trends in Endocrinology & Metabolism* **2012**, *23*, 1–8, doi:10.1016/J.TEM.2011.10.005.
3. Gerhart-Hines, Z.; Lazar, M.A. Circadian Metabolism in the Light of Evolution. *Endocrine Reviews* **2015**, *36*, 289–304, doi:10.1210/ER.2015-1007.
4. Bhadra, U.; Thakkar, N.; Das, P.; Pal Bhadra, M. Evolution of Circadian Rhythms: From Bacteria to Human. *Sleep Medicine* **2017**, *35*, 49–61, doi:10.1016/J.SLEEP.2017.04.008.
5. Sukumaran, S.; Almon, R.R.; DuBois, D.C.; Jusko, W.J. Circadian Rhythms in Gene Expression: Relationship to Physiology, Disease, Drug Disposition and Drug Action. *Advanced Drug Delivery Reviews* **2010**, *62*, 904–917, doi:10.1016/J.ADDR.2010.05.009.
6. Jordan, S.D.; Lamia, K.A. AMPK at the Crossroads of Circadian Clocks and Metabolism. *Mol Cell Endocrinol* **2013**, *366*, 163, doi:10.1016/J.MCE.2012.06.017.
7. Eckel-Mahan, K.L.; Patel, V.R.; Mohney, R.P.; Vignola, K.S.; Baldi, P.; Sassone-Corsi, P. Coordination of the Transcriptome and Metabolome by the Circadian Clock. *Proc Natl Acad Sci U S A* **2012**, *109*, 5541–5546, doi:10.1073/PNAS.1118726109/SUPPL_FILE/SD04.XLSX.
8. Zhang, R.; Lahens, N.F.; Ballance, H.I.; Hughes, M.E.; Hogenesch, J.B. A Circadian Gene Expression Atlas in Mammals: Implications for Biology and Medicine. *Proc Natl Acad Sci U S A* **2014**, *111*, 16219–16224, doi:10.1073/PNAS.1408886111.
9. Yang, X.; Downes, M.; Yu, R.T.; Bookout, A.L.; He, W.; Straume, M.; Mangelsdorf, D.J.; Evans, R.M. Nuclear Receptor Expression Links the Circadian Clock to Metabolism. *Cell* **2006**, *126*, 801–810, doi:10.1016/J.CELL.2006.06.050.
10. Roenneberg, T.; Allebrandt, K. v.; Merrow, M.; Vetter, C. Social Jetlag and Obesity. *Curr Biol* **2012**, *22*, 939–943, doi:10.1016/J.CUB.2012.03.038.

11. Ruger, M.; Scheer, F.A.J.L. Effects of Circadian Disruption on the Cardiometabolic System. *Reviews in Endocrine and Metabolic Disorders* **2009**, *10*, 245–260, doi:10.1007/S11154-009-9122-8/FIGURES/1.

12. Froy, O. The Relationship between Nutrition and Circadian Rhythms in Mammals. *Frontiers in Neuroendocrinology* **2007**, *28*, 61–71, doi:10.1016/J.YFRNE.2007.03.001.

13. Vasam, G.; Reid, K.; Burelle, Y.; Menzies, K.J. Nutritional Regulation of Mitochondrial Function. *Mitochondria in Obesity and Type 2 Diabetes: Comprehensive Review on Mitochondrial Functioning and Involvement in Metabolic Diseases* **2019**, 93–126, doi:10.1016/B978-0-12-811752-1.00004-3.

14. Li, S.; Tan, H.Y.; Wang, N.; Cheung, F.; Hong, M.; Feng, Y. The Potential and Action Mechanism of Polyphenols in the Treatment of Liver Diseases. *Oxidative Medicine and Cellular Longevity* **2018**, *2018*, doi:10.1155/2018/8394818.

15. Terra, X.; Montagut, G.; Bustos, M.; Llopiz, N.; Ardèvol, A.; Bladé, C.; Fernández-Larrea, J.; Pujadas, G.; Salvadó, J.; Arola, L.; et al. Grape-Seed Procyanidins Prevent Low-Grade Inflammation by Modulating Cytokine Expression in Rats Fed a High-Fat Diet. *The Journal of Nutritional Biochemistry* **2009**, *20*, 210–218, doi:10.1016/J.JNUTBIO.2008.02.005.

16. Montagut, G.; Bladé, C.; Blay, M.; Fernández-Larrea, J.; Pujadas, G.; Salvadó, M.J.; Arola, L.; Pinent, M.; Ardévol, A. Effects of a Grapeseed Procyanidin Extract (GSPE) on Insulin Resistance. *The Journal of Nutritional Biochemistry* **2010**, *21*, 961–967, doi:10.1016/J.JNUTBIO.2009.08.001.

17. Pons, Z.; Margalef, M.; Bravo, F.I.; Arola-Arnal, A.; Muguerza, B. Chronic Administration of Grape-Seed Polyphenols Attenuates the Development of Hypertension and Improves Other Cardiometabolic Risk Factors Associated with the Metabolic Syndrome in Cafeteria Diet-Fed Rats. *British Journal of Nutrition* **2017**, *117*, 200–208, doi:10.1017/S0007114516004426.

18. Yang, J.; Xiao, Y.Y. Grape Phytochemicals and Associated Health Benefits. *http://dx.doi.org/10.1080/10408398.2012.692408* **2013**, *53*, 1202–1225, doi:10.1080/10408398.2012.692408.

19. Quesada, H.; del Bas, J.M.; Pajuelo, D.; Díaz, S.; Fernandez-Larrea, J.; Pinent, M.; Arola, L.; Salvadó, M.J.; Bladé, C. Grape Seed Proanthocyanidins Correct Dyslipidemia Associated with a High-Fat Diet in Rats and Repress Genes Controlling Lipogenesis and VLDL Assembling in Liver. *International Journal of Obesity 2009 33:9* **2009**, *33*, 1007–1012, doi:10.1038/ijo.2009.136.

20. Pajuelo, D.; Fernández-Iglesias, A.; Díaz, S.; Quesada, H.; Arola-Arnal, A.; Bladé, C.; Salvadó, J.; Arola, L. Improvement of Mitochondrial Function in Muscle of Genetically Obese Rats after Chronic Supplementation with Proanthocyanidins. *Journal of Agricultural and Food Chemistry* **2011**, *59*, 8491–8498, doi:10.1021/jf201775v.

21. Pajuelo, D.; Quesada, H.; Díaz, S.; Fernández-Iglesias, A.; Arola-Arnal, A.; Bladé, C.; Salvadó, J.; Arola, L. Chronic Dietary Supplementation of Proanthocyanidins Corrects the Mitochondrial Dysfunction of Brown Adipose Tissue Caused by Diet-Induced Obesity in Wistar Rats. *British*

Journal of Nutrition **2012**, *107*, 170–178, doi:10.1017/S0007114511002728.

22. Ribas-Latre, A.; Baselga-Escudero, L.; Casanova, E.; Arola-Arnal, A.; Salvadó, M.J.; Arola, L.; Bladé, C. Chronic Consumption of Dietary Proanthocyanidins Modulates Peripheral Clocks in Healthy and Obese Rats. *The Journal of Nutritional Biochemistry* **2015**, *26*, 112–119, doi:10.1016/J.JNUTBIO.2014.09.006.

23. Hatori, M.; Vollmers, C.; Zarrinpar, A.; DiTacchio, L.; Bushong, E.A.; Gill, S.; Leblanc, M.; Chaix, A.; Joens, M.; Fitzpatrick, J.A.J.; et al. Time-Restricted Feeding without Reducing Caloric Intake Prevents Metabolic Diseases in Mice Fed a High-Fat Diet. *Cell Metabolism* **2012**, *15*, 848–860, doi:10.1016/J.CMET.2012.04.019/ATTACHMENT/7B05100A-A251-4932-AB75-1C551D89FE42/MMC2.XLS.

24. Branecky, K.L.; Niswender, K.D.; Pendergast, J.S. Disruption of Daily Rhythms by High-Fat Diet Is Reversible. *PLOS ONE* **2015**, *10*, e0137970, doi:10.1371/JOURNAL.PONE.0137970.

25. Ribas-Latre, A.; Baselga-Escudero, L.; Casanova, E.; Arola-Arnal, A.; Salvadó, M.-J.; Bladé, C.; Arola, L. Dietary Proanthocyanidins Modulate BMAL1 Acetylation, Nampt Expression and NAD Levels in Rat Liver OPEN. *Scientific RepoRts* | **2015**, *5*, 10954, doi:10.1038/srep10954.

26. Jacobi, D.; Liu, S.; Burkewitz, K.; Kory, N.; Knudsen, N.H.; Alexander, R.K.; Unluturk, U.; Li, X.; Kong, X.; Hyde, A.L.; et al. Hepatic Bmal1 Regulates Rhythmic Mitochondrial Dynamics and Promotes Metabolic Fitness. *Cell Metabolism* **2015**, *22*, 709–720, doi:10.1016/j.cmet.2015.08.006.

27. Martínez-reyes, I.; Chandel, N.S. Mitochondrial TCA Cycle Metabolites Control. *Nature Communications* **2020**, 1–11, doi:10.1038/s41467-019-13668-3.

28. Froy, O. Metabolism and Circadian Rhythms—Implications for Obesity. *Endocrine Reviews* **2010**, *31*, 1–24, doi:10.1210/ER.2009-0014.

29. Zhang, Y.; Papazyan, R.; Damle, M.; Fang, B.; Jager, J.; Feng, D.; Peed, L.C.; Guan, D.; Sun, Z.; Lazar, M.A. The Hepatic Circadian Clock Fine-Tunes the Lipogenic Response to Feeding through RORα/γ. *Genes Dev* **2017**, *31*, 1202–1211, doi:10.1101/GAD.302323.117.

30. Lamia, K.A.; Storch, K.-F.; Weitz, C.J. Physiological Significance of a Peripheral Tissue Circadian Clock. *Harvard Medical School* **2008**.

31. Pan, X.; Bradfield, C.A.; Hussain, M.M. Global and Hepatocyte-Specific Ablation of Bmal1 Induces Hyperlipidaemia and Enhances Atherosclerosis. *Nature Communications 2016 7:1* **2016**, *7*, 1–15, doi:10.1038/ncomms13011.

32. Gnocchi, D.; Pedrelli, M.; Pedrelli, M.; Hurt-Camejo, E.; Parini, P. Lipids around the Clock: Focus on Circadian Rhythms and Lipid Metabolism. *Biology (Basel)* **2015**, *4*, 104–132, doi:10.3390/BIOLOGY4010104.

33. Sinturel, F.; Gerber, A.; Mauvoisin, D.; Wang, J.; Gatfield, D.; Stubblefield, J.J.; Green, C.B.; Gachon, F.; Schibler, U. Diurnal Oscillations in Liver Mass and Cell Size Accompany Ribosome Assembly Cycles. *Cell* **2017**, *169*, 651-

663.e14, doi:10.1016/J.CELL.2017.04.015/ATTACHMENT/C0BF0EEE-43F1-400B-A84A-FA2B40FA2E17/MMC1.DOCX.

34. Anand, U.; Anand, C. v. Connecting Links between the Urea Cycle and the TCA Cycle: A Tutorial Exercise. *Biochemical Education* **1999**, *27*, 153–154, doi:10.1016/S0307-4412(99)00041-2.

35. Ajaz, S.; McPhail, M.J.; Gnudi, L.; Trovato, F.M.; Mujib, S.; Napoli, S.; Carey, I.; Agarwal, K. Mitochondrial Dysfunction as a Mechanistic Biomarker in Patients with Non-Alcoholic Fatty Liver Disease (NAFLD). *Mitochondrion* **2021**, *57*, 119–130, doi:10.1016/J.MITO.2020.12.010.

36. Zhou, J.; Tang, L.; Shen, C.L.; Wang, J.S. Green Tea Polyphenols Boost Gut-Microbiota-Dependent Mitochondrial TCA and Urea Cycles in Sprague–Dawley Rats. *The Journal of Nutritional Biochemistry* **2020**, *81*, 108395, doi:10.1016/J.JNUTBIO.2020.108395.

37. Rajput, S.A.; Sun, L.; Zhang, N.; Khalil, M.M.; Gao, X.; Ling, Z.; Zhu, L.; Khan, F.A.; Zhang, J.; Qi, D. Ameliorative Effects of Grape Seed Proanthocyanidin Extract on Growth Performance, Immune Function, Antioxidant Capacity, Biochemical Constituents, Liver Histopathology and Aflatoxin Residues in Broilers Exposed to Aflatoxin B1. *Toxins 2017, Vol. 9, Page 371* **2017**, *9*, 371, doi:10.3390/TOXINS9110371.

38. Bian, J.T.; Bhargava, H.N. Protective Effects of Grape Seed Proanthocyanidins and Selected Antioxidants against TPA-Induced Hepatic and Brain Lipid Peroxidation and DNA Fragmentation, and Peritoneal Macrophage Activation in Mice. *General Pharmacology: The Vascular System* **1998**, *30*, 771–776, doi:10.1016/S0306-3623(97)00332-7.

39. Devi, S.A.; Jolitha, A.B.; Ishii, N. Grape Seed Proanthocyanidin Extract (GSPE) and Antioxidant Defense in the Brain of Adult Rats. *Medical Science Monitor : International Medical Journal of Experimental and Clinical Research* **2006**, *12*, BR124-9.

40. Puiggròs, F.; Llópiz, N.; Ardévol, A.; Bladé, C.; Arola, L.; Salvadó, M.J. Grape Seed Procyanidins Prevent Oxidative Injury by Modulating the Expression of Antioxidant Enzyme Systems. *Journal of Agricultural and Food Chemistry* **2005**, *53*, 6080–6086, doi:10.1021/JF050343M.

41. Rongvaux, A.; Andris, F.; van Gool, F.; Leo, O. Reconstructing Eukaryotic NAD Metabolism. *BioEssays* **2003**, *25*, 683–690, doi:10.1002/BIES.10297.

42. Lin, S.J.; Guarente, L. Nicotinamide Adenine Dinucleotide, a Metabolic Regulator of Transcription, Longevity and Disease. *Current Opinion in Cell Biology* **2003**, *15*, 241–246, doi:10.1016/S0955-0674(03)00006-1.

43. Aragonès, G.; Suárez, M.; Ardid-Ruiz, A.; Vinaixa, M.; Rodríguez, M.A.; Correig, X.; Arola, L.; Bladé, C. Dietary Proanthocyanidins Boost Hepatic NAD + Metabolism and SIRT1 Expression and Activity in a Dose-Dependent Manner in Healthy Rats. *Nature Publishing Group* **2016**, doi:10.1038/srep24977.

44. Kalender, Y.; Yel, M.; Kalender, S. Doxorubicin Hepatotoxicity and Hepatic Free Radical Metabolism in Rats: The Effects of Vitamin E and Catechin. *Toxicology* **2005**, *209*, 39–45, doi:10.1016/J.TOX.2004.12.003.

45. Baranwal, A.; Aggarwal, P.; Rai, A.; Kumar, N. Pharmacological Actions and Underlying Mechanisms of Catechin: A Review. *Mini-Reviews in Medicinal Chemistry* **2021**, *22*, 821–833, doi:10.2174/1389557521666210902162120.

46. Kobayashi, H.; Tanaka, Y.; Asagiri, K.; Asakawa, T.; Tanikawa, K.; Kage, M.; Yagi, M. The Antioxidant Effect of Green Tea Catechin Ameliorates Experimental Liver Injury. *Phytomedicine* **2010**, *17*, 197–202, doi:10.1016/J.PHYMED.2009.12.006.

47. Jiang, Y.; Ding, S.; Li, F.; Zhang, C.; Sun-Waterhouse, D.; Chen, Y.; Li, D. Effects of (+)-Catechin on the Differentiation and Lipid Metabolism of 3T3-L1 Adipocytes. *Journal of Functional Foods* **2019**, *62*, 103558, doi:10.1016/J.JFF.2019.103558.

48. Helm, B.; Lincoln, G.A. Circannual Rhythms Anticipate the Earth's Annual Periodicity. *Biological Timekeeping: Clocks, Rhythms and Behaviour* **2017**, 545–569, doi:10.1007/978-81-322-3688-7_26.

49. Heideman, P.D.; Sylvester, C.J. Reproductive Photoresponsiveness in Unmanipulated Male Fischer 344 Laboratory Rats. *Biology of Reproduction* **1997**, *57*, 134–138, doi:10.1095/BIOLREPROD57.1.134.

50. Tavolaro, F.M.; Thomson, L.M.; Ross, A.W.; Morgan, P.J.; Helfer, G. Photoperiodic Effects on Seasonal Physiology, Reproductive Status and Hypothalamic Gene Expression in Young Male F344 Rats. *Journal of Neuroendocrinology* **2015**, *27*, 79–87, doi:10.1111/JNE.12241.

51. Ross, A.W.; Helfer, G.; Russell, L.; Darras, V.M.; Morgan, P.J. Thyroid Hormone Signalling Genes Are Regulated by Photoperiod in the Hypothalamus of F344 Rats. *PLOS ONE* **2011**, *6*, e21351, doi:10.1371/JOURNAL.PONE.0021351.

52. Patel, S.R.; Hu, F.B. Short Sleep Duration and Weight Gain: A Systematic Review. *Obesity* **2008**, *16*, 643–653, doi:10.1038/OBY.2007.118.

53. Rockall, A.G.; Sohaib, S.A.; Evans, D.; Kaltsas, G.; Isidori, A.M.; Monson, J.P.; Besser, G.M.; Grossman, A.B.; Reznek, R.H. Hepatic Steatosis in Cushing's Syndrome: A Radiological Assessment Using Computed Tomography. *European Journal of Endocrinology* **2003**, *149*, 543–548, doi:10.1530/EJE.0.1490543.

54. Amatruda, J.M.; Livingston, J.N.; Lockwood, D.H. Cellular Mechanisms in Selected States of Insulin Resistance: Human Obesity, Glucocorticoid Excess, and Chronic Renal Failure. *Diabetes/Metabolism Reviews* **1985**, *1*, 293–317, doi:10.1002/dmr.5610010304.

55. Dentin, R.; Pé, J.-P.; Benhamed, F.; Foufelle, F.; Ferré, P.; Ronique Fauveau, V.; Magnuson, M.A.; Girard, J.; Postic, C. Hepatic Glucokinase Is Required for the Synergistic Action of ChREBP and SREBP-1c on Glycolytic and Lipogenic Gene Expression*. **2004**, doi:10.1074/jbc.M312475200.

56. Kim, Y.R.; Lee, E.J.; Shin, K.O.; Kim, M.H.; Pewzner-Jung, Y.; Lee, Y.M.; Park, J.W.; Futerman, A.H.; Park, W.J. Hepatic Triglyceride Accumulation via Endoplasmic Reticulum Stress-Induced SREBP-1 Activation Is Regulated by Ceramide Synthases. *Exp Mol Med* **2019**, *51*, doi:10.1038/S12276-019-0340-1.

57. Ribas-Latre, A.; del Bas, J.M.; Baselga-Escudero, L.; Casanova, E.; Arola-Arnal, A.; Salvadó, M.J.; Arola, L.; Bladé, C. Dietary Proanthocyanidins Modulate Melatonin Levels in Plasma and the Expression Pattern of Clock Genes in the Hypothalamus of Rats. *Molecular Nutrition & Food Research* **2015**, *59*, 865–878, doi:10.1002/MNFR.201400571.

58. Bonomini, F.; Borsani, E.; Favero, G.; Rodella, L.F.; Rezzani, R. Dietary Melatonin Supplementation Could Be a Promising Preventing/Therapeutic Approach for a Variety of Liver Diseases. *Nutrients 2018, Vol. 10, Page 1135* **2018**, *10*, 1135, doi:10.3390/NU10091135.

59. Zhang, J.-J.; Meng, X.; Li, Y.; Zhou, Y.; Xu, D.-P.; Li, S.; Li, H.-B. Molecular Sciences Effects of Melatonin on Liver Injuries and Diseases. **2017**, doi:10.3390/ijms18040673.

60. Ohta, Y.; Kongo, M.; Sasaki, E.; Nishida, K.; Ishiguro, I. Therapeutic Effect of Melatonin on Carbon Tetrachloride-Induced Acute Liver Injury in Rats. *Journal of Pineal Research* **2000**, *28*, 119–126, doi:10.1034/J.1600-079X.2001.280208.X.

61. Tahan, G.; Akin, H.; Aydogan, F.; Ramadan, S.S.; Yapicier, O.; Tarcin, O.; Uzun, H.; Tahan, V.; Zengin, K. Melatonin Ameliorates Liver Fibrosis Induced by Bile-Duct Ligation in Rats. *Canadian Journal of Surgery* **2010**, *53*, 313.

62. Chojnacki, C.; Walecka-Kapica, E.; Romanowski, M.; Chojnacki, J.; Klupinska, G. Protective Role of Melatonin in Liver Damage.

63. Pascual-Serrano, A.; Arola-Arnal, A.; Suárez-García, S.; Bravo, F.I.; Suárez, M.; Arola, L.; Bladé, C. Grape Seed Proanthocyanidin Supplementation Reduces Adipocyte Size and Increases Adipocyte Number in Obese Rats. *International Journal of Obesity 2017 41:8* **2017**, *41*, 1246–1255, doi:10.1038/ijo.2017.90.

64. Pascual-Serrano, A.; Bladé, C.; Suárez, M.; Arola-Arnal, A. Grape Seed Proanthocyanidins Improve White Adipose Tissue Expansion during Diet-Induced Obesity Development in Rats. *International Journal of Molecular Sciences 2018, Vol. 19, Page 2632* **2018**, *19*, 2632, doi:10.3390/IJMS19092632.

65. Pons, Z.; Margalef, M.; Bravo, F.I.; Arola-Arnal, A.; Muguerza, B. Chronic Administration of Grape-Seed Polyphenols Attenuates the Development of Hypertension and Improves Other Cardiometabolic Risk Factors Associated with the Metabolic Syndrome in Cafeteria Diet-Fed Rats. *British Journal of Nutrition* **2017**, *117*, 200–208, doi:10.1017/S0007114516004426.

66. Serrano, J.; Casanova-Martí, À.; Gual, A.; Maria Pérez-Vendrell, A.; Teresa Blay, M.; Terra, X.; Ardévol, A.; Pinent, M. A Specific Dose of Grape Seed-Derived Proanthocyanidins to Inhibit Body Weight Gain Limits Food Intake and Increases Energy Expenditure in Rats. *Eur J Nutr* **2017**, *56*, 1629–1636, doi:10.1007/s00394-016-1209-x.

67. Ross, A.W.; Russell, L.; Helfer, G.; Thomson, L.M.; Dalby, M.J.; Morgan, P.J. Photoperiod Regulates Lean Mass Accretion, but Not Adiposity, in Growing F344 Rats Fed a High Fat Diet. **2015**, doi:10.1371/journal.pone.0119763.

68. Enooku, K.; Tsutsumi, T.; Kondo, M.; Fujiwara, N.; Sasako, T.; Shibahara, J.; Kado, A.; Okushin, K.; Fujinaga, H.; Nakagomi, R.; et al. Hepatic FATP5

Expression Is Associated with Histological Progression and Loss of Hepatic Fat in NAFLD Patients. *Journal of Gastroenterology* **2020**, *55*, 227–243, doi:10.1007/S00535-019-01633-2/TABLES/5.

69. Garbacz, W.G.; Lu, P.; Miller, T.M.; Poloyac, S.M.; Eyre, N.S.; Mayrhofer, G.; Xu, M.; Ren, S.; Xie, W. Hepatic Overexpression of CD36 Improves Glycogen Homeostasis and Attenuates High-Fat Diet-Induced Hepatic Steatosis and Insulin Resistance. *Molecular and Cellular Biology* **2016**, *36*, 2715–2727, doi:10.1128/MCB.00138-16/ASSET/881F280B-A2F4-4C5C-8996-A74C0CB54D83/ASSETS/GRAPHIC/ZMB9991013350007.JPEG.

70. Yang, S.C.; Shieh, K.R. Implications of Circadian Rhythms on Metabolic Disorders. *Tzu Chi Medical Journal* **2009**, *21*, 285–288, doi:10.1016/S1016-3190(09)60057-4.

71. Duez, H.; Staels, B. Rev-Erb-α: An Integrator of Circadian Rhythms and Metabolism. *Journal of Applied Physiology* **2009**, *107*, 1972–1980, doi:10.1152/JAPPLPHYSIOL.00570.2009/ASSET/IMAGES/LARGE/ZDG01 20987720003.JPEG.

72. Zhang, D.; Tong, X.; Arthurs, B.; Guha, A.; Rui, L.; Kamath, A.; Inoki, K.; Yin, L. Liver Clock Protein BMAL1 Promotes de Novo Lipogenesis through Insulin-MTORC2-AKT Signaling. *Journal of Biological Chemistry* **2014**, *289*, 25925–25935, doi:10.1074/JBC.M114.567628.

73. Wu, G.; Bazer, F.W.; Burghardt, R.C.; Johnson, G.A.; Kim, S.W.; Knabe, D.A.; Li, P.; Li, X.; McKnight, J.R.; Satterfield, M.C.; et al. Proline and Hydroxyproline Metabolism: Implications for Animal and Human Nutrition. *Amino Acids* **2011**, *40*, 1053, doi:10.1007/S00726-010-0715-Z.

74. Arutyunov, D.Y.; Muronetz, V.I. The Activation of Glycolysis Performed by the Nonphosphorylating Glyceraldehyde-3-Phosphate Dehydrogenase in the Model System q.

75. Toews, C.J.; Lowy, C.; Ruderman, N.B. The Regulation of Gluconeogenesis: THE EFFECT OF PENT-4-ENOIC ACID ON GLUCONEOGENESIS AND ON THE GLUCONEOGENIC METABOLITE CONCENTRATIONS OF ISOLATED PERFUSED RAT LIVER. *Journal of Biological Chemistry* **1970**, *245*, 818–824, doi:10.1016/S0021-9258(18)63338-1.

76. Ray, P.D.; Hanson, R.L.; Lardy, H.A. Inhibition by Hydrazine of Gluconeogenesis in the Rat. *THE JOURNAL cm BIOLOGICAL CHEMISTRY* **1970**, *245*, 690, doi:10.1016/S0021-9258(18)63317-4.

77. Harkness, D.R.; Ponce, J.; Grayson, V. A Comparative Study on the Phosphoglyceric Acid Cycle in Mammalian Erythrocytes. *Comparative Biochemistry and Physiology* **1969**, *28*, 129–138, doi:10.1016/0010-406X(69)91327-9.

78. Nie, C.; He, T.; Zhang, W.; Zhang, G.; Ma, X. Branched Chain Amino Acids: Beyond Nutrition Metabolism. *International Journal of Molecular Sciences 2018, Vol. 19, Page 954* **2018**, *19*, 954, doi:10.3390/IJMS19040954.

79. Martínez, Y.; Li, X.; Liu, G.; Bin, P.; Yan, W.; Más, D.; Valdivié, M.; Hu, C.A.A.; Ren, W.; Yin, Y. The Role of Methionine on Metabolism, Oxidative Stress, and Diseases. *Amino Acids* **2017**, *49*, 2091–2098, doi:10.1007/S00726-017-2494-2/TABLES/1.

80. Liu, T.T.; He, X.R.; Xu, R.X.; Wu, X.B.; Qi, Y.X.; Huang, J.Z.; Chen, Q.H.; Chen, Q.X. Inhibitory Mechanism and Molecular Analysis of Furoic Acid and Oxalic Acid on Lipase. *International Journal of Biological Macromolecules* **2018**, *120*, 1925–1934, doi:10.1016/J.IJBIOMAC.2018.09.150.

81. Li, B.; Hong, Y.; Gu, Y.; Ye, S.; Hu, K.; Yao, J.; Ding, K.; Zhao, A.; Jia, W.; Li, H. Functional Metabolomics Reveals That Astragalus Polysaccharides Improve Lipids Metabolism through Microbial Metabolite 2-Hydroxybutyric Acid in Obese Mice. *Engineering* **2022**, *9*, 111–122, doi:10.1016/J.ENG.2020.05.023.

82. Cardoso, C.M.P.; Moreno, A.J.M.; Almeida, L.M.; Custódio, J.B.A. Comparison of the Changes in Adenine Nucleotides of Rat Liver Mitochondria Induced by Tamoxifen and 4-Hydroxytamoxifen. *Toxicology in Vitro* **2003**, *17*, 663–670, doi:10.1016/S0887-2333(03)00106-1.

83. Rao, G.A.; Riley, D.E.; Larkin, E.C. Fatty Liver Caused by Chronic Alcohol Ingestion Is Prevented by Dietary Supplementation with Pyruvate or Glycerol. *Lipids* **1984**, *19*, 583–588, doi:10.1007/BF02534715.

84. Ur-Rehman, S.; Mushtaq, Z.; Zahoor, T.; Jamil, A.; Murtaza, M.A. Xylitol: A Review on Bioproduction, Application, Health Benefits, and Related Safety Issues. *https://doi.org/10.1080/10408398.2012.702288* **2015**, *55*, 1514–1528, doi:10.1080/10408398.2012.702288.

V. CONCLUSIONS

UNIVERSITAT ROVIRA I VIRGILI
THE INFLUENCE OF BIOLOGICAL RHYTHMS ON THE BENEFICIAL EFFECTS OF GRAPE SEED PROANTHOCYANIDIN EXTRACT (GSPE) ON LIVER METABOLISM IN HEALTH AND DISEASE
Romina Mariel Rodriguez

CONCLUSIONS

The main conclusions of the present thesis are:

1- An obesogenic diet intake leads to hepatic circadian disturbances affecting rhythmic expressions of liver clock and clock-controlled genes in rats.

2- Chronic consumption of 25 mg/kg of GSPE can restore these circadian liver clock disruptions, and this effect is dependent on the timing of administration. This beneficial effect is especially relevant when GSPE is administered at the beginning of the active phase.

2- Chronic consumption of 25 mg/kg of GSPE improves mitochondrial function, by regulating mitochondrial dynamics and increasing the activity of mitochondrial respiratory complexes and levels of TCA cycle metabolites in diet-induced obese rats.

3- The intake of a high-palatable CAF diet impairs hepatic rhythmic expressions of key metabolic genes involved in lipid and glucose metabolism, as well as alters metabolites ´concentrations and rhythmic oscillations in the liver of rats.

4- Chronic administration of 25 mg GSPE/kg modulates and partially restores diurnal oscillations of metabolic genes and metabolites, as well as metabolites concentrations, in a time-of-day-dependent manner.

5- Chronic consumption a dietary dose of GSPE is able to restore the disruption of diurnal oscillation of liver mass caused by the CAF diet intake in rats.

6- GSPE chronic administration at the beginning of the dark phase (ZT12) reduces hepatic triglyceride accumulation and lipid droplets formation ameliorating CAF-induced NAFLD in rats.

7- The improvement in the lipid liver profile obtained only when GSPE is administered at ZT12, might be related to the increase of hepatic NAD+ levels, owing to the fact that NAD+ operates as a link between circadian clocks and liver metabolic function through *Nampt*, *Sirt1* and PCG1α expression.

8- (+)-Catechin restores *Bmal1* circadian expression and improves glucose and lipid related metabolic genes expressions in mouse hepatocyte cell line (AML12) exposed to palmitate treatment (*in vitro* NALFLD model). Thus, it emerges as one of the main GSPE compounds involved in its hepatic clock and metabolic regulation,

9- The exposure to different photoperiods, representing the season's variations on day length, modulates GSPE effect on the hepatic glucose and lipid metabolism in healthy rats.

10- Chronic consumption of GSPE improves metabolic fitness of rats exposed to long photoperiod (L18) by acting on: (a) hepatic clock genes; (b) liver metabolic and ER stress genes; and (c) increasing plasmatic melatonin levels.

11- The effects observed for chronic GSPE consumption at L18 are not observed in rats subjected to a short photoperiod (L6) and treated with GSPE, demonstrating a clear season-dependent influence on the GSPE action on metabolism.

12- The beneficial effects of GSPE chronic consumption against MS-associated disorders vary due to photoperiod exposure.

13- Although GSPE was found to ameliorate some metabolic disturbances caused by the intake of an obesogenic diet in the three different photoperiods, its efficacy was greater in the standard 12 h light-12 h dark condition, indicating that seasonal variations in day length may influence its metabolic effects against MS and obesity.

Based on the results obtained in this thesis, it is suggested that the beneficial effects of GSPE dietary intake against MS-associated disorders, such as obesity, dyslipidaemia and NAFLD, are influenced not only by the time-of-day but also by the time-of-season consumption. Greater benefits are observed when it is consumed at the beginning of the active phase in a 12 h daylight condition.

UNIVERSITAT ROVIRA I VIRGILI
THE INFLUENCE OF BIOLOGICAL RHYTHMS ON THE BENEFICIAL EFFECTS OF GRAPE SEED PROANTHOCYANIDIN EXTRACT (GSPE) ON LIVER METABOLISM IN HEALTH AND DISEASE
Romina Mariel Rodriguez

LIST OF PUBLICATIONS

- **Published articles**

Rodríguez, R. M., Cortés-Espinar, A. J., Soliz-Rueda, J. R., Feillet-Coudray, C., Casas, F., Colom-Pellicer, M., Aragonès, G., Avila-Román, J., Muguerza, B., Mulero, M., & Salvadó, M. J. (2022). Time-of-Day Circadian Modulation of Grape-Seed Procyanidin Extract (GSPE) in Hepatic Mitochondrial Dynamics in Cafeteria-Diet-Induced Obese Rats. *Nutrients*, *14*(4), 774. https://doi.org/10.3390/nu14040774

Colom-Pellicer, M., **Rodríguez, R. M.**, Navarro-Masip, È., Bravo, F. I., Mulero, M., Arola, L., & Aragonès, G. (2022). Time-of-day dependent effect of proanthocyanidins on adipose tissue metabolism in rats with diet-induced obesity. *International Journal of Obesity*, 1-9.

Colom-Pellicer, M., **Rodríguez, R. M.**, Soliz-Rueda, J. R., Assis, L. V. M. de, Navarro-Masip, È., Quesada-Vázquez, S., Escoté, X., Oster, H., Mulero, M., & Aragonès, G. (2022). Proanthocyanidins Restore the Metabolic Diurnal Rhythm of Subcutaneous White Adipose Tissue According to Time-Of-Day Consumption. *Nutrients*, *14*(11), 2246. doi.org/10.3390/nu14112246

Rodríguez, R. M., Colom-Pellicer, M., Blanco, J., Calvo, E., Aragonès, G., & Mulero, M. (2022). Grape-Seed Procyanidin Extract (GSPE) Seasonal-Dependent Modulation of Glucose and Lipid Metabolism in the Liver of Healthy F344 Rats. *Biomolecules*, *12*(6), 839. https://doi.org/10.3390/biom12060839

- **Articles in preparation**

Rodríguez, R. M., Assis, L. V. M. de, Colom-Pellicer, M., Quesada-Vázquez, S., Cruz-Carrión, Á., Escoté, X., Oster, H., Aragonès, G., & Mulero, M. Grape-Seed Procyanidin Extract (GSPE) modulates diurnal oscillations of key hepatic metabolic genes and metabolites alleviating hepatic lipid deposition in cafeteria-fed obese rats in a time-of-day-dependent manner. Prepared for submission to Molecular Metabolism

Rodríguez, R. M., Ruiz de Azua, Ma. J., Sain, J., Gerstner, C., Fariña, A., Bernal, C. A., Muguerza, B., Suárez, M. & Mulero, M. Beneficial effects of bioactive compounds on the prevention or attenuation of liver steatosis induced by diets in experimental animal models.

Rodríguez, R. M., Colom-Pellicer, M., Hernandez-Baixauli, J., Quesada-Vázquez, S., Aragonès, G., & Mulero, M. Photoperiod modulates the metabolic beneficial effect of Grape-Seed Proanthocyanidin Extract (GSPE) in cafeteria-fed obese rats.

POSTER COMUNICATIONS

López-Fernández Sobrino, R., **Rodríguez, R. M**., Mulero, M., Bravo, F. I., Muguerza, B. (2019) A Phenol-enriched Grape-derived decreases Blood Pressure via Sirtuin-1 in spontaneously hypertensive Rats. Conference poster, *NuGOweek 2019, 16th edition From foodomics to nutrigenomics*. September 9-12, 2019. Bern, Switzerland.

López-Fernández Sobrino, R., **Rodríguez, R. M**., Mulero, M., Bravo, F. I., Muguerza, B. (2019) Involvement of endothelial-relaxing factors in the blood pressure lowering effect of a phenol-enriched grape-derived in spontaneously hypertensive rats. Conference poster, *Alimentòmica, XI Seminar on Food and Healthy Lifestyles*. July 23-24, 2019. Barcelona, Spain.

Cortés-Espinar, A. J., **Rodríguez, R. M**., Soliz-Rueda, J. R., Muguerza, B., G., Avila-Román, J., Mulero, M. (2021) Grape Seed Proanthocyanin Extract modulates circadian rhythms of clock genes and inflammation mediated by oxidative stress in dietary obese rats. *The 43rd Congress of the Spanish Society of Biochemical and Molecular Biology*. July 19-22, 2021. Barcelona, Spain.

Rodríguez, R. M., Soliz-Rueda, J. R., Colom-Pellicer, M., Muguerza, B., Aragonès, G., & Mulero, M. (2022). Impacto del consumo del extracto de procianidina de semilla de uva (GSPE) sobre el reloj circadiano hepático en ratas obesas *I Jornadas sobre Nutracéutica: Compuestos bioactivos y Nutracéuticos.* March 3-4, 2022. Tarragona, Spain.

Colom-Pellicer, M., **Rodríguez, R. M**., Mulero, M., & Aragonès, G. (2022). Las proantocianidinas reestablecen el ritmo circadiano del tejido adiposo blanco dependiendo del momento del día en el que se consuman*. I Jornadas sobre Nutracéutica: Compuestos bioactivos y Nutracéuticos.* March 3-4, 2022. Tarragona, Spain.

Rodríguez, R. M., Colom-Pellicer, M., Blanco, J., Aragonès, G., & Mulero, M. (2022). Seasonal dependent effects of Grape Seed Proanthocyanidin Extract (GSPE) on hepatic metabolism of healthy F344 rats. *The 10th International Conference on Polyphenols and Health.* April 20-23, 2022. London, UK.

UNIVERSITAT ROVIRA I VIRGILI
THE INFLUENCE OF BIOLOGICAL RHYTHMS ON THE BENEFICIAL EFFECTS OF GRAPE SEED PROANTHOCYANIDIN EXTRACT (GSPE) ON LIVER METABOLISM IN HEALTH AND DISEASE
Romina Mariel Rodriguez

UNIVERSITAT ROVIRA I VIRGILI
THE INFLUENCE OF BIOLOGICAL RHYTHMS ON THE BENEFICIAL EFFECTS OF GRAPE SEED PROANTHOCYANIDIN EXTRACT (GSPE) ON LIVER METABOLISM IN HEALTH AND DISEASE
Romina Mariel Rodriguez

UNIVERSITAT ROVIRA I VIRGILI
THE INFLUENCE OF BIOLOGICAL RHYTHMS ON THE BENEFICIAL EFFECTS OF GRAPE SEED PROANTHOCYANIDIN EXTRACT (GSPE) ON LIVER METABOLISM IN HEALTH AND DISEASE
Romina Mariel Rodriguez

Biological rhythms are internal timing mechanisms that allow organisms to adapt and anticipate cyclical changes in the environment caused by the rotation of the earth around its axis (circadian rhythms) and around the sun (circannual rhythms). Disruption of these mechanisms have been associated with impairment of metabolic homeostasis. Nowadays, excessive consumption of high-calorie foods has not only been shown to promote metabolic dysfunction, but also to cause circadian disturbances leading to Metabolic syndrome (MS) and non-alcoholic fatty liver disease (NAFLD). Proanthocyanidins, including grape seed proanthocyanidin extract (GSPE), are secondary plant metabolites that are considered beneficial in treating metabolic diseases. It has been reported that GSPE is able to modulate the circadian clock machinery, thus influencing the internal rhythmicity of metabolic processes. Therefore, the main aim of the present thesis was to evaluate if diurnal rhythms (day/night) and seasonal rhythms (photoperiods) can influence the beneficial effects of GSPE consumption on liver metabolism. To fulfill this objective, we carried out animal experiments and analyzed lipid and glucose-related parameters in blood and liver in relationship with the liver clock function. Firstly, we assessed the alteration of the hepatic metabolic rhythms caused by an obesogenic diet intake and demonstrated that the restorative effect of GSPE depends on the timing of administration. Most of its beneficial effects were found when GSPE was administered at the onset of the dark phase, the beginning of the active phase in rats. Secondly, we determined the photoperiod-dependent response of GSPE effects over serum hormones and liver metabolism under physiological conditions. Finally, we evidenced the strong influence of day length on the beneficial effects of GSPE consumption to treat MS and NAFLD. These findings highlight the importance of considering biological rhythms when studying the therapeutic actions of proanthocyanidins in MS-associated diseases in order to maximize their benefits.